





**THE BRITISH COTTON INDUSTRY  
RESEARCH ASSOCIATION**

**THE SHIRLEY INSTITUTE, DIDSBURY,  
MANCHESTER**

Please return before the date given below:

30.3.53.

*Books and journals must be returned by  
Registered Post.*











KONINKLIJKE NEDERLANDSE AKADEMIE  
VAN WETENSCHAPPEN

---

PROCEEDINGS OF THE  
SECTION OF SCIENCES

VOLUME LIV

SERIES B  
PHYSICAL SCIENCES

1951  
NORTH-HOLLAND PUBLISHING COMPANY  
(N.V. NOORD-HOLLANDSCHE UITGEVERS MAATSCHAPPIJ)  
AMSTERDAM





ELASTIC VISCOUS OLEATE SYSTEMS CONTAINING KCl. XV \*)

*Note on the relation between  $n$  and  $\Delta$ .*

BY

H. G. BUNGENBERG DE JONG

(Communicated at the meeting of November 25, 1950)

1. *Introduction*

In part I section 9 we drew attention to the fact that the  $n$  (the total number of turning-points which are observable through the telescope) of a given oleate system in a given spherical vessel, strangely enough appears to be independent of the intensity of the impulse which produces the damped rotational oscillation (only in the case of very weak impulses  $n$  becomes smaller, see part VII). Though in many tables in the parts I—IX  $n$  values have been inserted next to values of  $\Delta$  (logarithmic decrement), a general discussion of the correlation between  $n$  and  $\Delta$  has not yet been given. It was only known

1. that  $n$  represents some measure for the reciprocal of  $\Delta$ , as  $n$  always decreases when  $\Delta$  increases, and conversely;
2. that with a certain type of experiments (constant oleate concentration, constant radius of the vessel, variation of the KCl concentration, or when KCl is kept constant too, addition of organic substances) graphs which give the changes of  $n$  resemble very much those which give the changes of  $1/\Delta$  (Examples in parts VI, VII and VIII).

This is of great practical importance because  $n$  can easily be determined, whereas the measurement of the decrement does not only require experience but also special observational gifts. It enabled to continue in the parts X—XIII, the investigations which were begun in the parts VI—IX (on the connection between the action of an organic substance and its structure) by means of measurements of the period and  $n$  only.

It is the aim of the present communication to determine from the available data how  $n$  depends on  $\Delta$ . This dependency will prove to be more complicated than is expressed by the equation  $n \cdot \Delta = \text{constant}$ . One of the points of discussion will be, why nevertheless in the above mentioned types of investigations (comparison of organic substances, comparison of salts), the changes in  $n$  can successfully be used instead of

---

\*) Part I has appeared in these Proceedings 51, 1197 (1948); Parts II—VI in these Proceedings 52, 15, 99, 363, 377, 465 (1949); Parts VII—XIV in these Proceedings 53, 7, 109, 233, 743, 759, 975, 1122, 1319 (1950).

the changes in  $1/\Lambda$ . The discussion will further lead to the question what is happening during the giving of impulse used for producing the damped oscillation.

2. *The simultaneous change of  $n$  and  $1/\Lambda$ , when only one parameter is varied. General character of the  $n-1/\Lambda$  curve for the rotational oscillation <sup>1)</sup>*

We will consider successively the effects of a change in the oleate concentration, the KCl-concentration, the radius of the vessel and the temperature <sup>2)</sup>. When not stated otherwise the other parameters which are kept constant, have the following values: 1.2 % oleate from MERCK <sup>3)</sup>, a KCl concentration corresponding to the one of minimum damping, a temperature of 15°, a  $R$  of approxim. 5 cm (vessels of nominally 500 ml capacity).

Fig. 1 gives the simultaneous change of  $n$  and  $1/\Lambda$  when the oleate concentration is varied (see table I in part III). The  $(n, 1/\Lambda)$  points lie on a kinked curve, which consists of two straight branches. We will mark the lower of these branches with "branch a", the upper which is less steep, with "branch b". Fig. 1 shows that, though  $n$  is a rough measure for the reciprocal of  $\Lambda$ , it is erroneous simply to describe this relation by the equation  $n \cdot \Lambda = \text{constant}$ . In the latter case we would obtain one straight line through the point of intersection of the coordinate axis. It is only branch a of the  $n-1/\Lambda$  curve which nearly fulfils this equation, but there

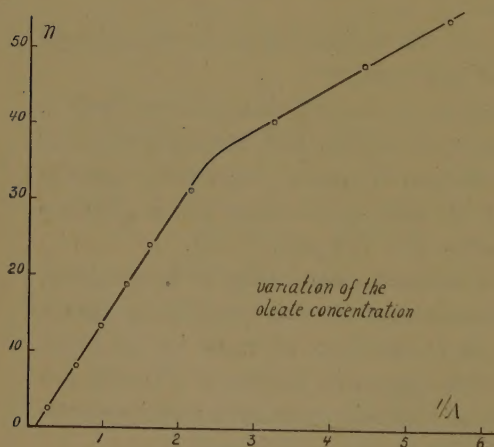


Fig. 1

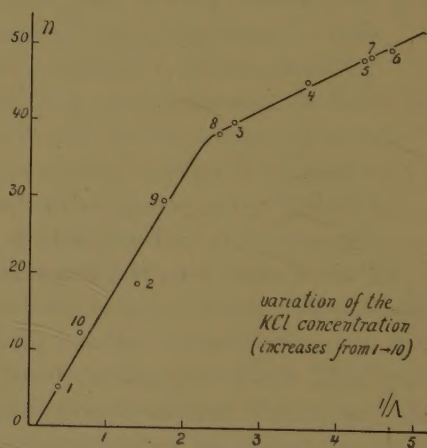


Fig. 2

<sup>1)</sup> As the rotational oscillation is the only one which has practical importance, we will not discuss the scarce data of the parts II and III relating to the quadrantal and meridional oscillation.

<sup>2)</sup> The experiments have been performed partly with completely filled vessels and partly with exactly half filled vessels. As no systematic differences could be detected between them, we have not introduced the degree of filling as a separate parameter.

<sup>3)</sup> Below we will meet an example in which nevertheless the  $(n, 1/\Lambda)$  point may move along branch a by varying the radius. See fig. 14.



is as yet this difference that branch *a* cuts the abscissa at a finite, though small, value of  $1/\Lambda$ .

Fig. 2 gives the  $n-1/\Lambda$  diagram for the blank series of the experiments in part VI, table 1). In this series the KCl concentration is increased at constant oleate concentration (1.2 % oleate). The shape of the  $n-1/\Lambda$  curve is the same as in fig. 1. We have numbered the experimentally determined points with 1 up to and including 10. In this sequence the KCl concentration increases. We see that the  $(n, 1/\Lambda)$  point first moves upwards along branch *a*, then upwards along branch *b*, reaches a final point here (at the KCl concentration corresponding with the one of minimum damping) and then returns along the same path (first downwards along branch *b*, then downwards along branch *a*).

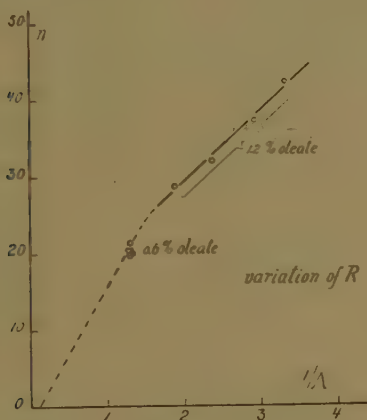


Fig. 3

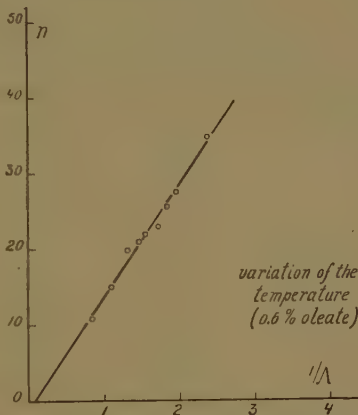


Fig. 4

We now turn to the variation of the radius of the spherical vessel. In none of the experiments in the parts II and V relating to 1.2 % oleate systems at  $15^\circ$  the radius has been varied so much as to obtain a complete  $n-1/\Lambda$  curve showing the characteristic two branches. The experimentally determined points are always lying on branch *b*. Compare fig. 3, which represents the results of the experiment of part II, table I.

Analogous experiments with 0.6 % oleate systems are not even capable to give  $n-1/\Lambda$  curves, because here  $\Lambda$  is independent of  $R$  (see part III, section 3)) and  $n$  hardly varies ( $n$  increases slightly with increasing  $R$ ). Therefore the results plotted in a  $n-1/\Lambda$  diagram will, only give a group of points lying close together at the same value of  $1/\Lambda$ .

Tentatively we have plotted the results of the experiment of part III, table III in the same figure 3 and have drawn a dotted line through this group of points and a point on the abscissa at  $1/\Lambda = 0.1$ . If the dotted line is combined with the drawn line through the experimentally determined points for the 1.2 % oleate system we get the usual shape of the  $n-1/\Lambda$  curve. The dotted line then represents branch *a*, but because  $\Lambda$  is independent of  $R$  for the 0.6 % oleate system, it is impossible to move

along this branch by varying  $R$ . This is only possible when other oleate concentrations are chosen. As we would enter the subject of section 4 with this (the effects of the variation of two parameters at the same time), a further discussion of this problem can better be postponed till later.

The last parameter to be discussed in this section is the temperature.

The only experiment till now published relates to a 1.2 % oleate system (table V in part II). But we have reasons to mistrust this experiment as being representative, and will therefore not represent it graphically <sup>4</sup>).

In table I the results have been given of an experiment together with Mr H. VAN DEN BERG on the influence of the temperature on the 0.6 % oleate system at the KCl concentration of minimum damping, which experiment has not yet been published.

TABLE I

*Influence of the temperature on  $T$  and  $\Delta$  of the 0.6 % oleate system (Na-oleate from MERCK, at 1.43 N KCl, exactly half filled 500 ml vessel)*

Temp.	$10 T/2$	$n$	$\Delta$	$1/\Delta$
3.27	12.65	34.8	0.421	2.38
5.38	12.65	27.6	0.511	1.96
7.27	12.56	25.6	0.547	1.83
8.83	12.52	23.3	0.583	1.72
11.27	12.38	22.0	0.644	1.55
13.79	12.12	21.0	0.685	1.46
15.09	12.15	19.8	0.761	1.31
17.90	12.15	15.0	0.920	1.09
20.69	12.06	10.8	1.190	0.84

The results have been plotted in fig. 4. Obviously the experimentally determined points are situated on branch  $a$  of the  $n-1/\Delta$  curve. With a statistical method we calculated 14.9 to be the slope of the best fitting straight line and 0.08 for the value of  $1/\Delta$ , where this line cuts the abscissa.

Summarizing the discussion of this section, we find that for each of the varied parameters the  $n-1/\Delta$  curve has the same character. Attempts to explain its shape will be postponed until section 5. Here we will only discuss why branch  $a$  cuts the abscissa. When the  $(n, 1/\Delta)$  point moves downwards to the left, the oscillations become more and more damped. At last we will reach such a high value of  $\Delta$  (i.e. small value of  $1/\Delta$ ) that the oscillation is so-called critically damped. There is then just no turning point left and we have to write  $n=0$ , though  $\Delta$  is not yet infinite, (i.e.  $1/\Delta$  has still a finite, though small value, which is in the order of 0.1 in our graphs).

When branch  $a$  is further lengthened downwards, it cuts the ordinate

<sup>4</sup>) The marked change in the temperature coefficient of the decrement at 19.5°, found with the used oleate sample, has not been met with in other cases. Neither is it present with oleate from BAKER. Therefore the sample of oleate used in table V of part II, must have been in an exceptional state (an advanced state of chemical deterioration?).

axis as values of about  $n = -1$  or  $-2$  or  $-3$ . Therefore a formula of the type  $(n + 2) \cdot \Lambda = \text{constant}$ , gives a better representation of the dependence of  $n$  on  $\Lambda$  for points on branch  $a$  than  $n \cdot \Lambda = \text{constant}$ .

3. *The addition of organic substances as the only parameter being varied.*  
*The utility of  $n$  in comparing the action of organic substances*

In the following experiments the oleate concentration (1.2 % or 0.6 %), the KCl concentration (at or near that corresponding to the one of minimum damping) the radius of the vessel (500 ml vessels) and the temperature ( $15^\circ$ ) are kept constant. In each experiment a number of organic substances which have been added in different concentrations have been investigated. The results with the first six  $n$ -primary alcohols (table I and II in part VIII), with the Na salts of the fatty acids  $C_8$ ,  $C_9$ ,  $C_{10}$ ,  $C_{11}$ ,  $C_{12}$  and  $C_{14}$  (table II in part IX) and with six hydrocarbons (table I in part VII) have been plotted in the figures 5, 6, 7 and 8.

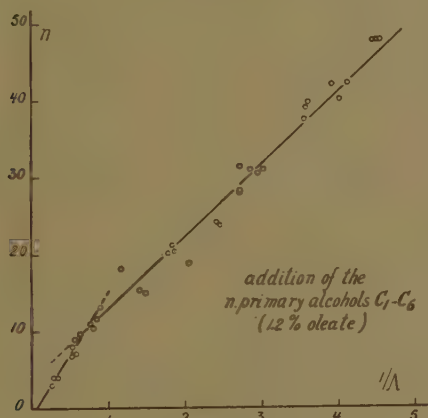


Fig. 5

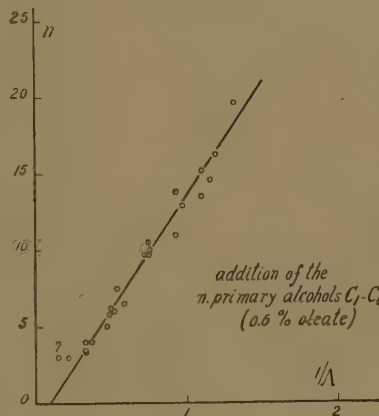


Fig. 6

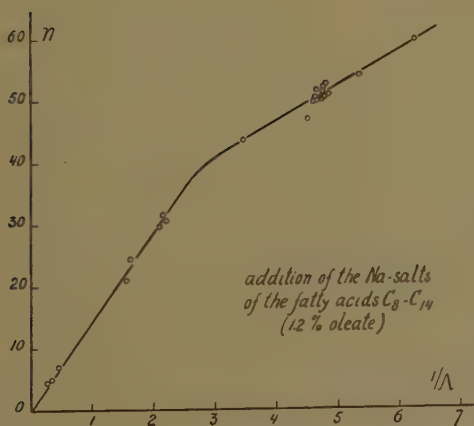


Fig. 7

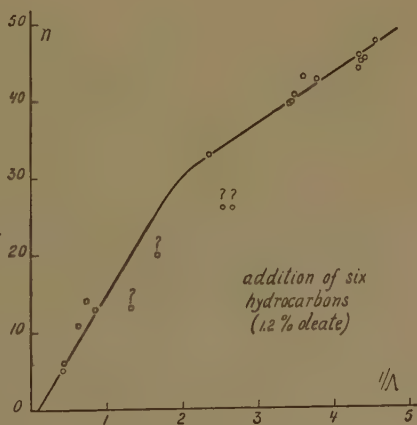


Fig. 8



It is believed that the irregular position of the  $(n, 1/\Lambda)$  points is due to experimental errors and to other circumstances<sup>5)</sup>.

For that reason we have drawn only one  $n-1/\Lambda$  curve through the points. The comparative regular position of the experimentally determined points in fig. 7 induces one to consider this experiment to be the most representative<sup>6)</sup>. The point representing the blank oleate system lies on branch *b* here and addition of each of the 6 organic substances causes the  $(n, 1/\Lambda)$  point to shift along one and the same  $n-1/\Lambda$  curve. The differences in action between the six organic substances which were investigated solely concern the direction in which this point is shifted (upwards to the right along branch *b* with  $C_{14}$ , downwards to the left along branch *b* and thereafter downwards along branch *a* with  $C_8, C_9, C_{10}, C_{11}$  and  $C_{12}$ ) and the rate of displacement (at equal concentrations of the added substances the positions of the  $(n, 1/\Lambda)$  point are very much different).

This explains why the graphs which give  $n$  or  $1/\Lambda$  as a function of the concentration of the organic substances resemble one another so much. Compare the figures 9 and 10 (taken from figure 6 in part VI). All the

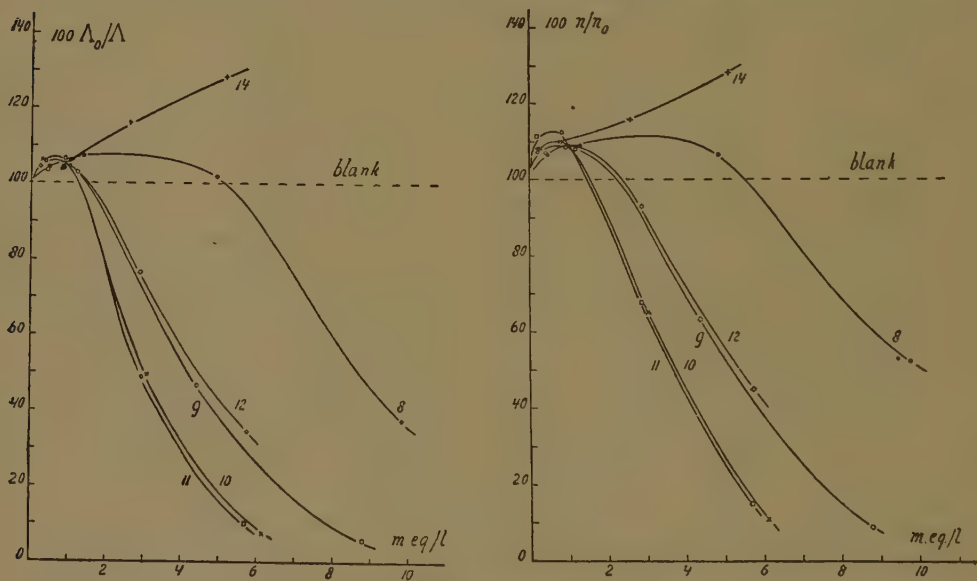


Fig. 9 and 10. Influence of the Na salts of the fatty acids  $C_8, C_9, C_{10}, C_{11}, C_{12}$  and  $C_{14}$  on  $\Lambda$  and  $n$  of the 1.2 % oleate system

<sup>5)</sup> The experiments have been made with the large volumes of the KCl containing oleate systems which had already served in previous experiments and had been kept in store. At the performance of each of these four series of experiments the stock oleate had a different age, and slow chemical alterations of the oleate in solution may have proceeded in different degrees. It is our experience that the errors with such long kept oleate systems are larger than with freshly prepared ones.

<sup>6)</sup> In one respect the experiment is not representative, viz the fact that branch *a* is proceeding here through the point of intersection of the coordinate axis. As this does not occur in any of the remaining figs. in this communication, experimental errors with regard to the position of the points on branch *a* must have been in play.

details of the  $1/A$  diagram (increase or decrease of  $1/A$ , relative position of the  $1/A$  curves) are given qualitatively by the  $n$  diagram <sup>7)</sup>.

Such a close resemblance is also present between the  $n$ -graphs and  $1/A$  graphs in the case of the experiments represented by the figs 5, 6 and 8, (compare for the series of the alcohols fig. 5 in part VI and the fig. 1 and 2 in part VIII; for the series of the hydrocarbons fig. 5 in part VII), though in view of the irregular position of the  $(n, 1/A)$  points in the figures 5, 6 and 8 the presence of relative large experimental errors in the determination of  $n$  or  $1/A$  is evident.

That these errors do not disturb the above mentioned close resemblance comes from the large differences between the successive terms of the homologous alcohols respectively the investigated six hydrocarbons with regard to the rate of displacement of the  $(n, 1/A)$  point downwards along the  $n-1/A$  curve (the blank point is the topmost one at the right side in fig. 5, 6 and 8).

4. *The simultaneous change of  $n$  and  $1/A$ , when two parameters are varied in the same experimental series. The position of branch  $b$  of the  $n-1/A$  curve*

In the preceding figures the  $n-1/A$  curve always has the same character, but the slopes of its branches are not the same (slightly different for branch  $a$ ; sometimes very much different for branch  $b$ ).

Now these experiments have been performed at different times with the contents of different flasks of Na oleate from MERCK. As the oleate changes with time (slow chemical deterioration) and this change proceeds with different rates in the individual flasks, the differences in slope in particular of branch  $b$  may be due to the samples of used oleate being no longer strictly comparable. Indeed in some separate experimental series in which quite the same parameter had been varied, the slopes of the branches  $b$  differed considerably (examples below in the notes 8 and 9).

We are now interested in the question if, for a given oleate sample, there exists only one  $n-1/A$  curve for all the five parameters that are considered.

It will be clear that no answer can be given to this question by comparing the  $n-1/A$  curves obtained from separate experimental series.

Happily we have a number of experiments where two parameters have been varied in the same experimental series. Only they allow to compare safely the  $n-1/A$  curves, due to each of these parameters apart.

---

<sup>7)</sup> Of course in the vertical direction the  $n$  diagram is distorted, because the  $n-1/A$  curve is no straight line but a kinked curve. In fig. 9 and 10 this distortion is not easily observable at first sight. In graphs in which the  $1/A$  curve is a characteristic maximum curve the distortion of the  $n$ -curve is at once plainly visible. Compare in part VI the figures 1, 2 and 4, from which it appears that the  $n$  curves have a much flatter maximum than the  $1/A$  curves, and further that the depression of the maxima of the  $n$  curves by added  $n$ -hexanol or ethanol is percentually less than the depression of the maxima of the  $1/A$  curves.

All experimentally determined points of the experiment of table I in part VI (in which the KCl concentration has been varied and *n*-hexanol has been added in different concentrations) have been designed in the  $n-1/\Lambda$  diagram of fig. 11. Similarly all experimentally determined points of table I in part IX (in which the KCl concentration has been varied and ethanol has been added in different concentrations) have been designed in fig. 12.

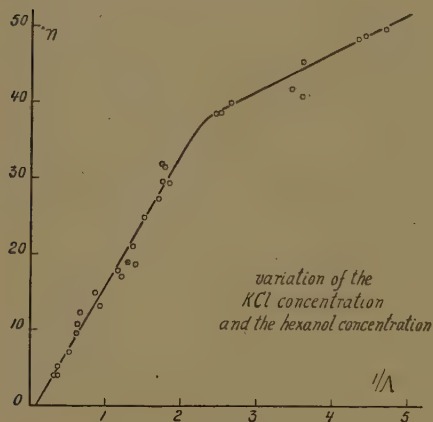


Fig. 11

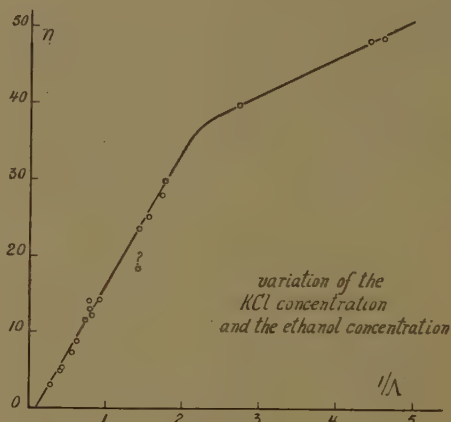


Fig. 12

Apart from a somewhat irregular position of some points on the *b* branch in fig. 11, all points (which represent systems with different KCl concentrations for the blank, and systems with different KCl concentrations which also contain hexanol or ethanol in different concentrations) lie close to only one  $n-1/\Lambda$  curve. Therefore there is no indication whatever that there should exist different  $n-1/\Lambda$  curves, or even different *b* branches for the two varied parameters viz. the addition of an organic substance and the variation of the KCl concentration<sup>8)</sup>.

We have still another example in which the same applies for the case that two parameters are varied at the same time, namely the addition of an organic substance and the variation of the radius of the spherical vessel.

Compare fig. 13 (data of table I in part V) and fig. 14 (data of table III in part V), which represent the variation of *R* for the blank 1.2 % oleate system<sup>9)</sup> and for the same system containing two different *n*-hexanol

<sup>8)</sup> The slope of the *b* branch in fig. 5 is exceptionally steep, compared to that of the *b* branches in fig. 7 and 8. That this difference is not due to a separate position of the *b* branch for the class of the alcohols, but to a different state of the used oleate sample (compare note 5), follows from the slopes of the *b* branches in fig. 11 and 12, which figures just like fig. 5 give the influence of ethanol and *n*-hexanol on the 1.2 % oleate system.

<sup>9)</sup> Comparison of fig. 13 with fig. 3 gives another instance of different slopes for quite the same kind of experiment. Once more we must conclude to different properties of the oleate samples which were used for the two experiments.



concentrations. The branches *b* have been drawn in exactly the same position in fig. 13 and 14. It therefore appears that for the two varied parameters viz. the addition of an organic substance and the variation of the radius, there exists only one *b*-branch along which the ( $n$ ,  $1/\lambda$ ) point can shift.

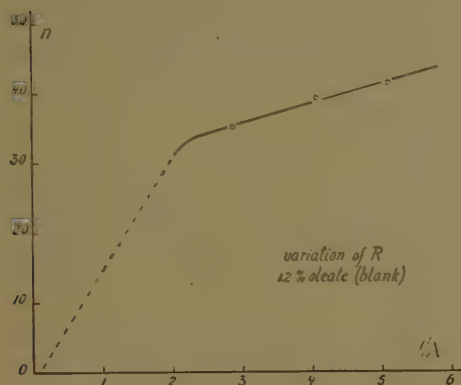


Fig. 13

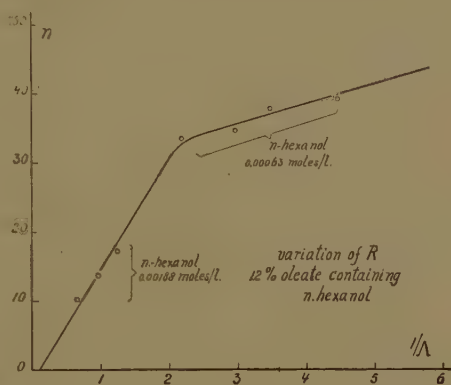


Fig. 14

The data at our disposal show that a generalization of the above to every two combinations of parameters is not allowed. A first example is given by fig. 15, in which the influence of the radius has been investigated for 4 oleate systems of different concentrations (data from table I in part V). The group of points for the 0.3 % oleate system and the group of points for the 0.6 % oleate system lie on a dotted line, the slope of which corresponds to the one of branch *a* of the usual  $n-1/\lambda$  curve. We perceive, however, that the experimentally determined points for the 1.2 % and the 1.8 % oleate systems are not situated on the same branch *b*, but on separate branches of the type *b* with different slopes.

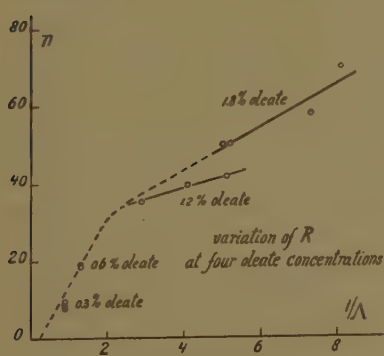


Fig. 15

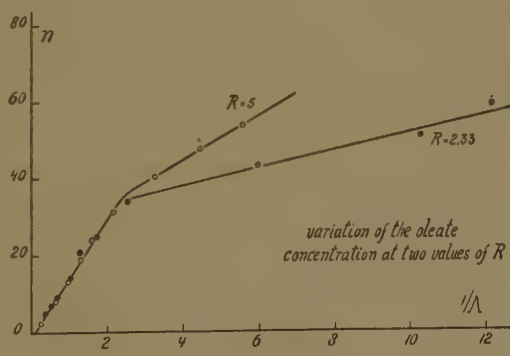


Fig. 16

A second example is given by fig. 16, in which the influence of the oleate concentration on the elastic properties has been investigated in two vessels of different radii (combined data of the tables I and II in part III).

The experimentally determined points for both vessels lie on typical kinked curves consisting of two (probably) straight parts.

The  $a$ -branches of both  $n-1/\Delta$  curves coincide, but the  $b$ -branches have different slopes.

We have therefore recognized that the position of the second branch depends on the oleate concentration when  $R$  is varied (fig. 15) and — what is the same in principle — on  $R$  when the oleate concentration is altered (fig. 16).

### 5. *The shape of the $n-1/\Delta$ curve*

In part V of this series it was found that the 0.3 % and 0.6 % oleate systems, which lie on branch  $a$  in fig. 15, are characterized by a  $\Delta$  which is independent of  $R$ , whereas the 1.2 % and 1.8 % systems which lie on branch  $b$  in fig. 15 have a  $\Delta$  which is proportional to  $R$ . This leads to the question whether the kink in the  $n-1/\Delta$  curve might generally indicate a change in the nature of the damping.

The results of the experiments represented in fig. 14 do not support this supposition. In this figure the influence of a variation of  $R$  for the 1.2 % oleate system is shown at two concentrations of  $n$ -hexanol. For the lower hexanol concentration the  $(n, 1/\Delta)$  points lie on branch  $b$ , but for the higher hexanol concentration they lie on branch  $a$ . But, as was shown in part V of this series, for both hexanol concentrations  $\Delta$  was found to be proportional to  $R$  (just as in the blank series represented in fig. 13). Therefore it is not true that in the most general sense the kink in the  $n-1/\Delta$  curve indicates a change in the character of the damping.

From the following it will appear that the kink in the curve probably indicates a change in what happens during and immediately after the giving of impulse for producing the damped oscillation.

To explain the independence of  $n$  (of a given oleate system in a given vessel) from the intensity of the impulse, it was supposed (in part I, section 9) that these happenings consist of liquefaction of the oleate system at the glass-wall, slip along the wall and resolidification into the maximally deformed elastic system (compare the flow curves in parts IV and V). The damped oscillation which is now setting in will show (dependent on the  $\Delta$  of the considered oleate system) a definite number  $n$  of turning points. This number is limited because the amplitude following the  $n$ th turning point is just no longer observable.

It seems appropriate now to limit this explanation to systems situated on branch  $a$  of the  $n-1/\Delta$  curve. But we must add a very remarkable conclusion concerning the initial maximum deformation after the impulse is given for all oleate systems on branch  $a$ .

This initial deformation must always be practically the same, because branch  $a$  is characterized by  $n \cdot \Delta$  being approximately constant (why  $\Delta \cdot n$  cannot be exactly constant has been explained at the end of section 2). For, the number of observable turning-points  $n$  between the same

initial deformation and the same last observable deviation is then inversely proportional to  $\Delta$ , that is  $n \cdot \Delta = \text{constant}$ .

It follows from the smaller slope of branch  $b$  that the initial deformation to the right of the bend in the  $n-1/\Delta$  curve is no longer the same after the impulse is given, but becomes smaller as the  $(n, 1/\Delta)$  point lies more to the right on branch  $b$ .

The above-mentioned happenings during the giving of impulse therefore, no longer occur or at least change profoundly in character.

### *Summary*

1. From data in the parts I—IX of this series the correlation between  $n$  (the maximum number of observable turning-points) and  $\Delta$  (the logarithmic decrement) has been discussed with the aid of  $n-1/\Delta$  graphs.

2. For experimental series in which only one parameter had been varied (oleate concentration, KCl concentration, radius of the vessel, temperature, addition of organic substances) the  $n-1/\Delta$  curve consists of two probably straight lines,  $a$  and  $b$  of different slopes.

3. The lower and at the same time steeper, branch  $a$  cuts the  $1/\Delta$  axis at a finite, though small value of  $1/\Delta$  (corresponding to the "critically damped" oscillation). The position of branch  $a$  may differ slightly in the separate experimental series. It must be due to differences between the samples of the used oleate, as in experimental series in which two parameters had been varied at the same time, the  $(n, 1/\Delta)$  points only moves along one and the same branch  $a$ .

4. The position of the upper, less steep, branch  $b$  is much more influenced by the above-mentioned differences between the separate samples of the used oleate (different stages of the slow deterioration of the oleate). It is only from experimental series in which two parameters had been varied at the same time, that safe conclusion can be drawn whether as a consequence of a variation of each of the two parameters the  $n, 1/\Delta$  point shifts along the same branch  $b$  or not. The first applies for 1) variation of the KCl concentration and addition of an organic substance, 2) variation of the radius and addition of an organic substance. Different branches of the type  $b$  exist for the variation of the radius and the variation of the oleate concentration.

5. It has been explained why, in the type of experiments performed in the parts X—XIII with the aim to compare the action of organic substances or of salts, the changes in  $n$  can successfully be used in practice instead of the changes in  $1/\Delta$ .

6. The kink in the  $n-1/\Delta$  curve does not necessarily indicate a change in the character of the damping. The character may be the same ( $\Delta \sim R$ ) on both branches or it may be different ( $\Delta$  independent of  $R$  on branch  $a$  and  $\Delta \sim R$  on branch  $b$ ).

7. From the equation  $n \cdot \Delta = \text{approximately constant}$ , which characterizes branch  $a$ , follows that the initial elastic deformation resulting from

the impulse which is given, has practically the same magnitude for oleate systems situated on branch *a*. The happenings during and directly after the giving of impulse are supposed to consist of liquefaction at the glass-wall, slip and resolidification into a maximally deformed elastic system here.

8. It follows from the smaller slope of branch *b* that to the right of the bend in the  $n-1/A$  curve the initial deformation after giving of impulse is no longer the same, but becomes smaller as the  $(n, 1/A)$  point lies more to the right on branch *b*.

The above-mentioned happenings are supposed to occur no longer here or to have changed profoundly in character.

*Department of Medical Chemistry,  
University of Leiden*



A NEW HOMOLOGUE OF PROVITAMIN D<sub>3</sub>

BY

J. STRATING AND H. J. BACKER

(Communicated at the meeting of January 27, 1951)

Several homologues of provitamin D<sub>3</sub> have been synthesised by varying its side chain <sup>1</sup>). Their interest lies in the possibility of studying the influence of these variations on the vitamin properties of the irradiated products.

Now we have studied a new type of homology, where the alteration refers to carbon atom 3 of the sterol molecule. In order to introduce a methylene group in this position, we may replace the 3-hydroxyl group by intermediance of the carboxylic methyl ester, which is finally reduced with lithium aluminium tetrahydride:



In this way we can transform 7-dehydrocholesterol (provitamin D<sub>3</sub>) into its homologue 7-dehydro-3-homocholesterol.

7-Dehydrocholesteryl chloride (II) prepared by bromination of cholesteryl chloride (I) and elimination of hydrobromic acid <sup>2</sup>), can be converted into the Grignard derivative, which by means of carbon dioxide is transformed into 7-dehydrocholesteryl-3-carboxylic acid (m.p. "in vacuo" 214–215°, clear liquid at 260°).

Diazomethane gives, in nearly theoretical yield, the methyl ester (III), which melts at 118.5–119.5° and gives a clear liquid at 127°;  $[\alpha]_D^{20} = -70.9^\circ$  (CHCl<sub>3</sub>). Its ultra-violet absorption-spectrum is the same as that of 7-dehydrocholesteryl acetate, so that we may conclude that the conjugated system of double bonds in ring B is unchanged.

The selective reduction of this methyl ester was effected by means of LiAlH<sub>4</sub>. In this way is formed 7-dehydro-3-homocholesterol (IV) or 3-homoprovitamin D<sub>3</sub> (m.p. "in vacuo" 125–126°, slight alteration at 120°).  $[\alpha]_D^{20} = -103.4^\circ$  (CHCl<sub>3</sub>).

The absorption spectrum of this compound (IV) shows that the conjugated system has not changed during the reaction. This homoprovitamin has been characterised by its acetate (m.p. 97.5–99°;  $[\alpha]_D^{18} = -87.2^\circ$ ), benzoate (m.p. 98–100°;  $[\alpha]_D^{18} = -59.9^\circ$ ) and 3,5-dinitrobenzoate (m.p. 183–184°;  $[\alpha]_D^{18} = -24.3^\circ$ ).

<sup>1</sup>) HARMEN DE VRIES and H. J. BACKER, Rec. trav. chim. **69**, 759, 1252 (1950).

<sup>2</sup>) J. STRATING and H. J. BACKER, Rec. trav. chim. **69**, 904 (1950).

All melting points were taken "in vacuo". The absorption spectra show that the conjugated system is still present. In the case of the benzoate and the dinitrobenzoate the absorption due to the acid rest has to be eliminated before this comparison is possible.

Now the question arises about the steric configuration at carbon atom 3. The configuration at the asymmetric carbon atom 3 is usually expressed by the position of the hydroxyl group with regard to the axillary methyl group, linked to carbon atom 10.

In cholesterol, where the OH-3 and the CH<sub>3</sub>-10 ly on the same side of ring A, the position of the OH group is called  $\beta$ , whereas for epicholesterol the position is  $\alpha$ .

In order to decide on the position of the hydroxymethyl group in the 3-homoprovitamin D<sub>3</sub> (IV), we can try an alternative synthesis from 3-homocholesterol, for which we can examine the configuration by means of the digitonine test.

One of the conditions for this test is that the position of the 3-hydroxyl group is the same ( $\beta$ ) as in cholesterol. When the homologue gives a digitonide, we may assume that the CH<sub>2</sub>OH group has the same position as the OH group of cholesterol. If, however, no digitonide separates, the problem cannot be resolved in this way.

The synthesis of 3-homocholesterol (VI) can be realised by means of the carboxylic acid, which is obtained by reacting carbon dioxide on the Grignard derivative of cholesteryl chloride. As a rule, this reaction yields a mixture of the two possible epimers <sup>3)</sup>.

The methyl ester (V), formed by methylation of cholesteryl 3-carboxylic acid with diazomethane and purified by recrystallisation from methanol, is, however, a single compound with a sharp and constant melting point (101.5—102.5°.)

This appears from the quantitative reduction with LiAlH<sub>4</sub> to 3-homocholesterol (VI, m.p. 129—130°,  $[\alpha]_D^{15} = -35.5^\circ$ ), which forms a digitonide.

From the mother liquor of this digitonide, which is rather soluble and partly dissociated, the rest of the sterol could be isolated. By the melting (and "mixed melting") points — before and after acetylation — this sterol proved to be identical with the sterol present in the digitonide. Thus 3-homocholesterol (VI), as well as the methyl ester (V) from which it is prepared, are single compounds.

From the fact that the 3-homocholesterol obtained gives a digitonide, we may conclude that its CH<sub>2</sub>OH group occupies the same steric position as the OH group of cholesterol.

In the acetate of 3-homocholesterol (VII) we can introduce a double bond 7—8 by using the same method as mentioned above for the preparation of 7-dehydrocholesteryl chloride (bromination and elimination

<sup>3)</sup> R. E. MARKER and coll., J. Am. Chem. Soc. **58**, 481 (1936).  
C. W. PORTER, *ibid.* **57**, 1436 (1935).

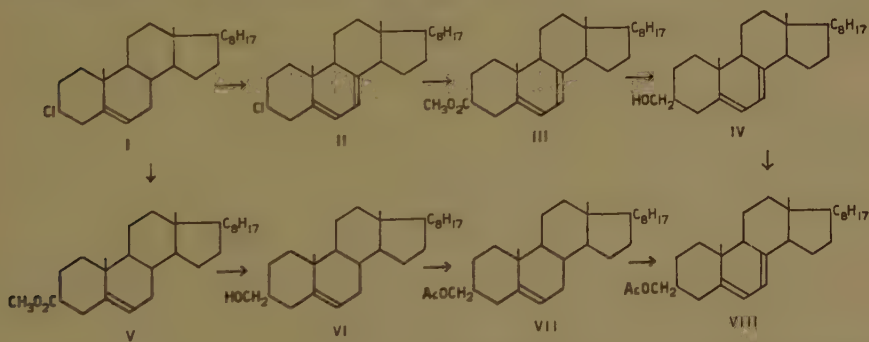
of HBr). Thus in the diene obtained (VIII) the position of the 3-CH<sub>2</sub>OH group is also known ( $\beta$ ).

The 7-dehydro-3-homocholesteryl acetate (VIII) so obtained, which is difficult to purify, has a melting point of 97—97.5°;  $[\alpha]_D^{18} = -83.8^\circ$ . The absorption spectrum shows that this product is pure for 98 %. The melting point (97—97.5°) is the same as that of the acetate, prepared from the carboxylic acid by the first method. The somewhat smaller rotation ( $-83.8^\circ$  in stead of  $-87.2^\circ$ ) may be ascribed to the slight impurity (2 %), which, on account of the small quantity available, could not be completely removed.

From these facts and from the observation that the free 7-dehydro-3-homocholesterol (IV) also gives a digitonide (according to the absorption spectrum an equimolecular combination of digitonine and 7-dehydro-3-homocholesterol), we may conclude that the homoprovitamin D<sub>3</sub> possesses the  $\beta$ -configuration at carbon atom 3.

The separation of the epimers of cholesteryl-3-carboxylic acid has been effected by recrystallisation of the methyl ester. For the 7-dehydrocholesteryl-3-carboxylic acid, the elimination of the epimer must have occurred during the purification of the acid itself. For all the various transformations (acid  $\rightarrow$  ester  $\rightarrow$  sterol  $\rightarrow$  acetate) are nearly quantitative reactions and they yield finally the single compound with  $\beta$  configuration.

The details of this research will be published elsewhere.



Molecular extinction coefficient at the maxima and minima of the ultra-violet absorption-spectrum (alcoholic solution, effective band width 1.5 m $\mu$ )

$\lambda$ (m $\mu$ )	271.3	276.3	281.8	289.6	293.4
P.A. *)	11500	9800	12160	6270	6820
IV	11260	9800	11970	6380	6850
VIII from IV	11720	10100	12400	6550	7050
VIII from VII	11740	10120	12310	6540	7080
III	11670	10020	12250	6430	6930
IV-benzoate minus VI-benzoate	11440	9580	12100	6670	7080
IV-dinitrobenzoate minus VI-dinitrobenzoate	11210	9830	11920	6590	6960

\*) P.A. = Provitamin D<sub>3</sub> acetate (7-dehydrocholesteryl acetate).

# DETERMINATION OF ABSOLUTE CONFIGURATION OF OPTICAL ACTIVE COMPOUNDS BY MEANS OF X-RAYS

BY

A. F. PEERDEMAN, A. J. VAN BOMMEL AND J. M. BIJVOET

(Communicated at the meeting of December 23, 1950)

## § 1. Introduction

It has been remarked<sup>1)</sup> that X-rays should be able to determine the absolute configuration of optically active compounds by using X-rays exciting one of the atoms.

Indeed this procedure is known to invalidate<sup>2)</sup> FRIEDEL's law of the equivalence of  $hkl$  and  $\bar{h}\bar{k}\bar{l}$  reflection, thus enabling us to determine a polar sequence<sup>3)</sup>. With this fact in mind the common statement that X-rays should be incapable of distinguishing between optical antipodes evidently needs revision. Our attention was drawn to the problem of the determination of absolute configuration in determining the phases of the FOURIER-waves by the isomorphous substitution method in the non-centrosymmetrical case. The mutual comparison of the intensities of two isomorphous compounds makes the determination possible of the phase differences from the density waves of the heavy atom configuration<sup>4)</sup>. (In this paper the latter configuration is supposed to be centrosymmetrical). The *signs* of these phase angles remain unknown as long as  $hkl$  and  $\bar{h}\bar{k}\bar{l}$  reflections are equivalent.

Fig. 1 shows how the introduction of a phase "lag" in the scattering of the heavy atom, destroying this equivalence, enables us to distinguish positive and negative wave phases. This phase "lag" relative to the scattering by a free electron is negative. The sign determination for all or the greater part of the phase angles should reveal the structure in every respect, absolute configuration included. When a structure has been determined already except for absolute configuration, the phase sign determination of a single reflection suffices to decide between the two inverted-mirror-images. In the following, the result of the latter procedure will be given for the ordinary — dextrarotating — tartaric acid. It may be remarked that other methods of determining the absolute con-

<sup>1)</sup> J. M. BIJVOET, These Proceedings 52, 313 (1949).

<sup>2)</sup> M. v. LAUE, Ann. Physik, 50, 33 (1916).

<sup>3)</sup> D. COSTER, K. S. KNOL and J. PRINS, Z. für Physik 63, 345 (1930).

<sup>4)</sup> C. BOKHOVEN, J. C. SCHOONE and J. M. BIJVOET, These Proceedings 52, 120 (1949).



figuration — viz. from the theoretical calculation of the rotatory power <sup>5)</sup> or from the relation between crystal structure and face development <sup>6)</sup> — led to no conclusive results <sup>5)</sup>, at least until recently <sup>7)</sup>.

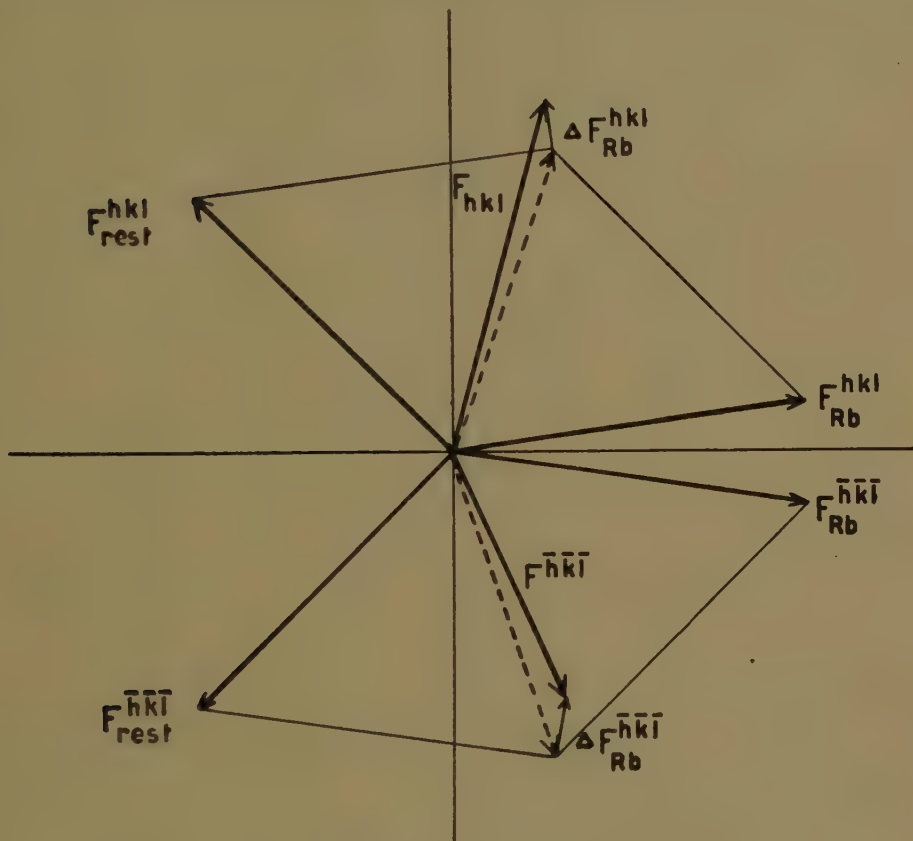


Fig.1

Fig. 1. The vectors  $F_{Rb}$  and  $F_{rest}$  are combined for the reflections  $hkl$  and  $\bar{h}\bar{k}\bar{l}$  resp. neglecting the imaginary part of the structure factor of  $Rb$ . The resultant (dotted) amplitudes are of equal modulus but opposite phase. The introduction of the term  $\Delta F''_{Rb}$  with phase increment  $\pi/2$  in respect to  $F_{Rb}$  is seen to destroy this equality of the resultant modulus.

§ 2. Using monochromatized  $Zr K_\alpha$ -rays which excite the  $Rb$ -atom a first layer (001) WEISSENBERG diagram of  $Na-Rb$  tartrate has been made

<sup>5)</sup> See e.g. S. GLASSTONE, Textbook of Physical Chemistry, (New York), pg. 607, (1947).

<sup>6)</sup> J. WASER, J. Chem. Phys. 17, 498 (1949). F. E. TURNER and K. LONSDAK, ibid. 18, 156 (1950).

<sup>7)</sup> The authors were glad to learn quite recently that Prof. KIRKWOOD achieved new calculations of the rotatory power, the results of the latter and the X-ray method being concordant as to the assignment of absolute configuration.

(oscillation angle,  $60^\circ$ , exposure time 72 hours)<sup>8)</sup>. The imaginary part of the anomalous scattering effect<sup>9)</sup> in this case amounts to  $\Delta f''_{K_{Rb}} = 3.2$ .

In the table experimental and calculated relation between  $I_{hkl}$  and  $I_{\bar{h}\bar{k}\bar{l}}$  are compared, the latter by symmetry being equal to  $I_{\bar{h}\bar{k}\bar{l}}$ . The visual

TABLE

$h$ $k$ $l$	Calculated		Observed
	$I_{hkl}$	$I_{\bar{h}\bar{k}\bar{l}}$	
1 4 1	361	377	?
1 5 1	337	313	?
1 6 1	313	241	>
1 7 1	65	78	<
1 8 1	185	148	>
1 9 1	65	46	>
1 10 1	248	208	>
1 11 1	27	41	<
2 6 1	828	817	>
2 7 1	18	8	>
2 8 1	763	716	>
2 9 1	170	166	?
2 10 1	200	239	<
2 11 1	159	149	?
2 12 1	324	353	<

estimations of the last column were made by a few persons independently. The calculated values are based on the structure model determined by BEEVERS and HUGHES<sup>10)</sup> — after some refinement of the parameter values — and corresponding in a positive coordinate system to the chemical convention of EMIL FISCHER (see fig. 2) as to absolute configuration. It has been verified that using *Cu*-rays no such differences between  $I_{hkl}$  and  $I_{\bar{h}\bar{k}\bar{l}}$  are found.

Of course one must take care to use the same — e.g. positive — coordinate system in indexing the WEISSENBERG diagram and in taking the atomic coordinates from the model.

The concordance of inequality signs in the observed and calculated intensities seen in the table *proves the chemical convention (fig. 2) to answer reality*.

The calculation of the difference, though small, between  $F_{hkl}$  and  $F_{\bar{h}\bar{k}\bar{l}}$  does not need very accurate  $F$  values. The sign of the inequalities in the table depends only on the fact whether the projection of  $F_{hkl}$  on  $\Delta F''_{Rb}$  has the same direction as the latter vector or opposite.

<sup>8)</sup> Our thanks are due to Mr. J. W. RENKEN for the construction of the Zr-tube and to Mr. E. VERBOOM and H. P. DE JONG for cooperation in the exposures.

<sup>9)</sup> R. W. JAMES, *The crystalline State II*, Appendix III (London 1948).

<sup>10)</sup> C. A. BEEVERS and W. HUGHES, *Proc. Roy. Soc. A* **177**, 251 (1941).

Full details will be published in Acta Crystallographica. We wish to thank the Netherlands Organization for Pure Research (Z.W.O.) for

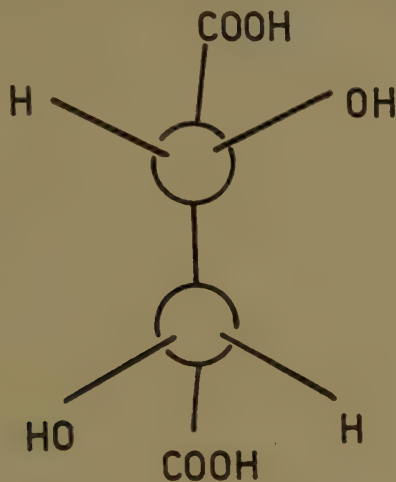


Fig. 2

Fig. 2. Convention according to EMIL FISCHER for the structure of natural, dextrorotating tartaric acid.

their assistance, embodied in the excellent technical help of its preparator Mr. A. KREUGER.

*Van 't Hoff-Laboratorium der  
Rijks-Universiteit, Utrecht*

## PHYSICS

### SIMILARITY OF INITIAL PROCESSES OF CONTINUOUS COSMIC RADIATION AND SHOWERS

BY

J. CLAY

(Communicated at the meeting of January 27, 1951)

#### *Summary*

Two largely different phenomena present themselves in cosmic radiation: the continuous radiation and the showers.

	Density penetrating part. to density soft particles	Increase of intensity from 0 to 7000 m	Barometric coeff. per cm Hg
cont. rad.	3	6	2 %
showers	0.1	600	15 %

The mesons are mostly produced in the upper layer of the atmosphere, but the particles produced in one nuclear reaction conserve their coherence coming down. It is shown to be impossible for an electron producing a shower at high level to cause the density of the showers observed below, neither can this be produced by mesons. But when a nucleon of high energy comes down low in the atmosphere, it can give rise to densities as observed with frequencies of the right order. That nucleons do sometimes penetrate deep into the atmosphere we can prove by the barometric coefficient of penetrating particles of 15 %, by the increase of showers with decreasing barometric pressure of 17 % per cm Hg and by the absorption found for protons.

§ 1. In cosmic radiation we distinguish at present two rather dissimilar processes. There is, firstly, the uninterrupted basic intensity of the radiation, depending upon the latitude and longitude of the place of observation and upon the thickness of the layer of material above the site of the experimental apparatus. The latter dependency implies that the variations of atmospheric pressure and of temperature will influence the observations, but the ensuing fluctuations will be small in comparison with the total radiation and be limited to a few percents.

Secondly, in addition to this continuous intensity we get every now and then concentrated showers, sometimes of very large density and containing particles of high energy. The frequency of these showers varies about inversely as the square (the value lies between 1,4 and 3) of the density of the particles. This means that the frequency has



approximately the same spectrum as the energy spectrum of the continuous radiation. The composition of these showers, however, differs largely from that of the continuous c.r. For while the latter consists of a mixture of roughly 3/4 mesons (penetrating particles) and 1/4 electrons with a number of photons on an average exceeding ten times that of the electrons, the showers contain 10 till 20 times as many electrons as mesons and high energy showers will contain moreover a much higher but very variable number of photons

For the penetrating particles in continuous radiation we find the ratio of the intensity at sea-level to that at 7000 m to be 1 : 6, for the number of penetrating showers this ratio is 1 : 600. The barometric variation for 1 cm Hg is for penetrating continuous radiation 18 %, for the penetrating showers it is of the order of 15 %.

§ 2. Yet we think there is reason to presume that the showers originate in a similar process as the continuous radiation. COCCONI [1] raised the relevant question recently in *Physical Review* 79, 1950.

It is at present a matter of common knowledge that practically all primary mesons in c.r. arise in a concentrated production by the collision of protons (which form the vast majority of the primary incident particles) with nucleons in the upper layers of the atmosphere. The number of mesons produced depends on the energy of the incident particle. At our latitude the energy of the primary particles lies upwards of  $2 \times 10^9$  eVolt, as we conclude from the geo-magnetic cut-off. Towards the equator this limit moves upwards till  $15 \times 10^9$  eVolt.

According to SCHEIN [2], who investigated the number of protons and mesons in the upper atmosphere, the multicentricity of production for primary particles of the minimum energy is in the first nuclear reaction of the order of 5. For higher energies, however, this multiplicity increases. We conclude this from photographs taken at high altitudes with plates coated very thickly with emulsion, a method to which we shall revert presently (photos by SCHEIN and other scientists).

As long as these processes occur between the utmost boundary of the atmosphere (which after the experiments with the  $V_2$  we may put at 50 km) and the height of 110 cm equiv. water or 14 km, this local production will not be very noticeable at the bottom of the atmosphere. For the number of mesons formed in each proton/nucleon collision is small and the divergency will cause the down-coming coherent particles to disperse more and more. Yet a phenomenon of coherence remains unmistakably demonstrable, as we have been able to prove in various experiments.

§ 3. The first precise investigation was made with a system of three counters 5—6—7 connected in parallel under a layer of lead of 20 cm thickness. On top of that two pairs of counters, 1—2 and 3—4, were arranged, one pair crosswise to the other, their resp. levels allowing

of 10 cm *Pb* to be placed between the pairs. We could measure 5-fold coincidences between 1, 2, 3, 4 and (5—6—7). At least two particles were always needed and the cases where more particles were engaged proved to be few in comparison to those where two sufficed. If one particle

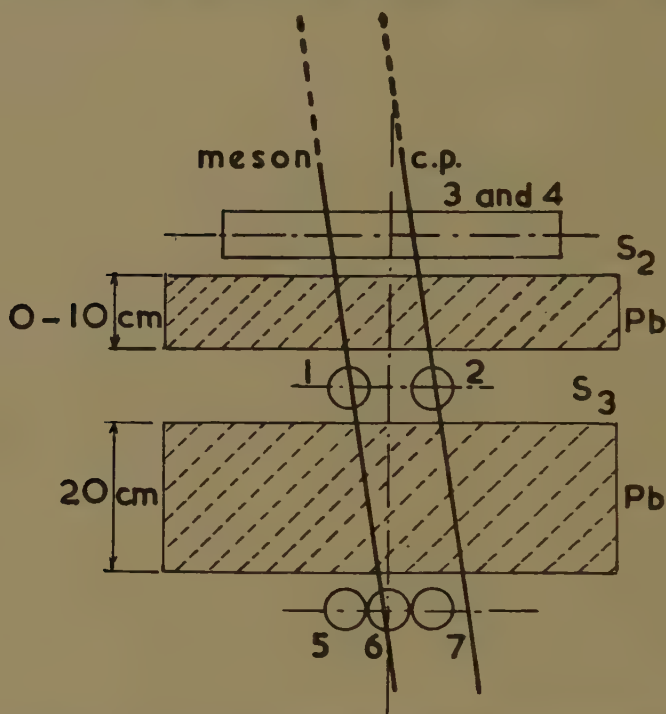


Fig. 1. Arrangement of the 5-fold coincidence apparatus to count coherent mesons (c.p.) produced in the atmosphere. *S* 2 is a layer of *Pb* of between 0 and 10 cm. 1, 2, 3 and 4 are four crossed counters (vide fig. 2). 5, 6 and 7 are connected in parallel.

traverses two crossed counters in any of the surfaces *A*, *B*, *C* or *D*, the co-operating particle will have to traverse the remaining two crossed counters in the crossing situated diagonally opposite. So the distance between these two particles will always be the same, and sufficiently large with regard to the surface of the crossings. For a 5-fold coincidence to happen, one of the particles has to be penetrating, as it has to traverse 20 cm of *Pb* before it can operate (5—6—7). Unless lead is put between the crossed counters, there is no need for the second particle to be penetrating.

With 10 cm *Pb* between the crossed counters, however, we only register the simultaneous arrival of 2 penetrating particles. (The dissolving time of our apparatus is of the order of  $5 \times 10^{-4}$  sec). Particles of this kind we have called coherent mesons and the only possibility for their occurrence is their having been produced in one and the same collision. In a coincidence between a hard and a soft particle, the soft particle will in most cases be an electron yielded by a collision of a coherent meson with the air

of the atmosphere (approximately 2/3 of the cases) or by the decay of a coherent meson (1/3 of the cases).

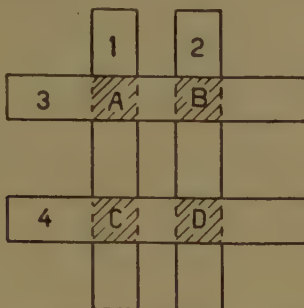


Fig. 2. Arrangement of the crossed counters. Coherent particles will be observed when A and D or B and C are hit.

By increasing the distance between the counters 1 and 2, and equally between the counters 3 and 4, the variation with distance of the number of observed mesons (resp. mesons + electrons) could be measured which proved to be an approximately exponential decrease with increasing distance. From this circumstance it is possible to calculate the total

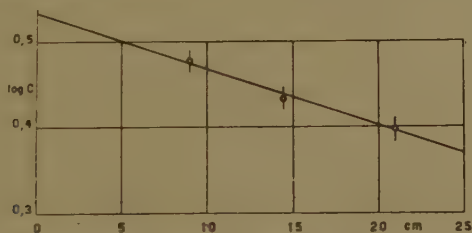


Fig. 3. Logarithmic decrease of the number of coincidences of the two penetrating particles produced in the atmosphere at different distances A—D (B—C).

number of coherent mesons. If the decrease with the distance is given by  $N = N_0 e^{-ax}$ , the total number is  $T = \frac{2\pi N_0}{a^2}$ . In our investigations we once found  $a$  to be  $0,011 \text{ cm}^{-1}$  and the coherence 40 % and in another series of experiments, under exceptionally favourable conditions both barometer and temperature remaining very constant during the 900 hours of the investigation, the frequency of the coincidences was found to be 100 %. This means that practically every meson coming down is accompanied by another meson.

§ 4. We made a second experiment with greater precision in an arrangement consisting of 2 piles of 3 counter-trays (the counters in each tray connected in parallel) using more sensitive and larger counters. 6-fold coincidences were counted, with the piles at 3 different distances. (The increased total sensitive surface of the counters, however, augmented the uncertainty about the distance). In this way the coherence of soft

rays could be determined and, by putting 10 cm *Pb* between the upper trays, also that of hard rays. At distances of 40, 110 and 170 cm we found 30, 27.5 and 25 coincidences per h. resp.

In this manner a coherence of 80 % was found for the mesons.

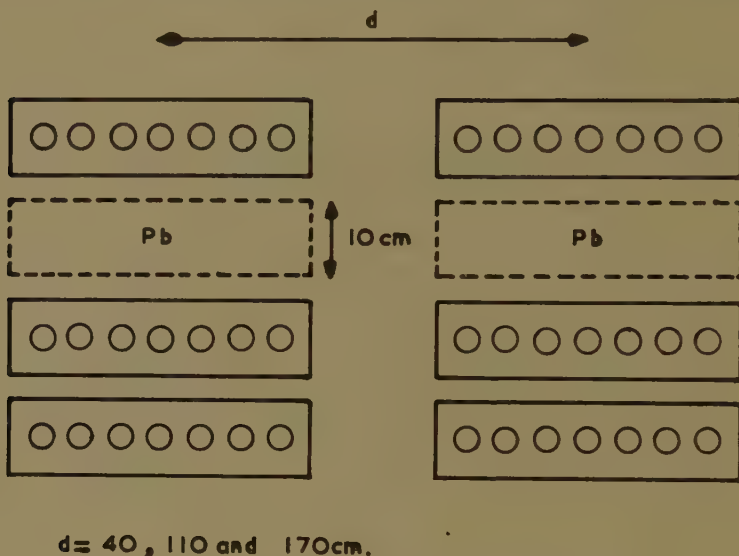


Fig. 4. Arrangement of the two countersets in which coherent particles were observed at distances of 40, 110 and 170 cm.

§ 5. Before we give an opinion on the origin of the big showers it will be proper to examine more closely the characteristic conduct of electron and meson.

Experiments at *high altitudes* have proved that *electrons* of over  $10^9$  eV hardly ever occur there. Even in that very rarefied atmosphere electrons of this energy and upwards lose their energy soon by Bremsstrahlung and pair formation.

Some *electrons* of  $10^9$  eV do occur there, however. Those may come down a few km, but this exhausts their energy and they will scarcely be found below 14 km and certainly not in our apparatus at sea-level.

An *electron* of  $10^9$  eV at an altitude of 20 km will, by Bremsstrahlung and pair-formation, without vanishing itself, produce 2 new electrons per 43.4 cm water (Bhabha unit for water). It will therefore be able to descend from 55 to 98 cm equiv. water i.e. to a height of 17 km, its energy being reduced to  $1/3$ . This applies if we neglect the ionisation loss, which does not become considerable until the energy has decreased to  $10^8$  eV. By the two processes of Bremsstrahlung and pair-formation the original electron and the two resulting from the first pair-formation will again share each their energy with 2 new particles. In the most favourable situation this may occur still once more so that 27 particles will have arisen of abt  $3 \times 10^7$  eV each. These particles may subsequently lose all



their energy in ionisation processes, but multiplication is no longer possible.

If the process wherein electrons are produced happens *lower* in the atmosphere, high energy electrons may also happen lower, but the chance of very high energy ones is here still smaller than at greater altitudes and even the  $10^8$  eV ones are few in number. All circumstances being favourable, electrons of  $10^8$  eV will still have a range of 2 Bhabha units (1 cm Pb or 600—700 m air) and cause a shower of 9 or 10 particles of abt  $10^7$  eV each.

In the *lowest layers* of the atmosphere an electron of  $10^7$  eV will lose approximately 2000 eV per cm air of its path, which therefore cannot exceed  $\frac{10^7}{2 \times 10^3} = 5000$  cm in air. Seeing the rate of their loss of energy electrons of  $10^7$  and  $10^8$  will not be able to appear in great density in the lower atmosphere, like they do in the showers we find, unless they have been produced at a relatively small distance.

To be able to penetrate a counter and if necessary one or two counters more for the registration of a 2- or 3-fold *coincidence*, an electron has to possess a **minimum energy** of  $5 \times 10^6$  eV.

To estimate the initial energy of an electron which, produced at the top of the atmosphere, at the bottom has an energy left *just insufficient to give a multiplication* (i.e. an electron of  $10^7$  à  $10^8$  eV, which would still be amply sufficient to give a coincidence in counters) we can reason as follows:

the Furry unit being 26 cm equiv. water and the atmosphere having 10 m e.w., if the particle has come down in an cascade process, there will have been 40 multiplications. The initial energy must therefore have been  $10^{12}$  times as large as the one left here below, making  $10^{19}$  eV. As already remarked, extremely high energy electrons are exceedingly rare because of their great loss of energy. It is highly improbable that a process of this nature should be the cause of the observed big showers at sea-level.

§ 6. Quite a different possibility may still be considered. The energy might come down conveyed by mesons. As the multiplication would then have to happen by nuclear reactions in the air, the total of particles produced could not be very large either. The free path between two nuclear reactions in the atmosphere is estimated by BROWN & KAY [5] at  $316 \text{ gr cm}^{-2}$  of matter, by FRETTER [6] however at  $750 \text{ gr cm}^{-2}$  and by PICCIONI [7] at  $1000 \text{ gr cm}^{-2}$ . This large divergence we may confidently attribute to the fact that it is extremely difficult to make an exact estimation from experiments in the Wilson chamber. If we take the most favourable case (BROWN & KAY) the opportunity for a meson to multiply in the atmosphere (abt  $1000 \text{ gr cm}^{-2}$ ) will offer 3 times. We have further to assume that the most usual multiplicity with these processes results in 2 particles. So the mean multiplicity along the whole distance of the atmosphere will be an 8-fold one. A process like the one LORD, FAIBERG & SCHEIN [8] observed, where at 30 km altitude

16 particles were produced, will give 128 particles down below. Taking into account the angular distribution to be inferred from the photo and to be put at 1 : 100, the dispersion is 250 m, which gives 128 particles on  $67.500 \text{ m}^2$  at sea-level, and an inferred mean density of  $2 \times 10^{-3} \text{ m}^{-2}$ . However, in a systematic investigation of penetrating showers, executed earlier with counter-trays at distances of up till 27 m, we found a total of 20.000 particles on a surface of 100 m radius or abt  $30.000 \text{ m}^2$ . This was calculated as indicated in § 3:

For a circular surface with radius  $R$  in which 90 % of the particles may be considered to be contained,  $R = \frac{4}{a}$  being in our case 100 m. The total of particles found was 20.000, giving a density of  $2/3 \text{ m}^{-2}$ . the centre of the bundle was found to be roughly 10 times the mean one, making  $6 \text{ m}^{-2}$ , but the entire area of high density was only abt  $27 \text{ m}^2$  and contained 160 mesons, This did not noticeably influence the mean density of roughly 0,6 upon the total surface, where a density of 0,003 would be expected if the shower was caused in a reaction like the one SCHEIN C. S. registered in his photo. We made several experiments with single counters, recording 3-, 4- and 6-fold coincidences below thick shielding, finding densities of 20 to 40 particles. Of course other processes with a higher yield might have played a part in our case, but the phenomena detected up to date do not leave much probability of that.

From this impasse we can escape by assuming the primary proton to have a 200 times higher energy than SCHEIN's particle, which would come to  $6 \times 10^{15}$ . Considering that particles of  $3 \times 10^{13} \text{ eV}$  have been calculated to arrive at the top of the atmosphere with a frequency of  $4.1 \times 10^{-4} \text{ min}^{-1} \text{ cm}^{-2}$ , we may conclude from the spectrum that particles of  $6 \times 10^{15}$  will occur sometimes, but only with a frequency of the order  $2.5 \times 10^{-8} \text{ min}^{-1} \text{ cm}^{-2}$ . This, however, differs widely from the observed frequency of the showers in question, being 5 per 24 hours.

§ 7. We must rather form quite a different picture of the events occurring here. Of the primaries, which are practically all protons, a certain number, especially those of very high energy, may accidentally have occasion to penetrate deeper, and if our registering apparatus happens to find itself at not too great a depth below the point where the proton causes a nuclear explosion and in the bundle of mesons produced there, a large density of particles may be expected in our counters or ionisation vessel. If a production process, as was found by LORD, FAINBERG and SCHEIN [8] at 30 km, occurs at a height of 2 km above our instrument, with the same number of mesons (16) of high energy and the same dispersion, the mesons have a chance of two multiplying processes, so that the number of particles will become 64 over a surface of  $300 \text{ m}^2$ , that is a density of  $0.2 \text{ m}^{-2}$ . This is of the same order as we have sometimes found in our experiments for penetrating particles over

large surfaces [9]. Now, what will be the frequency of such an event? The total number of protons entering the atmosphere will be, according to SCHEIN [2], 10 per  $\text{cm}^2$  per min. If we take that the frequency for high energies is going down with  $f = \frac{C}{N^{1.4}}$  (a relation we found for high energy events) [10], with the energy going up from  $2 \times 10^9$  to  $3 \times 10^{13}$ , the frequency will change with a factor  $2.5 \times 10^{-6}$ . In the atmosphere there is a great absorption, the free path being about 100 g  $\text{cm}^2$ . As the atmosphere is 1000 gr, we estimate that the number goes down by a factor of  $2^{10}$  or about  $10^3$ . We get the influence on a surface of 300  $\text{m}^2$ . Thus  $10 \times 2.5 \times 10^{-6} \times 300 \times 10^4 \times 10^{-3} \times 60$  per hour = 4.5 p. h. For penetrating showers with densities between 6 and 0.6 p.  $\text{m}^2$  we found a frequency of between 0.19 and 3.4 p. h., which is of the same order.

Similar values were found lately when measuring 6-fold coincidences in our counters below thick layers of material.

§ 8. A number of experiments will be cited below to prove the occasional presence of primary incident particles (practically all protons) at low levels in the atmosphere, which presence is necessary if the above assumptions shall apply. We know that at great altitudes extensive and intensive showers like the ones that occupy us down here, are produced by protons. In experiments in an areoplane up till 7000 m we [11] could record that the number of these showers decreases rapidly with increasing depth in the atmosphere, so that at sea-level there is only  $1/27^{\text{th}}$  left of the number at 7000 m. However, even at quite low levels these showers are still found, evidently produced in a similar process. We therefore conclude that a nucleon may sometimes penetrate very deeply into the atmosphere.

A striking fact is, that SCHEIN [2], when investigating the absorption of protons, found for the variation with altitude a value of the same order as the one we found for the variation of the frequency of the penetrating showers.

A further experimental proof is, that the barometric coefficient for the frequency of extensive showers is 14 % per cm Hg [12]. This means that, if the barometric pressure decreases by 1 cm, the effect is the same as if our apparatus had been removed to a height of 100 m. At this distance the relative increase of protons, according to SCHEIN, is of the same order as that of the showers in question. Our aeroplane measurements showed that, with an increase in height of 3000 m, corresponding to a decrease in atm. pressure of 23 cm Hg, the number of protons will rise from 3 to 118, which comes to 17 % per cm Hg.

In agreement with these experimentally obtained values are the most recent results of our counter-measurements in Amsterdam at sea-level and in Kenya at 3000 m, (not yet published), which show for showers of about the same density a ratio of 1 : 20. The density was determined from the relation between 6- and 4-fold coincidences in Amsterdam



and between 6- and 3-fold coincidences in Kenya. The barometric coefficient for the frequency was in agreement with the value quoted above.

Consequently we can assume that the way of arising of the big showers and bursts is qualitatively of the same character as that of the con-

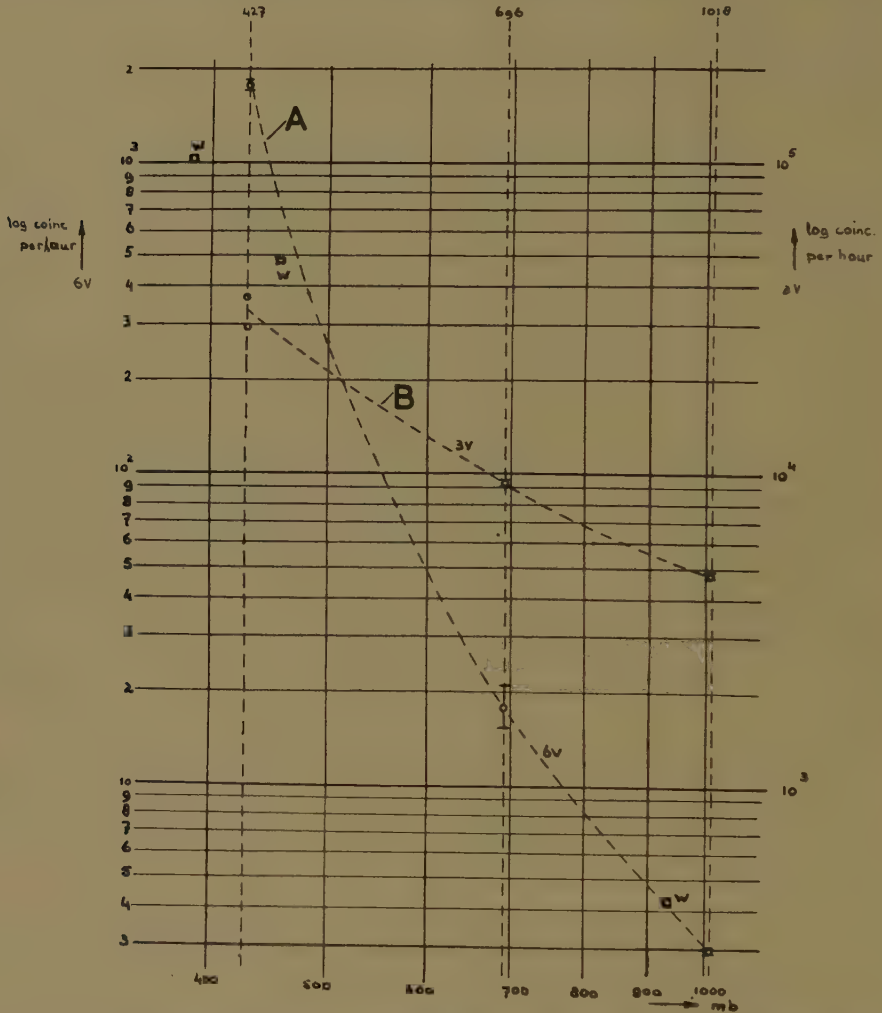


Fig. 5. Log frequency of coherent penetrating particles versus log of atm. pressure.  
A = 6 fold.

Log of frequency of single penetrating particles versus log of atm. pressure.  
B = 3 fold. W. observations of Wataghin.

tinuous radiation. The difference is that the showers and bursts only appear down here, when protons of high energy have come down exceptionally low. The only supposition we have to make is to assume e.g. that the number of mesons produced by the nucleons incident in the atmosphere increases with the energy. But as we used the value of the energy of the particle observed by LORD, FAIRBERG and SCHEIN



and the multiplicity they observed and further on our direct observations, we had not to make a supposition about the exponent of the energy.

If we assume the increase of the production of mesons to take place with the  $1/4$  power of energy as was found by FERMI (13) in his newly given theory, (of which he sent us an advance-copy, for which we are very thankful) then we think that in the dependence of the frequency on  $N$  (the density) the exponent has to be still smaller than the 1.4, we found as an approximation, otherwise the observed frequency of dence showers could not be explained.

§ 9. Further, about the electrons, there are three possibilities for the production of the electrons contained in the showers:

1. by collision of mesons with electrons,
2. by decay of mesons into electrons and
3. by decay of neutral mesons into photons of high energy, with subsequent production of electron pairs. A proof of this process has now been found by LORD, FAINBERG and SCHEIN. As both the first and second cases comprise only a small percentage of the mesons, the third case will have to be the most effective. And this is possible as the high energy protons will produce high energy electrons, which cannot happen but at a little distance under the spot where the explosion occurred. Nor will the photons and electrons produced be able to penetrate much farther under that spot. Consequently the ratio of electronic rays to mesonic ones increases rapidly with increasing height.

#### LITERATURE

1. COCCONI, G., Phys. Rev. **79**, 1006 (1950).
2. SCHEIN, M., Princeton Lecture.
3. CLAY, J., Physica **13**, 433 (1947).
4. ———, Physica **14**, 278 (1949).
5. BROWN and KAY, Phys. Rev. **77**, 392 (1950).
6. FRETTER, B., Phys. Rev. **76**, 511 (1949).
7. PICCIONI, O., Phys. Rev. **77**, 6 (1950).
8. LORD, J. J., J. FAINBERG and M. SCHEIN, 1950 not yet published. We are very thankful than they sent us the proof before publishing.
9. CLAY, J., Rev. of Modern Physics **21**, 94 (1949).
10. ——— and H. SWIERS, Versl. Ned. Akad. v. Wetensch. Amsterdam **53**, 380 (1944).
11. ——— and E. v. ALPHEN, Physica **16**, 393 (1950).
12. ———, Physica **16**, 278 (1950).
13. FERMI, E., Progress of Th. Physics **5**, 570 (1950).

# PERIODICITIES IN LUNAR ECLIPSES

BY

A. PANNEKOEK

(Communicated at the meeting of January 27, 1951)

## I

Astronomical literature from olden times mentions an 18 years period called the saros, which was first used by the Babylonian astronomers to predict lunar eclipses. Usually it was assumed that this is the only period that can be used for the purpose of prediction, so that the earliest cases of prediction which we meet with in the past must have been based upon knowledge of the saros. In later times, when the origin of the eclipses was exactly known, they were computed for the past and the future by means of the elements of the moon's and the sun's (apparent) orbit without making use of any period.

SCHIAPARELLI has pointed out <sup>1)</sup> that there are other and more simple means to forecast eclipses, regularities that must have been noticed and used at a time of more primitive knowledge. When a lunar calendar is used, with months equal to the moon's synodic period of 29.5 days, it is easy to perceive that the lunar eclipses — if, of course, the eclipses visible at night are completed by the eclipses occurring at day time, hence invisible — always follow one another with an interval of six months. In this way they form a group or series of 5 or 6 consecutive eclipses; then the series ceases. But after an interval of 17 or 23 months a new series starts, of which the eclipses occur 41 or 47 months after the corresponding ones of the former series. Each series begins with one or two partial eclipses, then in the midst come 2, 3, or sometimes 4 total eclipses, and the series ends with again one or two partial eclipses.

In a paper "The Origin of the Saros" <sup>2)</sup> the author has shown how the knowledge of the saros must have developed out of the knowledge of the small series. First the appearance of these series was explained by the fact that after six synodic periods the longitude of the sun and, hence, of the full moon has advanced  $4^{\circ}.023$  relative to the moon's node. Eclipses are only possible when the distance  $P$  between full moon and node is not greater than  $10^{\circ}$ — $12^{\circ}$ , total eclipses are only possible when this distance is not larger than  $5^{\circ}$ — $6^{\circ}$ . So a series of consecutive eclipses takes place when the difference of longitude  $P$  from say —  $10^{\circ}$  every

<sup>1)</sup> SCHIAPARELLI G. V., I primordi dell' astronomia presso i babilonesi. (Scientia IV. p. 36).

<sup>2)</sup> These Proceedings 20, 943 (1917).

six months increases to nearly  $-6^\circ, -2^\circ, +2^\circ, +6^\circ, +10^\circ$ ; then the series ceases because the next differences are  $+14^\circ, +18^\circ$  etc. But then soon the preceding full moon, with a longitude relative to the node  $30^\circ.67$  smaller, comes into action and shows successive differences  $-12.67, -8.65, \dots$  etc.

Thus the lunar eclipses occur in an array of consecutive series, in such a way that within each series the intervals are six months, and between the series the interval is one less than a multiple of six months. Each series shows a different character of the aspect of the partial and the duration of the total eclipses, due to the different values of  $P$  fluctuating over  $4^\circ$ . But after five series they return to nearly the same value, being in the sixth series only  $0^\circ.48$  different from the first series. Thus a larger period embracing five series appears, containing 223 lunar months. This period is the saros. Mathematically the saros is the nearest common multiple of the synodic and the draconitic revolutions of the moon. In the paper mentioned it was shown how by continued observation a knowledge of this saros must come forth out of the knowledge of the series, and that probably in Babylon it originated in this way.

The discovery of the saros-periodicity was facilitated by two circumstances. Firstly the period of 223 lunar months, i.e.  $6585\frac{1}{3}$  days, is only 11 days more than 18 years, so that the sun (and also the node that then has retrograded over nearly one circumference) returns to nearly the same longitude; this brings about that the effects caused by the excentricity of the earth's orbit return to nearly the same values after one saros. Secondly the saros is only  $\frac{1}{3}$  year longer than twice the period of revolution of the moon's perigee, so that the inequalities due to the excentricity of the lunar orbit (e.g. in the lunar parallax) also return nearly to the same values. Hence the irregularities occurring in the aspects of the consecutive series return in nearly the same way after every five series.

Since the purpose of the former paper was only to show the origin of the saros out of the more simple periodicity of the series, the irregularities due to the excentricities of the orbits have not been treated there. The most important is the influence of the apparent motion of the sun. Because in the syzygies the rapidly moving moon overtakes the slowly moving sun, the place of the meeting, the longitude of the full moon, chiefly depends on the sun, whereas the time of the meeting chiefly depends on the moon. The sun at an anomaly of  $90^\circ$  (in spring) is  $2^\circ$  advanced, at an anomaly of  $270^\circ$  (in autumn) is  $2^\circ$  back relative to the mean longitude. This brings about that the distance between full moon and node then is increased or diminished by an amount of  $2^\circ.28$ ; and thereby the character of the eclipse may be considerably changed. The effect of the excentricity of the moon's orbit, though it may change the moon's longitude by more than  $5^\circ$ , is diminished to circa  $1/12$  of this amount,  $0^\circ.43$  in the longitude of the full moon.

## II

SCHIAPARELLI remarked that it happens in certain centuries that a tetrad of four total eclipses follow one another in the midst of a series, whereas in other centuries such sequences are absent. This can be easily confirmed by looking through TH. VON OPPOLZER's *Canon der Finsternisse*<sup>3)</sup>. Then more irregularities present themselves. When only two eclipses in the midst of a series are total, their magnitude, expressed by the number of "digits" (Zoll, 1/12 of the moon's diameter), is high, up to more than 20, indicating a long duration of the totality. Where, however, four eclipses follow one another in the midst of a series, the first and the fourth, though remaining below 17, have a larger magnitude usually than the second and the third, just the reverse of what normally might be expected. It even happens that for the second or the third of this middle group the magnitude falls below 12 digits, hence the eclipse is

TABLE I  
Number of total eclipses

Mean year	Nr. of series	Number with 4, 4 imp, 3, 2 total eclipses	Average number per series	Mean year	Nr. of series	Number with 4, 4 imp, 3, 2 total eclipses	Average number per series
- 1174	18	0 0 4 14	2.22	512	18	0 0 3 15	2.17
1111	17	0 1 4 12	2.32	575	17	0 0 4 13	2.24
1047	18	3 2 2 11	2.61	636	17	0 0 3 14	2.18
980	19	4 3 7 5	3.03	700	18	0 1 4 13	2.31
912	19	5 3 10 1	3.29	763	17	2 2 1 12	2.47
844	18	5 2 7 4	3.11	828	19	6 2 9 2	3.26
780	18	2 3 1 12	2.53	895	17	4 3 10 0	3.32
715	18	0 0 6 12	2.33	962	19	5 1 5 8	2.87
652	17	0 0 3 14	2.18	1027	17	1 3 1 12	2.44
588	18	0 0 3 15	2.17	1090	18	0 0 5 13	2.28
525	17	0 0 3 14	2.18	1153	17	0 0 3 14	2.18
461	18	1 3 3 11	2.53	1217	18	0 0 3 15	2.17
396	18	2 3 9 4	2.97	1280	17	1 1 2 13	2.32
330	19	7 1 11 0	3.39	1345	19	4 2 3 10	2.74
263	18	5 2 11 0	3.33	1412	18	4 2 9 3	3.11
197	18	4 2 5 7	2.89	1479	19	5 2 11 1	3.26
134	17	1 2 2 12	2.41	1546	18	5 1 5 7	2.86
71	18	0 0 3 15	2.17	1611	18	1 2 3 12	2.44
- 8	17	0 0 4 13	2.24	1674	17	0 0 4 13	2.24
+ 56	18	0 0 3 15	2.17	1736	17	0 0 2 15	2.12
119	17	0 1 3 13	2.26	1799	18	0 0 5 13	2.28
182	18	3 3 0 12	2.58	1863	17	1 3 2 11	2.50
249	19	7 0 8 4	3.16	1926	18	4 0 7 7	2.83
318	19	4 4 11 0	3.32	1993	19	4 4 11 0	3.32
385	18	4 2 6 6	2.94	2063	20	6 0 9 5	3.05
448	17	3 3 1 10	2.68	2132	18	3 4 0 11	2.67

<sup>3)</sup> Denkschriften der Kais. Akad. der Wissensch. 52 (Wien, 1887).



only partial, though it is near the centre of the series. We could call such cases mutilated or imperfect tetrads.

A closer examination of OPPOLZER's Canon reveals a remarkable periodicity in the occurrence of these tetrads. In Table I for consecutive numbers of circa 100 eclipses is indicated how many series they embrace and how many among these show in the middle part two, three or four consecutive total eclipses or imperfect tetrads. We see a regular alternating: between the years  $-773$  and  $-472$ ,  $-111$  and  $+143$ ,  $475$  and  $729$ ,  $1050$  and  $1286$ ,  $1608$  and  $1854$  the tetrads are lacking and most of the series have only two total eclipses. On the contrary about  $-900$ ,  $-300$ ,  $+300$ ,  $900$ ,  $1500$ ,  $2000$  the series with only two total eclipses are almost lacking and tetrads of total eclipses show a maximum frequency. To express this periodicity numerically we may for each group of years compute an average number of total eclipses per series (counting the imperfect tetrads for  $3\frac{1}{2}$ ). These numbers are represented in Fig. 1. Though they do not run entirely regularly, we may deduce epochs of maximum and minimum:

Maximum  $-900, -310, +300, 860, 1460, 2010$

Minimum  $-600, +20, 600, 1180, 1730$

from which follows a mean period of circa 580 years. At present we are in an epoch of increasing tetrads; we had one embracing four total eclipses from 1949 April 13 to 1950 Sept. 26, and the next one will consist of the four eclipses 1960 March 13 to 1961 Aug. 26.

### III

In order to elucidate the origin of this periodicity a number of lunar eclipses had to be approximately computed by means of OPPOLZER's "*Syzygientafeln für den Mond*"<sup>4)</sup>. A total eclipse takes place when the latitude of the moon's centre is smaller than the semidiameter of the shadow diminished by that of the moon itself. If this quantity is expressed by  $i \sin l_0$  ( $l_0$  indicating some distance to the node and  $i$  the inclination) then the condition of totality can be thus expressed that  $P$ , the full moon's distance to the node, must be below  $l_0$ . This limiting longitude difference  $l_0$  varies between  $5^\circ.83$  (for the perigee) and  $4^\circ.75$  (for the apogee).

When (Case I) the regular part of  $P$ , which we will denote by  $P_0$ , for one eclipse is  $0^\circ$ , then for the next preceding and following ones it is  $-4^\circ$  and  $+4^\circ$ , both falling within the limits  $\pm l_0$ ; so there are 3 total eclipses, provided that the solar correction is small (which is the case in summer and winter). When the solar correction is large, when e.g. the middle eclipse falls in autumn and the two others fall in spring, the latter are displaced  $+2^\circ.28$  (at most) due to the sun's anomaly; so their relative longitudes  $P$  change into  $-2^\circ$  and  $+6^\circ$ , so that only 2 of the 3 total

<sup>4)</sup> Publication XVI der Astronomischen Gesellschaft (1881).

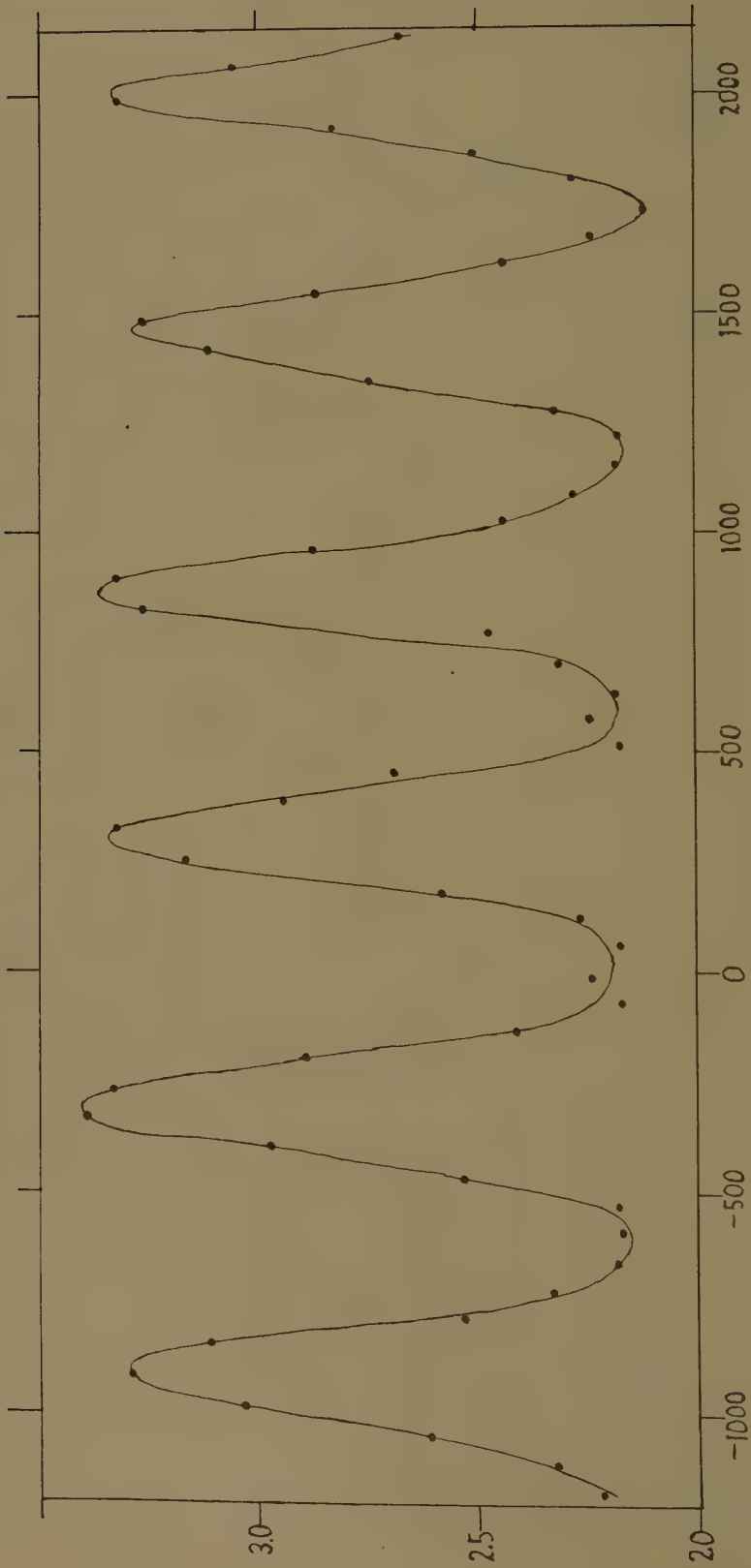


Fig. 1. Average number of total eclipses per series.

eclipses remain. The same holds for the opposite seasons with correction  $-2^{\circ}.28$ .

When (Case II) we take  $P_0 = -2^{\circ}.01$  and  $+2^{\circ}.01$  for the eclipses nearest to the node, and  $-6^{\circ}.03$  and  $+6^{\circ}.03$  for the adjacent ones, we have again two total eclipses only, if the sun's anomaly is near  $0^{\circ}$  or  $180^{\circ}$  and the solar correction is nearly zero. But the matter is different if the sun's anomaly is near  $90^{\circ}$  (spring) or  $270^{\circ}$  (autumn). In the case IIa with

	(autumn)	(spring)	(autumn)	(spring)
$P_0 = -6^{\circ}.03$	$-2^{\circ}.01$	$+2^{\circ}.01$	$+6^{\circ}.03$	
the corrections	$-2.28$	$+2.28$	$-2.28$	$+2.28$
producing $P = -8^{\circ}.31$	$+0^{\circ}.27$	$-0^{\circ}.27$	$+8^{\circ}.31$	

throw the first and last value farther from the node and the two middle values nearer to it, so that only two total eclipses of long duration occur. In the opposite case IIb with

	(spring)	(autumn)	(spring)	(autumn)
$P_0 = -6^{\circ}.03$	$-2^{\circ}.01$	$+2^{\circ}.01$	$+6^{\circ}.03$	
the corrections	$+2.28$	$-2.28$	$+2.28$	$-2.28$
producing $P = -3^{\circ}.75$	$-4^{\circ}.29$	$+4^{\circ}.29$	$+3^{\circ}.75$	

bring the first and last values within the boundary values for totality, whereas the two middle ones remain within them at a larger distance. So here we have four consecutive total eclipses, all of moderate magnitude. With somewhat different values of  $P_0$  and the solar correction it may happen that the second or third  $P$  is thrown outside the boundary value  $l_0$ ; then an imperfect tetrad is formed.

The various values which  $P_0$  can assume for the full moons nearest to the nodes are all situated between these limiting cases I and II; hence they will present intermediate results. A tetrad further on will be indicated in short by the quantities and arguments belonging to its first member; then we know that another with negative and two others with positive  $P_0$  will follow, in alternating seasons and with arguments of the inequalities (sun's or moon's anomaly) alternately in opposite quadrants.

In order to get an idea of the course of the phenomena we give in Tables II and III the data and results for an array of eclipses embracing two saros periods <sup>5)</sup>, first for the years 1732—66 when the tetrads are lacking, then for the years 2010—2044, when they have a maximum frequency. The regularly varying  $P_0$  in the 4th column was found by increasing the values of OPPOLZER's "Cyclentafel" by  $2^{\circ}.89$  (the amount he had subtracted to make all corrections positive) and adding the values of his "Periodentafel für Vollmonde". The "Empirische Korrekturen", being small in these centuries, have been neglected. The arguments  $g$  for the corrections, (2d and 3d column) i.e. the anomaly of sun and moon

<sup>5)</sup> It must be remarked that a saros period has no definite beginning or end, but is only a duration (of five series); it may start with any series.

expressed in centesimal degrees (0—400) are taken from the same source, rounded to full degrees. The 5th and 6th columns give the corrections themselves which must be added to  $P_0$ . The resulting corrected  $P$  shows the character of the eclipse; when necessary for dubious cases the boundary value of  $l_0$  is given in the next column. For comparison the last column gives the magnitude of the eclipse in digits, taken from OPPOLZER's Canon.

The table shows that in the years 1732—66 we meet repeatedly with Case IIa, where for the first and fourth full moon the distance to the node is increased by the solar inequality, and that in the years 2010—2044 we have twice in each saros period Case IIb, where the distance to the node is diminished by the solar inequality by such an amount as to bring about total eclipses. Moreover we see here how after five series, each with different values of  $P_0$  and of the corrections, hence with a different aspect in the sequence of partial and total eclipses, the next five series show a repetition of nearly the same values and circumstances.  $P_0$  has decreased by only  $0^\circ.48$ , and the argument of the solar inequality has increased by only 12 c.d. (centesimal degrees). The same holds for the border parts of the series with partial eclipses, which have been omitted here, and which in their aspects are still more sensitive to such differences. So we can understand how the larger period of five series forced itself into the attention of the observers and led to the discovery of the saros.

Nevertheless we can see by comparing the two consecutive saros periods how these small changes already bring about changes in the aspect: the fourth series (2021—22) drops out (2039—40) from the tetrads and in the fifth series (2043—44) a new tetrad comes into being. Thus gradually the character of the consecutive saros periods changes. After 18 such periods the argument of the solar inequality has increased by 200 c.d., and the solar correction has changed from a maximal positive to a maximal negative value, i.e. from case IIb to case IIa. Expressed in more exact figures:  $P_0$  the longitude of the full moon relative to the node decreases  $0^\circ.476$  per saros period; the sun's anomaly in one synodic period increases by  $29^\circ.1054$ , in one saros period increases by  $10^\circ.497$ . Hence relative to  $P_0$  the argument of the sun's inequality increases each saros period by  $10^\circ.97$ . It returns to the same value after  $360 : 10.97 = 32.8$  saros periods =  $32.8 \times 18.03 = 591$  years. This then is the theoretical value of the period for which our countings in the Canon gave an amount of nearly 580 years.

#### IV

Here we must go somewhat deeper into the causes which produce the sharp contrast between the maximum and minimum conditions. The five successive series of a saros follow one another rather regularly, so that their middle parts with small  $P_0$  — because the lunar node retrogrades  $350^\circ$  per saros — fall upon longitudes of the node, hence of



TABLE II

Date			$g \odot$	$g \circlearrowright$	$P_0$	Correction $\odot \quad \circlearrowright$		$P$	$l_0$	$m$
1732 June	8	176	289	$-3^\circ.39$	$+0.86$	$+ .45$	$-2^\circ.08$			$t$ 18.3
32 Dec.	1	370	61	$+0.64$	$-1.06$	$-.25$	$-0.67$			$t$ 21.2
33 May	28	164	233	$+4.66$	$+1.25$	$+ .31$	$+6.22$			$p$ 9.1
35 Oct.	2	302	265	$-5.90$	$-2.28$	$+ .46$	$-7.72$			$p$ 6.3
36 Mrch	27	96	37	$-1.87$	$+2.28$	$-.14$	$+0.27$			$t$ 22.0
36 Sept.	20	290	209	$+2.15$	$-2.26$	$+ .09$	$-0.02$			$t$ 21.7
37 Mrch	16	84	381	$+6.17$	$+2.22$	$+ .06$	$+8.45$			$p$ 6.7
39 July	20	222	14	$-4.38$	$-0.79$	$-.05$	$-5.22$	5.81		$t$ 13.3
40 Jan.	13	16	186	$-0.36$	$+0.58$	$-.15$	$+0.07$			$t$ 21.5
40 July	9	210	358	$+3.66$	$-0.37$	$+ .15$	$+3.44$			$t$ 16.1
41 Jan.	1	4	130	$+7.69$	$+0.15$	$-.48$	$+7.36$			$p$ 6.8
42 Nov.	12	348	390	$-6.89$	$-1.69$	$+ .03$	$-8.55$			$p$ 6.7
43 May	8	142	162	$-2.87$	$+1.83$	$-.35$	$-1.39$			$t$ 19.2
43 Nov.	2	336	334	$+1.16$	$-1.95$	$+ .26$	$-0.53$			$t$ 21.4
44 Apr.	26	130	106	$+5.18$	$+2.06$	$-.45$	$+6.79$			$p$ 8.6
46 Aug.	30	268	138	$-5.38$	$-2.02$	$-.47$	$-7.87$			$p$ 6.1
47 Febr.	25	62	310	$-1.35$	$+1.91$	$+ .38$	$+0.94$			$t$ 20.3
47 Aug.	20	256	82	$+2.67$	$-1.79$	$-.35$	$+0.53$			$t$ 21.2
48 Febr.	14	50	254	$+6.69$	$+1.64$	$+ .43$	$+8.76$			$p$ 3.6
50 June	19	188	286	$-3.86$	$+0.44$	$+ .46$	$-2.96$			$t$ 16.4
50 Dec.	23	382	58	$+0.16$	$-0.65$	$-.23$	$-0.72$			$t$ 21.2
51 June	9	176	230	$+4.18$	$+0.86$	$+ .28$	$+5.32$	4.81		$p$ 10.9
53 Oct.	12	314	262	$-6.37$	$-2.24$	$+ .25$	$-8.36$			$p$ 5.2
54 Apr.	7	108	34	$-2.35$	$+2.27$	$-.12$	$-0.20$			$t$ 22.4
54 Oct.	1	302	206	$+1.67$	$-2.28$	$+ .06$	$-0.55$			$t$ 20.8
55 Mrch	28	96	378	$+5.70$	$+2.28$	$+ .07$	$+8.05$			$p$ 7.6
57 July	30	233	10	$-4.86$	$-1.16$	$-.04$	$-6.06$			$p$ 11.7
58 Jan.	24	27	182	$-0.84$	$+0.96$	$-.19$	$-0.07$			$t$ 21.8
58 July	20	221	354	$+3.19$	$-0.76$	$+ .06$	$+2.49$			$t$ 17.6
59 Jan.	13	15	126	$+7.21$	$+0.55$	$-.48$	$+7.28$			$p$ 6.9
60 Nov.	22	360	386	$-7.38$	$-1.37$	$+ .04$	$-8.71$			$p$ 6.3
61 May	18	153	159	$-3.35$	$+1.56$	$-.37$	$-2.16$			$t$ 17.7
61 Nov.	12	348	331	$+0.68$	$-1.69$	$+ .28$	$-0.73$			$t$ 21.1
62 May	2	142	103	$+4.70$	$+1.83$	$-.44$	$+6.09$			$p$ 10.3
64 Sept.	10	279	135	$-5.86$	$-2.18$	$-.47$	$-8.51$			$p$ 4.9
65 Mrch	7	78	307	$-1.83$	$+2.10$	$+ .40$	$+0.67$			$t$ 21.1
65 Aug.	30	267	79	$+2.19$	$-2.01$	$-.34$	$-0.16$			$t$ 22.4
66 Febr.	24	61	251	$+6.21$	$+1.89$	$+ .42$	$+8.52$			$p$ 4.0

TABLE III

Date	$g \odot$	$g \ominus$	$P_0$	Correction $\odot \quad \ominus$	$P$	$l_0$	$m$
2010 Dec. 21	385	311	$-3^{\circ}.49$	$-0.55 + .38$	$-3^{\circ}.66$		$t$ 15.2
11 June 15	179	83	$+0.54$	$+0.76 - .36$	$+0.94$		$t$ 20.6
Dec. 10	373	255	$+4.56$	$-0.96 + .44$	$+4.04$		$t$ 13.7
14 Apr. 15	111	287	$-6.00$	$+2.26 + .46$	$-3.28$		$t$ 15.4
Oct. 8	305	59	$-1.97$	$-2.28 - .24$	$-4.49$		$t$ 14.0
15 Apr. 4	99	231	$+2.05$	$+2.28 + .39$	$+4.72$		$t$ 12.3
Sept. 28	293	3	$+6.07$	$-2.27 - .02$	$+3.78$		$t$ 15.6
18 Jan. 31	31	35	$-4.48$	$+1.09 - .13$	$-3.52$		$t$ 16.1
July 27	225	207	$-0.46$	$-0.89 + .07$	$-1.28$		$t$ 19.4
19 Jan. 21	19	379	$+3.56$	$+0.69 + .07$	$+4.32$		$t$ 14.5
July 16	213	151	$+7.59$	$-0.48 - .42$	$+6.69$		$p$ 8.0
21 May 26	157	11	$-6.99$	$+1.45 - .04$	$-5.58$	5.82	$t$ 12.3
Nov. 19	351	183	$-2.97$	$-1.62 - .18$	$-4.77$	4.77	$t?$ 11.9
22 May 16	145	355	$+1.06$	$+1.76 + .16$	$+2.98$		$t$ 17.1
Nov. 8	339	128	$+5.08$	$-1.88 - .48$	$+2.72$		$t$ 16.3
25 Mrch 14	77	159	$-5.48$	$+2.15 - .37$	$-3.70$		$t$ 14.1
Sept. 7	271	331	$-1.45$	$-2.07 + .38$	$-3.14$		$t$ 16.5
26 Mrch 3	65	103	$+2.57$	$+1.97 - .44$	$+4.10$		$t$ 14.1
Aug. 28	259	275	$+6.59$	$-1.85 + .47$	$+5.21$	5.06	$p$ 11.5
28 Dec. 31	396	308	$-3.96$	$-0.15 + .39$	$-3.72$		$t$ 14.9
29 June 26	190	80	$+0.06$	$+0.37 - .34$	$+0.09$		$t$ 22.5
Dec. 20	385	252	$+4.08$	$-0.55 + .42$	$+3.95$		$t$ 13.6
32 Apr. 25	122	284	$-6.47$	$+2.16 + .46$	$-3.85$		$t$ 14.3
Oct. 18	316	56	$-2.45$	$-2.22 - .22$	$-4.89$	5.62	$t$ 13.3
33 Apr. 14	110	228	$+1.57$	$+2.26 + .27$	$+4.10$		$t$ 13.2
Oct. 8	304	0	$+5.60$	$-2.28 - .00$	$+3.32$		$t$ 16.4
36 Feb. 11	42	32	$-4.96$	$+1.43 - .11$	$-3.64$		$t$ 15.7
Aug. 7	236	204	$-0.94$	$-1.25 + .04$	$-2.15$		$t$ 17.6
37 Jan. 31	30	376	$+3.09$	$+1.06 + .08$	$+4.23$		$t$ 14.6
July 27	224	148	$+7.11$	$-0.86 - .43$	$+5.82$	4.91	$p$ 10.0
39 June 6	168	8	$-7.47$	$+1.12 - .03$	$-6.38$		$p$ 10.7
Nov. 30	362	180	$-3.45$	$-1.31 - .20$	$-4.96$	4.78	$p$ 11.5
40 May 26	156	352	$+0.58$	$+1.48 + .18$	$+2.24$		$t$ 18.7
Nov. 18	350	124	$+4.60$	$-1.64 - .48$	$+2.48$		$t$ 17.1
43 Mrch 25	88	156	$-5.96$	$+2.25 - .39$	$-4.10$		$t$ 13.3
Sept. 19	282	328	$-1.93$	$-2.21 + .30$	$-3.84$		$t$ 15.0
44 Mrch 13	76	100	$+2.09$	$+2.14 - .43$	$+3.80$		$t$ 14.7
Sept. 7	270	273	$+6.11$	$-2.06 + .47$	$+4.52$		$t$ 12.7

the sun, that are retrograding nearly one fifth of a circumference; every next series comes  $2\frac{1}{2}$  month earlier than the preceding one. So we might expect that in one of them an eclipse with  $P_0$  circa  $-6^\circ$  must fall within the spring season, so that the conditions of case IIb, producing a tetrad of total eclipses should be present once every saros. Their complete absence about 1700 and their abundance about 2000 therefore need a further explanation.

The consecutive series are following one another with unequal intervals. Within a saros period there is twice an interval of 7, thrice an interval of 8 halfyears (the term halfyear here indicates 6 synodic periods). In 8 halfyears  $P_0$  changes by  $+1^\circ.514$ , in 7 halfyears by  $-2^\circ.509$ ; so the sequence of (rounded) values of  $P_0$  will run as follows (taking 1735—51 as an instance):

— 6	— 4.5	— 7	— 5.5	— 4.0	— 6.5
— 2	— 0.5	— 3	— 1.5	0	— 2.5
+ 2	+ 3.5	+ 1	+ 2.5	+ 4.0	+ 1.5
+ 6	+ 7.5	+ 5	+ 6.5		+ 5.5
8 h.y.	7 h.y.	8 h.y.	8 h.y.	7 h.y.	

If the first of each group should fall in autumn, with a large negative solar correction there is no possibility of getting a sequence of four total eclipses; if they should fall in spring, then in the first and the fourth group a tetrad of total eclipses may result. Now with an interval of 7 halfyears the nodes of the first eclipse, hence also the seasons interchange, whereas after an interval of 8 halfyears they remain the same. So e.g. as a sequence of season dates (retrograding 73 and 67 days) and of centesimal arguments of the solar correction (decreasing 80 and 74 c.d.)

in stead of Oct. 20	Aug. 8	June 2	Mrch 21	Jan. 7	Nov. 1
and 317	237	164	84	4	330 c.d.
we have Oct. 20	Aug. 8	Dec. 1	Sept. 20	July 8	Nov. 1
and 317	237	364	284	204	330 c.d.,

so that the spring cases IIb all drop out and the solar corrections are all negative. So under such conditions — as prevailed in the 18th century — there is no possibility for any tetrad of total eclipses to appear. The same, in opposite direction, takes place about 2000. When the first group of eclipses begins with a spring date, by the same occurrence twice of a 7 halfyears interval it remains in the spring, and the solar argument remains in or near the two first quadrants. Here e.g.

in stead of April 15	Jan. 31	Nov. 25	Sept. 13	July 2	April 26
and 111	31	357	277	196	122 c.d.
we have April 15	Jan. 31	May 26	Mrch 14	Dec. 31	April 26
and 111	31	157	77	396	122 c.d.

The result is that in every saros there are one or two series with tetrads of total eclipses.

Thus the sharp contrast between centuries with multitudes and

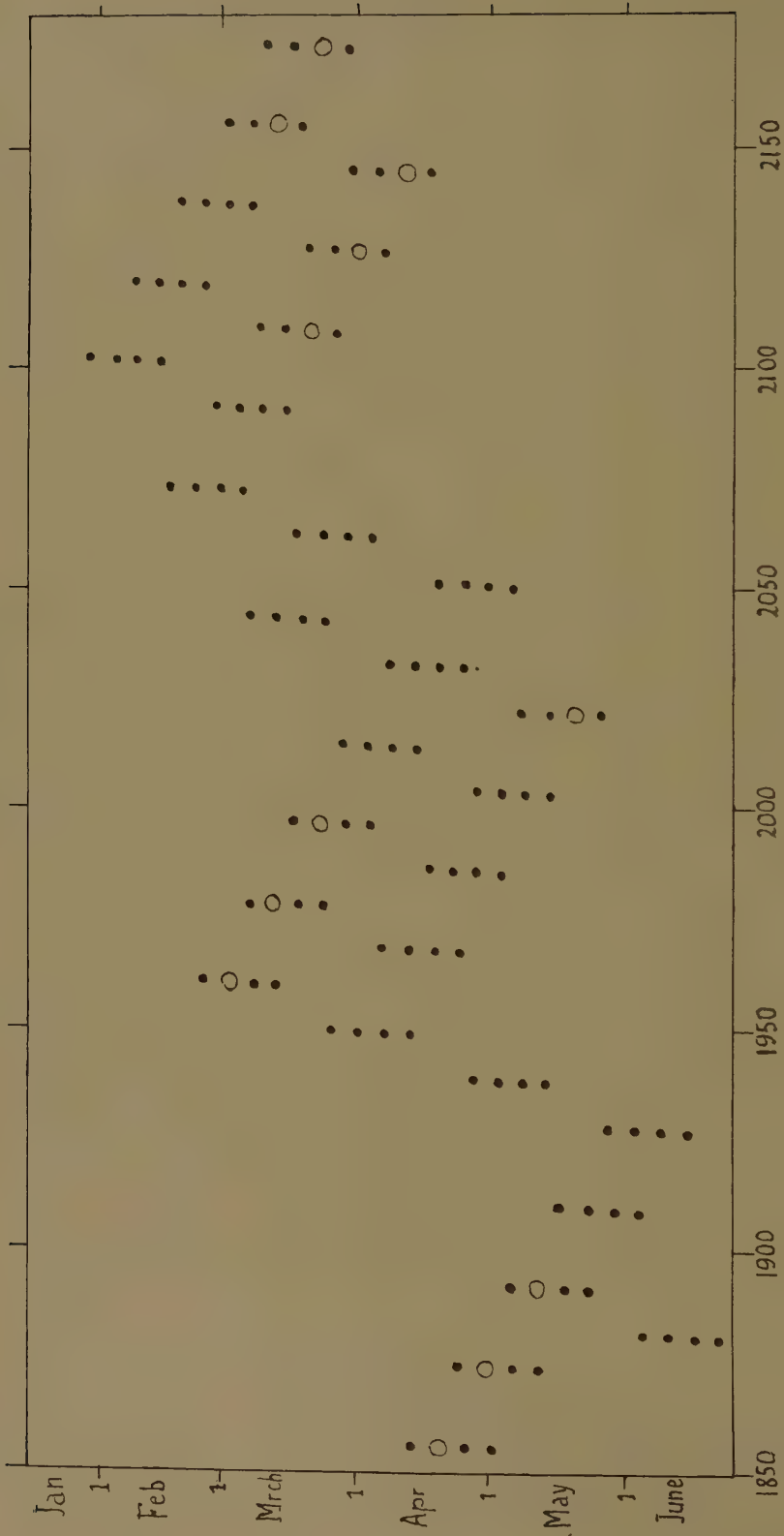


Fig. 2. Arrangement of tetrads of total lunar eclipses.



centuries with complete absence of tetrads of total eclipses is explained. Gradually, however, the conditions are changing. The (rounded) relative longitudes  $P_0$  after one saros have decreased by  $0^\circ.5$ ; exactly they return after 8 series (5 jumps of  $+1^\circ.5$  and 3 jumps of  $-2^\circ.5$ ) so that the jumps  $-2^\circ.5$  with the 7 halfyears interval per one saros will occur on the average  $15/8$  instead of 2 times. Hence the 7 halfyears intervals with their reversion of season gradually will come later in the five series of a saros, the decrease of the argument into the region with opposite sign (below 200 in the first, below 400 in the second case) will not be undone by the reversion of season, and ever more among the successive series will pass to the season with a solar correction small or of opposite sign. Thus gradually after a time of abundance the conditions for tetrads of total eclipses disappear, or conversely, after a time of absence, they gradually come into being.

It will be necessary now to consider more in detail the structure of the periodically appearing multitudes of tetrads of total eclipses. When in one series we have the favourable conditions of  $P_0$  say  $-5^\circ$  to  $+7^\circ$  and the solar argument somewhat below 100, then in each following saros period the latter will increase by 12 while the former decreases by  $0^\circ.5$ ; thus the favourable conditions persist and an array of tetrads will appear, following one another with 18 years interval. When finally the arguments run too near to 200 this array is extinguished. Then, however, other series come into play; after 8 series the values of  $P_0$  return and bring about a new array of tetrads, at dates 21 days earlier and with a solar argument smaller by 23 c.d. In such a way, when a first array of tetrads is extinguishing, new arrays come forth, each taking place 11 years after the former. Till at last they decline and disappear when the eclipses fall too early in the year. This arrangement of the tetrads of total eclipses in the years 1855—2174 has been reproduced in Fig. 2. The autumn eclipses have been transposed to the spring, to put them into one row with the spring eclipses of the same tetrad; open circles represent partial eclipses, hence indicate imperfect tetrads.

The irregularities shown in this arrangement of tetrads are chiefly due to the influence of the lunar terms. Though they are small (at most  $0^\circ.48$ ) and play a secondary role only, they sometimes are operative in making eclipses near the limit total or destroying the totality. Since the argument of the lunar inequality in one saros period decreases by 3.1 c.d. only, the lunar corrections persist with nearly the same amount during an entire array of tetrads, either stabilizing or effacing it.

ELECTRIC AND CHEMICAL POTENTIALS; DIFFERENT METHODS  
OF TREATMENT AND THEIR RELATION

BY

S. R. DE GROOT AND H. A. TOLHOEK

(Communicated by Prof. J. M. BIJVOET at the meeting of January 27, 1951)

*Synopsis*

Two methods are discussed for the treatment of problems of conduction of electricity in continuous media (especially electrolytes) in which also flows of matter, conduction of heat and chemical reactions are possible. The two methods differ in the respect that the electric potential and the electric potential energy are included or not in the chemical potentials respectively the internal energy.

It is shown that both methods are physically equivalent. The interest of the comparison of the methods concerns the controversy on the significance of electric and chemical potential taken separately or together. In our second formulation it becomes clear that in the combination  $\tilde{\mu}_k = \mu_k + e_k \varphi$  ( $\mu_k$  chemical potential of the  $k^{\text{th}}$  component,  $e_k$  specific charge of the  $k^{\text{th}}$  component  $\varphi$  electric potential),  $\mu_k$  and  $\varphi$  cannot be measured separately as long as no space charge occurs. (This condition is satisfied in normal electrolytes in a very good approximation, if the electric conductivity is not too small). This confirms a statement made by GUGGENHEIM.

This result does not mean that  $\mu_k$  and  $\varphi$  have no physical significance separately. For instance  $\varphi$  is defined as a mean value of the microscopic potential. While  $\varphi$  is inaccessible to direct measurement if no space charge exists, it can be measured separately from the  $\mu_k$ , if we have media that are (nearly) insulating, so that space charge can occur.

§ 1 *Introduction*

In connection with the problem of physical chemistry of measuring potentials in electric cells with electrolytes the question has arisen if the chemical potential  $\mu_k$  of the  $k^{\text{th}}$  component and the electric potential  $\varphi$  can be measured separately, or only in the combination  $\tilde{\mu}_k = \mu_k + e_k \varphi$ , which is called the electrochemical potential ( $e_k$ , charge per unit mass of the  $k^{\text{th}}$  component). It was especially envisaged by GUGGENHEIM<sup>1)</sup> who claimed that only the combinations  $\tilde{\mu}_k$  are to be considered and that the  $\mu_k$  and  $\varphi$  separately have neither thermodynamical nor physical importance. He showed this explicitly for isothermic systems of electrolytes in which diffusion and electric conduction can take place, and for which potential differences are measured at electrodes.

We have taken up this question for the case that a larger class of phenomena is considered according to the methods of the thermodynamics of irreversible processes<sup>2)</sup>. In § 2 the general formalism is developed and a first treatment of systems with electric conduction is given in which  $\mu_k$  and  $\varphi$  do not occur in the combinations  $\tilde{\mu}_k$ . In § 3 a treatment is given

in which the  $\tilde{\mu}_k$  are used. § 4 gives the conclusions drawn by comparison of the two methods.

§ 2. *A first treatment of continuous systems in which electric phenomena can occur*

In this section we give the first treatment of a system which consists of a number of components ( $k = 1, \dots, n$ ) and in which the following processes are possible: *a*) motion of the mixture as a whole (bulk motion), *b*) diffusion, *c*) electric conduction, *d*) heat conduction, *e*) a number  $r$  of chemical reactions. We formulate the laws as is done in the thermodynamics of irreversible processes, in which also the influence of the mentioned processes on each other is considered.

In the thermodynamics of irreversible processes the entropy production is calculated, for which four fundamental laws are used viz.: I, the law of conservation of mass, II, the force equation (equation of motion), III, the energy equation, IV, the second law of thermodynamics.

We shall start this section by supposing that a force  $\mathbf{F}_k$  is acting on the  $k^{\text{th}}$  component: afterwards we specialize to electric phenomena by taking the force  $\mathbf{F}_k$  of a purely electric character.

We begin with a quantitative formulation of the four fundamental equations.

I. *The law of conservation of mass* can be written as follows for the component  $k$

$$(1) \quad \partial \varrho_k / \partial t = -\operatorname{div} \varrho_k \mathbf{v}_k + \sum_{j=1}^r \nu_{kj} J_j^c,$$

where  $\varrho_k = M_k/V$  is the mass of component  $k$  per unit of volume ( $M_k$  mass of  $k$ ;  $V$  the volume),  $\partial/\partial t$  the local time derivative,  $\mathbf{v}_k^1$  the velocity of  $k$ , and  $\sum_j \nu_{kj} J_j^c$  the chemical production of  $k$  per unit of volume.

$$(2) \quad \sum_j \nu_{kj} J_j^c = (1/V) d_i M_k / dt,$$

where  $d_i M_k$  is the change in the amount of substance  $k$  caused by the chemical reactions; we have  $\sum_k d_i M_k = 0$ . The quantities  $\nu_{kj}$  divided by the molecular mass of substance  $k$  are proportional to the stoichiometric numbers of these components in the chemical reaction; we have  $\sum_k \nu_{kj} = 0$ ;  $J_j^c$  is the chemical reaction rate for the  $j^{\text{th}}$  reaction in mass per unit of volume per unit of time. The equation (1) has the form of a so-called balance equation: the local change on the left hand side is equal to the negative divergence of a flow plus a source term giving the production or destruction of substance  $k$ . Summed over all substances  $k = 1, 2, \dots, n$ , equation (1) becomes

$$(3) \quad \partial \varrho / \partial t = -\operatorname{div} \varrho \mathbf{v},$$

where  $\varrho$  is the total density

$$(4) \quad \varrho = \sum_k \varrho_k = (\sum_k M_k)/V = M/V = 1/v$$

(with  $v$  specific volume) and  $\mathbf{v}$  the center of mass velocity.

$$(5) \quad \mathbf{v} = (\sum_k \varrho_k \mathbf{v}_k) / \varrho.$$

The mass equation can be written in an alternative form by introducing the (barycentric) substantial time derivative

$$(6) \quad d/dt = \partial/\partial t + \mathbf{v} \cdot \text{grad}$$

and the flow of substance  $k$  defined with respect to the center of mass movement

$$(7) \quad \mathbf{J}_k = \varrho_k (\mathbf{v}_k - \mathbf{v}).$$

From (5) and (7) it follows that

$$(8) \quad \sum_{k=1}^n \mathbf{J}_k = 0.$$

With the help of (5), (6) and (7) equation (1) becomes

$$(9) \quad d\varrho_k/dt = -\varrho_k \text{div } \mathbf{v} - \text{div } \mathbf{J}_k + \sum_j \nu_{kj} J_j^c$$

or still simpler

$$(10) \quad \varrho dc_k/dt = -\text{div } \mathbf{J}_k + \sum_j \nu_{kj} J_j^c,$$

where  $c_k = \varrho_k/\varrho = M_k/M$  is the concentration of  $k$ . Equation (3) takes the form

$$(11) \quad d\varrho/dt = -v^{-2} dv/dt = -\varrho \text{div } \mathbf{v}.$$

II. *The force equation* can be written as

$$(12) \quad \varrho d\mathbf{v}/dt = \nabla \cdot \boldsymbol{\pi} + \sum_{k=1}^n \mathbf{F}_k \varrho_k,$$

where  $\boldsymbol{\pi}$  is the pressure tensor (with components  $\pi_{ik}$ ;  $i, k = 1, 2, 3$ ) and  $\mathbf{F}_k$  is the external force per unit of mass on substance  $k$ . (We have denoted the vector with components  $\sum_i \partial \pi_{ik} / \partial x_i$  as  $\nabla \cdot \boldsymbol{\pi}$ ).

We put for  $\pi_{ik}$

$$(13) \quad \pi_{ik} \equiv -p \delta_{ik} + p_{ik},$$

$p$  is the hydrostatic pressure;  $\delta_{ik}$  is the Kronecker symbol, 0 when  $i \neq k$ , 1 when  $i = k$ ;  $p_{ik}$  is the viscous pressure tensor. If we neglect viscous forces, as we shall do below, we can put  $p_{ik} = 0$  and (12) reduces to

$$(14) \quad \varrho d\mathbf{v}/dt = -\text{grad } p + \sum_{k=1}^n \mathbf{F}_k \varrho_k.$$

Mechanical equilibrium (absence of bulk motion of the matter) has consequences that allow different forms and simplifications for the equations. We have given the equations for the general case that bulk motion of the matter exists. We will not go into the details of the special forms of the equations for the case of mechanical equilibrium at this place.



III. *The energy equation* for  $u$  the energy per unit of mass with the exclusion of the barycentric kinetic energy

$$(15) \quad \varrho d(\tfrac{1}{2} \mathbf{v}^2 + u)/dt = -\operatorname{div}(p\mathbf{v} + \mathbf{J}_q) + \sum_{k=1}^n \mathbf{F}_k \cdot \mathbf{v}_k \varrho_k,$$

where  $\mathbf{J}_q$  is called the flow of heat.

IV. *The second law.* As second law we can use Gibbs' equation

$$(16) \quad TdS/dt = dU/dt + pdV/dt - \sum_k \mu_k dM_k/dt,$$

where the differentials are substantial derivatives with respect to the motion of the center of gravity (6) and where  $S$  is the total entropy,  $U$  the total energy and  $\mu_k$  the chemical potential of substance  $k$ . This equation can be used for open as well as for closed systems, as it can also be written entirely with intensive quantities, viz., specific entropy  $s = S/M$  ( $M$  = total mass), specific energy  $u = U/M$ , specific volume  $v = V/M$  and concentrations  $c_k = M_k/M = \varrho_k/\varrho$ . Formula (16) becomes

$$(17) \quad Tds/dt = du/dt + pdv/dt - \sum_k \mu_k dc_k/dt.$$

In the proof of the equivalence of (16) and (17) one must keep in mind that  $M$  is variable and the Euler relation

$$(18) \quad Ts = u + pv - \sum_k \mu_k c_k.$$

The mean specific chemical potential (specific Gibbs function) is

$$(19) \quad g = \sum_k \mu_k c_k = (\sum_k \mu_k \varrho_k)/\varrho = u - Ts + pv.$$

*The entropy balance.* Starting with the four fundamental equations we can calculate the entropy balance equation. When we subtract the force equation (14) multiplied by  $\mathbf{v}$  from the energy equation (15) we eliminate the kinetic energy of the center of gravity and thus obtain an expression for the change of  $u$

$$(20) \quad \varrho du/dt = -p \operatorname{div} \mathbf{v} - \operatorname{div} \mathbf{J}_q + \sum_k \mathbf{F}_k \cdot \mathbf{J}_k,$$

where (7) has been used. Introducing (11) we obtain

$$(21) \quad du/dt = -pdv/dt - \varrho^{-1} \operatorname{div} \mathbf{J}_q + \varrho^{-1} \sum_k \mathbf{F}_k \cdot \mathbf{J}_k.$$

Now it is easy to deduce the entropy balance by introducing (10) and (21) into (17)

$$(22) \quad \varrho Tds/dt = -\operatorname{div} \mathbf{J}_q + \sum_k \mathbf{F}_k \cdot \mathbf{J}_k + \sum_k \mu_k \operatorname{div} \mathbf{J}_k - \sum_{k,j} \mu_k v_{kj} J_j^c.$$

An alternative form of (22) is

$$(23) \quad \varrho \frac{ds}{dt} = -\operatorname{div} \left( \frac{\mathbf{J}_q - \sum_k \mu_k \mathbf{J}_k}{T} \right) + \frac{\mathbf{J}_q \cdot \mathbf{X}_q + \sum_k \mathbf{J}_k \cdot \mathbf{X}_k + \sum_j A_j J_j^c}{T} = -\operatorname{div} \mathbf{J}_s + \sigma,$$

where

$$(24) \quad \mathbf{X}_a = -(\text{grad } T)/T,$$

$$(25) \quad \mathbf{X}_k = \mathbf{F}_k - T \text{grad } (\mu_k/T),$$

$$(26) \quad A_j = - \sum_k \mu_k \nu_{kj}.$$

The latter quantity is called the chemical affinity. Formula (23) has clearly the form of a balance equation: the change of the specific entropy is due to two causes, the negative divergence of an entropy flow

$$(27) \quad \mathbf{J}_s = (\mathbf{J}_a - \sum_k \mu_k \mathbf{J}_k)/T$$

and an entropy production with a source strength

$$(28) \quad \sigma = (\mathbf{J}_a \cdot \mathbf{X}_a + \sum_k \mathbf{J}_k \cdot \mathbf{X}_k + \sum_j A_j J_j^c)/T,$$

which is obviously the sum of the products of two sets of variables, viz., the first set:  $\mathbf{J}_a$ ,  $\mathbf{J}_k$  and  $J_j^c$ , the second set:  $\mathbf{X}_a$ ,  $\mathbf{X}_k$  and  $A_j$ . These variables are mostly called respectively the "fluxes" and the "forces" in the thermodynamics of irreversible processes.

When one prefers to have the local time derivative instead of the substantial time derivative written at the left hand side of (23) one must apply (6). It is then more convenient to use the entropy expressed per unit of volume  $s_v = S/V = s_0$ , because (6) and (11) give the simple relation

$$(29) \quad \rho ds/dt = \partial s_v / \partial t + \text{div } s_v \mathbf{v}$$

valid, by the way, for any arbitrary specific quantity. Insertion of (29) into (23) gives, when the abbreviations (27) and (28) are used, for the change of the entropy at a fixed point

$$(30) \quad \partial s_v / \partial t = - \text{div } (\mathbf{J}_s + s_v \mathbf{v}) + \sigma.$$

The total entropy flow contains now, besides  $\mathbf{J}_s$ , also a convective part  $s_v \mathbf{v}$ . The source term is still the same  $\sigma$  (28).

The entropy production  $\sigma$  (28) is seen to be the result of the action of irreversible processes as heat conduction, diffusion and chemical reactions. The velocity of the center of gravity does not figure in the source of entropy. The bulk motion of the system is therefore to be considered as a reversible phenomenon. This is also what is wanted of course, because the motion of the center of gravity obeys the force equation (14). The theory is now completely consistent since the result of the reversibility of the barycentric motion is a consequence of the supposition that the Gibbs equation was valid in our continuous, non-uniform system, when the differentials were supposed to be substantial derivatives with respect to the velocity of the center of gravity  $\mathbf{v}$  (see formula (6)).

#### *The phenomenological relations and Onsager's theorem*

In (28) we have written the source strength  $\sigma$  of the entropy production as the sum of two sets of variables, called the "fluxes" and the "forces".

In a first approximation linear relations can be assumed between the fluxes and the forces. These relations are called the phenomenological equations

$$(35) \quad \mathbf{J}_i = \sum_{k=1}^n L_{ik} \mathbf{X}_k + L_{iq} \mathbf{X}_q,$$

$$(36) \quad \mathbf{J}_q = \sum_{k=1}^n L_{qk} \mathbf{X}_k + L_{qq} \mathbf{X}_q,$$

$$(37) \quad J_j^c = \sum_{m=1}^r L_{jm}^c A_m.$$

We have not taken up a relationship between the flows of matter and energy on the one hand and the chemical affinities on the other hand; also we have taken the chemical reaction rates independent of the forces  $\mathbf{X}_i$  and  $\mathbf{X}_q$ . That this procedure is correct is a consequence of the fact that the fluxes and forces in (35) are vectors, whereas those in (37) are scalars. It is impossible for a force of a certain tensorial character to give rise to a flow of a different tensorial character. Symmetry considerations of this type have already been given by CURIE<sup>3)</sup>.

We have supposed isotropy in (35) and (36); otherwise the separate components of the fluxes would be linear functions of the components of the forces.

According to ONSAGER'S theorem<sup>4)</sup> the coefficient matrix in the phenomenological relations (35), (36) and (37) is symmetrical; hence we have

$$(38) \quad L_{ik} = L_{ki} \quad \text{and} \quad L_{iq} = L_{qi}$$

and analogously for the "chemical" coefficients

$$(39) \quad L_{jm}^c = L_{mj}^c.$$

### *Electrical forces*

After having developed a slightly more general formalism we will now specialize to the systems mentioned in the beginning of this section; this means that we take  $\mathbf{F}_k$  of an electric character; hence we put

$$(40) \quad \mathbf{F}_k = -e_k \text{grad } \varphi,$$

where  $e_k$  is the charge of component  $k$  per unit of mass and  $\varphi$  the electric potential. Substituting (40) in the equations of this section we obtain the specialization to the systems under consideration. The expression for the forces  $\mathbf{X}_k$  becomes, e.g.,

$$(41) \quad \mathbf{X}_k = -e_k \text{grad } \varphi - T \text{grad } (\mu_k/T)$$

or

$$(42) \quad \mathbf{X}_k = -\text{grad } (\mu_k + e_k \varphi) + (\mu_k/T) \text{grad } T.$$

The force equation (14) becomes

$$(43) \quad \rho d\mathbf{v}/dt = -\text{grad } p - \sum_{k=1}^n \varrho_k e_k \text{grad } \varphi.$$

### § 3. *A different method in dealing with electric phenomena*

In literature the cases including electric phenomena are almost in variably treated by means of the combination  $\mu_k + e_k\varphi$  as "electro-chemical potential". However, it is clear that the formulae obtained in § 2 do not contain  $\mu_k$  and  $e_k\varphi$  exclusively in the combination  $\mu_k + e_k\varphi$ , when we consider the general case of non-uniform temperature (cf. (41) and (42)). Yet we will prove in this section that the procedure of using this combination can be justified by the thermodynamical theory of irreversible processes. In fact we shall see that by a particular linear transformation of fluxes and forces we can obtain expressions for the flow and the production of entropy and therefore also for the phenomenological equations which contain  $\mu_k$  and  $e_k\varphi$  only in the combination  $\mu_k + e_k\varphi$ . All these expressions and equations contain the transformed fluxes and forces, but have otherwise completely the same form as the original expressions and equations. This is also true for the fundamental equations: the force equation, the energy equation and the second law, when we neglect the total charge of the system. In the following we give the derivation of these statements. Thus it is possible to settle the question of the use of  $\mu_k + e_k\varphi$ , i.e., to indicate the circumstances under which the application of this function can be justified.

We introduce first the partial specific energy of component  $k$ , including the electrical energy

$$(44) \quad \tilde{u}_k = u_k + e_k\varphi.$$

As a consequence of this we can write

$$(45) \quad \tilde{u} = u + \sum_k e_k c_k = u + e\varphi$$

for the specific energy, including electric energy. We used the abbreviations  $c_k = \varrho_k/\varrho$  for the concentration and  $e = \sum_k e_k c_k$  for the total charge per mass unit. We also have now from (44)

$$(46) \quad \tilde{\mu}_k = \mu_k + e_k\varphi$$

for the chemical potential, including the electrical energy. We write the external force

$$(47) \quad \mathbf{F}_k = \tilde{\mathbf{F}}_k - e_k \text{grad } \varphi$$

separating it into a non-electrical part  $\tilde{\mathbf{F}}_k$  and an electrical force  $-e_k \text{grad } \varphi$ . (We will retain here the possibility that non-electric forces exist; hence we take (47) instead of (40)).

We introduce at this point the new thermodynamical flux

$$(48) \quad \tilde{\mathbf{J}}_q = \mathbf{J}_q + \sum_k e_k \mathbf{J}_k \varphi = \mathbf{J}_q + \mathbf{I}\varphi,$$

which is the heat flow including the flow of electrical energy. The total electrical current is written as

$$(49) \quad \mathbf{I} = \sum_k e_k \mathbf{J}_k.$$



We continue using the material flows  $\mathbf{J}_k$  as thermodynamical fluxes. We might proceed as in the preceding section to find immediately the corresponding thermodynamical forces. It is preferable to repeat the derivation of § 2 in order to show the physical consequences of the introduction of quantities which include electrical terms. We get from the force equation (14) and the relation (47)

$$(50) \quad \varrho d\mathbf{v}/dt = -\text{grad } p + \sum_k \tilde{\mathbf{F}}_k \varrho_k - \varrho e \text{grad } \varphi,$$

where the abbreviations mentioned after equation (45) have been used. The energy equation (15) takes the form

$$(51) \quad \varrho d(\tfrac{1}{2} \mathbf{v}^2 + \tilde{u})/dt = -\text{div}(p\mathbf{v} + \tilde{\mathbf{J}}_q) + \sum_k \tilde{\mathbf{F}}_k \cdot \mathbf{v}_k \varrho_k + \varrho e \partial\varphi/\partial t$$

when (44), (47) and (48) are introduced. To prove the equivalence of (15) and (51) one needs equations (6) applied to  $\varphi$ , (7), (10) and

$$(52) \quad \sum_k e_k v_{kj} = 0,$$

which expresses the conservation of electrical charge during a chemical reaction. Finally we have the second law (17) which becomes, when (45) and (46) are inserted

$$(53) \quad Tds/dt = d\tilde{u}/dt + pdv/dt - \sum_k \tilde{\mu}_k dc_k/dt - ed\varphi/dt.$$

We can deduce an equation for total quantities analogous to (53). (45) becomes for total quantities

$$(54) \quad \tilde{U} = U + eM\varphi$$

with

$$(55) \quad eM = \sum_k e_k M_k.$$

Using (54), (55) and (46), equation (16) gives the formula, which is analogous to (53)

$$(56) \quad TdS/dt = d\tilde{U}/dt + p dV/dt - \sum_k \tilde{\mu}_k dM_k/dt - eM d\varphi/dt.$$

The equation for  $\tilde{u}$  is obtained first by multiplying (50) by  $\mathbf{v}$  and then subtracting it from (51). With the aid of equation (6) one gets

$$(57) \quad \varrho d\tilde{u}/dt = -p \text{div } \mathbf{v} - \text{div } \tilde{\mathbf{J}}_q + \sum_k \tilde{\mathbf{F}}_k \cdot \mathbf{J}_k + \varrho e d\varphi/dt.$$

This equation is equivalent to (20). Finally the entropy balance is found by inserting (10) and (57) into (53). Using also (11) one obtains

$$(58) \quad \varrho \frac{ds}{dt} = -\text{div} \left( \frac{\tilde{\mathbf{J}}_q - \sum_k \tilde{\mu}_k \mathbf{J}_k}{T} \right) + \frac{\tilde{\mathbf{J}}_q \cdot \mathbf{X}_q + \sum_k \mathbf{J}_k \cdot \tilde{\mathbf{X}}_k + \sum_j \tilde{A}_j J_j^c}{T} = -\text{div } \tilde{\mathbf{J}}_s + \sigma,$$

where

$$(59) \quad \tilde{\mathbf{X}}_k = \tilde{\mathbf{F}}_k - T \text{grad } (\tilde{\mu}_k/T) = \mathbf{X}_k - e_k \varphi \mathbf{X}_q.$$

To obtain the last member, formulae (47), (44), (24) and (25) have been used. Furthermore the chemical affinity is

$$(60) \quad \tilde{A}_j = - \sum_k \tilde{\mu}_k \nu_{kj} = - \sum_k \mu_k \nu_{kj} - \varphi \sum_k e_k \nu_{kj} = A_j,$$

according to (46), (52) and (26). It is interesting to note also that

$$(61) \quad \tilde{\mathbf{J}}_s = \tilde{\mathbf{J}}_q - \sum_k \tilde{\mu}_k \mathbf{J}_k = \mathbf{J}_q - \sum_k \mu_k \mathbf{J}_k = \mathbf{J}_s,$$

$$(62) \quad \tilde{\sigma} = (\tilde{\mathbf{J}}_q \cdot \mathbf{X}_q + \sum_k \mathbf{J}_k \cdot \tilde{\mathbf{X}}_k + \sum_j \tilde{A}_j J_j^c) / T = (\mathbf{J}_q \cdot \mathbf{X}_q + \sum_k \mathbf{J}_k \cdot \mathbf{X}_k + \sum_j A_j J_j^c) / T = \sigma,$$

where (46), (48), (59), (60), (27) and (28) have been used.

We can draw some important conclusions from the above equations. In the first place we note that all equations leading to the "thermodynamical properties" of the system, viz., the balance equation for the entropy (58), the entropy flow (61) and the entropy production (62) are invariant under the linear transformation (48) and (59) of the fluxes and forces. As phenomenological equations we have

$$(63) \quad \mathbf{J}_i = \sum_k \tilde{L}_{ik} \tilde{\mathbf{X}}_k + \tilde{L}_{iq} \mathbf{X}_q,$$

$$(64) \quad \mathbf{J}_q = \sum_k \tilde{L}_{qk} \tilde{\mathbf{X}}_k + \tilde{L}_{qq} \mathbf{X}_q,$$

$$(65) \quad J_j^c = \sum_m L_{jm}^c A_m$$

with

$$(66) \quad \tilde{L}_{ik} = L_{ik},$$

$$(67) \quad \tilde{L}_{iq} = L_{iq} + \sum_k L_{ik} e_k \varphi,$$

$$(68) \quad \tilde{L}_{qi} = L_{qi} + \sum_k L_{ki} e_k \varphi,$$

$$(69) \quad \tilde{L}_{qq} = L_{qq} + \sum_i (L_{qi} + L_{iq}) e_i \varphi + \sum_{i,k} L_{ik} e_i e_k \varphi^2.$$

These coefficients are found when the old forces and fluxes are solved from (48) and (59) and the results inserted into (35) and (36). Quite generally we can say that all "thermodynamical" equations (58), (61), (62), (63) and (64) are formally the same as the corresponding equations (23), (27), (28), (35) and (36), but with the new quantities (with tildes) instead of the old ones. (The form of (59) is also the same as (25)). We thus found a system of fluxes and forces from which we can formally derive the same results as before and which includes  $\mu_k$  and  $e_k \varphi$  only in the combination  $\mu_k + e_k \varphi$ .

#### § 4 Conclusions

From the treatment of § 3 we come to the conclusion that it is possible to justify the use of the combination  $\mu_k + e_k \varphi$  throughout the "thermo-

dynamical" part of the theory, provided one takes as forces and fluxes  $\mathbf{J}_k$ ,  $\tilde{\mathbf{J}}_q$  defined by (48),  $\tilde{\mathbf{X}}_k$  expressed by (59) and  $\mathbf{X}_q$ . We stress this latter point because the thermodynamics of irreversible processes leads to this result, at the same time justifying the  $\mu_k + e_k\varphi$ -method and giving the framework of physical quantities to be used in a consistent and rigorous theory.

So far we discussed the "thermodynamical" results of the new system. Let us now consider the basic equations: the force equation (50), the energy equation (51) and the second law (53) in the new variables. Then it turns out that these equations do not have exactly the same form as the corresponding ones (14), (15) and (17) in the old system, but that all three contain a new term, proportional to the total electric charge per unit mass  $e$  and also including the electrical potential  $\varphi$ . These terms will in practice be extremely small as the total charge  $e$  will be negligible due to the strong Coulomb forces between charged particles when the materials are not very poor conductors. In this approximation of electrical neutrality the basic equations in the new system all have the same form as the corresponding ones in the old system.

GUGGENHEIM<sup>1)</sup> has expressed a principle underlying the sole use of the combination  $\tilde{\mu}_k = \mu_k + e_k\varphi$  as: "The electric potential difference between two points in different media can never be measured and has not yet been defined in terms of physical realities; it is therefore a conception which has no physical significance". Also some "microscopic" considerations are given to illustrate this principle: electricity does not exist as an imaginary fluid "electricity" but "only electrons and ions have physical existence". The equilibrium of these particles is thermodynamic and the driving chemical force — grad  $\mu_k$  and the electric force — grad  $(e_k\varphi)$  act always together on an ion and only the combination  $\tilde{\mu}_k = \mu_k + e_k\varphi$  can be observed.

However, in electron theory and also in the quantum mechanical theory of matter there is a well defined mean charge distribution that determines a microscopic electric field and potential, the mean values of which can be taken as the macroscopic field and potential. Hence electric field and potential must have some physical significance even in heterogeneous media according to the accepted principles of physics, although it may be that no direct methods of measurement could be given<sup>5)</sup>.

If we now consider the case of a medium which is nearly insulating the formalisms of §§ 2 and 3 can still be used. However, in (nearly) insulating media space charges can occur ( $e = \sum_k e_k c_k \neq 0$ ). Since  $\mathbf{v}$  and  $p$  are uniquely determined physical quantities we see that in this case grad  $\varphi$ , hence potential differences, can be determined according to (14), (43) or (50). In (43) it is certainly not possible to replace

$$\sum_{k=1}^n \varrho_k e_k \text{grad } \varphi = \sum_k \varrho_k \text{grad } (e_k \varphi)$$

by the expression  $\sum_k \varrho_k \text{grad} (\mu_k + e_k \varphi)$  containing  $\tilde{\mu}_k$ . For then it should result from equation (43) thus modified that we have in case of mechanical equilibrium in an uncharged medium  $\text{grad } p = - \sum_k \varrho_k \text{grad } \mu_k$ , so that generally pressure differences had to exist in this situation without electric space charge. This result is, however, not confirmed by experiment. Hence we must conclude that  $\text{grad } \varphi$  can be measured separately from the  $\text{grad } \mu_k$  in a (nearly) insulating medium.

The importance (and necessity) of the last term  $-eM d\varphi/dt$  in (56) is clearly demonstrated, if we consider a system with space charge and a change, that consists of a change  $d\varphi$  in the electric potential (and no chemical changes). This change  $d\varphi$  may be a purely formal change of the gauge of  $\varphi$  (the field that follows from  $\varphi$  does not change if a term  $at$  is added to  $\varphi$ ;  $a$  is a constant), or it may result from a displacement of the entire system in an electric field. As a consequence of the change  $d\varphi$  we have:  $dU=0$ ,  $d\tilde{U} = eM d\varphi$ . Both from (16) and (56) it follows then that  $dS=0$ . In (56) the change of  $d\tilde{U}$  is just compensated by the term  $-eM d\varphi$ . Of course  $dS=0$  must be demanded for these formal or reversible changes of  $\varphi$ .

As to the difference in treatment with GUGGENHEIM<sup>1)</sup> the following can be said:

a. A different method is used in "measuring" potential differences. We allow for the measurement of acceleration of a moving fluid, which gives  $\text{grad } \varphi$ . GUGGENHEIM restricts measurements of potentials to measurements with an ideal "Voltmeter" between two points of the same material.

b. The chemical "forces"  $-\text{grad } \mu_k$  and the electric force  $-e_k \text{grad } \varphi$  are different in character. The molecular forces, which give a contribution to  $\mu_k$ , are short range forces (range of molecular dimensions). The momentum transfer by molecular forces is already included in (12) in the pressure-tensor (for which the tensor representing an isotropic pressure can be taken if viscosity is neglected); the electric forces are, however, not included in this tensor. As the pressure can be measured directly, a separation of both parts of  $\tilde{\mu}_k = \mu_k + e_k \varphi$  is performed in this way.

*Summarizing, we see that the theory of media, which allow flows of matter, conduction of electricity and heat, and chemical reactions, can be formulated according to the thermodynamics of irreversible processes using only the combination  $\tilde{\mu}_k = \mu_k + e_k \varphi$  and not  $\mu_k$  and  $e_k \varphi$  separately, if no space charge exists. This is practically always the case for media with a reasonable electric conductivity. It implies that this field of phenomena does not allow separate measurements of  $\mu_k$  and  $\varphi$ , confirming GUGGENHEIM's results for these cases. If, however, (nearly) insulating media are investigated  $\varphi$  can be measured separately from the  $\mu_k$  if space charge exists.*

The authors wish to express their sincerest thanks to Prof. GUGGENHEIM for pointing their attention to his paper and the underlying problem.

*Institute for theoretical Physics,  
The University, Utrecht, Netherlands.*



## REFERENCES

1. GUGGENHEIM, E. A., *J. phys. Chem.* **33**, 842 (1929).  
———, *Thermodynamics*, (especially Chapter X) (North-Holland Publishing Company, Amsterdam, 1949).
2. GROOT, S. R. DE, *Thermodynamics of Irreversible Processes* (North-Holland Publishing Company, Amsterdam, 1951).
3. CURIE, P., *Oeuvres*, p. 127 (Gauthier-Villars, Paris, 1908).
4. ONSAGER, L., *Phys. Rev.* **37**, 405 (1931) and **38**, 2265 (1931).  
CASIMIR, H. B. G., *Philips Research Reports* **1**, 185 (1946) or *Rev. mod. Phys.* **17**, 343 (1945).
5. WIEBENCA, E. H., *Tweede symposium over sterke elektrolyten*, p. 90 (Netherlands chem. Soc., The Hague, 1945).

## PALEONTOLOGY

### FORAMINIFERA FROM THE TERTIARY OF ANGUILLA, ST. MARTIN AND TINTAMARRE (LEEWARD ISLANDS, WEST INDIES)

BY

C. W. DROOGER

(Communicated by Prof. G. H. R. VON KOENIGSWALD at the meeting of Nov. 25, 1950)

#### *Introduction*

Some samples from the islands of Anguilla, St. Martin and Tintamarre have become available for investigation of their foraminiferal contents. The samples were taken by ROBERT A. CHRISTMAN (Princeton University, N.J., U.S.A.) and J. H. WESTERMANN (Amsterdam, The Netherlands). CHRISTMAN collected samples from all three islands during a geological survey in 1948 and 1949<sup>1)</sup>. WESTERMANN took some additional samples on St. Martin, when visiting the island in 1950.

The samples containing Foraminifera have been derived from the Anguilla formation at Crocus Bay, Anguilla; the Simson Bay formation and Low Lands formation of St. Martin; and the small island Tintamarre, north-east of St. Martin.

The age of these formations will be discussed on the basis of the observed Foraminifera, whereas part of the species will be considered more closely.

#### *Tintamarre formation*

So far no geological or paleontological data concerning Tintamarre have been published.

The following larger Foraminifera could be identified: *Operculinoides antiquensis* VAUGHAN and COLE, *O. forresti* VAUGHAN and COLE, *Lepidocyclina* (*Lepidocyclina*) *canellei* LEMOINE and DOUVILLÉ, *L. (L.) supera* (CONRAD) and *Miogypsina* ? *M. hawkinsi* HODSON. These species occur in large numbers in two samples, whose faunas are identical.

*Operculinoides antiquensis* and *O. forresti* have originally been described from the Middle Oligocene Antigua formation in Antigua, but they are known to range upwards into the Upper Oligocene. The above mentioned species of *Lepidocyclina*, were both described from Upper Oligocene deposits in America, but likely they occur in deeper parts of the Oligocene as well. *L. supera* is reported as a typical species for the Upper Oligocene (Chattian ?) Byram Calcareous Marl of the southern United States.

---

<sup>1)</sup> A complete account of the geology of the islands will be published in the near future by ROBERT A. CHRISTMAN.

Variants of *L. canellei* in the Tintamarre material closely resemble *L. (L.) parvula* CUSHMAN, which is known from several Middle Oligocene (Rupelian ?) deposits in tropical America. The features of the early chambers of the *Miogypsina* specimens probably have some relation to their stratigraphical position. However, our knowledge regarding this interrelationship is still limited, in particular as far as concerns the American *Miogypsinae*. Outside America, the observed arrangements in the early chambers of the *Miogypsinae* of Tintamarre would place them at a distinctly higher level (probably Burdigalian) than the one concluded from the other larger Foraminifera. However, it should be kept in mind that the stratigraphical place of the *Miogypsinae* as a whole is considered to be lower in America than in the Western Pacific and the Mediterranean area.

As the genus *Lepidocyclina* in America is generally thought not to occur above the Upper Oligocene (Chattian ?), we can safely assume an Oligocene age for the Tintamarre formation, Upper Oligocene (Chattian ?) being most likely.

Smaller Foraminifera are scarce in the Tintamarre samples. Among them the following species of rare occurrence could be determined: *Robulus americanus* (CUSHMAN), *R. subpapillosus* (NUTTALL), *Dentalina pauperata* (D'ORBIGNY), *Elphidium sagra* (D'ORBIGNY), *Eponides umbo-natus* (REUSS), *Amphistegina lessonii* D'ORBIGNY, *A. angulata* (CUSHMAN), *A. angulata* (CUSHMAN) var. *christmani* DROOGER n. var., *Cibicides americanus* (CUSHMAN) and *Planorbulinella trinitatensis* (NUTTALL).

### *Anguilla formation*

The Anguilla formation is generally considered to be distinctly younger than the Middle Oligocene Antigua formation. This is based mainly on the fauna of Echinoids, Corals, Molluscs and Foraminifera, determined respectively by R. T. JACKSON, T. W. VAUGHAN, C. W. COOKE and J. A. CUSHMAN.

In 1919 CUSHMAN reported from Crocus Bay, Anguilla, the following species: *Gypsina globulus* (REUSS), *Heterosteginoides* (= *Miogypsina*) *antillea* CUSHMAN, *Orbitolites* (= *Sorites*) *duplex* CARPENTER and representatives of *Textularia*, *Nonionina*, *Quinqueloculina* and *Alveolina*, not specifically determined.

From all paleontological data VAUGHAN concluded an Aquitanian or Burdigalian age for the Anguilla formation; presumably Burdigalian.

The sample from Crocus Bay, Anguilla, collected by CHRISTMAN, yielded a small foraminiferal fauna (see below). The sole possibly diagnostic species in this assemblage is *Miogypsina* ? *M. antillea* (CUSHMAN). A fairly high percentage of specimens shows the early chambers arranged according to TAN SIN HOK's symmetrical *indonesiensis* type. Outside America this type is only known from strata referred to the Lower Miocene (Burdigalian and possibly younger). Its stratigraphic range in America is unknown, but it is present, though only in small numbers and with a

slightly higher number of nepionic chambers, in the Upper Oligocene (Chattian ?) Tintamarre formation.

This small positive evidence, together with the complete absence of typical Oligocene Foraminifera, is thought to strengthen VAUGHAN's opinion that the Anguilla formation is of Lower Miocene (Burdigalian) age.

*Simson Bay formation and Low Lands formation*

So far very few fossils have been recorded from these formations, i.e. the Foraminifera *Orbitolites* (= *Sorites*) *duplex* CARPENTER, *Spiroloculina* sp. and *Alveolina* sp. by CUSHMAN (1919) from Simson Bay Point, and the Echinoid *Echinolampas lycopersicus* GUPPY by G. A. F. MOLENGRAAFF (1931) from the Low Lands.

Thin sections of the Simson Bay limestones show abundant Foraminifera, among which *Peneroplidae* and *Miliolidae* are predominant. Some species of these families could be determined also from the washed samples, which contain in addition other Foraminifera, mainly representatives of *Amphistegina* and *Elphidium*. Thin sections of the more calcareous parts of the Low Lands formation show an assemblage completely identical to that in the Simson Bay limestones.

All species identified from the Anguilla and Simson Bay formations have been listed below:

	Anguilla formation	Simson Bay formation	Low Lands formation
<i>Clavulina tricarinata</i> D'ORBIGNY		X	
<i>Quinqueloculina candeiana</i> D'ORBIGNY		X	
<i>Quinqueloculina laevigata</i> D'ORBIGNY		X	
<i>Quinqueloculina maculata</i> GALLOWAY and HEMINWAY	X	X	X
<i>Quinqueloculina polygona</i> D'ORBIGNY	X	X	
<i>Quinqueloculina seminula</i> (LINNAEUS)		X	
<i>Triloculina oblonga</i> (MONTAGU)	X		
<i>Elphidium sagra</i> (D'ORBIGNY)	X	X	X
<i>Elphidium poeyanum</i> (D'ORBIGNY)	X	X	
<i>Elphidium lanieri</i> (D'ORBIGNY)		X	X
<i>Elphidium owenianum</i> (D'ORBIGNY)	X		
<i>Peneroplis carinatus</i> D'ORBIGNY		X	X
<i>Peneroplis proteus</i> D'ORBIGNY		X	X
<i>Archaias angulatus</i> (FICHEL and MOLL)	X	X	X
<i>Sorites duplex</i> (CARPENTER)	X	X	X
<i>Marginopora</i> sp.	X	X	X
<i>Discorbis bertheloti</i> (D'ORBIGNY) var. <i>floridensis</i> CUSHMAN	X		X
<i>Carpenteria proteiformis</i> GOËS	X		
<i>Amphistegina angulata</i> (CUSHMAN)	X	X	X



Anguilla Simson Bay Low Lands  
formation formation formation

<i>Amphistegina angulata</i> (CUSHMAN)			
var. <i>christmani</i> DROOGER n. var.	X	X	X
<i>Gypsina globulus</i> (REUSS)	X		X
<i>Miogypsina</i> ? <i>M. antillea</i> (CUSHMAN)	X		

In addition to the above Low Lands fossils a large number of species was observed in small quantities in the marly samples of this formation. The following list of species may be considered to represent a good picture of the fauna, though some of the determinations are based on very few or sometimes poorly preserved specimens. The species of *Amphistegina* are most common.

- Textularia leuzingeri* CUSHMAN and RENZ  
*Vulvulina pennatula* (BATSCH)  
*Karrerella bradyi* (CUSHMAN)  
*Karrerella subcylindrica* (NUTTALL)  
*Schenckella nodulosa* (CUSHMAN)  
*Sigmoilina sigmoidea* (BRADY)  
*Pyrgo murrhina* (SCHWAGER)  
*Robulus americanus* (CUSHMAN)  
*Robulus clericii* (FORNASINI)  
*Saracenaria arcuata* (D'ORBIGNY) var. *ampla* CUSHMAN and TODD  
*Nodosaria* cf. *N. nuttalli* (CUSHMAN and JARVIS)  
var. *gracillima* (CUSHMAN and JARVIS)  
*Nodosaria paucistriata* (GALLOWAY and MORREY)  
*Nodosaria verneuili* (D'ORBIGNY)  
*Lagena* (*Entosolenia*) *orbignyana* (SEGUENZA)  
*Nodosarella subnodosa* (GUPPY)  
*Ellipsoidina abbreviata* SEGUENZA  
*Borelis pulchra* (D'ORBIGNY)  
*Bolivina tectiformis* CUSHMAN  
*Uvigerina rustica* CUSHMAN and EDWARDS  
*Angulogerina* cf. *A. cojimarensis* PALMER  
*Gyroidina soldanii* D'ORBIGNY  
*Eponides campester* PALMER and BERMUDEZ  
*Eponides umbonatus* (REUSS)  
*Eponides ventricosus* GALLOWAY and HEMINWAY  
*Rotalia beccarii* (LINNAEUS) var. *tepida* CUSHMAN  
*Siphonina pulchra* CUSHMAN  
*Carpenteria bulloides* GALLOWAY and HEMINWAY  
*Globigerina* cf. *G. conglomerata* SCHWAGER  
*Globigerinella aequilateralis* (BRADY)  
*Globigerinoides conglobatus* (BRADY)  
*Globigerinoides grimsdalei* (KEYZER)

- Globigerinoides* cf. *G. trilobus* (REUSS)  
*Orbulina bilobata* (D'ORBIGNY)  
*Orbulina universa* D'ORBIGNY  
*Sphaeroidinella* cf. *S. seminulina* (SCHWAGER)  
*Globorotalia menardii* (D'ORBIGNY)  
*Amphistegina lessonii* D'ORBIGNY  
*Asterigerina carinata* D'ORBIGNY  
*Pullenia bulloides* (D'ORBIGNY)  
*Cassidulina carapitana* HEDBERG  
*Cassidulina subglobosa* BRADY  
*Anomalina alazanensis* NUTTALL var. *spissiformis* CUSHMAN and  
STAINFORTH  
*Cibicides io* CUSHMAN  
*Cibicides mexicanus* NUTTALL  
*Laticarinina bullbrooki* CUSHMAN and TODD  
*Planulina subtenuissima* (NUTTALL).

The similarity of Simson Bay and Low Lands faunas, from outcrops not far apart, strongly favours the opinion that we are dealing with components of one and the same formation, deposited under tropical shallow water conditions. The marly part of the Low Lands formation also contains *Peneroplidae* and *Miliolidae*, but here the representatives of these families are much less dominant than in the more calcareous parts. Obviously the facies was rather more marine, resulting in the presence of numerous species in small numbers, among which are several representatives of the family *Globigerinidae*.

An indication of the age of these sediments is given by the combination of the known time-ranges of the latter Low Lands species. This points to Upper Oligocene or Lower Miocene. The complete absence of diagnostic larger Foraminifera, however, favours a Lower Miocene age. This places these formations of St. Martin at about the same time-level as the near-by Anguilla formation. Excepting the occurrence of *Miogypsina* in Anguilla, its fauna indeed shows the same composition of tropical shallow water species. Moreover MOLENGRAAFF reports the Echinoid *Echinolampas lycopersicus* GUPPY from the Low Lands formation. This is also a well-known species of the Anguilla formation in Anguilla.

Concluding we may say that in all likelihood Anguilla formation, Simson Bay formation and Low Lands formation are of about equal Lower Miocene age.

Similar shallow water sediments with about the same fauna (*Peneroplidae* and *Miliolidae*) and of about equal age are known from tropical America, especially of the Greater Antilles. These are the Lower Miocene Los Puertos formation in Porto Rico (GALLOWAY and HEMINWAY, 1941), the Upper Oligocene-Lower Miocene Florentino formation in the Dominican Republic (BERMUDEZ, 1949), the Upper Oligocene-? Middle Miocene

Paso Real formation and the Lower Miocene Güines formation of Cuba (BERMUDEZ, 1950). In Cuba the lower part of the Paso Real formation contains, in addition to *Peneroplidae* and *Miliolidae*, *Miogypsina*. This part is considered Upper Oligocene. Through the kindness of Dr P. J. BERMUDEZ several *Miogypsinae* of the Cuban Upper Oligocene could be studied. In the sectioned specimens of these Cuban *Miogypsinae* the symmetrical *indonesiensis* type is extremely rare. This may be another indication that the Anguilla formation is younger than Upper Oligocene.

The following facts should be considered in evaluating the age problem. The stratigraphical distribution of many American larger Foraminifera is still a matter of conjecture, whereas correlation of American Middle Tertiary units with European subdivisions of Oligocene and Miocene deserves careful re-study.

#### *Remarks on some Foraminifera*

##### *Miliolidae*

Though representatives of the *Miliolidae*, especially of *Quinqueloculina*, are quite numerous in the samples from Anguilla and St. Martin, a large part of them cannot be determined. The most common form is the peculiarly ornamented *Q. maculata* GALLOWAY and HEMINWAY (1941; p. 303, pl. 2, f. 3).

##### *Peneroplidae*

Representatives of the genera *Archaias* and *Sorites* are common to abundant in the samples from Anguilla and St. Martin, especially in their more calcareous parts. Neither the specimens from the washed samples, nor those in the thin sections show sufficient characteristics for detailed comparison with the species, described in literature. Moreover descriptions of genera and species of this family are often rather confused. As far as could be ascertained there is hardly any difference between these fossil specimens and representatives, living in recent seas.

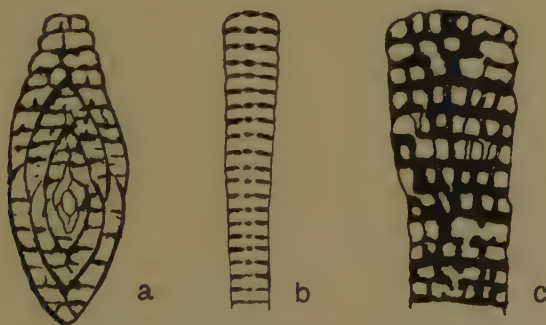


Fig. 1. Schematic drawings of transverse sections of:  
 a. *Archaias angulatus* (FICHTEL and MOLL),  
 b. *Sorites duplex* (CARPENTER), marginal portion,  
 c. *Marginopora* sp., marginal portion.  
 Simson Bay formation, St. Martin; 20 ×.

The specimens of *Archaias* show much variation. All of them can be considered to belong to *A. angulatus* (FICHTEL and MOLL), including under this name those forms known as *A. aduncus* (FICHTEL and MOLL) and *A. compressus* (FICHTEL and MOLL). Specimens intermediate between these three types are abundantly present. No doubt *Alveolina* sp. (?), reported by CUSHMAN from Simson Bay Point, St. Martin (1919, p. 71, pl. 5, f. 14) should be regarded as a transverse section of *A. angulatus*.

Most specimens of *Sorites* show the simple type, which is usually referred to as *S. duplex* (CARPENTER).

Some fragments with complicated interior resemble *Marginopora* BLAINVILLE. In the thin sections similar structures may partly be referable to specimens of the *compressus* type of *Archaias angulatus*. The presence of *Marginopora*, however, is quite obvious, but a specific determination lacks sufficient evidence.

### *Operculinoides antiquensis* VAUGHAN and COLE

*Operculinoides antiquensis* VAUGHAN and COLE, 1936, Proc. U.S. Nat. Mus., Wash., vol. 83, no. 2996, p. 492, pl. 38, f. 7—10; WRIGHT BARKER, 1939, Proc. U.S. Nat. Mus., Wash., vol. 86, no. 3052, p. 313, pl. 14, f. 1, 2, pl. 16, f. 3, pl. 17, f. 1, pl. 21, f. 10, 11.

This species is abundant in the Tintamarre samples. The specimens distinctly show the characteristics that distinguish *Operculinoides antiquensis* and *O. semmesi* from the other species of the genus *Operculinoides*. They vary widely in diameter from 1.0—3.4 mm.

About 50 of them were sectioned, including specimens of all sizes. The larger diameter of the test was measured, whereas the number of chambers in the final coil was counted. From this it became clear that all specimens from Tintamarre belong to one species, *O. antiquensis*, also the smaller ones, which should be considered immature individuals.

The number of chambers increases with increasing size. According to the original description of the species from Antigua by VAUGHAN and COLE, there is a variation of diameter from 2.5—3.7 mm. One Antiguan specimen of 3 mm diameter showed 29 chambers, another of 3.5 mm 33 chambers in the final convolution. WRIGHT BARKER gives a variation of 2.4—3.5 mm for the diameter and a number of 23—29 chambers in the last-formed whorl in his Mexican material.

From the numerous specimens of Tintamarre it became clear that specimens of equal size may differ 3—5 chambers on the total number in the final coil. Specimens with a diameter larger than 3.25 mm are rare, showing 27—29 chambers in the last-formed whorl. Specimens, having a diameter of 2.4 mm and more, in our material, have 22—29 chambers in the final convolution, these numbers being about the same as those observed by WRIGHT BARKER in *O. antiquensis* from Mexico. On the other hand specimens referable to *O. semmesi* are absent in our material. VAUGHAN and COLE, as well as WRIGHT BARKER, give a range of variation



of 1.75–2.8 mm for the diameter of this species and respectively 14–19 and 18–19 for the number of chambers in the final coil. The Tintamarre specimens of 1.75–2.8 mm diameter possess 18–26 chambers, whereas those having 14–19 chambers in the final convolution vary between 1.1 and 1.8 mm in diameter. Thus it can be concluded that in specimens of equal size *O. semmesi* has a distinctly lower number of chambers in the final whorl (including variation deviations) than *O. antiguensis*.

*Operculinoides forresti* VAUGHAN and COLE

*Operculinoides forresti* VAUGHAN and COLE, 1936, Proc. U.S. Nat. Mus., Wash., vol. 83, no. 2996, p. 493, pl. 37, f. 1–3; COLE, 1938, Florida State Dept. Conserv., Geol. Bull. 16, p. 37, pl. 5, f. 8–13.

In the samples from Tintamarre this species is less frequent than *O. antiguensis*, but a large number of typical specimens were found. They agree with the original description and figures. The larger diameter of the Tintamarre specimens varies between 1 and 4 mm. The number of chambers in the final whorl becomes higher with increasing size from 13 in the smallest specimens to 27 in those of the largest diameter. As in *O. antiguensis* also *O. forresti* shows variation in the number of chambers in the final whorl in all cases that sufficient numbers of specimens of equal size could be investigated. This variation proved to amount to 2–4 chambers.

*Amphistegina angulata* (CUSHMAN)

*Asterigerina carinata* CUSHMAN, 1919, Carnegie Inst., Wash., Publ. 291, p. 45, pl. 13, f. 1.

*Amphistegina angulata*, GALLOWAY and HEMINWAY, 1941, New York Ac. Sci., Sci. Survey Porto Rico and the Virgin Islands, vol. 3, pt. 4, p. 407, pl. 28, f. 6; BERMUDEZ, 1949, Cushman Lab. Foram. Res., Spec. Publ. 25, p. 261, pl. 19, f. 19–21.

This species is common to abundant in all marly samples of the three islands. Most specimens, especially those of the Low Lands formation, show an extremely thick calcareous wall of lamellar structure. In these specimens the interior characteristics are usually hardly if at all visible. Some variation occurs in the relative thickness of the test. Both the



Fig. 2. *Amphistegina angulata* (CUSHMAN); a. ventral view, b. peripheral view. Low Lands formation, St. Martin; 25 ×.

ventral and the dorsal umbo are closed, whereas the ventral one often shows a thickened mass of clear shell-material.

*Amphistegina angulata* (CUSHMAN) var. *christmani* DROOGER n. var.

Description: Variety differing from the typical in having ventrally the lamellae of the wall not covering the entire test, leaving a shallow open umbilicus.

Diameter. up to 3 mm.

Remarks: About half the number of specimens of *Amphistegina* from the Low Lands marls belongs to this variety. In these the lamellae of the later whorls do not close over the ventral side, thus leaving a more or less open umbilical region, bordered by the usually almost circular inner sides of the lamellae. Often these inner sides of the lamellae run from the umbilicus to the periphery in irregular lines. Occasionally similar, but less pronounced, characteristics are shown on the dorsal side of the test. Specimens of both species and variety are found in all sizes, thus obviously excluding the possibility of one being the adult form of the other.

Occurrence: Holotype from the Lower Miocene, Low Lands marls of St. Martin (S 66, Christman collection), deposited in the collection of the

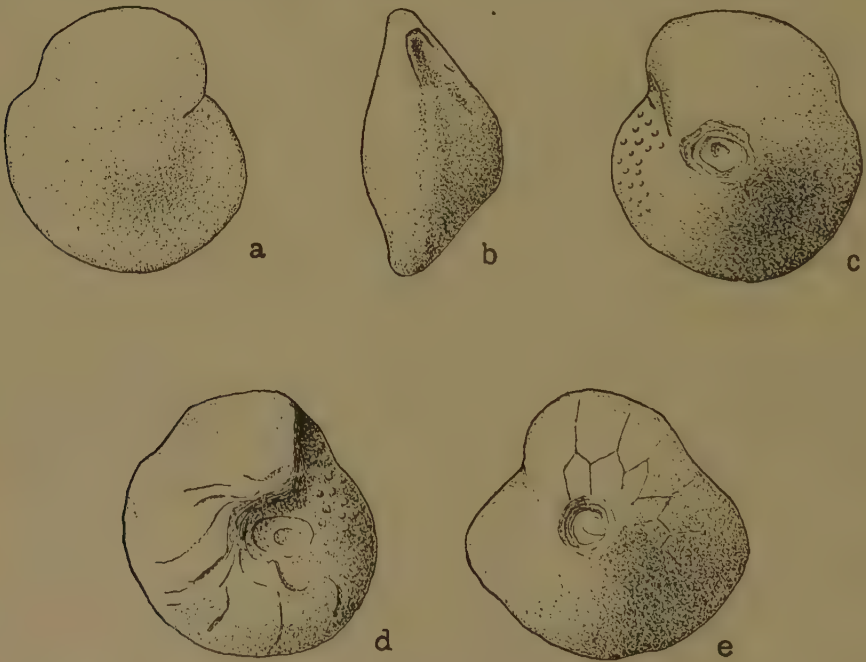


Fig. 3. *Amphistegina angulata* (CUSHMAN) var. *christmani* DROOGER n. var.  
 a, b, c: Holotype, 28 ×; a. dorsal view, b. peripheral view, c. ventral view;  
 d. ventral view of a specimen, showing the edges of the lamellae, running from the  
 umbilicus to the periphery, 15 ×; e. ventral view of another specimen of which  
 the lamellae are partly removed, showing the arrangement of the chambers, 35 ×.  
 Low Lands formation, St. Martin.

Geological Department of Princeton University, Princeton, N.J., U.S.A. <sup>2</sup>). The variety is present in all marly samples of the three islands (Upper Oligocene and Lower Miocene), but it is most abundant in the Low Lands marls of St. Martin.

*Lepidocyclina (Lepidocyclina) canellei* LEMOINE and R. DOUVILLÉ

*Lepidocyclina canellei* LEMOINE and R. DOUVILLÉ, 1904, Mém. Soc. Géol. France, tome 12, fasc. 2, no. 32, p. 20, pl. 1, pl. 3, f. 5; CUSHMAN, 1920 U.S. Geol. Survey, Prof. Paper 125 D, p. 75, pl. 32, f. 1–5; VAUGHAN, 1933, Smiths. Misc. Coll., vol. 89, no. 10, Publ. 3222, p. 14, pl. 6, f. 1–5.

Many specimens, completely resembling those of the references, cited above, occur in the samples from Tintamarre. However, there is a gradual change to specimens with the same inner characteristics, but with heavy pillars in the central portion of the test. According to VAUGHAN (p. 15) the latter should be referred to as *L. (L.) parvula* CUSHMAN.

*Lepidocyclina (Lepidocyclina) supera* (CONRAD)

*Orbitolites supera* CONRAD, 1865, Proc. Ac. Nat. Sci., Philadelphia, no. 2, p. 74.

*Lepidocyclina supera*, CUSHMAN, 1920, U.S. Geol. Survey, Prof. Paper 125 D, p. 69, pl. 26, f. 5–7; VAUGHAN, 1933, Smiths. Misc. Coll., vol. 89, no. 10, Publ. 3222, p. 12, pl. 29, f. 1–3.

In the samples from Tintamarre numerous fragments of rather flat and papillate *Lepidocyclinae* were encountered, which can be referred to *L. supera*. Only in few cases the isolepidine arrangement of the early chambers could be ascertained. The observed interior characteristics agree with those described by CUSHMAN.

*Miogypsina* ? *M. antillea* (CUSHMAN)

*Heterosteginoides antillea* CUSHMAN, 1919, Carnegie Inst., Wash., Publ. 291, p. 50, pl. 5, f. 5, 6.

Numerous specimens belonging to *Miogypsina* s.str. occur in the sample of Crocus Bay, Anguilla.

Description: Test irregularly fan-shaped, considerably varying in appearance, the apical portion usually protruding, the frontal side often more or less deeply indented. One side is often more strongly convex than the other. Size of macrospheric specimens usually less than 2 mm, microspheric specimens may attain a size of 3 mm. Thickness varying between 0.4 and 1 mm, the latter situated excentrically near the early portion of the test. Surface with irregular mesh work of the lateral chambers and variously papillate, the papillae usually not strongly protruding. The diameter of the papillae varies between 25 and 75  $\mu$ , the larger ones having their strongest development near the thickest portion of the test.

<sup>2</sup>) Excepting the holotype of this new variety, all Foraminifera, mentioned in this paper, have been deposited in the collection of the Geological Institute of the State University at Utrecht.

In transverse sections the layer of median chambers is usually straight and regular, sometimes slightly curved or irregular. Height fairly constant: 100—140  $\mu$ . The lateral chambers are arranged in regular layers with a height of 20—40  $\mu$ . The length of these chambers never exceeds the length of the equatorial chambers. They are arranged in tiers only where pillars are present. Up to 5 layers on each side occur in the thickest portion of the test; towards the edges this number gradually decreases, whereas on the frontal side the lateral chambers are sometimes absent. Near the initial part of the test the layers of lateral chambers bend around the early portion. Usually only the horizontal walls are present here, forming a kind of collar around the initial part, the cavities of the lateral chambers being not or only slightly developed.

In longitudinal sections the initial chambers appear to lie very close to the border of the test. The first chamber is more or less spherical, the second hemispherical to rheniform, embracing the first one in section for a quarter to one third of its circumference. The diameter of the protoconch averages 160  $\mu$  (130—190  $\mu$ ); the smaller diameter of the deuterococonch is of about the same size, the larger diameter averages 210  $\mu$  (150—240  $\mu$ ). The arrangements of the nepionic chambers show different forms of the *bifida* and *indonesiensis* types, the latter being proportionately better represented. The spirals around the deuterococonch are incomplete or obscure, the deuterococonch usually being for the greater part directly overlain by the collar. In few specimens accessory auxiliary chambers are possibly present. The total number of chambers around the protoconch, including the auxiliary chambers, varies between 5 and 8.



Fig. 4. Schematic drawings of the arrangement of the early chambers in horizontal sections of 6 specimens of *Miogypsina* ? *M. antillea* (CUSHMAN); approx. 17  $\times$ ; The apical-frontal line is vertical. Crocus Bay, Anguilla.

In horizontal sections form and size of the equatorial chambers vary widely. They are usually diamond-shaped, the apical-frontal diameter being largest. This longer dimension varies between 80 and 240  $\mu$  (usually 120 and 180  $\mu$ ), the tangential dimension between 60 and 200  $\mu$  (usually 100 and 170  $\mu$ ).

Stolons in the walls of embryonic and equatorial chambers could only occasionally be observed in our material.

These specimens are probably identical with *Miogypsina antillea* (CUSHMAN), also from Crocus Bay, Anguilla, which is, however, inadequately described and pictured. No material of CUSHMAN's collection could be investigated.

#### *Miogypsina* ? *M. hawkinsi* HODSON

*Miogypsina hawkinsi* HODSON, 1926, Bull. Am. Paleont., vol. 12, no. 47, p. 28, pl. 7, f. 9, pl. 8, f. 1, 2.



In the Tintamarre samples a number of specimens of *Mio-gypsina* s. str. were found, which show much resemblance to those of Crocus Bay, Anguilla. The main differences are that none of the Tintamarre specimens shows an indented frontal side of the test, whereas the symmetrical *indonesiensis* type is proportionately less strongly represented. In none of the sectioned specimens, having this type, the number of nepionic chambers round about the protoconch is less than seven (the lowest number in the Anguilla specimens is five).

As hardly anything is known about the variability of the arrangements of the nepionic chambers in *M. hawkinsi* from its original locality in Venezuela, no certain comparison of our specimens with HODSON's species can be made.

### Acknowledgements

The author wishes to express his thanks to Mr ROBERT A. CHRISTMAN and Dr J. H. WESTERMANN for placing their samples at his disposal and for their valuable information and suggestions; to Mr P. MARKS for drawing some of the figures.

### REFERENCES

- BERMUDEZ, P. J., Tertiary smaller Foraminifera of the Dominican Republic, Cushman Lab. Foram. Res., Spec. Publ. 25 (1949).
- , Contribucion al estudio del Cenozoico Cubano, Mem. Soc. Cub. Hist. Nat., 19, no. 3 (1950).
- COOKE, C. W., Tertiary Mollusks from the Leeward Islands and Cuba, Carnegie Inst., Wash., Publ. 291 (1919).
- CUSHMAN, J. A., Fossil Foraminifera from the West Indies, Carnegie Inst., Wash., Publ. 291 (1919).
- GALLOWAY, J. J. and HEMINWAY, C. E., The Tertiary Foraminifera of Porto Rico, New York Ac. Sci., Sci. Survey of Porto Rico and the Virgin Islands, 3, pt. 4 (1941).
- JACKSON, R. T., Fossil Echini of the West Indies, Carnegie Inst., Wash., Publ. 306 (1922).
- MOLENGRAAFF, G. A. F., Saba, St. Eustatius (Statia) and St. Martin, Leidsche Geol. Meded. (Feestbundel K. Martin) (1931).
- VAUGHAN, T. W., Fossil corals from Central America, Cuba and Porto Rico, etc., U.S. Nat. Mus., Bull. 103 (1919).
- , Stratigraphic significance of the species of West Indian fossil Echini, Carnegie Inst., Wash., Publ. 306 (1922).
- , Criteria and status of correlation and classification of Tertiary deposits, Bull. Geol. Soc. Am., 35, 677—742 (1924).
- , Notes on the igneous rocks of the Northeast West Indies and on the Geology of the Island of Anguilla, Journ. Wash. Ac. Sci., 16, no. 13 (1926).
- WESTERMANN, J. H., Overzicht van de geologische en mijnbouwkundige kennis der Nederlandse Antillen, Kon. Ver. Ind. Inst., Meded. no. 85 (with a summary in English) (1949).

## PALEONTOLOGY

### UPPER CRETACEOUS FORAMINIFERA OF THE MIDDEN-CURAÇAO BEDS NEAR HATO, CURAÇAO (N.W.I.)

BY

C. W. DROOGER

(Communicated by Prof. G. H. R. VON KOENIGSWALD at the meeting of Dec. 23, 1950)

In 1929 G. J. H. MOLENGRAAFF gave the name of Midden-Curaçao Beds to a series of sediments of Curaçao, whose thickness proved to be more than a thousand meters. The outcrops of this formation occur in the central part and in scattered places of the eastern portion of the island. L. W. J. VERMUNT and M. G. RUTTEN described in more detail the lithologic characteristics of these sediments in Central Curaçao. From the base upwards they distinguished the following three zones: conglomerates, sandstones and shales, and shales only.

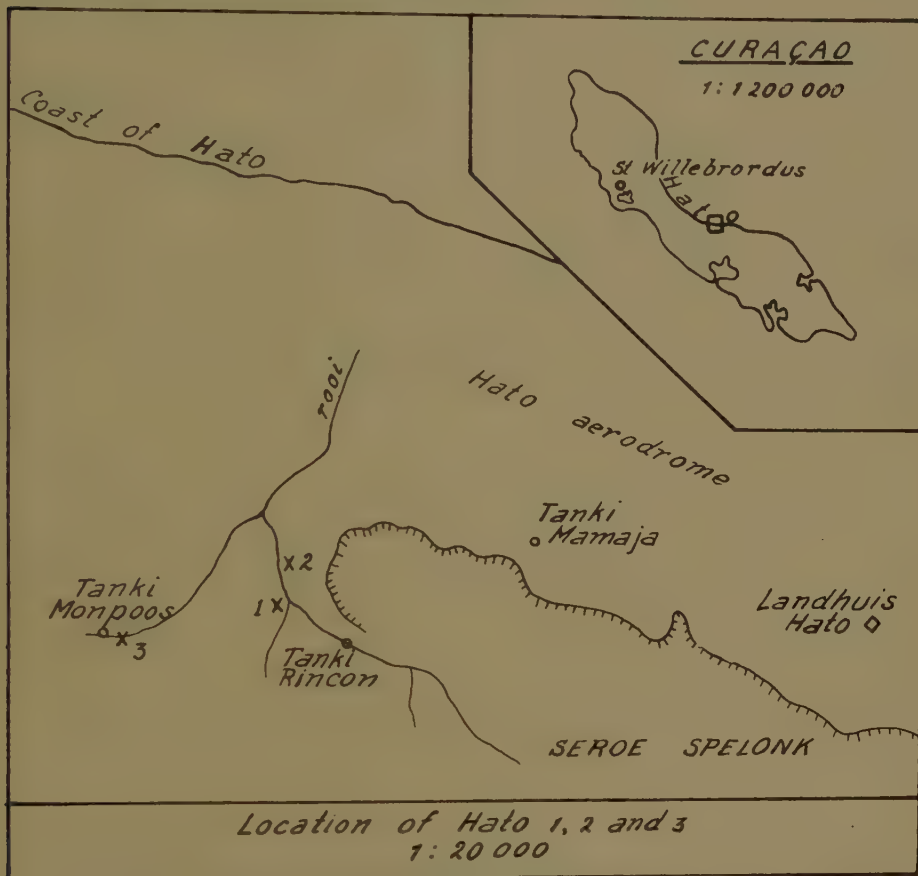
Locally the conglomerates of the Midden-Curaçao Beds contain pebbles of the Seroe Teintje Limestones, which are considered to be of Upper Cretaceous age. The corals of these limestones were determined by H. GERTH, who concluded a Lower Senonian age for them. H. J. MAC GILLAVRY described two Rudists from the same formation, remarking: "Everything considered the facts agree quite well with the Lower Senonian age given by GERTH on account of the corals." He added: "The age certainly is Senonian, probably Campanian or even Maestrichtian."

The Midden-Curaçao Beds, together with the older sediments, were folded, probably in Lower Eocene time, after which the Upper Eocene Seroe di Cueba Limestone was formed.

From these data it appears that the Midden-Curaçao Beds should be placed in the Upper Cretaceous and (or) Lowermost Tertiary. There are some general records of fossils in the Midden-Curaçao Beds (MOLENGRAAFF, 1929; VERMUNT and RUTTEN). According to P. J. PIJERS (p. 37—38) C. T. TRECHMANN examined some fossils of this formation, collected by L. RUTTEN and his students in 1930. From these fossils TRECHMANN thought it most likely that the Midden-Curaçao Beds are of Eocene age.

In 1949 some shallow wells were drilled by the Water Supply Service in the Hato Valley, west of Hato aerodrome. The samples of two of these borings were investigated (Borings Hato 1 and Hato 2). A surface sample was taken by J. H. WESTERMANN in the Hato Valley, near Tanki Monpoos, in 1950 (Hato 3). Probably all the samples were derived from the upper shaly part of the Midden-Curaçao Beds. Moreover samples of another boring (St. Willebrordus-Jan Kok 2) of the Water Supply Service were examined. The latter samples proved to be completely devoid of identi-

fiable organic remains. According to the geological sketch map, published by VERMUNT and RUTTEN, this well was drilled in the sandstone and shale zone of the Midden-Curaçao Beds.



The surface sample Hato 3 yielded a large number of moderately preserved smaller Foraminifera. Ten species could be determined, three of which also occur in the samples of boring Hato 1 (9.00—17.50 m below the surface level). Only one of the species has been observed in boring Hato 2 (depth 12.50 m). The specimens of the borings are considerably corroded.

The species occurring in Hato sample 3 are all known from Upper Cretaceous strata. Considering their established stratigraphical ranges in America, an Upper Taylor to Lower Navarro age is most suitable to the fauna as a whole. From the occurrence of *Spiroplectamina grzybowskii*, which is known in particular from the Uppermost Cretaceous and from transitional strata between Cretaceous and Tertiary, a Lower Navarro (Maestrichtian) age is most probable. Most frequent in this fauna are *Globotruncana fornicata* and *Globigerinidae*, among which could be identified *Globigerina voluta*.

The poor fauna of boring Hato 1 is of Upper Cretaceous age, but cannot be determined more specifically; presumably its age does not differ much from that of the fauna of the surface sample. In the drilling samples of Hato 1 *Planulina taylorensis* is predominant. At some levels over 90 % of the entire number of specimens belong to this species. Its presence was also ascertained in one sample of boring Hato 2.

It is unlikely that we are dealing with reworked Foraminifera in any of these Hato samples. This is evidenced by the fact that the whole assemblage constitutes a distinct Upper Cretaceous fauna. It would also appear from the observation that the majority of the specimens are undamaged. They do not even show the slightest traces of transport. Of each species specimens have been found of different individual development and size. It should be remarked that in nearly all species the individuals are smaller than the sizes recorded from other localities. This possibly points to the fact that life conditions during deposition were rather unfavourable.

Concluding it may be assumed that at least part of the Midden-Curaçao Beds is of Upper Senonian age. Accordingly these sediments were deposited immediately after the forming of the Seroe Teintje Limestones. It is however possible, that sedimentation of the uppermost strata took place during early Tertiary time.

### Description of the species

*Spiroplectammina grzybowskii* FRIZZELL (fig. 1)

*Spiroplectammina grzybowskii* FRIZZELL, 1943, Journ. of Pal., vol. 17, p. 337, pl. 55, f. 12, 13 (see for ref.).

This species is recorded mainly from the Uppermost Cretaceous and from Cretaceous-Tertiary transitional strata. WHITE reports it from the Middle Mendez up to the Lower Velasco of Mexico (1929, Journ. of Pal., vol. 3, p. 32).

The initial coiled stage is rather obscure in our material, due to the poor preservation of the specimens.

Rare at Hato 3.

*Robulus pseudo-secans* CUSHMAN (fig. 2)

*Robulus pseudo-secans* CUSHMAN, 1938, Contrib. Cushman Lab. Foram. Research, vol. 14, p. 32, pl. 5, f. 3; CUSHMAN, 1941, *ibid.*, vol. 17, p. 59, pl. 15, f. 7.

Originally described from the Selma Chalk of Tennessee.

In some of the Curaçao representatives of this species the sutures are straighter than in the typical, whereas the umbilical boss is sometimes distinctly separated from the raised sutures. The keel is variously developed, occasionally almost entirely wanting, which may be due to the corrosion of the specimens.

Rare at Hato 1 and 3.



*Bulimina kickapooensis* COLE (fig. 3)

*Bulimina quadrata*, CUSHMAN and PARKER (non PLUMMER), 1935, Contrib. Cushman Lab. Foram. Research, vol. 11, p. 100, pl. 15, f. 13, 14, 16.

*Bulimina kickapooensis* COLE, 1938, Florida State Dept. Conserv., Bull. 16, p. 45, pl. 3, f. 5; CUSHMAN and HEDBERG, 1941, Contrib. Cushman Lab. Foram. Research, vol. 17, p. 94, pl. 22, f. 28.

Reported from Taylor and Navarro.

Both microspheric and macrospheric specimens were observed.

Rare at Hato 3.

*Bulimina reussi* MORROW (fig. 4)

*Bulimina reussi* MORROW, 1934, Journ. of Pal., vol. 8, p. 195, pl. 29, f. 12; CUSHMAN and PARKER, 1935, Contrib. Cushman Lab. Foram. Research, vol. 11, p. 99, pl. 15, f. 8, 10.

This is a well-known species of American Upper Cretaceous deposits, ranging from Austin to Navarro.

Rare at Hato 3.

*Gümbelina striata* (EHRENBERG) (fig. 5)

*Textularia striata* EHRENBERG, 1838 (1840), Abh. K. Ak. Wiss., Berlin, p. 135, pl. 4, f. 1—3, 9.

*Gümbelina, striata* CUSHMAN, 1938, Contrib. Cushman Lab. Foram. Research, vol. 14, p. 8, pl. 1, f. 34—40.

Originally described from the Upper Senonian of Germany. In America occurring from Austin to Lower Navarro.

A number of our specimens are very small and do not clearly show the peculiar striate characters of the early chambers.

Rare at Hato 3.

*Gyroidina girardana* (REUSS) (fig. 6a, b)

*Rotalina girardana* REUSS, 1851, Zeitschr. d.d. geol. Ges., Band 3, p. 73, pl. 5, f. 34.

*Gyroidina girardana*, CUSHMAN and TODD, 1943, Contrib. Cushman Lab. Foram. Research, vol. 19, p. 68, pl. 12, f. 3.

Originally described from the Eocene of Germany. Widely recorded from the Upper Cretaceous in America.

Rare at Hato 3.

*Stensiöina americana* CUSHMAN and DORSEY (fig. 7a—c)

*Cibicides excolata* CUSHMAN (non *Truncatulina excolata*, CUSHMAN), 1926, 1931, Journ. of Pal., vol. 5, p. 315, pl. 36, f. 8.

*Stensiöina americana* CUSHMAN and DORSEY, 1940, Contrib. Cushman Lab. Foram. Research, vol. 16, p. 5, pl. 1, f. 7.

Reported from Upper Taylor and Lower Navarro.

The ventral sutures in our specimens are moderately limbate.

Rare at Hato 3.

*Globigerina voluta* WHITE (fig. 8a, b)

*Globigerina voluta* WHITE, 1928, Journ. of Pal., vol. 2, p. 197, pl. 28, f. 5.



WHITE described this species from the Mendez formation of Mexico.

Part of our specimens are more or less asymmetric, often showing on one side faint traces of the previous whorls. Thus they are morphologically intermediate between *G. voluta* and *G. cretacea* D'ORBIGNY. The same features were observed by WHITE in the fauna of the Mendez formation. The number of chambers in the final convolution varies between 4 and 6.

Rather common at Hato 1 and 3.

*Globotruncana fornicata* PLUMMER (fig. 9a—c)

*Globotruncana fornicata* PLUMMER, 1931, Texas Univ. Bull. 3101, p. 130, pl. 13, f. 4—6.

Recorded from Upper Taylor and Navarro.

The majority of the specimens of Curaçao closely resemble the type from Texas. Part of the individuals differ from the typical in having the dorsal sutures more or less strongly raised. Others show a highly elevated ventral side with in many cases a partial reduction of the ventral keel. The latter specimens approach the type of *G. cretacea* CUSHMAN (1938, Contrib. Cushman Lab. Foram. Research, vol. 14, p. 67, pl. 11, f. 6).

Rather common at Hato 3.

*Planulina taylorensis* (CARSEY) (fig. 10a, b)

*Anomalina taylorensis* CARSEY, 1926, Texas Univ. Bull. 2612, p. 47, pl. 6, f. 1.  
*Planulina taylorensis*, CUSHMAN, 1940, Contrib. Cushman Lab. Foram. Research, vol. 16, p. 35, pl. 6, f. 10; CUSHMAN, 1942, *ibid.*, vol. 18, p. 66, pl. 15, f. 28—31.

Recorded from Austin to Lower Navarro.

The number of chambers in the final whorl of the Curaçao specimens usually amounts to 10 or 11. The representatives of this species in Hato 1

---

#### EXPLANATION OF THE PLATE

- Fig. 1. *Spiroplectammina grzybowskii* FRIZZELL; Hato 3; 66 ×.  
Fig. 2. *Robulus pseudo-secans* CUSHMAN; Hato 3; 66 ×.  
Fig. 3. *Bulimina kickapooensis* COLE; Hato 3; 66 ×.  
Fig. 4. *Bulimina reussi* MORROW; Hato 3; 194 ×.  
Fig. 5. *Gumbelina striata* (EHRENBERG); Hato 3; 66 ×.  
Fig. 6a, b. *Gyroidina girardana* (REUSS); a. dorsal view, b. peripheral view; Hato 3; 66 ×.  
Fig. 7a—c. *Stensiöina americana* CUSHMAN and DORSEY; a. dorsal view, b. ventral view, c. peripheral view; Hato 3; 66 ×.  
Fig. 8a, b. *Globigerina voluta* WHITE; a. side view, b. peripheral view; Hato 3; 66 ×.  
Fig. 9a—c. *Globotruncana fornicata* PLUMMER; a. dorsal view, b. ventral view, c. peripheral view; Hato 3; 66 ×.  
Fig. 10a, b. *Planulina taylorensis* (CARSEY); a. dorsal view, b. ventral view; Hato 3; 124 ×.

and 2 are partly somewhat thicker than the typical, whereas the majority are quite indistinct by corrosion of the surface.

Common to abundant at Hato 1, rare at Hato 2 and 3.

*Acknowledgements*: The author wishes to thank Dr J. H. WESTERMANN and the Water Supply Service, Curaçao, for generously placing the samples at his disposal; the Foundation for Scientific Research in Surinam and Curaçao, Utrecht, for its valued financial support; Mr P. MARKS for his careful drawing of the figures.

#### REFERENCES

- GERTH, H., Beiträge zur Kenntnis der mesozoischen Korallenfaunen von Südamerika. I. Korallen aus den oberkretazischen Rudistenkalken von Curaçao. Leidsche Geol. Meded., 3, afl. 1 (1928).
- MAC GILLAVRY, H. J., The Rudist fauna of Seroe Teintje limestone (Northern Curaçao). Proc. Kon. Ak. v. Wetensch. Amsterdam, 35, no. 3 (1932).
- MOLENGRAAFF, G. J. H., Geologie en Geohydrologie van het eiland Curaçao. Acad. Thesis (Delft, 1929).
- , Curaçao. Leidsche Geol. Meded., 5, Feestbundel K. Martin (English text) (1931).
- PIJPERS, P. J., Geology and Paleontology of Bonaire (D.W.I.). Geogr. en Geol. Meded. Utrecht, Physiogr. Geol. Reeks, no. 8 (1933). (also: Acad. Thesis Utrecht).
- VERMUNT, L. W. J. and M. G. RUTTEN, Geology of Central-Curaçao. Proc. Kon. Ak. v. Wetensch. Amsterdam, 34, no. 3 (1931).
- WESTERMANN, J. H., Overzicht van de geologische en mijnbouwkundige kennis der Nederl. Antillen (with summary in English). Kon. Ver. Ind. Inst., Meded. no. 85 (Amsterdam, 1949).



SOME REMARKS ON THE DEVELOPMENT OF THE COMPOUND  
MICROSCOPES IN THE 19TH CENTURY

BY

P. H. VAN CITTERT AND J. G. VAN CITTERT-EYMERS

(Communicated by Prof. A. J. KLUYVER at the meeting of December 23, 1950)

More than 15 years ago one of us published The Descriptive Catalogue of the Collection of Microscopes in charge of the Utrecht University Museum<sup>1)</sup>, referred to as D.C., which differed from similar catalogues that it not only gave a description of the mechanical construction and of the various accessories, but also of the magnifications (measured for 25 cm eye-distance) and the resolutions of all microscopes described. The last of these were determined with the aid of a "Grayson Rulings" (compare D.C. 7) and parallel beams of light, so that  $\lambda/A$  was measured. Parallel beams were namely necessary because by using a condensor one never measures the resolution  $\lambda/2A$  (as is erroneously found in most of the literature), but a much inferior value, depending on the ratio between the breadth and the distance of the lines of the Grayson rulings and on the skill and experience of the observer (viz.  $\lambda/1,2 A$  or  $\lambda/1,3 A$ ).<sup>2)</sup>

From the dates given in the D.C. it follows clearly that until about 1830 the resolution of the single microscopes greatly surpassed that of the compound ones. Up to about 1800 only non-corrected microscopes were in use. It was especially the chromatic aberration that limited the optical power. In consequence, only few 18th century compound microscopes had a magnification surpassing  $200 \text{ à } 300 \times$  and a resolving power of more than  $1/200 \text{ mm}$ . There were exceptions: the famous microscope of Hooke must certainly have been of better quality, judging from his observations. Before 1830 the single microscope was far superior in optical respect to the compound one. This explains why scientific observers invariably fell back on the former type of instrument for their more important investigations (for example VAN LEEUWENHOEK, BROWN, DARWIN). The successful construction and the development of the achromatic objective opened the period of increasing resolving power of the compound microscope.

In 1791 the amateur F. BEELDSNIJDER at Amsterdam (1755—1808) was the first to succeed in making an achromatic microscope-objective (D.C. p. 63), that formed a satisfactory image. This objective was very

---

<sup>1)</sup> Edition P. Noordhoff N.V. (Groningen 1934).

<sup>2)</sup> P. H. VAN CITTERT, Proc. Kon. Akad. v. Wet. Amsterdam 39, 182 (1936).

weak; it resolved only 1/100 mm. About 1806 HARMANUS VAN DEYL, also at Amsterdam, was the first to introduce achromatic microscopes on the market. These had a magnification of about  $150\times$  and a resolution of 1/200 mm (comp. D.C. p. 64 etc.). After this the optical power of the compound microscope increased steadily; especially when one succeeded in diminishing the spherical aberration as well. AMICI<sup>1)</sup> showed that in order to arrive at a high resolving power the objective must be composed of different parts, each of which separately still gives rise to aberrations, but which are so computed that they neutralize each others impairing influence.

Now, of a number of 19th-century microscopes in the Utrecht collection, the years of purchase are known from the catalogue of the Utrecht Physical Institute, from the files of the Utrecht Physical Society and from HARTING's well-known standardwork "Het Mikroskoop". Thus it was possible to trace the increase of the resolution and of the magnification of these microscopes as a function of the years, using the measurements, published in the D.C. In Table I are given the max. resolutions and the max. magnifications of 13 microscopes.

TABLE I

No.	Name	Year	Max. magnification	Max. resolution
1	Beeldsnijder (Obj.) . . . . .	1791	—	1/100 mm
2	v. Deyl . . . . .	1807	100 à 150 $\times$	1/200 mm
3	Ch. Chevalier . . . . .	1837	1000 $\times$	1/600 mm
4	Amici . . . . .	1837	6000 $\times$	1/1000 mm
5	Lerebours-Secretan . . . . .	1840	1100 $\times$	1/800 mm
6	Plössl . . . . .	1845	1320 $\times$	1/1200 mm
7	Oberhäuser . . . . .	1845	1200 $\times$	1/1400 mm
8	Amici . . . . .	1849	2500 $\times$	1/1200 mm
9	Nachet No. 7 . . . . .	1849	1400 $\times$	1/1400 mm
10	A. Chevalier . . . . .	1869	1200 $\times$	1/1600 mm
11	Hartnack . . . . .	1870	1550 $\times$	1/1600 mm
12	Zeiss . . . . .	1890	—	1/1800 mm
13	Zeiss . . . . .	1920	950 $\times$	1/1900 mm

The table gives rise to the following remarks:

- ad 4 To the microscope of CHARLES CHEVALIER (D.C. p. 72) belongs a still stronger objective. The object-distance of this objective, however, is smaller than the thickness of the cover glass of the GRAYSON-rulings, so that it was impossible to determine the resolution. Therefore, the max. resolution of this microscope is probably somewhat larger than indicated.

<sup>1)</sup> In this study only continental microscopes are subjected to an examination; British ones of the 19th century are practically absent in the Utrecht collection. The reason for this is that through Napoleons Continental System the English microscopes disappeared from the European market.

- ad 5 The strongest objective that belonged to the microscope of AMICI, which was discussed in D.C. p. 68 was lost at the time of writing the D.C. It has since been found again. This is why the figures given here do not agree with those mentioned in the D.C. p. 68.
- ad 8 Besides, nearly the whole system of objectives of the AMICI-microscope bought by the Utrecht Physical Society in 1849 has also been retrieved (P. H. VAN CITTERT, Proc. Amsterdam, **50**, 554, 1947).
- ad 9 The box of the Oberhäuser Microscope (number 7 above) contains a still stronger lens, viz. a lens "Nacht No. 7", which was not put on the market before 1849. The microscope itself had already been bought in 1845.
- ad 13 Of number 13 the max. magnification has not been measured, but calculated. In 1920 it was well-known, that a magnification, larger than  $1000 \times \text{N.A.}$  had no sense: the strongest oculars present and corresponding with an immersion-objective have, therefore, not been taken into account.

When we plot the resolutions (fig. 1) and the magnifications (fig. 2) against the years of the 19th century, we obtain for the first diagram an

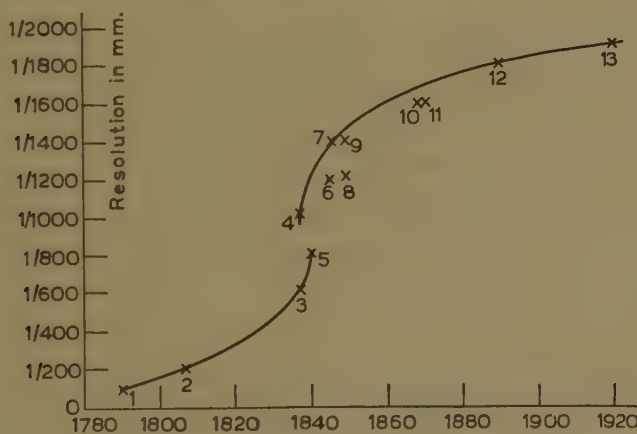


Fig. 1

upward line, which for the AMICI-microscope 1837 shows a distinct discontinuity. There the resolution jumps up considerably. After 1837 the curve is continuous again and at the end of the 19th century reaches the theoretical value ( $1/1800$  mm and  $1/1900$  mm for the ZEISS-microscopes of 1890 N.A. 0,9 and of 1920 N.A. 0,95 respectively).

It should here be remarked that the curve for the measured resolution should at least pass through the highest points found by the measurements, since the GRAYSON rulings make it only possible to state that the resolution is for instance larger than  $1/800$  mm and smaller than  $1/1000$  mm.

One can ask to what causes this rise of the resolving power in the 19th

century and the jump near 1837 are due. In the 18th and in the beginning of the 19th century one was generally convinced that the optical power of a microscope was determined by the magnification. As regards the 19th century, this can be clearly seen in fig. 2, in which the magnification is

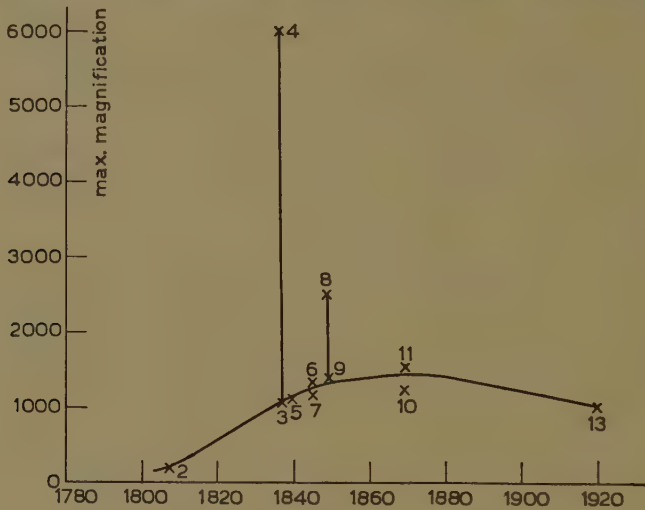


Fig. 2

plotted against time. In the first part of the curve one can see a fairly strong rise of the magnification, which shows for the AMICI-microscope of 1837 a sharp peak. As the resolution shows a jump here, this seems indeed to confirm the prevailing conviction. But after 1837 the magnification falls back again to its former value, to remain practically constant. As the resolution is then still rising, the above conviction can no longer be maintained. There must have been other reasons for the increase of the resolving power.

Nowadays we know that two more causes are possible, namely the increase of the (numerical) aperture and other improvements of the lens-systems. As regards the increase of the aperture we believe that AMICI indeed first tried to improve the microscope by increasing the magnification, but that when this proved unsuccessful, he realized that those objectives that gave the largest resolutions had in most cases also the largest aperture. In that way he found, without any theoretical reason the increase of the aperture to be fundamental for the improvement of the optical properties of the microscope. Still it seems that he could not dissociate himself entirely from the idea of the importance of large magnifications. The AMICI-microscope of 1849 (no. 8) shows namely also a very decided peak in the magnification (fig. 2), though not so high as that of 1837. As already mentioned above, AMICI improved the quality of the lens-systems too.

One can ask which of the two causes: the increase of the N.A. or the further improvement of the lens-systems has had the greatest influence



on the amelioration of the microscopes. To answer this question we measured also the max. N.A. of the microscopes, mentioned in table I, with the apertometer of ABBE. Now this apertometer can only be used directly for microscopes with small magnifications. For those with larger magnifications one must use an auxiliary microscope, screwed into the tube of the original one. This device made it necessary to provide auxiliary tubes or other implements for most of our microscopes. But we always took care that the required object-distance for such a rebuilt microscope, was the same as for the microscope in its original form. The results of our measurements are given in table II and are plotted as a function of the years in fig. 3.

TABLE II

No.	Name	Year	Max. N.A.
1	Beeldsnijder (Obj.) . . . . .	1791	0,1
2	van Deyl . . . . .	1807	0,1
3	Ch. Chevalier . . . . .	1837	0,39
4	Amici . . . . .	1837	0,54
5	Lerebours-Secretan . . . . .	1840	0,42
6	Plössl . . . . .	1845	0,63
7	Oberhäuser . . . . .	1845	0,66
8	Amici . . . . .	1849	0,68
9	Nachet No. 7 . . . . .	1849	0,70
10	A. Chevalier . . . . .	1869	0,82
11	Hartnack . . . . .	1870	0,88
12	Zeiss. . . . .	1890	0,90
13	Zeiss. . . . .	1920	0,95

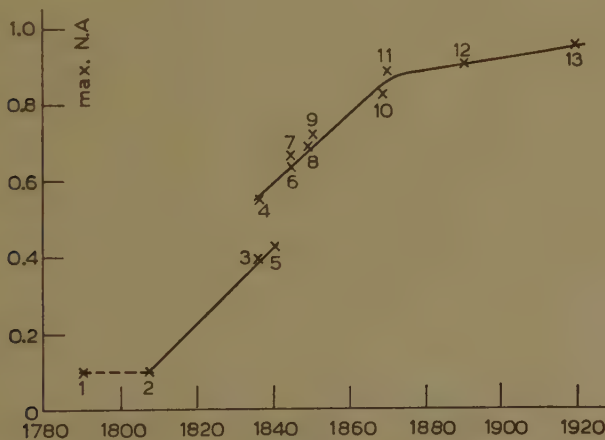


Fig. 3

The resemblance of the curve in fig. 3 with that in fig. 1 is very remarkable, the two curves at first rising steadily, and showing a pronounced jump in 1837 (AMICI). The influence of the increase of the N.A. on the resolving power is very apparent. The curves for the N.A. and for the

resolution are, however, not exactly similar, as should be the case if the N.A. were the only determining factor. The choice of the units in the fig. 1 and 3 is namely such that the value 1/2000 mm for the resolution corresponds to the value 1 for the N.A. (The resolution =  $\lambda/\text{N.A.} = 1/2000$  mm for N.A. = 1, if we take  $\lambda = 5000 \text{ \AA}$ , white light being used). The scales of the two diagrams are, therefore, the same, so that we should expect a straight line with an inclination of about  $45^\circ$ , if we plot the max. resolution against the max. measured N.A., at least, if the increase of the resolution should be determined only by  $\lambda/\text{A.}$  In reality, however, the line given in fig. 4 was found, which shows a deviation from the

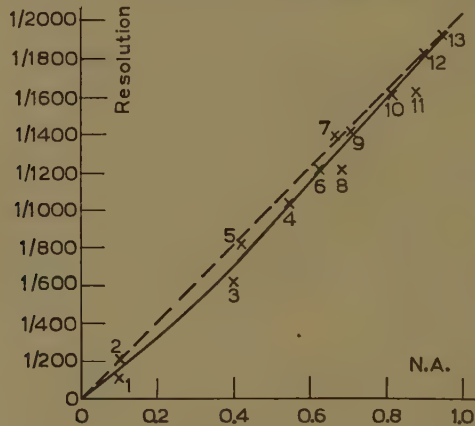


Fig. 4

theoretical line. This deviation is largest at the beginning of the 19th century (about 1830). This shows that it was not only the increase of the N.A., but also the other amplifications of the lens-systems, that influenced the improvement of the microscopes. But it is undeniable that the former was the more important one. It must be remarked that no apochromates were measured. Had that been the case, the curve in fig. 4 would have been somewhat higher about 1900.

We also tried to measure the progress of the N.A. of the non-corrected objectives in the 18th century, but these attempts failed. We employed various methods, but they all gave different results:

1. we used for instance the apertometer of ABBE,
2. we measured directly the diameter of the objective and the object-distance,
3. we sent a beam of light through the tube of the microscope, which converged from an illuminated plane on the place of the original image, formed between the two lenses of the Huyghenian eyepiece and measured the small circular patch of light, formed just outside the objective and the object-distance, and
4. we applied the method of LISTER <sup>1)</sup>.

<sup>1)</sup> See: P. HARTING: Nieuwste verbetering van het mikroskoop 1858 (further referred to as N.V.), p. 18 and following pages.

As already stated, these various methods gave different results, due to the fact, that the observed edges of the various fields of view were unsharp. The N.A., as far as could be observed was, however, seldom much above 0,1.

As mentioned above, only continental microscopes were measured. In the third part of HARTING's book (further referred to as III) and in HARTING's N.V. we found some dates concerning the progress of the N.A. of the British microscopes during the 19th century. TULLEY in 1824 was the first to put a corrected microscope on the market (III, p. 176 and p. 229). The angular aperture was only  $18^\circ$  (N.A. 0,16). Later on, in 1830, he managed to increase the aperture to  $38^\circ$  (N.A. 0,32). After him came PRITCHARD (III p. 234) who between 1840 and 1850 seems to have attained a max. aperture of  $70^\circ$  (N.A. 0,57). England owes the greatest progress, however, to the work of ROSS, as is illustrated very clearly in table III.

TABLE III  
Microscopes of ROSS

	Year	Max. aperture	Max. N.A.
Harting III page 258 . . . . .	1832	$14^\circ$	0,12
„ III „ 258 . . . . .	1833	$18^\circ$	0,16
„ III „ 258 . . . . .	1834	$55^\circ$	0,46
„ III „ 258 . . . . .	1836	$64^\circ$	0,53
„ III „ 258 . . . . .	1842	$74^\circ$	0,60
„ III „ 258 . . . . .	1850	$120^\circ$	0,87
„ N.V. „ 67 . . . . .	1851	$135^\circ$	0,92
„ „ „ 67 . . . . .	1853	$155^\circ$	0,975

In fig. 5 the max. N.A. of the microscopes of TULLEY, PRITCHARD and ROSS are plotted against the years of the 19th century. The curve of fig. 3, giving the progress for the continental microscopes, is given also. In the first place fig. 5 makes it clear, that the greatest progress of the British microscopes falls exactly in the same period as that of the continental ones. In the second place, one gets the impression that the British microscopes were very much better than the continental ones. One may, however, not draw this conclusion rashly from fig. 5, as there is a large difference between the given N.A. of the British microscopes and that of the continental ones. The N.A. of the English microscopes are mostly geometrical apertures, calculated from object-distance and lens diameter, those of the continental microscopes, however, are effective apertures, measured on objectives having an average age of 80 years. Moreover, there was very often a large difference between the geometrical aperture given by the manufacturer and the effective one measured by the customer. Nachet for example supplied HARTING (N.V. p. 49) with a lens having an aperture of  $148^\circ$  (N.A. 0,96), which turned out to have an effective aperture of only  $120^\circ$  (N.A. 0,87). Sometimes very large apertures are mentioned, for example for a microscope made by SPENCER (1852, N.V.

p. 9), which was supposed to have an aperture of  $174\frac{1}{2}^\circ$ , that is N.A. 0,999, a very improbable value for a N.A. This case was no exception, one meets with several large apertures in the relevant literature. HARTING mentions for example (N.V. p. 53) that AMICI in 1856 sold a microscope-objective

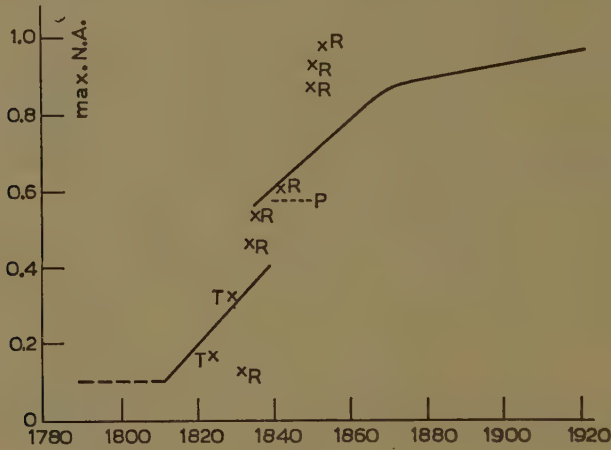


Fig. 5

with N.A. 0,985. HERTING remarks, however, (N.V. p.23) that in most cases such large apertures do not give a corresponding increase in the resolution. Often, only the central parts of the objectives contribute to the image. The boundary regions can often give only an unsharp image. In consequence the large aperture is often harmful instead of being advantageous. HARTING gives (N.V. p. 27) a small table concerning measurements by ROBINSON (Table IV) showing very considerable differences between the geometrical apertures and the effective ones.

TABLE IV

Geometrical aperture	Effective aperture
160° (N.A. 0,985)	110°,8 (N.A. 0.82)
129° (N.A. 0.90)	109°,5 (N.A. 0.82)
156° (N.A. 0.98)	114°,6 (N.A. 0.84)
170° (N.A. 0.995)	122°,8 (N.A. 0.88)

HARTING himself found for an objective with geometrical aperture  $150^\circ$  (N.A. 0,97) an effective one of  $120^\circ$  (N.A. 0,87). From all this it is clearly not allowed to conclude from our measurements that the continental microscopes were inferior to the British ones.

This investigation was concluded in June 1949; owing to private circumstances it was impossible for us to publish the results before now.

*Physical Institute of the University  
of Utrecht*



# SOAP COACERVATES WITH SPECIAL PROPERTIES, HITHERTO ONLY KNOWN IN COACERVATES OF PHOSPHATIDES

## III <sup>1)</sup>

BY

H. G. BUNGENBERG DE JONG AND W. W. H. WEYZEN \* <sup>2)</sup>

(Communicated at the meeting of March 31, 1951)

### 1. *Direct observation of the vesicle wall*

P-coacervate drops often have peculiar shapes, which must be due to superficially attached vesicles. As a rule the latter are not visible with transmitted light (see for arguments in favour of the presence of such vesicles Part I).

It has now been found that with dark field illumination the attached vesicles can easily be observed. The borders of the coacervate drops appear as intensely illuminated zones, or at a somewhat other position of the microscope mirror as two broad intensely illuminated circles. All coacervate drops which show defects of the spherical form in transmitted light, now show clearly attached vesicles, the walls of which appear as thin and faint lines (fig. 1A and B). Closely situated drops with nearly parallel plane faces, appear in reality to be as was already concluded in Part. I united by one vesicle membrane (fig. 1C).



Fig. 1

Units consisting of more than two coacervate drops united by one vesicle membrane may also be observed. The case depicted in fig. 1 D, in which a number of lens-shaped small coacervate drops are suspended in a vesicle membrane which is attached laterally to a large coacervate drop with a nearly plane face is relatively frequent.

\*) Aided by grants from the „Netherlands Organization for Pure Research (Z.W.O.)”

<sup>1)</sup> Part I has appeared in these Proceedings 52, 783 (1949), Part II in these Proceedings 52, 794 (1949).

<sup>2)</sup> Publication No. 12 of the Team for Fundamental Biochemical Research (under the direction of H. G. BUNGENBERG DE JONG, E. HAVINGA and H. L. BOOY).

These composite forms are generated from originally free coacervate drops with attached vacuoles of the types of fig. 1A and B at contact of their vesicle membranes.

To observe the vesicle membranes with dark field illumination, the emulsion of P-coacervate drops (obtained as described in Part I by adding the precisely required amount of iso-amylalcohol to the KCl-containing oleate solution) is brought into an appropriate observational cell. The latter consists of a sufficiently large glass square of for instance  $9 \times 9$  cm as a bottom, four coverglasses and a somewhat smaller glass square resting on the cover glasses. Both glass squares have previously been prepared by wetting them with a 1 % solution of soluble starch and drying them afterwards. The starch film on the glass plates prevents the coacervate drops from spreading over the glass surfaces, so that the drops retain their spherical form.

The advantage of a large observational cell is that disturbances caused by evaporation (especially of iso-amylalcohol) at the open edges of the cell are not soon felt in the middle of the cell.

Such disturbances, which may consist for instance of the growth of myeline tubes from the surface of the coacervate drops, can be studied conveniently near the edges of the observational cell.

## 2. *Shape of the coacervate drops bearing attached vesicles*

Though we have not yet performed accurate measurements of the angles between the three meeting surfaces (the vesicle membrane and the two surfaces of the coacervate drop) we got the impression, that they are about equal. This explains, why the deviations from the spherical form of the coacervate drops may bear different characters, which depend on the relative volumes of the coacervate drops and the attached vesicles. Compare fig. 2, in which we have assumed arbitrary that the three angles are equal.

When a small vesicle is attached to a large coacervate drop, then the deviation must necessary appear as a curved incision in the surface of the coacervate drop (fig. 2 A).

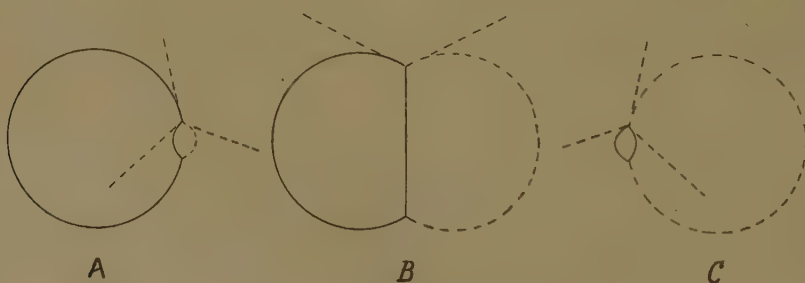


Fig. 2

With nearly equal volumes of coacervate drop and vesicle, the coacervate drop will appear as a sphere from which a segment has been cut away (fig. 2 B).

Finally when the volume of the vesicle is very much larger than that of

the coacervate drop, the latter must assume the shape of a biconvex lens (fig. 2 C).

Units of the last mentioned type, in which therefore only one small coacervate drop takes part, have not yet been observed actually. But lens-shaped coacervate drops forming parts of units which consist of one large, one or more small drops and one common vesicle are not infrequent. (Compare fig. 1 D.)

One may ask why the units which are depicted in fig. 2 C have not been met with so far. Referring to Part I for the details, we remember here that vesicles arise when a vacuole meets the inner surface of the coacervate drop. The vacuole now may arise in two ways: *a*) by proper vacuolisation, e.g. as a consequence of a change in the composition of the total system or of a change in temperature (the latter is discussed in the following section), *b*) by haphazard inclusion of equilibrium liquid in coacervate drops during the shaking of the coacervated system.

Just before the formation of units of the type of fig. 2 C we must have had a small coacervate drop, which had a large included vacuole. With proper vacuolisation such a large vacuole can hardly arise. The haphazard inclusion of a large volume of equilibrium liquid in a very small coacervate drop is also rather improbable.

Therefore the answer to the question why units of the type of fig. 2 C have not been met with so far, seems to be that the chance of their formation is very small. The relative frequency of the composite units depicted in fig. 1 D, in which lens-shaped small coacervate drops are suspended in the membrane of a vesicle which is attached to a large coacervate drop, is easily understood. These composite units arise from the meeting of simple units, with extended vesicle membranes. Now the simple units do not need to possess a vesicle whose volume is many times that of the coacervate drop. For instance all of them may be of the type *B* in fig. 1. After fusion of the vesicles into one common vesicle the small coacervate drops participating in the composite unite will change their form into the lens-shaped one, whereas the large coacervate drop may nearly retain its original shape.

### 3. *Direct observation of the formation of articulated vacuoles and of attached vesicles*

With the technique which is used one may also observe the formation of vesicles. We choose a coacervate drop in the preparation which is perfectly spherical in form, and with dark field illumination we observe when a jet of warm air (from an electrical hair-dryer) is directed on the observational cell. One then observes the formation of vacuoles, their eventual union into articulated vacuoles and their incomplete exit from the coacervate drop under formation of protruding vesicles. Thus the conclusion reached in Part I of this series: attached vesicles arise from contact of vacuoles with the inside of the drop surface, is fully confirmed.

### 4. *P-coacervation of oleate at pH values in the neighbourhood of neutrality*

With regard to O-coacervation with KCl, oleates only behave in an uncomplicated way if the pH is high enough (e.g. at pH = 12 or higher) to exclude all hydrolysis.

Therefore it seemed advisable to start the study of P-coacervation (part I and II, and the sections 2 and 3 in the present communication) under the same precautions.

The effects of the lowering of the pH on O-coacervation can be ascribed to the presence of oleic acid, which acting as a "salt-sparing substance" lowers the KCl concentration just required for the coacervation. This effect is already strongly felt below  $\text{pH} = 10$ .

A still further lowering of the pH is even deleterious to O-coacervation, which finally becomes no longer possible. The pH limit lies approximately at  $\text{pH} = 8.7$ .

We were therefore much surprised to find that P-coacervation of oleate is not suppressed at this pH, but could still be realized typically at  $\text{pH} = 7.5$ ,  $7.3$  and in some cases even at  $\text{pH} = 6.8$ .

Typical examples are for instance: P-coacervation (in the presence of KCl, or NaCl and a small amount of phosphate buffer) with iso-amylalcohol, benzylalcohol, meta-cresol and aniline (with the latter only at an appropriate not to high salt concentration).

We do not need to repeat here the description of the morphology of the P-coacervate drops at these lower pH values, a description which would differ in no way from that given in Part I and in the sections 2 and 3 of the present communication for P-coacervates obtained at  $\text{pH} > 12$ .

In Part II we have determined from the amount of isoamyl alcohol just required at  $\text{pH} > 12$  to start P-coacervation the number of molecules iso-amylalcohol bound to one molecule of oleate.

This number was found to lie between 2 and 4, dependent on the chosen KCl concentration.

We were interested if, at a pH value near neutrality, the number of bound molecules of iso-amylalcohol per molecule of oleate (eventually present free oleic acid reckoned as oleate) would be of the same order of magnitude, or if it would be totally different.

For the method which is used we refer to Part II, the differences being a slightly higher temperature ( $25^\circ$  instead of  $20^\circ$ ), a two times larger total volume of the mixtures (40 ml instead of 20 ml) and the additions of buffer to obtain a pH of approximately 7.5 (10 ml of a buffer obtained by mixing 1 volume 0.2 mol/l  $\text{KH}_2\text{PO}_4$  and 5 volumes 0.2 mol/l  $\text{Na}_2\text{HPO}_4$  are always present in the 40 ml mixture). Of course the stock oleate solutions which were used were *not* provided with an excess of KOH to obtain a  $\text{pH} > 12$  as in Part II.

The results at pH 7.5 for two KCl concentrations have been given in Table I and have been plotted in fig. 3.

This figure shows that the amount of iso-amylalcohol needed for P-coacervation is a linear function of the oleate concentration and that at a higher KCl concentration the straight line lies below the one at a smaller KCl concentration and that it has a smaller slope. In all these points we have quite the same behaviour as was found in Part II for the P-coacervation at  $\text{pH} > 12$ .



Even quantitatively there is close similarity. The values, calculated from the slopes of the straight lines in fig. 3, for the number of molecules iso-amylalcohol per molecule of oleate, (3.50 at 0.56 N. KCl and 2.59 at 1.13 N.KCl) come near to those found at  $\text{pH} > 12$  in Part II.

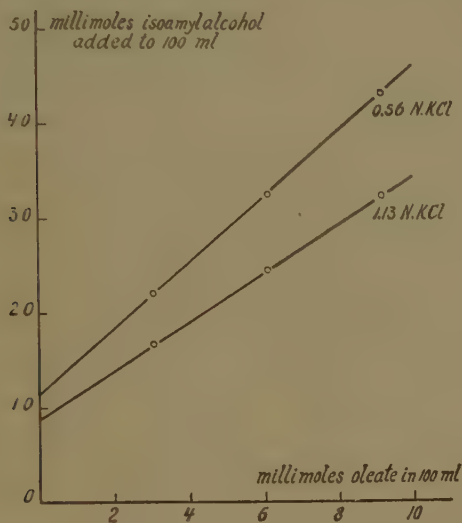


Fig. 3

In this calculation we have reckoned all oleate to be really oleate and thus not to be partially hydrolyzed. The similarity of the above numbers found at  $\text{pH} 7.5$  and those found at  $\text{pH} > 12$  suggests that under the circumstances of P-coacervation — that is when a large amount of iso-amylalcohol is bound to the oleate micelles — the tendency to hydrolysis is much reduced. This may explain why P-coacervation is still possible at  $\text{pH}$  values round about the neutrality point, though O-coacervation is no longer possible below  $\text{pH} = 8.7$ .

TABLE 1

Determination of the number of molecules of iso-amylalcohol bound to one molecule of Na-oleate when P-coacervation is obtained at  $\text{pH} 7.5$ . Temperature  $25^\circ \text{C}$ .

KCl concentration = 0.56 N			KCl concentration = 1.13 N		
millimoles iso-amylal- cohol added to 100 ml system	millimoles oleate present in 100 ml system	bound iso-amylalcohol oleate	millimoles iso-amylal- cohol added to 100 ml system	millimoles oleate present in 100 ml system	bound iso-amylalcohol oleate
22.1	3.04	3.50	16.7	3.04	2.59
32.5	6.09		24.6	6.09	
43.4	9.13		32.5	9.13	

### 5. *P-coacervation of K-palmitate*

All previous measurements have been made with Na-oleate of BAKER, a preparation which contains as impurities other soaps (e.g. palmitate) as well. It seemed advisable also to perform some measurements starting from a single soap, especially with regard to the number of molecules of iso-amylalcohol bound per molecule of soap. We decided to perform such an investigation with K-palmitate, as we had a sample of reasonably pure palmitic acid (melting point 61—62°) at our disposal <sup>1)</sup>.

Before performing these measurements, we located at approximately 20° in a KCl—iso-amylalcohol diagram the regions in which the different states of the palmitate system occur.

For the method we refer to Part II, section 4.

The results who are obtained, compare fig. 4, apply to 20 ml systems containing  $\frac{3}{4}$  % K. palmitate and 0.025 N free KOH (thus pH > 12) and different KCl concentrations.

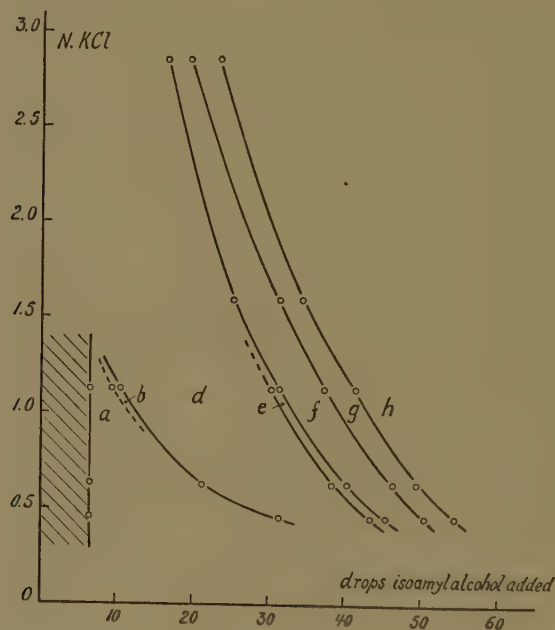


Fig. 4

In this figure the letters *a—h* have the same meaning as in the analogous diagram for oleate at pH > 12 given as fig. 5 in Part II.

Comparison of both diagrams will reveal that they are very much alike. The curves in both diagrams mount upwards to the left and the succession of the regions from left to right (i.e. from *a* to *h*) is the same.

As we were especially interested in the relative position of the regions *d* (flocculated system), *e* (homogeneous system), *f* (P-coacervate + equilibrium liquid), *g* (double drops consisting of P-coacervate shells which

<sup>1)</sup> We thank Dr H. VELDSTRA for putting this sample at our disposal.

are surrounding drops rich in iso-amylalcohol, the compound drops being suspended in the equilibrium liquid) and *h* (drops rich in iso-amylalcohol suspended in the equilibrium liquid which is rich in water and KCl, the P-coacervate being no longer present) we have not taken so much care to locate the boundaries of the remaining regions: *a* (homogeneous, often elastic system), *b* (ordinary coacervate + equilibrium liquid) and *c* (coacervate + equilibrium liquid + a denser soap system, which is also present in *d*).

The boundaries of *b* have been determined at only one KCl concentration, those of *c* at none at all. The latter region should lie between *b* and *d*, but because it is presumably very narrow we have not perceived it in the actual experiment.

The only difference between the diagram of fig. 4, and the analogous one for oleate in Part. II, is the presence of an extra region along the ordinate axis (shaded in fig. 4). In this region the palmitate system has a milk-white appearance, because the K-palmitate is insoluble at 20°. After adding a small amount of iso-amylalcohol the turbidity disappears and we enter the homogeneous region *a*, in which the palmitate system may be elastic in a pronounced way.

We further investigated at three palmitate concentrations the amount of iso-amylalcohol required to obtain P-coacervation.

This investigation was performed at only one KCl concentration (1.20 N.), but at two temperatures in order to gain a deeper insight into the influence of temperature on P-coacervation.

Using once more the same method as in Part II (section 4) we obtained the results recorded in Table II and given in fig. 5.

TABLE 2

Determination of the number of molecules of iso-amylalcohol bound to one molecule of K-palmitate when P-coacervation is obtained at 20° C and at 39.4° C.  
KCl concentration = 1.20 N;  $\text{PH} > 12$ .

20° C			39.4° C		
millimoles iso-amylal- cohol added to 100 ml system	millimoles K-palmitate present in 100 ml system	bound iso-amylalcohol K-palmitate	millimoles iso-amylal- cohol added to 100 ml system	millimoles K-palmitate present in 100 ml system	bound iso-amylalcohol K-palmitate
19.35	3.40	2.25	17.16	3.40	2.20
23.33	5.10		20.93	5.10	
27.00	6.80		24.65	6.80	

The figure bears quite the same character as the two analogous figures for oleate (fig. 3 in this communication and fig. 7 in Part II).

Once more we obtain for the number of iso-amylalcohol molecules bound per molecule of soap a value (see table) lying between 2 and 4.

### 6. Influence of the temperature on the P-coacervation

Qualitative observations during the microscopic investigation of P-coacervate drops allow already to draw the conclusion that increase of temperature favours P-coacervation. We found for instance in Part I, section 3, that homogeneous P-coacervate drops suspended in their

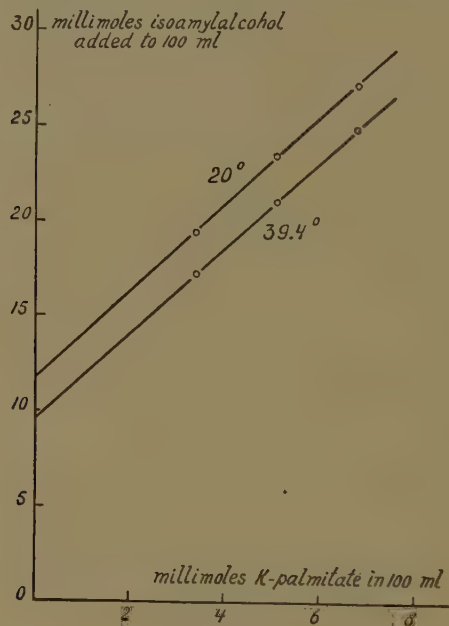


Fig. 5

equilibrium liquid, change on heating into P-coacervate drops with enclosed drops of the phase rich in iso-amylalcohol. At further heating the outer shell of P-coacervate disappears, thus leaving only the inner-drops.

Using the same letters as in the iso-amylalcohol—KCl diagrams (fig. 5 in Part I and fig. 4 in the present communication) we may say that the morphological state of the soap system, which was *f* originally, changes into *g* upon heating and finally into *h*. Upon colling we obtain once more the original state. Therefore the system changes back from *h* into *g* and finally into *f*.

Starting from a soap system in the state *e*, (homogeneous system) we may observe P-coacervation on heating, which disappears on cooling. As these observations refer to a soap system of constant total composition (therefore constant KCl concentration and a constant amount of added iso-amylalcohol) we must conclude that the regions *f* and *g* in a KCl—iso-amylalcohol diagram are shifted to the left at increase of the temperature and back to their original position after restoring the original temperature.



In order to gain more insight into the influence of the temperature on P-coacervation, the measurements recorded in fig. 5, have been performed at two temperatures. We perceive in this figure that indeed increase of temperature favours P-coacervation, for at each K-palmitate concentration, a smaller total amount of iso-amylalcohol is needed to reach P-coacervation at  $39^{\circ},4$  than at  $20^{\circ}$ . The salient point in fig. 5 is, that the straight lines at  $39.4^{\circ}$  and at  $20^{\circ}$  have practically the same slope. From this we conclude that the temperature has no influence on the number of molecules bound per molecule of palmitate when P-coacervation is just obtained.

Therefore the marked influence of the temperature on P-coacervation only resides in the influence of the temperature on the solubility of iso-amylalcohol in the KCl-water medium bathing the soap micelles. This solubility (indicated in fig. 5 by the intersection point of the straight line with the ordinate axis, compare Part II) decreases with increasing temperature.

It is well known that the phenomenon of a decreasing solubility with increasing temperature already occurs in the binary system iso-amylalcohol water.

### *Summary*

1. Dark field illumination provides a means to observe easily, the presence of attached vesicles on the surface of P-coacervate drops which show deviations from the spherical form.

2. The three meeting surfaces (vesicle membrane and two surfaces of the coacervate drop) include angles which are about equal.

3. The fact sub 2) explains why the deviations of the coacervate drops from the spherical form may have different characters and why this depends on the ratio of volume of the vesicle and the volume of the coacervate drop. With a ratio much smaller than one, the coacervate drop shows a curved incision in its surface; with a ratio of about one the coacervate drop appears as a sphere from which a segment has been cut off; with a ratio much larger than one the coacervate drop assumes the shape of a biconvex lens.

4. It was argued in Part I from observations with transmitted light that articulated vacuoles arise from the meeting of vacuoles inside the coacervate and that attached vesicles arise from the contact of vacuoles with the inside of the surface of the coacervate drop. These conclusions have been confirmed by direct observation with dark field illumination.

5. Whereas O-coacervation is (by the disturbing effect of hydrolysis) no longer possible below pH 8.7, P-coacervation is still possible near the neutrality point. The number of molecules of iso-amylalcohol which are bound to one molecule of oleate when P-coacervation is just obtained is nearly the same at pH 7.5 and at pH  $> 12$ . This suggests that the uptake

of a large amount of iso-amylalcohol in the soap micelles appreciably diminishes the tendency to hydrolysis.

6. P-coacervation of relatively pure K-palmitate has been studied at  $\text{pH} > 12$ . The results do not differ essentially from those obtained with commercial Na-oleate. Here too the number of molecules of iso-amylalcohol which are bound to one molecule of the soap when P-coacervation is just obtained is relatively large and not much different from that obtained with oleate.

7. P-coacervation is favoured by increase of the temperature. From an investigation on the amount of iso-amylalcohol needed for P-coacervation as a function of the K-palmitate concentration follows that this influence of the temperature solely resides in the decrease of the solubility of iso-amylalcohol in the KCl-water medium bathing the soap micelles. The number of molecules iso-amylalcohol which are bound to one molecule of K-palmitate when P-coacervation is just obtained is not changed by increase of the temperature (from  $20^\circ$  to  $39.4^\circ$ ).

*Department of Medical Chemistry  
University of Leiden*

## INFLUENCE OF EXPOSURE OF A GELATIN SOLUTION TO VARIOUS TEMPERATURES OR TO THE ACTION OF PEPSIN ON THE SUBSEQUENT COMPLEX COACERVATION WITH GUM ARABIC

BY

H. G. BUNGENBERG DE JONG AND A. M. VAN LEEUWEN

(Communicated at the meeting of March 31, 1951)

1. *Previous exposure of the gelatin solution to various temperatures*

It is well known, that the properties of gelatin solutions are irreversibly altered by prolonged exposure to higher temperatures.

The problem arose which might be the effect on the subsequent complex coacervation with gum arabic<sup>1</sup>). We started with gelatin F 00 extra (Lym and Gelatine Fabriek, Delft, at Delft, Holland) and a very good grade of gum arabic (Gomme Senegal petite boule blanche I, from ALLAND et ROBERT, Paris). Buffered 2 % stock solutions of gelatin and gum arabic were made, each containing 0.1 N acetic acid and 0.01 N Na-acetate, giving a pH of approximately 3.7. In preparing the gelatin solution the suspension of the already swollen gelatin powder was heated to only 40° (2 hours), in order to prevent heat damage at the start of the experiments already.

In a number of sedimentation tubes (wide tube with a calibrated narrow tube at the lower end) standing in a thermostate of 40°, mixtures were made of a ml gum arabic solution and (20-a) ml gelatin solution. After mixing thoroughly, the tubes were left until the following morning, whereupon the coacervate volumes were read. The results expressed in 0.1 ml have been plotted in fig. 1 (see curve *a*) as a function of the mixing proportion of the two colloids (the mixing proportion is expressed in percentages of the gum arabic solution).

The rest of the stock gelatin solution was put in a thermostate of 60° (glass stoppered flask) and after 23.5 hours it was used for a mixing series with Gum Arabic at 40°, in exactly the same way as is described above. The remaining stock gelatin solution was left in the thermostate of 60° and 24 hours later it was used for a third mixing series at 40°.

The results after a heat treatment of the stock gelatin solution of 23.5 hours at 60° are represented by curve *b* in fig. 1, those after a heat

---

<sup>1</sup>) For complex coacervation see H. G. BUNGENBERG DE JONG in Chapter X of H. R. KRUYT, Colloid Science II. (Elsevier Publishing Company, Inc. New York, Amsterdam, London, Brussels; 1949).

treatment of  $23.5 + 24 = 47.5$  hours at  $60^\circ$  are given by curve *c* in fig. 1.

We perceive that at all mixing proportions the coacervate volume decreases as a consequence of the previous heat treatment of the gelatin solution. However the mixing proportions corresponding to the maxima

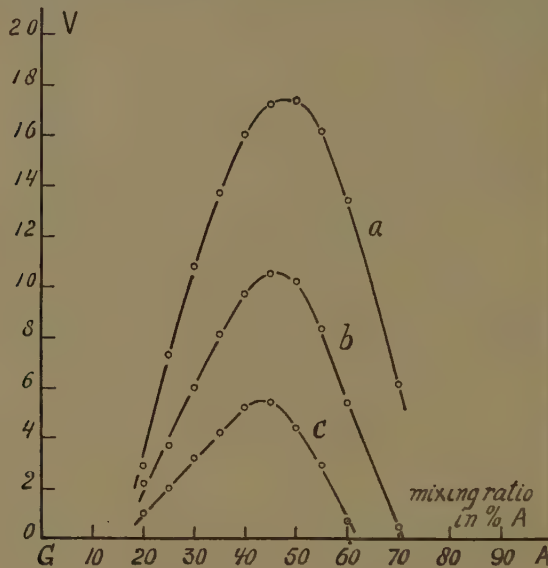


Fig. 1. Influence of exposure of a buffered 2 % gelatin solution to  $60^\circ$  on the subsequent complex coacervation with a buffered 2 % gum arabic solution at  $40^\circ$ .  $v$  = volume of the coacervate in 0,1 ml from 20 ml mixture. Curve *a* = blank, curve *b* = 23,5 hours at  $60^\circ$ , curve *c* = 47,5 hours at  $60^\circ$ .

of the curves are not much different (curve *a* = 47.5 %; curve *b* = 46 %; curve *c* = 44 %).

To simplify the next series of experiments, which deal with the influence of temperature on the rate of the change of the gelatin solution, we restricted ourselves to measuring the coacervate volume at the mixing proportion of 50 % gum arabic solution (always at  $40^\circ$ ).

For this series of experiments 2 l stock solutions of the above mentioned composition were made. Because of the acid reaction of these solutions ( $\text{pH} = 3.7$ ) bacterial growth is practically suppressed, but growth of mould colonies may still occur. To prevent this we have added  $\text{CCl}_4$  as a preservative to those solutions which had to be kept during a long period at temperatures below  $25^\circ$ . To the 2 l stock gum arabic solution, which was stored at room temperature ( $18^\circ$ – $20^\circ$ ), we added 1 ml  $\text{CCl}_4$ . At the conclusion of the experiments (after  $\pm 6$  months) this solution was still clear, and free from mould colonies. The stock gelatin solution was divided in smaller portions into glass stoppered bottles. To a number of them, which were used for the storage experiments at  $16^\circ$  and  $4^\circ$ , we added 1 drop of  $\text{CCl}_4$  per 50 ml. After 6 months these were still free from mould colonies.



For the experiments at 100°, 80°, 60°, 40°, and 25° no  $\text{CCl}_4$  was added. These experiments were started within a few days after the preparation of the stock solutions, which were kept in the meantime in the refrigerator. During the experiments at 100°, 80°, 60°, 40°, no mould growth was observed. The absence of  $\text{CCl}_4$  in the experiment at 25°, however, was seriously felt, so that the exposure could not be extended any longer than 490 hours.

In the experiment at 25° a few small colonies were present after 228 hours, but this did not yet have an influence upon the normal course of the decrease of the coacervate volume with time. Even after 490 hours this was not yet the case, though the number and size of the colonies had increased. After 800 hours the coacervate volume was very much lower than could be expected, which is obviously due to the proteolytic action of the increased quantity of fungi being present now. For this reason the experiments at 25° only give reliable results up to 490 hours exposure. The results at 16° and 4°, in which we used gelatin samples with and without  $\text{CCl}_4$  also lead to the conclusion that the presence of a few colonies of

TABLE 1

Coacervate volume  $V$ , after a heat treatment of the gelatin stock solution (pH 3.7) during the time  $t$  at different temperatures, and the velocity of the initial decrease of the coacervate volume  $-dV/dt$  in 0.1 ml per hour.

100° C		80° C		60° C		40° C	
$t$ (min)	$V$ in 0.1 ml	$t$ (min)	$V$ in 0.1 ml	$t$ (hours)	$V$ in 0.1 ml	$t$ (hours)	$V$ in 0.1 ml
0	16.9	0	17.2	0	17.2	0	17.25
3.5	15.7	18.5	16.4	1.5	16.7	22	16.5
7	14.8	36	15.7	3	16.25	43	15.8
13.75	13.5	72	14.0	6	15.05	115.5	13.4
21	11.4	108	12.45	8.9	14.3	195	10.7
28	9.2	144	10.7	11.9	13.4	308	7.3
56	3.3	288	5.3	24	9.5	354	6.1
85	1.1	432	1.9	33.5	6.9	456	3.5
112	0	576	0	75	0.7	500	2.6
						552	1.55
						625	0.6
$-dV/dt = 16.1$		$-dV/dt = 2.71$		$-dV/dt = 0.321$		$-dV/dt = 0.033$	
25° C		16° C			4° C		
$t$ (hours)	$V$ in 0.1 ml	$t$ (hours)	$V$ in 0.1 ml	$V$ in 0.1 ml (+CCl <sub>4</sub> )	$t$ (hours)	$V$ in 0.1 ml	$V$ in 0.1 ml (+CCl <sub>4</sub> )
0	17.25	0	17.25	17.25	0	17.25	17.25
22	17.1	43	17.13	17.29	23	17.33	17.23
41	17.0	237	16.95	17.07	237	17.13	17.15
228	15.6	4080	—	13.25	4080	16.31	16.35
490	14.2						
$-dV/dt = 0.0062$		$-dV/dt = 0.00098$			$-dV/dt = 0.00022$		

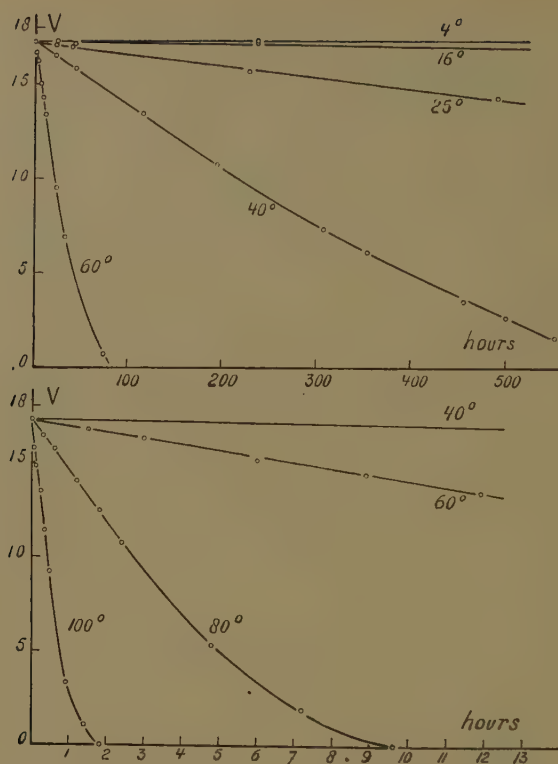


Fig. 2. Influence of exposure of a buffered 2 % gelatin solution during various times at various temperatures on the subsequent complex coacervation with a buffered 2 % gum arabic solution at 40°.  $V$  = volume of the coacervate in 0,1 ml from a mixture of 10 ml gelatin solution and 10 ml gum arabic solution.

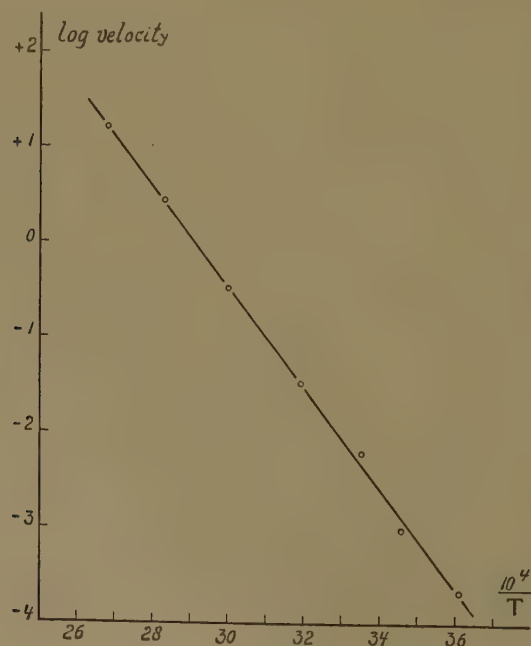


Fig. 3. Validity of the formula of Arrhenius for the rate of decrease of the coacervate volume. Ordinates: the logarithms of the values  $-dV/dt$  from table 1. Abscissa:  $10^4 \times 1/T$

fungi has no influence but that a larger growth gives a too low coacervate volume.

After 6 months storage at 4° the sample without  $\text{CCl}_4$  only had a few colonies ( $\pm 6$ ). This sample gave the same coacervate volume as the sample with  $\text{CCl}_4$  which was free from colonies.

The same applies for the experiments at 16°. Up to 237 hours the samples without (moulds present) and with  $\text{CCl}_4$  (moulds absent) gave the same coacervation volumes. But after 6 months the sample without  $\text{CCl}_4$  (abundant moulds and totally liquefied gelatin) did not give complex coacervation any longer, whereas the sample with  $\text{CCl}_4$  (moulds absent) gave the expected coacervate volume.

The general method which was used in these experiments was the following: Directly after the preparation of the stock solutions, we determined in quadruple, the coacervate volume at 40° and at the mixing proportion of 50 % gum arabic solution. The gelatin solutions were exposed to the different temperatures. At the times given in table I we pipetted 10 ml from the gelatin solutions held at 100°, 80°, 60° and 40°, which we added to 10 ml of the gum arabic solution standing in the thermostate of 40°. As a rule the results given in table I are the means of a duplo determinations.

The samples which had been exposed to lower temperatures were first heated up to 40°, kept at this temperature during 2 hours and then used for the complex coacervation. Here the given results are the means of four determinations.

The results have been plotted in fig. 2. We perceive that the coacervate volume decreases with time and that the temperature has a very great influence on the rate of this decrease.

In general the curves have the same character. They begin with a linear decrease of the coacervate volume with the time of exposure but after approximately half of the original volume is left the coacervate volume decreases more slowly with the time of exposure.

Besides this, the appearance of the heated gelatin solution alters with the time of exposure. They remain clear at first, but with increasing exposure they become opalescent, turbid and even small flocculations may be formed (these didn't have much influence on the coacervate volume). For a comparison of the rates of decrease of the coacervate volume at various temperatures we used the initial slopes of the curves. Compare the values  $-dV/dt$  given in the table. As the rate of the decrease of the coacervate volume with the temperature of exposure of the stock gelatin solution enormously increases with increase of the temperature (at 100° the rate is approx. 70.000 times that at 4°) we cannot but conclude that a chemical reaction underlies the decrease of the coacervate volume with time.

According to the formula given by ARRHENIUS for the dependence of the velocity of a chemical reaction on the temperature, the logarithms of the velocities plotted against the reciprocal values of the absolute temperature must give a straight line. Fig. 3 shows that indeed a straight line is obtained if the logarithms of the values  $-dV/dt$  of the table are plotted against reciprocal values of the absolute temperature.

## 2. *Previous exposure of the gelatin solution to proteolytic action*

We may now ask which chemical reaction underlies the decrease of the coacervate volume as a consequence of a prolonged exposure of the gelatin solution to various temperatures. One may suppose that a hydrolytic break up of peptide bonds takes place. Therefore it was obvious to investigate if similar results can be obtained by previous exposure of the gelatin solution to a proteolytic enzyme, for which we choose a commercial sample of pepsin.

Two stock solutions were made, one of which contained 2 % gum arabic and 0.01 N Na acetate, the other 2 % gelatin and 0.1 N acetic acid. The two components of the acetate buffer are thus divided over the two stock solutions. This has the advantage that the exposure to pepsin could take place at a low pH (at which pepsin acts rapidly), and that by mixing 10 ml of both solutions the pH (3.7) is reached which is most favourable for the complex coacervation.

50 ml of the gelatin solution (of 40°) were pipetted into four flasks which were standing in the thermostate of 40° and provided with 0, 35, 65 and 98 mg of the pepsin preparation. By rotation of the flasks the pepsin powder was rapidly dissolved. At various times 10 ml samples were taken from the flasks and put into sedimentation tubes which were standing in the thermostate and filled beforehand with 10 ml gum arabic solution. After mixing the tubes were left until the following morning, whereupon the coacervate volumes were read.

Fig. 4 A gives the results. It is seen that the blank gelatin solution gives the same coacervate volume during the 510 minutes that it was exposed to 40°. With pepsin, the coacervate volume decreases with the time of exposure and the slope of the curves is approximately proportional to the pepsin concentration. Compare fig. 4 B.

The same effects as were reached in thermolysis by increasing the temperature (compare fig. 2) are here reached at a constant temperature by the presence of a biocatalyst which is known to hydrolyze peptide bonds.

A further similarity between thermolysis and proteolysis is that also in the latter case the gelatin solution becomes gradually turbid and a small amount of flocculation may be formed.

A peculiar point of difference between fig. 2 and fig. 4 is, that in the former the curves take origin at one point on the ordinate axis, whereas in the latter it seems that there is a momentary decrease at the time zero.

The explanation of the abnormal course of the curves in fig. 4 is to be sought in the fact that at the moment we mix the gelatin solution with the gum arabic solution the proteolytic action does not stop but still continues at pH 3.7. The lowering influence on the coacervate volume will therefore continue to manifest itself during the time that the greater part of the formed coacervate drops are still in suspension. As soon as these drops have coalesced for the greater part to one homogeneous layer proteolytic action has no longer influence on the volume of this layer. Therefore the coacervate volumes which are read off belong to exposures to proteolytic action which are somewhat longer than recorded on the abscissa.



This explains why the curves in fig. 4 seem to take their origine at a „negative time”.

As we had observed meanwhile that also at pH 3.7 the proteolytic action proceeds with sufficient rate, the possibility was opened to in-

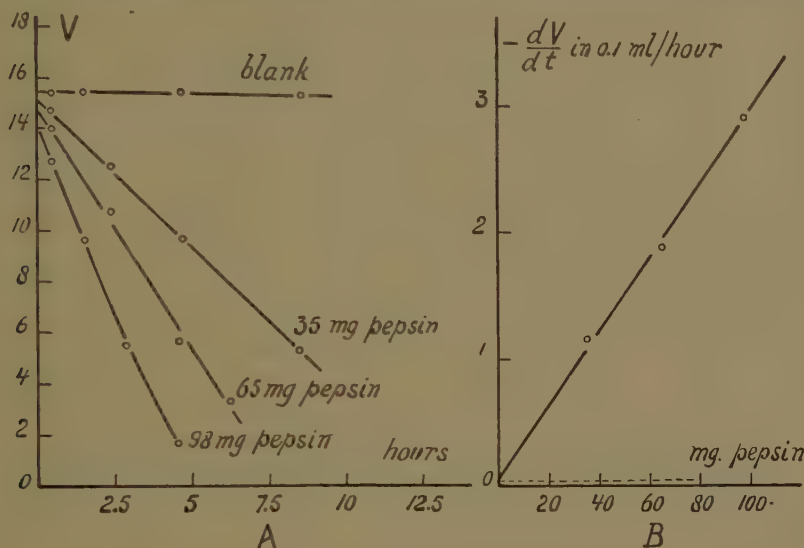


Fig. 4. Influence of exposure of a gelatin solution to the action of pepsin at 40° on the subsequent complex coacervation with a gum arabic solution.

Fig. 4A. Ordinates: volume of the coacervate in 0,1 ml from mixtures of 10 ml gelatin solution and 10 ml gum arabic solution.

Fig. 4B. Slope of the curves in fig. 4A as a function of the concentration of the pepsin. Dotted line:  $-\frac{dV}{dt}$  for the thermolysis at 40°.

investigate if the decrease of the coacervate volume just as with thermolysis is present at all mixing proportions. We could therefore return to the kind of stock solutions used in the experiments on thermolysis (2 % solutions of gelatin or of gum arabic containing each 0.1 N acetic acid and 0.01 N Na acetate). As the preparation of a mixing series takes considerable time, it was necessary to inactivate the pepsine in the gelatin solution beforehand.

We took two 1 l flasks, brought in each one 200 mg pepsin powder, pipetted in each one 100 ml stock gelatin solution, and dissolved the powder rapidly by rotating the flask. The first flask was put in a thermostat of 40° during 2 hours, thereafter the flask was dipped in boiling water during 5 minutes to inactivate the pepsin, cooled down rapidly to 40° and the contents were used for a mixing series at 40° with the stock gum arabic solutions. See curve *D* in fig. 5. The second flask was inactivated in the same way and used for a blank mixing series directly after the pepsin was dissolved. See curve *A* in fig. 5. We see that curve *D* (pepsin has acted upon the gelatin during 2 hours at 40° before inactivation) lies

much lower than the blank curve *A* (pepsin has acted during 2 minutes at 40° before inactivation). The lowering influence of proteolytic action on the coacervate volume has the same character as that of thermolytic action. Compare fig. 5 and fig. 1.

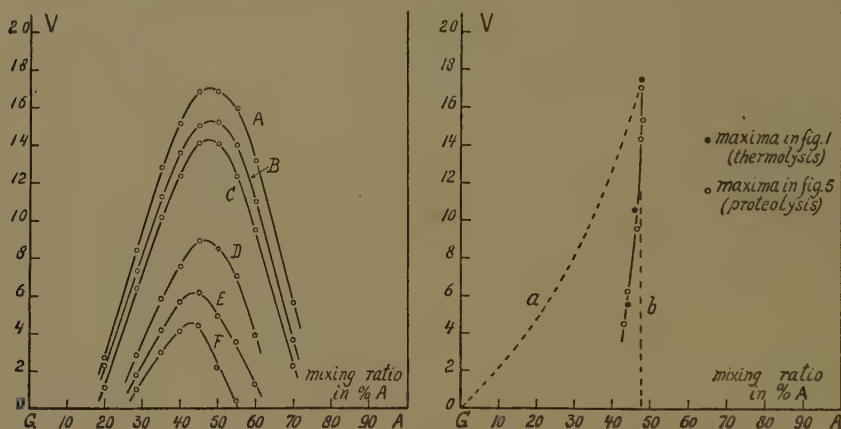


Fig. 5. Influence of exposure of a buffered 2 % gelatin solution to the action of pepsin at 40° on the subsequent complex coacervation with a buffered 2 % gum arabic solution. Ordinates: volume of the coacervate in 0,1 ml from 20 ml mixture. Curve *A* and *D*, inactivation of the pepsin after 2 min. and 2 hours respectively. Curve *B*, *C*, *E* and *F* see text.

Fig. 6. Path followed by the maxima of the curves in fig. 1 and 5. Ordinates: Volume of the coacervate from 20 ml mixture. *a* and *b*, paths followed according to two different explanations of the decrease of the volume of the coacervate (see text).

After standing 27 hours both series of sedimentation tubes were shaken anew and left to sedimentation, after which we obtained the curves *B* and *E*. This was repeated 23 hours later, after which the curves *C* and *F* were obtained.

To explain this further lowering with time at 40°, one will of course think at first of thermolysis during these 27 and 50 hours at 40°. If we compare however, the rate of decrease of the coacervate volume at 50 % mixing ratio with the experiments in section 1 for pure thermolysis at 40°, it appears that this rate is too big. We must conclude that during the inactivation a small fraction of the pepsin (approximately 1 % for the "blank series" and 3 % for the series in which pepsin acted on the gelatin for 2 hours) had actually escaped inactivation. Considering that the original amount of added pepsin gave a proteolytic action that was approx. 130 times as fast as the thermolytic action at the same temperature, it is no wonder that these small fractions still have a considerable influence.

With the full amount of pepsin being active a decrease of the coacervate volume (at 50 % mixing proportion) from 16.8—8.4 occurred in two hours. With pure

thermolysis, also at  $40^\circ$ , the same decrease takes 261 hours, (compare fig. 2). Hence the proteolytic action was approx. 130 times as fast as the thermolytic action at the same temperature.

After inactivation of the pepsin-gelatine mixture used for the blank series, (curves A, B, C) the coacervate volume at 50 % mixing proportion decreased from 16.8 to 14.0 in 50 hours, whereas pure thermolysis also at  $40^\circ$  takes 90 hours for the same decrease (compare fig. 2). Hence the inactivation of the pepsin had not been complete, the rate of decrease of the coacervate volume in fig. 5 being 1.8 times the one that occurs with pure thermolysis. The fraction of the pepsin which had escaped inactivation therefore amount to  $(1.8-1)/130 = 0.006$ , or 0.6 %.

Similarly one can calculate for the pepsin-gelatine mixture which was used for the other series (curves D, E, F), which fraction of the pepsin has escaped inactivation. The coacervate volume at 50 % mixing proportion decreased from 8.4 to 4.9 in 27 hours, whereas pure thermolysis also at  $40^\circ$  takes for the same decrease 130 hours. The rate of decrease of the coacervate volume in fig. 5 is therefore  $130/27 = 4.8$  times the one that occurs with pure thermolysis. The fraction of the pepsin which has escaped the inactivation here therefore amounts to  $(4.8-1)/130 = 0.029$ , or 2.9 %.

### 3. Discussion

The similarity of the results obtained in the sections 1 and 2 strongly points to the same mechanism underlying the decrease of the coacervate volume as a consequence of a previous heat treatment of the gelatin and as a consequence of a previous proteolytic action on the gelatin. We now have to seek an explanation why the coacervate volume diminishes when by one of the two above causes peptide bonds are hydrolyzed. A peculiar detail occurring both in the figures 1 and 5 is that the situation of the maximum of the curve expressed in the mixing ratio does not change very much when the curve is lowered as a consequence of thermolysis or proteolysis of the gelatin. Compare the following survey and fig. 6, in which the data of the survey have been plotted. The drawn curve gives the path followed by the maximum in the figures 1 (black dots) and 5 (open circles).

In addition two dotted curves, *a* and *b* have been drawn in fig. 6 which

*Ordinates and abscissa of the maxima of the coacervate volume curves in fig. 1 (thermolysis) and fig. 5 (proteolysis).*

Fig. 1			Fig. 5		
Curve	Ordinate (in 0.1 ml)	Abscissa (in % gum arabic sol)	Curve	Ordinate (in 0.1 ml)	Abscissa (in % gum arabic sol)
a	17.2	47.5	A	17.0	47.5
b	10.5	46	B	15.5	48
c	5.5	44	C	14.2	47.5
			D	8.9	46.5
			E	6.2	44
			F	4.5	43

give the paths that would be expected when two different points of view concerning the cause of the decrease of the coacervate volume are taken in consideration.

Curve *a* represents the path of the maximum when it is supposed that the decrease of the coacervate volume is a direct measure for the amount of destroyed gelatin. The maximum originally lies at 47.5 % gum arabic, that is 19 parts of negative gum arabic just compensate 21 parts of positive gelatin. When the maximal coacervate volume has been decreased down to half the original value, 19 parts of the gum arabic solution now will need  $2 \times 21 = 42$  parts of the modified gelatin solution. The maximum will now be found at the ratio 19 (19 + 42), that is at a mixing proportion of 31.2 %.

It is characteristic of curve *a* that a distinct shift to smaller mixing ratios directly manifests itself when the coacervate volume begins to decrease.

Curve *b*, a dotted vertical line, depicts the path taken by the maximum of the coacervate volume curve, when it is assumed that the decrease of the coacervate volume is the result of an increase of the solubility of the coacervate, an increase which already occurs at the very first beginning of the hydrolytic break up of peptide bonds. When one bond in the very large gelatin macromolecule is hydrolized, two smaller macromolecules will be formed, which certainly will increase the mutual solubility of the two layers, the coacervate layer and the equilibrium liquid. This will lead to a decrease of the coacervate volume. But the scission of the original macromolecule into two smaller macromolecules, will leave the total amount of positive charges practically unaltered (the increase of the basic groups with one is very small compared to the total number in the arginine, lysine and histidine side chains).

The second point of view therefore leads to a decrease of the coacervate volume without changing of the mixing ratio at which the maximum of the coacervate volume is situated. The path followed by the maximum is a straight vertical line (dotted curve *b*) then.

The actually determined path (curve through the experimentally determined points) coincides in its upper part with the vertical line *b*, and only when the coacervate volume has decreased considerably a slight shift to smaller mixing ratios occurs.

We may conclude that the decrease of the coacervate volume is mainly due to the mechanism proposed in the second point of view, and that a destruction according to the first point of view plays only a very minor part.

In this connection it is worth while to mention the following observation. When the gelatin solution is heated so long that it just does not give complex coacervation with the gum arabic solution any longer, addition of distilled water to the clear mixture at once causes complex coacervation. This fact is not compatible with the first explanation (gelatin as a complex



component is destroyed), but it gives no difficulties when the second explanation is accepted (increase of the mutual solubility of coacervate and equilibrium layer).

To explain the reappearance of the coacervate after addition of distilled water it must be remembered that our systems contain a small concentration of a salt (0.01 N. Na acetate of the buffer) and that by dilution with distilled water this concentration will therefore diminish. Now addition of salts increases in general the mutual solubility of a complex coacervate and its equilibrium liquid. Therefore dilution of a salt containing coacervate system will decrease the mutual solubility of the layers. When after previous heating of the gelatin solution complex coacervation just no longer occurs, this means that in the presence of 0.01 N salt the two layers have just become miscible. By dilution with distilled water they are no longer miscible and coacervation will occur.

#### 4. *Summary*

1. Buffered gelatin and gum arabic solutions ( $\text{pH} = 3.7$ ) can be stored at room temperature (or lower temperature) for at least 6 months without (visible) development of bacteria and moulds when some  $\text{CCl}_4$  is added.

2. Prolonged exposure of the gelatin solution to various temperatures diminishes the volume of the coacervate volume of the subsequent complex coacervate with gum arabic (at  $\text{pH} 3.7$  and at  $40^\circ$ ). A study of the rate of this change as a function of the temperature points to a chemical reaction being the underlying cause. The formula of ARRHENIUS applies in the investigated range of temperatures ( $4^\circ$ — $100^\circ$ ).

3. The great similarity of the results obtained with the exposure of the gelatin solution both to proteolytic action (pepsin) and to heat, points to the conclusion that the chemical reaction mentioned sub 2 also consists of a hydrolysis of peptide bonds.

4. The decrease of the coacervate volume must, however, take place at the very beginning of the hydrolysis of peptide bonds. This follows from the path taken by the maximum of the coacervate volume curve in a mixing diagram gelatin gum arabic.

5. The decrease of the coacervate volume itself is mainly due to increased mutual solubility of the two layers (coacervate and equilibrium liquid) as a consequence of the cleavage of the macromolecule of gelatin into a few smaller ones during the beginning of the hydrolysis.

*Department of Medical Chemistry.  
University of Leiden.*

# AUTOXIDATION OF SATURATED HYDROCARBONS IN THE LIQUID PHASE

(First communication)

## I

BY

J. P. WIBAUT AND A. STRANG

(Communicated at the meeting of March 31, 1951)

### 1. Introduction and purpose

A great many investigations have been carried out concerning the "slow combustion" of gaseous hydrocarbons, i.e. the partial oxidation by molecular oxygen at elevated temperatures, from which important conclusions have been drawn as to the mechanism of the reactions.

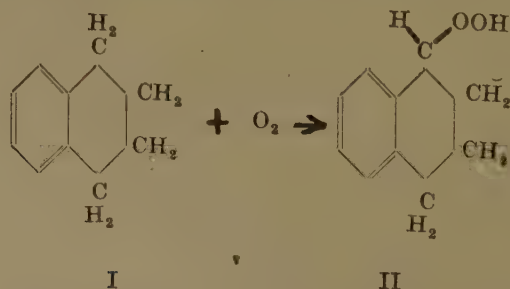
As regards autoxidations of liquid hydrocarbons, the investigations mainly concerned the action of air or oxygen on unsaturated hydrocarbons, in some cases with the aid of catalysts.

Much less is known about the action of molecular oxygen on saturated hydrocarbons with 6 or more C atoms.

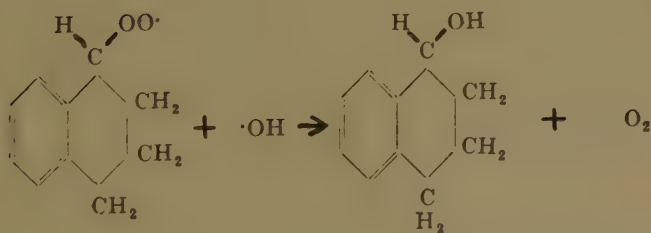
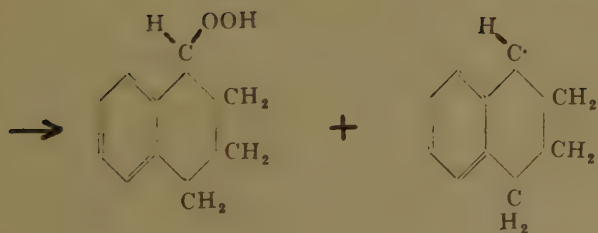
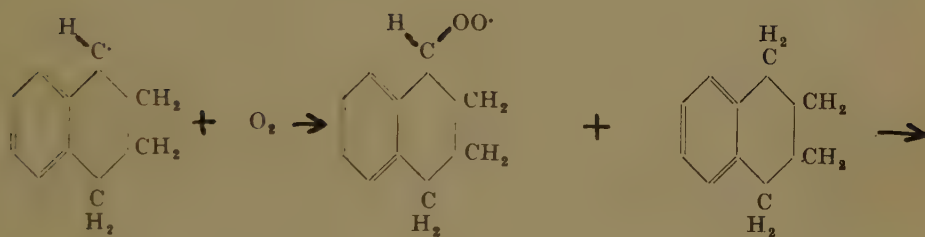
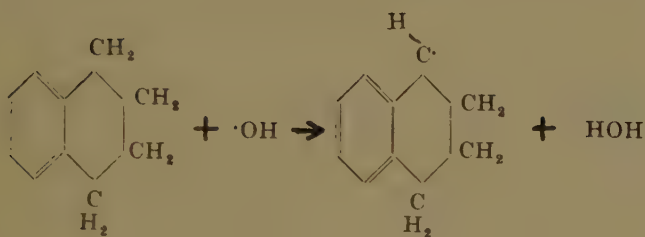
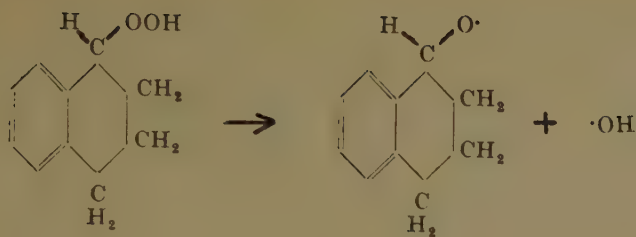
CHAVANNE (1) oxidized *n*-octane, *n*-nonane and *n*-decane with molecular oxygen at 120°. He obtained from octane methyl hexyl ketone besides other non-identified ketones and a mixture of fatty acids. From nonane he obtained, besides other ketones, methyl heptyl ketone and various fatty acids. This shows that in the case of normal alkanes oxidation starts in different places in the chain.

No conclusions as to the mechanism of the oxidations can be drawn from experiments on the catalytic oxidation of white oils (mixtures of alkanes) stated in the patent literature.

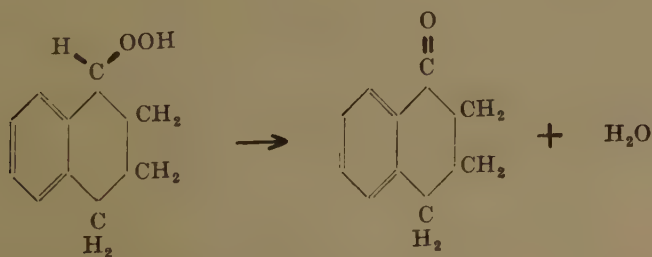
The autoxidation of tetrahydronaphthalene (I) in the liquid phase has been investigated very extensively. According to WATERS, ROBERTSON and GEORGE's investigations (2) a hydroperoxide (II) is formed:



which splits up into radicals, which enter into a chain reaction:



Side reaction:



According to WATERS and ROBERTSON the part played by the catalyst in the catalytic oxidation of tetraline consists in the strong acceleration of the decomposition of the peroxide by the catalytically acting metal ion, after which the radicals formed react according to the above scheme.

We have carried out an investigation into the oxidation by molecular oxygen of a number of normal alkanes with 8 to 22 carbon atoms, of some alkanes with branched carbon chain and of some homologues of cyclohexane.

We made it our object

1. to ascertain whether there is a relation between the structure of the hydrocarbon and the rate of oxidation;
2. to collect data on the mechanism of the reaction.

For our purpose it was therefore of importance to examine the oxidation products primarily formed, so that the oxidation reactions had to take place at the lowest possible temperature.

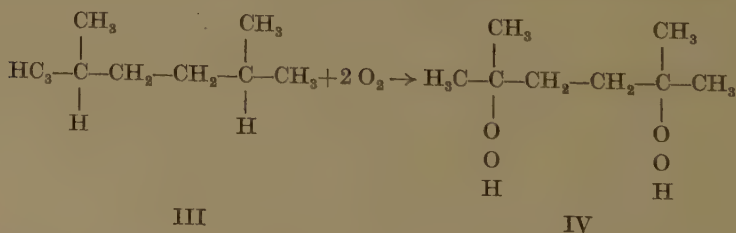
## 2. *Formation of peroxides*

Most of the hydrocarbons examined by us are not or very slowly attacked by molecular oxygen at temperatures below the boiling point. However, after addition of a small quantity of an organic cobalt salt which is soluble in the hydrocarbon, the oxidation proceeds at a measurable rate.

Some other metal salts, too, have a catalytic effect; in most of our experiments we used cobalt stearate as the catalyst.

It has been found that the first stage of the oxidation reaction consists in the formation of a hydroperoxide.

In a sample of 2,5-dimethylhexane (III) ( $C_8H_{18}$ ), which had been kept for some years in a stoppered bottle partly filled with air, white crystals had deposited, which melted at  $106.5^\circ$  and the composition of which corresponded with the formula  $C_8H_{16}O_4$  (found 53.79 % C; 9.97 % H; calculated 53.91 % C; 10.17 % H). This substance has the formula (IV).



The dihydroperoxide IV liberates the calculated quantity of iodine from an acidified potassium iodide solution and passes over into 2,5-dimethylhexanediol-2,5, melting point  $88^\circ$ ; we have prepared this peroxide synthetically by the action of hydrogen superoxide on 2,5-dimethylhexanediol-2,5.



*As far as we know, this is the first example of autoxidation of an alkane in which the hydroperoxide formed is isolated.*

The presence of small quantities of peroxides can also be detected in samples of other saturated hydrocarbons which have been kept for a long time, for instance in 3,4-dimethylhexane, 2,5-dimethylhexane, 3-methylheptane, *n*-nonane, *n*-hexadecane and methylcyclohexane. Some peroxide contents calculated from the quantity of separated iodine are given below:

TABLE 1

Hydrocarbon	<i>n</i> -nonane	<i>n</i> -heptane	3-methylheptane
peroxide content in mg eq. per mol. hydrocarbon . . . . .	1.05	1.70	0.98

The primarily formed peroxide is decomposed under the influence of the catalyst; the radicals thus formed start a chain mechanism, so that the oxidation reaction proceeds.

### 3. *Experimental procedure* (see figure 1)

The glass reaction vessel (A) has the shape of a cylinder with a flat bottom and is provided with a mercury-sealed stirrer (B), a feed tube for oxygen and a side tube with ground stopper (C) to which a spoon has been fused. A thin-walled glass basin containing a weighed quantity of the catalyst can be placed on this spoon. A measured quantity of hydrocarbon is introduced into the reaction vessel filled with oxygen and the feed tube is connected with a gas burette filled with oxygen. The reaction vessel is kept at a constant temperature by means of the vapour of a boiling liquid contained in the boiling vessel.

When the desired temperature has been adjusted, the required quantity of catalyst is added to the hydrocarbon by turning the stopper. This point of time is assumed to be the starting point of the reaction. The height of the mercury in the gas burette is noted down at given points of time and from this the quantity of oxygen absorbed can be found.

An absorption curve for the oxidation of *n*-octadecane ( $C_{18}H_{38}$ ) at  $110.4^{\circ}C$  is represented in figure 2; the quantities of oxygen are given in ml ( $0^{\circ}$  and 760 mm) per 61.7 millimols *n*-octadecane to which 0.112 millimol. cobalt stearate has been added.

This curve shows that after a certain induction period the quantity of oxygen absorbed per unit of time is constant. From the maximum slope of the curve it is evident that this quantity is about 50 ml per hour per 61.7 millimols of hydrocarbon; this is a measure of the maximum rate of oxidation.

The following is observed in the oxidation with cobalt stearate as catalyst. The dissolved cobalt stearate gives the hydrocarbon a pink colour; after some time this colour changes into a deep green due to the

presence of a cobalt III ion. From this point of time the oxygen is absorbed at a constant rate. After some time (1 to 2 hours) the red colour of the

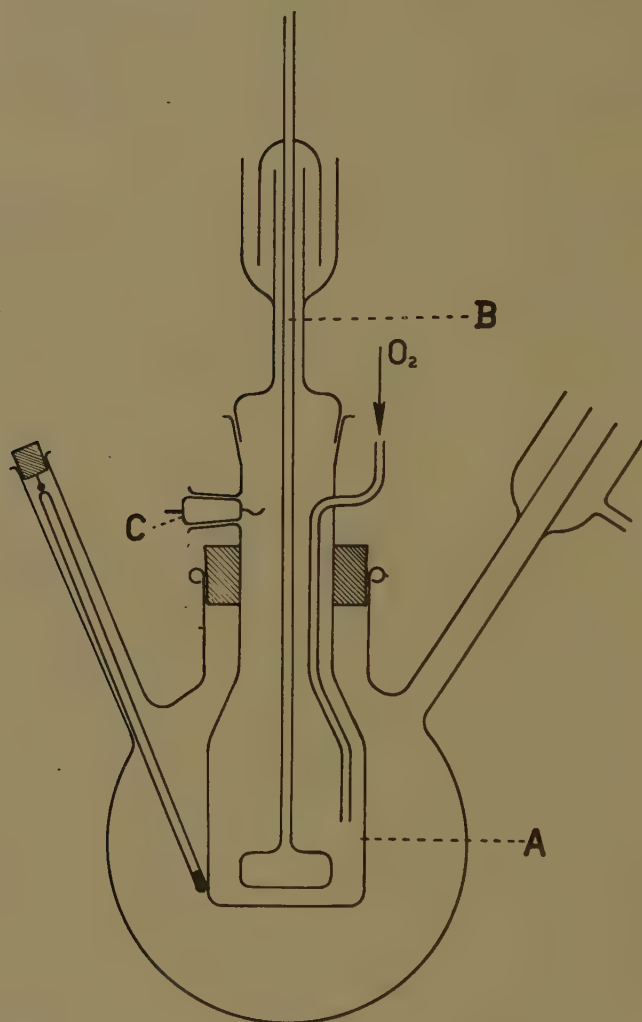


Figure 1

lowest stage of oxidation of cobalt reappears and the catalyst begins to flocculate. This is caused by the presence of lower fatty acids and water formed during oxidation, as a result of which the cobalt stearate is converted into cobalt compounds which are insoluble in the reaction medium. From this point of time the curve begins to bend down.

For the calculation of the initial rate we have only considered the straight part of the curve, thus when only a small quantity (about 1 %) of the hydrocarbon has been oxidized.

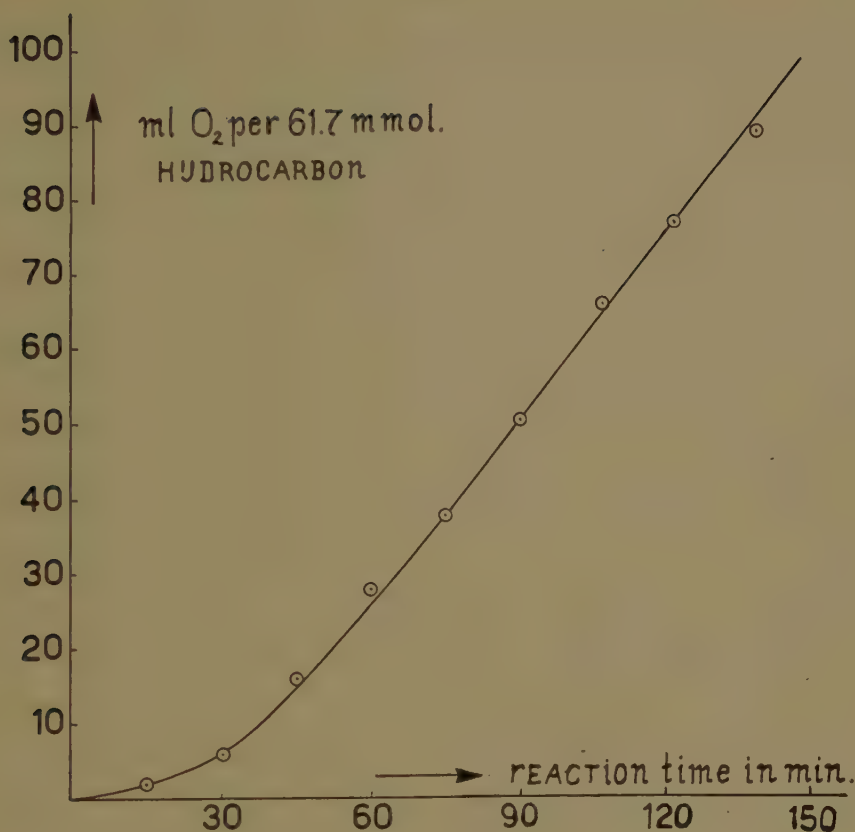


Figure 2

To obtain reproducible results it is necessary that the hydrocarbon samples are very pure<sup>1)</sup>.

#### 4. Initiation of the oxidation by decomposition of peroxides

From what is said below it is clear that a small quantity of peroxide in the hydrocarbon sample is required for initiation of the oxidation reaction.

*N*-nonane, which has been distilled over sodium immediately before the oxidation test and in which no peroxide can be detected iodometrically, does not absorb oxygen at 110.4°, even in the presence of cobalt stearate. When 12 mg 2,5-dimethylhexane-dihydroperoxide per 61.7 m.mol hydrocarbon is added, oxidation sets in.

<sup>1)</sup> A number of very pure hydrocarbons originating from an investigation into the physical constants of alkanes carried out in Amsterdam Laboratory was at our disposal (J. P. WIBAUT, H. HOOG, S. L. LANGEDIJK, J. OVERHOFF and J. SMITTENBERG, *Rec.* 58, 329 (1939). A second and third group originated from Kon./Shell-Lab. and from an investigation carried out by WIBAUT and SCHUH-MACHER, which has not yet been published. A fourth group was prepared synthetically by us. The origin, purity and synthesis are described extensively in STRANG's thesis, which will be published in April 1951.

*N*-hexadecane shows the same phenomena as *n*-nonane. Branched alkanes show similar phenomena. 3-methylheptane, 3,4-dimethylhexane, 2,5-dimethylhexane and methylcyclohexane were examined.

With these hydrocarbons the peroxides could not always be sufficiently removed by a simple distillation over sodium to prevent oxidation under the influence of cobalt stearate. The removal was effected by washing the hydrocarbon successively with potassium permanganate solution, bisulphite solution, alkali and strong sulphuric acid, followed by distillation over sodium in a column of approximately twenty theoretical plates.

2,5-dimethylhexane, freed from peroxides in the above-described manner, forms a peroxide so rapidly at 78.1° in an oxygen atmosphere that in the presence of cobalt stearate the oxidation process soon proceeds at its maximum rate.

After purification 3,4-dimethylhexane is so slow in the thermal formation of hydroperoxide that no noticeable oxygen absorption is observed in the presence of cobalt stearate for three hours; after this period oxidation starts.

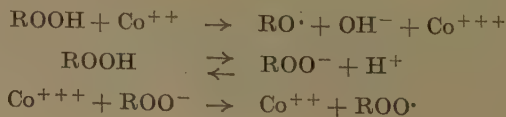
3-methylheptane and methylcyclohexane are extremely slow in the thermal formation of peroxides, so that no autoxidation was initiated during the time of the experiment (about 5 hours).

A last interesting sample is *n*-octane: At first this freshly prepared hydrocarbon could not be made to oxidize. Iodometrically, no peroxide could be detected in this preparation. After passing oxygen through the boiling liquid (125°) — which contained 1 % cobalt stearate — for ten hours, oxidation was initiated. By distillation of the preparation thus oxidized a *n*-octane was obtained which could not be oxidized. This excludes the possibility that the non-oxidizability of the purified hydrocarbon should be due to the presence of inhibitors. Addition of 12 mg 2,5-dimethylhexane-dihydroperoxide-2,5 to 61.7 mmol of a non-oxidizing preparation makes the oxidation of *n*-octane proceed at the maximum rate already after an induction period of 45 minutes.

When oxygen is passed through at 125° while excluding a catalyst, a measurable quantity of peroxide is formed in the *n*-octane in course of time. When cobalt stearate is added to a preparation thus treated, the hydrocarbon is oxidized at a measurable rate.

##### 5. Part played by the catalyst

For the decomposition of the hydroperoxides under the influence of cobalt ions we use as a basis the scheme drawn up by HABER and WEISS for the decomposition of hydrogen peroxide by ferrous ions.





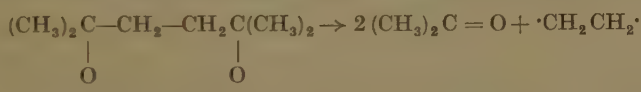
This reaction mechanism is supported by the following experiments:

a. When 2,5-dimethylhexanedihydroperoxide-2,5 dissolved in benzene, 2,5-dimethylhexane or diphenylmethane is decomposed catalytically, the liquid shows the green colour of the trivalent cobalt. Since this reaction was carried out in a nitrogen current, the occurrence of trivalent cobalt must be attributed to the action of hydroperoxide.

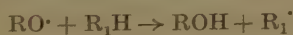
b. It is found that a given quantity of cobalt stearate is able to decompose a more than equivalent quantity of peroxide, so that the cobalt II ion must be regenerated in one way or another. Considering the weakly acid properties of hydroperoxides, the above reaction does not seem improbable.

c. If the decomposition is carried out in different solvents the reaction products mainly consist of 2,5-dimethylhexane-diol-2,5 and acetone. The acetone can be determined quantitatively when the decomposition is carried out in a nitrogen current (free from oxygen). The acetone formed is entrained by the current and collected in water after which it is determined as *p*.nitrophenylhydrazone.

It is difficult to think of this acetone being formed in another way than by decomposition of the alkoxy radical RO· which has the following structure in the case of 2,5-dimethylhexane-dihydroperoxide-2,5:



The alkoxy radical can react, not only according to a monomolecular decomposition, but also with the solvent:



In contrast with the monomolecular decomposition the latter reaction greatly depends on the solvent. According as the hydrogen atoms are more reactive, the alcohol formation will proceed at a higher rate and consequently the chance of decomposition of the alkoxy radical will be smaller.

This is confirmed by the experiments represented in table II.

TABLE 2

Solvent	Acetone from 4 mmol peroxide
benzene (50 ml) . . . . .	1.70 mmol
2,5-dimethylhexane (50 ml) . . . . .	1.20 „
diphenylmethane (30 ml) . . . . .	— „

Reaction temperature: 78°

Catalyst: 70 mg cobalt stearate

Benzene, in which the hydrogen atoms are firmly linked, promotes the formation of acetone; in diphenylmethane, in which the hydrogen atoms of the methylene group are very reactive, no acetone is formed.

## THE HEAT CONDUCTIVITY OF SCALES IN EVAPORATORS

BY

P. HONIG<sup>1)</sup>

(Communicated at the meeting of January 27, 1950)

1. For the calculation of the capacity of multiple evaporators, which are frequently applied in the chemical industries, it is customary to use a number of data for the total heat transfer: "heating steam—solution to be evaporated", based on practical experience and on a number of systematically performed determinations.

In the cane sugar industry, where the clarified juice has to be concentrated from 15–20 % to 60–70 % dry solids a quadruple or quintuple effect, the professional literature mentions a number of data which are considered to be a useful foundation for the calculation of the capacity of evaporator sets.

In table no. I the most important data for quadruple effects are summarized as used in different countries.

TABLE I  
Heat transmission coefficients ( $\text{Cal}/\text{m}^2/\text{h}/^\circ\text{C}$ ) of multiple evaporators

1st body	2nd body	3rd body	4th body	Source
2400–3000	1800–2400	1200–1800	600–900	Claassen <sup>2)</sup>
2250	1750	1250	750	Tromp <sup>3)</sup>
2000	1400	900–1000	400–500	Hugot <sup>4)</sup>
2400	1800	1200	600	Coutanceau <sup>5)</sup>

2. In practice it can be observed that the total heat transfer changes gradually, caused by the formation of scales on the side of the evaporator tubes of the concentrated juice, mainly composed of inorganic components present in the juice, partly becoming insoluble during the concentration process and partly by the precipitation of some of the inorganic constituents; the occurring phenomena cannot yet be explained by well defined solubility data. The magnitude of scaling is a subject of permanent interest and discussion in professional circles. However, the progress that

<sup>1)</sup> Dr P. HONIG, Technical Research Director, West Indies Sugar Corporation, 60 East 42nd Street, New York 17, N.Y.

<sup>2)</sup> Dr H. CLAASSEN, *Die Zuckerfabrikation* (Schallehn und Wohlbrück, Magdeburg, 1940).

<sup>3)</sup> L. A. TROMP, *Sugar Machinery and Equipment* (Norman Rodger, London, 1946).

<sup>4)</sup> E. HUGOT, *La Sucrierie de Cannes* (Dunod, Paris, 1950).

<sup>5)</sup> L. J. COUTANCEAU, *Heaters and Evaporators* (Port Louis, Mauritius, 1944).

has been made in the past thirty years towards the objective and quantitative interpretation of the occurring facts is limited. The intensity of scaling, in regard to the thickness of the scale, is usually judged visually and the method of classification is subjective.

The following quantitative classification can be used for the terminology, to be applied in scaling phenomena.

TABLE II

Very light scaling . . .	< 100 g/m <sup>2</sup>	evaporating surface
Light to medium scaling	100—1000 g/m <sup>2</sup>	„
Heavy scaling . . . . .	1000—1500 g/m <sup>2</sup>	„
Very heavy scaling . .	> 2000 g/m <sup>2</sup>	„

3. The intensity of scaling in evaporators of cane sugar factories varies from country to country and in the same country from year to year; one can observe in the same year and in the same country great differences between different areas. The cause of these differences can be found in the composition of the processed raw material, i.e. the cane juice. It is a well-known fact that a raw material as sugar cane produces in the recovery of the extracted juice a mixed juice with wide fluctuations in the quantities of the organic components present.

According to experiences collected in Java over a period of 14 years (1927—1941) and related to more than 1000 mixed juice analyses, the variations in the quantities of the different inorganic non-sugars, present per liter of mixed juice, are within the following limits.

TABLE III

Cations:	in mg per 1 of mixed juice	Anions:	in mg per 1 of mixed juice
K <sub>2</sub> O . . . . .	600—4000	Cl . . . . .	50—400
Na <sub>2</sub> O . . . . .	200—500	SO <sub>3</sub> . . . . .	300—1000
CaO } . . . . .	300—1600	P <sub>2</sub> O <sub>5</sub> . . . . .	100—800
MgO } . . . . .		SiO <sub>2</sub> . . . . .	300—1000
Fe <sub>2</sub> O <sub>3</sub> } . . . . .	150—500		
Al <sub>2</sub> O <sub>3</sub> } . . . . .			

These fluctuations are related to the composition of the soil, to the cane variety, to the amount and method of applied fertilizers and to the agricultural techniques; furthermore to the composition of the irrigation water and to the climatic conditions. Of special significance is the condition under which the cane has grown and the physiological condition of the cane at the time of harvesting. It is altogether a very complicated system of relations.

There are positive indications that cane grown on certain types of soil always produces juices with a low phosphate content, caused by a low percentage of available phosphate in the soil. Other soils always produce

juices with a high calcium and magnesium content, also related to the soil composition.

At the present moment positive facts about the assimilation of silicic acid and sesquioxides by the cane plant and the way it is present in juices, are practically not available.

4. In practical sugar manufacture it is customary that the mill juice is mixed with milk of lime, in order to obtain a certain alkalinity (pH), and heated, by which a considerable part of the inorganic constituents, together with some organic non-sugars, are precipitated, and become removable by sedimentation and filtration. The resulting clarified juice, being the raw material for the recovery of the commercial sugar, still contains a relatively high amount of inorganic impurities.

In Java, where during the years before the 2nd world war a large number of determinations on the occurrence of these impurities were made, the amounts were classified as follows:

TABLE IV

Cations:	Per liter of clarified juice in mg		
	low	normal	high
CaO . . . . .	< 300	300—600	> 600
MgO . . . . .	< 100	100—200	> 200
Fe <sub>2</sub> O <sub>3</sub> . . . . .	< 20	20—45	> 45
Al <sub>2</sub> O <sub>3</sub> . . . . .	< 5	5—25	> 25
Anions:			
SO <sub>3</sub> . . . . .	< 300	300—500	> 600
P <sub>2</sub> O <sub>5</sub> . . . . .	< 30	30—70	> 70
SiO <sub>2</sub> . . . . .	< 150	150—250	> 250

5. While concentrating clarified juice a part of the inorganic non-sugars are separated from the solution as an incrustation on the heating and evaporating surface. During the time an evaporator is in operation the thickness of the formed scale increases correspondingly and the heat transfer decreases in the same relation, making it necessary for the evaporator to be stopped for cleaning after a certain period of operation. The cleaning is done by mechanical means, like scraping and brushing, evt. in combination with a chemical treatment which usually consists of boiling the scales with a diluted solution of lye or acid in order to dissolve certain incrustating components, resp. to transfer them in such a way that they can easily be removed mechanically. The chief purpose of the chemical treatment is to change the physical structure of the scales so that they will lose their mechanical coherence and can be removed completely by a washing, a spray or brushing and that consequently the evaporating surface can be restored to its original condition.

5. The quantity of scale formed in the different vessels of a multiple evaporator set shows considerable fluctuations. Relatively speaking the



largest quantities of scale are always formed in the first and last bodies. The scaling in the first body is partly caused by a flocculation and precipitation, resulting from the high temperature of the juices to be evaporated; in the last body it is mainly caused by the insolubility of certain non-sugars as a result of the concentration process in the evaporators.

The scaling can be expressed as the quantity of formed scale in grams per ton of cane processed:

scale in g per ton of cane =

$$A_g = \frac{\text{amount of scale in kg in evaporators} \times 1000}{\text{amount processed cane in tons}}$$

Practical determinations have shown that the quantity of scale in raw cane sugar mills varies from 3—15 g per ton of cane, usually 15 g and higher. This means that in a modern sugar mill with a daily capacity of 3000 tons of cane, an amount of 9—45 kg scale is formed in the evaporators. This is a considerable quantity. In most cane sugar producing countries, where the scaling is one of the normal phenomena in the manufacturing process, it is necessary for an evaporator set to be taken out of operation once a week and cleaned.

6. Assuming that the heating surface, which the normal sugar factory has installed for the concentration of juices, is 90—150 m<sup>2</sup> per 100 tons of cane processed per 24 hours, it is possible to get an idea of the amount of scale formed per m<sup>2</sup> heating surface per unit of time (per hour or per day). As has been remarked already the scaling is not distributed equally over all bodies. Under practical conditions the highest scaling is usually in the last body. Of the total scale formed in an evaporator set the amount of scale formed in the last body may account for 40—50 % of the total scaling. This can be expressed by the following formula:

$$A_{m^2}^t = \text{scale in grams per m}^2 = \frac{A_g \cdot 100}{\text{evap. surface per 100 tons process cane/24 hours}} \cdot \text{total operating days.}$$

For a specific body as f.i. the fourth body of a quadruple evaporator set this formula is:

$$A_{m^2}^4 = \frac{A_g \cdot (\% \text{ of the total scaling, in the 4th body}) \cdot 100}{\text{evap. surface 4th body per 100 tons processed cane/24 h}} \cdot \text{total operating days.}$$

It has been proven possible to study the scaling in a quantitative manner in this way, by determining the amount of scale formed on a specific heating surface in a known period of time, corresponding to a certain amount of cane processed. In this way we know accurately the magnitude of scaling. However, this is not yet sufficient for a quantitative

analysis of the incrustation problem from a chemical engineering standpoint.

7. The quality of the scale is in many cases more important than the amount of scale formed per  $\text{m}^2$  heating surface or per ton of cane processed. Through a large number of determinations and analyses, collected by the Java sugar industry over a number of years, it has been possible to classify scales in regard to composition and the influence on the heat transfer. Similar observations can be found for boiler scales in the professional literature. Here too, in the same way as with sugar evaporator scales, it has been found that the porosity of the scale is more important in regard to the way it influences the heat transfer than the chemical composition. Evaporator scales can be classified as follows:

TABLE V

	Main components	Porosity <sup>1)</sup>	Calculated specific heat conductivity $\lambda$
crystalline scales . . . .	$\text{CaSO}_3 \cdot 2\text{aq}$ , Ca. organates (oxalate and aconitate), $\text{CaCO}_3$	25—50	0.60—1.0
micro-crystalline scales .	$(\text{CaO} \cdot \text{MgO})_a \cdot (\text{P}_2\text{O}_5)_b$ $(\text{CaO} \cdot \text{MgO})_n \cdot (\text{SiO}_2)_m$	40—65	0.30—0.70
amorphous scales . . . .	$\text{SiO}_2$ $\text{R}_2\text{O}_3(\text{Al}_2\text{O}_3 \text{ and } \text{Fe}_2\text{O}_3)$	50—80	0.10—0.35

In order to calculate the specific heat transfer of formed scales through the use of determined data, the thickness of the scale per  $\text{m}^2$  should be used and not the weight of scale per unit of heating surface.

8. Heat transfer in an evaporator is a complicated phenomena. At the present moment a specific knowledge exists in regard to the way the heat is transferred from heating steam unto a boiling and evaporating liquid, separated by a metal wall. The condensation of the heating steam takes place as a so-called film condensation, in which a thin layer of condensate covers the condensating surface. This condensate flows off under the influence of the gravity and forms a transitional layer for the heat transfer. Film condensation is the normal form of condensation of steaming heat in the technical evaporators in the sugar industry. The so-called drop condensation about which much has been studied and published on account of its great theoretical significance and the possibility

<sup>1)</sup> Porosity =  $100 \left( \frac{\text{specific gravity} - \text{apparent specific gravity}}{\text{specific gravity}} \right)$

to increase the heat transfer, is not being realized under practical conditions of a sugar factory. However, the overall heat transfer is partly reduced by the resistance of the condensate film. The heat resistance of the construction material of the evaporator tubes, either brass or red copper, is of a limited significance. The heat conductivity on the juice side, where the water in the juices to be concentrated has to be evaporated, is essential for the overall heat transfer. The normal form of evaporation in sugar juices is the nuclear evaporation; evaporation starts with certain nuclei which can either be suspended solids, dissolved gases or certain points and areas of the evaporating surface. The main phenomena taking place consists of the solid wall transferring heat on the liquid to be evaporated through convection and the liquid transferring the heat to the developing vapor bubbles. In order to explain this transfer it is

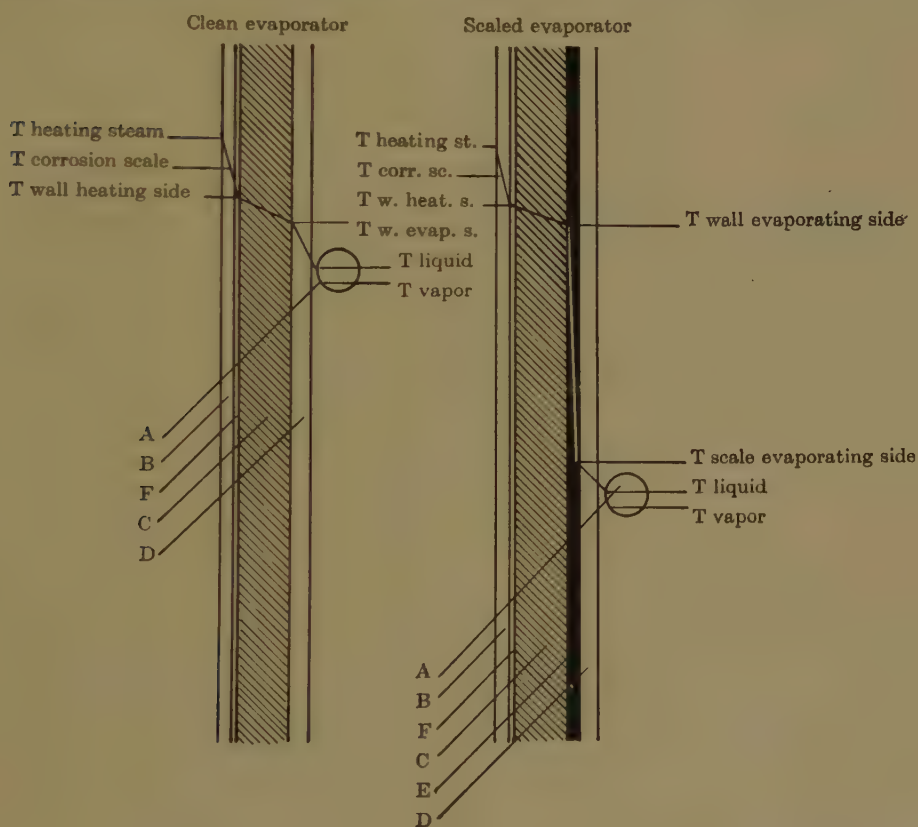


Fig. 1

Heat transfer and temperature drop in evaporators.

A = vapor bubble formed in evaporating liquid

B = condensate film

C = wall construction material evaporator (brass or red copper)

D = transitional layer evaporating liquid

E = scale formed on liquid side

F = corrosion scale on heating side

necessary to assume a certain difference of temperature between the boiling liquid and the saturation temperature of the vapor bubbles in the juices to be evaporated. This means that the solid surface and the liquid, in relation to the temperature of the vapor, are slightly overheated.

In a schematic way the heat transfer can be given as indicated in figure no. 1.

In order to calculate the influence of formed scales on the heat transfer, we assume that all heat transfers remain the same as: heating vapor — condensate film; condensate film — wall; wall — scale; scale — liquid; liquid — vapor, and that the only change taking place in the total heat transfer is the result of the incrustation as such. Furthermore it is assumed that the scale formation takes place as a linear function continuously and gradually with the time the evaporator is in operation. In this way it is possible, knowing the total heat transfer, to calculate the specific influence of the incrustation:

$$H_{\text{incrustated evaporation}} = \frac{1}{\frac{1}{H_{\text{clean evap.}}} + \frac{d}{\lambda}}$$

$H_{\text{clean evaporation}}$  in Cal/m<sup>2</sup>/h/°C can be calculated from the amount of formed condensate, m<sup>2</sup> evaporating surface, temp. from the evaporating juice and temp. condensate.

$H_{\text{scaled evaporators}}$  can be determined and calculated in the same way.  $d$  = amount of scale in meters, to be calculated from the amount of scale in grams per m<sup>2</sup> and the apparent specific gravity. With these data  $\lambda$  can be calculated from the relation:

$$\lambda = \frac{d \text{ in meters}}{\frac{1}{H_{\text{scaled}}} - \frac{1}{H_{\text{clean}}}}$$

9. The data calculated and collected on the heat transfer in the described way can be correlated with the chemical composition and the porosity of scales of evaporators in sugar mills. For the calculation of the correlation between the composition, the porosity and the specific heat transfer we have found the following data for 14 determinations of scales of the fourth bodies of quadruple effects for which the necessary technical data were available. (Table VI)

The specific heat transfer of scales, formed in the fourth body of evaporators in cane sugar mills, using the normal liming process as purification method, can, according to these data, be expressed by the following empirical formula:

$$\lambda = \frac{(\% \text{ mol. cryst. comp.}) 0.8 + (\% \text{ mol. microcryst. comp.}) 0.4 + (\% \text{ mol. amorphous comp.}) 0.1}{100}$$



TABLE VI  
Procentual molar ratio of incrustation components

no. of incr. sample	crystalline ( $\text{CaSO}_4 \cdot 2\text{aq.}$ Ca-organates)	microcrystalline ( $\text{CaO} \cdot \text{MgO})_3(\text{P}_2\text{O}_5)_2$ ( $\text{CaO} \cdot \text{MgO})(\text{SiO}_2)$	amorphous $\text{SiO}_2, \text{Fe}_2\text{O}_3,$ $\text{Al}_2\text{O}_3$	determined specific heat transfer scales $\lambda$
1	24	18	58	0.28
2	33.5	14.5	52	0.40
3	69	23	18	0.69
4	67	23	10	0.72
5	65	17.5	17.5	0.67
6	28	26	46	0.40
7	38	10.5	41.5	0.41
8	50	20	30	0.51
9	57	15	28	0.38
10	56	27	17	0.40
11	17	24	58	0.22
12	43	24	33	0.43
13	47	26	27	0.42
14	44	10.5	45.5	0.29

The determined total heat transfer for fourth bodies of evaporators in a clean state, free of any incrustation, varied from 910—1540 Cal/m<sup>2</sup>/h/°C. The heat transfer of the same, but scaled, evaporators varied from 400—950. The result of these quantitative figures enables us to calculate the influence of specific incrustations on the heat transfer, if we know the composition resp. the porosity of the scales. The classification of these observations indicates, although the number of determinations is limited, that the influence of the different components of a scale on the heat transfer is additive: by calculation it is possible, when the quantity and composition of a scale are known, to estimate the influence on the total heat transfer.

The results of these scale samples are summarized in figure 2.

10. The principles laid down for the quantitative determination and classification of the scaling problem are of a direct practical significance. In recent years a number of methods and aids have been developed and introduced, attempting to reduce scaling, resp. to increase the time that an evaporator can be kept in operation without the necessity of cleaning. This is of practical significance for the economy of the sugar manufacture. The proposed methods are partly based on the addition of phosphates to the juices to be concentrated, eliminating the formation of calcium sulphate as a scaling component, which addition can be combined with vegetable mucilages as alginates, cactus extracts and sulphonated lignine, which substances influence the crystallization and scale formation of inorganic components in such a way that the formed scale has only a very loose coherence. This may result either in a continuous removal of formed

scale by the circulating juices in the evaporators, or, if scales are formed, they are removable by simple methods in a mechanical way. Another method consists of applying an alternating electric current to the juices to be concentrated. It is stated by the inventors and promoters of such systems that this current does change the scaling components such as

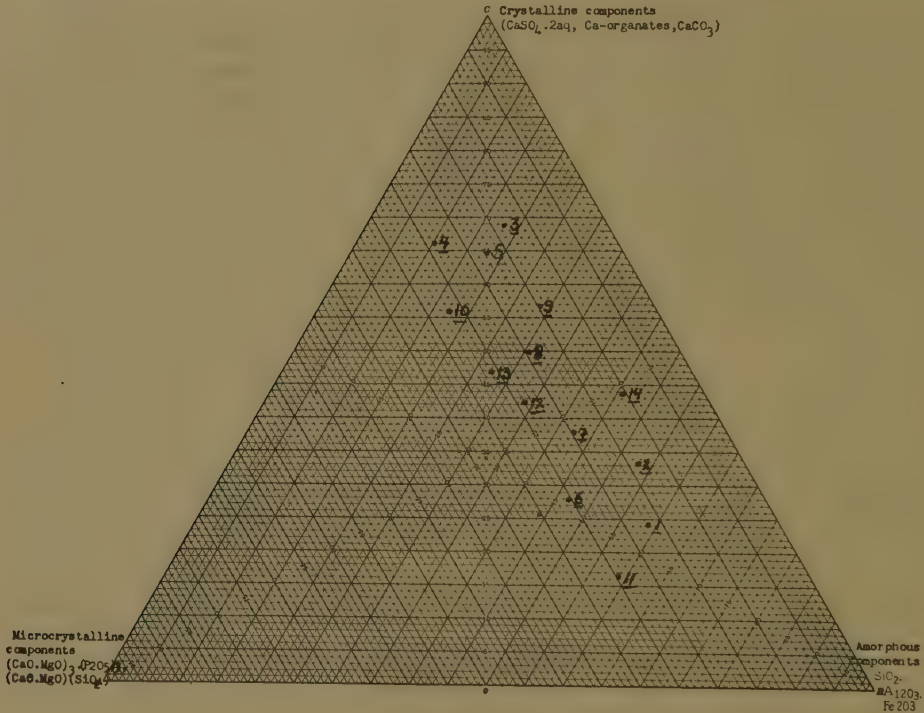


Fig. 2

silicic acid and sesquioxides in such a way that they do not adhere to the evaporating surface, but remain in suspension.

A fundamental knowledge in regard to the action and effect of this proposed and in many cases already applied method, is lacking.

A quantitative research study in regard to the obtained effects has, as far as is known to the author of this article, not been undertaken anywhere in the sugar industry. Through the application of the method as described above, it is possible to discuss the scaling phenomena quantitatively and also to collect experience in regard to what may happen by changing the methods of operation in the field of scaling.

The data mentioned in this study have resulted from research studies undertaken by the Experimental Station for the Java Sugar Industry and have partly been published in the Communications (Mededeelingen) and Proceedings (Verhandelingen) of the Java Sugar Industry, published in the years 1930—1941.

11. The following publications among the general available literature

have to be mentioned for the analytical methods to be used on scale compositions:

Handboek voor de suikercultuur en de rietsuikerfabricage, Methoden van Onderzoek bij de Java Suikerindustrie, 6de druk, VAN INGEN, Surabaja, (1931).

BOGTSTRA, J. F., Het afzetseelvraagstuk in de suikerindustrie. Med. Proefstation Java Suikerindustrie, 911, (1932).

HONIG, P., Proceedings 7th Congress I.S.S.C.T. Queensland (1950).

———, Incrustations in Evaporators, Proceedings 24th Annual Meeting of the Association of Sugar Technologists of Cuba, Habana, Cuba, (1950).

———, The efficiency of Evaporators and the scaling problem, Azucar, I, Lima, Peru (1951).

*New York, January 1951.*

## ELASTICITY

### ELEMENTARY DERIVATION OF THE SHEARING STRESS DISTRIBUTION, THE ANGLE OF TWIST AND THE WARPING IN A PRISMATICAL SHAFT OF ELLIPTICAL CROSS SECTION TWISTED BY A TORQUE

BY

O. BAX STEVENS

(University of Indonesia)

(Communicated at the meeting of February 24, 1951)

#### Summary

In a prismatical shaft of elliptical cross section twisted by a torque, the shearing stress distribution is derived from the well-known geometrical relation existing between the ellipse and its major circle.

From the linear variation of the shearing stress components along lines parallel to the principal axes of the ellipse, an elementary method is developed to determine the angle of twist and the warping of the cross section.

#### Introduction

In a prismatical shaft of circular cross section (of radius =  $a$ ) twisted by a torque  $M$ , the *resultant* shearing stress ( $= \tau_{tc}$ ) varies linearly along any radius from:  $\tau_{tc} = 0$  at the centre to:  $\max. \tau_{tc} = (2M/\pi a^3)$  at the boundary.

The direction of  $\tau_{tc}$  is perpendicular to this radius.

If in fig. 1  $x_c$  and  $y_c$  denote the coordinates of any point  $P_c$  of the circular cross section with respect to an orthogonal system of axes through its centre  $O$ , then the *horizontal* ( $= \tau_{hc}$ ) and *vertical* ( $= \tau_{vc}$ ) shearing stress component respectively at this point is:

$$(1a) \quad \tau_{hc} = \frac{2M}{\pi a^4} y_c \quad \text{and:} \quad (1b) \quad \tau_{vc} = \frac{2M}{\pi a^4} x_c$$

From Eq. (1a) follows, that at points equidistant from the  $X$ -axis, the *horizontal* component ( $= \tau_{hc}$ ) is independent of  $x_c$  and equal to the *resultant* shearing stress at the point of the  $Y$ -axis with ordinate:  $y = y_c$ , whereas from Eq. (1b) follows that at points equidistant from the  $Y$ -axis, the *vertical* component ( $= \tau_{vc}$ ) is independent of  $y_c$  and equal to the *resultant* shearing stress at the point of the  $X$ -axis with abscissa:  $x = x_c$ .

It is evident that the sum of the moments of the *horizontal* elemental shearing forces ( $= dx_c \cdot dy_c \cdot \tau_{hc}$ ), with respect to the centre  $O$  of the circle,



is equal to:  $\frac{1}{2}M$ , which is also the case for the *vertical* elemental shearing forces ( $= dx_c \cdot dy_c \cdot \tau_{vc}$ ), hence:

$$\iint dx_c \cdot dy_c \cdot \tau_{hc} \cdot y_c = \iint dx_c \cdot dy_c \cdot \tau_{vc} \cdot x_c = \frac{1}{2} M.$$

A. *The distribution of shearing stresses in a twisted shaft of elliptical cross section*

An area with circular boundary defined by the equation:  $x^2 + y^2 = a^2$  can be transformed in an elliptical one defined by the equation:  $(x^2/a^2) + (y^2/b^2) = 1$  ( $a > b$ ) by reducing the ordinates  $y_c$  of all the points of

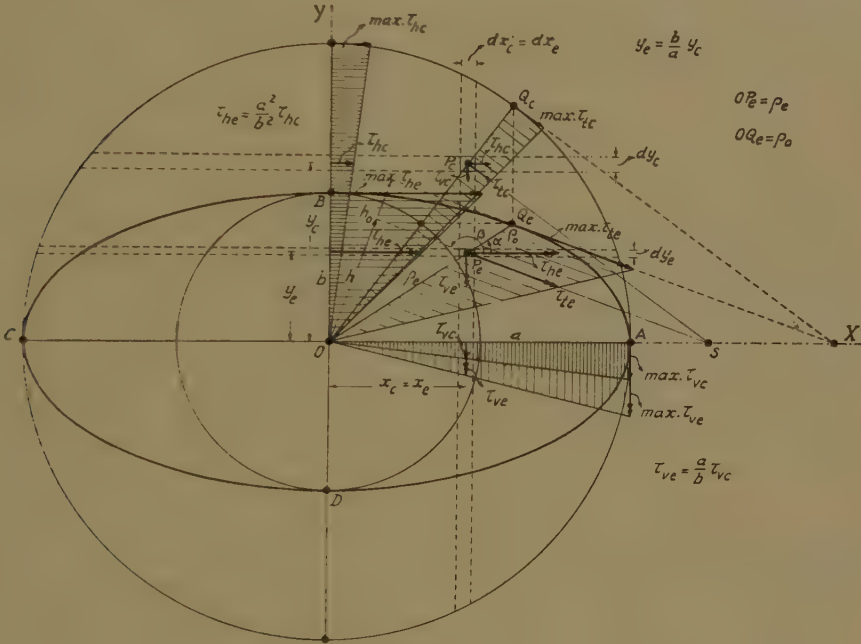


Fig. 1

this circular area in the ratio  $b/a$ , so that for instance any point  $P_c$  is shifted to  $P_e$  (see fig. 1). Hence the rectangular coordinates of  $P_e$  expressed in those of  $P_c$  become:

$$(2) \quad x_e = x_c \quad \text{and:} \quad y_e = \frac{b}{a} y_c.$$

If this transformation is applied to an originally circular cross section of a twisted shaft, then the *vertical* component of the elemental shearing force:  $dx_c \cdot dy_c \cdot \tau_{vc}$  at  $P_c$  is shifted parallel to the  $Y$ -axis to  $P_e$ . The elemental area:  $dx_c \cdot dy_c$  becomes therewith:  $dx_e \cdot dy_e$  or referring back to Eqs (2):  $dx_c \cdot (b/a) dy_c$ . The distance from the  $Y$ -axis and the direction (parallel to the  $Y$ -axis) of this *vertical* component of the elemental shearing force remain unchanged through this transformation, so that it may be concluded that the sum of the moments of the *vertical* components of the elemental

shearing forces with respect to the centre 0 of the elliptical cross section remains unchanged too and hence:

$$\iint dx_c \cdot dy_c \cdot \tau_{vc} \cdot x_c = \iint dx_e \cdot dy_e \cdot \tau_{ve} \cdot x_e = \frac{1}{2} M$$

and referring back to Eqs (2) we obtain:

$$\iint dx_e \cdot dy_e \cdot \tau_{ve} \cdot x_e = \iint dx_c \cdot \frac{b}{a} dy_c \cdot \tau_{ve} \cdot x_e = \frac{1}{2} M$$

from which follows:

$$\tau_{vc} = \frac{b}{a} \tau_{ve} \quad \text{or:} \quad \tau_{ve} = \frac{a}{b} \tau_{vc}$$

then from Eqs (1b) and (2):

$$(3) \quad \tau_{ve} = \frac{a}{b} \cdot \frac{2M}{\pi a^4} x_e = \frac{2M}{\pi a^3 b} x_e.$$

Thereby an expression is found for the distribution of the *vertical* components of the shearing stresses over an *elliptical* cross section.

Through this transformation the *horizontal* components of the elemental shearing forces:  $dx_c \cdot dy_c \cdot \tau_{hc}$  are displaced parallel to themselves and an expression for the magnitude of the *horizontal* components of the shearing stresses  $\tau_{he}$  in the elliptical cross section may be derived by observing that the sum of the moments of the *horizontal* components of the elemental shearing forces will also remain unchanged and is consequently equal to:  $\frac{1}{2}M$ . Hence:

$$\iint dx_c \cdot dy_c \cdot \tau_{hc} \cdot y_c = \iint dx_e \cdot dy_e \cdot \tau_{he} \cdot y_e = \frac{1}{2} M$$

and referring back to Eqs (2):

$$\iint dx_c \cdot dy_c \cdot \tau_{hc} \cdot y_c = \iint dx_c \cdot \frac{b}{a} dy_c \cdot \tau_{he} \cdot \frac{b}{a} y_c = \frac{1}{2} M$$

from which follows:

$$\tau_{hc} = \frac{b^2}{a^2} \tau_{he} \quad \text{or:} \quad \tau_{he} = \frac{a^2}{b^2} \tau_{hc}$$

then from Eqs (1a) and (2):

$$(4) \quad \tau_{he} = \frac{a^2}{b^2} \cdot \frac{2M}{\pi a^4} y_e = \frac{a^2}{b^2} \cdot \frac{2M}{\pi a^4} \cdot \frac{a}{b} y_e = \frac{2M}{\pi a b^3} y_e.$$

The formulas (3) and (4) together determine the distribution of the shearing stresses over the *elliptical* cross section. Formula (3) in particular determines the variation of the *resultant* shearing stress along the *major* axis of the ellipse (= *X*-axis), whereas formula (4) in particular determines the variation of the *resultant* shearing stress along the *minor* axis (= *Y*-axis).

The magnitudes of the shearing stresses along the principal axes of the ellipse being known, the *resultant* stress in any point of the elliptical

cross section can be graphically constructed. From this construction follows evidently a *linear* variation of the *resultant* shearing stress  $\tau_{te}$  along any radius of the ellipse.

To establish the relation which expresses this linear variation, we refer back to Eqs (3) and (4) from which follows that the *resultant* shearing stress at any point  $P_e$  is (see fig. 1):

$$(5) \quad \tau_{te} = \sqrt{\tau_{he}^2 + \tau_{ve}^2} = \frac{2M}{\pi ab} \sqrt{\frac{x_e^2}{a^4} + \frac{y_e^2}{b^4}}.$$

Changing from rectangular coordinates:  $x_e, y_e$  to polar coordinates  $\varrho_e$  and  $\alpha$  by substituting into Eq. (5) the relations:

$$x_e = \varrho_e \cos \alpha \quad \text{and:} \quad y_e = \varrho_e \sin \alpha$$

we obtain:

$$(6) \quad \tau_{te} = \frac{2M\varrho_e}{\pi ab} \sqrt{\frac{\cos^2 \alpha}{a^4} + \frac{\sin^2 \alpha}{b^4}}$$

thus for:  $\alpha = \text{constant}$   $\tau_{te}$  varies linearly along any radius from zero at the origin 0 to  $\text{max. } \tau_{te}$  at  $Q_e$  on the boundary.

Between the direction  $\alpha$  of the radius  $\varrho_e$  to  $P_e$  and the direction  $\beta$  of the *resultant* shearing stress at that point the following relation exists (see fig. 1):

$$\text{tg } \beta = \frac{-\tau_{ve}}{\tau_{he}} = -\frac{b^2}{a^2} \cotg \alpha$$

or:

$$(7) \quad \text{tg } \alpha \cdot \text{tg } \beta = -\frac{b^2}{a^2}$$

thus the direction of  $\tau_{te}$  at  $P_e$  is conjugate in the ellipse to the direction of the radius  $\varrho_e$  to  $P_e$  and independent of the position of the point on this radius, i.e. *the resultant shearing stresses in the consecutive points of any radius are parallel to each other and their direction coincides with the direction of the tangent through point  $Q_e$  on the elliptical boundary.*

If  $x_0$  and  $y_0$  denote the coordinates of point  $Q_e$  on the boundary, then from Eq. (5):

$$(8) \quad \text{max. } \tau_{te} = \frac{2M}{\pi ab} \sqrt{\frac{x_0^2}{a^4} + \frac{y_0^2}{b^4}}.$$

Thereby the variation of the *resultant* shearing stress along the elliptical boundary is found as a function of its coordinates.

It should be noted that the length of the normal drawn from the origin 0 onto the tangent through  $Q_e$  on the elliptical boundary is equal to:

$$h_0 = \frac{1}{\sqrt{\frac{x_0^2}{a^4} + \frac{y_0^2}{b^4}}}$$

so that:

$$(8a) \quad \text{max. } \tau_{te} = \frac{2M}{\pi ab h_0}.$$

It may be shown that the foregoing conclusions relating to the shearing stress components along any line parallel to one of the principal axes of the elliptical boundary holds also for any other line which is *not* parallel to one of the principal axes provided the components of the shearing stress are now taken in the direction of this line and in the direction *conjugate* to it (see fig. 2).

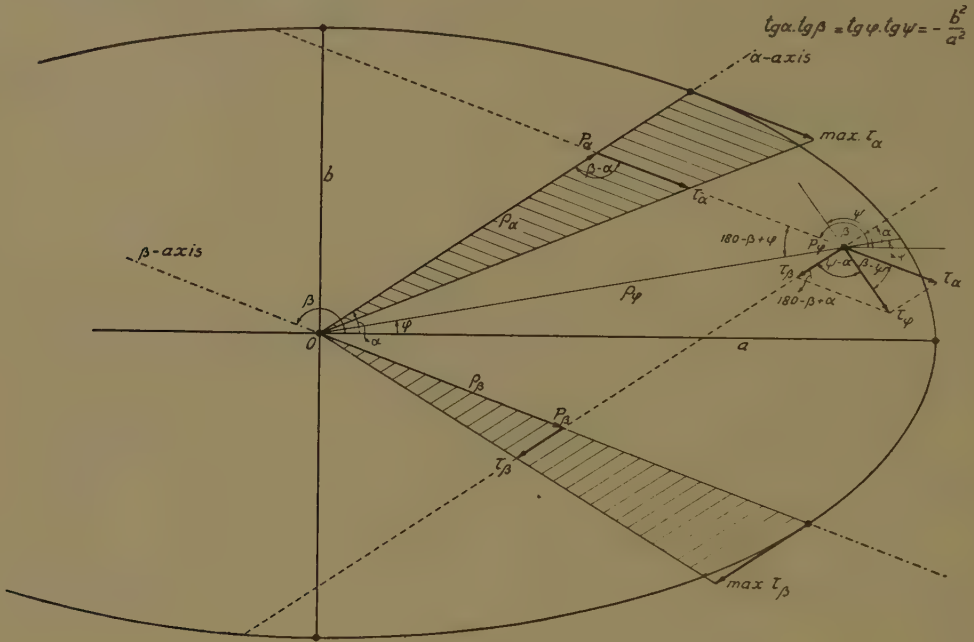


Fig. 2

### B. Determination of the angle of twist

The distribution of the shearing stress components  $\tau_{he}$  (see Eq. 4) over the cross section being known, we may now determine the *angle of twist* per unit length produced by these components exclusively.

Taking into consideration the remarkable variation of the  $\tau_{he}$ -components over the cross section it may be imagined that an element of the bar of unit length ( $dz = 1$ ) is cut out of a rectangular plate with sides equal to  $2a$  and  $2b$  (see fig. 3). This plate in turn may be imagined to be subdivided by planes perpendicular to the  $X$ -axis in a number of similar elemental bars of square cross section and unit area and length equal to  $2b$  (see figs 3 and 4).

The linear distribution of the shearing stress components  $\tau_{he}$  over the lateral sides of all these elemental bars being the same, it is evident that their distortion under *free* deformation will be similar and consequently will fit together after their distortion as portions of the rectangular plate without any interference of additional stresses so that the condition of continuity of deformation is satisfied (see fig. 3).

Due to the  $\tau_{he}$ -component at a point  $x_e, y_e$  (see fig. 5) of the upper plane



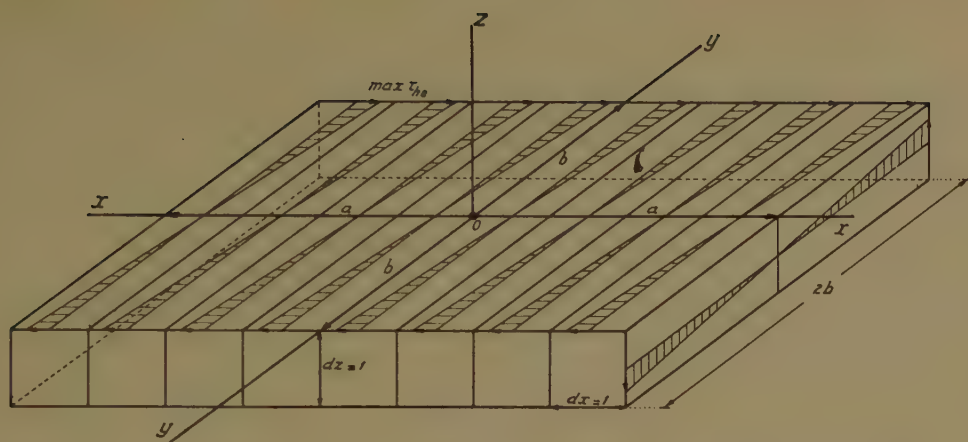


Fig. 3

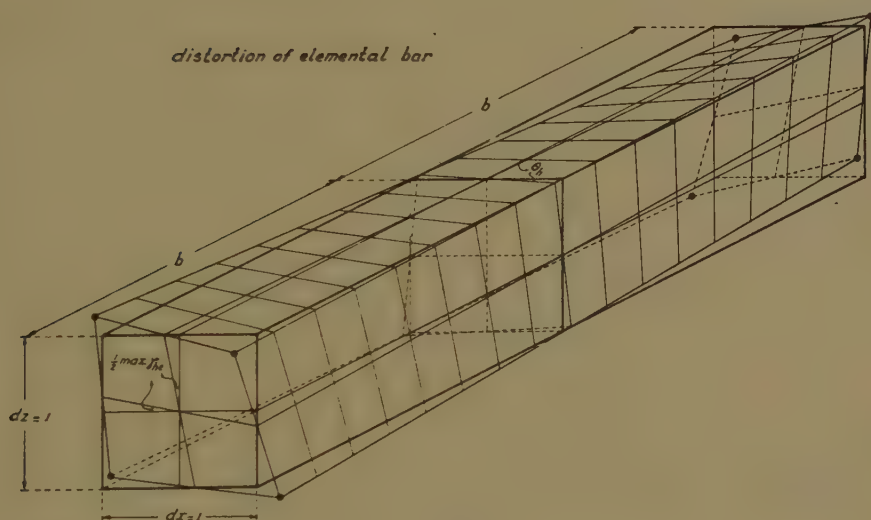


Fig. 4

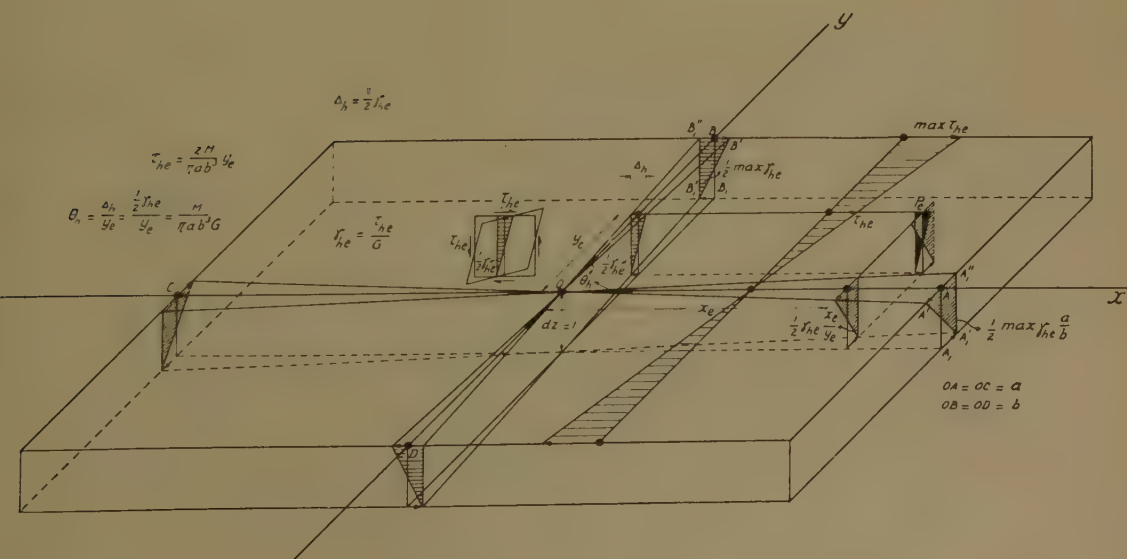


Fig. 5

of the rectangular plate, this point will be displaced with respect to the corresponding point  $x_e, y_e$  of the lower plane in the first instance perpendicular to the  $Y$ -axis. This relative displacement is by virtue of Hooke's law:

$$\Delta_h = \frac{1}{2} \gamma_{he} = \frac{1}{2} \frac{\tau_{he}}{G} \quad (\text{for } dz = 1)$$

in which:  $\gamma$  = shearing strain and:  $G$  = modulus of elasticity in shear, and from Eq. (4):

$$\Delta_h = \frac{M}{\pi a b^3 G} y_e$$

hence proportional to  $y_e$ .

*Consequently lines initially parallel to the  $Y$ -axis remain straight after free deformation through the action of  $\tau_{he}$ .*

The angular rotation:  $\theta_h = (\Delta_h/y_e) = (\frac{1}{2} \gamma_{he}/y_e)$  of the line:  $x = x_e$  is consequently:  $\theta_h = (M)/(\pi a b^3 G)$  and equal to the angular rotation of the  $Y$ -axis and this is the case for any line parallel to the  $Y$ -axis.

Since the  $\tau_{he}$ -components are considered exclusively, there are no shearing stresses acting in the planes perpendicular to the  $Y$ -axis and consequently the lines:  $y = y_e$  will rotate together with the lines:  $x = x_e$  through an equal angle  $\theta_h$ .

However, due to the additional angular rotation  $\theta_h$  of the lines:  $y = y_e$ , an additional relative displacement:  $\Delta_v = \theta_h \cdot x_e$  of  $P_e$  parallel to the  $Y$ -axis will result, so that the total relative displacement will be:

$$\begin{aligned} \Delta_t &= \sqrt{\Delta_h^2 + \Delta_v^2} = \sqrt{(\theta_h \cdot y_e)^2 + (\theta_h \cdot x_e)^2} = \\ &= \theta_h \sqrt{x_e^2 + y_e^2} = \theta_h \cdot \rho_e \end{aligned}$$

i.e. proportional to the distance of  $P_e$  to the centroid.

The direction of  $\Delta_t$  is:

$$\frac{\Delta_v}{\Delta_h} = \frac{-\theta_h \cdot x_e}{\theta_h \cdot y_e} = -\frac{x_e}{y_e}$$

i.e. perpendicular to the direction of  $\rho_e$ , so that it can be concluded that each radius, and consequently, the whole cross section, rotates about  $O$  through the same angle.

Likewise it may be concluded that due to the action of the  $\tau_{re}$ -components, the whole cross section will rotate about its centroid through the angle:

$$\theta_e = \frac{M}{\pi a^3 b G}.$$

Hence according to the principle of superposition the resultant angle of twist per unit length of the bar  $\theta_t$  will be obtained by adding the angular rotations  $\theta_h$  and  $\theta_v$  thus:

$$\theta_t = \theta_h + \theta_v = \frac{M (a^2 + b^2)}{\pi a^3 b^3 G}.$$

The relative resultant displacement of  $P_e$  is:

$$\theta_i \cdot \varrho_e$$

and perpendicular to the direction of  $\varrho_e$ .

### C. *Warping of the cross section*

It has been shown that lines initially parallel to the principal axes of the ellipse remain straight after deformation and rotate through an angle  $\theta_i$  and about their point of intersection with the axis to which they are perpendicular.

Considering the free deformation it can furthermore be concluded that besides this angular rotation  $\theta_i$  in the plane of the cross section, the lines perpendicular to the principal axes of the ellipse moreover rotate in planes perpendicular to the axis which they intersect and about their point of intersection with this axis.

This may readily be understood if the free deformation of the square cross sections of the elemental bars be considered (see fig. 4). For any line  $y = y_e$  along which  $\tau_{he}$  acts, rotates about the  $Y$ -axis (condition of symmetry) through an angle (see fig. 6):

$$\frac{1}{2} \gamma_{he} = \frac{1}{2} \frac{\tau_{he}}{G} = \frac{M}{\pi a b^3 G} y_e$$

and thus the vertical displacement:  $z_h$  of  $P_e(x_e, y_e)$  is:

$$z_h = \frac{1}{2} \gamma_{he} \cdot x_e = \frac{M}{\pi a b^3 G} x_e y_e.$$

Likewise it may be shown that  $\tau_{re}$  acting along any line:  $x = x_e$  produces a rotation of the line about its intersection with the  $X$ -axis and consequently a vertical displacement  $z_v$  of  $P_e$  which may be expressed by:

$$z_v = \frac{-M}{\pi a^3 b G} x_e y_e$$

and in a plane perpendicular to the  $X$ -axis but now in a direction opposite to  $z_h$  as can be easily verified.

Thus the resultant vertical displacement  $z_t$  of  $P_e$  will be:

$$z_t = \frac{M(a^2 - b^2)}{\pi a^3 b^3 G} x_e y_e.$$

From this expression it may be seen that the warped cross section is an *hyperbolic paraboloid*. Such a surface is also called a *ruled surface* because it consists of two systems of straight lines which are here the intersections of the curved surface with planes perpendicular to the principal axes of the cross section.

Intersections of this surface with planes through the longitudinal axis of the twisted bar ( $Z$ -axis) are parabolas whereas intersections with planes perpendicular to this axis are hyperbolas with their asymptotes parallel to the principal axes of the cross section.

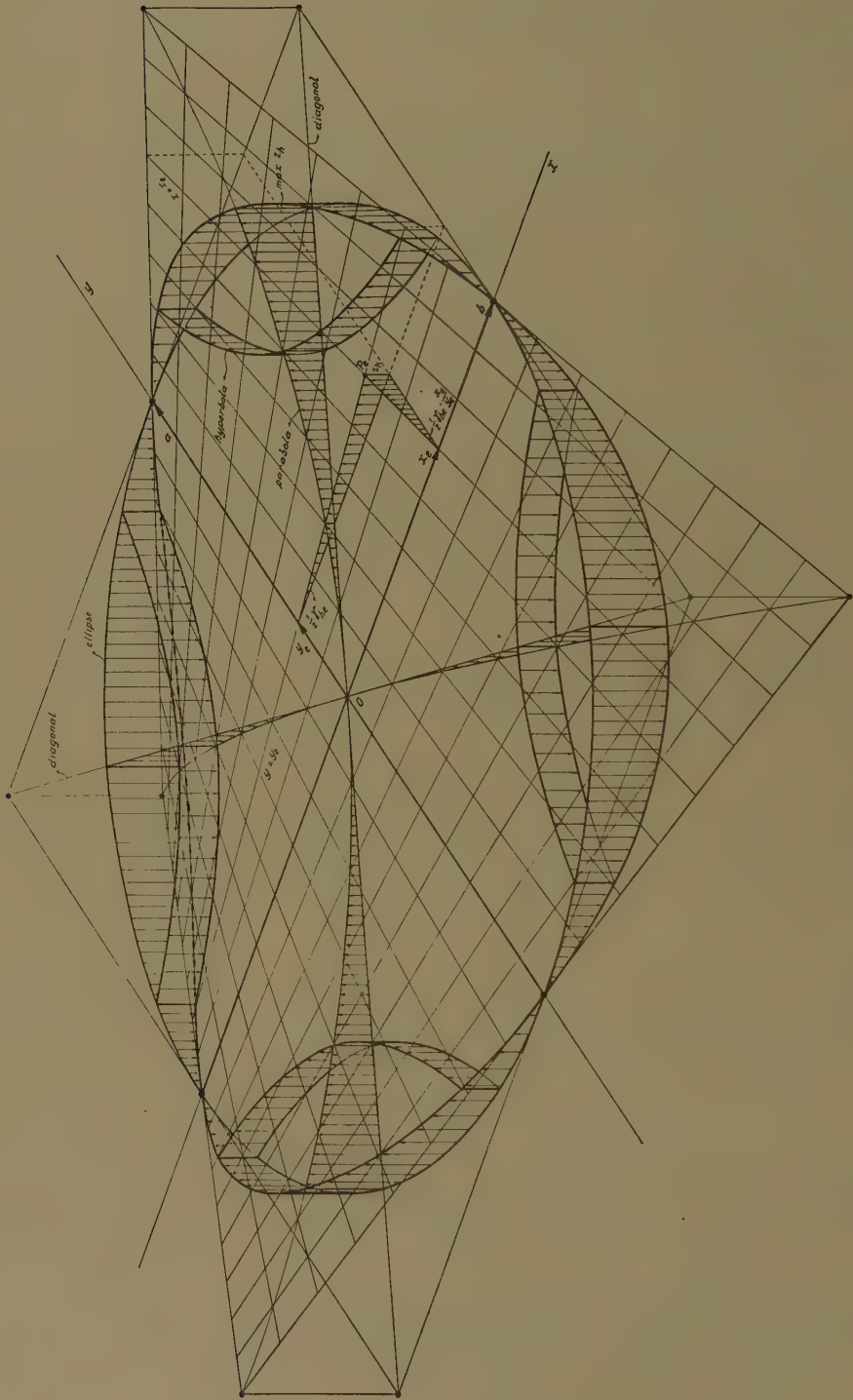


Fig. 6



O. BAX STEVENS: *Elementary derivation of the shearing stress distribution, the angle of twist and the warping in a prismatical shaft of elliptical cross section twisted by a torque.*

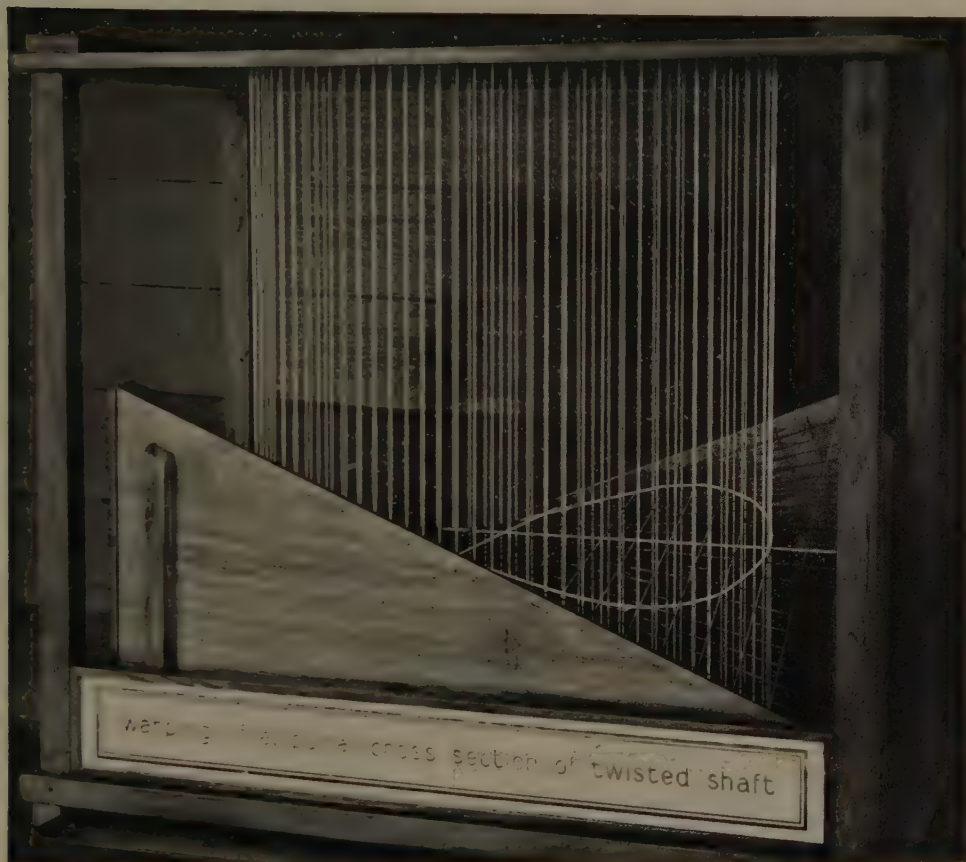


Fig. 7

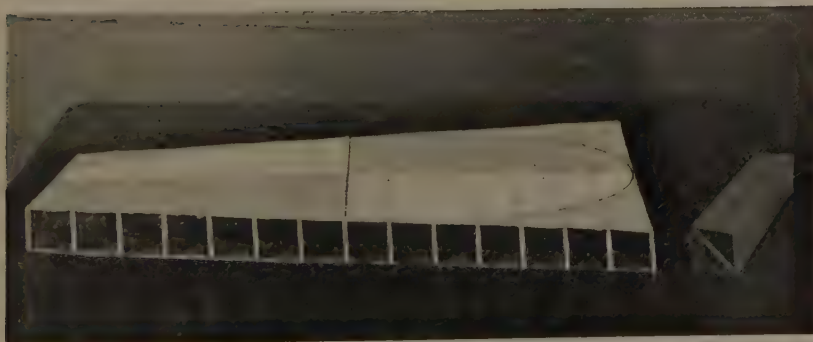


Fig. 8



The principal axes of the ellipse divide the cross section in quadrants which are warped alternately *upward* and *downward* as may be easily checked.

It is furthermore interesting to note that the points at which  $z_i$  is maximum are found at the intersections of the diagonals of the circumscribed rectangle and the elliptical boundary. This maximum displacement is:

$$\max. z_i = \frac{M(a^2 - b^2)}{2\pi a^2 b^2 G}.$$

To visualize the warping of the cross section a string model may be constructed as shown on the picture (see fig. 7). The free deformation of an elemental bar as discussed previously may be demonstrated by means of a square tube constructed of tin-plate as shown on the picture (see fig. 8).

By placing any number of these tubes side by side a rectangular plate is obtained showing the actual total distortion (i.e. rotation about the longitudinal axis of the shaft together with the warping of the cross section) due to the action of the shearing stresses (see fig. 8).

*Bandung, February 1950.*

SUR LE MÉTAMORPHISME À GLAUCOPHANE DANS LA NAPPE  
DES SCHISTES LUSTRÉS DE LA CORSE

PAR

H. A. BROUWER ET C. G. EGELER

(Communicated at the meeting of March 31, 1951)

Les roches à amphiboles et pyroxènes sodiques dont il sera question dans les pages suivantes font partie de la nappe des schistes lustrés, qui est charriée de l'Est à l'Ouest vers le massif autochtone de la Corse occidentale <sup>1</sup>). Ces roches métamorphiques sont issues de roches éruptives (gabbros, dolérites, spilites) et de roches sédimentaires, le plus souvent riches en produits de projections volcaniques.

Les roches à amphiboles et pyroxènes sodiques ont une grande extension dans la partie orientale de la Corse. On les trouve à divers endroits au Cap Corse, dans la région à l'Ouest de Bastia, dans la vallée de l'Insecca au Sud-Ouest de Biguglia, dans une zone d'une longueur de plus de 50 kilomètres au Nord et au Sud de Morosaglia, dans les environs de Cervione et Moita, à l'Ouest de Piedicorté, à plusieurs endroits près de Vezzani et au Nord-Est de Lugo <sup>2</sup>).

Notre étude du groupe des roches à glaucophane de la Corse a été faite avec l'aide financière de l'Organisation Néerlandaise des Recherches Pures (Z.W.O.). Nos recherches sur le terrain furent exécutées pendant l'été de 1949. Nos études préliminaires en 1947 <sup>3</sup>) et les renseignements qui nous ont été donnés par des étudiants de l'Université d'Amsterdam, travaillant en Corse, ont facilité nos investigations.

Dans les pages suivantes nous donnerons un aperçu de nos observations dans trois régions caractéristiques: la région à l'Ouest de Vezzani, la région du San Pétrone au Sud de Morosaglia et la région de la Serra di Pigno à l'Ouest de Bastia.

---

<sup>1</sup>) Localement des roches à amphiboles sodiques (surtout crossite) ont été trouvées aussi dans la partie orientale du massif autochtone, jusqu'à une distance assez grande du pays de nappes, entre autres dans des roches dioritiques qui montrent l'influence des dislocations alpines.

<sup>2</sup>) Voir la Carte Géologique de la France 1 : 80.000 (feuilles Bastia et Corte) et la Carte no. 1 de PILGER (Abh. Ges. der Wiss. Göttingen, Math. Phys. Kl. III Folge, 19, 1—43, (1939)).

<sup>3</sup>) H. A. BROUWER et C. G. EGELER. Sur les granites alpins de la Corse. Proc. Kon. Ned. Akad. v. Wetensch. Amsterdam, 51, No. 3, 302—307 (1948); C. G. EGELER, On glaucophane-bearing rocks from Corsica, Ibid, No. 5, 556—564.



### Région de Vezzani

Nos recherches ont été faites dans la région à l'Ouest de Vezzani, où les collines rocheuses d'ophiolites descendent du chemin de Vezzani à Vivario, jusqu'à la mine de cuivre abandonnée près du chemin de Rospigliani à Noceta (fig. 1). La plupart des roches étudiées sont des

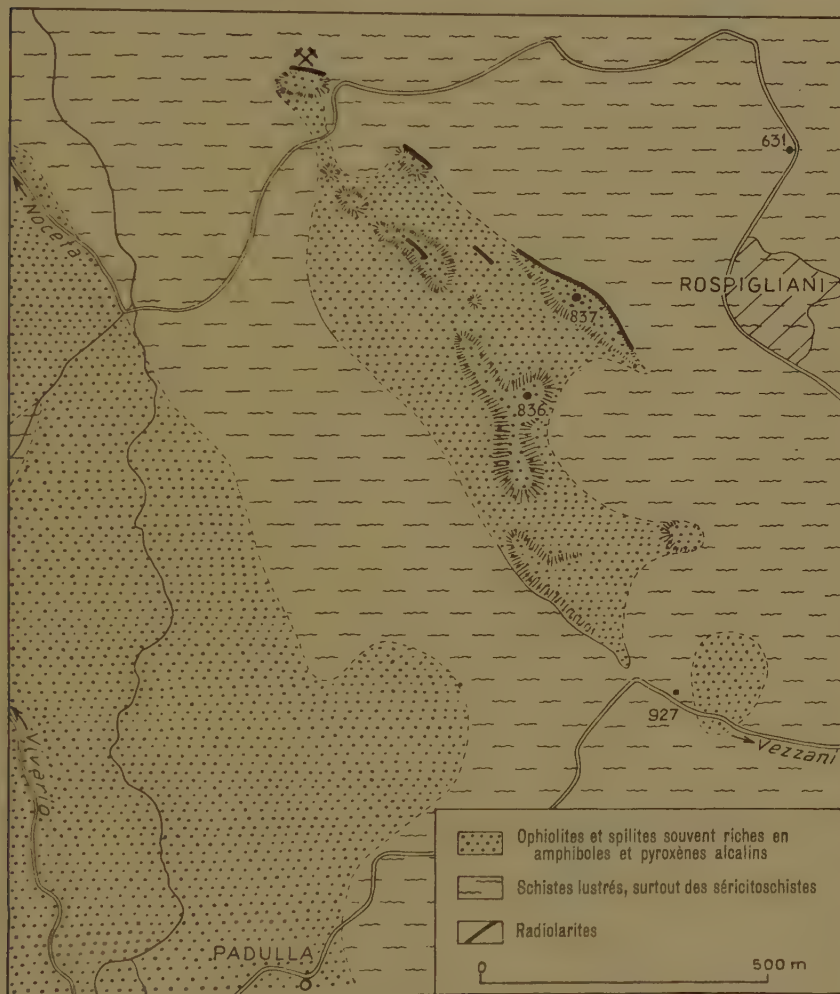


Fig. 1. Région à l'Ouest de Vezzani (par S. B. SPIJER)

dolérites et des spilites plus ou moins métamorphisées en types riches en amphiboles et pyroxènes alcalins. Au sud du chemin de Vezzani à Vivario on trouve des dolérites, en partie porphyriques, qui ont encore complètement conservé leur structure ophitique et dans lesquelles le métamorphisme s'est limité à une conversion des feldspaths en pumpellyite et albite et un commencement d'altération d'augite en aegyrine. Associé aux dolérites et spilites métamorphisées on trouve au Sud et au Nord

de la route de Vezzani à Vivario des roches leucocrates, formant le plus souvent un réseau de veines et quelquefois des masses plus grandes qui peuvent contenir des inclusions irrégulières des roches basiques métamorphiques. Ces roches leucocrates montrent surtout des types riches en feldspath et aussi des transitions à des types quartzo-feldspatiques, qui tous les deux contiennent généralement des amphiboles et pyroxènes sodiques d'origine métamorphique. La structure est presque toujours reconnaissable comme une structure magmatique. Nous pensons qu'elles représentent les portions acides et résiduelles du magma ophiolitique. Leur cristallisation était antérieure au métamorphisme glaucophanitique. MM. TH. A. F. NETELBEEK et S. B. SPIJER, qui ont étudié ces roches dans la même région et dans d'autres, sont d'accord avec nous sur cette interprétation.



Fig. 2. Veines leucocrates quartzo-feldspathiques à crossite dans une crossite à albite; petite colline au Sud de la mine de cuivre abandonnée, près de la route de Rospigliani à Noceta

Pour comparer la composition chimique d'une crossite à albite avec celle d'une veine leucocrate quartzo-feldspatique à crossite de la même localité (fig. 2), nous donnons ci-dessous les analyses I et II.

La colline 837 est composée de roches basiques métamorphisées dans une masse carbonatée riche en trémolite, qui est souvent associée à des amphiboles alcalines. On trouve aussi des masses carbonatées riches en

	I	II
SiO <sub>2</sub>	54.65	74.19
Al <sub>2</sub> O <sub>3</sub>	12.52	13.99
Fe <sub>2</sub> O <sub>3</sub>	5.55	0.81
FeO	5.97	0.92
MgO	5.32	0.94
CaO	3.87	0.68
Na <sub>2</sub> O	6.30	7.32
K <sub>2</sub> O	0.21	0.08
H <sub>2</sub> O <sup>+</sup>	2.15	0.64
H <sub>2</sub> O <sup>-</sup>	0.07	0.07
CO <sub>2</sub>	—	0.02
TiO <sub>2</sub>	2.99	0.28
P <sub>2</sub> O <sub>5</sub>	0.36	0.03
MnO	0.15	0.03
	100.11	100.00

I. *Crossitite à albite riche en chlorite*; petite colline au Sud de la mine de cuivre abandonnée, près de la route de Rospigliani à Noceta. Anal. Lab. Lobry de Bruyn.

II. *Roche leucocrate quartzo-feldspatique à crossite*, formant des veines irrégulières dans la roche I. Anal. Lab. Lobry de Bruyn.

pyroxènes alcalins quelquefois englobants des reliques d'augite magmatique. La couleur rougeâtre du carbonate résulte de la présence d'hématite. Localement on trouve de la picotite et nous supposons que ces roches sont formées par calcification d'une masse hétérogène de serpentine, dolérites et spilites, la calcification ayant principalement influencé les zones fortement brisées.

### Région du San Petrone

Le San Petrone (1766 m.) est le plus haut sommet de la nappe des schistes lustrés en Corse. La base de cette montagne est formée de serpentine, les parties plus élevées sont formées d'une série épaisse de schistes à glaucophane avec une direction N-S et un plongement assez fort vers l'Ouest (fig. 3 et 4).

Cette série se compose principalement de schistes à glaucophane et lawsonite souvent avec du grenat et un pyroxène alcalin. Quelquefois les roches contiennent des pseudomorphoses de phénocristaux de feldspath, pour la plus grande partie en lawsonite accompagnée de muscovite. Dans d'autres roches des concentrations lenticulaires de lawsonite sont considérées comme de même origine, indiquant que ces roches sont issues de roches éruptives porphyriques.

Dans la partie Nord-Est de la région, près de la ruine de la chapelle de San Pietro d'Accia, on trouve un petit massif de gabbro à glaucophane. Ces roches montrent des degrés variés de transformation. Les types les moins altérés contiennent des reliques de diallage, généralement entouré

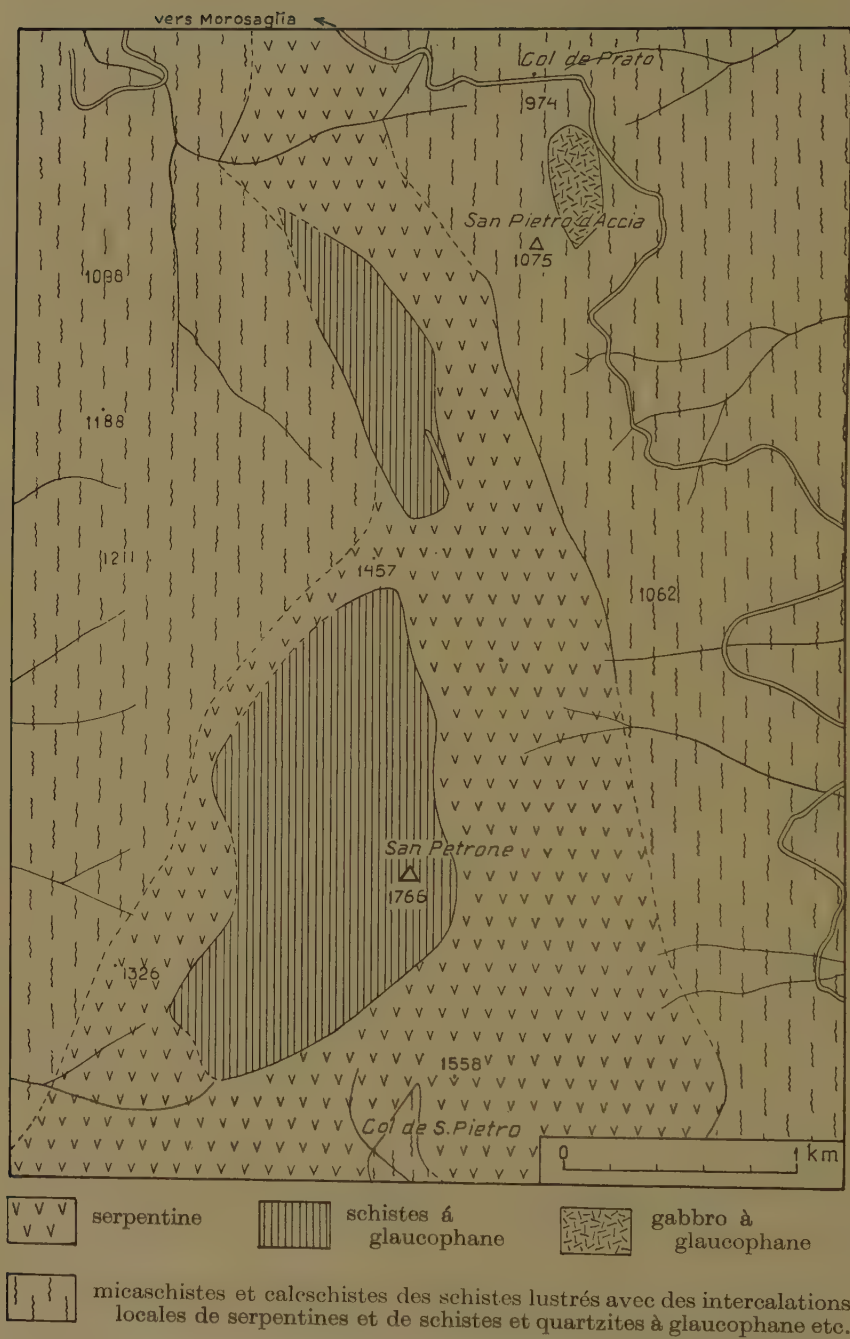


Fig. 3. Région du San Pedrone (par W. M. J. LINCKENS).



d'aggrégats de glaucophane. Des pyroxènes alcalins, de la chlorite et du talc ont été observés aussi. Les plagioclases calciques sont maintenant représentés par de l'albite avec de la lawsonite et de l'épidote. Les types plus schisteux sont plus riches en amphiboles sodiques, accompagnées de pyroxènes alcalins, de lawsonite et d'épidote.

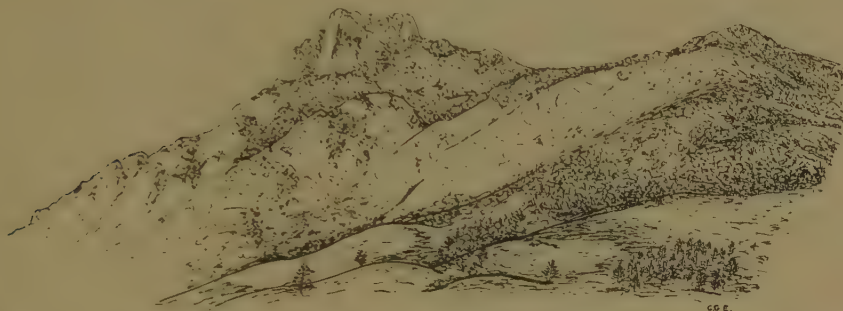


Fig. 4. *Le San Petrone vu de l'Est*. Les sommets se composent de schistes à glaucophane, reposant sur une grande masse de serpentine.

Près du point 1188 dans la partie Nord-Ouest de la région se trouvent des quartzites blancs à glaucophane et crossite alternant avec des schistes bleus à glaucophane et crossite, riches en albite et lawsonite. Ces quartzites, qui sont très schisteux, contiennent des porphyroblastes d'amphiboles alcalines quelquefois dépassant 5 mm. Les autres minéraux, qui accompagnent le quartz et les amphiboles alcalines, sont la muscovite, la chlorite, l'épidote (souvent avec un noyau d'allanite), la lawsonite, l'albite, le sphène, le rutile, la tourmaline, l'apatite, la pyrite et la calcite. Souvent les amphiboles alcalines sont brisées; quelquefois elles sont chloritisées et la chlorite forme parfois des pseudomorphoses complètes.

Dans la partie méridionale de la région, au-dessus du Col de San Pietro, des types de composition variables, riches en amphiboles et pyroxènes alcalins, forment des intercalations d'une épaisseur très variée dans les quartzoschistes et calcschistes des schistes lustrés, constituant un complexe très plissé. On peut distinguer entre autres des schistes à crossite, chlorite, calcite et muscovite, des schistes quartzifères à crossite, épidote et chlorite, des types extrêmes à lawsonite et pyroxène riche en jadéite, des types à muscovite et pyroxène alcalin contenant souvent du grenat et de la crossite et des roches riches en grenat avec albite, muscovite et pyroxène alcalin. Il semble que ces roches contenaient originalement une assez grande quantité de matériaux tuffogènes.

### *Région de la Serra di Pigno*

La base orientale du massif de la Serra di Pigno (Fig. 5) à l'Ouest de Bastia est formée principalement par une série de schistes à glaucophane avec des intercalations de micaschistes. Ces schistes à glaucophane



Fig. 5. *La Serra di Pigno vue de l'Est*. Le plateau à la base est formée principalement par des schistes à glaucophane. Les roches au dessus du plateau se composent de gneiss albitiques associés à des schistes à glaucophane et des glaucophanites plus ou moins granitisées

sont d'une composition variée; on trouve entre autres des schistes à glaucophane et lawsonite en partie grenatifères et des schistes à glaucophane et épidote, en partie avec de la chlorite et souvent très riches en muscovite. La teneur en albite d'origine métasomatique est très variable. Plus haut ces roches, que nous considérons pour la majeure partie comme d'origine tuffogène, passent à des glaucophanites plus massives d'origine magmatique (localement on trouve encore des gabbros à glaucophane), tandis que près du sommet recommencent les schistes à glaucophane avec des intercalations de schistes lustrés. Surtout la partie supérieure de la série inférieure et les roches en-dessus ont subi l'influence intensive d'une granitisation. Dans les roches schisteuses une infiltration lit par lit a donné lieu à une alternance de gneiss à albite et muscovite ("granite alpin")<sup>1)</sup> et des schistes à glaucophane qui sont souvent feldspatisés. On trouve aussi des roches gneissiques ocellées et des roches plus massives, qui sont des glaucophanites plus ou moins granitisées.

Dans les schistes à glaucophane de la partie inférieure de la série inférieure on ne trouve généralement que des porphyroblastes d'albite. La ressemblance des porphyroblastes avec ceux des schistes plus fortement granitisés nous amène à considérer leur formation comme un début de granitisation.

### *Considérations sur le métamorphisme*

La formation des roches métamorphiques dans lesquelles la soude est entrée en partie ou totalement dans des amphiboles ou pyroxènes alcalins, a été discutée depuis longtemps. Il paraît que ces roches peuvent être produites par un métamorphisme régional sans influence directe d'intrusions magmatiques, mais qu'en d'autres cas le métamorphisme peut être plus locale, limité à des zones d'addition pneumatolitique ou hydrothermale au contact de roches magmatiques.

En Corse nos investigations indiquent que le métamorphisme à glaucophane est un métamorphisme régional, contrôlé principalement par des conditions physiques. Nous n'avons pas trouvé d'indications d'une relation directe entre ce métamorphisme et les intrusions des magmas ultra-basiques, pour lesquelles on peut même prouver en quelques cas que leur intrusion a précédé le métamorphisme régional. Il est évident que c'est aussi le cas pour les gabbros, dolérites et spilites, desquels est issue la majeure partie des roches à glaucophane. Ceci n'exclut pas un apport sodique prémétamorphique dans les roches au contact des ophiolites. Nous n'avons pas trouvé non plus des indications que la granitisation alpine est en relation causale avec la formation des roches à glaucophane, ce qui ne veut pas dire que ces roches métamorphiques ne peuvent pas être influencées par cette granitisation avant leur cristallisation finale (formation de schistes à

---

<sup>1)</sup> Le nom granite alpin pour ces roches a été introduit par PILGER (loc. cit).



porphyroblastes d'albite et de gneiss à glaucophane). La distribution des roches à glaucophane est telle qu'on les trouve aussi dans des régions où il n'y a pas trace de granitisation à la surface. Il est d'ailleurs certain que, dans les régions où on trouve les roches à glaucophane et la granitisation ensemble, la formation de la glaucophane et des minéraux associés était déjà avancée au commencement de la granitisation.

Nous réservons pour une publication ultérieure la discussion de la composition chimique des roches à amphiboles et pyroxènes sodiques.

### *Granitisation et métamorphisme dans l'histoire orogénique*

Quoique certaines veines donnent l'impression d'être injectées, l'origine la plus fréquente des gneiss albitiques ("granites alpins") semble être une transformation des roches préexistantes, imprégnées ou infiltrées par des solutions de granitisation. Dans la région à l'Ouest de Bastia on trouve toutes les transitions entre des roches à glaucophane ne montrant aucun signe de granitisation et des variétés qui sont presque complètement granitisées. Des observations, quoique locales, indiquent que les mouvements tectoniques ont commencé avant la granitisation (inclusions de trainées à glaucophane plissées dans les porphyroblastes d'albite), qu'ils ont continué pendant la granitisation (inclusions sigmoïdes dans les porphyroblastes d'albite) et qu'ils ont continué souvent encore après la granitisation (cataclase intensive de quartz et feldspath et plissement des roches après la granitisation). Que la granitisation a certainement eu lieu en partie en même temps qu'une phase relativement tardive des mouvements et peut avoir continué après, est indiqué par le fait qu'on observe aussi des porphyroblastes d'albite non cataclastiques et des filons discordants de pegmatite et de quartz en relation avec les roches granitisées. Le fait que des "granites alpins" et des phénomènes de granitisation dans les schistes lustrés sont souvent localisés dans la zone de bordure de la nappe des schistes lustrés, touchant au pays autochtone ou parautochtone<sup>1)</sup>, pourrait indiquer une relation entre les plans de charriage et l'ascension de solutions de granitisation, ce qui serait en concordance avec ce que nous avons dit sur l'âge relatif des mouvements et de la granitisation.

Quant à l'âge de la formation des roches à glaucophane par rapport à la granitisation, il est évident que la plupart des minéraux formés par ce métamorphisme sont antérieurs à la granitisation. Mais on constate souvent que les minéraux de ce métamorphisme se sont formés pendant la granitisation et même postérieurement à elle (cristallisation simultanée de cristaux de glaucophane et de quartz de granitisation, cristallisation de lawsonite dans les gneiss granitiques, formation de glaucophane dans des zones granuleuses dans le quartz de granitisation, enrichissement de glaucophane le long de veines quartzo-feldspatiques et autour d'imprégnations de

<sup>1)</sup> H. A. BROUWER. Sur la tectonique de la Corse. Proc. Kon. Ned. Akad. v. Wetensch. 53, No.1, 3—8 (1950).



quartz). Ainsi la granitisation se serait effectuée au moins en partie sous des conditions qui permettent à la glaucophane de se former. En considérant l'âge de la granitisation par rapport aux mouvements, on peut conclure que la formation de minéraux du métamorphisme à glaucophane a continué dans une phase assez avancée des mouvements orogéniques. On peut considérer le métamorphisme rétrograde, qui a été observé en plusieurs endroits (déformation et chloritisation des amphiboles alcalines, altération de lawsonite en chlorite, séricite ou épidote) comme accompagnant des mouvements plus tardifs.

*Institut de Géologie  
de l'Université d'Amsterdam.*

## GEOLOGY

# THE WATER BORE OF ORANJESTAD 1942—1943, AND ITS IMPLICATION AS TO THE GEOLOGY AND GEOHYDROLOGY OF THE ISLAND OF ARUBA (*Netherlands West Indies*) I

BY

J. H. WESTERMANN

(Communicated by Prof. G. H. R. VON KOENIGSWALD at the meeting of Jan. 27, 1951)

### *Summary*

In 1942—1943 a water test well was drilled by the Government of Curaçao within the limits of Aruba's capital Oranjestad, following the "discovery" of an underground fresh water flow by two French friars operating a detector or divining rod. A depth of 927' was reached without encountering the predicted fresh water. However, abundant salt water under pressure was struck in a sand bed at 830'. Its salt concentration proved to be twice that of sea water. It may be assumed that rain water entering the outcrop area of weathered diorite and diorite detritus further inland, percolates down through a dipping sand bed, locked in by impervious clay layers, thus constituting an artesian water system. The high salinity of this water is tentatively explained by a process of solution of salts adsorbed in the sands and clays during their deposition in a marine or coastal environment.

Practically all sediments penetrated by the bore carry salt water. A survey of ground water localities all over the island reveals a generally high salinity, coupled with a limited supply, offering unfavourable conditions for intensive ground water production.

The test well has considerably increased our knowledge of the Tertiary and Quaternary formations of the island. Clayey and sandy deposits of marine origin were encountered, so far unknown in Aruba. Quaternary coral limestones, totalling some 300 feet, overlie unconformably foraminiferal clays and sands of (presumably Lower to Middle) Miocene age, the latter series reaching down to 830'. From 830' to 930' a probably non-marine mica sand, carrying the above-mentioned artesian salt water, was penetrated. A Schlumberger survey, measuring electrical resistivities in rocks, has determined the depth of the basement under the drill-hole location as approximately 1610'. Most likely this basement is of a dioritic character.

Further drilling unto the basement would probably meet with more water-bearing sand beds. The prospects are that this water will be likewise salt water.

### *General*

On the 1st September of the year 1941 the people of Curaçao and Aruba were greatly stirred by the newspaper announcement that two French friars from Venezuela, Frères APPOLLINAIRE and JUAN, predicted the occurrence of an underground fresh water flow in the island of Aruba. Their detection was based on a research carried out with divining rod and pendulum. According to the friars the water flow would be in easy drilling reach, just below the capital Oranjestad<sup>1</sup>). It was believed that this fresh water would originate in the Sierra Nevada de Santa Marta of Colombia, moving subsequently below the Caribbean Sea and rising somewhat after reaching Aruba. Its further course should be sought in the direction of Curaçao and beyond.

In view of the great need of fresh water the Government of Curaçao undertook to drill a hole at a location opposite the Roman Catholic church of Oranjestad marked carefully by the friars (550 m. NE of the coast; altitude 4.5 m). The drilling was carried out by an American contractor, with a cable tool drilling outfit, and lasted from June 29th until September 11th, 1942.

Abundant salt water was encountered below 666' and below 830'. On September 11th, after reaching a depth of 937' drilling work was interrupted owing to shortage of equipment and pending the arrival of new material. It was resumed on 18th January 1943. Because of technical set-backs and taking into account geological advice, it was finally decided to abandon the project (17th April 1943). There had been practically no progress since the depth of 937' was reached.

*Outline of the geology of Aruba, with particular reference to the subsoil of Oranjestad as revealed by the water bore and the electrical sounding survey.*

The oldest rocks of Aruba are found in the centre; they consist of a diabase and diabase tuff series, presumably of Cretaceous age. Orogenic processes and the simultaneous intrusion of a quartz-dioritic magma — occurring in older Tertiary time — have metamorphosed this series to a large extent. The intruding magma differentiated into a variety of igneous rocks of which in particular quartz-diorite occupies large areas of the present island surface.

These two older formations are covered unconformably by limestone of Tertiary and Quaternary age. The older beds of this limestone show

---

<sup>1</sup>) According to the friars there would be two fresh water flows below the capital, one to the Northwest of the Roman Catholic church at a depth of 902 feet (water displacement would amount to 45 cubic meters per minute), and a second flow in the neighbourhood of Companasji, not far from the R.C. school, at a depth of 738 feet (water displacement 53 cubic meters per minute). The newspaper *Amigoe di Curaçao* of 1st April 1942, from which the above figures are quoted, does not mention the dimensions of the transverse section of the supposed water "channels".

distinct dipping and are remnants of a slightly arched limestone cap which in earlier times appears to have covered a great part of the island. Younger limestone beds at the periphery of the previously existing cap are present as horizontal terraces, bordering on the sea. The facies of the limestone is predominantly coralline, *Lithothamnium* being widespread.

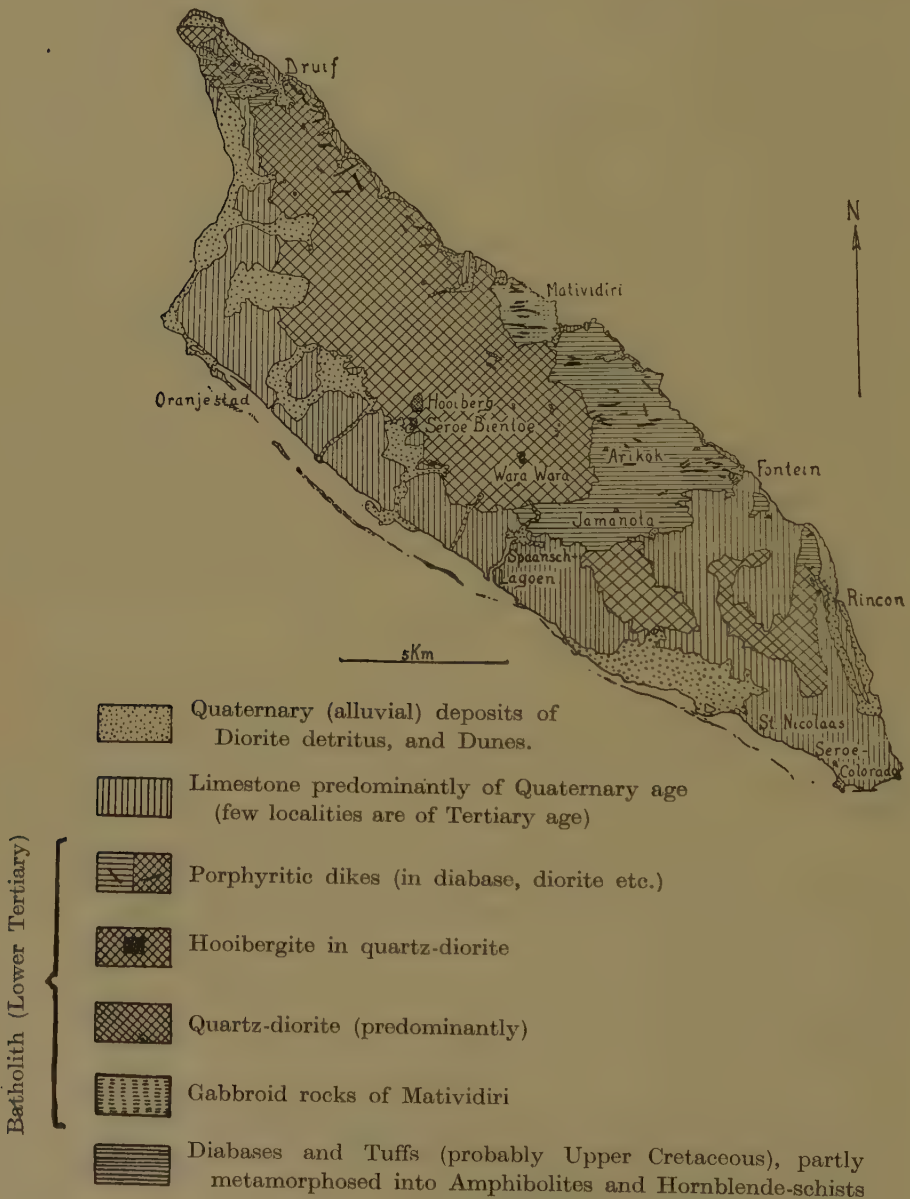


Fig. 1. Geological sketch-map of Aruba.



Large deposits of diorite detritus occur along the South and West coast. Their deposition was begun as soon as the magmatic rock series reached the erosion level, and is still in force. Hence, this material is found both underlying and overlying the limestone beds; the Quaternary limestone itself also contains a fair amount of diorite minerals, indicating that only part of the island was submerged during that period.

For a full description of the geology and petrography reference is made to WESTERMANN 1932. A small sketch-map will serve for general orientation (fig. 1).

The water bore of Oranjestad has considerably increased our knowledge of the Tertiary and Quaternary formations in that particular area. The unexpected result of the drilling was that under the Quaternary limestone clayey and sandy deposits were encountered, so far unknown in Aruba.

The surroundings of the capital show a low-lying, flat limestone plateau rising from the coast to some 65 feet. The "rooi" systems (a "rooi" — Spanish: "arroyo" — is a water course carrying water only after heavy rains) which cut through the limestone, contain large deposits of diorite detritus derived from the dioritic hinterland, the nearest outcrop of which is situated some 2 kilometers ( $1\frac{1}{4}$  mile) from the coast. The border between diorite and the younger limestone & detritus deposits runs somewhat parallel to the shore line (fig. 2).

Previous to 1942 the thickness of the limestone bed near Oranjestad was unknown. In the extreme Southeastern corner of Aruba (Mangle Corá) a bore had penetrated from 50 to 70 feet into limestone before reaching diorite, and a similar thickness was assumed for the coastal plain around the capital. Solely from the surface geology it would appear that the Quaternary limestone is underlain by diorite detritus which gradually merges into diorite. The prediction of the friars would, on the face of it, seem to relate to normal ground water accumulated below the limestone in the diorite detritus or weathered diorite, and this conception seemed to be corroborated by data obtained from shallow water wells in Western Aruba, dug by the Eagle Petroleum Company. However, the depths of the water flow predicted by the friars (902', 738') exceeded by far any estimate which could have been based solely on the surface geology.

Thanks to Frère ANTOON, in Aruba, and Frater REALINO in Curaçao — whose diligence is greatly appreciated — a complete set of "bailer" samples<sup>2)</sup> of the water bore, down to 930', was collected and placed at the disposal of the author of

---

<sup>2)</sup> After crushing the rock with the drilling bit (cable tool drilling), the crushed material is pulled up by means of a "bailer", a metal cylinder fitted with a valve. It is obvious that such "bailer" samples could be easily contaminated with rock material derived from beds slightly higher in the drilling hole and not yet cased off by casing.

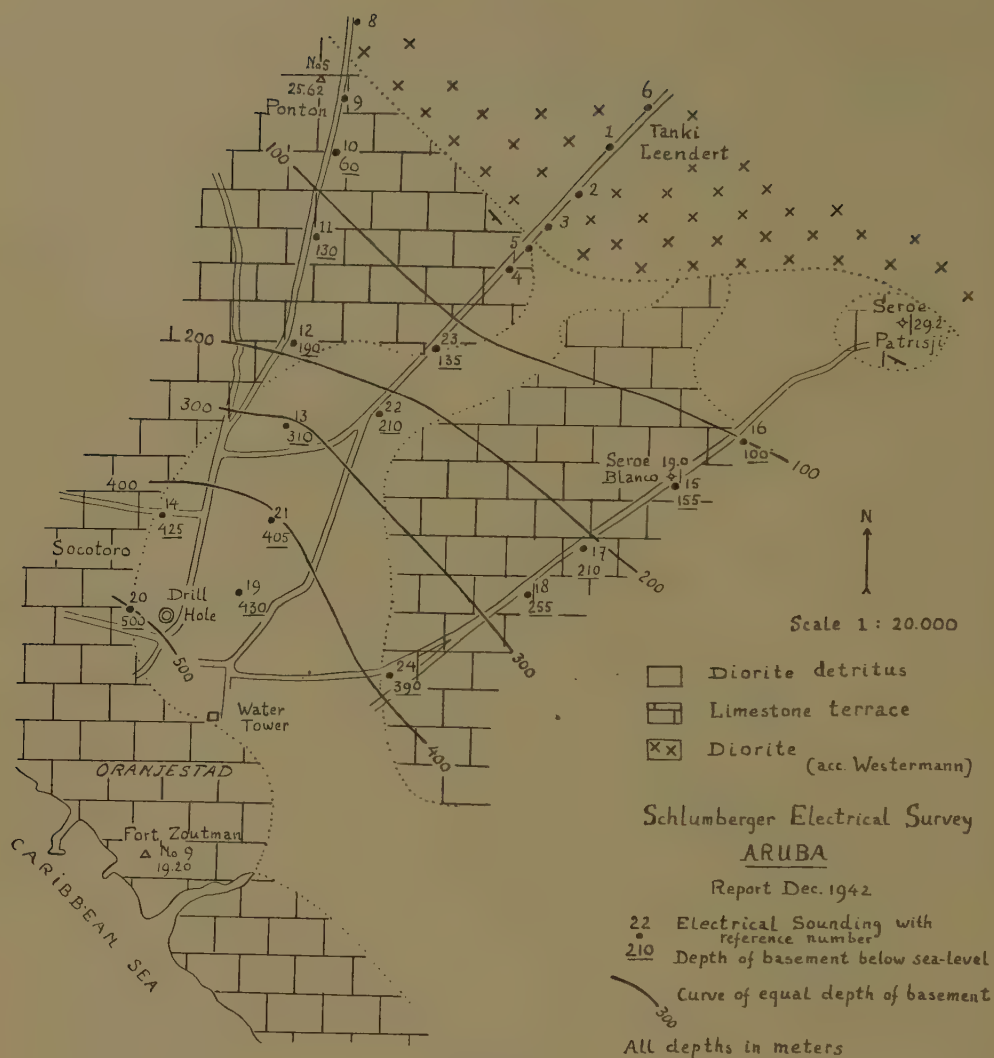


Fig. 2

this article, at that time working with the Caribbean Petroleum Company at Maracaibo, Venezuela. The geological investigation of the samples was carried out with the approval of the said Company and of the Government of Curaçao. A preliminary article was published in the Weekly Periodical "Curaçao" (WESTERMANN 1943).

In 1949–1950 the foraminifera were investigated by C. W. DROOGER (Lit), at the Mineralogical-Geological Institute of the University of Utrecht, Holland.

Fairly complete sample collections of the water bore are being kept at three places: a) St. Dominicus College at Oranjestad, Aruba, under the care of Frère ANTOON; b) St. Thomas College at Willemstad, Curaçao, under the care of Frater REALINO; c) Mineralogical-Geological Institute of the University of Utrecht, Holland.

The geological and palaeontological evidence of the 49 "bailer" samples is shown in table 1. Data of the driller's report have been added (H. SMITH).

From the stratigraphical column it is evident that below the subrecent

	Depth in feet and meters	Lithological remarks	Faunal remarks		Sample numbers
Holocene	0—20' 0—6 m	Weathered debris of diorite . . . . .			1
	20—320' 6—97 m	White limestones with few quartz grains (salt water) . . . . .		Coral remains, <i>Lithothamnium</i> , <i>Amphistegina</i>	2—16
Pleistocene	320—330' 97—100 m	Grey marl with few quartz grains . . . . .	Many Foraminifera and other fossils	<i>Planulina ariminensis</i> , dominant species	17
	330—390' 100—119 m	Fine calcareous gravel with pebbles of quartz, diorite, etc. . . . .	Few Foraminifera		18—20

## Unconformity

Miocene	Upper Zone	{ 390—430'	Fine sand with mica and	Foraminifera		21—22
		{ 119—131 m	glauconite . . . . .			
		{ 430—470'	Light-grey marly clay			
		{ 131—143 m	with glauconite . . .			
		{ 470—666'	Light- and dark-grey			
	Lower Zone	{ 143—203 m	marly clays with glauconite . . . . .	Many Foraminifera		25—34
			At 480' (146 m) pyritised micaceous sandstone.			
		{ 666'	Pyritised micaceous sandstone with pyritised wood remains . . . .			
		{ 203 m				
		{ 666—720'	Fine sand with mica and glauconite (abundant salt water) . . . . .			
		{ 203—220 m		Foraminifera		36—38
		{ 720—830'	Light- and dark-grey			
		{ 220—253 m	marly clays with glauconite . . . . .			
		{ 800—830'	Semi-carbonized wood remains . . . . .			
		{ 244—253 m			Shallow? water fauna	44
?		{ 830—930'	Fine sand rich in mica; small lignitic fragments (abundant salt water under high pressure)	No Foraminifera or other fossils		45—49
		{ 253—284 m				

detritus deposits of Oranjestad, measuring some 20 feet, the bore has penetrated into 300 feet of coralline *Lithothamnium* limestone and has subsequently struck beds of marl and conglomeratic limestone (calcareous gravel). At 390' a true marine series is reached, beginning with fine grained foraminiferal sands rich in mica and glauconite. From 430' down to 830' this

series consists of marine clays, with marine sands interbedded. The latter formation rests on a mica sand of presumably non-marine character: 830'—930'.

Although there is no strict palaeontological evidence it may be assumed that the upper diorite detritus and the underlying limestone series belong to the Quaternary. No distinction, however, can be made between Holocene and Pleistocene. It should be noted, that we have no data on dips, and that, as a consequence, the stratigraphical thickness remains uncertain for the time being. Most probably the dip does not exceed 30° in the lower limestones and may be nearly horizontal in the higher beds.

For the interval between 390' and 830', consisting of typical foraminiferal sands and clays, DROOGER (Lit. in press) — after careful correlation with similar strata in Northern South-America and the Caribbean area — has determined a Miocene age; the faunal evidence points with about equal strength to both Lower and Middle Miocene, whereas no conclusion can be drawn as to the presence of Upper Miocene. Attention is also drawn to the determination of the Ostracod *Cytheromorpha minuta* from the same formation, by VAN DEN BOLD (1946); this species was found earlier in the Miocene of Cuba.

The Miocene sands are largely composed of terrigenous material derived in all likelihood from the diorite massif to the Northeast: quartz-mica-sands. Quartz and mica are also found in the clays; whether these minerals have been washed in exclusively by natural processes or are to be considered partly as contaminated material (due to the "bailer" sampling method) remains questionable.

The mica sands of 830'—930' prove to be devoid of fossils, and no particular age can be attached to them. There is no sign of a stratigraphical gap at 830' and for the time being they may be included in the Miocene. A stratigraphical gap should be assumed, however, between the Miocene series and the overlying Pleistocene beds of predominantly calcareous facies.

Thanks to the diligence of R. J. BEAUJON, former Chief of 's Lands Water-voorzienings Dienst (Government Water Supply Service), the Schlumberger Sureenco S.A. at Caracas was contracted to carry out an electrical investigation which had for sole aim the study of the structure of the Oranjestad "basin" and an approximation of the depth of the basement. The prospect was conducted by the engineers R. LELEU and C. AYNARD, and lasted from 9th to 28th November, 1942 (SCHLUMBERGER 1942).

As the Schlumberger report has only a very limited distribution it is deemed advisable to reprint the most important parts of it, thus giving the reader an idea of the general principles and the results of this "electrical sounding" survey.

„Numerous measurements taken during the last twenty years inside drill-holes as well as on outcrops have shown that the different rocks, considered as electrical conductors, behave very unequally. It has been proven too that the conductivity of rocks derives from their water content, whether the water is saturating a porous medium such as in a sand or held by capillarity as in a clay. Consequently the various rocks present widely separated electrical resistivities, the lowest corre-



sponding to a high amount of water together with a high percentage of salts in solution. It must be noticed that, as long as a given geological formation keeps the same composition, its electrical resistivity remains approximately constant. As an example the following values were observed in Curaçao and Aruba:

Igneous rocks: quartz-diorite Aruba . . . . .	100—200 ohms/m <sup>2</sup> /m
diabase Curaçao . . . . .	70—300
Metamorphic rocks . . . . .	70—300
Weathered zone covering the igneous rocks:	
quartz-diorite Aruba . . . . .	20—30
diabase of Curaçao . . . . .	10—40
Blue clay (found in drill-hole Aruba) . . . . .	I
Salt water sands (id) . . . . .	I
Superficial beds of Quaternary limestone, not impregnated	
with sea-water . . . . .	50—300
Quaternary limestone impregnated with sea-water . . . . .	I

A physical parameter of the rocks showing such important variations lends itself readily to underground prospection by means of a simple technique".

After presenting a cursory outline of the geological problem of the bore the report continues: "To remain within a practical point of view the question which is of immediate importance is that of the total thickness of these formations, because the original idea is that the fresh water is to be found in the basement not far from the contact between the sedimentary deposits and the igneous or metamorphic rocks.

It must be understood that the electrical investigation has for sole aim the study of the structure of the basin and cannot give direct indication concerning the wateryielding capacity of the different formations involved. In the whole area which has been prospected we can foretell with a fairly good approximation the depth at which lies the basement, at the drilling location we predict how many hundred meters of hole must be dug before striking the basement. Whether potable water would be finally obtainable when the hole is completed can no more be ascertained by the resistivity method than by any other scientific geophysical process.

Before taking any measurements it could be assumed that the igneous and metamorphic rocks would act as a basement of resistivity practically infinite compared to that of the sedimentary formations above. This was confirmed by the field observations".

The observations are subject to the general limitations of the resistivity method. After indicating these limitations the authors expressed as their opinion: "Altogether, we estimate that our determinations of depth are obtained with an approximation of 10 %.

The results are represented essentially by a map (fig. 2) in which each center of electrical sounding has been marked down with its reference number. The denseness of the observations could not be exactly as great as we desired in the very vicinity and to the south of the drill-hole, because of the impossibility of extending the cables amidst the houses of Oranjestad. Consequently the drill-hole itself is on the edge of the surveyed area. However, the disposition of the stations along profiles converging towards the drill-hole enables us to check the final results on different cross-sections.

The electrical measurements clearly indicate that salted water is impregnating the limestone everywhere below sea-level. This phenomenon is already known in the water-wells dug close to the shore in certain parts of this island; it was observed at the time the upper section of the hole in Oranjestad was drilled; we can state that it persists even to a distance of two kilometers from the sea.

On the map, besides each electrical sounding the calculated depth below sea-level of the basement is plotted. Curves of equal depth have been construed with an interval of 100 meters. They give, inside a strip about one kilometer wide, a picture of the sedimentary basin which lies along the South-West coast of the island. The basement has roughly the shape of a plane dipping towards the sea under an average angle of 18 degrees.

A cross-section (fig. 3) has been drawn along a line following a North-East to South-West direction in the central part of the surveyed area. It runs from Tanki Leendert to Oranjestad and includes the location of the drill-hole. From a point located between station 3 and 5 the contact plunges gradually to reach its greatest recorded depth under station 20<sup>3)</sup>.

On this section, the depth of the basement under the location of the drill-hole is found to be 490 meters (1610 feet). It should be borne in mind that an approximation of 10 % is attached to the above figures<sup>3)</sup>.

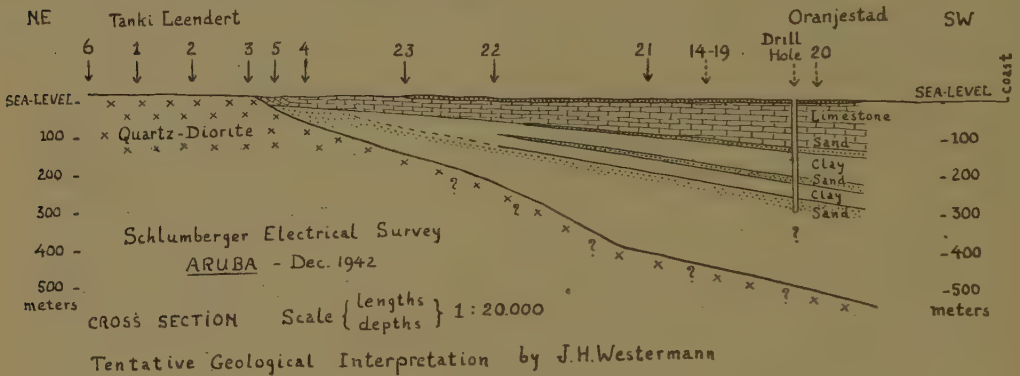


Fig. 3

From the Schlumberger survey described above it is apparent that no conclusion can be drawn as to the character of the sediments above the basement, nor can the kind of basement rock be ascertained. In fig. 3 we have assumed a dioritic basement rather than a (metamorphosed) diabase & diabase tuff formation, owing to the relative proximity of outcropping diorite. This of course remains conjectural. Although we have no indication as to the kind of sediments in the interval between the bottom of the well (937') and the basement (measured by the Schlumberger engineers at approximately 1610') it may be surmised that here too an alternation of sandy and clayey beds obtains: the water-bearing sands below 830' supposedly are confined above and below by clay beds.

*Tentative reconstruction of the geological history of Aruba during Tertiary and Quaternary.*

The surface geology, the examination of the sediments of the water bore and the electrical survey throw some light on the geological processes prevailing in Caenozoic time.

<sup>3)</sup> The fairly steep slope of the basement below the stretch 22-21 may indicate faulting, more or less parallel to the Southwest coast (note by the author).

After the period of orogenesis and magmatic intrusion in Old Tertiary time the older volcanic and magmatic formations became subjected to a relatively high tectonical uplift and subsequent denudation.

A *Lepidocyclina* limestone whose age may range from Upper Eocene to Upper Oligocene, collected in Southeast Aruba (Butucoe) testifies of the occurrence of at least one marine ingression in Middle Tertiary time. Besides, a number of fossils of questionable Tertiary age has been found in various places (WESTERMANN 1932, 1949).

More definite data on marine transgressions are presented by the clay and sand sediments of the Oranjestad water bore whose age has been determined as (probably Lower to Middle) Miocene. The non-marine mica-sands below the foraminiferal series (830'—930') may be considered as diorite detritus deposited as a deltaic sediment bordering the diorite outcrop: fragments of lignite encountered in the 830'—850' interval support the assumption of a predominantly terrestrial or coastal deposition.

The overlying alternating series of marine clays and sands gives evidence of positive and negative changes in level, while to all appearance the shore was situated Northeast of the present location of Oranjestad. Terrestrial material in the clay, i.e. quartz grains, mica and few semi-carbonized wood fragments, prove that the marine sedimentation took place not far from land. The main transgression appears to have taken place at the time of deposition of the darkgray clays in the interval 666'—470'.

It is not known whether this transgression covered the whole of contemporary Aruba or only part of it. According to WAGENAAR HUMMELINCK (1940) zoögeographical data indicate partial submergence, and this would seem to be corroborated by the fact that elsewhere in Aruba Miocene sediments are found to be absent between the "basement" formations and the overlying Quaternary limestones. Although there is always the possibility that such Miocene beds have been removed in a later period, it is equally possible that the Miocene transgression has been confined entirely to the SW portion of Aruba.

The beds between 470' and 390' are indicative of regression, a South-westward movement of the shoreline and increased transport of terrestrial material into the sea at the location of Oranjestad, which was getting shallower continuously.

As far as can be determined there is a definite stratigraphical gap between the Miocene clay & sand series below 390' and the overlying calcareous beds which are to be classed as probably Pleistocene. Therefore, during Pliocene time Southwest Aruba seems to have been marked by a strong regression causing a gap in the sedimentation. This regression was followed by a transgression in the Pleistocene period. On top of the Miocene beds a conglomeratic limestone, with pebbles of quartz and diorite, was deposited and subsequently covered by a thin marl and thick coral reef deposits. The thickness of the coralline limestone of maximum 300 feet indicates a gradual subsidence of the island.

It was pointed out before, that elsewhere in Aruba the limestone has been deposited directly upon the old volcanic and magmatic formations. It is very likely that during the Pleistocene transgression not all of Aruba was submerged since the limestone contains quartz material throughout the section; this conception is supported by zoögeographical data.

The coral limestones of the water bore cannot be subdivided into a Pleistocene and Holocene section. The surface geology of Aruba gives evidence of a slight upwarping of the Pleistocene limestone. During the Holocene this limestone cap was covered at its periphery by younger reef limestones. Subsequently diorite detritus was deposited on top of these limestones. A subrecent lowering of the sea level caused renewed erosion of outcropping formations; there is a possibility that at the location and in the surroundings of the bore the younger limestone has been (partly) removed by erosion and replaced by "rooi" deposits of diorite detritus (compare fig. 2).

For a more detailed account of the Quaternary history of Aruba and the influence of the Glacial oscillation of the ocean level, reference is made to WESTERMANN 1932 and 1949.

*(To be continued.)*



## GEOLOGY

# THE WATER BORE OF ORANJESTAD 1942—1943, AND ITS IMPLICATION AS TO THE GEOLOGY AND GEOHYDROLOGY OF THE ISLAND OF ARUBA (*Netherlands West Indies*) II

BY

J. H. WESTERMANN

(Communicated by Prof. G. H. R. VON KOENIGSWALD at the meeting of March 31, 1951)

### *Geohydrological Data*

The outcome of the bore viewed with respect to fresh water supply, proved to be disappointing. No fresh water was encountered at the depth of 902', where it had been predicted by the friars. However, an abundant supply of salt water was struck by the drill at a depth of 830' when penetrating the non-marine mica sand. Considerable pressure, suddenly released by the drill, converted the sand bed into quick sand which ascended into the drilling hole over a distance of some 200 feet, at the same time dislocating the heavy drilling outfit and dragging it along over more than 50 feet.

The drilling work below 830' was greatly hampered on account of the drilling hole being choked continuously by ascending quick sand.

The salt water at 858' was tested by the chemical laboratories of the "Openbare Gezondheids Dienst", Curaçao, the Eagle Petroleum Co. and the Lago Oil & Transport Cy, Aruba. It proved to contain 6.3 % of salts, and the total hardness was measured at 501.2 D° (i.e. equivalent to 5012 milligrams of CaO per Liter). The temperature was about 90° F, density 1.039 <sup>1</sup>). A more detailed chemical analysis of the salt water obtained from the bore, is not available.

Another salt water horizon was penetrated in the marine sands between 666' and 720'. For some unknown reason abnormal pressure was not observed at this particular occurrence. In the driller's report this interval is marked down as "quick sand".

As to the salt water below the depth of 830' three points need some explanation, i.e. the high pressure, the medium temperature, and high salt content.

The general impression is gained that the water bore at Oranjestad can be viewed as an artesian well. Studying the geological section, tentatively drawn on the basis of the lithology of the well and the data of the

---

<sup>1</sup>) The approximate figures of sea water are given for comparison: 3.5 % of salts, 370 D°, density 1.0223 at 76.6° F.

Schlumberger Electrical Survey (fig. 3), it seems quite feasible to interpret the sedimentary basin of Oranjestad as an artesian basin. Porous sands carrying water alternate with impervious clay beds, and this series is covered by limestones and marls. As far as we can ascertain the strata dip gently seaward, and it may be assumed that there exists a direct connection between the deep-lying sands and the diorite in the interior. Owing to this configuration rain water entering the outcrop area of weathered diorite and detritus, will percolate down through the dipping permeable sand beds locked in above and underneath by impermeable clay layers. Meanwhile the hydrostatic pressure is increasing with the depth, and it seems quite feasible — even considering internal and external friction — that a pressure of some tens atmospheres was released when the waterbody at 830' was struck.

It is interesting to remind the reader of MARTIN's statement as to the impossibility of artesian wells on the islands of Curaçao, Aruba and Bonaire (1888, p. 115): „Zur Anlage von artesischen Brunnen, welche auf den Inseln so sehr gewünscht wird, liefert die Kreideformation — die einzige, welche überhaupt in Betracht kommen könnte — jedenfalls keine Handhabe; ihre zusammengestauchten und verworfenen Schichten, welche mit complicirter Lagerung tiefe Zerklüftung verbinden, müssen jeden Gedanken daran sofort zurückdrängen". Although this statement can be upheld without reservation as far as the Cretaceous formations are concerned, it is pointed out that on the other hand the tectonic configuration in the coastal basin of Oranjestad — made up of Tertiary and Quaternary sediments — has given sufficient evidence of artesian possibilities.

It may be remarked here that the assumption by frères APPOLLINAIRE and JUAN as regards an artesian connection between Colombia and Aruba can be dismissed without further comment. Earlier a similar thought was expressed by H. VAN KOL (*Een noodlijdende kolonie*, 1901, p. 22) who figured such a connection between the mountains of Venezuela and the Curaçao island group.

The salt water struck at 253 m. (830') proved to be tepid. A temperature of approximately 90° F (i.e. 32.2° C) was measured in the drilling hole but we have no data on the exact depth of measurement! 32.2° C is only slightly less than the theoretical temperature expected at such a depth, taking into account an average geothermic gradient of 3° C per 100 meters, and an average temperature on the surface of 27° C.

The third item to be discussed is the high salt content of the artesian water. This water proved to have a concentration almost twice that of sea water (6.3 % : 3.5 %). According to RUSSELL (1933) brines having a higher concentration than sea water are commonly found in horizons not closely associated with salt deposits, and likewise we need not assume the nearby presence of such a salt body in the case of the Aruba bore. As a matter of fact most of the sand and clay samples obtained with the bailer contain a fair amount of salt, betraying itself by the salty taste and by typical salt precipitations covering the dried material.

Failing a chemical analysis of the water in question we can only guess at the nature and quantity of the dissolved salts. The total hardness of

501.2 D° (equivalent to 5012 mg/L CaO) indicates a high concentration of Ca and Mg salts (carbonates, sulphates, chlorides). The remainder of the 63,000 mg/L supposedly consists largely of chlorides and sulphates of Na (and perhaps K). The actual figure of Cl' mg/L is unknown, but, judging from the taste, we may safely consider the water as a chloride brine.

RUSSELL has discussed critically the evidence regarding all the processes which may have produced chloride brines more concentrated than sea water. Of these processes concentration by hydration, osmosis or adsorption seems to be most evident. Special attention is paid here to concentration by *adsorption*. In order to get somewhat acquainted with RUSSELL's train of thought, the reader is referred to the following quotations from his contribution (p. 1225—1227):

„It has long been known that clays and very fine-grained soils will adsorb salts from solution. The amount adsorbed is probably proportional to the total surface area of all the particles in the material. Since the total surface area of very fine-grained rocks is enormously greater than that of coarse-grained rocks, it is evident that adsorption would be important only in the fine-grained rocks, and in a given sediment the finest portion would contain nearly all the adsorbed salts.

Very fine sediments laid down in sea water should contain considerable adsorbed bases, but it is not clear whether the chlorine would accompany these bases, or whether all or a portion of it would be released and escape before burial. If some or all of the chlorine remains in the marine deposits, certain agencies, such as recrystallization, cementation, and the effects of heat and pressure, may cause the liberation of the adsorbed materials as chlorides. The effect of these agencies should increase with depth. As most of the adsorbed salts or ions are held on the finest particles of the sediment, and as the finest grains are the first to recrystallize into larger masses, it is obvious that recrystallization would liberate most of the ions or chlorides held on the surfaces by adsorption. The chlorides thus released would increase the concentration of the solutions occupying the pore spaces of the rocks, and after further compaction they might be expelled into the associated water-bearing horizons.

Until more definite knowledge is available regarding the amounts of chlorides that are adsorbed during the deposition of fine sediments in sea water, it is difficult to apply a quantitative test to this theory. However, if, for example, a quantity of sodium chloride amounting to 0.1 per cent of the weight of a shale were expelled without accompanying water into a reservoir containing sea water and having a thickness of 50 feet and a porosity of 20 per cent, it would require a stratum of shale only 140 feet thick to furnish enough salt to double the concentration of the solution in the reservoir. A bed of shale 560 feet thick would furnish enough salt to raise the concentration to five times that of sea water.

If it could be shown that sufficient quantities of chlorine are entombed with the fine sediments as a result of adsorption, this theory would be very promising. Until further investigations have furnished additional information bearing on this point, it is difficult to estimate the importance of adsorption in producing concentrated chloride brines”.

The sands and clays as encountered in the water bore of Aruba, are clearly of marine and deltaic origin, and — according to the above quotation — they could have adsorbed considerable amounts of salts



during their deposition. Part of these adsorbed salts may have become fixed in the sediments and another part may have been released subsequently — and is still being liberated — by certain agencies, acting after sedimentation and burial, such as heat, pressure, compaction and other physical or chemical processes. As has been pointed out by RUSSELL it may be accepted that these salts are adsorbed (and partly released) by the fine clays in particular, rather than by the adjoining sands. Assuming a direct connection between the water-bearing sand beds in the bore and the diorite and detritus in the outcrop area further inland, enabling slow but steady percolation of rain water through the pore spaces of these dipping sand beds, one would logically expect this fresh water to dissolve the salts expelled from the adjacent clay beds. Thus, it would gradually change from fresh into brackish and salt water, surpassing even the salt concentration of sea water. The high hardness may be explained partly by solution of calcium carbonate from the fossiliferous beds, partly by liberation of other Ca and Mg salts.

Besides the artesian salt water in the Miocene sands there is abundant saline water in the overlying coral limestone (according to the drilling report: "plenty of salt water"). The electrical measurements also clearly indicate salt water impregnation of the limestone everywhere below sea level. Generally speaking this ground water originates from rain water penetrated through the cavernous reef limestones until stopped by impervious clay beds.

Before attempting to explain the high salinity of the limestone ground water, it is useful to present some data on 40 shallow water wells drilled or dug by the Eagle Petroleum Company in the young limestone terrace of Western Aruba <sup>2)</sup>. These water wells, situated along a line averaging 800 meters from the coast, have a depth of 15 to 20 feet; their bottom lies somewhat below sea level whereas their maximum water level is some 4 feet above the bottom. Water analyses show a chlorine content varying between about 330 and 2555 milligrams per liter, depending on the well and the time of sampling (see table 2). Thus, the average (1215 milligrams) chlorine content surpasses that of ordinary local drinking-water (200—500 milligrams) considerably. Excavating a well further below sea level incurs increasing chlorine content.

No chemical analysis is available of the limestone ground water encountered in the bore. From the driller's report one gets the impression that this water is true "salt water", having a salinity much higher than that of the average Eagle well. This would stand to reason because the limestone beds are — geologically speaking — very young and are situated largely below sea level. Leaching of the sea water salts left behind in the pores of the limestones has by no means proceeded very far, and as a consequence the water is still salt.

<sup>2)</sup> Data obtained in November 1942 from R. J. BEAUJON, former Chief of 's Lands Watervoorzienings Dienst, Curaçao.



At this instance it is interesting to draw the attention to the "warm mineral spring" observed by VAN KOOLWIJK (1884) which according to him flowed into the sea at the base of the limestone terrace, just South of Fort Zoutman, Oranjestad (fig. 2). No recent observations are available. If we leave the temperature out of account (there are no specific data on the so-called "warm" water), then this particular spring could be explained as just one of the places where the saline ground water of the limestone terrace drains off into the sea. On the other hand, a temperature higher than normal would suggest a deeper origin of the water (ascending along a fault plane?).

No particular problem is raised by the fresh water spring at Fontein, in Northeastern Aruba, making its appearance at the outcrop of the plain of abrasion separating the volcanic formation and the overlying Caenozoic limestone. In all probability this plain of abrasion dips in a Northerly direction, thus draining the rain water percolating through the limestone down to the said contact. The water production of the spring is small and depends entirely on the rainfall at the limestone plateau South of Fontein. The salinity of the Fontein spring varies between 200 and 460 Cl' mg/L; total hardness is 17—19 D° (see table 2). Thus it compares favourably with the ground water in the neighbourhood of Oranjestad and in the Eagle concession. The difference is easily explained by the difference in topographical situation: the limestone plateau South of Fontein has an altitude varying between 80' and 330' above sea level, whereas the terrace limestone around Oranjestad reaches from a few feet above sea level to well below it.

It may be assumed that the salt content of the Fontein water — however small — is derived mainly from the tuffaceous beds of the old volcanic formation forming the plain of abrasion, rather than from the plateau limestone. This assumption is based on the theory that the salts adsorbed during marine transgressions in the finegrained tuffaceous rocks are more difficult to dissolve than those left behind in the cavernous and porous limestone. It would seem, therefore, that the leaching of the plateau limestone has made far more progress than that of the underlying volcanic rocks. Similar geohydrological conditions were met by MOLENGRAAFF (1929) around the springs of Hato, Curaçao. Quaternary limestone overlies here unconformably the shales of the Midden-Curaçao formation. Where the Northward dipping plain of abrasion, separating both rock types, is outcropping, fresh water springs are appearing. The salinity of the Hato springs is still lower than that of the Fontein spring, and varies between approximately 140 and 360 mg. Cl' per liter, the total hardness from 12 to 22 D° (see also LIEFRINCK 1937, p. 36, enclosure 13). MOLENGRAAFF has observed that the salinity is highest in those springs situated farthest from the outcropping plain of abrasion i.e. from the limestone cliff, owing to the longer transport of the water through the shales which are relatively rich in adsorbed sea water salts.

The limestone plateau South of Fontein has been surveyed more than once with a view to increasing its water supply, so far without satisfactory results. DALLMUS (1943) paid a short visit to Aruba (16—18 November, 1942) and favoured the idea of utilizing the cavernous limestone of Fontein and Quadirikiri, along the North side of the plateau, as artificial ground water reservoirs, by constructing underground dams. The drainage areas at these localities were estimated at 10, respectively 5 square kilometers. He also reported on the water supply of the Mangle Corá well system in Southeastern Aruba: drainage area about 3 sq. kms. Its quality did not improve appreciably after the seaward side of the well had been cemented off<sup>3</sup>). Many years ago, in 1888, it was stated by MARTIN "dass das östliche Kalkplateau für die Wasserfrage bedeutungslos ist, da die Schichten sich hier in schwebender Lage als Hangendes der Felsenmeere von Diorit und nur in geringer Höhe über dem Meeresspiegel befinden", a rather indistinct statement to which no particular significance can be attached.

No attention is paid to this limestone area by LIEFRINCK (1937) and SANTING (in KRUL 1949).

Contrary to the poorly founded opinion expressed by the geologist WESTERMANN in 1932 (p. 127), that the rather deeply weathered diabasic and dioritic subsoil of Aruba would act as a fairly good water reservoir, the hydrologists LIEFRINCK, DALLMUS and SANTING report on this soil as having very limited permeability and thus greatly impeding infiltration of rain water. Thus, according to these specialists, precipitation would add little to the ground water reservoir<sup>4</sup>). Consequently there are no possibilities of an adequate ground water supply for the present dense population. If in view of changing economic conditions sea water distillation and foreign import of fresh water would of necessity be abandoned, a reduced population will have to fall back upon rain water cisterns and reservoirs besides the few wells suitable for drinking-water.

---

<sup>3</sup>) Aruba Esso News Vol. 11, no. 20 of September 29, 1950, p. 4, published a popular article "Water for All Time. Mangel Cora Well", containing a photograph and a sketch map of the 2134 foot water-collecting tunnel in the coral. The concrete underground dam or "grout line" between the tunnel and the sea, acting as a barrier to water seepage from the basin to the sea, and vice versa, is also shown on the map. The article mentions an increase in the supply of fresh water from 1000 to approximately 5000 barrels a day, but does not have any record of improvement in quality.

G. SANTING informed the author that after the completion of the grout line the Cl' content decreased from 6750 to approximately 5000 mg/L (data obtained during his visit in the year 1948).

<sup>4</sup>) The impermeability of the dioritic soil is reflected in the high salinity of the ground water (see table 2). This impermeability relates to the extensive areas swept barren by soil erosion, and as much to the comparatively rare places where a fairly thick soil profile has developed through weathering. In the latter case the weathered zone makes a poor reservoir in view of the fact that the already low porosity is further reduced by the fine material resulting from the decomposition of feldspar (DALLMUS 1943).

TABLE 2

Location	Approx. Altitude in meters	Geological Formation	Cl' mg/L	Total Hardness D°	Date of Sampling
<i>Northeast &amp; North coast</i>					
Bron di Fontein . . . .	10	Quaternary limestone/ Diabase & Diabase-tuff formation	210 400 460	— 19 17	2 July 1930 (W.H.) 23 Dec. 1936 (W.H.) 30 Dec. 1948 (W.H.)
Pos di Fontein . . . .	10	ditto	400	18	23 Dec. 1936 (W.H.)
Bron di Rooi Prins . .	20	Diabase-tuffs	1300 1345	36 40	9 Jan. 1937 (W.H.) 26 Aug. 1949 (W.H.)
Cueba di Andicouri . .	sea-level	Quaternary limestone/ Diabase & Diabase-tuff formation	780	4	26 Aug. 1949 (W.H.)
Bron di Andicouri . . .	15	Quartz-diorite	6640	—	1883 (de Loos, Van Koolwijk)
Bron di Pos di Noord .	10	Quartz-diorite	3250	55	30 Dec. 1936 (W.H.)
Pos di Noord . . . . .	10	Quartz-diorite	3300	60	30 Dec. 1936 (W.H.)
<i>Central part of island</i>					
Rooi Juditi, SE of Seroe Kabaai (temporary)	50—60	Diabase-tuffs	2260	—	28 Dec. 1948 (W.H.)
Puddle in Rooi Kabaai, SSW of Miralamar (temporary, excavated)	55	Diabase-tuffs, strongly metamorphosed	1860	—	28 Dec. 1948 (W.H.)
Bron di Rooi Bringamosa	15	Quartz-diorite	3150 4910	50 —	6 Jan. 1937 (W.H.) 18 Jan. 1949 (W.H.)
<i>South &amp; Southwest coast</i>					
Well Mangle Corá . . .	sea-level	Quaternary limestone/ Quartz-diorite	6750	—	Nov. 1942 (D)
Pos Grandi (Rooi Lamoenchi) . . . . .	sea-level	Quaternary limestone terrace	960	26	12 Feb. 1937 (W.H.)
Pos W. of Rooi Lamoenchi	sea-level	Quaternary limestone terrace	720	26	11 Feb. 1937 (W.H.)
Pos di Balashi (Wesoe)	7	Quaternary limestone terrace	1645 1595	53.3 —	July 1937 (L.) 10 May 1940 (S.)
Well in Rooi upstream of Balashi. . . . .	?	?	5106	87.9	July 1937 (L.)
<i>West coast</i>					
40 Wells of Eagle Petroleum Co's Concession	sea-level	Quaternary limestone terrace	min. 330 max. 2555 (averages 1180/1250)	—	Jan./Feb. 1942
Bubali no. 1 . . . . .	sea-level	Quaternary limestone	1940/2065	—	Jan./Feb. 1942
„ „ 2 . . . . .		terrace	dry/2015	—	Jan./Feb. 1942



In order to give a general idea of the composition of Aruba ground water, analyses of several springs and wells are listed in table 2. The figures are borrowed chiefly from LIEFRINCK 1937 (L), WAGENAAR HUMMELINCK 1940 (W.H.), DALLMUS 1943 (D), and SANTING (KRUL) 1949 (S), as well as from Eagle Petroleum Co's reports 1942. Dr WAGENAAR HUMMELINCK kindly supplied additional figures of samples collected during his 1948—1949 visit, and tested by F. W. KLEVE (W. H.).

*Prospects of finding potable water when drilling deeper*

The question may be raised whether fresh water would be struck by extending the water bore of Oranjestad down to the basement (calculated by the Schlumberger engineers at approximately 1610'). For the time being we cannot express any definite opinion as to the nature of the sediments between 937' and 1610'. Either the non-fossiliferous mica sands of 830'—930' might be found extending down to the basement, or a series of alternating marine and non-marine clays and sands (as observed in the present drilling hole) would be encountered. In all likelihood more water-bearing sand beds would be reached, at least some of them connected with the outcrop area inland and thus constituting artesian systems. Our experience with the water bodies of the present drilling does not warrant any optimistic prediction as regards the quality of water yet to be struck. There is indeed no geohydrological indication whatsoever of fresh water in the sediments below Oranjestad. Although for purely scientific purposes further drilling would be highly recommendable, this should be definitely dissuaded from an economic standpoint, notwithstanding Frère Appollinaire's confidence in ultimately finding the much desired fresh water flow.

#### REFERENCES

- BOLD, W. A. VAN DEN, *Contribution to the study of Ostracoda with special reference to the Tertiary and Cretaceous microfauna of the Caribbean region*. Amsterdam, 1946 (Aruba, p. 105).
- DALLMUS, K. F., *Report on the fresh water supplies and geology of the islands of Curaçao and Aruba*, submitted to the Lago Oil & Transport Cy., Aruba. March 1943 (p. 17—28).
- DROOGER, C. W., Miocene and Pleistocene Foraminifera of Oranjestad, Aruba (Netherlands Antilles). *Contributions from the Cushman Foundation for Foraminiferal Research* (in press).
- (KOOLWIJK, A. J. VAN), Bronnen van mineraalwater op Aruba. *Tijdschr. Ned. Aardr. Gen.* (2). 1. Afd. Verslagen en Aardr. Meded. 1884, p. 600—601. (See also p. 369).
- KRUL, W. F. J. M., *Rapport inzake de Waterhuishouding van Curaçao en Aruba* (with 3 enclosures). Rijksinstituut voor Drinkwatervoorziening, The Hague. 1949.
- Enclosure II: SANTING, G., *Nota inzake de Hydrologie van Curaçao en Aruba*. (p. 11, 19, 56, 75; bijlage II-5, p. 13—14).
- A convenient synopsis of this report has been published in the Caribbean Commission's publication *Caribbean Economic Review*, Vol. 1, Nos. 1 & 2, December, 1949: Survey of Water Supplies in the Caribbean—Netherlands West Indies, p. 58—63.



- (LIEFRINCK, F. A.), *Rapport inzake de Gouvernements-Waterleidingen op Curaçao en Aruba* (with 44 enclosures). Rijksbureau voor Drinkwatervoorziening, The Hague. 1937. (chapter II, XIV–XVIII; enclosure 39).
- LOOS, D. DE, Bitterwater van Aruba. *Tijdschr. uitgeg. door de Nederl. Maatsch. ter bev. v. Nijverheid*, 46, 1883, p. 321.
- , Aruba-Bitterwasser. *Berichte d. Deutsch. Chem. Ges.* 17. 7. Berlin 1884, p. 250.
- , Bitterwater van Aruba. *Natuurk. Tijdschr. voor Nederl. Indië* 44, 1885, p. 86.
- MARTIN, K., *Bericht über eine Reise nach Niederländisch West-Indien und darauf gegründete Studien. 2. Geologie*. Leiden. 1888. (p. 113–118).
- MOLENGRAAFF, G. J. H., *Geologie en Geohydrologie van het eiland Curaçao*. Delft. 1929. (p. 111–126).
- RUSSELL, WILLIAM L., Subsurface Concentration of Chloride Brines. *Bull. Am. Ass. Petr. Geol.* 17. 10. 1933, p. 1213–1228.
- SCHLUMBERGER SURENCO, S. A. (Caracas), *Report on the Schlumberger Electrical Survey carried out in Aruba (November 9 to November 28, 1942)*. Government of Curaçao (N.W.I.), Landswatervoorzieningsdienst. Dec. 1942.
- WAGENAAR HUMMELINCK, P., *Studies on the fauna of Curaçao, Aruba, Bonaire and the Venezuelan Islands*. No. 1–3. (General information. A survey of the mammals, lizards and mollusks. Zoogeographical remarks). Utrecht. 1940. (p. 28, table 5; p. 32; p. 53, fig. 15). See also: Vol. II. 4. 1940 (p. 17–19; p. 21, table 1).
- WESTERMANN, J. H., *The Geology of Aruba*. *Geogr. en Geol. Meded. Utrecht. Physiogr. Geol. Reeks* 7. 1932.
- , De Waterboring op Aruba. Voorloopige beschouwingen door een geoloog. *Curaçao, Weekbl. Staatk. Ec. en Cult. Belangen Gebiedsd. Curaçao*. 5. Nos. 6–7, 9–16 Jan. 1943, p. 1–5, 1–3.
- See also: *Jaarb.* 1945–1946, *Natuurwetensch. Studiekring Sur. Curaçao*. Utrecht 1946, p. 68–69, en *De West-Indische Gids* 27. 12. 1946, p. 372–375 (P. WAGENAAR HUMMELINCK: *Literatuur betreffende het natuurwetenschappelijk onderzoek in Curaçao gedurende de oorlogsjaren*).
- , Overzicht van de Geologische en Mijnbouwkundige Kennis der Nederlandse Antillen, benevens voorstellen voor verdere exploratie. *Meded.* 85. *Afd. Trop. Prod.* 35. *Ind. Inst. Amsterdam*. 1949. (p. 31–39; 116–119).

## INSULIN AND GROWTH

BY

A. P. MAASSEN \*)

(Communicated by Prof. S. E. DE JONGH at the meeting of November 25, 1950)

With YOUNG <sup>1)</sup> we agree, that the experiments of MIRSKY <sup>2)</sup> on the protein-accumulating effect of insulin are promising for an influence of this hormone on body growth as a whole.

After the observations of GAARENSTROOM *cs.* <sup>3)</sup> we are inclined to believe, that the pituitary growth hormone has a direct pancreatropic as well as a secondary influence on insulin production, by its tendency to elevate the bloodsugar level. According to VAN WIERINGEN <sup>4)</sup> the increased insulinproduction, though not indispensable <sup>5)</sup>, may play a rôle in the mechanisms of growth.

BRAND observed <sup>6)</sup> after injection of small doses (0.5 I.U.) of insulin a decreased loss of body weight in hypophysectomized rats but no real body growth could be achieved.

In our series of experiments we tried to prove that small doses of insulin have a growth promoting effect in normal and adrenalectomized rats.

*Methods*

Increase of body weight and taillength of young normal female rats (60 g) injected with insulin (0.02 I.U. daily) were compared with those of normal controls (saline). Both series were held on 17 g of "governmental food" (20 % protein) daily.

As no effect of insulin administration could be detected, a second experiment was done under the same conditions; to increase the need for protein, this time a daily diet of 12 g "governmental food" was given.

We <sup>7)</sup> observed that under certain conditions (0.1 mg Doca subc. daily and 1 % NaCl as drinkwater) adrenalectomy may stimulate growth after 5 days, in rats. An experiment was done to investigate if insulin could still increase the extra growth-rate of adrenalectomized animals. Because of a high deathrate in young adrenalectomized animals and a lesser need for food after adrenalectomy we carried this experiment out on rats of 80 g on a diet of 10 g "governmental food" daily.

*Results* (tables 1 and 2).

Only on a considerable limited diet insulin injections have a significant stimulating effect on tail growth ( $t = 3.0$ ) in normal rats, whereas the body weight seems to react also ( $t = 1.9$ ). After adrenalectomy we observed an increase in tailgrowth only ( $t = 2.1$ ).

For the surprisingly low growth rates of the adrenalectomized animals

---

\*) Supported by a grant from the Netherlands Organization for Pure Research (Z.W.O.).

TABLE I  
Growth of normal rats (60 g) after insulin administration for 5 days

Number	Food intake daily	Treatment daily	Body growth in g	Tail growth in mm
10	17 g	insulin 0.02 I.U.-subc.	9.1 $\pm$ 1.1	5.3 $\pm$ 0.4
10	17 g	saline 0.2 cc subc.	8.6 $\pm$ 1.2	5.4 $\pm$ 0.3
10	12 g	insulin 0.02 I.U.-subc.	8.2 $\pm$ 0.8	5.5 $\pm$ 0.4
9	12 g	saline 0.2 cc. subc.	6.1 $\pm$ 0.8 $t = 1.9$	4.0 $\pm$ 0.3 $t = 3.0$

TABLE II  
Growth of adrenalect. rats (80 g) after insulin administration for 5 days (both series treated daily with 0.1 mg Doca subc. and 1 % NaCl as drinkwater)

Number	Food intake daily	Treatment daily	Body growth in g	Tail growth in mm
12	10 g	insulin 0.02 I.U.-subc.	3.3 $\pm$ 0.9	4.8 $\pm$ 0.5
12	10 g	saline 0.2 cc subc.	3.1 $\pm$ 1.2	3.3 $\pm$ 0.5 $t = 2.1$

compared with those of the normal controls, the circumstances under which the third experiment was done, may be held responsible (less food, bigger animals).

The results mentioned suggest that the observed growth effect of insulin has been achieved in the animal by increasing the influence of circulating growth hormone.

An attempt to attain final proof for this hypothesis by investigating the effect of insulin on hypophysectomized rats injected with a certain amount of growth hormone, failed because of premature death after insulin administration.

### *Summary*

An increase in tailgrowth (significant) and in body weight (nearly significant) has been observed in normal animals on a restricted diet after daily injections of insulin (0.02 I.U. subc.) for 5 days.

In adrenalectomized animals insulin has a stimulating effect on tail growth only.

*Pharmacological Laboratory; State University of Leiden.*

### BIBLIOGRAPHY

1. YOUNG, F. G., *Bioch. J.* **39**, 515 (1945).
2. MIRSKY, I. A., *Endocrinology* **25**, 52 (1939); *Am. J. Physiol.* **124**, 596 (1938).
3. GAARENSTROOM, J. H., J. HUBLÉ and S. E. DE JONGH, *Acta endocrin.* **2**, 317 (1949).
4. G. VAN WIERINGEN, *Archiv. intern. pharmacodyn.* **76**, 450 (1948).
5. GAARENSTROOM, J. H. and S. E. DE JONGH, *Proc. Kon. Ned. Ak. v. Wetensch.* **51**, 166 (1948).
6. BRAND, M., personal communication.
7. MAASSEN, A. P., to be published.

## GEOLOGY

### POSTGLACIALE LAND- EN ZEENIVEAU-VERANDERINGEN

DOOR

H. J. ZWART

(Communicated by Prof. I. M. VAN DER VLERK at the meeting of February 24, 1951)

De hypothese, dat de Holocene afzettingen langs de kust van Nederland bij een continu rijzende zeespiegel zouden zijn ontstaan, telt weinig aanhangers meer. Onlangs gaf UMBGROVE (1947) een uiteenzetting over de vorming van Nederlands kust in verband met de bewegingen van het zeeniveau en de daling van de bodem.

Uit de resultaten van de pollenanalyse kon worden afgeleid, dat de ontwikkeling van de postglaciale bossen in geheel Noordwest-Europa op nagenoeg dezelfde wijze is verlopen. Dit maakte het mogelijk, een schema van die bosgeschiedenis te ontwerpen, dat een basis van de indeling van het Holoceen is geworden. Veelal gebruikt men daarbij de Blytt-Sernanderse terminologie en spreekt dan van Praeboreaal, Borea, Atlanticum, Subborea en Subatlanticum. Door middel van archaeologische vondsten, die „ijking” van pollendiagrammen toelieten, kon bij benadering de duur van die tijden worden vastgesteld. Zo wordt, volgens de jongste schattingen, (WOLDSTEDT 1950, FIRBAS 1949, GODWIN 1945) aangenomen, dat b.v. het Atlanticum ongeveer 5500 j. v. Chr. begon en tot  $\pm 2500$  j. v. Chr. duurde, terwijl het aansluitende Subborea enige eeuwen voor het begin van onze jaartelling een einde nam.

Vrijwel algemeen wordt aangenomen, dat het Westelijk deel van Nederland sinds lange tijd in dalende beweging is. Deze beweging is niet alleen relatief, d.w.z. ten opzichte van de zeespiegel, maar ook absoluut, (ESCHER 1940, KUENEN 1940 en 1945, UMBGROVE 1947). Evenmin wordt betwijfeld, dat sinds de laatste ijstijd het zeeniveau is gestegen. Beide bewegingen vergroten het verschil tussen land- en zeeniveau.

Wanneer een mariene afzetting op een terrestrische ligt, is dit als regel het gevolg van overstroming van het land door de zee. De oorzaak van dit verschijnsel is een relatieve stijging van de zeespiegel. Zijn deze mariene afzettingen steeds in een zeer ondiepe zee gedeponneerd, dan stelt de dikte van de laag de totale relatieve zeespiegelstijging voor. In ons land zijn alle mariene sedimenten, die op het „veen op grotere diepte” liggen, afzettingen in ondiep water. Veelal wordt een groot deel van deze afzettingen als wadsediment beschouwd.

Blijkens de Toelichting bij de Geologische Kaart van Nederland No. 2 (1947) laten de samenstellers van die kaart het Holocene lagencomplex in het Westen van ons land beginnen met het „veen op grotere diepte”.



Daarop heeft zich een pakket, volgens hen oud-Holocene, wadsediment afgezet, dat in jong-Holocene tijd bedekt werd met Oud Zeezand en Oud Duinzand in de kuststrook, en oostelijker met Oude Zeeklei. Hierop kan weer Zandig Moerasveen (in de duinstreek) of Laagveen (ten Oosten daarvan) rusten.

EDELMAN (1950) duidt het gehele complex mariene afzettingen tussen „veen op grotere diepte” en „oppervlakteveen” aan met de naam Oude Zeeklei. Daar deze laatste naam in de geologische literatuur reeds een bepaalde en beperkende betekenis had gekregen, noemen wij dit complex afzettingen „Oud Wadsediment”.

Het ontstaan van dit Oude Wadsediment is dus mogelijk geweest door een daling van het land of een stijging van het zeeniveau, of door samenwerking van beide.

Het begin van de afzetting van het Oude Wadsediment is niet precies te dateren, maar viel blijkbaar in het Atlanticum. In die gevallen, waarbij het mogelijk was, een volledige serie monsters van het onderliggende „veen op grotere diepte” te analyseren, bleek de overgang Boreaal-Atlanticum in dit veen te liggen. Het werd daar dus gevormd tijdens het Laat-Boreaal en Vroeg-Atlanticum. (FLORSCHÜTZ 1939 en 1944; ZWART (nog niet gepubl.)). Het veen ligt op laagterraszand, dat gewoonlijk voor jong-Pleistoceen wordt gehouden. De stijging van het zeeniveau bracht een stuwing van het grondwater mee, waardoor op het laagterras moerassen ontstonden, waaruit het „veen op grotere diepte” is ontstaan. Daar dit veen gevormd is als indirect gevolg van de stijging van het zeeniveau, beschouwen wij een serie sedimenten, waarvan de basis in het „veen op grotere diepte” ligt en waarvan de afzetting in het begin van het Atlanticum een aanvang genomen heeft.

Het eind-tijdstip van de vorming van dit Oude Wadsediment kan eveneens bij benadering bepaald worden en wel door pollenanalytisch onderzoek van het erop liggende veen. Uit een vijftal pollendiagrammen van dit veen kon worden afgeleid, dat de grens Atlanticum-Subboreaal ongeveer aan de basis van dit oppervlakteveen ligt. Veelal wordt aangenomen, dat de overgang Atlanticum-Subboreaal bij een snelle afname van het *Ulmus*percentage ligt. In de door ons onderzochte monsters van dit veen bleek inderdaad het *Ulmus*-percentage zeer klein te zijn, terwijl in een diagram, dat zich over een deel ook tot de onderliggende oude wadsedimenten uitstreckte, de betrokken spectra een duidelijk hoger *Ulmus*gehalte te zien gaven. Globaal genomen mag het einde van de afzetting van het Oude wadsediment geacht worden ongeveer samen te vallen met de overgang Atlanticum-Subboreaal of met het eerste gedeelte van het Subboreaal.

Voor de vorming van dit Oude Wadsediment en een gedeelte van het „veen op grotere diepte” is dus een tijdsduur, die het gehele Atlanticum beslaat, beschikbaar. In jaren uitgedrukt is dit bij benadering  $5500 - 2500 = 3000$  jaar.

Bij de bepaling van de oorspronkelijke dikte van dit laagpakket stuiten wij op de moeilijkheid, gelegen in de bepaling van de mate, waarin het is ingeklonken. Bekend is, dat de inklinking van zand gering is en meestal niet meer dan enkele cm, ook bij een meerdere meters dik pakket, bedraagt. Een kleilaag is aan een grotere diktevermindering t.g.v. klink onderhevig. Zo berekende HUIZINGA (1940) voor een kleilaag van 2 m dikte een belast met 5 m zand onder water na 270 jaar een zetting van 30 cm en na bijna 3000 jaar van 33 cm. Een veenlaag verliest onder deze omstandigheden ongeveer de helft van zijn dikte. Ook de snelheid van de inklinking is verschillend. Veen bereikt in betrekkelijk korte tijd zijn maximale zetting, terwijl de klink van klei zeer lang voortduurt.

Het is nog niet goed mogelijk, om op het ogenblik de klink van een laag Oud Wadsediment te berekenen, eendeels doordat een dergelijk pakket niet homogeen van samenstelling is, anderdeels doordat niet voldoende bekend is, onder welke omstandigheden zo'n pakket tijdens en na de afzetting ervan heeft verkeerd. Voor het bepalen van de klink zijn wij dus aangewezen op schattingen, met als basis de berekeningen van HUIZINGA.

Om de dikte van het Oude Wadsediment aan het einde van het Atlanticum te leren kennen, moet die klink in twee gedeelten gesplitst worden, de klink tijdens het Atlanticum en die na deze tijd tot heden. Het „veen op grotere diepte” is waarschijnlijk reeds tijdens het Atlanticum bijna geheel tot de tegenwoordige dikte ingeklonken, want het werd in het Atlanticum met een minstens 10 m dikke laag sediment bedekt. Ook het Oude Wadsediment zal tijdens het Atlanticum reeds belangrijk zijn ingeklonken, maar een hernieuwde sterke zetting is waarschijnlijk na het drooglopen van het wad aan het einde van het Atlanticum opgetreden, omdat nu de wateronttrekking aan het sediment sneller kon gaan. Voor een 10 m dikke laag Oud Wadsediment, bestaande uit klei en zand zal naar schatting de inklinking tijdens het Atlanticum 2 m bedragen hebben. Voor de inklinking gedurende de 4500 jaar daarna nemen wij eenzelfde bedrag van twee meter. De top van het Oude Wadsediment lag aan het einde van het Atlanticum in dit geval dan 2 m hoger dan thans.

Bij Rotterdam, Velzen en Nootdorp, waar het „veen op grotere diepte” pollenanalytisch gedateerd kon worden, is de dikte van het Oude Wadsediment tot aan het oppervlakteveen (in Nootdorp tot aan een stuifzandlaag) resp. 10.50, 12 en 9.50 m, gemiddeld 11 m. Indien de post-Atlantische klink 2 m bedroeg, was de dikte aan het einde van het Atlanticum  $\pm 13$  m.

Eenzelfde benaderde waarde kunnen wij berekenen voor het hoogteverschil tussen „veen op grotere diepte” en de oude strandvlakten tussen de Oude duinen in Zuid-Holland. De Westelijkste strandvlakte, die waarschijnlijk aan het einde van het Atlanticum is ontstaan, ligt op  $\pm 2$  m — N.A.P. Het „veen op grotere diepte” ligt daar op 14–16 m — N.A.P., zodat de dikte van dit pakket 12 à 14 m bedraagt. Hier werd

de dikte door klink minder beïnvloed, omdat onder de duinen het pakket uit zand bestaat, voor zover de bovenste meters betreft, n.l. uit het Oude Zeezand van de Geologische Kaart.

Ook hier zal het „veen op grotere diepte” reeds tijdens het Atlanticum belangrijk ingeklonken zijn.

Bij benadering bedroeg de relatieve zeespiegelstijging tijdens het Atlanticum 13 m. Deze relatieve zeespiegelstijging bestaat dus uit de werkelijke stijging van het zeeniveau, vermeerderd met de daling van het land.

Andere omstandigheden treffen wij in Denemarken aan. Ontlast van de druk van het landijs van de laatste ijstijd is het Noord-oostelijke deel van dit land isostatisch gestegen. Daar zijn pollenanalytisch gedateerde mariene sedimenten, waarvan de afzetting in het begin van het Atlanticum een aanvang heeft genomen. De dikte van de tijdens het Atlanticum afgezette mariene sedimenten, meestal gyttja's, stelt dus een minimum-waarde voor van de relatieve zeespiegelstijging gedurende deze tijd. Deze relatieve zeespiegelstijging bestaat in Denemarken uit de werkelijke zeeniveaustijging, verminderd met de rijzing van het land. IVERSEN (1943) vond bij Søborg Sø en Klampenborg Fjord 3.80 en 4 m mariene gyttja, die tijdens het Atlanticum is afgezet. Ook hier weer rekening houdende met de post-Atlantische klink van dit zeer fijnkorrelige sediment, mogen wij de dikte aan het einde van het Atlanticum op 5 m stellen. Bovendien is er voor de afzetting van een gyttja een minimum-waterdiepte van  $\pm 1$  m nodig. zodat in dit gedeelte van Denemarken een relatieve zeespiegelstijging van 6 à 7 m heeft plaats gehad. Hierbij moet nog worden opgemerkt, dat deze mariene gyttja's op terrestrische afzettingen liggen en dat de zee aan het begin van het Atlanticum hierover getransgreedeerd is.

De zeeniveaustijging gedurende het Atlanticum ligt dus vermoedelijk tussen 7 en 13 m. Voorlopig is een gemiddelde waarde als het meest waarschijnlijk te beschouwen, zodat wij een bedrag van 10 m voor de absolute stijging van het zeeniveau gedurende het Atlanticum als een benaderde waarde zullen mogen beschouwen.

Ook op grond van enkele andere gegevens is het mogelijk tot een positieve niveauverandering van  $\pm 10$  m tijdens het Atlanticum te concluderen. MIKKELSEN (1949) vond in de Praestø-fjord een zeespiegelstijging van 9 m. Volgens A. JESSEN (1928) bedraagt de post-Atlantische opheffing van de bodem op deze plaats ongeveer 1 m, zodat aan het einde van het Atlanticum de totale zeeniveaustijging hier 10 m bedroeg.

Met behulp van deze gegevens is het mogelijk de bodemdaling van Nederland althans bij benadering te bepalen. Deze zal vermoedelijk  $13 - 10 = 3$  m bedragen hebben, gedurende het Atlanticum, welke tijd ongeveer 3000 à 3500 jaar besloeg. Per eeuw berekenen wij derhalve een bodemdaling van  $\pm 9$  cm. Wij nemen aan, dat de bodemdaling in een geologisch zo korte tijd als van het begin van het Atlanticum tot heden niet aan grote schommelingen onderhevig is geweest en stellen dus



de bodemdaling van Zuid-Holland gedurende het Holocene op  $\pm 9$  cm per eeuw. Deze uitkomst is een goede overeenstemming met de resultaten van KUENEN, die op een geheel andere wijze voor West-Nederland een daling van 5 cm per eeuw vond, maar voor beide provincies Holland tot een hoger bedrag kwam, n.l. 10 cm.

Wanneer het mogelijk zou zijn, een curve van de relatieve beweging van de zeespiegel te construeren, dan zou door aftrekking van de bodemdaling de werkelijke verandering van het zeeniveau in een grafische voorstelling kunnen worden weergegeven.

Hierbij ondervinden wij enkele moeilijkheden. Zo is het bekend, dat ongeveer 4000 jaar geleden een belangrijke regressie heeft plaats gehad. Van deze regressie zijn over de gehele aarde sporen terug gevonden. DALY (1943) vond op talrijke plaatsen abrasievlakken, brandingsnissen, opgeheven strandterrassen en andere fenomenen, die op een hogere zeespiegel dan de tegenwoordige, wijzen. In Engeland zijn op het 25 ft beach, dit is het post-glaciale strandterras, sporen van Neolithische bewoning gevonden. Daly neemt aan, dat dit terras nog tijdens het Neolithicum boven de zeespiegel is komen te liggen, ongeveer 2000 j. v. Chr. Dit zou dan in het eerste gedeelte van het Subboreaal gebeurd zijn. Zoals UMBGROVE (1947) reeds opmerkte, weerspiegelt deze gebeurtenis zich in Nederland in het drooglopen van het wad en de groei van het oppervlakteveen. Wij zagen, dat pollenanalytisch onderzoek van dit veen waarschijnlijk maakte, dat het vroeg in het Subboreaal is begonnen te groeien.

De grootte van deze regressie is niet bekend. Wel zegt DALY, dat de tegenwoordige stand van het zeeniveau 6 m onder de hoogste post-glaciale ligt, maar later kwam hij hier op terug. In 1934 schrijft DALY: „The many low benches do, in fact, show emergence varying from 1 to 6 meters”.

Na deze regressie is het zeeniveau waarschijnlijk weer gestegen. Zo zijn er in ons land verscheidene aanwijzingen voor verschillende transgressie-fasen omstreeks het begin van onze jaartelling en later. Weliswaar werkte de bodemdaling dit verschijnsel in de hand, maar o.i. moeten deze transgressies toch duidelijk het gevolg zijn van een absolute stijging van het zeeniveau. Bovendien is in recente tijd een zeespiegelstijging geconstateerd, die samenhangt met het afsmelten van gletschers (KUENEN 1945).

Hoe groot de totale daling van het zeeniveau omstreeks 2000 j. v. Chr. is geweest, kan uit Nederlandse gegevens dus nog niet worden bepaald. Wel is waarschijnlijk, dat deze daling enkele meters heeft bedragen; dit blijkt ook reeds uit de snelle verzoeting van het milieu, waarin het „oppervlakteveen” ontstond.

Uit waarnemingen in Denemarken (IVERSEN 1937) en bij Nootdorp (Z.H.) (ZWART, nog niet gepubl.) is gebleken, dat er tijdens het Atlanticum nog een drietal kleine regressies is geweest. De verkregen gegevens waren echter niet voldoende voor het construeren van een curve, die de bewegingen van de zee aangeeft.



Uit proeven, door TIMMERMANS (1935) gedaan in het Rijksmuseum van Geologie te Leiden, is gebleken, dat door de branding op een zandkust een strandwal wordt opgeworpen. In het algemeen zal een dergelijke strandwal niet boven vloedhoogte komen te liggen. VAN DER MEER (1949) maakte waarschijnlijk, dat bij een regressie deze strandwal boven het zeeniveau komt te liggen, zodat duinvorming, dus ophoging, op de strandwal mogelijk wordt. Bij een volgende transgressie ontstaat vóór de eerste een nieuwe strandwal, die bij de volgende regressie ook tot een duinrug wordt omgevormd. VAN DER MEER onderscheidde twee zulke duinruggen, waarvan de Oostelijkste, die waarop Lisse en Hillegom liggen, de oudste is en bij een midden-Atlantische regressie zou zijn gevormd. Tijdens een tweede regressie ontstond de volgende duinrug, die waarop Noordwijkerhout ligt. Volgens de Geologische Kaart is echter de rug van Voorschoten — Voorburg de oudste, terwijl Westelijk van de rug van Noordwijkerhout nog een brede strandvlakte ligt, waarop nogmaals een oude duinrug, bijna geheel bedekt door jong duin, volgt. In totaal zijn er dus vier brede duinruggen, waarvan de oudste drie met de drie Atlantische regressies te correleren zijn, terwijl de jongste met de regressie van DALY overeenkomt. Zo zien wij, dat het rythme, dat wij soms kunnen waarnemen in een verticaal profiel in Hollands veengebied, n.l. een afwisseling van veen- en kleilagen, gelijkenis vertoont met een rythme in een horizontaal vlak, in de vorm van afwisseling van duinruggen en strandvlakten.

Het is helaas nog niet mogelijk, om de Atlantische regressies goed te dateren, zodat wij ook hier met schattingen zullen moeten volstaan. Daar in het Atlanticum een gedeelte van het „veen op grotere diepte” is gevormd en een vrij dik pakket Oud Wadsediment (n.l. de Oud-Holocene wadafzettingen van de Geologische Kaart), moet er een vrij lange tijd zijn verlopen vanaf het begin van het Atlanticum tot aan de eerste regressie. Anderzijds moet er ook tijd beschikbaar zijn geweest voor de vorming van het Oude Duin, dat immers voor het grootste deel tijdens het Atlanticum is ontstaan. Om deze redenen plaatsen wij de eerste Atlantische regressie midden in het Atlanticum, op  $\pm 4000$  j. v. Chr. Voor de vorming van het Oude Duin is dan een tijd van 2000 jaar beschikbaar.

De hoogte van de strandvlakten tussen de oude duinruggen stelt de gemiddelde vloedhoogte van de zee tijdens de vorming van de strandwal voor. Het lijkt ons niet waarschijnlijk, dat deze hoogten na het Atlanticum door inklinking belangrijk beïnvloed zijn, omdat hier de afzettingen op het „veen op grotere diepte” grotendeels zandig zijn, en in ieder geval het bovenste gedeelte uit zand bestaat. De Oostelijkste strandvlakte, waardoor de spoorlijn Den Haag—Leiden loopt, ligt op 2.80 m — N.A.P., waarbij de jongere bedekking met veen buiten beschouwing is gelaten. De tweede strandvlakte ligt op 2.20 m — N.A.P. de derde op 1.60 m — N.A.P. en de vloedhoogte vóór de vierde strandwal zal dan ongeveer 1 m — N.A.P. bedragen hebben. Daar de gemiddelde vloedhoogte bij Katwijk nu 80 cm

+ N.A.P. bedraagt, is het verschil tussen de stand van het zeeniveau tijdens de vorming van de strandwallen en het tegenwoordige gemiddelde zeeniveau resp. 3.60, 3.00, 2.40 en 1.80 m.

Uit deze getallen zou volgen, dat de relatieve zeespiegelstijging van — 4000 tot — 2000:  $3.60 - 1.80 = 1.80$  m bedroeg. Zoals wij reeds hebben berekend, bedroeg de bodemdaling in 2000 jaar  $20 \times 9 \text{ cm} = 1.80 \text{ m}$ .

Wij komen dus tot de conclusie, dat gedurende het tweede gedeelte van het Atlanticum en het begin van het Subboreaal het zeeniveau nage-noeg op een constant peil is gebleven, omdat de bodemdaling gelijk is aan de relatieve zeespiegelstijging. In het eerste gedeelte van het Atlanticum daarentegen zal de eustatische stijging van de zee vrijwel geheel de berekende waarde van 10 m bedragen hebben.

Tijdens het eerste deel van het Atlanticum vinden wij dus een belangrijke en snelle transgressie van omstreeks 10 m, gedurende de laatste helft blijft het zeeniveau ongeveer op gelijke hoogte, maar er zijn enkele schommelingen, waarvan de grootte o.i. niet veel meer dan een halve meter heeft bedragen. Waren de regressies in het Atlanticum van grotere afmeting geweest, dan zouden er veel meer en veel belangrijker veenlagen in het Oude Wadsediment moeten liggen. Zij zijn echter schaars en vrij dun.

Bij een belangrijke regressie, zoals die van omstreeks 2000 j. v. Chr., begon overal op het Oude Wadsediment, veengroei.

Dat in het tweede deel van het Atlanticum de afzetting van het Oude Wadsediment toch is doorgegaan, is het gevolg van het inklinken van de reeds afgezette veen- en kleilagen. Door deze inklinking ontstond dus de plaats voor nieuwe sedimenten. Klink heeft dus wel het effect van bodemdaling, maar toch is de totaal bereikbare dikte van zo'n pakket gebonden aan de relatieve zeeniveaustijging.

De oude duinen zouden dus gevormd zijn bij een vrijwel constante zeespiegel; de verschillende ruggen zijn te danken aan kleine regressies. Het hoogteverschil tussen de strandvlakten is het gevolg van de bodemdaling tijdens het ontstaan van de duinruggen.

In verband met de vele waarnemingen van DALY lijkt ons een vrijwel constant zeeniveau gedurende lange tijd in het Atlanticum zeer waarschijnlijk. Vooral de abrasievlakken, die langs vele kusten voorkomen, doen toch wel een tijdelijk constant zeeniveau veronderstellen. Bij een snel stijgende of dalende zeespiegel zal niet licht een duidelijk abrasievlak gevormd worden. Ook strandterrassen, die op vele plaatsen gevonden zijn, duiden op een stilstandstijd van het zeeniveau. Bij een constant stijgende zeespiegel gedurende het Atlanticum en een plotselinge daling daarna, zouden deze strandterrassen niet zo fraai ontwikkeld zijn. DALY zegt dan ook: „Thus, the different regions must have had sea-level nearly constant for a considerable time, during which the strand marks were well incised.”

Ook in West-Europa komen wij verschijnselen tegen, die op een vroegere hoge stand van de zeespiegel wijzen. Voornamelijk zijn dit strand-

terrassen. In Noord-Engeland en Schotland is het 25 ft beach een dergelijk terras. Naar het Zuiden gaande ligt dit terras steeds lager als gevolg van de isostatische opheffing na het verdwijnen van de gletschers. In werkelijkheid bevindt dit terras zich op een hoogte van 0—10 m boven de zeespiegel. In Denemarken en Zweden kent men een dergelijk strandterras, daar het Litorina-strand genoemd. Ook dit terras ligt, naar het Zuiden gaande, steeds lager.

In Nederland, waar het land sinds de ijstijd is gedaald, ligt het „Litorina-strand” dus tussen de oude duinruggen, onder het tegenwoordige zeeniveau.

Zoals wij gezien hebben, is het wel waarschijnlijk, dat de zee tijdens het laatste gedeelte van het Atlanticum en in het begin van het Subboreaal hoger stond dan tegenwoordig. Dit komt ook tot uiting in de curve, die de werkelijke bewegingen van het zeeniveau weergeeft. Hieruit kan worden afgeleid, dat de zeespiegel tegenwoordig slechts 1 à 2 m lager staat dan tijdens het Atlanticum. Hoeveel de zeespiegel in het Subboreaal gedaald is, is onbekend. Dit vraagstuk hangt ten nauwste samen met de oorzaak van de daling van het zeeniveau in het algemeen.

Er zijn aanwijzingen gevonden, dat in het postglaciaal van 4000—2000 j. v. Chr. het klimaat een optimum bereikte. (FLINT, 1947). Eveneens zijn er tekenen, dat in het Subboreaal een zekere klimaats-verslechtering heeft plaats gevonden (IVERSEN, MIKKELSEN 1949). Anderzijds echter waren de Alpen in de tweede helft van het Subboreaal minder vergletscherd dan nu (GAMS en NORDHAGEN 1923), terwijl in de laatste honderd jaar de gletschers duidelijk aan het terugtrekken zijn.

Zouden de schommelingen van het zeeniveau alleen door het smelten en weer aangroeien van gletschers veroorzaakt worden, dan is een hoge zeestand tijdens het klimaatoptimum van 4000—2000 j. v. Chr. heel aannemelijk, terwijl het aangroeien van de gletschers na die tijd inderdaad met een daling van het zeeniveau samenvalt. In de tweede helft van het Subboreaal toen het zeeniveau mogelijk zijn laagste stand na de hoogste postglaciale bereikte, was de gletscherstand hoger dan de tegenwoordige, maar lager dan in het Atlanticum. Toch stond de zeespiegel in de tweede helft van het Subboreaal lager dan thans. Een tweede moeilijkheid zien wij in de stilstand van de zeespiegel tijdens het klimaatoptimum in het Atlanticum en in het eerste gedeelte van het Subboreaal, terwijl ook de hoge ligging van vele abrasievlakken en strandterrassen, n.l. 6 m boven het tegenwoordige zeeniveau, niet met onze conclusies in overeenstemming is; wij vonden slechts een verschil tussen hoogste postglaciale stand en tegenwoordige, van 1—2 m.

DALY schrijft de daling van de zee in het Subboreaal niet toe aan het aangroeien van gletschers, maar aan het isostatisch zakken van de oceaanbodems, die door het vrijkomende smeltwater aan een zwaardere belasting onderhevig waren. DALY is van mening, dat de vrij snelle daling van het zeeniveau hierop wijst. In dit geval zou hij het dalen van de



oceanbodems het omgevende land isostatisch moeten rijzen, waardoor strandterrassen en abrasievlakken eveneens omhoog zullen gaan. Een relatieve daling van 5 à 6 m zou dan niet alleen op rekening mogen worden gesteld van een beweging van het zeeniveau. Deze verklaring lijkt ons niet geheel bevredigend: waarom zal de zeespiegel na een stilstand van  $\pm 2000$  jaar plotseling gaan dalen, omdat pas dan de oceanbodems snel isostatisch zullen inzakken?

Een combinatie van deze twee factoren, wisselingen in de stand der gletschers en bewegingen van de oceanbodems, lijkt ons het meest waarschijnlijk. Toen na de laatste ijstijd de gletschers snel inkrompen, en het peil van de zeeën snel steeg door het vrijkomende water, zullen naar alle waarschijnlijkheid de bodems van die zeeën door de grotere waterdruk zijn gaan dalen. Dit proces zal ook in het Atlanticum zijn doorgegaan, maar, daar aan het einde van deze tijd het klimaat zijn optimale toestand had bereikt, zal er een evenwicht tussen de stand van de gletschers en dit klimaat tot stand zijn gekomen. In de loop van het Atlanticum zal het smelten van de gletschers steeds langzamer gegaan zijn om aan het einde van deze tijd of in het eerste gedeelte van het Subboreaals tot stilstand zijn gekomen. Daarna zouden de gletschers weer zijn gaan aangroeien met als gevolg het dalen van de zeespiegel. Daar het evenwicht tussen de isostatische daling van de zeebodems en de daarop door het water uitgeoefende druk waarschijnlijk met een zekere vertraging tot stand kwam, zal deze daling zijn doorgegaan, terwijl als gevolg hiervan de omliggende kusten door isostatische compensatie zullen zijn gerezen.

Wanneer nu in het tweede gedeelte van het Atlanticum de plaats, die vrij kwam door de daling van de oceanbodems, juist door het aangevoerde smeltwater werd gevuld, dan komt dit neer op een stilstand van de zeespiegel. In de tijd, daaraan voorafgaand zal de hoeveelheid smeltwater, die aan de zee werd toegevoegd, groter zijn geweest dan de plaats, die vrij kwam door de daling van de zeebodem. Ná deze tijd werden de gletschers weer groter, terwijl door het nog enige tijd doorgaan van de daling van de zeebodem een snelle regressie optrad. Te zelfder tijd rezen de kusten nog, zodat een vrij groot verschil tussen de hoogste zeestand en die aan het einde van de regressie kan zijn ontstaan.

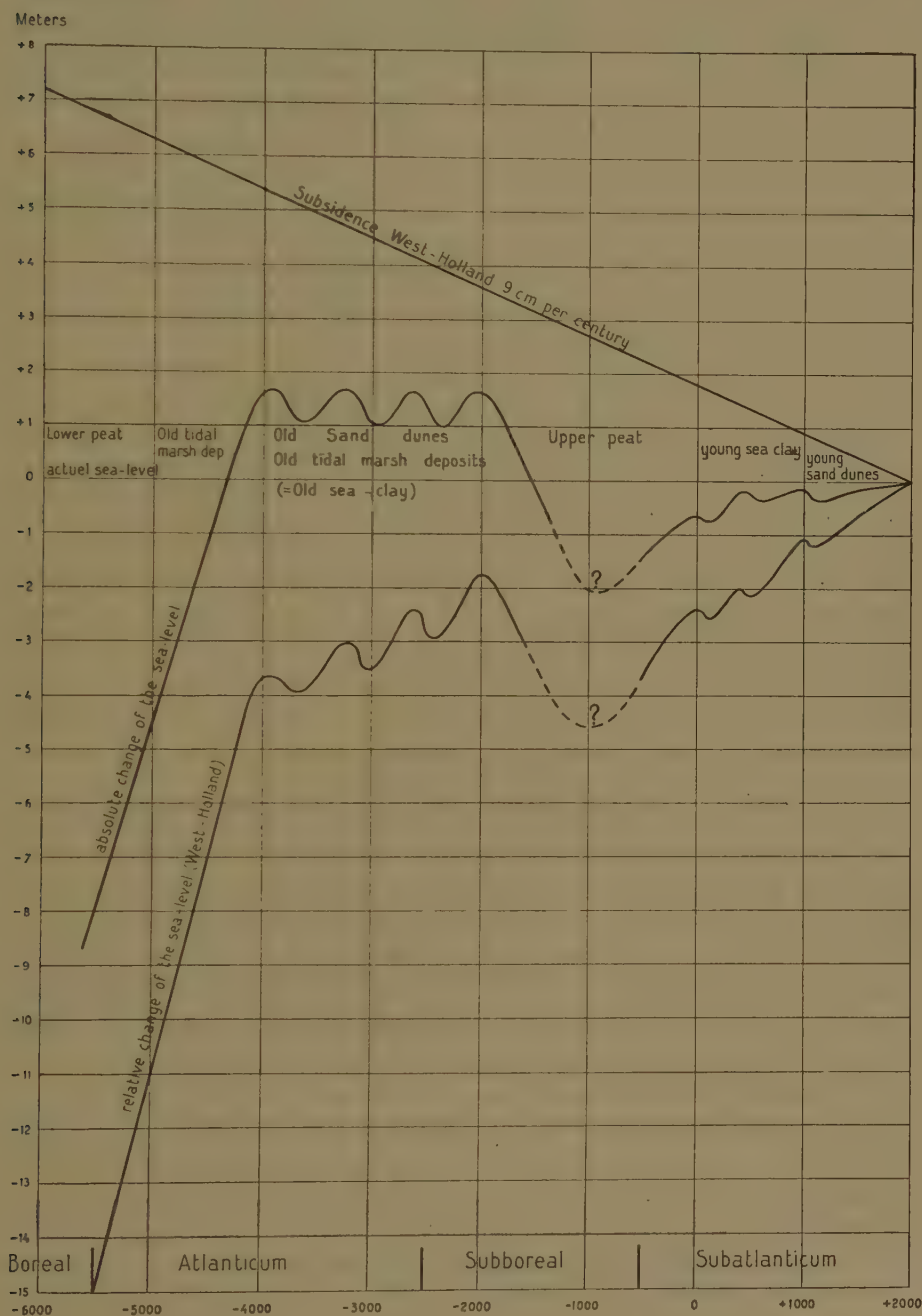
In de loop van het Subboreaals kunnen de gletschers verder zijn aangegroeid en eventueel in het Subatlanticum een hoogste stand bereikt hebben. In betrekkelijk recente tijd trad weer een afsmelting op, gepaard gaande met een stijging van het zeeniveau.

In bijgaande grafiek zijn de bewegingen van het zeeniveau sinds het begin van het Atlanticum weergegeven, zoals die volgens onze mening is verlopen. Door de bodemdaling af te trekken van de curve voor de relatieve zeeniveaustijging, is de lijn, die de echte beweging van de zeespiegel aangeeft, gevonden.

Van de bestaande curven, gelijkt die van NILSSON (1948) vrij veel



op de onze. Zijn curve geeft echter alleen de relatieve beweging van de zeespiegel weer en is minder gedetailleerd.



Zeer veel dank ben ik verschuldigd aan Prof. F. FLORSCHÜTZ, die het manuscript critisch doorlas en mij vele belangrijke en nuttige aanwijzingen gaf.

### *Summary*

For a comparison of strata in different countries it is necessary to know their age. For post-glacial beds we can make use of pollen-analysis. According to ESCHER, KUENEN and UMBGROVE, it has been established that the coast of Holland has been sinking since the last ice-age. We presume that the sea-level has risen after the Würm-glacial. As for a marine sediment, covering a terrestrial deposit, the top being settled at the actual sea-level, the thickness of the bed represents the sum of the rise of the sea-level and the subsidence of the land during the sedimentation. For the thickness of the sediments, deposited in the Atlanticum in West-Holland we found 11 m. Considering the compaction, the thickness at the end of the Atlanticum will have been about 13 m.

In Danmark land and sea were both rising. Therefore, the thickness of an Atlantic marine bed in that country represents the rise of the sea-level reduced by the rise of the land. For some marine gyttja's there was found a thickness of 4 m. Considering the compaction and the minimum depth of water for settling a gyttja, the relative rise of the sea-level during the Atlanticum will have been 6 or 7 m. The absolute rise of the sea-level during the Atlanticum lies between 7 and 13 m, average 10 m.

Hence in the Netherlands the subsidence of the land during the Atlanticum was 3 m in 3500—3000 years, or 9 cm per century.

According to DALY, there was an important regression some 4000 years ago, so in the beginning of the Subboreal. In Holland this regression is represented by the growth of the upper peat. The extent of this regression is still unknown.

It appears from dutch and danish data that in the second part of the Atlanticum three regressions have taken place. In contrast with the regression of 2000 years b. C. these three regressions were of a small extent. We can correlate them with the formation of the old dunes, of which we can distinguish four ridges. From the height of the old beaches between the sandbars, we know the height of high tide during the formation of the offshore bar, which has been blown up to a dune ridge during the following regression.

The difference in height between the first and the last beach level is 1.80 m, representing just the subsidence of the land in the 2000 years of formation of old dunes.

Hence the sea rose the whole value of 10 m in the first part of the Atlanticum, and in the second part the sea stayed on the same level, with some little changes, regression- and transgressionphases. Our conclusions are in agreement with the observations of DALY. The many wave-cut benches, undercuts and raised beaches, caused by the sea in the Atlanticum, have undoubtedly been formed with a temporary constant sea-level. This sea-level is the highest after the last glaciation. The same conclusion can be drawn from our curve for the absolute rise

of the sea. After the regression in the Subboreal the sea rose anew in Subatlantic times.

The cause of the changes of the sea-level will be a combination of the melting and growing on of the glaciers and the subsidence of the bottom of the oceans by the weight of the water.

#### L I T E R A T U U R

- DALY, R. A., A recent Worldwide sinking of the Ocean-level. *Geological Magazine*, **57**, (1920).
- , The changing world of the Ice age. (1934).
- ESCHER, B. G., Het vraagstuk van de daling van de bodem van Nederland. *Geologie en Mijnbouw*, **2** (1940).
- FLINT, R. F., Glacial geology and the Pleistocene Epoch. (1947).
- FIRBAS, F., Spät- und nacheiszeitliche Waldgeschichte Mitteleuropas. (1949).
- FLORSCHÜTZ, F., „Laagterras” en „veen op grotere diepte” onder Velzen. *Tijdschrift K.N.A.G.* 2e reeks, **61**, (1944).
- en VLERK, I. M. VAN DER, Duizend eeuwen geschiedenis van de bodem van Rotterdam. *De Maastunnel*, **2**, no. 6, (1939).
- GAMS, H. en NORDHAGEN, R., Postglaziale Klimaänderungen und Erdkrustenbewegungen in Mitteleuropa. *Geog. Ges. in München, Landeskundliche Forschungen*, no. 25, (1923).
- GODWIN, H., Coastal peatbeds of the British isles and North sea. *Journal of Ecology*, **31**, (1943).
- , Coastal peatbeds of the North Sea region as indices of land- and sea-level changes. *New phytologist*, **44**, (1945).
- HUIZINGA, T. K., De bodemdaling van Nederland, bezien van grondmechanisch standpunt. *Geologie en Mijnbouw*, **2**, no. 5, (1940).
- IVERSEN, J., Undersogelser over Litorinatrangressioner i Danmark. *Medd. Dansk. geol. för.*, **2**, heft 2, (1937).
- JESSEN, A., Niveauveränderungen. In Uebersicht über die Geologie von Dänemark.” *Danmarks geol. Unders.*, V Raekke, no. 4 (1928).
- KUENEN, PH., De relatieve en absolute daling van onze bodem. *Geologie en Mijnbouw*, **3**, no. 7, (1941).
- , De zeespiegelrijzing der laatste decennia. *Tijdschrift K.N.A.G.* 2e reeks, **62**, (1945).
- MEER, K. VAN DER, De vorming der duinen, Boor en Spade III, (1949).
- MIKKELSEN, V. M., Praestø-fjord. *Dansk Bot. Arkiv*. Bd. 13, no. 2, (1949).
- NILSSON, T., Versuch einer anknüpfung der Postglazialen Entwicklung des nord-westdeutschen und niederländischen Flachlandes an die Pollenfloristische Zonengliederung Südkandinaviens. *Medd. Lunds Geol. mineral. Institution*, nr. 112, (1948).
- TIMMERMANS, P. D., Proeven over de invloed van golven op een strand. *Diss.* (Leiden, 1935).
- UMBROVE, J. H. F., Origin of the dutch coast. *Proc. Kon. Ned. Ak. v. Wetenschappen*, **50**, no. 3, (1947).
- WOLDSTEDT, P., Norddeutschland und angrenzende Gebiete im Eiszeitalter. (1950).

## PALAEONTOLOGY

## DESCRIPTION DE QUELQUES ALVEOLINES DE TIMOR; RESULTAT D'UNE ELABORATION DE LA METHODE DES COURBES D'INDICE DE REICHEL

PAR

L. RITSEMA

(Communicated by Prof. H. A. BROUWER at the meeting of March 31, 1951)

Les calcaires à Alvéolines, récoltés par F. P. VAN WEST (litt. 18, p. 29) pendant l'expédition aux Petites Iles de Sonde sous la direction du professeur H. A. BROUWER, ont été soumis à une analyse plus détaillée qu'ils ne l'avaient été par lui. Ils proviennent tous de la région de Miomaffo dans la partie occidentale de l'île de Timor. Les échantillons sont conservés à l'Institut de Géologie à Amsterdam.

Voici la liste des échantillons en question avec leur faune:

No. de la collection	Roches	Espèces	Quantité	Gisements
B 5956	calcaire à Alvéolines, gris	<i>A. oblonga</i> <i>A. javana</i> <i>A. pygmaea</i>	très nombreuse rare très rare	Sentier Noil Toko-K. Seoam à l'Est de P 18.
B 6034	calcaire à Alvéolines, gris	<i>A. oblonga</i> <i>A. javana</i> <i>A. wichmanni</i>	très nombreuse rare rare	Noil Noni P 57 près de Noil Toko.
B 6104	calcaire à Alvéolines, gris foncé, compact	<i>A. oblonga</i>	très nombreuse	à l'Ouest du Pasan Graham, Noil Toko, en amont de N. Niti, sur la rive droite entre Tertiaire sup. et schistes cristallins.
B 6242	calcaire à Alvéolines, beige	<i>A. wichmanni</i> flosculinisée <i>A. oblonga</i>	très rare  rare	Noil Noni P 54 près de Noil Toko
B 6243	calcaire à Alvéolines, marneux, gris foncé	<i>A. oblonga</i>	assez fréquente	Noil Noni P 54 près de Noil Toko.
B 6245	calcaire à Alvéolines, écrasé, beige	<i>A. javana</i> flosculinisée <i>Alveolina spec.</i>	rare  rare	Noil Noni P 54 près de Noil Toko.
B 6248	calcaire à Alvéolines, marneux, gris bleuâtre	<i>A. wichmanni</i>	très rare	Noil Noni P 55 près de Noil Toko.



L'auteur tient à exprimer ici sa profonde reconnaissance envers M. le professeur H. A. BROUWER qui lui a prêté sa précieuse collection de fossiles, et envers M. le professeur M. G. RUTTEN qui l'a encouragé à entamer cette étude et qui a montré beaucoup d'intérêt pour ce travail.

Puisqu'il était impossible de détacher les Alvéolines de la roche et qu'il n'y avait aucune orientation dans la disposition des individus, on a dû, dans l'analyse, recourir aux lames minces, présentant toutes les sections possibles.

REICHEL donne dans son ETUDE SUR LES ALVÉOLINES (litt. 11, fig. 2) un tableau des différentes sections montrant de façon schématisque l'aspect de la spire et des *septa*. Pour compléter ce tableau il faudrait mentionner la section oblique non-centrée, qui se trouve plus près de la section axiale que de la section équatoriale. Cette section se présente très souvent dans les lames minces des roches examinées. On trouve au centre d'une telle section des anneaux concentriques, tout comme dans la section tangentielle, tandis que plus à l'extérieur on retrouve la spire normale, présentée aussi par la section oblique-centrée et par la section équatoriale. (fig. 1).

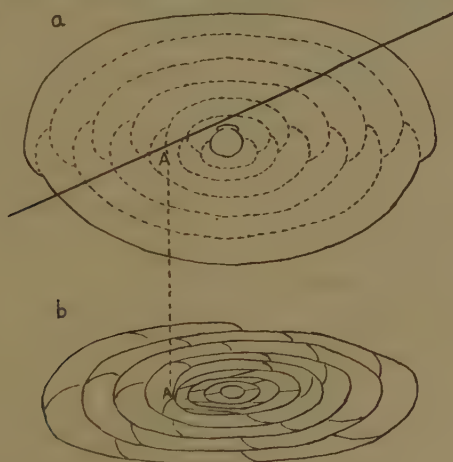


Fig. 1

- a) La section axiale montrant la direction de la section oblique non -- centrée.
- b) La section oblique non — centrée.
- A. L'endroit où l'axe traverse la section.

Nous n'avons pas pu constater le dimorphisme, indiqué par REICHEL comme trait caractéristique du genre *Alveolina*. Les roches examinées, quelque approfondie qu'ait pu être l'expérience, ne présentaient que des formes mégasphériques.

Les quatre premiers caractères du genre *Alveolina* donnés par REICHEL (litt. 11, p. 77) ont bien été observés, à savoir:

- 1) le canal postseptal
- 2) les deux rangées d'ouvertures dans les septa
- 3) les cloisonnettes alternantes
- 4) la flosculinisation.

Nous n'avons pu observer ni le pelotonnement des premiers tours de la spire ni les logettes supplémentaires dans l'épaississement basal de la région axiale.

Bien que selon les règles internationales le nom générique *Fasciolites* (et éventuellement *Borelis*) soit plus exact, nous sommes d'avis qu'il faut préférer comme "nomen conservandum" *Alveolina*, nom consacré par un usage tout à fait général.

#### LES ESPÈCES

Ce qui pour la détermination des espèces se révéla tout d'abord particulièrement important, ce fut la relation qui dans un individu existe entre le numéro d'ordre des tours de la spire et l'indice (c'est-à-dire la proportion longueur : largeur) de chaque tour (cf. déjà aussi REICHEL litt. 11, p. 18). Nous avons représenté cette relation au moyen de graphiques, indiquant en abscisse les tours de la spire et en ordonnée l'indice. Ces COURBES D'INDICE, donnant une idée fort exacte de la croissance d'un individu, sont caractéristiques pour une espèce déterminée.

Il n'y a, en théorie, que la section axiale qui se prête à la construction d'une courbe d'indice. Cependant, dans la pratique, on peut avoir recours aussi aux sections qui coupent l'axe sous un angle aigu.

Nous avons ensuite déterminé le nombre des tours de la spire à un rayon de 1 mm d'autant d'individus que possible, ce à quoi peut servir chaque section à travers la loge initiale. Le nombre des logettes secondaires sur une longueur de méridien de 1 mm à un rayon de 1 mm ne se laisse déterminer que dans une section axiale.

Enfin nous avons mesuré la hauteur des logettes secondaires dans le dernier tour.

La loi d'enroulement, établie et employée par BAKX (litt. 1, p. 219) dans sa détermination des espèces, paraît à peu près sans valeur, à cause des différences assez grandes entre les individus appartenant à une seule espèce et de la différence peu saillante entre les relevés numériques donnés pour les espèces différentes.

#### DESCRIPTION DES ESPÈCES

##### *Alveolina oblonga* d'Orbigny (fig. 2 A, 3 A)

- 1826 *Alveolina oblonga* D'ORBIGNY. Tableau méthodique. Ann. des Sc. nat. Tome VII p. 306.
- 1883 *Alveolina oblonga* D'ORBIGNY. C. Schwager: Die Foraminiferen aus dem Eozän-abl. der lib. Wüste und Aeg. Palaeontografica Bd. 30, 1 p. 99.
- 1896 *Alveolina timorensis* VERBEEK. Verbeek en Fennema: Java en Madoera. p. 1094.
- 1916 *Alveolina oblonga* D'ORBIGNY. H. Douvillé: Le Crétacé et l'Eocène du Tibet central. Pal. Indica N. S. 5 Mem. 3 p. 42.

- 1925 *Alveolina oblonga* D'ORBIGNY. W. F. Nuttall: The Stratigraphy of the Laki Series. Quart. Journ. Geol. Soc. 81, p. 440.  
 1932 *Fasciolites oblonga* D'ORBIGNY. L. Bakx: De Genera Fasciolites en Neoalveolina. Verh. Geol. Mijnb. Gen. 9, p. 218.  
 1934 *Fasciolites oblonga* D'ORBIGNY. H. Henrici: Foraminiferen aus dem Eozän und Altmiozän von Timor. Palaeontogr. Suppl. IV, Abt. 4, p. 40.

La courbe de l'indice (fig. 3 A) présente un maximum variant de 2.0 à 2.3 entre le 8<sup>me</sup> et le 10<sup>me</sup> tour.

La forme varie entre la forme cylindrique et l'ellipsoïde tronqué.

Les tours sont très réguliers.

Le nombre des tours, à un rayon de 1 mm, est de 10 à 12.

Le nombre des logettes secondaires à un rayon de 1 mm est de 14 par 1 mm de méridien.

La hauteur des logettes secondaires au dernier tour est de 100  $\mu$  environ.

#### *Alveolina timorensis* Verbeek

Comme BAKX l'a déjà indiqué, l'espèce *Alveolina timorensis* ne peut être admise. VERBEEK (litt. 17, p. 1094 et fig. 39, Pl. II) a créé cette espèce, se basant sur une coupe qui n'était pas axiale, ni même centrée. Aussi n'a-t-il pas pu en donner une description suffisante. D'ailleurs la figure montre clairement qu'il s'agit ici d'une *Alveolina oblonga* aux extrémités tronquées, aux tours réguliers et aux logettes secondaires assez grandes.

#### *Alveolina javana* Verbeek (fig. 2 B, 3 B)

- 1896 *Alveolina javana* VERBEEK. Verbeek en Fennema: Java en Madoera. p. 1091.  
 1932 *Fasciolites javana* VERBEEK. L. Bakx: De Genera Fasciolites etc. Verh. Geol. Mijnb. Gen. 9, p. 231.  
 1934 *Fasciolites cf. javana* VERBEEK. H. Henrici: Foraminiferen etc. Palaeontogr. IV, Abt. 4, p. 39.

La courbe de l'indice croît graduellement jusqu'au 11<sup>me</sup> ou 12<sup>me</sup> tour, et ensuite encore plus lentement. Elle ne décroît pas aux derniers tours, comme c'est le cas pour *Alveolina oblonga*.

La forme est elliptique avec des pôles assez aigus.

Les tours sont moins réguliers que ne sont ceux d'*Alveolina oblonga*.

Le nombre des tours à un rayon de 1 mm est de 12.

Le nombre des logettes secondaires à un rayon de 1 mm est d'environ 17 par 1 mm de méridien.

La hauteur des logettes secondaires au dernier tour est d'environ 50  $\mu$ .

#### *Alveolina wichmanni* Rutten (fig. 2 C, 3 C)

- 1914 *Alveolina wichmanni* n. sp. L. RUTTEN: Nova Guinea, p. 45, Pl. IX, fig. 1, 2.  
 1918 *Alveolina wichmanni* RUTTEN. Newton: Foraminifera in tertiary rocks of New Guinea. Geol. Mag. 1918, p. 207. Pl. VIII, fig. 1 (non pas Pl. VIII, fig. 3, 4a!).  
 1932 *Fasciolites wichmanni* RUTTEN. L. Bakx: De Genera Fasciolites etc. Geol. Mijnb. Gen. 9, p. 234.



A

1 mm



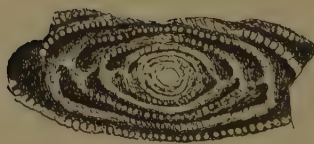
B

1 mm



C

1 mm



D

1 mm

Fig. 2

- A. *A. oblonga* D'ORBIGNY B 6034, 4 (18, 5 ×)
- B. *A. javana* VERBEEK B 6034, 6 (20 ×)
- C. *A. wichmanni* RUTTEN B 6248 (12, 7 ×)
- D. *A. pygmaea* HANZAWA B 5956, 17 (15, 8 ×)



La courbe de l'indice (fig. 3 C) croît considérablement jusqu'au 6<sup>me</sup> tour (indice de 3.0 environ), et présente un maximum de 3.6 au 9<sup>me</sup> ou 10<sup>me</sup> tour.

La forme est allongée, aux extrémités très aigües.

Les tours sont très irréguliers.

Le nombre des tours à un rayon de 1 mm est de 10.

Le nombre des logettes secondaires à un rayon de 1 mm est de 18 par 1 mm de méridien.

La hauteur des logettes secondaires au dernier tour est inférieure à 50  $\mu$ .

### *Alveolina pygmaea* Hanzawa (fig. 2 D, 3 D)

- 1929 *Borelis* sp. indet. Yabe and Hanzawa: Tertiary rocks of the Philippines. Sc. Rep. Tohoku Imp. Univ. Sendai vol. 11, 3. p. 181. Pl. XV, fig. 12.
- 1930 *Borelis (Fasciolites) pygmaea* sp. nov. Hanzawa: Note on Foraminifera found in the Lep. limestone from Pabeasan Java. Sc. Rep. Tohoku Imp. Univ. Sendai, vol. 14, 1. p. 94. Pl. 26, fig. 14, 15.
- 1932 *Neovalveolina pygmaea* HANZAWA. L. Bakx: De Genera Fasciolites etc. p. 237, Pl. III fig. 18, 19.
- 1934 *Fasciolites pygmaea* HANZAWA. H. Henrici: Foraminiferen etc. p. 44, Pl. III, fig. 1.
- 1947 *Borelis pygmaea* HANZAWA. Hanzawa: *Borelis* pygm. from the Mariana Islands, Jap. Journ. of Geol. and Geogr. vol. 20, p. 9. Pl. V, fig. 3, 4.

L'indice (fig. 3 D) croît très légèrement dans les 4 ou 5 premiers tours et ensuite plus rapidement, ne décroissant pas aux derniers tours.

La forme est elliptique; les tours sont réguliers.

Le nombre des tours à un rayon de 1 mm est de 8.

Le nombre des logettes secondaires à un rayon de 1 mm est de 16 par 1 mm de méridien.

La hauteur des logettes secondaires au dernier tour est de 50  $\mu$ .

La forme que nous venons de décrire coïncide dans tous ses caractères avec *Borelis pygmaea* HANZAWA (litt. 5), sauf en ce qui concerne les premiers tours. Ceux-ci sont réguliers, contrairement à la description faite par HANZAWA.

BAKX (litt. 1, p. 238) observait chez cette même espèce un *proloculum* triloculaire, ce qui l'a amené à la considérer comme appartenant au genre *Neovalveolina*.

L'individu que nous venons de décrire possède un *proloculum* normal (une seule loge initiale ronde) aux premiers tours régulièrement enroulés. Ceci nous conduit à suivre le jugement énoncé par HENRICI (litt. 6, p. 44) et à considérer donc cette espèce comme appartenant au genre *Alveolina*.

### FLOSCULINISATION

Le phénomène de la flosculinisation se rencontre rarement parmi les Alvéolines examinées, (seulement dans les roches B 6242 et B 6245). Néanmoins nous avons pu constater qu'il est impossible de classer les

formes flosculinisées en une seule espèce; au contraire, l'une d'entre elles est sans doute une *Alveolina wichmanni* et une autre pourrait être très vraisemblablement une *Alveolina javana*. Bien qu'*Alveolina oblonga* soit l'espèce la plus fréquente, elle ne montre pas de traces de flosculinisa-

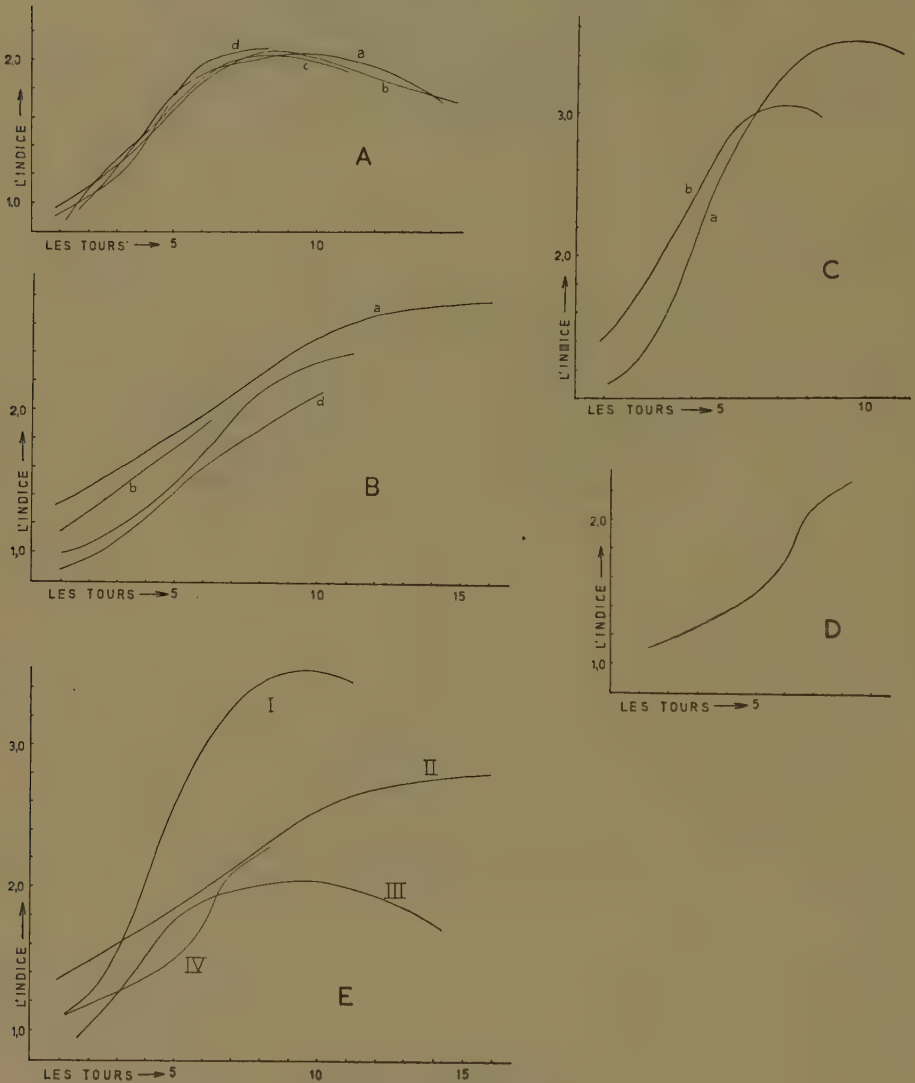


Fig. 3

Les courbes d'indice.

- A. *A. oblonga* D'ORBIGNY (a. B 6034, 4; b. B 5956, 26; c. B 6104, a; d. B 6104, c)
- B. *A. javana* VERBEEK (a. d'après la figure 35, Pl. II de VERBEEK (1896); b. B 5956, 6; c. B 6034, 6; d. B 6034, d)
- C. *A. wichmanni* RUTTEN (a. B 6248; b. 6034, 2)
- D. *A. pygmaea* HANZAWA (B 5956, 17)
- E. Quatre courbes d'indice des différentes espèces. I. *A. wichmanni* RUTTEN; II. *A. javana* VERBEEK; III. *A. oblonga* D'ORBIGNY; IV. *A. pygmaea* HANZAWA.

tion. En outre nous avons observé des individus flosculinisés à côté d'individus normaux dans la même roche (par exemple B 6242).

Il en résulte donc que l'abondance de calcaire ne saurait être admise comme la cause la plus probable de ce phénomène, ainsi que l'entendait BAKX en 1932.

### L'accroissement selon la spirale logarithmique

Mlle CURRIE a démontré, en 1941 (litt. 2), que l'accroissement de l'ammonite *Promicroceras marstonense* SPATH s'effectue selon une spirale logarithmique. Il paraît en être de même pour *Alveolina oblonga*.

Pour faire ressortir cet accroissement régulier d'un individu, on détermine le rayon à chaque demi-tour à partir du centre du proloculum. Toute section à travers l'appareil embryonnaire peut y servir, pourvu que les mesures soient faites dans la direction perpendiculaire à l'axe d'allongement.

En représentant ces mesures à l'aide d'un graphique (le nombre des tours en abscisse, et les rayons respectifs en ordonnée), on trouve une courbe qui paraîtra logarithmique. Car, en indiquant en ordonnée les logarithmes naturels des rayons mesurés, on obtient une courbe (juxtaposition de segments droits) dont les coefficients angulaires varient tant soit peu pour des valeurs croissantes de l'ordonnée (fig. 4).

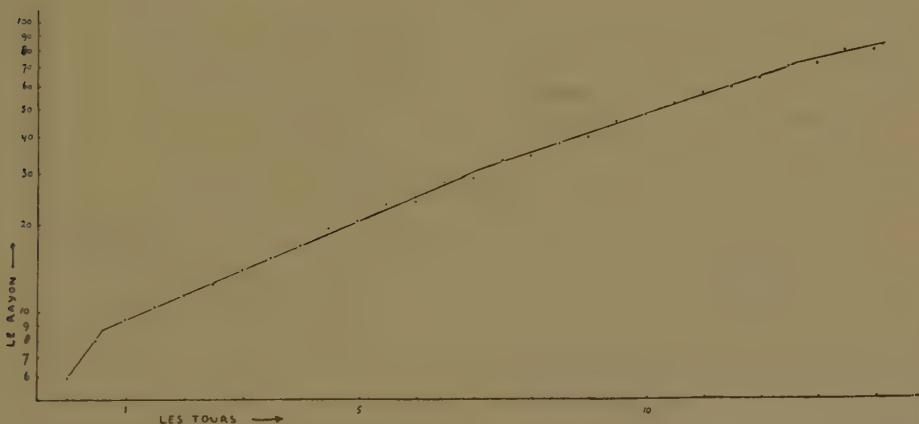


Fig. 4

Courbe logarithmique, démontrant l'accroissement d'un individu selon une spirale logarithmique. (*A. oblonga* D'ORBIGNY, B 6034, 4)

Ces variations de coefficients angulaires désignent des phases d'accroissement différentes. Pendant la formation des premiers tours l'accroissement était relativement rapide, puis, à chaque variation de coefficient angulaire il s'effectuait plus lentement. Tout au long d'une seule phase cependant, la courbe est une droite; l'accroissement se fait donc suivant la spirale logarithmique.

## CONCLUSION

Les espèces du genre *Alveolina* se prêtent remarquablement bien à une description à l'aide de graphiques. Les courbes d'indice (M. REICHEL) des individus montrent des traits bien caractéristiques, qui facilitent largement la distinction des différentes espèces. C'est de cette façon que nous avons décrit les espèces *Alveolina oblonga*, *Alveolina javana*, *Alveolina wichmanni* et *Alveolina pygmaea*.

L'accroissement d'*Alveolina oblonga* s'effectue à peu près selon une spirale logarithmique.

De rares individus fosculinisés se trouvent à coté d'individus normaux de sorte que la fosculinisation ne s'explique pas par une teneur en carbonate élevée de l'ambiance de ces individus.

## L I T T E R A T U R E

1. BAKX, L., De Genera Fasciolites en Neovalveolina in het Indo-Pacifische gebied. Verh. Geol. Mijnb. Gen. IX. (1932).
2. CURRIE, ETHEL D., Growth stages in the Ammonite *Promicroceras marstonense* Spath. Proc. Roy. Soc. Edinburgh. B 61, 344. (1941).
3. DOUVILLE, H., Calcaire à Fusulines de l'Indochine. Bull. Soc. Géol. de France. Série IV, 6, 576 (1906).
4. HANZAWA, S., Note on Foraminifera found in the *Lepidocyclina* limestone from Pabeasan Java. S. Rep. Tohoku Imp. Univ. Sendai. 14, 1. 94 (1930).
5. ———, *Borelis pygmaea* Hanzawa from the Mariana Islands. Jap. Journ. of Geol. and Geogr. 20, 9 (1947).
6. HENRICI, H., Foraminiferen aus dem Eozän und Altmiozän von Timor. Palaeontographica Suppl. IV, Abt. 4 (1934).
7. NEWTON, R. B., Foraminifera in tertiary rocks of New Guinea. Geol. Mag. 207 (1918).
8. NUTTALL, W. F., The Stratigraphy of the Laki Series. Quart. Journ. Geol. Soc. 81, 440 (1925).
9. D'ORBIGNY, Tableau méthodique de la classe des Céphalopodes. Ann. des Sc. nat. 7, 306 (1826).
10. REICHEL, M., Sur la structure des Alvéolines. Ecl. Geol. Helv. 24, 289 (1931).
11. ———, Etude sur les Alvéolines. (1936—37).
12. RUTEN, L., Einige Foraminiferen aus dem O. Arm von Celebes. Samml. Geol. Reichsmuseum Leiden. Serie 1, 9, 307 (1911).
13. ———, Nova Guinea (1914).
14. SCHWAGER, C., Die Foraminiferen aus den Eozän-Ablagerungen der lib. Wüste und Aegyptens. Palaeontographica 30, Abt. 1 (1883).
15. UMBROVE, J. H. F., Tertiary Foraminifera. Feestbundel Martin (1931).
16. VERBEEK, R. D. M., Voorlopig bericht over Numm. enz. Natuurk. Tijdschrift voor Ned. Indië 51.
17. ——— en FENNEMA, R., Geologische Beschrijving van Java en Madoera. Deel II, 1091 (1896).
18. WEST, F. P. VAN, Geological Investigations in the Miomaffo Region (Netherlands Timor). voir: Geological Expedition to the Lesser Sunda Islands under leadership of H. A. Brouwer, vol. III, (1941).
19. YABE, H. and HANZAWA, S., Tertiary Rocks of the Philippines. Sc. Rep. Tohoku Imp. Univ. Sendai. 11, no. 3, 181, (1929).



FOSSIL PLANTS OF THE ISLAND OF BINTAN

BY

W. J. JONGMANS

with a contribution by J. W. H. ADAM <sup>1)</sup>

(Communicated by Prof. J. H. F. UMBGROVE at the meeting of March 31, 1951)

Some time ago I received a small collection of fossil plants from the island of Bintan in the Rhio (Riouw) archipelago, east of Sumatra, which had been found and gathered by Mr BARTELS and Dr ADAM, respectively Mining Engineer and Chief-geologist of the Billiton Company. The General Management of the Billiton Company at The Hague gave me the permission to publish the results of my examination of this small flora for which courtesy I desire to express herewith my sincere thanks.

At my request Dr ADAM has kindly put at my disposal a geological description of the locality with his comments on it illustrated by a map, showing the exact position of the locality and the distribution of rocks of its environment. My description of the fossil material will be preceded by his notes, from which it appears that, although the sediments in which the fossil plants occur had generally been considered as of Tertiary age (see VAN BEMMELEN, *Geology of Indonesia*, p. 309); the geologists of the Billiton Company were always doubtful of it.

*I. The Geological Position of the "Bintan Beds" on the Island of Bintan*

Along the entire south coast of the island of Bintan, with certainty at least from the Bintan bay to beyond Tg. Tili, including the small islands of Los, Penjengat and Dompok, but probably also west of the Bintan Bay (see geological sketch), very low dipping, almost horizontal, beds of alternating shale and sandstone occur in which, until recently, no fossils have been found and which, merely by reason of their almost undisturbed position, have always been regarded as of tertiary age. For the sake of brevity, this formation, so typical for the southern part of Bintan, may provisionally be called the "Bintan formation". The measured dips of the visible beds are in all places so low (at the most about 10°, usually directed to the south, but sometimes also to the north or to some other direction), moreover clean cliff-sections on the shore so narrow that possible thick individual beds would not be directly observable. But from the widespread occurrence, in the interior of the island, of

---

<sup>1)</sup> Published by courtesy and with the cooperation of the N.V. Billiton Maatschappij, The Hague.

laterite which can only be formed from shale it must be concluded that the shale beds are, as a rule, much thicker than the sandstone beds, so that the Bintan-formation may be said to consist chiefly of shale and subordinately of interstratified sandstone. As the determination of the prevailing strike of nearly horizontal beds by averaging measurements on beds is attended with liabilities of error, it had to be concluded from the trends of the sandstone outcrops in the interior of the island, that the Java-direction, i.e. an azimuth of about  $110^{\circ}$  was to be taken as the most probable general strike of the formation. As so often can be observed in the Rhio-archipelago with its weakly folded sedimentary formation, the coastline approximately follows the local strike of the folding even where this strike might deviate considerably from the main tectonic direction being that of Sumatra or the Malayan peninsula. Evidently, this is also the case with the most southern part of the coastline of Bintan. Although, in the inland, all rocks are deeply weathered, there are sufficient indications that the sedimentary part of South Bintan consists of the same formation as along the coast where marine erosion has made the rocks only more easily recognisable.

The idea of the possible occurrence of a rather extensive tertiary formation in a peneplained region with considerable exposures of pre-tertiary granites and their accompanying contact-rocks has always given a feeling of embarrassment in the geological investigation of Bintan. No evidence is found of the existence of an older formation between the granites and this Bintan-formation. The intensely contact-metamorphosed sedimentary rocks with andalusitehornfels on the island of Kelong might be assigned without inconvenience to the Bintan-formation if this could only be proved to be older than the granite. Those occurrences that resemble eruptive aphanites and are indicated as such on the accompanying sketch may, if they are not, as Dr R. W. VAN BEMMELEN believes, contact-rocks as well, be regarded as intrusives (f.i. sills) or extrusives in the Bintan-formation. Further it must be remarked that lithological identity affords some ground to the belief that also the sandstone beds on the islands of Mantang and Siolong are but a southward continuation of the Bintan-formation, that is to say, of a younger conformable portion of it. On Siolong these sandstone beds attain a height of more than 400 feet whereas the adjacent granite hills of Mantang are much lower.

Moreover, the latest more extended investigations of the Rhio-Lingga archipelago by the geologists of the Billiton Company have disclosed the remarkable fact that on these islands by far the greater part of the common sedimentary "Rhio"-formation consisting of shales, sandstones, and conglomerates and hitherto unscrupulously regarded as entirely Triassic is rather characterized by very weak folding or slight tilting of the beds. There are only two exceptions. Firstly: Some portions of a comparatively narrow strip the median line of which may be represented by the Bulan Strait between the islands of Bulan and Batam show the

shale and sandstone beds to be so strongly compressed that they resemble quartzite- and mica schist. But both to the east and to the west of this strip there is only very slight folding. Secondly: In the westernmost N.W.-S.E. belt of the Rhio-Lingga archipelago including the islands of Karimun and Singkep there comes to the surface in isolated patches, probably from underneath the Triassic, a wholly different formation consisting of the most silky and contorted phyllites with occasional amphibolites (islands between Karimun and Kundur, Posik group and Singkep). That this formation is certainly of higher antiquity than the common Rhio-formation is proved by the occurrence, on the west coast of the island of Sanglang (Dutch name: Valsch Doerian) S. E. of Kundur, of a typical basal conglomerate containing very large boulders — many of them at least three feet in diameter — of the same kind of contorted phyllite as that of which the bed-rock of Singkep is constituted. These basal conglomerates pass upward into conformable less coarse conglomerates, sandstones and shales of the common Rhio-formation, here dipping about  $15^{\circ}$  to the North-East. This is an instructive instance of slightly disturbed beds reposing directly on the oldest known formation of the Rhio archipelago.

All these indications throw doubt on the correctness of the view that only the Bintan-formation should be considered as tertiary and the remaining part of the Rhio-formation as triassic.

In the time of the Japanese occupation of Indonesia, Mr BARTELS, then mining engineer of the bauxite mines on Bintan, whom the Japanese had allowed to carry out geological investigations on the island, discovered, in a carbonaceous shale bed of the Bintan-formation on the coast at Tanjung Batu Itam (somewhat south of the principal town Tanjung Penang), some fossil plant-remains in which at first sight he believed to see some resemblance with the permo-carboniferous plant-remains from the Merangin region on Sumatra as pictured in Rutten's handbook on the Geology of the Neth. East Indies. This led him to the suspicion of a carboniferous age for the Bintan-formation, the more so as also the Merangin beds were known to be but slightly disturbed. From the first collection of the Bintan fossils formed by him in that time and considered by him to have been a valuable one, he, unfortunately, did not find back a single piece on his return on the island after the war. About two years ago our geologists formed, at his urgent request, a new collection, a part of which was selected and laid apart for future determination.

Up to the present, these plant fossils have been found only at that single locality, Tg. Batu Itam. This place is particularly favourable to the search for them, for, with low tide, a rather extensive platform is here laid bare, the surface of which lies exactly in the thin fossiliferous bed. Owing to the almost horizontal position of the beds, it is invariably platforms that emerge of the Bintan-formation with low water, but,



as a rule, they consist of sandstone, this rock offering a longer resistance to marine erosion than the soft shale beds. It is to a rare exception of this rule that the cape of the fossil locality owes its name, for Batu Itam means "black rock" and only here has the coast a dark appearance from the carbonaceous shales, whereas the sandstone platforms look white or gray.

A characteristic of all platforms is the fact that their surfaces are sharply divided into squares or rectangles by two sets of vertical joints and this is most markedly the case with the platform of Tg. Batu Itam. Unfortunately, all photographs taken of this place were spoiled by an unexpected defect of the camera used. But to have a clear idea of how this platform on the sea-coast looks like, it is fully sufficient to see in A. HOLMES' book "Principles of Physical Geology" plate.14 A representing "Well-developed jointing in sandstone, Eagle hawk Neck, Tasmania". Owing to a speaking likeness one might take this picture for one of Tg. Batu Itam. There can be no doubt that the sea-floor of the shallow gulf of Bintan mainly consists of the Bintan-formation. It is on the coasts of the small island of Penjengat that the best cross-sections of the carbonaceous layers of the Bintan-formation are found and even a coal-seam, about one foot in thickness, has here been observed, but, unfortunately nowhere with perceptible fossils. It must be remarked, however, that in geological investigations for mining purposes, there is very little time available for the search for fossils. It is quite possible that with long-continued patient searching and careful scrutiny fossils will yet be found on Penjengat and even at all other places where the Bintan-formation is exposed in a sufficiently unweathered condition.

As the platforms along the coast repeatedly come to be submerged with high water, whereas the erosion by wave action at Tg. Batu Itam is always feeble, the fossiliferous shale bed is always found in a very wet and soft condition in consequence of which the samples taken become crumbly on drying and liable to break into pieces during the transport. Further, it must be borne in mind that we, economic geologists and non-specialists in palaeontology, are not the most efficient fossil-collectors: we have no ability to recognize in a fossil those characters that make it valuable for determination. We have primarily searched for specimens with distinctly recognizable plant remains. The surface of the platform of Tg. Batu Itam is marked by the presence of numerous stripes suggestive of flattened plant-stalks but made up of siderite and an unknown black colloidal mineral.

Mr BARTELS and myself consider it as most probable that the same beds as those of the Bintan-formation also occur at other places in the Rhio-Lingga archipelago for instance on the northernmost islands of the Lingga-group, west of Strait Pengelap. On one of these small islands where we stopped on a hasty excursion to Lingga, we found a black carbonaceous shale similar to that of Tg. Batu Itam and also in nearly horizontal beds. Unfortunately, we could not find fossils in it.



## II. Description of the plants found in the Bintan-formation

So far as the plants of the available collection can be identified they all belong to the Cycads and may, in the main, be compared with the genus *Pterophyllum*. In this genus are included numerous forms which, either formerly or still now by some investigators are classed under various other genera. At any rate it is certain that a suchlike flora can never have been Tertiary but must be attributed to the Mesozoic. As, further, this group attained its maximum development during the passage from Upper-Triassic to Jurassic, i.e. in the Rhaeto-Liassic formation, it is quite natural to make a comparison with the numerous Rhaeto-Liassic plants described from E. and S.E. Asia and particularly with the flora of Tonkin which has so excellently been described and illustrated by ZEILLER (ZEILLER, Flore fossile des gîtes de Charbon du Tonkin, 1903). Rhaetic floras have also been described from China by SZE (Die mesozoische Flora aus der Hsiangchi Kohlen-Serie in Westhupeh, Palaeontologia sinica, N.S.A., No. 2, 1949. This work also contains the fairly complete bibliography on the Rhaeto-Liassic flora from China) and from Japan, especially by OISHI and his collaborators (OISHI, The rhaetic plants from the Nariwa district, Prov. Bitchu (Okayama Prefecture), Japan, Journ. Fac. Sci. Hokkaido Imp. Univ., Series 4, I, 3—4, 1932; OISHI, The mesozoic floras of Japan, Journ. Fac. Sci. Hokkaido Imp. Univ., Series 4, V, 2—4, 1940).

### *Pterophyllum bintanense* n. sp.

Fig. 1, 1a; 2, 2a; 3, 3a.

This species is most abundantly represented in the flora. Whereas only one specimen is present of each of the plants to be described hereafter, of this species there are available ten, though mostly very fragmentary, specimens.

#### *Description*

Leaves incomplete. The fragments are at the most 6 cm long. The leaves lack top or base almost entirely, only in the small fragment of fig. 2 the top seems to be nearly reached.

The leaf-segments are small, at the most 6 or 7 mm long and, at their greatest width, at the most 2 or 3 mm broad. The segments stand on the axis at a fairly large angle, in some cases nearly at a right angle. In very small specimens the segments are directed slightly more upward. The axis is not broader than 1 mm and is well visible in fig. 3, 3a. Except for a scarcely visible longitudinal striation no ornamentation is visible on it. On the portion, shown in fig. 1, which is about 4.7 cm long, 15 segments are found. From this it follows that the segments stand closely together, nearly without interspaces. So far as can be judged the size of the segments is constant for great lengths. In one single case an up-

ward decrease in length of the successive segments is perceptible (fig. 2, 2a). The segments have parallel margins, they are implanted with their entire base and there is not a trace of any constriction. At the top the segments are abruptly truncated and but feebly arched. Unfortunately, the venation is not quite well preserved. So far as can be judged the veins are all parallel, both to each other and to the sides of the segments. One gets the impression that, at some places, the veins are once divided at the base. Whether this is a rule, cannot be decided.

#### *Discussion*

At any rate this species must belong to the small-leaved forms. It may be compared with some of the figures of *Pt. muensteri* in ZEILLER's work, f.i. Pl. 45, f. 5, but also here the dimensions are much greater. As to the size, most to be taken into consideration is a comparison with *Pt. rosenkrantzi* HARRIS, Fossil Flora of Scoresby Sound, East Greenland, Meddel. om Groenland, 85, 5, 1932, p. 55, Textf. 25. Also some of the figures of *Pt. nathorsti* SCHENK in SZE, 1949, p. 14, particularly the comparatively small-leaved forms of Pl. 2, and Pl. 9, fig. 3b, may more or less be taken for comparison. The plant from Bintan, however, has much smaller leaves and the separate segments are smaller than in the forms mentioned.

Hence, there is every reason to describe this plant as a new species, *Pterophyllum bintanense* JONGM. n. sp.

#### *Pterophyllum cf. contiguum* SCHENK

fig. 4, 4a

There is only one good specimen of this species in the collection. Another specimen, which possibly belongs to it, is so badly preserved that there is no doing anything with it.

#### *Description*

The leaf-segments are at the most 13 mm long, the length decreasing towards the top of the leaf. The width is at the most 2 mm. Hence the segments are comparatively very long and narrow. They are somewhat sickle-shaped, with upward convexity, stand closely together and are implanted with their full breadth. The axis of the leaf is very narrow. At the place of their implantation the segments are directed slightly upwards but for far the greatest part they are nearly horizontal. The top is rounded. The veins are parallel to each other and to the sides of the segments; 7 or 8 veins per segment. Whether they are divided at the base, cannot be decided.

#### *Discussion*

So far as can be judged this form corresponds with *Pt. contiguum* in ZEILLER on Pl. 48, especially with f. 4 and 6. A striking difference is

that on ZEILLER's figures the segments have upward convexity, whereas the segments in the specimen of Bintan have downward convexity. To what extent this character has to be considered as a difference cannot be judged on the basis of the insufficient material. None of the figures in ZEILLER, HARRIS or SZE shows this upward convexity of the segments.

*Pterophyllum* sp.

fig. 5, 5a.

Of this species there is likewise only one fragment present in the collection.

This form possesses somewhat sickle-shaped segments. The top is distinctly blunted. As to the nervation it can be said only that the veins run parallel. The segments are 1 cm long and 3 or 4 mm wide.

The fragment rather resembles *Pt. inconstans* BRAUN, Pl. 44 in ZEILLER. This species, however, is on the whole much larger and also the shape of the segments is a different one. It may also be compared with *Pt. cf. inconstans* in SZE. but this is, like the figures in ZEILLER, much larger.

*Cycadolepis* sp.

Fig. 8

Besides these Cycad-leaves there are a few squamiform remains in the collection, which may be compared with *Cycadolepis*, for instance *C. granulata* ZEILLER, Pl. 50, f. 5, p. 202.

Doubtful are the specimens of Fig. 6, 6a and 7, 7a. These may be scales also, or perhaps seeds.

An absolutely undeterminable fragment has been figured in Fig. 9, 9a for the sake of completeness.

*Conclusions*

It appears from the descriptions and figures here given that a perfectly certain determination is in almost none of the cases possible. Nor are coal films found on the imprints, so that a cuticula-examination, which in so many cases of mesozoic plants has led to important results, has not been possible.

The most important result is, that a flora in its composition comparable with those from Keuper, Rhaet and Lias but especially with one of Rhaet, has been found in a formation the age of which has been hitherto, though with some reserve, considered as Tertiary. The small flora of Bintan is well comparable with other floras of approximately the same age from East Asia (Tonkin, China, Japan). This is, as far as I know, the first example of a mesozoic flora from Indonesia. It is true that some kinds of wood have been found in mesozoic (perhaps also Upper-Triassic) formations, but with the exception of *Protocupressinoxylon malayense* which

has been described by ROGGEVEEN (*Mesozoisches Koniferenholz von der Insel Soegi im Riouw-Archipel, Niederl. Ost-Indien, Proceedings Kon. Ak. v. Wetensch., Amsterdam, XXXV, 4, 1932, p. 1—7*) these kinds of wood have not been described as yet.

It is much to be hoped that further investigations should be undertaken with a special view to obtain better material and more species which would permit the age of the Bintan-formation and, if possible, also of other parts of the Rhio-formation, to be fixed with more certainty.

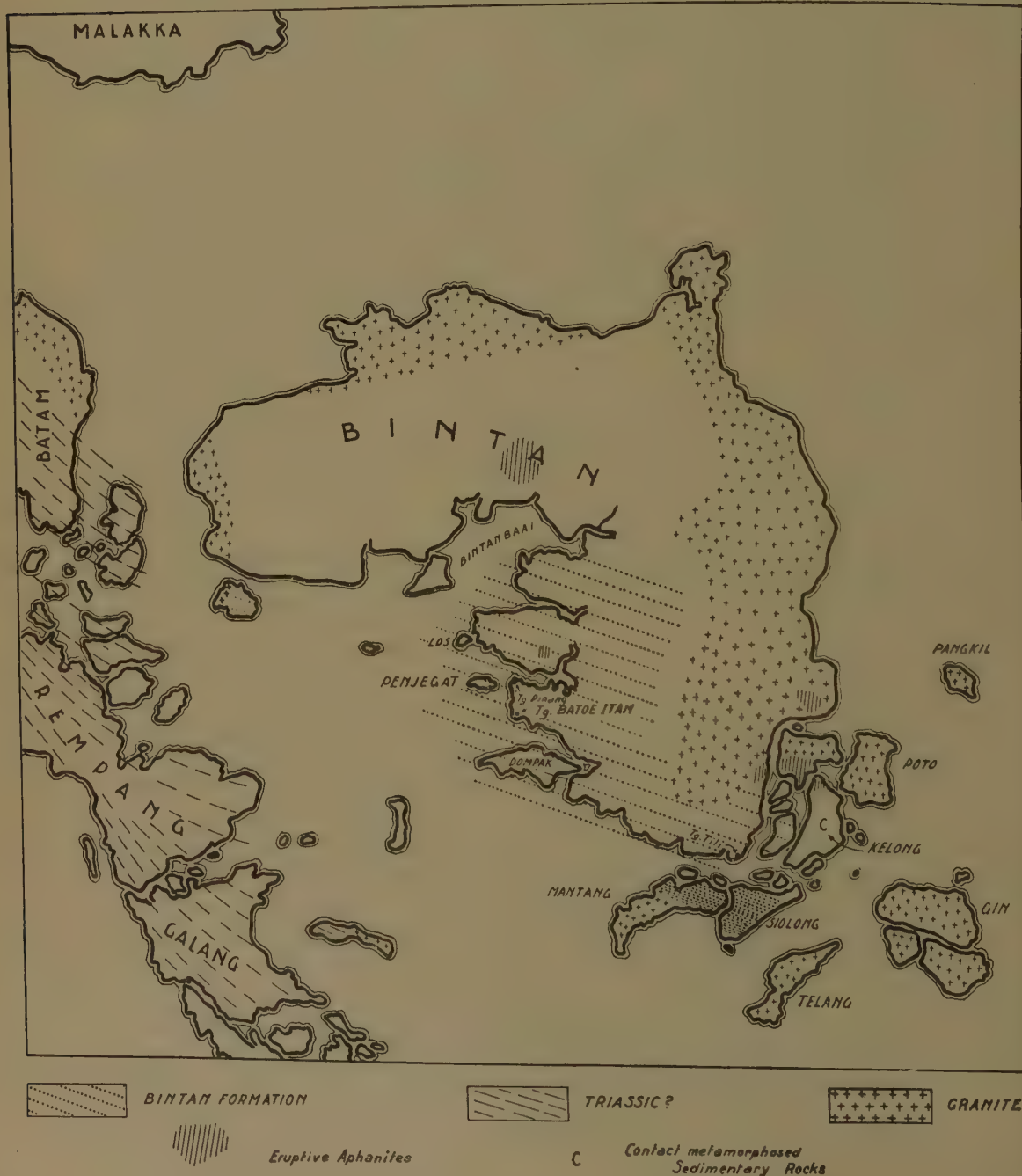






FOTO V. VOSKUYLEN

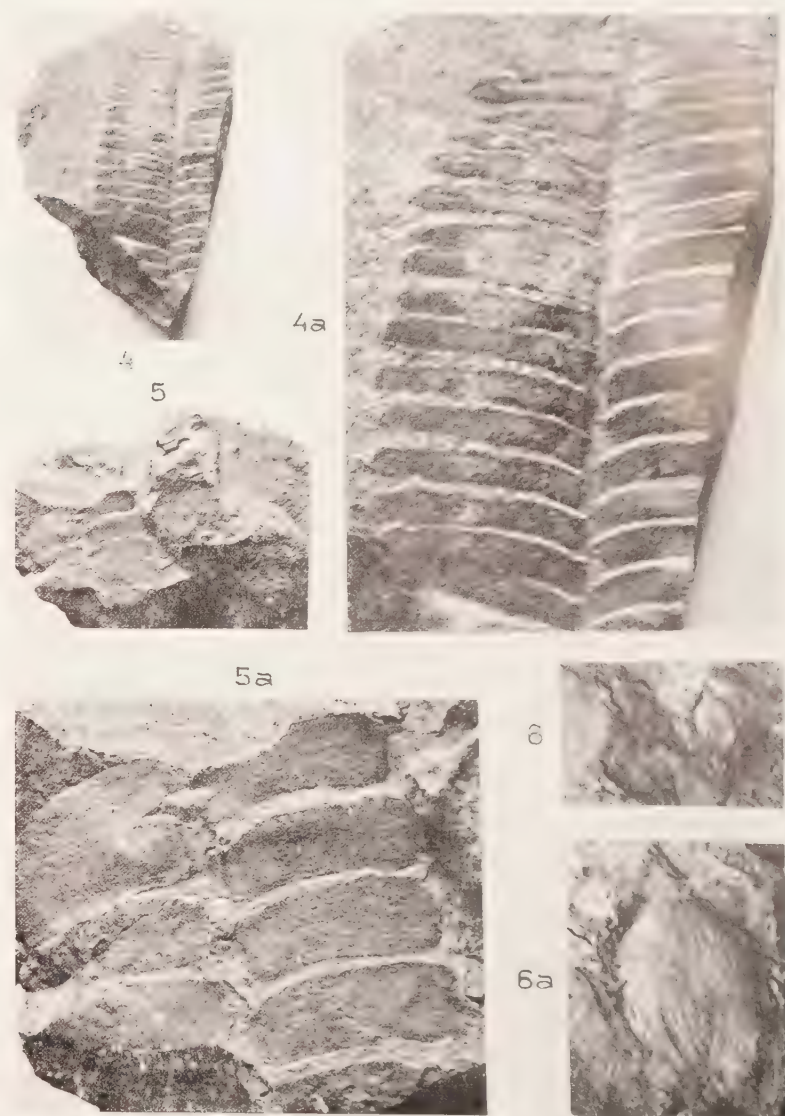


FOTO V. VOSKUYLEN









## A NEW METHOD FOR THE PREPARATION OF DIAZOMETHANE

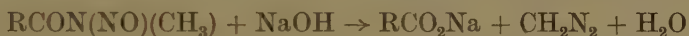
BY

H. J. BACKER AND TH. J. DE BOER

(Communicated at the meeting of May 26, 1951)

The yellow gas which KLOBBIE<sup>1)</sup> discovered when decomposing methylnitroso-urethane with NaOH could not be studied further by him, as it set up a serious irritation of the mucous membranes of his eyes and respiratory organs. When VON PECHMANN<sup>2)</sup> had shown that it was diazomethane and that it was a practical methylating agent, it found its way into all laboratories of organic chemistry<sup>3)</sup>.

The hydrolysis of methyl-nitroso-acylamides is a general reaction<sup>4)</sup>.



One problem is the instability of methylnitroso-urethane. Therefore the more stable nitrosomethylurea<sup>5)</sup> was introduced.

JONES, ADAMSON and KENNER<sup>6)</sup> recommended the derivative of mesityloxide. In this case the diazomethane should be eliminated immediately in order to prevent its action on the non-saturated ketone which is formed at the same time.

All the methods so far described have thus various disadvantages.

In search of a better basic material for diazomethane we prepared *p*-tolylsulphomethylnitrosamide (*p*-tosylmethylnitrosamide). This compound has the following advantageous properties:

- 1) It is stable: even after being kept for a year it is practically unchanged.
- 2) It gives diazomethane with an excellent yield (80—90 %).
- 3) Its synthesis from cheap commercial products is very simple and gives a high yield.

It is curious that this and analogous compounds have not as yet drawn much attention. We have found one patent<sup>7)</sup>, in which this and other

<sup>1)</sup> E. A. KLOBBIE, 57, 69, Thesis Leyden (1890).

<sup>2)</sup> H. v. PECHMANN, Ber. 27, 1888 (1894); 28, 855 (1895).

<sup>3)</sup> Cf A. B. GREVENSTUK, Chem. Weekblad 37, 48 (1940).

<sup>4)</sup> H. J. BACKER, J. Chem. Soc. 101, 592 (1912).

<sup>5)</sup> Org. Syntheses 15, 3 (1935).

<sup>6)</sup> J. Chem. Soc. 1933, 363; 1935, 286; 1937, 1551.

<sup>7)</sup> D. R. P. 224388. FRIEDLÄNDER's Handb. d. Teerfarbenfabr. 10, 1216 (1913).

sulphomethylnitrosamides have been used for alkylating phenols ( $\beta$ -naphthol, morphine). It has not been claimed, and it is uncertain, that the alkylation takes place via a diazo compound<sup>8</sup>). For the analogous methylation with the methylnitrosamino derivative of mesityloxide ADAMSON and KENNER<sup>6</sup>) conclude that the intermediary formation of diazomethane under the conditions of the experiment (0°) is very improbable.

When a strong alkaline lye is added to the ethereal solution of *p*-tosylmethylnitrosamide, no trace of diazomethane is evolved, not even after standing for half an hour. It is still more remarkable that a strong alkaline lye does not decompose the solid nitrosamide. When heated up to 60°, the compound melts without being attacked by the NaOH. Other nitrosamides may explode under this treatment.

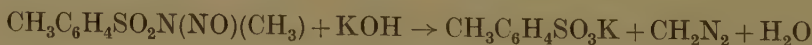
When however an alcoholic solution of KOH is added in the cold to an ethereal solution of the nitrosamide, so that a homogeneous mixture is formed, the solution immediately takes a canary yellow colour. Distillation gives an ethereal diazomethane solution with a yield of 80–90 %.

It may be asked if this surprising result is owing simply to the homogeneity of the reaction mixture. This supposition cannot, however, be correct. When reacting in dioxane and water (50–50 %), the mixture becomes homogeneous; but even after 3 hours no appreciable quantity of diazomethane is formed. The alcohol and the base both exert a chemical action.

It is possible to vary the quantity of the base considerably (from a great excess to the fraction of a molecule) without affecting the yield of diazomethane. Even a quantity of 0.15 mol. KOH still yields 80–90 %. When smaller molar quantities are used, the yield falls.

When the ethereal solution of the nitrosamide is decomposed by means of the equimolecular quantity of KOH in alcohol, the solution, after distillation of the diazomethane, still contains about half of the KOH, whilst the rest is transformed into potassium *p*-toluenesulphonate. At the same time a considerable amount of ethyl *p*-toluenesulphonate is formed.

Since the nitrosamide reacts very slowly with KOH in dioxane-water, potassium *p*-toluenesulphonate cannot be formed by direct hydrolysis in great quantity.



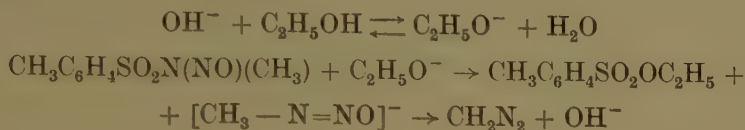
In that case one molecule of nitrosamide would require one molecule of KOH, whereas in fact a much smaller quantity is sufficient.

#### *Reaction mechanism*

All products and phenomena of the reaction are explained when we

<sup>8</sup>) C. M. SUTER, Org. Chem. of Sulfur, 595 (1945).

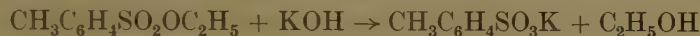
assume that the *ethylate ion*, formed from alcohol and KOH, reacts primarily on the nitrosamide:



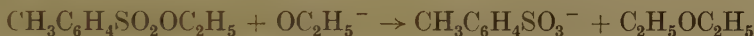
It is probable that such an unstable intermediary anion is formed first. The decomposition of methylnitroso-urethane with KOH at 0° gives  $\text{CH}_3\text{N}_2\text{OK} \cdot \text{H}_2\text{O}$ , which hydrolyzes into  $\text{CH}_2\text{N}_2$  and KOH <sup>9)</sup>.

That the decomposition of tosylmethylnitrosamide is not effected by an aqueous solution of KOH must be imputed to the insufficiently nucleophilic character of the hydroxyl ion. The ethylate ion, however, has much stronger nucleophilic properties.

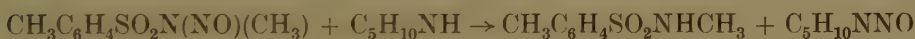
According to the given reaction schema the quantity of hydroxyl ions should not change during the reaction. Yet a part of the KOH is used up. This may be ascribed to a secondary reaction with the formed ester:



When decomposing the nitrosamide by means of an alcoholic solution of *sodium ethylate* one can also obtain a secondary reaction with the ester first formed:



The nitrosamide, when made to react with *piperidine*, is readily decomposed. However, not a trace of diazomethane is formed, not even in the presence of alcohol. The reaction is a double substitution with formation of nitrosopiperidine:



This research will be continued in various directions; the experimental details will be published elsewhere.

<sup>9)</sup> A. HANTZSCH and M. LEHMANN, Ber. 35, 897 (1902).

TREERING MEASUREMENTS AND WEATHER FLUCTUATIONS  
IN JAVA FROM A.D. 1514

I

BY

H. J. DE BOER

(Communicated at the meeting of May 26, 1951)

1. *Introduction*

Several years ago BERLAGE [1] published treering measurements of *Tectona grandis*, which contained widths of treerings from A.D. 1514 up to 1929 including. With the aid of these measurements he could show, that the well-known 3-year cycle in the barometric pressure and the rainfall, which is very active in the Indian and the Pacific Ocean, had been in operation from A.D. 1514 at least and that its mean length during that period was 3.4 years. Studying his series of widths of treerings we became convinced by some features in this series, that it would be worth while to investigate the data into more details.

2. *Working process*

In the Table at the end of this paper column 1, 2 and 3 have been taken from the above-mentioned article of BERLAGE. Column 1 contains the years for which the width of the corresponding treering has been measured. In column 2 the relative widths of the treerings for the various years, averaged from several measurements, have been collected. Column 3 indicates the numbers of measurements from which the averaged widths in the preceding column have been determined. After that BERLAGE has graduated the values in column 2 by calculating the overlapping 11-yearly means. As a consequence of this process a possible 11-year period hidden in the treering measurements has been wiped out. In order to avoid such a complication we have graduated the values by a different formula. We have chosen a formula of 13 terms of which the coefficients fit a quadratic curve and with which the fortuitous errors of the values in column 2 become a minimum [2]. This formula may be represented by

$$u'_0 = (25u_0 + 24u_{\pm 1} + 21u_{\pm 2} + 16u_{\pm 3} + 9u_{\pm 4} - 11u_{\pm 6})/143,$$

where  $u'_0$  is the graduated value of  $u_0$ .

If a series of data is adjusted by a symmetrical formula of 13 terms, then the first 6 and the last 6 data of the series remain ungraduated. In order to graduate these values too we have applied asymmetrical formulae, which suit the used symmetrical one [3].



The values graduated in the above-mentioned way have been collected in column 4. After that we have subtracted the data of column 4 from the corresponding ones of column 2. These differences have been multiplied by 100 and divided by the corresponding values of column 4. For short this process may be represented by  $100 (\text{column 2} - \text{column 4}) / \text{column 4}$ . The ratios thus obtained have been gathered in column 5. We may say now that the values of column 5 are very suitable to an investigation of shortperiod variations which occur in the values of column 2, as the longperiod variations happening in the data of column 2 have been excluded by the process which has lead to the values of column 5.

When studying the values of column 2 we have to think of the fact that these values show not only variations in the widths of treerings but also the influence of the growth of the tree. The relation between tree-growth and age is not a simple one, as tree-growth mainly depends on two factors, namely the properties of the soil in which a tree grows and the density of the tree-population in its immediate neighbourhood. Because the changes in the two mentioned factors are not known through the centuries we have solved this difficulty in the following way.

Through the values of column 4 from A.D. 1550 up to 1929 including we have fitted a quadratic curve with the aid of the method of least squares. We did the same to the values of column 4 from A.D. 1514 up to 1574 including. The two curves are overlapping during a period of 25 years and in order to get only one set of values we have interpolated between the corresponding values of both curves so that discontinuities could not arise on the transition from the values of the second curve to the interpolated values and on the transition from the interpolated values to those of the first curve. Column 6 contains the results of this process and we may say, that the values of column 6 represent the relative widths of the rings of a tree which started to grow in A.D. 1514, whilst the weather was always the same during these centuries or whose growth was not affected by weather variations.

Now we were able to calculate the influence of weather fluctuations on the graduated widths of treerings for each year of the whole considered period in this way:  $100 (\text{column 4} - \text{column 6}) / \text{column 6}$ . The results of this process have been collected in column 7 and the values of this column represent departures from the mean concerning the adjusted widths of the treerings corrected for the age of the tree. These values are very suitable to an investigation of longperiod variations occurring in the widths of the treerings.

Finally we have calculated the values  $100 (\text{column 2} - \text{column 6}) / \text{column 6}$ , which represent departures from the mean concerning the measured widths of the treerings corrected for the age of the tree. These values have been gathered in column 8 and may be used for investigation into longperiod and shortperiod variations.

### 3. Longperiod variations

Firstly we have analysed the data of column 7 in search of longperiod variations in the widths of tree-rings in Java. This analysis has been carried out by application of the signcoefficient method to the above-mentioned data [4]. This signcoefficient method is only a simple substitute of the method of autocorrelation. In this way we have found two well-developed cycles with a length of the period of 51 and 89 years respectively. The averaged shape of both periods, calculated from the 416 departures in column 7, has been represented respectively in fig. 1a and 1b, whilst the beginning of the representation of the 89-year period has been fixed at the year A.D. 1583 and that of the 51-year period at the year A.D. 1520. Though we could not detect the 36-year period with this first analysis, we have put the figures of column 7 in rows of 35 and of 36. We have found, that the figures in rows of 35 gave the most homogenous result. The 35-year period, derived from the 416 departures in column 7, has been represented in figure 1c, whilst the beginning of this period has been fixed at A.D. 1545. Concerning the three figures 1a, b and c we

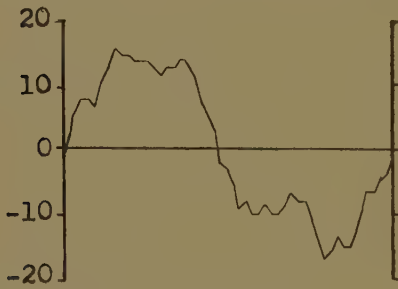


Fig. 1a. 51-year period.

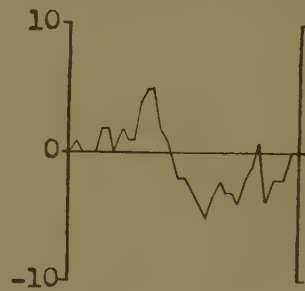


Fig. 1c. 35-year period.



Fig. 1b. 89-year period.

may remark, that their amplitudes have been plotted in the same relative units. The 51-year cycle is, as far as we know, a hitherto unknown one,

though it appeared to be well-developed. The 89-year cycle is a well-known one from the work of EASTON [5], VISSER [6] and others. Even without the signcoefficient method this period could be detected because the curve, representing the numbers of column 7 as a function of the time, shows deep valleys at A.D. 1548, 1637, 1726 and 1815. About 1904 we could not observe such a valley. The 89-year cycle is connected with the sunspot cycle in this way, that the duration of 8 sunspot cycles is exactly 89 years. Considering the table of WOLF-WOLFERS' mean yearly sunspot numbers we observed that the years 1816 and 1905 are maximum sunspot years with the smallest maximum sunspot numbers in a period of 89 year. When we put the successive maximum sunspot numbers of the sunspot cycle in rows of 8 in the way of Table I, we observed the appearance of a well-developed period.

Table I, The 89-year period in maximum sunspot numbers.

			83	86	106	154	132	48
1816. . . .	46	71	138	124	96	139	64	85
1905. . . .	64	104	78	114	155			
mean . . .	55	88	100	108	119	146	88	66
deviation .	— 41	— 8	4	12	23	50	— 8	— 30

Therefore we may assume, that the years 1905, 1816, 1727, 1637 and 1548 are maximum sunspot years with small sunspot numbers; perhaps we may even say: with minimal sunspot numbers during the corresponding 89-year cycle.

The 35-year period in the annual widths of treerings is not very well developed. This cycle has been the subject of discussion in literature so often, that there is no need to discuss it now.

#### 4. *Shortperiod variations*

BERLAGE [1] has shown, that the well-known 3-year cycle with an average length of the period of 3.4 years has been in operation from A.D. 1514. The signcoefficient method [4] applied to the values of column 5 has revealed, that a 6-year period was well-developed from A.D. 1514, though its phase was varying around its average value during the past centuries. Our opinion on the existence of the 6-year cycle is, that it is a consequence of the beating of the 3.4-year cycle by the  $7\frac{1}{3}$ -year cycle and that therefore it is a physically unreal period [7, 8]. But the presence of the 6-year period means, that the  $7\frac{1}{3}$ -year period, which has its origine in the North Atlantic Ocean [9], has also been in operation from A.D. 1514. Investigation of this cycle in treerings through the centuries has shown, that this cycle has not been well-developed in the neighbourhood of Java. Its amplitude, calculated from the 416 values of column 5, has been represented in fig. IIa. The averaged amplitude of the 6-year period has been represented in fig. IIb.

Another period, which is prominent in these regions, is the 6.8-year cycle. This cycle, called by BERLAGE the Pacific cycle [9], could not be detected with the aid of the signcoefficient method. We have calculated its average features from the values of column 5 and have represented the amplitude of this period in fig. IIc. The amplitude has been expressed

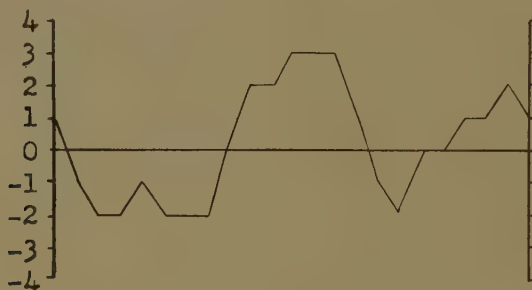


Fig. IIa.  $7\frac{1}{3}$ -year period.

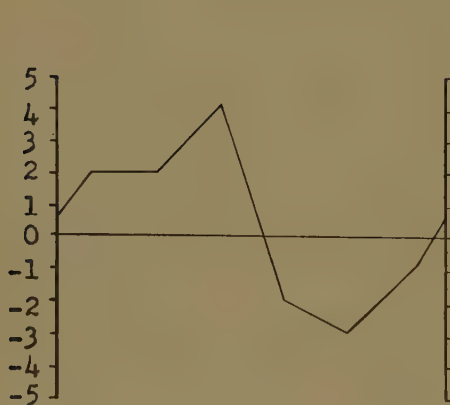


Fig. IIb. 6-year period.

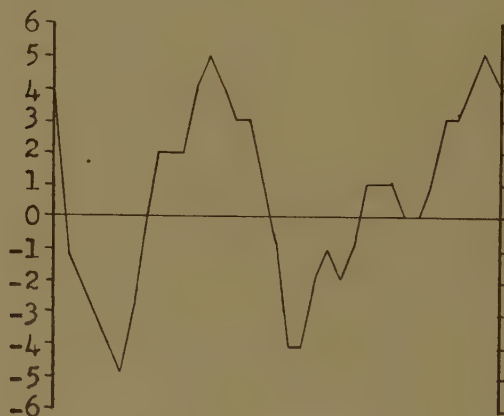


Fig. IIc. 6.8-year period.

in the same units as used for the 6-year and the  $7\frac{1}{3}$ -year period. Our opinion on the 6.8-year period in airpressure was, that this cycle has a double wave [7]. This opinion has been confirmed by BERLAGE, who has calculated the 6.8-year period in the Bombay airpressure and who has found, that this airpressure cycle appeared to have a double wave. The representation of the period of fig. IIc shows the same features. The first wave has a duration of exactly three years, just as the duration of the first wave of the 6.8-year period in the Bombay airpressure curve. We may assume therefore, that it has been sufficiently proved that the Pacific cycle or the 6.8-year cycle has a double wave.

##### 5. *Relation between treerings and weather in Java*

In order to learn something about weather fluctuations in Java through the centuries we have had to investigate the relation between the



variations in the widths of treerings and the weather fluctuations. Weather is composed of the various weather elements and we have chosen the weather elements of Djakarta (formerly called Batavia) for comparison, as Djakarta has the longest and most accurate series of observations. In order to judge the relationship between the variations in the widths of treerings and the fluctuations in the various weather elements we have calculated various correlation coefficients. As the variations in the widths of treerings we have chosen the procentual deviations, occurring in column 5, from 1864 up till 1929 including, because the observations at Djakarta have been started in 1864. The following weather elements of Djakarta have been taken into consideration: number of raindays, amount of clouds, amount of rainfall, temperature and number of dry months. With the exception of the last element we have fitted a quadratic curve through the annual figures of each element from 1864 up to 1929 including with the aid of the method of least squares. The differences between the actual annual figures of each element and their corresponding annual figures computed from the quadratic curve, have been called the departures from the mean. After that the correlation coefficients between the procentual deviations of the widths of treerings and the departures from the mean of each mentioned element have been determined. Concerning the number of dry months we have given different limits to a "dry month" in order to obtain the largest correlation coefficient. We have given the value 1 to a month, in which the amount of rainfall is  $\leq 30$  mm, and the value  $\frac{1}{2}$  to a month, in which the amount of rainfall is  $> 30$  mm but  $\leq 60$  mm. In this way we have determined the number of dry months for each year from 1864 up to 1929 including. After that we have computed the departures from the mean and the wanted correlation coefficient. The calculated correlation coefficients between the procentual deviations of the widths of treerings and the departures from the mean of the various weather elements at Djakarta are tabulated below:

number of raindays . . . . .	+ 0.48
amount of clouds . . . . .	+ 0.49
amount of rainfall . . . . .	+ 0.10
temperature . . . . .	— 0.26
number of dry months . . . . .	— 0.43

This means, that a wide treering corresponds with a large yearly number of raindays, a large yearly amount of clouds, a small number of dry months in that year and a yearly temperature below the average, whereas the influence of the yearly amount of rainfall is negligible. In the first place this conclusion is true for shortperiod variations. If we compare the course of the data of column 7 from 1864 up to 1929 including with the course of the decadal means of the yearly amounts of rainfall and of the yearly temperatures at Djakarta during the same

periode, then we may say that successively decreasing widths of treerings correspond with increasing temperatures and decreasing amounts of rainfall. If we now combine these properties, then in general we may say that rainy weather and temperatures below normal correspond with wide treerings, dry weather and temperatures above normal correspond with narrow treerings and vice versa.

#### 6. *Weather in Java compared with European weather*

As in the preceding paragraph we have determined the meaning of wide and narrow treerings we are now able to derive the successive types of weather occurring in Java from A.D. 1514 up till the present from the departures collected in column 7 of the Table at the end of this paper. We have chosen the following limits to the different weathertypes. If a departure is  $> -10$ , but  $< 10$ , then we have called the weather during that year normal. If the departure is  $> -25$ , but  $\leq -10$ , then the weather has been called dry; if a departure  $\leq -25$  the weather is very dry and hot; if a departure  $\geq 10$ , but  $< 25$  the weather is rainy and a departure  $\geq 25$ , the weather is very rainy and cool. With these different weathertypes we have been able to construct the following list, in which the first column indicates the successive periods, the second column the weathertypes in the corresponding periods and the third column data of comparison taken from a pattern concerning European weather constructed by D. J. SCHÖVE [11, 12].

1514—1520	dry to normal . . . . .	} preglacial
1521—1539	rainy . . . . .	
1540—1575	dry to very dry and hot . . . . .	} Ia
1576—1598	rainy to very rainy and cool . . . . .	
1599—1644	normal to dry . . . . .	Ib
1645—1677	very dry to dry and hot . . . . .	Ic
1678—1721	transition from normal to rainy to dry . . . . .	} interglacial
1722—1730	very dry and hot . . . . .	
1731—1734	dry to normal . . . . .	
1735—1764	normal to rainy . . . . .	II
1765—1795	very rainy and cool . . . . .	lull
1796—1812	normal . . . . .	} III
1813—1821	dry to very dry and hot . . . . .	
1822—1844	rainy to very rainy . . . . .	
1845—1857	dry to normal . . . . .	
1858—1892	normal to rainy . . . . .	
1893—1909	normal to dry . . . . .	} interglacial
1910—1929	dry to very dry and hot . . . . .	

From this list it appears that the period, in which is happening the beginning of the 89-year cycle as explained in § 3, is always dry or very dry.

SCHOVE has made his list of European weathertypes from A.D. 1451 up till now from several sources of information and these weathertypes specially concern that part of Western and Northern-Europe, which is situated between 40°—55° N.L.

For reasons of comparison we have taken the following general data from his list:

	<i>Glaciers</i>	<i>Weathertype</i>
1451—1540	preglacial . . . . .	very maritime
1541—1590	Little Ice Age phase I. . . . .	Ia continental
1591—1650		Ib moist, cool
1651—1680		Ic very continental
1681—1740	interglacial . . . . .	maritime
1741—1770	Little Ice Age phase II . . . . .	continental
1771—1800	lull . . . . .	very continental
1801—1890	Little Ice Age phase III . . . . .	continental
1891—1940	interglacial . . . . .	very maritime

After a rough survey of both lists it looks as if the weathertypes of Europe are in agreement with those of Java from A.D. 1678 in this way, that very continental weather in Europe coincides with very rainy weather in Java, continental weather in Europe with rainy weather in Java, maritime weather in Europe with dry weather in Java and finally very maritime weather in Europe with very dry weather in Java. Before A.D. 1678 however this concordance is not present and there may be two causes for this fact, if the agreement is not accidental. In the first place the treering measurements before 1678 are not reliable, in the second place the general aircirculation has been subject to a change at about 1678, so that before that year an other region in the tropics was in the above-mentioned concordance with European weather. The doubtful reliability of the treering measurements before 1678 is not a likely cause, as not only the 3-year, 6-year and 6.8-year period are present from A.D. 1514, but also the 51-year and the 89-year period.

#### 7. *Final remark*

Observations at Djakarta have been partly started in 1864 and in 1866. From these observations we have been able to determine limits to the weathertypes in Java, occurring during this instrumental period: normal, dry and very dry and hot. The difference between the normal and the dry weathertype is an increase in annual temperature of 0,1—0,3 centigrade degree and a decrease in the annual amount of rainfall of 50—75 mm. The very dry and hot weathertype means an increase in annual temperature of 0,5—0,7 centigrade degree and a decrease in the annual amount of rainfall of 150—200 mm with respect to the normal weathertype.

Bogor, April 1951.

*University of Indonesia,  
Faculty of Agricultural Science*

## REFERENCES

1. BERLAGE, H. P., *Tectona*, **24**, 939 (1931).
2. BOER, H. J. DE, Thesis Groningen, p. 8, 9 and 29 (1936).
3. ———, Thesis Groningen, p. 25 (1936).
4. ———, *Proc. Roy. Neth. Ac. Sc.*, **41**, 505 (1938).
5. EASTON, E. C., *Proc. Roy. Ac. Sc. Amsterdam*, **20**, 1092 (1917).
6. VISSER, S. W., *Proc. Roy. Neth. Ac. Sc.*, **53**, 172 (1950).
7. BOER, H. J. DE, *Verhandelingen K.M.M.O.*, Batavia, No. 29, (1941).
8. ———, *Verhandelingen K.M.M.O.*, Batavia, No. 30, (1947).
9. BERLAGE, H. P., *Verhandelingen K.M.M.O.*, Batavia, No. 26, (1934).
10. ———, *Verhandelingen K.M.M.O.*, Batavia, No. 31, (1947).
11. SCHOVE, D. J., *Quat. Journal*, **75**, 175 (1949).
12. ———, *Met. Mag.*, London, **7c**, 11 (1949).

*(To be continued).*



METEOROLOGY

TREERING MEASUREMENTS AND WEATHER FLUCTUATIONS  
IN JAVA FROM A.D. 1514

II

BY

H. J. DE BOER

(Communicated at the meeting of May 26, 1951)

TABLE

1	2	3	4	5	6	7	8
1514	33.57	10	28.18	19	32.92	— 14	2
15	20.61	10	27.23	— 24	32.13	— 15	— 36
16	24.93	10	26.37	— 5	31.35	— 16	— 20
17	26.58	10	25.98	2	30.58	— 15	— 13
18	25.53	10	27.79	— 8	29.82	— 7	— 14
19	32.46	10	28.13	15	29.07	— 3	12
1520	35.40	10	28.92	22	28.24	2	25
21	32.52	10	30.52	7	27.61	11	18
22	24.09	10	30.53	— 21	26.90	13	— 10
23	25.08	10	30.53	— 18	26.20	17	— 4
24	31.98	10	27.75	15	25.51	9	25
25	32.61	10	28.46	15	24.83	15	31
26	29.10	10	27.95	4	24.17	16	20
27	28.20	15	27.97	1	23.51	19	20
28	26.46	15	27.73	— 5	22.87	21	16
29	23.64	15	26.94	— 12	22.24	21	6
1530	27.00	15	23.74	14	21.62	10	25
31	26.01	15	25.26	3	21.01	20	24
32	24.21	15	25.14	— 4	20.42	23	19
33	24.12	15	24.36	— 1	19.83	23	22
34	27.00	15	23.88	13	19.26	24	40
35	22.50	15	23.22	— 3	18.75	24	20
36	22.14	15	21.58	3	18.15	19	22
37	20.22	15	20.75	— 3	17.61	18	15
38	18.36	15	19.79	— 7	17.08	16	7
39	17.52	15	18.83	— 7	16.56	14	6
1540	18.93	15	16.87	12	16.06	5	18
41	15.00	15	15.99	— 6	15.57	3	— 4
42	18.36	15	14.89	23	15.09	— 1	22
43	13.65	15	13.91	— 2	14.62	— 5	— 7
44	10.29	15	12.77	— 19	14.16	— 10	— 27
45	9.27	15	11.86	— 22	13.71	— 13	— 32
46	13.65	15	10.90	25	13.28	— 18	3
47	10.32	15	10.19	1	12.74	— 20	— 19
48	9.45	15	9.13	4	12.21	— 25	— 23
49	8.94	15	9.47	— 6	11.69	— 19	— 24
1550	10.14	15	9.15	11	11.19	— 18	— 9
51	7.38	15	8.45	— 13	10.70	— 21	— 31
52	6.93	15	7.85	— 12	10.22	— 23	— 32
53	8.01	14	8.11	— 1	9.75	— 17	— 18
54	11.16	14	7.95	40	9.29	— 14	20
55	4.08	14	7.32	— 44	8.84	— 17	— 54
56	7.56	14	7.24	4	8.41	— 14	— 10
57	8.91	14	6.97	28	8.02	— 13	11
58	7.11	14	6.63	7	7.68	— 14	— 7
59	4.14	14	5.92	— 30	7.43	— 20	— 44

TABLE (Continued)

1	2	3	4	5	6	7	8
1560	4.32	14	5.41	— 20	7.26	— 25	40
61	8.10	14	5.58	45	7.04	— 21	15
62	2.97	14	4.94	— 40	6.85	— 28	— 57
63	5.58	14	4.64	20	6.67	— 30	— 16
64	4.32	14	4.75	— 9	6.51	— 27	— 34
65	5.07	14	4.84	5	6.38	— 24	— 21
66	5.07	14	4.69	8	6.27	— 25	— 19
67	4.26	14	4.48	— 5	6.19	— 28	— 31
68	4.56	14	4.74	— 4	6.11	— 22	— 25
69	4.98	14	4.69	6	6.03	— 22	— 17
1570	4.68	14	4.98	— 6	5.96	— 16	— 21
71	5.37	14	5.24	2	5.90	— 11	— 9
72	5.07	14	5.54	— 8	5.85	— 5	— 13
73	5.52	14	6.22	— 11	5.81	7	— 5
74	7.38	14	6.60	12	5.77	14	28
75	6.66	14	6.22	7	5.74	8	16
76	6.93	14	6.19	12	5.72	8	21
77	6.57	14	6.21	6	5.71	9	15
78	7.44	14	6.41	16	5.69	13	31
79	3.84	14	6.28	— 39	5.67	11	— 32
1580	3.12	14	6.30	— 50	5.66	11	— 45
81	9.30	14	6.65	40	5.64	18	65
82	7.95	14	6.72	18	5.62	20	41
83	7.53	14	6.78	11	5.61	21	34
84	6.15	14	7.05	— 13	5.59	26	10
85	8.13	14	7.40	10	5.57	33	46
86	6.99	14	7.61	— 8	5.55	37	26
87	5.58	14	7.25	— 23	5.54	31	1
88	7.29	14	7.41	— 2	5.52	34	32
89	8.73	14	7.42	18	5.50	35	59
1590	7.62	14	7.38	3	5.49	34	39
91	9.00	14	7.24	24	5.47	32	65
92	5.73	14	7.09	— 19	5.45	30	5
93	5.94	14	6.95	— 15	5.44	28	9
94	5.85	14	6.42	— 9	5.42	18	8
95	6.12	14	6.07	1	5.40	12	13
96	5.91	14	5.88	1	5.38	9	10
97	7.53	14	5.54	36	5.37	3	40
98	4.50	14	5.18	— 13	5.35	— 3	— 16
99	4.68	14	4.80	— 3	5.34	— 10	— 12
1600	4.92	14	4.59	7	5.32	— 14	— 8
01	3.66	14	4.26	— 14	5.31	— 20	— 31
02	3.06	14	4.05	— 24	5.29	— 23	42
03	2.94	14	3.88	— 24	5.27	— 26	— 44
04	6.09	14	4.03	51	5.25	— 23	16
05	4.65	14	4.01	16	5.24	— 23	— 11
06	3.33	14	3.98	— 16	5.22	— 24	— 36
07	4.08	14	4.02	1	5.21	— 23	— 22
08	3.69	14	4.00	— 8	5.19	— 23	— 29
09	3.66	14	3.87	— 5	5.17	— 25	— 29
1610	3.99	14	3.71	— 8	5.16	— 28	— 23
11	3.42	14	3.71	— 8	5.14	— 28	— 33
12	3.99	14	3.96	1	5.12	— 23	— 22
13	4.38	14	3.92	12	5.11	— 23	— 14
14	4.17	13	4.06	3	5.09	— 20	— 18
15	4.05	13	4.16	— 3	5.08	— 18	— 20
16	3.27	13	4.26	— 23	5.06	— 16	— 35
17	5.64	13	4.49	26	5.05	— 11	12
18	3.75	13	4.56	— 18	5.03	— 9	— 25
19	5.13	13	4.70	9	5.01	— 6	2
1620	4.74	13	4.88	— 3	5.00	— 2	— 5
21	5.04	13	4.85	4	4.98	— 3	1
22	5.22	13	4.77	9	4.96	— 4	5

TABLE (Continued)

1	2	3	4	5	6	7	8
1623	4.44	12	4.57	— 3	4.95	— 8	— 10
24	4.92	12	4.56	8	4.93	— 8	— 0
25	4.29	12	4.67	— 8	4.92	— 5	— 13
26	3.72	12	4.91	— 24	4.90	0	— 24
27	5.07	12	5.16	— 2	4.89	6	4
28	5.46	12	5.47	— 0	4.87	12	12
29	5.61	12	5.39	4	4.86	11	15
1630	7.26	12	5.21	39	4.84	8	50
31	5.07	12	5.21	— 3	4.83	8	5
32	4.86	12	4.92	— 1	4.81	2	1
33	3.81	12	4.11	— 7	4.80	— 14	— 21
34	1.89	12	3.84	— 51	4.78	— 20	— 60
35	4.41	12	3.34	32	4.77	— 30	— 8
36	4.26	12	3.09	38	4.75	— 35	— 10
37	2.34	12	3.67	— 36	4.74	— 23	— 51
38	2.70	12	4.13	— 35	4.72	— 13	— 43
39	6.12	12	3.98	54	4.71	— 15	30
1640	3.15	12	4.72	— 33	4.69	1	— 33
41	6.30	12	4.55	38	4.68	— 3	35
42	6.72	12	4.56	— 47	4.66	— 2	44
43	3.42	12	4.54	— 25	4.65	— 2	— 26
44	2.73	12	4.23	— 35	4.63	— 9	— 41
45	3.84	12	3.21	20	4.62	— 31	— 17
46	3.00	12	3.40	— 12	4.60	— 26	— 35
47	3.36	12	2.88	17	4.59	— 37	— 27
48	3.24	12	2.61	24	4.57	— 43	— 29
49	3.00	12	3.32	— 10	4.56	— 27	— 34
1650	2.13	15	2.72	— 22	4.54	— 40	— 53
51	2.25	15	2.75	— 18	4.53	— 39	— 50
52	3.15	15	2.90	9	4.51	— 36	— 30
53	2.25	15	3.12	— 28	4.50	— 31	— 50
54	4.05	15	3.35	21	4.49	— 25	— 10
55	3.78	15	3.49	8	4.49	— 22	— 15
56	4.32	15	3.69	17	4.46	— 17	— 3
57	3.42	15	3.78	— 10	4.45	— 15	— 23
58	3.99	15	3.79	5	4.43	— 14	— 10
59	2.97	15	3.74	— 21	4.42	— 15	— 33
1660	2.97	15	3.02	— 2	4.40	— 31	— 33
61	3.93	15	2.95	33	4.39	— 33	— 10
62	3.33	15	2.74	22	4.37	— 37	— 24
63	2.61	15	2.77	— 6	4.36	— 36	— 40
64	1.68	15	2.63	— 36	4.34	— 40	— 61
65	1.41	15	2.66	— 47	4.33	— 39	— 67
66	3.69	15	2.40	54	4.32	— 44	— 15
67	3.39	15	2.77	22	4.31	— 36	— 21
68	3.33	15	3.08	8	4.29	— 28	— 22
69	2.43	15	3.42	— 29	4.28	— 20	— 43
1670	3.54	15	3.57	— 1	4.26	— 16	— 17
71	3.69	15	3.59	3	4.25	— 16	— 13
72	4.80	15	3.46	39	4.23	— 18	13
73	3.09	15	3.63	— 15	4.21	— 14	— 27
74	3.30	15	3.64	— 9	4.20	— 13	— 21
75	2.97	15	3.65	— 19	4.19	— 13	— 29
76	3.96	15	3.50	13	4.18	— 16	— 5
77	4.23	15	3.54	19	4.17	— 15	1
78	3.87	15	4.04	— 4	4.16	— 3	— 7
79	3.15	15	4.42	— 29	4.14	7	— 24
1680	4.29	15	4.62	— 7	4.13	12	4
81	5.25	15	4.78	10	4.11	16	28
82	5.76	15	4.60	25	4.10	12	40
83	6.45	15	4.59	41	4.08	13	58
84	2.67	15	4.70	— 43	4.07	15	— 34
85	4.23	15	4.58	— 8	4.06	13	4

TABLE (Continued)

1	2	3	4	5	6	7	8
1686	3.99	15	4.18	— 5	4.05	3	— 1
87	3.39	15	3.94	— 14	4.04	— 2	— 16
88	5.31	15	4.08	30	4.02	1	32
89	4.59	15	4.32	6	4.01	8	14
1690	3.33	15	4.68	— 29	4.00	17	— 17
91	4.33	15	4.69	— 7	3.99	18	9
92	5.79	15	4.81	20	3.98	21	45
93	5.88	15	4.80	23	3.96	21	48
94	4.05	15	4.64	— 13	3.95	17	3
95	3.87	15	4.51	— 14	3.93	15	— 2
96	4.80	15	4.35	10	3.92	11	22
97	4.11	15	4.09	0	3.91	5	5
98	3.60	15	3.81	— 6	3.90	— 2	— 8
99	3.63	15	3.59	1	3.88	— 7	— 6
1700	2.79	15	3.57	— 17	3.87	— 8	— 23
01	4.08	15	3.45	18	3.86	— 11	6
02	3.93	15	3.23	22	3.84	— 16	3
03	2.79	15	3.26	— 14	3.83	— 15	— 27
04	2.55	15	3.37	— 24	3.83	— 12	— 33
05	3.75	15	3.48	8	3.82	— 9	— 2
06	3.48	15	3.47	0	3.80	— 9	— 8
07	3.06	15	3.30	— 7	3.79	— 13	— 19
08	4.17	15	3.24	29	3.77	— 14	— 11
09	3.75	15	3.21	17	3.76	— 15	— 0
1710	2.91	15	3.06	— 5	3.74	— 18	— 22
11	2.16	15	3.01	— 28	3.73	— 19	— 42
12	2.61	15	3.08	— 15	3.72	— 17	— 30
13	2.91	15	3.16	— 8	3.71	— 15	— 22
14	3.24	15	3.10	5	3.70	— 16	— 12
15	3.70	13	3.09	20	3.69	— 16	0
16	4.22	13	3.15	34	3.68	— 14	15
17	3.04	13	3.30	— 8	3.67	— 10	— 17
18	2.84	13	3.23	— 12	3.66	— 12	— 22
19	2.30	13	3.18	— 28	3.64	— 13	— 37
1720	2.52	13	3.04	— 17	3.63	— 16	— 31
21	3.66	13	2.89	27	3.62	— 20	1
22	3.70	13	2.71	37	3.61	— 25	2
23	2.38	10	2.69	— 12	3.59	— 25	— 34
24	2.70	10	2.51	8	3.58	— 30	— 25
25	1.90	10	2.30	— 17	3.57	— 36	— 47
26	1.96	10	2.02	— 3	3.56	— 43	— 45
27	1.54	10	1.59	— 3	3.55	— 55	— 57
28	2.08	10	1.76	18	3.54	— 50	— 41
29	1.52	10	1.92	— 21	3.53	— 46	— 57
1730	2.08	10	2.15	— 3	3.52	— 39	— 41
31	2.38	13	2.79	— 15	3.50	— 20	— 32
32	2.66	13	3.06	— 13	3.49	— 12	— 24
33	4.50	13	3.22	40	3.48	— 7	29
34	3.10	13	3.40	— 9	3.47	— 2	— 11
35	4.56	13	3.58	27	3.46	3	32
36	4.52	13	3.67	23	3.45	6	31
37	1.52	13	3.80	— 60	3.44	10	— 56
38	3.44	13	3.81	— 10	3.43	11	0
39	3.84	13	3.55	8	3.42	4	12
1740	4.42	13	3.77	17	3.41	11	30
41	4.28	13	3.70	16	3.39	9	26
42	4.14	13	3.96	5	3.38	17	22
43	3.18	13	4.05	— 21	3.37	20	— 6
44	3.12	13	3.81	— 18	3.36	13	— 7
45	5.12	13	3.65	40	3.35	9	53
46	3.12	13	3.61	— 14	3.34	8	— 7
47	4.12	13	3.61	14	3.33	8	24
48	2.42	13	3.82	— 37	3.32	15	— 27



TABLE (Continued)

1	2	3	4	5	6	7	8
1749	4.24	13	3.87	10	3.31	17	28
1750	3.78	13	3.76	1	3.30	14	15
51	4.36	13	3.65	19	3.29	11	33
52	3.68	13	3.72	— 1	3.28	13	12
53	4.30	13	3.61	19	3.27	10	31
54	2.42	13	3.59	— 33	3.26	10	— 26
55	3.26	13	3.36	— 3	3.25	3	0
56	3.78	13	3.41	11	3.24	5	17
57	2.98	13	3.27	— 9	3.23	1	— 8
58	3.52	13	3.37	4	3.22	5	9
59	3.46	13	3.34	4	3.21	4	8
1760	3.70	13	3.45	7	3.20	8	16
61	3.76	16	3.48	8	3.19	9	18
62	2.66	16	3.49	— 24	3.18	10	— 16
63	4.14	16	3.62	14	3.17	14	31
64	3.20	16	3.87	— 17	3.16	22	1
65	4.06	16	3.95	3	3.15	25	29
66	4.64	22	4.01	16	3.14	28	48
67	3.96	22	3.92	1	3.13	25	27
68	4.82	22	4.06	19	3.12	30	54
69	3.60	22	3.96	— 9	3.11	27	16
1770	3.46	22	3.97	— 13	3.10	28	12
71	3.76	22	3.90	— 4	3.09	26	22
72	3.78	22	3.94	— 4	3.08	28	23
73	4.02	22	3.97	1	3.07	29	31
74	4.50	22	3.98	13	3.06	30	47
75	4.20	22	4.32	— 3	3.05	42	38
76	4.60	22	4.58	0	3.04	51	51
77	4.52	22	4.67	— 3	3.03	54	49
78	3.92	22	4.63	— 15	3.02	53	30
79	5.12	22	4.53	13	3.01	50	70
1780	5.62	22	4.51	25	3.00	50	87
81	4.36	22	4.45	— 2	3.00	48	45
82	3.46	22	4.20	— 18	2.99	40	16
83	3.66	22	4.28	— 14	2.98	44	23
84	4.40	22	4.27	— 3	2.97	44	48
85	4.52	22	4.02	12	2.96	36	53
86	3.56	22	3.89	— 8	2.95	32	21
87	3.92	22	3.99	— 2	2.94	36	33
88	5.42	22	3.98	36	2.93	36	85
89	3.14	22	3.77	— 17	2.92	29	8
1790	2.82	22	3.77	— 25	2.91	30	— 3
91	3.78	22	3.72	16	2.90	28	30
92	4.06	22	3.79	7	2.90	31	40
93	3.48	22	3.71	— 6	2.89	28	20
94	3.64	22	3.54	3	2.88	23	26
95	4.66	22	3.49	34	2.87	22	62
96	2.74	22	3.29	— 17	2.86	15	— 4
97	3.48	22	3.16	10	2.85	11	22
98	2.58	22	3.02	— 15	2.84	6	— 9
99	2.10	22	2.92	— 28	2.83	3	— 26
1800	2.44	22	2.83	— 14	2.83	0	— 14
01	3.74	13	2.77	35	2.82	— 2	33
02	3.68	13	2.93	26	2.81	4	31
03	2.30	13	2.83	— 19	2.80	1	— 18
04	2.80	13	2.96	— 5	2.80	6	0
05	3.06	13	2.94	4	2.79	5	10
06	2.68	13	2.81	— 5	2.78	1	— 4
07	2.68	13	2.65	1	2.77	— 4	— 3
08	2.44	13	2.75	— 11	2.76	— 0	— 12
09	3.34	13	2.84	18	2.75	3	21
1810	2.40	13	2.76	— 13	2.75	0	— 13
11	2.74	13	2.70	1	2.74	— 1	0

TABLE (Continued)

1	2	3	4	5	6	7	8
1812	2.74	13	2.59	6	2.73	— 5	0
13	2.90	21	2.38	22	2.72	— 13	7
14	1.90	15	2.09	— 9	2.72	— 23	— 30
15	2.02	13	1.88	7	2.71	— 31	— 25
16	1.74	13	1.92	— 9	2.70	— 29	— 36
17	1.30	13	1.80	— 28	2.69	— 33	— 52
18	1.58	13	1.88	— 16	2.68	— 30	— 41
19	1.90	13	2.08	— 9	2.67	— 22	— 29
1820	3.08	13	2.21	39	2.67	— 17	15
21	2.78	15	2.57	8	2.66	— 3	5
22	2.22	15	2.69	— 17	2.65	2	— 16
23	3.40	15	2.91	17	2.64	10	29
24	2.84	15	3.04	— 7	2.64	15	8
25	2.50	15	3.14	— 20	2.63	19	— 5
26	4.39	32	3.28	34	2.62	25	68
27	1.98	32	3.40	— 42	2.61	30	— 24
28	4.40	32	3.60	22	2.60	38	69
29	3.64	32	3.54	3	2.60	36	40
1830	3.76	32	3.59	5	2.59	39	45
31	3.79	32	3.62	5	2.58	40	47
32	2.98	32	3.47	— 14	2.58	34	16
33	3.90	32	3.48	12	2.57	35	52
34	2.70	32	3.12	— 13	2.56	22	5
35	3.17	32	3.13	1	2.56	22	24
36	3.66	32	3.14	17	2.55	23	44
37	2.67	32	3.05	12	2.54	20	5
38	2.77	32	3.06	— 9	2.53	21	9
39	2.80	32	3.01	— 7	2.53	19	11
1840	3.90	32	3.09	26	2.52	23	55
41	2.97	32	2.93	1	2.51	17	18
42	2.18	32	2.85	— 24	2.51	14	— 13
43	3.25	32	2.75	18	2.50	10	30
44	2.70	32	2.52	7	2.49	1	8
45	2.31	32	2.30	0	2.49	— 8	— 7
46	1.83	32	2.10	— 13	2.48	— 15	— 26
47	2.32	32	2.18	6	2.47	— 12	— 6
48	1.52	32	2.15	— 29	2.47	— 13	— 38
49	2.10	32	2.16	— 3	2.46	— 12	— 15
1850	2.47	32	2.17	14	2.45	— 11	1
51	2.51	32	2.15	17	2.45	— 12	2
52	2.64	32	2.12	25	2.44	— 13	8
53	1.81	32	2.13	— 15	2.44	— 13	— 26
54	2.45	32	2.28	7	2.43	— 6	1
55	1.16	32	2.19	— 47	2.43	— 10	— 52
56	2.17	32	2.28	— 5	2.42	— 6	— 10
57	2.64	32	2.31	14	2.41	— 4	10
58	3.15	32	2.50	26	2.41	4	31
59	2.82	32	2.68	5	2.40	12	18
1860	2.04	32	2.80	— 27	2.39	17	— 15
61	3.41	32	2.92	17	2.39	22	43
62	2.32	32	2.82	— 18	2.38	18	— 3
63	3.34	32	2.63	27	2.38	11	40
64	2.41	32	2.55	— 5	2.37	8	2
65	2.78	32	2.60	7	2.37	10	17
66	2.23	32	2.67	— 16	2.36	13	— 6
67	2.40	32	2.58	— 7	2.35	10	2
68	2.09	36	2.58	— 19	2.35	10	— 11
69	3.29	36	2.49	32	2.34	6	41
1870	2.95	36	2.59	14	2.33	11	27
71	2.65	36	2.61	2	2.33	12	14
72	2.10	36	2.59	— 19	2.32	12	— 9
73	2.18	36	2.43	— 10	2.32	5	— 6
74	2.73	36	2.40	14	2.31	4	18

TABLE (Continued)

1	2	3	4	5	6	7	8
1875	2.68	36	2.30	17	2.31	— 0	16
76	2.23	36	2.48	— 10	2.30	8	— 3
77	1.99	36	2.61	— 24	2.30	13	— 13
78	2.43	36	2.63	— 8	2.29	15	6
79	3.47	40	2.73	27	2.28	20	52
1880	2.82	40	2.73	3	2.28	20	24
81	3.21	40	2.65	21	2.27	17	41
82	2.13	40	2.74	— 22	2.27	21	— 6
83	2.25	56	2.68	— 16	2.26	19	— 0
84	3.33	56	2.62	27	2.26	16	47
85	1.95	56	2.51	— 22	2.25	12	— 13
86	2.15	56	2.51	— 14	2.25	12	— 4
87	3.44	56	2.51	37	2.24	12	54
88	2.20	89	2.58	— 15	2.24	15	— 2
89	2.93	89	2.56	14	2.23	15	31
1890	2.09	83	2.55	— 18	2.23	14	— 6
91	2.43	78	2.60	— 7	2.22	17	9
92	2.67	78	2.46	9	2.22	11	20
93	2.40	78	2.29	5	2.21	4	9
94	2.58	78	2.33	11	2.21	5	17
95	2.23	78	2.14	4	2.20	— 3	1
96	1.55	76	2.16	— 28	2.20	— 2	— 30
97	1.85	76	2.02	— 8	2.19	— 8	— 16
98	1.93	76	1.98	— 3	2.19	— 10	— 12
99	1.78	76	1.86	— 4	2.18	— 15	— 18
1900	2.89	76	1.85	56	2.18	— 15	33
01	1.48	76	1.98	— 25	2.17	— 9	— 32
02	1.48	76	2.07	— 29	2.17	— 5	— 32
03	1.79	76	2.07	— 14	2.17	— 5	— 18
04	2.95	76	2.04	45	2.16	— 6	37
05	1.96	76	2.13	— 8	2.16	— 1	— 9
06	2.43	76	2.16	13	2.16	0	13
07	1.86	76	2.34	— 21	2.15	9	— 13
08	2.07	76	2.28	— 9	2.15	6	— 4
09	2.15	76	2.09	3	2.15	— 3	0
1910	2.76	76	1.83	51	2.14	— 14	29
11	1.72	76	1.80	— 4	2.14	— 16	— 20
12	1.55	76	1.71	— 9	2.14	— 20	— 28
13	1.14	76	1.66	— 31	2.13	— 22	— 46
14	1.14	76	1.51	— 25	2.13	— 29	— 46
15	1.51	76	1.44	5	2.12	— 32	— 29
16	2.12	76	1.35	57	2.12	— 36	0
17	1.64	76	1.47	12	2.11	— 30	— 22
18	1.22	76	1.57	— 22	2.11	— 26	— 42
19	1.31	76	1.72	— 24	2.10	— 18	— 38
1920	1.80	70	1.70	6	2.10	— 19	— 14
21	1.40	65	1.59	— 12	2.10	— 24	— 33
22	2.09	65	1.44	45	2.09	— 31	0
23	1.89	61	1.56	21	2.09	— 25	— 10
24	1.57	53	1.54	2	2.08	— 26	— 25
25	0.68	53	1.37	— 50	2.08	— 34	— 67
26	1.15	53	1.45	— 21	2.07	— 30	— 44
27	1.53	53	1.41	9	2.07	— 32	— 26
28	2.29	53	1.39	65	2.06	— 33	— 11
29	0.91	29	1.39	— 35	2.06	— 33	— 56

## SIMILARITY OF INITIAL PROCESSES OF CONTINUOUS COSMIC RADIATION AND SHOWERS. II

BY

J. CLAY

*(University of Amsterdam)*

(Communicated at the meeting of April 28, 1951)

In their papers on "Nuclear Transmutations produced by Cosmic Ray Particles of great energy" CARLSON, HOOPER and KING<sup>1, 2)</sup> have published their investigation of processes in photographic emulsions and derived from 1300 cases the masses, the life-time and the frequencies of neutral  $\pi$  mesons. They determined the masses at  $295 \pm 20$  electron masses, the lifetime at  $2-5 \cdot 10^{-14}$  sec, and the number of neutral mesons at  $0.45 \pm 0.1$  of the charged mesons. It has also become a certainty that the neutral  $\pi$  meson decays into two photons and each photon into an electron pair. On this ground we may assume that at a very short distance of the nuclear explosions, the number of electrons produced by neutral mesons is in total about twice that produced by the charged mesons.

At present some cosmicians incline to think that all soft (electron) radiation proceeds from this source, just as formerly, after the decay of charged mesons had first been discovered, it was thought that all electrons came from these decay-mesons. Let us see what conclusions we have to draw.

We know from earlier measurements that in the higher regions of the atmosphere the total number of particles is 150 times that at sea-level, and that the number of penetrating particles there is 10 times that at sea-level. We also know that at sea-level the ratio of charged penetrating to soft (electronic) particles is as 3 : 1 (totalling 4). The corresponding number for the total in the high atmosphere is 600, and the corresponding number for the penetrating particles therein is 30, leaving 570 electrons in the total. Where did this number of electrons arise from?

According to the results of CARLSON, HOOPER and KING<sup>1)</sup> the ratio of neutral to charged mesons in the upper atmosphere is as 1 : 2. Considering the resp. life-times we may expect to find every neutral meson supplanted by 4 electrons, produced in the above-mentioned processes. This gives a ratio of electrons to the other particles as 2 : 1. If these were the only processes we could expect, we should find the 600 particles actually present to consist of 400 electrons and 200 other particles. As a matter of fact there are only 30 charged penetrating particles in a total



of 600, so that 170 appear to have decayed. As a product of this decay 170 electrons will have arisen, raising the number of electrons present to 570 (in the mean each decaying charged meson produces one electron). The ratio of the remaining (30) hard to the (570) soft particles is therefore as 1 : 19 in the high atmosphere.

Coming downwards into lower regions the number of soft particles goes down with that of the penetrating particles, because in the higher regions the range of the electrons of  $10^8$  eVolt is only 2 or 3 KM and in the lower atmosphere even only 600 M, but part of the mesons can persist till sea-level.

The most remarkable find is, that at sea-level where we measured for about 10 years <sup>3, 4</sup>), we have generally found that, provided the distances were not taken too small, the ratio of the number of penetrating particles (all charged, neutral ones being practically absent here) to the number of electrons in atmospheric showers was found to be of the order of 1 : 10—20. This is about the same ratio as that cited above for the production in the higher atmosphere. This supports the opinion we gave in the previous article on the same subject, namely that the continuous radiation and the atmospheric showers have similar origins. This was based on measurements for hard and soft showers as separate cases. But every time when in one and the same shower the density is measured of penetrating and of electronic particles, in counters at different distances, we find the density for penetrating particles somewhat greater in proportion to that of electrons than we should expect from the above calculations. We think the cause hereof is, that the bulk of the electrons is produced from the neutral mesons at very small distance from the point of explosion. The charged mesons however need a larger distance to decay. This was demonstrated in our measurements of coherent coincidences at different distances.

It is also comprehensible that at very short distances the number of photons (which will give rise to more electrons) can be very considerable.

By a closer examination of the relative numbers of mesons, electrons, and photons in the showers at sea-level we have now the possibility to find the correlation of the production processes in the high atmosphere.

#### REFERENCES

1. CARLSON, A. G., J. E. HOOPER and D. T. KING; Phil. Mag. Ser. 7, 41, 701 (1950).
2. HOOPER, J. E., and D. T. KING; Phil. Mag. Ser. 7, 41, 1194 (1950).
3. CLAY, J., Proc. Neth. Acad. Amst. 44, 888 (1941).  
     ———, Physica; 13, 433 (1947).  
     ———, Proc. Roy. Neth. Acad. Amst. B 54, 20 (1951).
4. ——— and E. v. ALPHEN; Physica 16, 393, (1950).

A REMARKABLE FEATURE OF THE EARTH'S TOPOGRAPHY <sup>1)</sup>,  
ORIGIN OF CONTINENTS AND OCEANS. I

BY

F. A. VENING MEINESZ

(Communicated at the meeting of December 23, 1950, manuscript at the  
meeting of May 26, 1951)

As he has already mentioned in a preliminary paper <sup>1)</sup>, the writer in studying the development in spherical harmonics of the Earth's topography by PREY <sup>2)</sup> found a remarkable result, the dominance of the low order terms over the higher order ones. This paper deals more in detail with this result and mentions some further curious features.

In examining the great number of coefficients of PREY's development we do not see much of a system. As, however, for many phenomena in the Earth, as e.g. convection, we obtain equations which, if expressed in spherical harmonics, depend only on the order  $n$  of the harmonic and not on the coefficients of the  $2n + 1$  constituent under-terms, it seemed worth while to try to derive for each order a value representative of all its under-terms together and to compare these values. For this purpose it appeared indicated to derive the mean over the Earth's surface of the squares of that part of the topographic elevation which is given by the combination of all the under-terms of a certain order or, still better, by the root of this mean square.

In doing so we find the curve of fig. 1 showing these roots for the first up to the sixteenth order terms; PREY's development does not go further. In examining this curve we see at once the remarkable fact mentioned above of the dominance of the first up to the sixth order terms over those of higher order and, besides, the curious regularity of this curve and its wave-character. Before looking further into these peculiarities we shall mention the formula's used for the computing of the ordinates of the curve.

For the first under-term <sup>3)</sup> of the general spherical harmonic of the order  $n$  which is only a function of  $z = \cos \vartheta$  ( $\vartheta$  = distance to the pole) we have the formula

$$(1a)^4) \quad \dots \int_{-1}^{+1} (P_n)^2 dz = \frac{2}{2n+1}$$

<sup>1)</sup> First paper in Proc. Kon. Ned. Akad. v. Wet., 53, 7 (1950).

<sup>2)</sup> A. PREY, Darstellung der Höhen und Tiefenverhältnisse der Erde, Abh. Ges. der Wissenschaften, Göttingen, Math. Phys. Kl. N. F., 11, 1 (1922).

<sup>3)</sup> Also called Legendre polynomial.

<sup>4)</sup> See e.g. WHITTAKER—WATSON, A course of Modern Analysis, p. 306.

and this leads to a mean value over the sphere of  $(P_n)^2$  of half of this value. For the following under-terms having the shape

$$P_n^m(z) \cos m\lambda \text{ and } P_n^m(z) \sin m\lambda \quad (m \text{ varying from } 1 \text{ to } n)$$

in which  $P_n^m$  is called an Associated Legendre function, we have

$$(1b)^1) \quad \int_{-1}^{+1} (P_n^m)^2 dz = \frac{2}{2n+1} \frac{(n+m)!}{(n-m)!}$$

and this gives a mean value over the sphere of  $(P_n^m)^2 \cos^2 m\lambda$  of a quarter of this value and for  $(P_n^m)^2 \sin^2 m\lambda$  of the same.

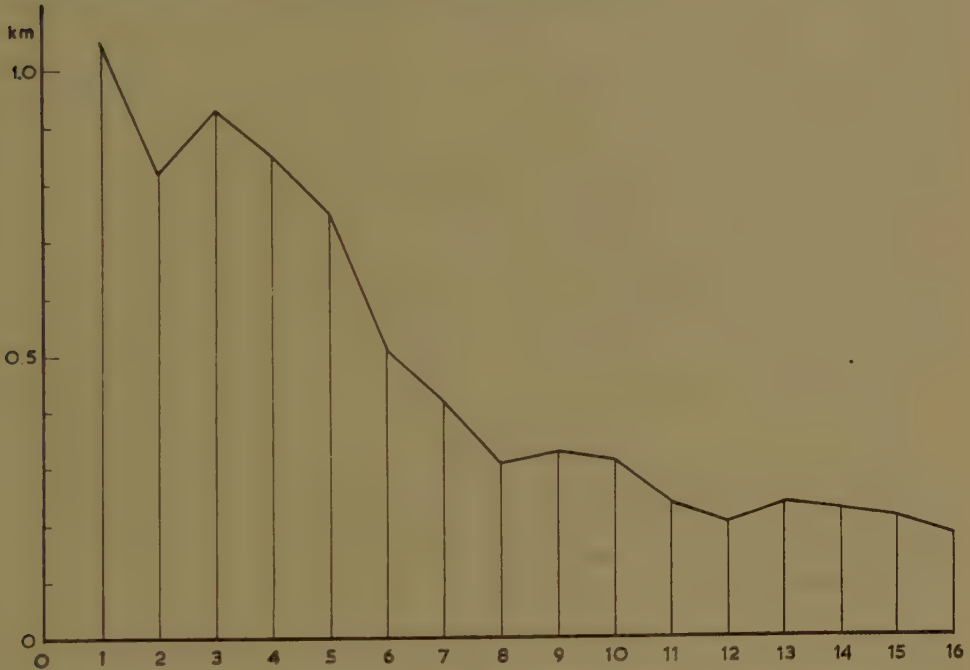


Fig. 1. Earth's topography, mean values of spherical harmonic terms of orders 1-16.

This provides us with the following value for the mean of the squares of that part of the topography that is given by the spherical harmonic of the order  $n$ . If this part of the topography is given by

$$(2) \quad \left\{ \begin{aligned} Y_n = & a_n P_n + a_n^1 P_n^1 \cos \lambda + \dots + a_n^m P_n^m \cos m\lambda + \dots + a_n^n P_n^n \cos n\lambda + \\ & + b_n^1 P_n^1 \sin \lambda + \dots + b_n^m P_n^m \sin m\lambda + \dots + b_n^n P_n^n \sin n\lambda. \end{aligned} \right.$$

we find for the mean square over the sphere

$$(3) \quad \left\{ \begin{aligned} |(Y_n)^2| = & \frac{1}{2n+1} (a_n)^2 + \frac{1}{2(2n+1)} \frac{(n+1)!}{(n-1)!} [(a_n^1)^2 + (b_n^1)^2] + \dots + \\ & + \frac{1}{2(2n+1)} \frac{(n+m)!}{(n-m)!} [(a_n^m)^2 + (b_n^m)^2] + \dots + \frac{(2n)!}{2(2n+1)} [(a_n^n)^2 + (b_n^n)^2]. \end{aligned} \right.$$

<sup>1)</sup> See WHITTAKER-WATSON, p. 325. In some publications these associated Legendre functions are provided with a further numerical factor  $n!/(n+m)!$ . The above formulas correspond to those used by PREY in his computations.

By means of this formula and of PREY's coefficients  $a$  and  $b$  the values entered in the second column of table I have been found; they thus represent the mean square of the parts of the topography corresponding to the different order terms. The roots of these mean squares are given by the third column; they are represented by the ordinates of fig. 1.

For these computations the coefficients  $a$  and  $b$  have been used of PREY's *A* table, i.e. those derived by him by developing the complete topography of the solid Earth's surface consisting of the continents and of the ocean-floors. For further studies he likewise developed the topography of the ocean-floors combined with zero elevation for the parts of the crust above sea-water; he thus found the  $a$  and  $b$  coefficients of his table *B*. We shall use these coefficients too in connection with the following problems dependent on the distribution of the topographic masses.

If we consider the load of the topography on the Earth's crust, the submarine topography has to be taken into account with a density equal to the rock-density diminished by the density of sea-water and if we follow the usual assumptions by putting the rock-density for all topographic features at 2.67 and that of sea-water at 1.028, we obtain a load-density for the submarine topography which is 0.615 times the load-density for the continental topography. We may conclude, therefore, that if we wish to develop the topographic load on the crust in spherical harmonics, we can do so by diminishing the sea-depths by 0.385 times their values and so we find the corresponding coefficients  $a$  and  $b$  for this development by subtracting 0.385 times the values of PREY's table *B* from the values of  $a$  and  $b$  of his table *A*. For getting the loads we should have to multiply the results by 2.67.

A similar line can be followed for developing the varying thickness of the Earth's crust according to the supposition of Airy of its floating in hydrostatic equilibrium on the plastic substratum. Taking the usual simplified assumption of a homogeneous crust of a density of 2.67 floating on a substratum of a density of 3.27 and assuming this equilibrium to be realized for each vertical prism of the crust independent of its surroundings, we find a deviation of the normal thickness of this floating crust which, for the continental parts, equals 5.45 times the elevation of the topography and, for the oceanic parts,  $1 + 4.45 \times 0.615 = 3.737$  times the topographic elevation. We find the development of this quantity in spherical harmonics by multiplying the coefficients of PREY's table *A* by 5.45 and by subtracting 1.713 times the coefficients of his table *B*, or we can diminish the coefficients of his table *A* by 0.3143 times those of table *B* and afterwards multiply the result by 5.45.

For simplifying the computation of the mean square of the different order terms of these and similar developments, all supposed to be a linear function of the complete topography as represented by the series  $Y_n$  with the coefficients of table *A*, and of the oceanic topography only,



as represented by a series which we shall indicate by  $Y'_n$  and which has the coefficients of table *B*, the writer, besides deriving the mean square of the terms  $Y_n$  in the way mentioned above, has done the same for the mean square of the terms  $Y'_n$  and for the mean product of the terms  $Y_n$  and  $Y'_n$ . These last two groups of results are shown by the 4th and 5th columns of table I. The 6th column gives the values of the terms

$$(4) \quad |(Y''_n)^2| = |(Y_n - 0.3143 Y'_n)^2| = |(Y_n)^2| - 0.6286 |Y_n \times Y'_n| + 0.3143^2 |(Y'_n)^2|$$

and the 7th column the roots of these values multiplied by 5.45 which thus represent the roots of the mean squares of the parts of the deviation in thickness of the Earth's crust corresponding to the terms of different order.

The values of this last column have been represented graphically by the ordinates of fig. 2. We see that it shows the same properties as the terms of the topography represented by fig. 1. The values of the 7th column have in fact a nearly constant ratio to those of the 3rd column; this ratio is close to 4 : 1. We may no doubt draw the conclusion that other similar linear combinations of the two developments  $Y_n$  and  $Y'_n$  as e.g. that which corresponds to the development of the topographic load on the crust, show likewise the same character.

TABLE I  
*List of spherical harmonic terms*  
( $Y''_n = Y_n - 0.3143 Y'_n$ )

$n$	$ (Y_n)^2 $ km <sup>2</sup>	$ [(Y_n)^2] $ km	$ (Y'_n)^2 $ km <sup>2</sup>	$ Y_n \cdot Y'_n $ km <sup>2</sup>	$ (Y''_n)^2 $ km <sup>2</sup>	$5.45 \sqrt{ (Y''_n)^2 }$ km	$\sqrt{n(n+1)} \times$ col. 7
0	—	-2.456	—	—	—	-8.791	—
1	1.1036	1.055	0.8556	0.9722	0.5770	4.140	5.86
2	0.6760	0.822	0.5315	0.5971	0.3532	3.239	7.93
3	0.8667	0.931	0.6477	0.7450	0.4625	3.706	12.83
4	0.7221	0.850	0.5293	0.6157	0.3924	3.414	15.28
5	0.5640	0.751	0.3948	0.4870	0.2969	2.970	16.27
6	0.2597	0.510	0.1801	0.2088	0.1462	2.034	13.51
7	0.1730	0.416	0.1610	0.1626	0.0867	1.605	12.02
8	0.09573	0.309	0.07720	0.08213	0.05072	1.228	10.42
9	0.10805	0.3287	0.07702	0.08750	0.06066	1.342	12.74
10	0.09880	0.3143	0.06941	0.08034	0.05514	1.278	13.40
11	0.05563	0.2359	0.03943	0.04475	0.03140	0.966	11.10
12	0.04194	0.2048	0.02913	0.03296	0.02410	0.846	10.57
13	0.05521	0.2350	0.04552	0.04864	0.02913	0.930	12.55
14	0.05186	0.2277	0.04188	0.04480	0.02784	0.910	13.19
15	0.04750	0.2179	0.03180	0.03790	0.02682	0.893	13.83
16	0.03276	0.1810	0.02202	0.02457	0.01950	0.761	12.55

The figures of the last column have been found by multiplying those of the 7th column by  $n^{\frac{1}{2}}(n+1)^{\frac{1}{2}}$ ; they are represented by fig. 3. We shall presently come back to the meaning of this curve but we can already

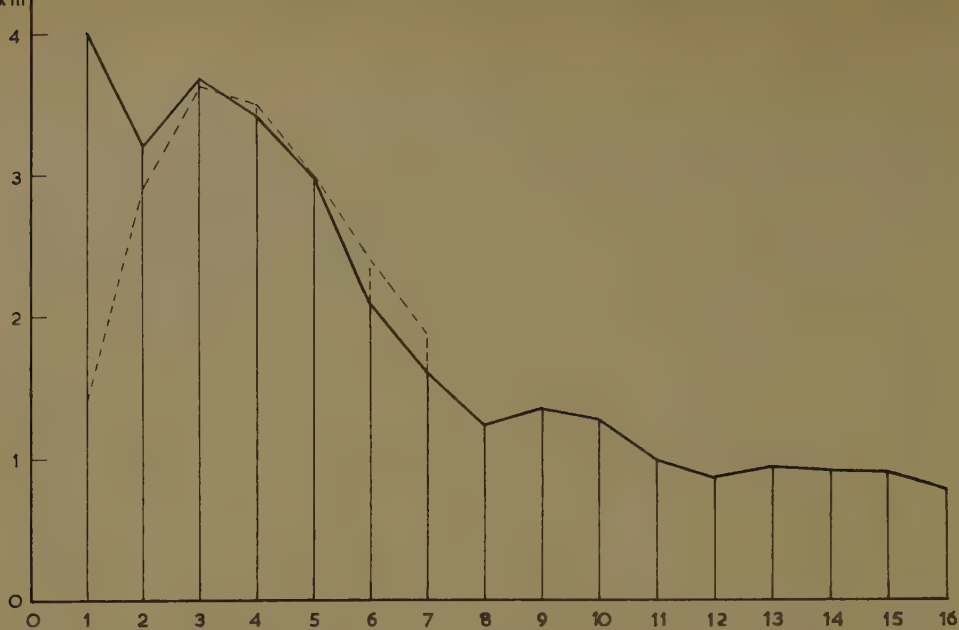


Fig. 2. Deviations of Earth's crust's thickness, mean values of spherical harmonic terms of orders 1–16.

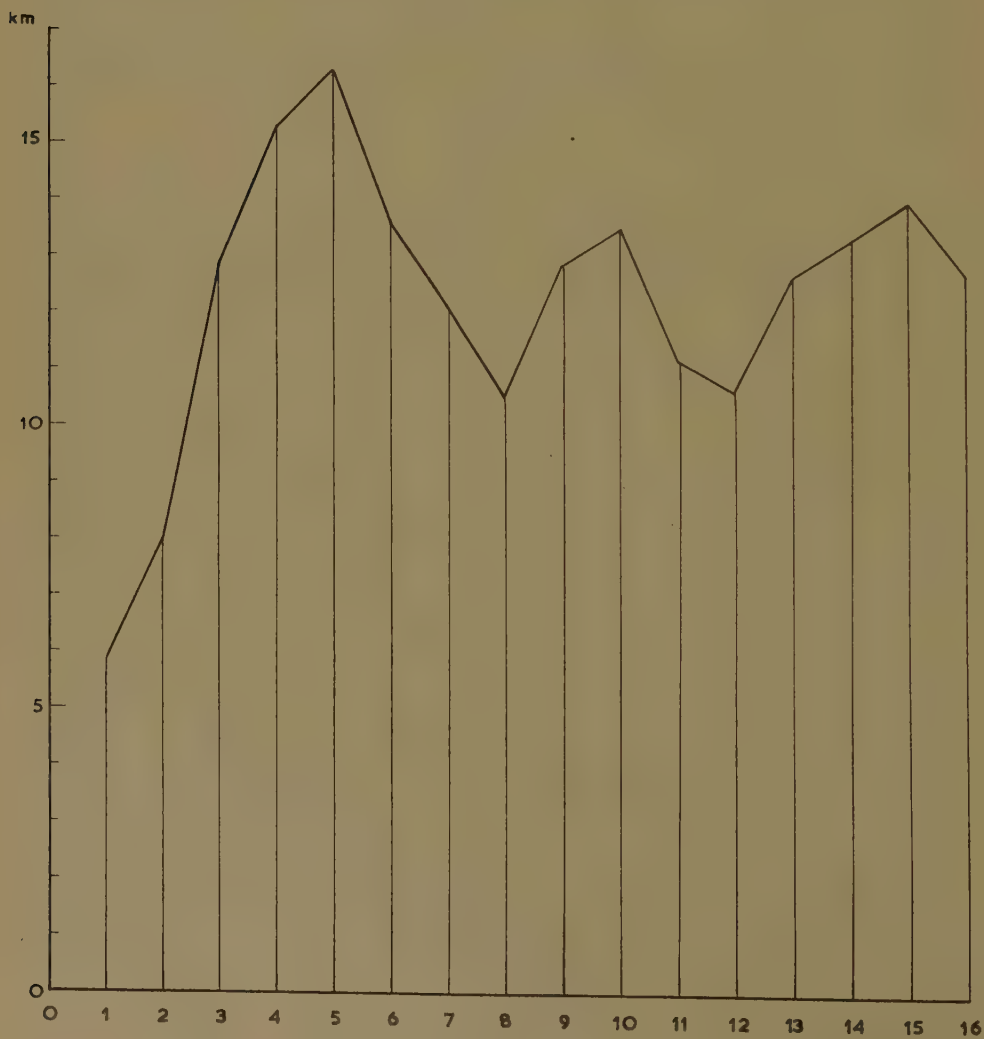


Fig. 3. Ordinates of fig. 2 multiplied by  $\sqrt{n(n+1)}$ .

notice its remarkable regularity, also for the higher values of  $n$ , and its curious periodic features.

That the regular character of the curves of fig. 1, 2 and 3 is not a common feature of the development in spherical harmonics of a quantity on the Earth's surface is shown by another curve given for comparizon in fig. 4.

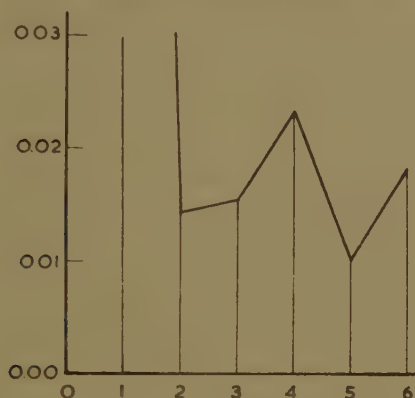


Fig. 4. Earth's magnetic potential, mean values of spherical harmonic terms of orders 1—6.

It represents the development in spherical harmonics of the potential of the terrestrial magnetism. It has been derived by S. W. VISSER by means of the same formula 3 from the coefficients given by DYSON and TURNER <sup>1)</sup> and taking into account that these coefficients refer to formulas for the Associated Legendre functions provided with the factor  $n!/(n+m)!$  as mentioned in the note on p. 213. The curve does not show the large first term corresponding to the main part of the Earth's magnetism but it gives the next terms. Although only a few are available we see clearly their irregular character. We notice likewise that it neither shows the large values of the terms for low values of  $n$  as shown by the curves of fig. 1 and 2.

Examining these last curves we see in the first place the large value of the first order term. This need not surprise us; it corresponds of course to the fact that the distribution of the continents shows a hemisphere rich in continental topography and one where the oceans dominate. It is clear that this must bring about a large first order term.

In contradiction to the curve for the terrestrial magnetism, however, the high first order term is followed by a series of large terms. After a slight sinking in the second order one we get a higher value again for the third order term and the following terms are likewise large. Besides, the whole group of the 2nd to the 8th terms shows a remarkably regular trend which can hardly be accidental and which, therefore, points strongly to some physical phenomenon dominating this whole group of terms. The same conclusion follows from the curve of fig. 3.

<sup>1)</sup> F. DYSON and H. TURNER, The Earth's Magnetic Potential, M.N.R.A.S Geoph. Suppl. 1, No. 3, 76 (1923).

The curves of fig. 1 and fig. 2 show two further waves between the 8th and the 16th order but their amplitudes are much smaller and so doubts might arise about their having a physical meaning. These doubts vanish, however, when examining the curve of fig. 3 which shows these waves so clearly; their shape shows a most curious similarity to that of the first wave. The tops in this curve moreover, occur at perfectly regular intervals, viz. at  $n = 5$ ,  $n = 10$  and  $n = 15$ . We can hardly escape the surmise that these waves are caused by similar physical phenomena or at least by closely related ones.

Before continuing our examination of the curves, we must first have a look at the meaning of our multiplying the ordinates of the curve of fig. 2 by  $n^{\frac{1}{2}}(n+1)^{\frac{1}{2}}$  by means of which we obtained the curve of fig. 3. It is based on the fact that a great many spherical problems governed by a spherical harmonic  $Y_n$  on a sphere with radius  $\varrho$  can be transformed in plane problems governed by the plane function  $K$  given by the equation

$$(5a) \quad \nabla^2 K + k^2 K = 0$$

if

$$(5b) \quad k^2 = \frac{n(n+1)}{\varrho^2}$$

This follows from the relation

$$(6) \quad \nabla^2 Y_n + \frac{n(n+1)}{\varrho^2} Y_n = 0$$

Adopting orthogonal coordinates  $x$  and  $y$  in the plane, the equation (5a) has a solution

$$(7a) \quad K = a \cos k_x x \cos k_y y \quad (k_x^2 + k_y^2 = k^2)$$

and if  $K$  is assumed constant in the sense of the  $Y$  axis

$$(7b) \quad K = a \cos kx$$

For this last case we may conclude that  $k$  is reciprocal to the wavelength and, for the more general case, to a quantity characterizing the dimensions of the periodic function. Going back to the case of spherical harmonics we may derive from 5b the same statement for the product  $n^{\frac{1}{2}}(n+1)^{\frac{1}{2}}$ , and so we may conclude that the multiplication of the ordinates of the curve of fig. 2 by this quantity has the effect of dividing these ordinates by a quantity proportional to the horizontal dimensions of the corresponding terms.

We thus come to the conclusion that the second and third waves of our development, being of about the same size in the curve of fig. 3, correspond to topographic features with elevations roughly proportional to their horizontal dimensions; the elevation of the first wave is somewhat larger.

For getting a rough idea of the horizontal extension of a spherical



harmonic of the order  $n$  on the Earth's surface, we may combine the formulas 7a and 5b and we find for the half wave-length  $L$  in both directions (putting  $k_x = k_y$ )

$$(8) \quad L = \frac{\pi \sqrt{2}}{k} = \frac{\pi R \sqrt{2}}{n^{\frac{1}{2}}(n+1)^{\frac{1}{2}}} = \frac{28300}{n^{\frac{1}{2}}(n+1)^{\frac{1}{2}}} \text{ km}$$

which gives for the three waves of fig. 2 and 3

$$1^\circ \quad n = 4 \quad L = 6300 \text{ km,}$$

$$2^\circ \quad n = 9 \quad L = 3000 \text{ km,}$$

$$3^\circ \quad n = 14 \quad L = 1900 \text{ km.}$$

The first wave is clearly of continental dimensions.

Returning to fig. 1 we see how strikingly the curve shows the result already mentioned in the previous paper, the dominance of the five first terms over all the following terms. We must, therefore, expect that the topography represented by these five first terms must provide a considerable part of the main topography of the Earth and that it will already show the distribution of the continents and oceans. This has been checked by means of the map.

This map shows the topography of the combined first five terms in contours. We see that all the main features are already represented. As may be expected, the smallest continent, Australia, shows least and also Europe does not give a pronounced picture. Its southern point excepted, South America comes out remarkably well although it is not one of the largest continents. Asia shows up strongest. Of the oceans, the Pacific, the Southern Atlantic and the Indian Ocean are most clearly expressed. In general we may notice that the southern hemisphere shows stronger contrasts in elevation than the northern one. The Mid Atlantic and Mid Indian Ocean ridges do not show up at all.

*(To be continued.)*

## GEOPHYSICS

### A REMARKABLE FEATURE OF THE EARTH'S TOPOGRAPHY<sup>1</sup>, ORIGIN OF CONTINENTS AND OCEANS. II

BY

F. A. VENING MEINESZ

(Communicated at the meeting of December 23, 1950, manuscript at the meeting of May 26, 1951)

In the foregoing the facts have been given and this is no doubt the more important part of this paper. We shall now try an attempt at an interpretation but it is necessary to emphasize beforehand its hypothetical character.

Examining again our figures it seems likely that the first order term is due to a separate phenomenon from that which brought about the group of terms from the second to the sixth order which forms the first wave of our curves. A first order term corresponds to one hemisphere of positive and one of negative elevations or, shortly expressed, to a hemisphere where land and one where sea abounds. Two explanations suggest themselves for accounting for such a configuration.

In the first place we may attribute it to the birth of the moon which, if originated by separation from the Earth, must have carried away much of the light surface matter from one side of the Earth. This supposition is in good harmony with the smaller density of the moon which is only 3.33. A similar hypothesis advocating the idea that the Pacific can be considered as the wound where the moon was released from the Earth, has already in 1882 been advanced by OSMOND FISHER. It was studied critically by JEFFREYS in "The Earth" who, especially in the 2nd edition (1929) came to favourable conclusions. More recently it was taken up by ESCHER<sup>2</sup>) who devoted much time to the study of the moon and its relations to the Earth and gave several arguments in favour of the idea<sup>3</sup>). The hypothesis supposes that the remaining part of the sialic cover of the Earth survived sufficiently the catastrophe for the present continents to be the remnants of this cover torn apart during their drift towards the wound. The writer will afterwards shortly deal with this hypothesis: it appears to him that it can be brought in harmony with the results

---

<sup>1</sup>) First paper in Proc. Kon. Ned. Akad. v. Wet., 53, 7 (1950).

<sup>2</sup>) B. G. ESCHER, Moon and Earth, Proc. Kon. Ned. Akad. v. Wet. Amsterdam, 42 (1939).

<sup>3</sup>) Other studies about this subject may be found in :

W. H. PICKERING, The place of origin of the moon, Journ. Geol. 15 (1907),

R. STAUB, Der Bewegungsmechanismus der Erde, (Berlin, 1928),

R. SCHWINNER, Lehrbuch der physikalischen Geologie, (Berlin, 1936),

H. QUIRING, Die irdische Mondnarbe, Forsch. u. Fortschr. 24, 211, (1948),

K. G. SCHMIDT, Mondablösung, Gebirgsbildung, Kontinentverschiebung, (Bonn, 1949).

studied in this paper. He wishes here only to mention that the plane of the moon's orbit does not contain the axis of the first order spherical harmonic, which points to a point south of Odessa, (for the first order term of the topography  $\varphi = 43^\circ 57'$ ,  $\lambda = 30^\circ 28'$ , for that of the thickness of the sialic layer  $\varphi'' = 43^\circ 57'$ ,  $\lambda'' = 30^\circ 57'$ ) but this seems to him no serious objection against assuming this first order term to have been caused by the moon's release; the crust of the Earth may since have moved around the Earth's interior and this may have brought about the discrepancy.

Another explanation of the first order spherical harmonic of the topography and of the thickness of the sialic cover of the Earth might perhaps be given by the assumption that during the beginning of the Earth's history, when the core had not yet differentiated, a convection current had originated in the whole Earth's interior, distributed corresponding to a first order spherical harmonic, i.e. sinking below one hemisphere, passing with its axis through the center and rising towards the other hemisphere. In two ways such a current might have brought about a thickening of the sialic crust in one of the two hemispheres and a thinning in the other, thus bringing about the first order spherical harmonic we have to explain. As we shall presently treat more in detail the two ways in which a convection-current in the Earth might be supposed to affect the sialic layer, we shall not go into this question here.

Comparing this hypothesis to that connected with the moon's release, the moon's hypothesis appears to be the most acceptable; a convection-current of the type as here supposed would be so fundamentally asymmetric in the Earth that the probability of its coming into being seems doubtful.

For the group of terms from the 2nd to the 6th order the writer feels inclined to attribute them to one or more systems of convection in the mantle during the first part of the Earth's history when the solidification of the crust was still going on. In a study about this subject which he hopes to publish shortly, he derived the minimum vertical gradient sufficient for allowing a stable convection-current in the mantle. Assuming that the temperature gradient  $\beta$  in the mantle diminishes downwards, he supposed the product of  $\beta$  by the vertical component  $w_0$  of the velocity in the axis of the rising and sinking currents and divided by the thermometric conductivity  $\mu$  to be given by

$$(9) \quad \frac{\beta w_0}{\mu} = C \varrho (R - \varrho) (\varrho - r)$$

in which  $R$  is the Earth's radius and  $r$  that of the core. This quantity, equal to  $\nabla^2 \Theta$ , in which  $\Theta$  is the deviation from the temperature before motion occurred, determines the distribution of the temperature in the mantle. From this assumption he derived the value for stable convection of the quantity  $\lambda$  given by

$$(10) \quad \lambda = \frac{\alpha \varrho' g \beta}{\eta \mu} (R - r)^4$$

in which  $\alpha$  is the thermal volume expansion,  $\rho'$  the density and  $\eta$  the viscosity. The quantity  $\lambda$  dominates the equation of motion of the convection. Its value for stable convection represents the lowest value for which convection is possible. For the mean value of  $\lambda$  over the whole height  $R - r$  of the current and for different values of the order  $n$  of its spherical harmonic distribution, he found the values of table II; the third column gives its reciprocal values multiplied by 2400; these values may provide us with a measure for the probability of terms of that order forming part of the current.

TABLE II

$n$	$\lambda_m$	$\frac{2400}{\lambda_m}$
1	1722	1.392
2	825	2.908
3	663	3.620
4	683	3.516
5	800	3.000
6	1000	2.400
7	1288	1.864

The values of the third column are represented by the hatched curve of fig. 2. We see that it shows a remarkable correlation to the ordinates of the main curve from the 2nd to the 7th order, i.e. for that part we are now investigating. As a connection of the thickness of the sialic layer and convection in the mantle would not be difficult to explain, there seems reason to consider such a connection at least as an acceptable possibility. We see that the second order ordinate of the main curve is somewhat larger than that of the hatched one, but as it can easily be explained that the moon's release, besides bringing about a first order term, must also have caused a smaller second order one, this does not offer difficulties.

As the writer has already put forward in previous papers <sup>1)</sup> the connection between a system of convection in the mantle and the thickness of the sialic crustal layer may have been brought about in two ways; the resulting effects of the two possibilities have opposed sign.

In the first place the rising currents may have brought the sial to the surface where, according to this hypothesis, it solidified in rigid shields above those currents and where we must suppose that it remained without being carried away by the diverging currents. This appears difficult to accept but on the other hand we must assume that during the whole ensuing history of the Earth higher temperatures must have reigned below the continents than below the oceans because of the sial being richer in

<sup>1)</sup> F. A. VENING MEINESZ, De Verdeeling van continenten en oceanen over het aardoppervlak, Versl. Ned. Akad. v. Wetensch. Amsterdam, 53, 4 (1944). (with English and French summaries).

F. A. VENING MEINESZ, Major Tectonic Phenomena and the Hypothesis of Convection Currents in the Earth, Quarterly Journal Geol. Soc. London, 103, 205 (1948).



radio-active constituents than the sub-oceanic crust and this might well have brought about rising currents below the continents which obviously have not succeeded in carrying away the sial. The only explanation could be that from the beginning the simatic crust under the adjoining areas has constituted a sufficient barrier to the spreading and has even been able to cause a steep edge to the sialic shield in the way the continents now show.

In the second place the sial might be supposed to have been concentrated by the converging currents in shields above the descending currents. This supposition appears more satisfactory; it also explains in a simpler way the steep and sudden edges of the sialic continents. Still we must realize that the concentration of sial must have tended to raise the temperature below it and so, after some time, this must have counteracted the current-system and favoured a rising current in this area where originally a descending one was assumed.

As for both hypotheses the sialic shields must have become distributed according to the same system of spherical harmonics as that which governed the distribution of the vertical component  $w$  of the convection-current — although the sign for both cases is opposite — we need not decide between the two possibilities, for affirming the correlation between the distribution of the thickness of the sialic layer and of the vertical component of a convection-current in the mantle.

So we thus have found a possible explanation of the large size of the group of terms from the second till the sixth order. A curious fact may perhaps give a further support to it. We have already mentioned that the Mid-Atlantic and Mid-Indian-Ocean ridges are not expressed by the combination of the 1st—5th order spherical harmonics as represented by map II but that on the contrary they coincide with the deepest parts of this map. This might well be explained by the two above hypotheses. In case the sial mainly solidified above the rising currents, we may assume that a small part of it was carried off towards the oceanic areas and was concentrated above the descending currents, thus forming the ridges in the middle of the oceans. In the second case where we supposed the continents to be the sialic concentrations swept together by the converging currents below this layer, we may well admit that above the rising currents a small part of the sial was staying above the middle of it without being carried off.

The fact that no pronounced ridge is found in the middle of the Pacific might be explained by the absence of sial in this area caused by the phenomenon bringing about the first order term which we discussed before.

The second and third waves of our curves are clearest expressed by fig. 3. This figure suggests their having the same character as the first wave, although they are much smaller, as we see clearly in fig. 1 and fig. 2. The similarity in type with regard to the first wave suggests a

similar cause and so this would lead to the supposition of their having been brought about by smaller systems of convection. The current-system correlated with the second wave must be supposed to have had about half the dimensions of that dealt with for the first wave and that connected with the third wave of one third of its size. As it does not seem likely that we have had periods during which there were discontinuity surfaces at a depth of about one half or one third of the thickness of the mantle, we cannot easily explain these smaller current-systems in this way. We might perhaps suppose that crustal phenomena have brought about temperature-distributions which have imposed these dimensions on the currents in the mantle but it is not easy to see the reason of such dimensions having the simple ratio mentioned to those of the system dealt with above for the first wave. Possibly also for some reason yet unknown a double or triple layer of convection-cells have developed in the mantle which thus would have the right size.

It is of course likewise possible that the simple ratio of 1 : 2 and 1 : 3 to the big system is no more than a fortuitous coincidence. As the writer has put forward elsewhere<sup>1)</sup> he thinks that there is evidence of still smaller systems of convection in the mantle brought about by temperature disturbances caused by crustal phenomena and we must expect such currents to lead to deeper temperature deviations which could well bring about larger convection-cells.

So the hypothesis of smaller convection systems having occurred in the mantle, also in more recent geological periods, can be tentatively accepted and there does not seem, therefore, to be any objection to the supposition of current-systems having likewise brought about the second and third waves of our curves. We can leave it an open question at what periods such phenomena could have taken place.

We still have to consider whether the great convection-system to which we have attributed the large terms of the orders 2—6 of our curves and, therefore, the origin of the continents and the oceans, could have been more or less simultaneous to the after-effects of the moon's separation from the Earth. This would involve the supposition that the great commotion of the Earth's resuming its new equilibrium position has also brought about the current-system responsible for the concentration of the remaining sial in the continental shields. We must no doubt assume that the moon's birth took place after there had been enough differentiation in the Earth for the moon's mainly carrying away light materials and so

---

<sup>1)</sup> F. A. VENING MEINESZ, Major tectonic phenomena and the hypothesis of convection-currents in the Earth, *Quart. J. Geol. Soc. of London*, **53**, 191—207 (1948).  
F. A. VENING MEINESZ, Gravity Expeditions at Sea, Vol. IV, p. 38 e.s., *Publ. Netherl. Geodetic Comm.*, (Delft 1948).

F. A. VENING MEINESZ, Deep-focus and intermediate earthquakes in the East Indies, *Proc. Kon. Ned. Akad. v. Wet. Amsterdam*, **49**, 8 (1946).

F. A. VENING MEINESZ, Convection-currents in the Earth, *Proc. Kon. Ned. Akad. v. Wet. Amsterdam*, **50**, 3 (1947).

it may be supposed that at that time the core had already been formed <sup>1)</sup>. Under these conditions it does not seem inadmissible to suppose that the commotion in the mantle during the resuming of the new equilibrium figure released a whole system of currents adapted to the thickness of the mantle and, therefore, corresponding in its distribution to the first wave of spherical harmonics of our figures. We may leave it an open question whether a temperature gradient caused by cooling has also played a part in the originating of these currents. It seems rather likely because otherwise it is somewhat difficult to understand the spreading of the movement throughout the whole mantle. It is remarkable, however, that on the map the topography on the side opposite to the South Pacific (where the moon must be supposed to have been released) shows much less contrast than elsewhere. We may perhaps consider this to be a good point in favour of our hypothesis <sup>2)</sup>.

If it is right we must no doubt accept the second view-point about the development of the continental shields and assume that the sial has been concentrated over the descending currents. As we may suppose that around the wound of the moon's birth descending currents occurred, we can easily explain the ring of continents surrounding the Pacific. We can likewise understand that in that ocean no mid-oceanic ridge is found but that in the Atlantic and the Indian Ocean where rising currents must be assumed, such ridges have come into being. The diverging currents, moreover, must have favoured the forming of crustal cracks in these ridges and this could explain the volcanic activity in those areas.

Lastly, the coming into being of the Atlantic Ocean might perhaps have occurred through the tearing apart of the sialic layer by the rising current below it and this might well explain the likeness of the continental edges on both sides which have already given rise to so many speculations, among which the theory of WEGENER is the most widely known.

We thus have arrived at a hypothesis practically coinciding with that of OSBORNE FISHER and ESCHER, although it differs somewhat in the mechanism of the formation of the continents and in some other details. The writer may refer to their publications for further arguments in favour of it. It seems an important asset of the hypothesis that the mathematical approach of this paper, although started quite independently, leads likewise towards this possibility.

We may, however, also keep in mind the possibility that the current-system occurred somewhat afterwards as a consequence of great temperature disturbances in the mantle. They may have been caused by the

---

<sup>1)</sup> In "The Earth", 1929, 3.21, JEFFERYS gives strong arguments in favour of this assumption; he proves that otherwise the moon's formation from the Earth would have been impossible.

<sup>2)</sup> It is possibly significant that at present this area shows only little seismic activity. The surrounding of the Pacific is on the contrary especially active and only there deep foci are found.



phenomenon of the moon's release itself or by the carrying off of the sialic layer on the Pacific side of the Earth and the resulting difference in radio-active heating. In any case the currents must be supposed to have come into being before that side of the Earth was covered by a sufficiently strong crust that it could no longer be engulfed by the descending currents; in that case the concentration of sialic continents, as e.g. N. and S. America, above those currents would not have been possible. The two hypotheses are not far apart; they more or less merge into each other.

We may perhaps ask whether it would be possible that the system of currents has taken place in a much more recent period and in such a way that the resulting movement and redistribution of the continental shields would fit in WEGENER's theory. It seems to the writer that such a hypothesis would be difficult to accept, mainly because of its being hard to believe that in a recent period the oceanic parts of the crust could have become sufficiently plastic <sup>1)</sup> to allow the transportation by the currents of the sialic shields as assumed in this paper without these shields being fundamentally deformed themselves. In a future paper the writer plans to come back to this and other questions connected with this paper.

A last point the writer wants to raise here is the question how the problem is affected when the two phenomena of the moon's release and the system of subcrustal currents which have caused respectively the first order term and the wave formed by the second to sixth order terms, have not been simultaneous. In this regard there is only one possibility, viz. that the moon has been separated first; in case of the reversed sequence it seems hardly possible that the regular configuration caused by the current-system could have survived after the upheaval contingent to the moon's birth.

The question now arises what current-system would have been needed for bringing about the present series of spherical harmonic terms, if the first order term was already there. The dragging process of the currents on the crust is difficult to analyse for this case but we may probably get a tentative idea of the result by supposing that it can be represented by the product of the series of terms corresponding to the current-system by the sum of a constant thickness of the crust and a term proportional to a first order harmonic. We have, therefore, to develop the product by the last term of this sum in spherical harmonics; the product by the constant term is already expressed in this way.

The general solution of the development of the product of two surface spherical harmonics  $Y_m$  and  $Y_n$  has been given by EMIL WAELSCH in 1909 <sup>2)</sup>. For our case,  $m = 1$ , and for our purpose we can simplify our

---

<sup>1)</sup> See also the well-known hypothesis of Joly (Phil. Mag. 45, (1923), 1167–1188, etc.) and JEFFREYS' opposition to it (The Earth 2nd Ed. (1929), p. 323, etc.).

<sup>2)</sup> EMIL WAELSCH, Über die Entwicklung des Produktes zweier Kugelfunktionen nach Kugelfunktionen, Sitz. Ber. K. Akademie d. Wiss. Wien, M. N. Kl. 118, IIa (1909).



formulas by choosing our coordinates  $\vartheta$  (spherical distance to the coord. axis) and  $\lambda$  (angle between a plane through this axis and a datum-plane through it) with regard to an axis coinciding with that of the first order term which thus reduces to the simple shape  $a_1^\circ \cos \vartheta$ . If  $A_n^\circ$ ,  $A_n^m$ ,  $B_n^m$  are the coefficients of  $Y_n$  (see form. 2) and  $a_n^\circ$ ,  $a_n^m$ ,  $b_n^m$  those of the development in spherical harmonics of the product, we find

$$(11a) \quad a_n^\circ = \frac{n}{2n-1} a_1^\circ A_{n-1}^\circ + \frac{n+1}{2n+3} a_1^\circ A_{n+1}^\circ$$

$$(11b) \quad a_n^m = \frac{n-m}{2n-1} a_1^\circ A_{n-1}^m + \frac{n+m+1}{2n+3} a_1^\circ A_{n+1}^m$$

$$(11c) \quad b_n^m = \frac{n-m}{2n-1} a_1^\circ B_{n-1}^m + \frac{n+m+1}{2n+3} a_1^\circ B_{n+1}^m$$

We see that the new coefficients are a linear function of those of  $Y_{n-1}$  and  $Y_{n+1}$ . Applying these formulæ and dividing by the common factor  $a_1^\circ$ , we obtain the coefficients of table III.

TABLE III  
Spherical harmonic coefficients of the product  $\cos \vartheta \times P_n$

$n$	$m=0$	$m=1$	$m=2$	$m=3$	$m=4$	$m=5$	$m=6$
0	$a_0^0$	$\frac{1}{3}A_1^0$					
1	$a_1^0 = A_0^0 + \frac{2}{3}A_2^0$	$a_1^1 = \frac{2}{3}A_2^1$					
2	$a_2^0 = \frac{2}{3}A_1^0 + \frac{3}{2}A_3^0$	$a_2^1 = \frac{1}{3}A_1^1 + \frac{4}{3}A_3^1$	$a_2^2 = \frac{5}{7}A_3^2$				
3	$a_3^0 = \frac{3}{5}A_2^0 + \frac{4}{3}A_4^0$	$a_3^1 = \frac{2}{5}A_2^1 - \frac{5}{9}A_4^1$	$a_3^2 = \frac{1}{3}A_2^2 - \frac{6}{9}A_4^2$	$a_3^3 = \frac{7}{9}A_4^3$			
4	$a_4^0 = \frac{4}{7}A_3^0 - \frac{5}{11}A_5^0$	$a_4^1 = \frac{3}{7}A_3^1 - \frac{6}{11}A_5^1$	$a_4^2 = \frac{2}{7}A_3^2 + \frac{7}{11}A_5^2$	$a_4^3 = \frac{1}{4}A_3^3 + \frac{8}{11}A_5^3$	$a_4^4 = \frac{9}{11}A_5^4$		
5	$a_5^0 = \frac{5}{9}A_4^0 - \frac{6}{13}A_6^0$	$a_5^1 = \frac{4}{9}A_4^1 - \frac{7}{13}A_6^1$	$a_5^2 = \frac{3}{9}A_4^2 - \frac{8}{13}A_6^2$	$a_5^3 = \frac{2}{9}A_4^3 + \frac{9}{13}A_6^3$	$a_5^4 = \frac{1}{9}A_4^4 + \frac{10}{13}A_6^4$	$a_5^5 = \frac{11}{13}A_6^5$	
6	$a_6^0 = \frac{6}{11}A_5^0 - \frac{7}{15}A_7^0$	$a_6^1 = \frac{5}{11}A_5^1 - \frac{8}{15}A_7^1$	$a_6^2 = \frac{4}{11}A_5^2 - \frac{9}{15}A_7^2$	$a_6^3 = \frac{3}{11}A_5^3 + \frac{10}{15}A_7^3$	$a_6^4 = \frac{2}{11}A_5^4 + \frac{11}{15}A_7^4$	$a_6^5 = \frac{1}{11}A_5^5 + \frac{12}{15}A_7^5$	$a_6^6 = \frac{13}{15}A_7^6$

Examining this table we see that as a rough approximation we may assume the new coefficients to be the mean of those of  $Y_{n-1}$  and  $Y_{n+1}$  but with the exception of the first column they are somewhat nearer to those of  $Y_{n+1}$  and more so for higher values of  $m$ . As a rough estimate we may, therefore, expect that a wave of terms, as e.g. the one here discussed for the orders 2 to 6, will, by multiplying by a first order term, become somewhat broader, with in most cases a tendency to shift to the right. It depends of course of the actual values of the coefficients of the original series of terms whether this will be true. When e.g. all the terms are Legendre functions (1st column of table III), i.e. when all the Associated Legendre functions are zero, it is slightly shifted to the left. A precise conclusion can, therefore, only been drawn after computing all the new coefficients. Besides complications to which we shall not refer here, this is a great work; it has not been undertaken by the writer.

Concluding we may state that probably the multiplication by a first order spherical harmonic will not much change the character of the curve of terms. In our case we need not, therefore, decide the ratio of the

constant part to the first order part of the factor by which we have to multiply the series of spherical harmonics representing the current-system for obtaining the series representing the thickness of the sialic crust; the character of the curve is probably not much affected by the multiplication. So it is likely that the explanation of the wave of terms from the second to the sixth order does not much depend on the question whether the phenomenon causing it occurred simultaneously with that bringing about the first order term or afterwards.

In this paper the crust of the Earth has been indicated as a "sialic layer". The real situation is no doubt more complicated than here presented. The crust is certain to consist of more than one layer below the sediment-cover, viz. a granite layer and, possibly, even more than one below it. It is not certain whether the difference between the crusts under the oceans and in the continents is especially caused by the difference in thickness of the granite layer which is probably absent in the deep parts of the oceans, or whether also the other layers differ in thickness. The gravity results over the continental shelves and the adjoining oceanic areas seem to point to the first assumption but the result is far from sure. If this is true the sialic layer dealt with in this paper must be the granite one and, if at least we admit the assumption that it was concentrated above the descending currents, we must suppose that at the time when the continents originated it was the only more or less rigid layer present.

### *Summary*

The investigation of the development in spherical harmonics of the Earth's topography by PREY shows that the first six terms are large; they practically dominate the great features, e.g. the distribution of the continents and the oceans, which thus appears to be founded on a mathematical base. The same is, therefore, true for the variability in thickness of the sialic layer.

The large first order term is probably caused by the moon's birth from the Earth while the wave of great terms from the 2nd to the 6th order can perhaps be explained by a system of currents in the mantle; this might possibly have been connected with the commotion in the Earth when it resumed its equilibrium figure after the release of the moon or it may have occurred in a slightly later phase as a consequence of temperature disturbances; we thus arrive at a hypothesis about the origin of continents and oceans closely approaching that of OSMOND FISHER, JEFFREYS and ESCHER (see for other studies on this matter the note on p. 220).

The higher order terms show two further waves of prominent values, viz. the 8th to 11th order and the 12th to 16th order terms which each point to some physical phenomenon behind it. Possibly they are likewise caused by currents in the mantle but of a smaller size than the first mentioned system.



O-5<sup>TH</sup> ORDER SPHERICAL HARMONICS OF WORLD-TOPOGRAPHY





# AUTOXIDATION OF SATURATED HYDROCARBONS IN THE LIQUID PHASE

(First communication)

## II

BY

J. P. WIBAUT AND A. STRANG

(Communicated at the meeting of May 26, 1951)

### 5. Relation between rate of oxidation and structure of the hydrocarbon

We ascertained the maximum rate of oxidation of a number of normal alkanes with 8, 9, 10, 12, 14, 16, 18, 20 and 22 carbon atoms. The results are represented in figure 3. The experiments were carried out at  $110.4^\circ$  and with 0.112 millimol cobalt stearate per 61.7 millimols hydrocarbon.

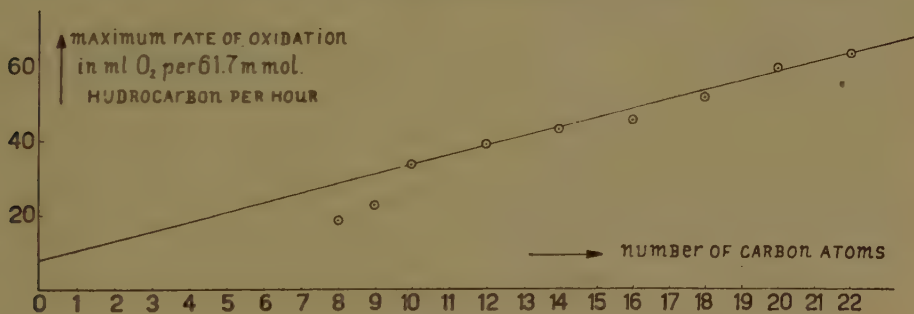


Figure 3

This figure shows that there is a linear relation between the number of carbon atoms and the maximum rate of oxidation from  $C_{10}H_{22}$  to  $C_{22}H_{46}$ . This can be explained by assuming that all the secondary carbon atoms have an equal chance of reacting; oxidation of a primary carbon atom is less probable since a greater bond energy is attributed to a primary C-H bond<sup>3)</sup> ( $CH_3$  group) than to a secondary C-H bond ( $CH_2$  group).

When the linear relation is merely the result of an increase in the number of secondary carbon atoms, the straight line should intersect the horizontal axis at 2 in extrapolating the curve in figure 3. The figure shows that this is certainly not the case.

The deviation may be due to an increase in the stability of the hydroperoxide with lengthening carbon chain, as a result of which the initiation reaction of the oxidation will proceed more slowly.

Measurements of hexadecane have shown that no change in rate of oxidation is observed when the oxygen pressure is reduced to 48 % of the original value; within wide limits therefore, this rate is independent of the oxygen concentration in the liquid. The rates measured for the

various hydrocarbons are therefore comparable, although these hydrocarbons have different vapour tensions at the reaction temperature, so that the partial tension of the oxygen in the reaction vessel is different from case to case.

In the case of *n*-octane and *n*-nonane, however, (boiling points 125° and 150° respectively) the hydrocarbon has a high vapour tension at the reaction temperature, so that the partial pressure of the oxygen in the reaction vessel is much lower than with decane and higher hydrocarbons. In this case the rate of oxidation may become dependent on the oxygen concentration, which results in too low a rate of oxidation at this low oxygen tension.

Moreover, part of the solution may evaporate as a result of the great volatility of these hydrocarbons and spread over the walls of the reaction vessel, where no oxidation can take place due to the absence of catalysts.

Quite different results are obtained in the oxidation of branched alkanes. As these oxidized much more easily than the isomers with normal chains, the comparative experiments were carried out at a lower temperature, namely at 78.1°.

The maximum rate of oxidation is stated in table III for six branched octanes and for one highly branched heptane (2,2,3-trimethylbutane).

TABLE 3

Maximum rate of oxidation of branched alkanes measured in ml O<sub>2</sub> per 61.4 mmol. hydrocarbon per hour. Catalyst: 70 mg cobalt stearate. Reaction temp. 78.1°.

Hydrocarbon	Maximum rate of oxidation
2-methylheptane. . . . .	5.0 <sup>1)</sup>
3-methylheptane. . . . .	3.0 <sup>1)</sup>
3, 4-dimethylhexane . . . . .	11.0
2, 5-dimethylhexane . . . . .	35.0
3-methyl-3-ethylpentane . . .	0.0
2, 2, 4-trimethylpentane . . .	0.0
2, 2, 3-trimethylbutane . . .	6.0 <sup>2)</sup>

<sup>1)</sup> at 100.2° these values are 34.0.

<sup>2)</sup> reaction temperature 72.0°.

Comparison with the behaviour of octane at 78.1° shows that *n*-octane is not oxidizable at this temperature, even when peroxide is added.

The absorption curves from which the above maximum rates of oxidation have been determined are represented in figure 4.

These results indicate that oxidation begins at a tertiary C-H bond, from which a hydroperoxide group is formed.

The fact that a considerable quantity of acetone is formed during the oxidation of 2-methylheptane, methylethylketone being formed during the oxidation of 3-methylheptane is in accordance with the above. These ketones were isolated as *p*-nitrophenylhydrazones.

We extensively ascertained what products are formed by the oxidation of 2,5-dimethylhexane. To this end pure oxygen was passed for six hours

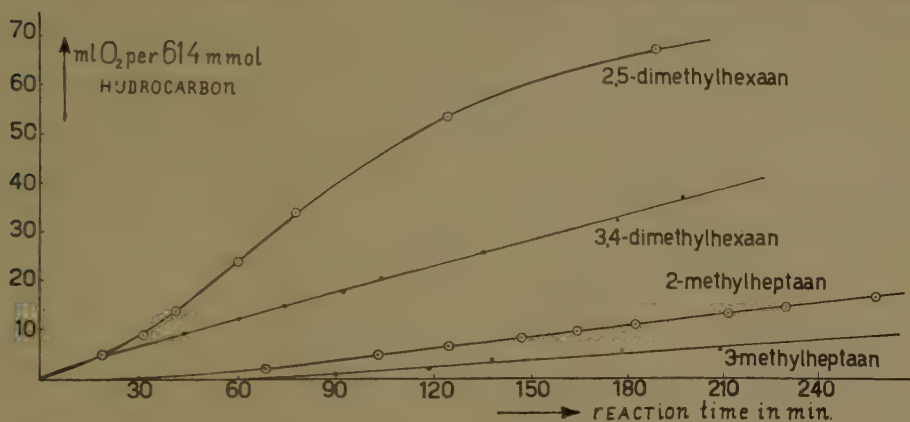


Figure 4. Relation between oxygen absorption and reaction time: Reaction temperature:  $78.1^{\circ}$ ; catalyst 70 mg cobalt stearate per 61.4 mmol. hydrocarbon.

at  $105^{\circ}$  through the hydrocarbon to be oxidized, in which 1 % cobalt stearate had been dissolved.

Starting from 439 mmol. hydrocarbon the most important oxidation products are: water (37.7 mmol.), acetone (15.8 mmol.), 2,5-dimethylhexane-diol-2,5 (13.2 mmol.), carbonic acid (6.6 mmol.). Further, a quantity of unidentified peroxide, which certainly contained the 2,5-dimethylhexane-dihydroperoxide-2,5 (calculated on this peroxide the quantity was 6.8 mmol.); formic acid (1.5 mmol.) and traces of formaldehyde.

Moreover, we isolated a fraction which, according to boiling range ( $75-85^{\circ}/12$  mm) and refractive index ( $n_D^{20} = 1.4211$ ) mainly consisted of 2,5-dimethylhexanol-2; this fraction showed a positive reaction with acidified mercuric sulphate, which reacts to tertiary alcohol groups. We did not succeed in preparing a crystalline derivative, however. The quantity of this alcohol is estimated at about 4.8 mmol.

Further we isolated about 3.9 mmol. of a fraction mainly consisting of isovaleric acid (characterized by its own smell and that of the ethyl ester) and a fraction which was considered as 2,2', 5,5'-tetramethyltetrahydrofuran (smell of camphor) (about 5.5 mmol.).

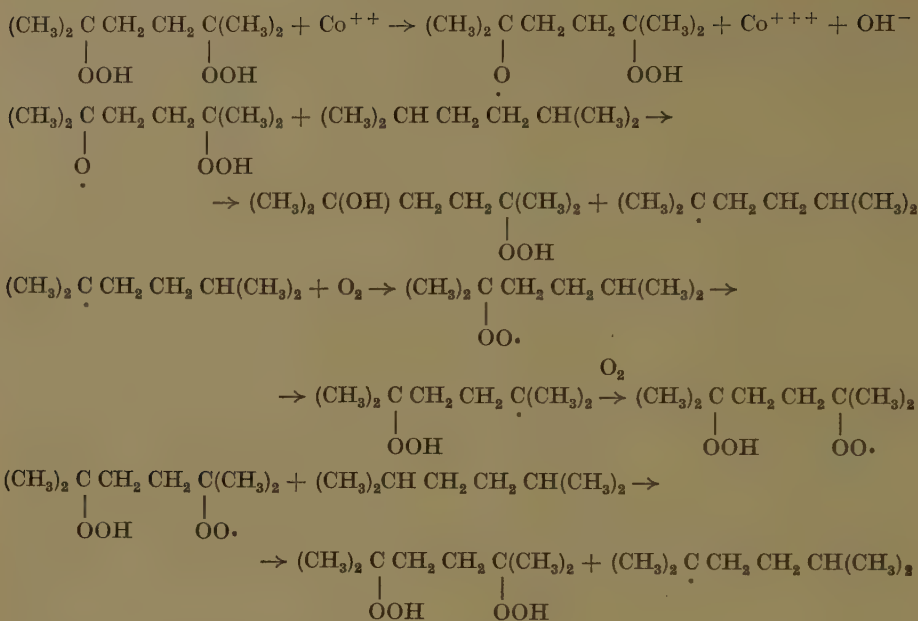
An oxygen balance was drawn up to check whether the analysis had been complete. It showed that 74 % of the absorbed oxygen was found in the reaction products.

With reference to the reaction products and the above-mentioned facts the following reaction scheme can be drawn up.

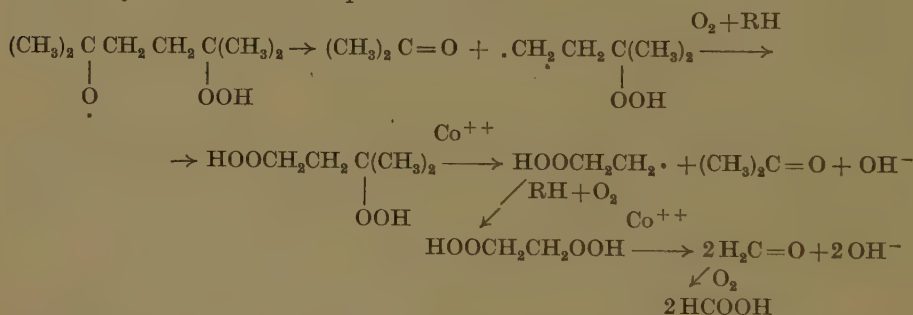
The characteristic feature of the reaction scheme for the catalytic oxidation of 2,5-dimethylhexane and of other branched alkanes is that the chain mechanism is initiated by an alkoxy radical. In the catalytic oxidation of tetraline on the other hand the reaction is assumed to be initiated by the hydroxyl radical.

# Reaction scheme

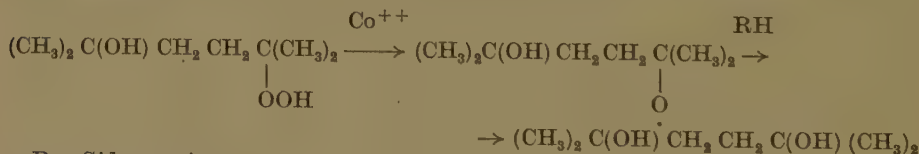
## A. Main reaction



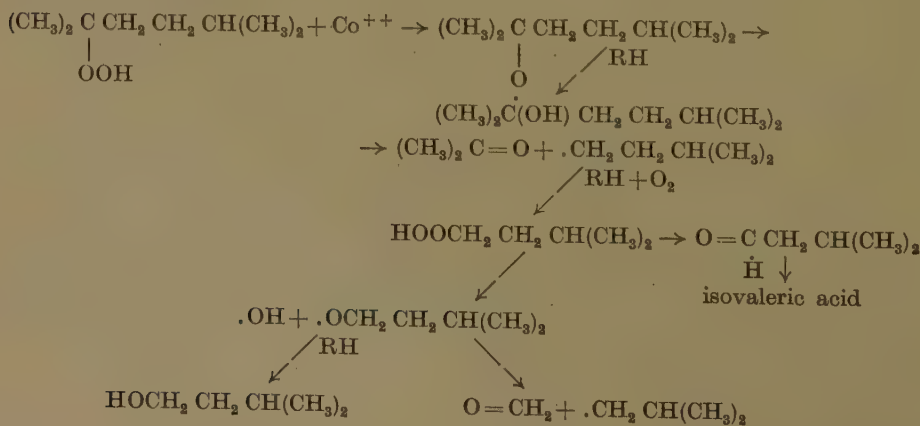
The alkoxy radical can decompose as follows:



The 2,5-dimethylhexane-diol-2,5 is formed from 2,5-dimethylhexane-2-oxy-5-hydroperoxide:



## B. Side reaction







With triptane, which is oxidizable, the quaternary carbon atom lies next to the tertiary atom. Screening by the quaternary carbon atom is impossible here.

A quaternary hydrocarbon such as 3-methyl-3-ethylpentane cannot be oxidized; this is in agreement with our reactions scheme, since this hydrocarbon does not contain a tertiary C atom.

In the case of cyclanes, a very distinct influence of the structure on the rate of oxidation is observed, as is shown in figure 5.

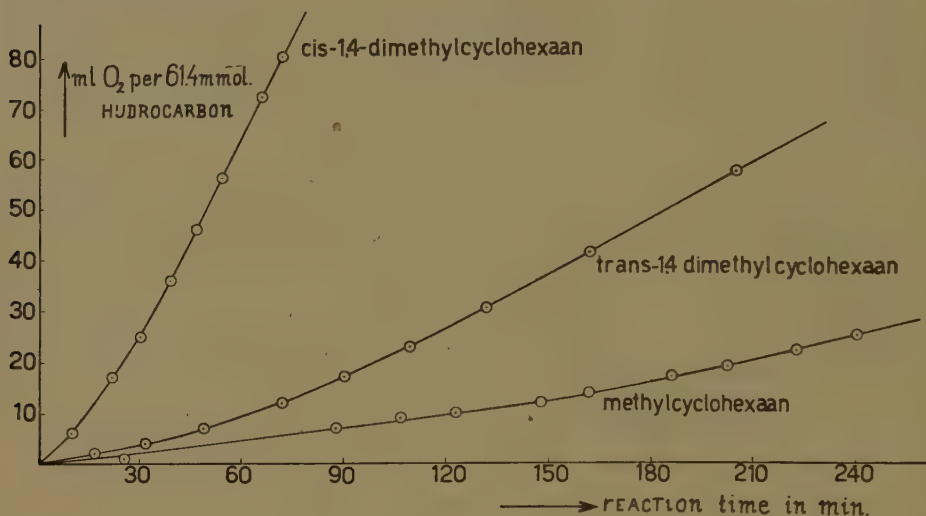


Figure 5

At 78.1° C we compared the rates of oxidation of methylcyclohexane, trans-1,4-dimethylcyclohexane and cis-1,4-dimethylcyclohexane. As catalyst we used again 0.112 mmol. cobalt stearate. The maximum rate of oxidation measured in ml O<sub>2</sub> per hour and per 61.4 mmol. hydrocarbon is 10 for methylcyclohexane; for trans-1,4-dimethylcyclohexane it is 23 and for cis-1,4-dimethylcyclohexane 80. Here, too, an increase in rate of oxidation is observed with increasing number of tertiary C atoms. The difference between trans- and cis-1,4-dimethylcyclohexane will probably be due to a difference in bond energy of the tertiary CH bond; the difference in combustion heat between these two isomers gives an indication in this direction.

In a subsequent article we shall deal with the kinetics of these oxidations and draw up a reaction mechanism with the aid of those data.

We wish to express our thanks to the Management of the Koninklijke Shell-Laboratory, Amsterdam for their assistance and support, which enabled us to carry out this investigation and to Prof. Dr L. J. OOSTERHOFF, Dr Ir A. J. WILDSCHUT and Dr E. C. KOOYMAN, who showed their interest in our work in informative and fruitful discussions.

*Laboratory of Organic Chemistry of  
the Amsterdam University*

## BIBLIOGRAPHY

1. CHAVANNE, G. & G. TOCK, Bull. Soc. Chim. Belg. 41, 630 (1932).
2. GEORGE, P., A. ROBERTSON, Proc. Roy. Soc. A 185, 309 (1946).  
ROBERTSON, A. and W. A. WATERS, J. Chem. Soc. 1574 (1948).
3. POLANYI, M., E. C. BAUGHAN, Nature 146, 685 (1940).  
STEINER, H., H. R. WATSON, Disc. Farad. Soc. 2, 88 (1947).

## SYNTHESIS OF A LOWER HOMOLOGUE OF CITRAL AND OF PSEUDO-IONONE

BY

J. F. ARENS AND P. MODDERMAN

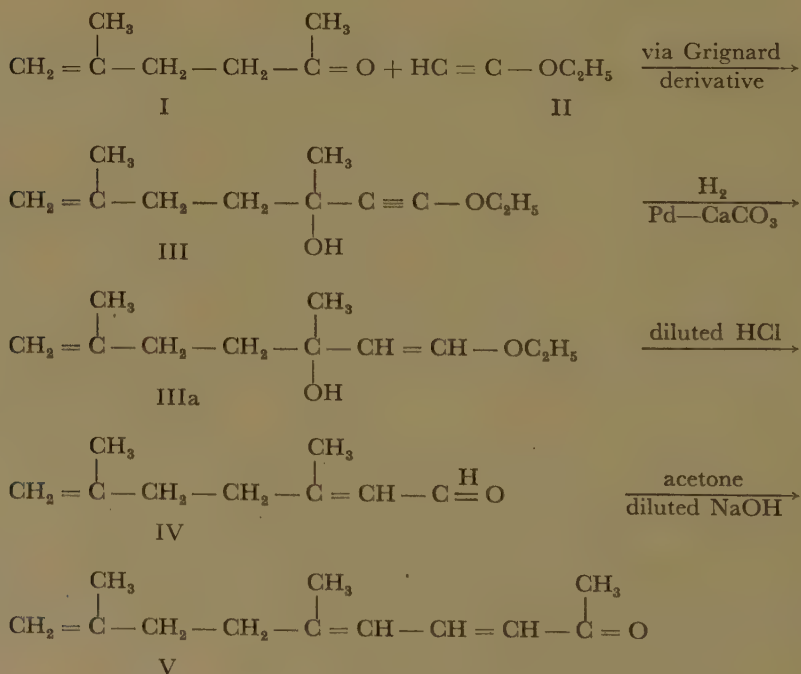
(Communicated at the meeting of May 26, 1951)

*Summary*

Methallylacetone I, prepared from ethyl aceto-acetate and methallylchloride, was coupled with ethoxy acetylene II. By partial reduction of the acetylenic carbinol III and rearrangement with diluted HCl we obtained a nor-citral IV. This could be condensed with acetone, yielding nor-pseudo-ionone V.

By alkalis the nor-citral V is easily hydrolysed into methallyl acetone I.

We prepared a homologue of pseudo-ionone, containing one  $\text{CH}_2$  group less, by the following series of reactions <sup>1)</sup>.



<sup>1)</sup> Compare for this method of synthesis: Rec. Trav. Chim. 67, 973 (1948).



The aldehyde IV can be obtained in a very satisfactory yield. It has an odour very similar to that of citral. The condensation of the aldehyde with acetone produces only low yields of V.

In spite of the fact that we modified the circumstances of the reaction in several ways, we were unable to improve this yield. A considerable part of the aldehyde was hydrolysed to methallylacetone, and other by-products were formed. The best results were obtained with acetone and 15 % aqueous NaOH (yield 27 %). The ketone V has a strong and pleasant, flowerlike odour.

### *Experiments* <sup>2)</sup>

#### 1. *Methallylacetone*. (2-methyl-hexen-1(or 2)-one-5)

This substance was prepared according to KIMEL and COPE <sup>3)</sup> by acetoacetic ester synthesis from methallylchloride and ethyl acetoacetate. As a by-product we obtained a substance with b.p. 64–68° (0,1 mm) and  $n_D^{25}$  1,4621;  $d_{25}^{25}$  0,9746.

Analysis of the by-product:

Found : 70,27 % C. 9.39 % H.

Calc. for  $C_{14}H_{22}O_3$ : 70,56 % C. 9.30 % H.

This is probably a product formed from 2 moles of methallylchloride and 1 mole of ethyl acetoacetate,  $[CH_2 = C(CH_3) - CH_2]_2C(COOC_2H_5) - CO - CH_3$  which is obviously not saponified during the ketonic hydrolysis of the mono-substituted aceto acetic ester.

#### 2. *2,5-dimethyl-5-hydroxy-7-ethoxy-hepten-1(or 2)-yn-6*. [III]

Caution:

We observed severe explosions during the distillation of the crude carbinol III, when the samples were stored for one night or longer. Such explosions never occurred when the total preparation was made without interruptions. Batches up to 60 gram were safely handled.

A solution of 25,5 g of ethoxy acetylene <sup>4)</sup> in 25 ml of dry ether was slowly added while stirring and with occasional cooling in ice, to 185 ml of ethereal ethyl magnesium bromide (2,1 molar).

Ethane escaped through the reflux condenser. The ethoxy ethynyl magnesiumbromide formed a dark oily layer. After 15 minutes the reaction was complete. The flask was cooled in ice-salt and a solution of 27 g methallylacetone (I) in 45 ml of dry ether was slowly added.

<sup>2)</sup> Our thanks are due to Mrs. SUPARWOTO and Yo KIM TEK for assistance in the laboratory and to Mr P. J. HUBERS, Amsterdam for performing the micro-analysis.

<sup>3)</sup> A. Soc. **65**, 1996 (1943).

<sup>4)</sup> Rec. Trav. Chim. **70**, 289 (1951).

After 15 minutes the mixture was poured into a great quantity of ice cold ammonium chloride solution. After filtration by suction, to remove some dirt, the ethereal layer was separated. The aqueous layer was twice extracted with ether and the combined extracts washed with some water (twice), dried with sodium sulfate, evaporated and finally distilled in a high vacuum in nitrogen atmosphere.

The carbinol III had a b.p.  $82-84^{\circ}$  (1 mm),  $n_D^{25}$  1,4605—1,4630.

In several experiments the yield varied from 80—90 %.

A redistilled sample showed the following constants:

$$n_D^{23} \quad 1,4635 \quad d_{23}^{23} \quad 0,9258$$

### 3. 2,5-dimethyl-5-hydroxy-7-ethoxy-heptadiene-1(or 2),6. [IIIa]

and rearrangement of this substance into

#### 2,5-dimethyl-heptadiene-1(or 2),5-al-7. [IV] ("nor-citra").

The substance III (40 g) was hydrogenated in ethylacetate (100 ml) with hydrogen and palladium-calcium carbonate ( $2\frac{1}{2}$  %, 1,0 g) at ordinary pressure. Sometimes the reduction started with difficulty, but once started, proceeded fairly rapidly. The hydrogenation was interrupted as soon as one mole of hydrogen was absorbed. Then the catalyst was centrifuged and the solution shaken with 0,2 n HCl (110 ml) during  $\frac{1}{2}$  hr. The upper layer was washed with sodium bicarbonate solution, dried and distilled in an atmosphere of nitrogen.

The aldehyde IV had a b.p.  $49-51^{\circ}$  (0,2 mm). Yield 85—90 %.

$$n_D^{26} \quad 1,4772 \quad d_{26}^{26} \quad 0,8909$$

The crude semicarbazone had m.p.  $160-166^{\circ}$ , but after two crystallisations from acetone it remained unchanged  $174-176^{\circ}$  (uncorrected). Analysis of the semicarbazone:

Found : 21,12 % N

Calc. for  $C_{10}H_{17}ON_3$ : 21,52 % N

### 4. 2,5-dimethyl-decatriene-1(or 2), 5,7-one-9. [V] ("nor pseudo-ionone").

10 g of the aldehyde IV was mixed with 6 ml of acetone and 14 ml of aqueous 15 % sodiumhydroxide. The mixture was shaken at room temperature during two days. Then the dark red emulsion was mixed with water and extracted with ether. The extract was washed with water, dried and distilled in an atmosphere of nitrogen.

After a considerable fore-running the desired ketone distilled at  $82-90^{\circ}$  (0,2 mm). The fore-running contained considerable amounts of methallyl-acetone.

The yield was  $3\frac{1}{2}$  g  $n_D^{26}$  1,5252,  $d_{26}^{26}$  0,9541.

The crude semicarbazone melted at 139—143°. After recrystallisation from alcohol white needles were obtained with m.p. 145—146°.

Analysis of the semicarbazone:

Found : 17,73 % N.

Calc. for  $C_{13}H_{21}ON_3$ : 17,90 % N.

The use of baryta or lime water as condensing agents did not improve the yield of the ketone V.

*Bandung, University of the Republic Indonesia.  
Laboratory for Organic Chemistry.*

ELASTIC-VISCOUS OLEATE SYSTEMS CONTAINING KCL. XVI <sup>1)</sup>

1. *The elastic properties as a function of the oleate concentration.*
2. *Hypothesis on the state of the oleate in the elastic viscous oleate system.*

BY

H. G. BUNGENBERG DE JONG, W. A. LOEVEN\*) AND W. W. H. WEYZEN \*) <sup>2)</sup>

(Communicated at the meeting of May 26, 1951)

1. *Introduction and methods*

In part III of this series, where we worked with Na-oleate from MERCK at a single KCl concentration and a single temperature, simple relationships were found to exist between the elastic properties and the oleate concentration.

The present communication deals with the question whether these relations are quite general, viz. if they retain the same character qualitatively with other oleate preparations, other KCl concentrations and other temperatures. The next step (two following communications) will be to use the above relations systematically in analysing the influence of parameters other than the oleate concentration (e.g. temperature, KCl concentration, added organic substances) on the elastic behaviour. The large quantity of oleate which is necessary for the realization of this program at once excludes the possibility to perform all experiments with K-oleate made from freshly prepared chemically pure oleic acid <sup>3)</sup>.

The available quantity of the latter only allowed for one single series of measurements (section 3). All remaining experiments were performed with Na-oleate from BAKER. <sup>4)</sup>

Though this preparation is by no means chemically pure (it contains e.g. palmitate), in some respects (KCl concentration corresponding to

---

\*) Aided by grants from the "Netherlands Organization for Pure Research (Z.W.O.)."

<sup>1)</sup> Part I has appeared in these Proceedings 51, 1197 (1948); Part II—VI in these Proceedings 52, 15, 99, 363, 377, 465 (1949); Parts VII—XIV in these Proceedings 53, 7, 109, 233, 743, 759, 975, 1123, 1319 (1950); Part XV in these Proceedings 54, Series B, 1 (1951).

<sup>2)</sup> Publication No. 13 of the Team for Fundamental Biochemical Research (under the direction of H. G. BUNGENBERG DE JONG, E. HAVINGA and H. L. BOOLJ).

<sup>3)</sup> We are much indebted to Mr C. A. DE BOCK for preparing the sample of chemically pure oleic acid. See for particulars of the preparation note 9 in part XIII of this series.

<sup>4)</sup> A generous gift of Na-oleate from The Rockefeller Foundation provided the means for the experiments described in this publication.



the minimum damping) it resembles much more pure oleate in its elastic behaviour than the preparation from MERCK used in part III (see part XIII section 5 and part X section 7).

For the experimental methods (rotational oscillation, contrivance to excite the oscillation, electrolytic  $H_2$ -mark) we refer to preceding parts of this series. The experiments have been performed with completely filled spherical vessels of approximately 500 ml, except in the series with chemically pure K-oleate in which for economical reasons the experiments had to be performed with completely filled 110 ml vessels.

As none of us could perform the difficult measurement of the decrement we had to content ourselves with the measurement of  $n$ , which quantity under certain restrictions is an approximate measure for  $1/A$  (particulars in part XV of this series).

The values for  $|G|$  in the tables have been calculated from the period  $T$  (without correction for  $\Delta$ ), the radius of the vessel  $R$  and the density  $\rho$  with the aid of the formula  $|G| = (2\pi/4.493) \times (R/T) \times \sqrt{\rho}$ , which formula follows from the one for the period of the rotational oscillation given in part II of this series. Because of the experimental errors the values of  $|G|$  may be 0.5 % wrong and consequently  $G$  may be 1 % wrong.

The omission of a correction for  $\Delta$  seems quite natural because no  $\Delta$  values were measured. Still this is not the real cause, for from the known relation between  $n$  and  $1/A$ , see part XV, we could have calculated  $\Delta$  approximately from the measured  $n$  values. Though these  $\Delta$  values would not have been very accurate, they would have been good enough to be used in the correction. Now there is no doubt how the correction must be applied when  $\Delta \propto R$ , that is at higher oleate concentrations. But here  $\Delta$  is so small usually that the correction is smaller than the experimental error. We just need the correction most at very low oleate concentrations. At lower oleate concentrations however (0.6 % and less) the character of the damping is quite another, viz.  $\Delta$  being independent of  $R$ . BURGERS has given a method to correct  $T$  in the case that  $\Delta$  being independent of  $R$ , resides in a slipping of the elastic system along the wall of the vessel. But in part XIV of this series it appeared that no such slipping is present. Therefore the mechanism of the damping at low oleate concentrations is still unknown and likewise the way in which  $T$  should be corrected for  $\Delta$ .

## 2. *The elastic properties as a function of the oleate concentration. Experiments with Na-oleate from Baker at a number of KCl concentrations and temperatures*

In a first series of experiments we kept the temperature constant (15° C) and investigated the elastic properties at 0.6, 0.9 and 1.5 N KCl. All mixtures contained 0.05 N KOH to provide for a  $pH > 12$  in order to exclude all hydrolysis. Besides, the total Na-ion concentration was kept constant by adding so much NaCl that the total Na-ion concentration corresponds to the one which prevails at the highest Na-oleate concentration being used. Fig. 1 gives the results. It appears that the  $|G|$  curves and the lower parts of the  $n$  curves are straight lines, which as a rule meet the abscissa at a finite, though small oleate concentration. The  $|G|$  curve

at 1.5 N KCl seems to proceed through the point of intersection of the coordinate-axis but we did not trust this result (when  $\sqrt{G}$  at 2 % oleate is too low, the calculated slope of the best fitting straight line will be somewhat less, and as a result the part cut off from the abscissa will be too small). Therefore it was decided to repeat the experiment at 1.5 N KCl using a much larger number of oleate concentrations. In this experiment too we kept the KOH concentration constant (0.05 N) but we did not provide for a constant total Na-ion concentration as this might possibly give complications. The results have been collected in Table I and have been represented in fig. 2. Now the  $\sqrt{G}$  curve has the same character as in fig. 1 at 0.6 and at 0.9 N KCl, as it meets the abscissa at a finite though small oleate concentration. We therefore believe that the strict proportionality between  $\sqrt{G}$  and the oleate concentration found in fig. 1 at 1.5 N KCl was due to experimental errors.

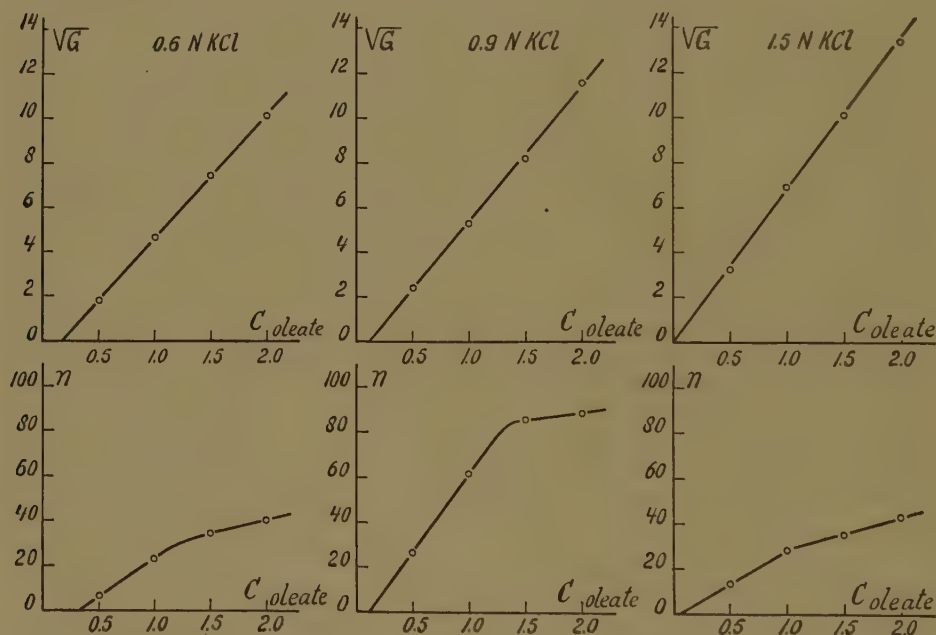


Fig. 1. Dependence of  $\sqrt{G}$  and of  $n$  on the oleate concentration at three KCl concentrations (15°).

The  $n$ - $C_{\text{oleate}}$  curve of fig. 2 also bears the same character as those in fig. 1. It is composed of two straight branches, the lower of which meets the abscissa at a finite though small oleate concentration.

In a next series of experiments we investigated the elastic properties as a function of the oleate concentration at three KCl concentrations and four temperatures. Because of the limited experimental possibilities we had to reduce the number of oleate concentrations at each KCl concentration to only three (0.8 %, 1.2 % and 1.6 % oleate). As KCl concentration we choose one which corresponds to the one of minimum

TABLE I

Elastic properties at 1.5 N KCl and 15° as a function of the oleate concentration (oleate from Baker)

Oleate concentration g/100 ml	$G$ (dyne/cm <sup>2</sup> )	$\sqrt{G}$	$n$
0.2	0.81	0.90	4.4
0.4	5.43	2.33	14.5
0.6	14.4	3.80	23.7
0.8	26.4	5.14	29.7
1.0	41.7	6.46	33.7
1.2	64.0	8.00	34.6
1.4	86.5	9.30	37.4
1.6	108.4	10.41	38.4

damping (1.05 N), one which is lower (0.75 N) and one which is higher (1.5 N) than the one of minimum damping. All systems contained 0.05 N KOH to provide for a pH > 12. The elastic systems were made in 1 l ERLEMEYER flasks by adding 300 ml of a stock oleate solution (of 3.2, 2.4 or 1.2 % Na-oleate in 0.1 N KOH) to 300 ml of a stock KCl solution (of 1.5, 2.1 or 3 N). After closing the flasks with rubber stoppers, the contents were shaken vigorously during several minutes and were used to fill the nine 500 ml spherical vessels (of known radii) completely, that is to stay high up into the neck. The vessels were put overnight in a thermostate of 15° to become completely free from enclosed air, whereafter the measurements were performed. Now the temperature of

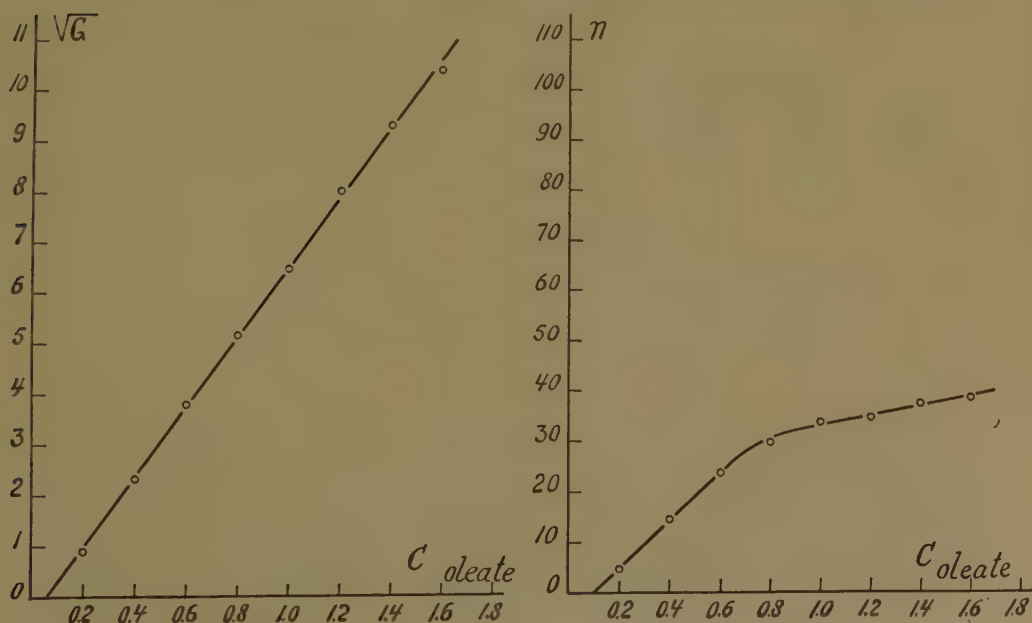


Fig. 2. Dependence of  $\sqrt{G}$  and  $n$  on the oleate concentration at 1.5 N KCl (15°).

the thermostat was altered and after standing overnight once more, measurements were performed. In this way the elastic properties of the nine elastic systems were measured at 15°, 34.6°, 25°, 20° and 15°, thus ending with the same temperature as the one with which we began. This enables us to discern between an eventual irreversible change of the elastic properties as a consequence of the exposure during four days to higher temperatures and a reversible change of the elastic properties with temperature. The latter change is interesting us in the first place. The results (compare table II) show that indeed an irreversible change has taken place, but that this change is relatively small compared with the measured differences in elastic properties at the four temperatures. Therefore these differences are mainly the expression of the reversible change of the elastic properties as a function of the temperature.

TABLE II

Elastic properties as a function of the oleate concentration at three KCl concentrations and four temperatures (oleate from Baker)

KCl conc.	temp. °C	$\sqrt{G}$			$G$ (dyne/cm <sup>2</sup> )			$n$		
		0.8 % oleate	1.2 % oleate	1.6 % oleate	0.8 % oleate	1.2 % oleate	1.6 % oleate	0.8 % oleate	1.2 % oleate	1.6 % oleate
0.75 N	15	3.84	6.28	8.67	14.7	39.5	75.2	28.6?	41.6	59.5
	20	3.58	6.14	8.48	12.8	37.7	71.9	17.7	37.5	50.3
	25	3.40	5.97	8.37	11.5	35.6	70.1	11.5	28.3	47.7
	34.6	—	5.44	8.09	—	29.6	65.4	3.6	12.8	24.6
	15	3.77	6.27	8.61	14.2	39.3	74.1	21.3	40.6	59.5
1.05 N	15	4.26	6.59	8.93	18.2	43.5	79.8	50.6	75.7	80.5
	20	4.28	6.64	9.04	18.3	44.1	81.8	41.5	60.4	73.4
	25	4.28	6.76	9.13	18.3	45.7	83.4	33.5	53.6	66.6
	34.6	4.28	6.77	9.24	18.3	45.8	85.3	13.7	25.6	30.5
	15	4.26	6.62	8.98	18.1	43.8	80.6	48.3	68.7	78.3
1.5 N	15	5.29	8.06	10.67	28.0	65.0	113.8	29.6	38.5	40.6
	20	5.36	8.42	11.41	28.8	70.9	130.2	16.6	22.5	23.4
	25	5.58	8.83	11.98	31.1	78.0	143.5	10.2	11.9	14.5
	34.6	—	—	—	—	—	—	1—2	2	2
	15	5.15	8.00	10.76	26.5	64.1	115.8	28.8	39.4	40.5

The irreversible change is probably the result of a slow chemical alteration of the oleate (oxidation?) and it is manifesting itself mainly in an increase of the damping (decrease of  $n$ ). The differences between the  $\sqrt{G}$  (and  $G$ ) values at the beginning and at the end of the experiment are relatively small and often do not exceed the experimental errors in the case of 0.75 N and 1.05 N KCl. The large differences in the case of 1.5 N KCl cannot be trusted to be real. Here the series of measurements at 15° at the beginning of the experiments is obviously quite erroneous. Probably at the preparation of the elastic systems these mixtures had not been shaken sufficiently long.



We known from previous experience that a slight deviation from complete homogenization may give serious errors. As at the following temperatures the mixtures with 1.5 N gave quite acceptable values, they must have become homogeneous afterwards.

Fig. 3 gives the results obtained for each of the three KCl concentrations (for those at 15° the measurements at the end of the series have been taken).

In all cases the  $\sqrt{G}$ - $C_{\text{oleate}}$  curves are straight lines intersecting the abscissa at finite, though small oleate concentrations. Details as to the influence of the KCl concentration or the temperature on the slope and on the part cut off from the abscissa will be discussed in the next communication of this series.

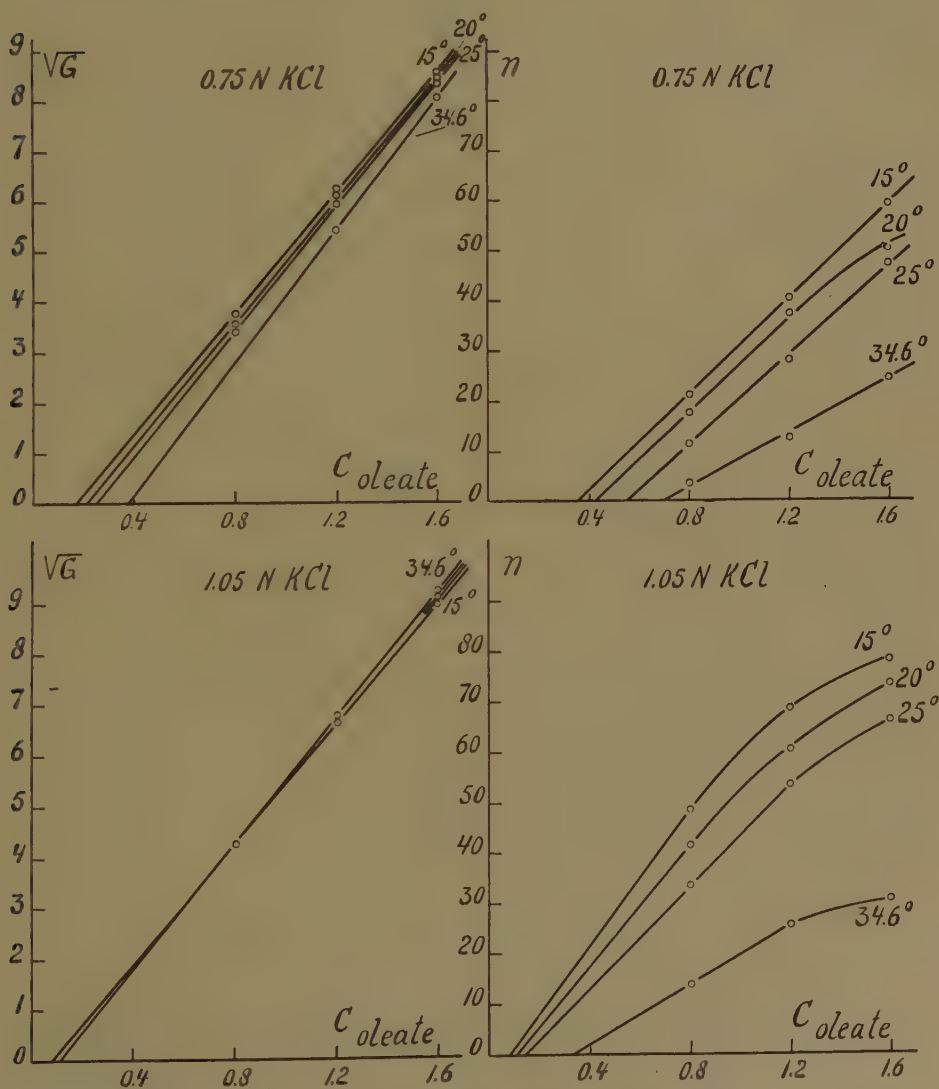


Fig. 3A. Dependence of  $\sqrt{G}$  and  $\eta$  on the oleate concentration at 0.75 N and 1.05 N KCl, at four temperatures.

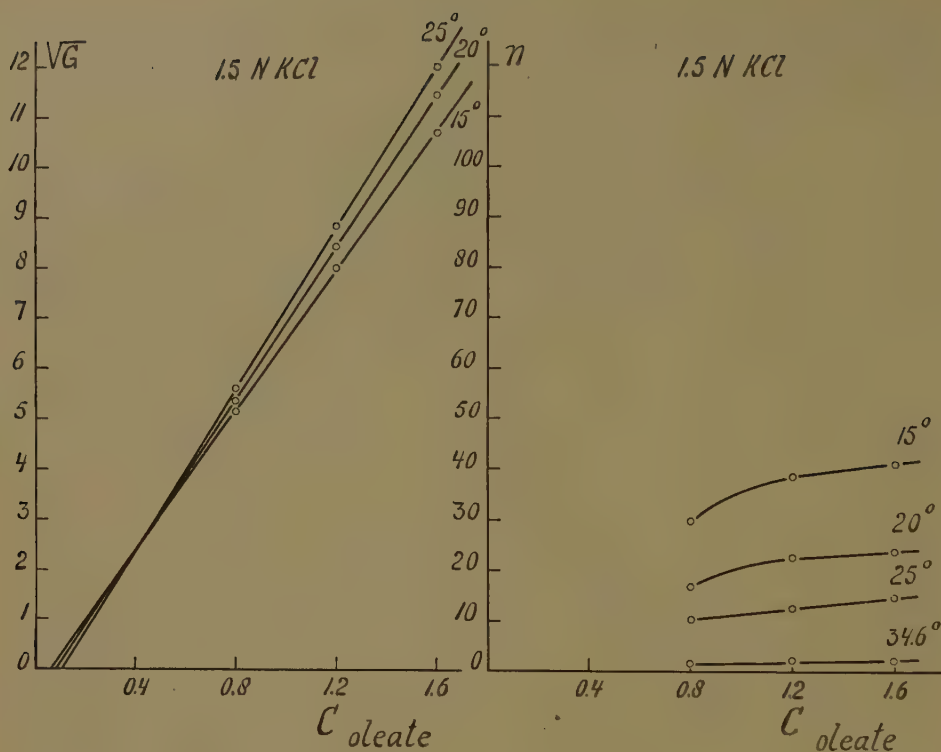


Fig. 3B. Dependence of  $\sqrt{G}$  and  $\eta$  on the oleate concentration at 1.5 N KCl, at four temperatures.

The results are not satisfactory as far as regards the  $n$ - $C_{oleate}$  curves. This does not surprise us very much, because we know already (see fig. 1 and 2) that the  $n$ - $C_{oleate}$  curves consist of two straight branches. Therefore three experimentally determined points will not suffice in general to locate the two branches with any accuracy.

For this reason fig. 3 only gives the approximate course of the  $n$ - $C_{oleate}$  curves. Still the influence of the KCl concentration and of the temperature on this course is so large, that as yet something can be said about the influence of the above parameters on the slope of the lower branch of these curves and on the part cut off from the abscissa. This will be postponed till the next communication.

### 3. The $\sqrt{G}$ - $C_{oleate}$ and $n$ - $C_{oleate}$ curves for potassium oleate prepared from pure oleic acid at one KCl concentration and four temperatures

To control that the very characteristic relationships found with the two commercial Na-oleate preparations (from MERCK in part III and from BAKER in the present communication) are not due to the presence of Na-ions or contaminating other fatty acids, we decided to perform also an investigation with K-oleate made from freshly prepared chemically

pure oleic acid (left from the control experiments in part XIII and used for the present experiments a few days later).

The available quantity of pure oleic acid only sufficed for a small scale experiment, namely at one KCl concentration only and when completely filled 110 ml vessels (instead of the usual 500 ml vessels) were used.

A stock K-oleate solution was made by dissolving, in a 1 l measuring flask, 21.15 gr pure oleic acid (0.0749 gram molecule) with the equivalent amount of KOH, and adding 50 ml KOH 2N and distilled water to make 1 l. This stock K-oleate solution contains approximately as much oleate as a 2.4 % stock Na-oleate solution <sup>5)</sup>.

For the experiment we chose the KCl concentration corresponding to the one of minimum damping found in part XIII, viz. 0.98 N KCl and we further provided for a constant KOH concentration in all systems, viz. that KOH concentration (= 0.067 N) which at the highest K-oleate concentration used is already present without extra added KOH. The measurements were made in completely filled 110 ml vessels at four temperatures. In table III, which gives the results, the K-oleate concentra-

TABLE III

Elastic properties of K-oleate systems prepared from chemically pure oleic acid as a function of the oleate concentration at 0.98 N KCl and four temperatures

K-oleate concentr. (arbitrary units)*	→ ° C	0.2	0.4	0.6	0.8	1.0	1.2	1.4	1.6
<i>G</i> (dyne/cm <sup>2</sup> )	17.8	0.52	3.8	9.3	19.1	29.3	43.3	63.0	81.2
	25.1	0.47	3.7	9.2	18.2	29.2	43.1	60.7	79.8
	34.7	—	3.5	9.4	18.0	29.4	43.3	60.3	79.2
	46.7	—	—	8.3	16.2	28.3	39.7	57.2	78.3
$\sqrt{G}$	17.8	0.72	1.94	3.05	4.37	5.41	6.58	7.94	9.01
	25.1	0.69	1.92	3.03	4.27	5.40	6.57	7.79	8.93
	34.7	—	1.87	3.07	4.24	5.42	6.58	7.77	8.90
	46.7	—	—	2.88	4.02	5.32	6.30	7.56	8.85
<i>n</i>	17.8	7.7	24.3	42.4	56.3	67.5	74.4	79.4	84.6
	25.1	6.7	20.5	33.7	46.9	57.6	66.7	73.7	78.3
	34.7	1	13.7	23.5	33.8	43.6	52.5	61.7	66.5
	46.7	—	1—2	6.6	13.6	19.6	22.5	24.8	26.3

\*) As unit of the oleate concentration was taken 10/24 that of the stock oleate solution, which contained 0.0749 grammolecules/l.

tion has been given in arbitrary units, calling 1.0 the concentration which is 10/24 from that of the stock K-oleate solution (see note 5).

The results have been plotted in fig. 4.

<sup>5)</sup> In preparing the usual 2.4 % stock solution of Na-oleate from BAKER, we dissolve 24 g. Na-oleate to make 1 L. which therefore contains 0.0789 gram molecule/l. Therefore the above stock K-oleate solution is somewhat less concentrated.

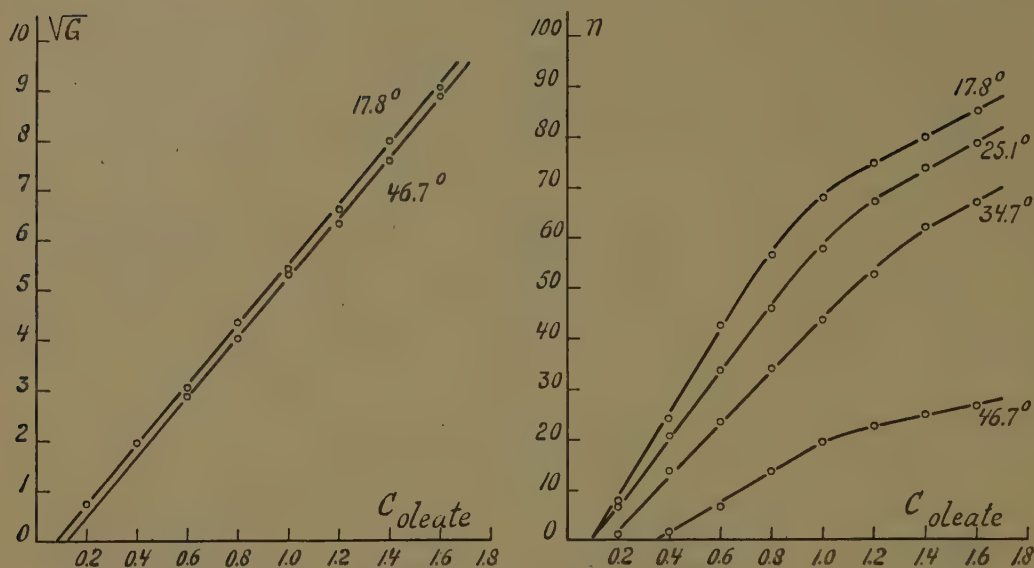


Fig. 4. Dependence of  $\sqrt{G}$  and  $n$  on the oleate concentration ( $K$  oleate from pure oleic acid) at four temperatures. Concentration in arbitrary units, compare text and note 5?

We meet quite the usual behaviour here,  $\sqrt{G}$  being a linear function of the oleate concentration and the straight line intersecting the abscissa at a finite, though small, oleate concentration.

The temperature has little influence on the position of the  $\sqrt{G}$ - $C_{oleate}$  curve, the slope being practically the same at the four investigated temperatures, whereas the part cut off from the abscissa becomes slightly larger only with certainty at the highest temperature. For this reason fig. 4 gives the  $\sqrt{G}$  curves only at  $17.8^\circ$  and  $46.7^\circ$ .

The  $n$ - $C_{oleate}$  curve consists of two branches just as is already found with oleate from BAKER. Here too the lower branch cuts the abscissa at a small oleate concentration. The influence of the temperature is also the same qualitatively, the slope of the lower branch decreasing and the part cut off from the abscissa increasing with temperature. Quantitatively the influence of the temperature on the damping (and also on  $\sqrt{G}$ ) is decidedly less than with the commercial preparation.

#### 4. Discussion

The simple relationships following from the experiments with Na-oleate from MERCK (compare table I in part III of this series) have been given in fig. 5<sup>6)</sup>.

<sup>6)</sup> The graph in Fig. 5 has been drawn while taking the roots of  $G$  given in table I of part III. The original graph in part III gave the dependence of  $1/T$  instead of  $\sqrt{G}$  on the oleate concentration. The formula for the period of the rotational oscillation shows that  $\sqrt{G} \sim 1/T$ , provided that the density remains constant.



The results in section 2 with Na-oleate from BAKER, and in section 3 with pure K-oleate confirm the generality of the relation between  $\sqrt{G}$  and the oleate concentration. This curve just as in fig. 5 is always a straight line intersecting the abscissa at a small oleate concentration.

The  $n$ - $C_{\text{oleate}}$  curves obtained in the section 2 and 3 are composed of two branches, the lower just as in fig. 5 being a straight line intersecting the abscissa at a low oleate concentration. Obviously the bend in the  $n$ - $C_{\text{oleate}}$  curve has not been reached in fig. 5.

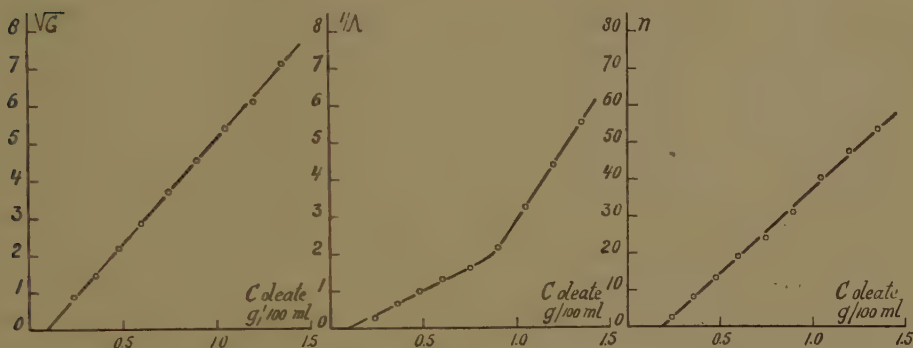


Fig. 5. Dependence of  $\sqrt{G}$ ,  $1/\Delta$  and  $n$  on the oleate concentration (at the KCl concentration corresponding to the minimum damping of the oleate preparation used- Na oleate from Merck). Data from part III of this series.

The dependence of  $n$  upon the oleate concentration was not given graphically in part III. The graph in fig. 5 has been drawn while using the values of  $n$  recorded in table I of part III.

The generality of the shape of the  $1/\Delta$ - $C_{\text{oleate}}$  curve could not be controled in the present investigation, as we were not able to perform the difficult measurement of the decrement. Recent investigations with the collaboration of Mr H. VAN DEN BERG have shown that the  $1/\Delta$ - $C_{\text{oleate}}$  curve for oleate from BAKER has in principle the same shape as given in fig. 5<sup>7)</sup>.

The lower, less steep branch is a straight line once more, intersecting the abscissa at a finite, though small value of the oleate concentration.

Therefore in general we can represent the  $\sqrt{G}$  curves, the lower branches of the  $1/\Delta$  curves and the lower branches of the  $n$  curves by linear

---

As the density remains practically constant with increasing oleate concentration at the small concentrations used, the  $1/T$ - $C_{\text{oleate}}$  curve in part III has the same character as the  $\sqrt{G}$ - $C_{\text{oleate}}$  curve given above in fig. 5.

<sup>7)</sup> To be published in a later communication of this series. In this investigation  $\Delta$  was measured at a much greater number of oleate concentrations in the neighbourhood of the bend in the  $1/\Delta$ - $C_{\text{oleate}}$  curve. This enabled us to ascertain that in reality the two branches are not connected by a rounded bend as is suggested in fig. 5, but that an additional branch with an intermediate slope is interposed.

relations of the same type:

$$\sqrt{G} = a (C_{\text{oleate}} - b)$$

$$1/\Delta = c (C_{\text{oleate}} - d)$$

$$n = e (C_{\text{oleate}} - f)$$

in which  $a$ ,  $b$ ,  $c$ ,  $d$ ,  $e$ , and  $f$  are depending on the oleate preparation, the KCl concentration, the temperature and other parameters.

For the present fig. 5 we found already in part III (constant oleate preparation and all parameters being kept constant), that the parts cut off from the abscissa by the  $\sqrt{G}$  and the lower branch of the  $1/\Delta$  curve are practically the same (we found 0.09 % oleate) Thus  $b = d$ .

This induces the hypothesis that the total amount of oleate in the viscous elastic system is present in two different states which are in equilibrium with one another, viz. oleate in extensive association forming the elastic structure and free oleate permeating the elastic structure and bearing the character of an equilibrium concentration.

When, starting from zero, the oleate concentration is gradually increased no elastic system (hence  $G = 0$  and  $1/\Delta = 0$ ) is produced as long as the oleate concentration is smaller than the critical concentration  $b$  (which is equal to  $d$ ). After passing this critical concentration, the excess oleate associates in order to form the elastic system.

This excess oleate, represented by the expression  $(C_{\text{oleate}} - b)$ , which is equal to  $(C_{\text{oleate}} - d)$ , may be called the "reduced oleate concentration". The elastic properties are connected in a very simple way with this latter concentration, *the shear modulus  $G$  being proportional to the square of the reduced oleate concentration* (with the square of  $a$  in the above formula as proportionality factor) *and the reciprocal value of the logarithmic decrement being proportional to the reduced oleate concentration* (only for the lower branch of the  $1/\Delta$  curve, and with  $c$  as proportionality factor).

An analogous formulation for  $n$ , however, can not be made, for if we determine  $f$ , the part cut off from the abscissa by the  $n$  curve in fig. 5, we find the value 0.18 %, which is decidedly higher than the value found for  $b$  and  $d$ , which are 0.09 %.

Therefore we must consider if this does not contradict the above hypothesis. The answer to this question is no, for one must bear in mind that  $n$  is only an imperfect measure of  $1/\Delta$  (for particulars see part XV of this series).

When in fig. 5 we move along the lower branch of the  $1/\Delta$  curve downwards to the left,  $\Delta$  increases more and more and will reach such a high value at last that we have obtained the so called critically damped oscillation. There is just no turning point left any longer and we have to write  $n = 0$ . Yet  $1/\Delta$  is not zero but has still a finite, though small, value. Therefore at this value of  $1/\Delta$  the  $n$  curve already meets the

abscissa in fig. 5. This explains why  $f > d$ . Combining this with  $b = d$ , we get the general expectation:

$$b = d < f,$$

which in fact was found in fig. 5 ( $b = d = 0.09\%$ ;  $f = 0.18\%$ ).

In the experiments in section 2 and 3, where logarithmic decrements were not determined, we can therefore only control that  $b < f$ .

The experiments<sup>1</sup> at 0.9 N KCl and 1.5 N KCl in fig. 1 are not accurate enough (too few points on the lower  $n$  branch to locate with certainty its position), but for the experiment at 0.6 N KCl we find indeed  $b < f$  ( $b = 0.16\%$ ,  $f = 0.32\%$ ).

The much more accurate experiment in fig. 2 (three points on the lower  $n$  branch) also confirms our expectation for 1.5 N KCl ( $b = 0.06\%$ ,  $f = 0.10\%$ ). We find the same for the experiments with pure K-oleate in fig. 4 (at 0.98 N KCl and at four temperatures). Both at  $17.8^\circ$  and  $25.1^\circ$  one finds  $b = 0.08\%$  and  $f = 0.12\%$ . At  $34.7^\circ$  these values are  $b = 0.08\%$  and  $f = 0.17\%$ , whereas at  $46.7^\circ$  one finds  $b = 0.12\%$  and  $f = 0.37\%$ .

The experiments at 0.75 N and 1.05 N KCl in fig. 3A give striking examples of  $b < f$  at four temperatures.

In the above we have mainly paid attention to the general character of the linear relations, but did not yet discuss in which way the values of  $a$ ,  $b$ ,  $e$  and  $f$  are depending on the KCl concentration and the temperature. This will be postponed till the next communication, in which further experiments of importance with regard to this question will be published.

## 5. Summary

1. The dependence of  $\sqrt{G}$  and of  $n$  on the oleate concentration has been investigated at a number of KCl concentrations and temperatures with Na-oleate from BAKER and with K-oleate made from chemically pure oleic acid.

2. The results, combined with those obtained in part III with Na-oleate from MERCK allow to conclude that quite generally the  $\sqrt{G}$ - $C_{\text{oleate}}$  curve, the lower branch of the  $1/A - C_{\text{oleate}}$  curve and the lower branch of the  $n$ - $C_{\text{oleate}}$  curve are straight lines intersecting the abscissa at small values of the oleate concentration.

3. Representing these straight lines by:

$\sqrt{G} = a (C_{\text{oleate}} - b)$ ;  $1/A = c (C_{\text{oleate}} - d)$  and  $n = e (C_{\text{oleate}} - f)$ , it appears that at a given oleate preparation, KCl concentration and temperature  $b = d$ , but that  $b < f$ . For the latter inequality an explanation has been given.

4. The hypothesis is brought to the fore that the total oleate in the elastic viscous system is present in two different states in dynamic equilibrium with one another, viz. "structural oleate", i.e. oleate participat-

ing in the elastic phenomena and "free oleate" i.e. oleate not participating in the elastic phenomena.

5. The concentration of the "free oleate" is indicated by  $b$ , which is equal to  $d$ . The elastic properties are depending on the concentration of the "structural oleate" given by the expression  $(C_{\text{oleate}} - b)$ , which is equal to  $(C_{\text{oleate}} - d)$ .

Calling this concentration the "reduced oleate concentration" and denoting it with  $C_{\text{red.oleate}}$ , we have

$$G \propto (C_{\text{red.oleate}})^2 \text{ and } A \propto (1/C_{\text{red.oleate}})$$

(the latter expression only applies to the lower branch of the  $1/A - C_{\text{oleate}}$  curve).

*Department of Medical Chemistry  
University of Leiden*



## SUDDEN INCREASE OF COSMIC RAY INTENSITY FOLLOWING LARGE METEORIC ACTIVITY

BY

H. F. JONGEN

*(Laboratory for Physics, University of Amsterdam)*

(Communicated by Prof. J. CLAY at the meeting of April 28, 1951)

*Summary.* On October 10, 11, 1946 with an interval of nearly one day, an increase of cosmic ray intensity was observed of 4 %—6 %, lasting several hours and apparently not correlated with a solar flare. It is suggested that the cause of this effect may be the passage of the earth in the early morning of October 10, 1946 through meteoric debris belonging to the Giacobini-Zinner comet, meteoric activity during several hours having augmented by a factor 5000.

1. The last few years the idea has been generally accepted that the greater part of the sudden increases of cosmic ray intensity is of solar origin. A large number of observational data <sup>1)</sup> is available, proving that in many cases solar flares (éruptions chromosphériques brillantes) of class 3 or 3<sup>+</sup> and even some smaller flares of class 2 and 1 are followed within from 20 minutes to 2 hours by a considerable increase of cosmic ray intensity. However, it must be admitted that this correlation is not found in most of the cases with flares of class 1 and 2<sup>2)</sup>.

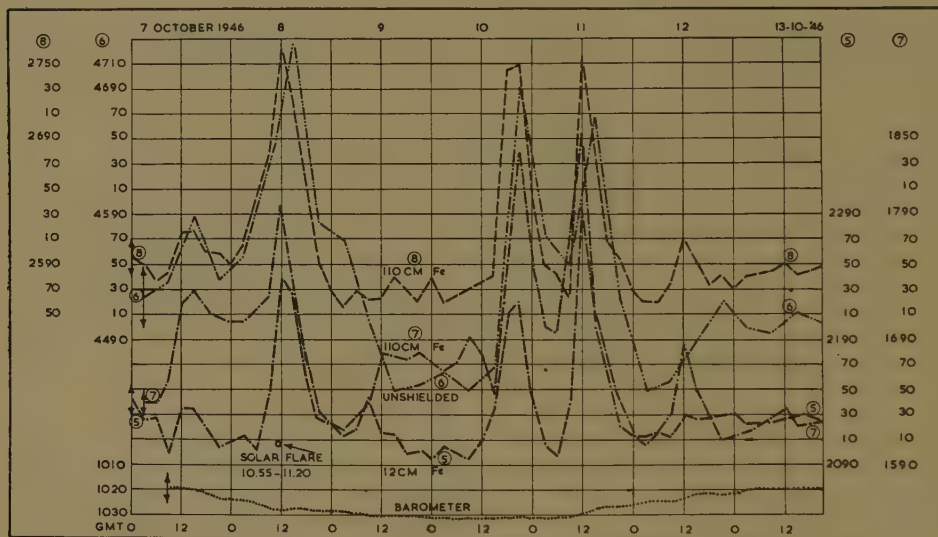
Various theories on the production process of cosmic radiation during solar flares have been given, but most of them fail to account for the occurrence, in the bursts originating in the flares, of cosmic ray particles with large energy. FORBUSH, GILL and VALLARTA predicted theoretically a small frequency for the increases caused by solar flares, basing themselves on the alleged scarcity of favorable conditions for particles to escape from the sun. This prediction is not borne out by our experimental results for the year 1947.

2. Should no direct flare observations have been made during an increase of cosmic radiation, owing to bad weather conditions or otherwise, we can nearly every time infer the presence of the flare from data about geomagnetic and ionospheric effects narrowly correlated with its occurrence, and starting practically at the same instant <sup>3)</sup> e.g. earth magnetic crochets, radio fade out observations in short wave transmission

(Dellinger effects), sudden phase anomalies in long wave transmission, also sudden enhancements of atmospherics.

3. However, in one case of observed considerable increase of c.r. intensity this method has failed to disclose a corresponding flare, namely on October 10, 11, 1946.

Our intensity records of cosmic rays in Amsterdam (at sea-level) extend over 15 years. The four vessels, containing Argon at 60 atmospheres are each provided with a central probe, one of them is unshielded, one shielded



with 12 cm Fe, two with 110 cm Fe, one of the latter has an Argon pressure of 100 atm. A zero method is used to establish the voltage change of the probe by means of an electrometer triode; accuracy of results 1–2  $\frac{0}{100}$ .

The results for Oct. 7–13, 1946 are given in the graph. Each time the mean value of 3 measurements is plotted, one point every 3 hours for the shielded vessels, one point every 6 hours for the unshielded one, which recorded once in 2 hours. On Oct. 8 an increase in intensity is registered, setting in at about 9.00 GMT with a maximum round 12.00 GMT. This might be caused by the solar flare of class 1 observed at Worthing observatory from 10.55–11.20 GMT, although it is not very clear, how a minor flare can give such a large effect (3–6 %). Moreover the increase sets in too early.

For the following days data of direct flare observations are very scarce, and no reports at all have been published about flare influence in the earthmagnetic field or in short wave radio transmission, so we have to assume that the increase of Oct. 10, 11 was not due to a solar flare. On Oct. 10 the intensity increased in all our vessels, beginning at 15.00 GMT with a maximum increase of 4–6 % at 21.00 GMT. On Oct. 11 these

effects repeated themselves at 9.00 and 11.00 resp., while a minor maximum, in the hard component only, occurred on Oct. 12 at 12.00.

4. The following suggestion is offered.

On Oct. 10, 1946 in the early morning the earth traversed the orbit of the Giacobini-Zinner comet, fifteen days after the passage of the comet. By means of the newly developed radio techniques LOVELL and co-workers<sup>5)</sup>, using a wavelength of 4.2 m, observed on Oct. 10 between 0.00 and 6.00 UT a meteoric activity of 5000 times normal with a maximum at 3.40 UT up to heights of 200 KM. They assume that this is meteoric debris associated with the above-mentioned comet. Their apparatus could only just detect a meteor producing  $5 \cdot 10^9$  electrons/cm at a range of 100 KM, while meteors producing  $8 \cdot 10^{10}$  electrons/cm at that range caused saturation of their apparatus. The bulk of the meteors traversed the atmosphere at a height of 100 KM. From these data we may conclude that during the passage of this debris the ionization is locally somewhat heightened in the higher atmosphere and it is possible that this ionization is the cause of the observed increment in cosmic radiation. It is not clear, however, how particles produced in this way can obtain the energy necessary to reach the earth and moreover penetrate the shielding of our vessels.

The same comet passed in the vicinity of the earth in 1933. We regret to possess no cosmic ray data for that period.

#### REFERENCES

1. FORBUSH, S. E., *Phys. Rev.* **70**, 771 (1946).  
NEHER, H. V. and W. C. ROESCH, *Rev. Mod. Phys.* **20**, 350 (1948).  
EHMERT, A., *Zeitschr. f. Naturforschung*, **3a**, 264 (1948).  
CLAY, J., H. F. JONGEN and A. J. DIJKER, *Proc. Kon. Ned. Ak. v. Wetensch.* **52**, 897, 923 (1949).  
BROXON, J. W., H. W. BOEHMER, *Phys. Rev.* **78**, 411 (1950).  
CLAY, J., and H. F. JONGEN, *Phys. Rev.* **79**, 908 (1950).
2. SWANN, W. F. G., *Phys. Rev.* **43**, 217 (1933).  
BAGGE, E. & L. BIERMANN, *Naturw.* **35**, 120 (1948).  
FORBUSH, S. E., P. S. GILL & M. S. VALLARTA, *Rev. Mod. Phys.* **24**, 44 (1949).
3. ELLISON, M. A., *Mon. Not. Roy. Astro. Soc.* **109**, 1 (1949).  
———, *Nature* **163**, 749 (1949).  
———, *Publ. Roy. Obs. Edinburgh* **1**, no. 4 (1950).
4. *Quarterly Bulletin on Solar Activity* **69–76**, 36 (1946, 1947).
5. LOVELL, A. C. B., C. J. BANWELL, J. A. CLEGG, *Mon. Not. Roy. Astro. Soc.* **107**, 164 (1947).  
———, *Nature* **167**, 94 (1951).

# SUR LA FONCTION DE DISTRIBUTION RADIALE D'UN GAZ IMPARFAIT ET LE PRINCIPE DE SUPERPOSITION

PAR

B. R. A. NIJBOER ET L. VAN HOVE

(Communicated by Prof. J. M. BIJVOET at the meeting of April 28, 1951)

*Summary*

The term proportional to the square of the density in the expansion of the radial distribution function of an imperfect gas in powers of the density is calculated exactly in the case of a gas consisting of hard spheres. The result can be checked by means of the value of the 4th virial coefficient, which is known since a long time for such a gas. The exact expression, being a function of the distance  $r$  between two molecules, is compared with the approximate one, obtained by applying the superposition principle introduced by KIRKWOOD.

Comme l'ont montré YVON, KIRKWOOD, DE BOER, et d'autres<sup>1)</sup>, la fonction de distribution radiale d'un gaz imparfait peut être développée en série de puissances de la densité:

$$g(r) = e^{-\frac{V(r)}{kT}} \cdot \{1 + \varrho g_1(r) + \varrho^2 g_2(r) + \dots\}$$

On désigne par  $r$  la distance entre molécules, par  $V(r)$  le potentiel intermoléculaire et par  $\varrho$  le nombre de molécules par unité de volume. Les fonctions  $g_1(r)$ ,  $g_2(r)$ , ... sont exprimées par des intégrales portant sur le potentiel  $V(r)$ <sup>2)</sup>.

Pour un gaz de sphères incompressibles sans forces attractives, la fonction  $g_1(r)$  a été calculée par KIRKWOOD<sup>3)</sup>, avec le résultat suivant

$$g_1(r) = \frac{2\pi}{3} \left( 2 - \frac{3}{2}r + \frac{r^3}{8} \right) \text{ pour } r \leq 2,$$

$$g_1(r) = 0 \text{ pour } r \geq 2,$$

où le diamètre des sphères est pris comme unité de longueur. Pour le même cas, nous avons calculé la fonction  $g_2(r)$  dont l'expression générale est la suivante

$$g_2(r) = \frac{1}{2} \{g_1(r)\}^2 + \varphi(r) + 2\psi(r) + \frac{1}{2}\chi(r),$$

<sup>1)</sup> On se reportera par exemple au travail d'ensemble de J. DE BOER, Reports on Progress in Physics, 12, 305 (1948-49).

<sup>2)</sup> BOER, J. DE, et A. MICHELS, Physica, 6, 97 (1939).

<sup>3)</sup> KIRKWOOD, J. G., J. Chem. Physics, 3, 300 (1935).



avec

$$\begin{aligned}\varphi(r_{12}) &= \int f(r_{13}) f(r_{24}) f(r_{34}) \vec{dr}_3 \vec{dr}_4, \\ \psi(r_{12}) &= \int f(r_{13}) f(r_{23}) f(r_{24}) f(r_{34}) \vec{dr}_3 \vec{dr}_4, \\ \chi(r_{12}) &= \int f(r_{13}) f(r_{14}) f(r_{23}) f(r_{24}) f(r_{34}) \vec{dr}_3 \vec{dr}_4.\end{aligned}$$

La fonction  $f(r)$ , dont l'expression générale est

$$f(r) = \exp \left\{ -\frac{V(r)}{kT} \right\} - 1,$$

prend pour des sphères incompressibles la forme

$$\begin{aligned}f(r) &= -1 \quad \text{pour } 0 \leq r < 1, \\ f(r) &= 0 \quad \text{pour } r \geq 1.\end{aligned}$$

Le calcul de  $\chi(r)$ , qui seul présente des difficultés, a été effectué par transformation de FOURIER. Les résultats obtenus sont

$$\varphi(r) = \pi^2 \left\{ -\frac{r^6}{1260} + \frac{r^4}{20} - \frac{r^2}{6} - \frac{r^2}{4} + \frac{9}{5}r - \frac{9}{4} + \frac{27}{70} \frac{1}{r} \right\} \quad \text{pour } 1 \leq r \leq 3,$$

$$\varphi(r) = 0 \quad \text{pour } r \geq 3;$$

$$\psi(r) = \pi^2 \left\{ \frac{r^6}{1260} - \frac{r^4}{20} + \frac{r^2}{6} + \frac{r^2}{4} - \frac{97}{60}r + \frac{16}{9} - \frac{9}{35} \frac{1}{r} \right\} \quad \text{pour } 1 \leq r \leq 2,$$

$$\psi(r) = 0 \quad \text{pour } r \geq 2;$$

$$\begin{aligned}\chi(r) &= -\{g_1(r)\}^2 + \pi \left\{ -\frac{3}{280}r^4 + \frac{41}{420}r^2 \right\} \sqrt{3-r^2} \\ &\quad + \pi \left\{ -\frac{23}{15}r + \frac{36}{35} \frac{1}{r} \right\} \arccos \frac{r}{\sqrt{3(4-r^2)}} \\ &\quad + \pi \left\{ \frac{3}{560}r^6 - \frac{1}{15}r^4 + \frac{1}{2}r^2 + \frac{2}{15}r - \frac{9}{35} \frac{1}{r} \right\} \arccos \frac{r^2+r-3}{\sqrt{3(4-r^2)}} \\ &\quad + \pi \left\{ \frac{3}{560}r^6 - \frac{1}{15}r^4 + \frac{1}{2}r^2 - \frac{2}{15}r + \frac{9}{35} \frac{1}{r} \right\} \arccos \frac{-r^2+r+3}{\sqrt{3(4-r^2)}} \\ &\quad \text{pour } 1 \leq r \leq \sqrt{3},\end{aligned}$$

$$\chi(r) = -\{g_1(r)\}^2 \quad \text{pour } \sqrt{3} \leq r \leq 2,$$

$$\chi(r) = 0 \quad \text{pour } r \geq 2.$$

On trouvera dans la figure 1 le graphique de la fonction  $g_2(r)$  ainsi obtenue. Le graphique de  $g_1(r)$  est donné dans DE BOER<sup>1)</sup>. A titre de vérification, on peut calculer le 4e coefficient du viriel  $B_4$  à l'aide de  $g_2(r)$ . Le théorème du viriel donne en effet

$$B_4 = \frac{2\pi}{3} g_2(1).$$

Alors on retrouve exactement le résultat de BOLTZMANN<sup>4)</sup>

$$B_4 = 0,2869 \, b^3,$$

<sup>4)</sup> BOLTZMANN, L., Versl. Akad. Wetensch. Amsterdam, 7, 484 (1899).

où  $\frac{1}{2}b$  est le volume de chaque particule. Une vérification supplémentaire portant sur la fonction  $g_2(r)$  pour toutes les valeurs de  $r$ , est obtenue en déduisant  $B_4$  de la formule de compressibilité relative

$$-\frac{p}{V} \left( \frac{dV}{dp} \right)_T = 1 + 4\pi\rho \int_0^\infty \{g(r) - 1\} r^2 dr.$$

Il est intéressant de comparer l'expression exacte de  $g_2(r)$  avec l'expression approchée qu'on obtient en appliquant le principe de superposition proposé par KIRKWOOD en théorie des liquides <sup>1)</sup>. Faisant usage

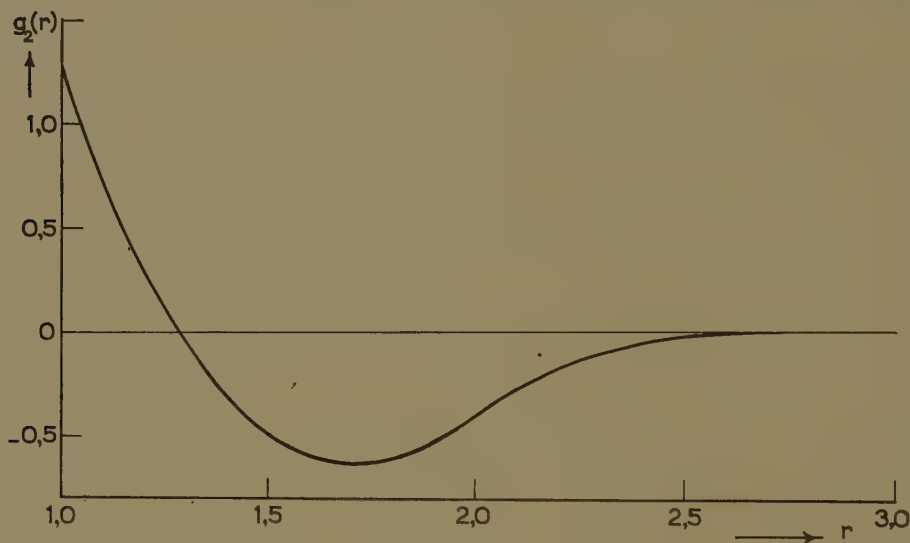


Fig. 1

de ce principe suivant la méthode de BORN et GREEN <sup>5)</sup>, on obtient pour  $g(r)$  une équation intégrale non linéaire que l'on peut résoudre par développement en série de puissances de  $\rho$ . L'expression approchée  $g'_2(r)$  qui en résulte ne diffère de  $g_2(r)$  que par le remplacement de  $\chi(r)$  par

$$\chi'(r) = \pi^2 \left\{ -\frac{1}{630} r^6 + \frac{1}{10} r^4 - \frac{19}{72} r^3 - \frac{1}{2} r^2 + \frac{12}{5} r - \frac{22}{9} + \frac{18}{35} \frac{1}{r} \right\} \text{ pour } 1 \leq r \leq 2,$$

$$\chi'(r) = 0 \quad \text{pour } r \geq 2.$$

La courbe en trait plein de la figure 2 représente la différence  $g_2(r) - g'_2(r)$ . Il est à noter qu'une approximation plus simple et meilleure est obtenue en remplaçant  $\chi(r)$  par  $-\{g_1(r)\}^2$ ; l'erreur introduite ainsi est représentée par la courbe pointillée.

Indiquons pour terminer les valeurs fournies pour le 4e coefficient du viriel par les approximations mentionnées. Dans l'approximation de

<sup>5)</sup> BORN, M. et H. S. GREEN, Proc. Roy. Soc. A 188, 10 (1946).

KIRKWOOD, le théorème du viriel donne  $B_4 = 0,2252 b^3$  <sup>6)</sup> et la formule de compressibilité relative  $B_4 = 0,3424 b^3$ , tandis que l'autre approxima-

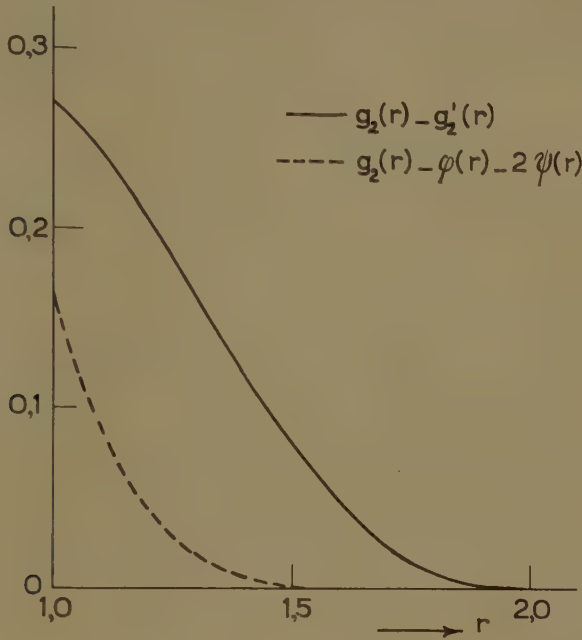


Fig. 2

tion, qui pose  $g_2 = \varphi + 2\psi$ , donne respectivement  $B_4 = 0,2500 b^3$  et  $0,2969 b^3$ .

Un compte rendu détaillé de ce qui précède sera publié ailleurs.

*Institut de physique théorique, Université, Utrecht, Pays-Bas  
et  
Université libre de Bruxelles, Belgique.*

<sup>6)</sup> Cette valeur a été obtenue récemment par R. W. HART, R. WALLIS et L. PODE, J. Chem. Physics, 19, 139 (1951), ainsi que par G. S. RUSHBROOKE et H. I. SCOINS, Nature, 167, 366 (1951).

GENERAL LINEARIZED THEORY OF THE EFFECT OF  
SURFACE FILMS ON WATER RIPPLES. I

BY

R. DORRESTEIN

(Communicated by Prof. F. A. VENING MEINESZ at the meeting of May 26, 1951)

§ 1. *Introduction*

That a rough sea can be calmed to a certain extent by pouring out minute quantities of adequate oils on the sea surface must have been well known among mariners since very, very long ago. At any rate, PLINIUS THE ELDER has already made mention of it. Although, certainly, this is a very striking phenomenon from a physical point of view, there have been, up to now, only relatively few physicists and chemists who have occupied themselves with the subject and have endeavoured to give a physical explanation. We mention BENJAMIN FRANKLIN (1774), O. REYNOLDS (1880), J. AITKEN (1883), Frau A. PÖCKELS (1891). The latter three authors are mentioned in the few pages devoted to the question in the text-books of N. K. ADAM: "The Physics and Chemistry of Surfaces, 3rd Edition (1941) p. 105, and of H. LAMB: "Hydrodynamics", 6th Edition (1932), Art. 351. Especially AITKEN (1883) gave, in an excellent account, a qualitative physical explanation of the phenomenon, supported by systematic laboratory experiments, which explanation may be considered up to now as essentially right. He showed that the calming effect of oil must be due to the *variations* of tension caused by the extensions and contractions of the contaminated surface.

Experience has made clear that an oil film on a water surface can manifest itself substantially in two ways: —

1. A suitable film prevents the formation of short waves (wave length a few centimeters and less) by the wind. As a consequence, in some way the development of the dangerous crests of large storm waves is hindered.
2. In the absence of wind, the damping of short waves is strongly increased when a suitable oil film is present on the water surface.

It is obvious that the second phenomenon must be important in the explanation of the first one.

By LAMB (Art. 351) only a few lines are devoted to the theory of the increase of the viscous damping of water waves caused by the presence of a surface film. This very brief treatment can be extended in such a way as to give the most complete *linearized* theory of waves travelling on water where some sort of surface film is present. This will be done in the next section of this paper.



## Notation

	Introduced in equation
$A, C$ complex constants . . . . .	(7)
$C$ phase-velocity of wave $= \lambda/P$ . . . . .	
$g$ acceleration of gravity . . . . .	(1)
$k$ wave-number . . . . .	(7)
$m$ complex constant . . . . .	(7 <sup>b</sup> )
$N$ real number . . . . .	(18)
$O$ surface area available for a certain material part of the film	(18)
$P$ wave-period . . . . .	(32 <sup>a</sup> )
$p$ pressure . . . . .	(1)
$p_{xx}, p_{xy}, p_{yy}$ Reynold's stresses in the fluid . . . . .	
$r = 2\pi \times$ wave-frequency . . . . .	(7)
$t$ time . . . . .	
$T$ surface tension, $T' = T/\varrho$ . . . . .	(11)
$T_{xx}, T_{xz}, T_{zz}$ surface stresses . . . . .	
$u(x, y, t), v(x, y, t)$ velocity componenets in $x$ - and $y$ -direction	(1)
$V$ group-velocity of wave . . . . .	(45)
$x, y, z$ orthogonal coordinates ( $y$ vertical upwards). . . . .	(1)
$\Delta$ Laplace-operator . . . . .	
$\varepsilon$ complex quantity (assumed $ \varepsilon  \ll 1$ ) . . . . .	(24)
$\eta$ elevation of fluid surface with respect to undisturbed state	(10)
$\theta = \nu k^2/\sigma$ (assumed $\theta \ll 1$ ) . . . . .	(23)
$\lambda$ wave-length . . . . .	
$\mu$ dynamic viscosity of fluid . . . . .	(12)(16)
$\mu_s$ surface viscosity of film . . . . .	(17)
$\nu$ kinematic viscosity of fluid $= \mu/\varrho$ . . . . .	(1)
$\nu_s = \mu_s/\varrho$ . . . . .	
$\xi$ phase-angle measuring hysteresis in surface tension (assumed $\ll 1$ ) . . . . .	
$\varrho$ density of fluid . . . . .	(1)
$\sigma = (gk + T'k^3)^{1/2}$ . . . . .	(14)
$\tau$ modulus of decay (characteristic time) . . . . .	(32/)
$\tau$ shearing stress at surface $\approx p_{xy}$ at surface . . . . .	(15)
$\Phi(x, y, t), \Psi(x, y, t)$ velocity potentials . . . . .	(3)
$\chi$ complex parameter . . . . .	(21)(38)

§ 2. *Theory.* Following LAMB (Art. 349), we take the  $y$ -axis vertically upwards; let the undisturbed surface of the fluid be given by  $y = 0$ . We assume that the fluid is incompressible and that the motion is confined to the dimensions  $x, y$ . If we consider only wave motions with such small velocities that we are allowed to neglect the terms in the equations of

motion which are quadratic in the velocities, we obtain the following equations of motion:

$$(1) \quad \frac{\partial u}{\partial t} = -\frac{1}{\varrho} \frac{\partial p}{\partial x} + \nu \Delta u, \quad \frac{\partial v}{\partial t} = -g - \frac{1}{\varrho} \frac{\partial p}{\partial y} + \nu \Delta v,$$

with

$$(2) \quad \frac{\partial u}{\partial x} + \frac{\partial v}{\partial y} = 0.$$

Any pair of functions  $u(x, y)$ ,  $v(x, y)$  can be written in the form

$$(3) \quad u = -\frac{\partial \Phi}{\partial x} - \frac{\partial \Psi}{\partial y}, \quad v = -\frac{\partial \Phi}{\partial y} + \frac{\partial \Psi}{\partial x},$$

where  $\Phi(x, y)$  and  $\Psi(x, y)$  are two new functions.

The solutions of the following equations lead, with (3), to solutions of (1) and (2):

$$(4) \quad \Delta \Phi = 0,$$

$$(5) \quad \frac{\partial \Psi}{\partial t} = \nu \Delta \Psi$$

$$(6) \quad \frac{p}{\varrho} = -gy + \frac{\partial \Phi}{\partial t}$$

(comp. Appendix 1)

Now, for the following it is convenient to write  $\Phi$ ,  $\Psi$ ,  $u$ ,  $v$ ,  $p$  etc. as complex quantities, of which we have to take the real part. We assume  $\Phi$  and  $\Psi$  to contain a common factor  $e^{i(\tau t + kx)}$  where  $k$  and  $r$  are two constants. According to (3),  $u$  and  $v$  will then contain the same factor. If  $k$  and  $r$  are real, or approximately real, the factor indicates a periodicity in  $t$  and in  $x$ . If we assume the fluid to be very deep, the solutions of (4) and (5) must be finite for  $y = -\infty$ . The following solutions obey the above conditions:

$$(7a) \quad \Phi = A e^{ky} e^{i(\tau t + kx)}$$

$$(7b) \quad \Psi = C e^{my} e^{i(\tau t + kx)}$$

where  $A$  and  $C$  are (complex) constants and  $k$  and  $m$  have positive real parts, with:

$$(8) \quad m^2 = k^2 + \frac{i\tau}{\nu}.$$

From (7) we have, by (3), for the velocity components:

$$(9a) \quad u = (-ikA e^{ky} - mC e^{my}) e^{i(\tau t + kx)}$$

$$(9b) \quad v = (-kA e^{ky} + ikC e^{my}) e^{i(\tau t + kx)}.$$

If  $\eta$  denote the elevation of the surface, we must have  $\partial\eta/\partial t + u\partial\eta/\partial x = v$  for  $y = \eta$ . Approximating by putting  $\partial\eta/\partial t = v$  for  $y = 0$  gives:

$$(10) \quad \eta = \frac{k}{r} (iA + C) e^{i(\tau t + kx)}.$$

The boundary-conditions at the surface will supply equations which are sufficient to give a relation between  $r$  and  $k$ . In the absence of internal friction ( $\nu = 0$ ), solutions appear to be possible with real values for the constants  $r$  and  $k$ . If  $r$  and  $k$  are assumed to be positive, we have then a simple harmonic wave travelling in the negative  $x$ -direction, with period  $P = 2\pi/r$  and wave-length  $\lambda = 2\pi/k$ . With internal friction, if not too large, we hope to find solutions in which  $r$  and  $k$  are in first approximation real and positive, so that in first approximation we have a simple harmonic wave travelling in the negative  $x$ -direction. We shall see, then, that either  $r$ , or  $k$ , must contain a (relatively small) imaginary part, and this imaginary part will determine the rate of decay of the wave.

The first boundary-condition concerns the normal pressure at the surface. Assuming zero pressure above the fluid, we must have for the normal stress,  $p_{vv}$ , within the fluid at the surface the following relation for all values of  $x$  and  $t$ :

$$(11) \quad 0 = p_{vv} - T \frac{\partial^2 \eta}{\partial x^2}.$$

This is true to the first order, since the inclination of the surface to the horizontal is assumed to be infinitely small. Now the relation between the stress  $p_{vv}$  and the pressure  $p$  is, according to the linear theory of viscosity in isotropic media (cf. LAMB, Art. 326):

$$(12) \quad p_{vv} = -p + 2\mu \frac{\partial v}{\partial y},$$

whence, by (6) and (10), and introducing the "specific" surface tension  $T' = T/\varrho$ :

$$0 = \frac{p_{vv}}{\varrho} - T' \frac{\partial^2 \eta}{\partial x^2} = (g + T' k^2) \eta - \frac{\partial \Phi}{\partial t} + 2\nu \frac{\partial v}{\partial y}.$$

From this we obtain by (7), (10) and (9), replacing  $e^{k\eta}$  and  $e^{m\eta}$  by 1, the condition:

$$(13) \quad 0 = \{A (ir^2 - i\sigma^2 + 2\nu k^2 r) - C (\sigma^2 + 2\nu kmr)\} e^{i(r t + kx)},$$

where we have put

$$(14) \quad gk + T' k^3 = \sigma^2.$$

Since the real part of the right-hand side of eq. (13) should be zero for all values of  $x$  and  $t$ , both the real and imaginary parts of the expression in brackets must be zero.

A second boundary-condition is given by the shearing stress at the surface,  $\tau$ . We shall first deal with the most general case. Afterwards, by simplifying the result obtained, we can consider different special cases.

Consider a rectangular surface element of the fluid with sides  $dx$  parallel to  $x$ , and  $dz$  parallel to  $z$ . We put  $\tau_a = x$ -component of shearing stress acting on the surface from the air above the surface,  $-\tau_w = x$ -component

of shearing stress acting on the surface from the water below the surface,  $(T_{xx}, T_{xz}, T_{zz})$  = tensor of surface stresses within the surface (see Appendix 2). Then, we have that the following sum of forces, all acting in the positive  $x$ -direction, must be zero:

$$0 = \tau_a dx dz - \tau_w dx dz + \left( \frac{\partial T_{xx}}{\partial x} dx \right) dz + \left( \frac{\partial T_{xz}}{\partial z} dz \right) dx.$$

We assume here the first and fourth terms to be zero, so that we have

$$(15) \quad 0 = \tau_w - \frac{\partial T_{xx}}{\partial x}.$$

The linear theory of isotropic viscosity gives, at the surface (cf. LAMB, Art. 326):

$$(16) \quad \tau_w \approx p_{xy} = \mu \left( \frac{\partial v_s}{\partial x} + \frac{\partial u_s}{\partial y} \right)$$

(where the index  $s$  indicates the surface), and the relation between the surface stress  $T_{xx}$  and the surface tension  $T$  is, according to the linear theory of "surface viscosity":

$$(17) \quad T_{xx} = T + \mu_s \frac{\partial u_s}{\partial x},$$

where  $\mu_s$  is the "surface viscosity" (see Appendix 2).

Now, any wave motion of the water surface will be connected with some periodic extensions and contractions along the surface. If we may assume that the molecules of the film are sticking firmly to the water beneath them, there must be consequent periodic variations in the area available for any small part of the surface film. This assumption is certainly valid if we have to do with films of aliphatic chain molecules with hydrophylic end-groups, such as fatty acids, their tri-glycerides (the fats), amides, amines, methylketones (see ADAM (1941)).

It is well known that the variations in area in general will involve variations in surface tension. Both variations can be assumed to be small with respect to the mean values. We assume a linear relation to exist between them:

$$(18) \quad \frac{\delta T}{T_0} = N \frac{\delta O}{O}$$

where  $T_0$  is the surface tension in the undisturbed state,  $O$  is the area available for a certain material part of the film (considered to be much smaller than one wave length), and  $N$  is a positive number, being inversely proportional to the compressibility of the film.

For  $\delta T \ll T_0$ , eq. (18) may, alternatively, be replaced by

$$(18a) \quad T \sim O^N.$$

$N$ , therefore, is given by the slope of the  $T(O)$ -curve in a double-logarithmic plot. According to the nature and the condition of the film, the value of  $N$  can vary from zero to very high values (see ADAM (1941)).



In our case we have:

$$(19) \quad \frac{1}{O} \frac{DO}{Dt} \approx \frac{\partial u_s}{\partial x} \approx \frac{1}{NT_0} \frac{DT}{Dt},$$

where  $D/Dt$  denotes a differentiation following the motion of the surface film.

Differentiating the condition (15) with respect to  $t$ , using (16), (17) and (19), and "linearizing" by putting  $\partial/\partial t$  for  $D/Dt$  we obtain:

$$0 = \mu \frac{\partial}{\partial t} \left( \frac{\partial v_s}{\partial x} + \frac{\partial u_s}{\partial y} \right) - NT_0 \frac{\partial^2 u_s}{\partial x^2} - \mu_s \frac{\partial^3 u_s}{\partial t \partial x^2}.$$

From this we have, by (9), replacing  $e^{k\eta}$  and  $e^{m\eta}$  by 1, using (8) and introducing the "specific" quantities  $T' = T_0/\rho$ ,  $\nu = \mu/\rho$  and  $\nu_s = \mu_s/\rho$ :

$$(20) \quad 0 = \{A(2i\nu k^2 r + \chi \sigma^2) + C(ir^2 + 2\nu k^2 r - i\chi \sigma^2 m k^{-1})\} e^{i(rt+kx)},$$

where we have put:

$$(14) \quad gk + T'k^3 = \sigma^2$$

$$(21) \quad k^3 (NT' + i\nu_s r) = \chi \sigma^2,$$

with  $\chi$  a dimensionless complex number.

Just as in (13), the total complex expression in brackets in (20) must be zero.

We see that the influences of limited compressibility ( $N$ ) of the film and of a surface viscosity ( $\nu_s$ ) appear together in the quantity  $\chi$ . Here, and in the following, the formulae valid for water waves without surface film can be easily obtained by omitting the terms with  $\chi$ .

Equations (13) and (20) represent two homogeneous linear equations for  $A$  and  $C$ . Therefore, in order to have a solution where at least one of these quantities differs from zero, the determinant of the coefficients has to be zero. This leads to the condition:

$$(22) \quad 0 = (ir^2 + 2\nu k^2 r)^2 + \sigma^2 r^2 - 4\nu^2 k^3 m r^2 + \chi \sigma^2 (m k^{-1} r^2 - m k^{-1} \sigma^2 + \sigma^2)$$

With given values of  $g$ ,  $T'$ ,  $\nu$ ,  $N$ ,  $\nu_s$ , this condition (with (14) and (21)) can be read as a relation between  $r$ ,  $k$  and  $m$ , and thus, by (8), as a relation between  $r$  and  $k$ . For  $\nu = 0$  and  $\chi = 0$ , we see from (22):  $r = \pm \sigma$ , and from (14) we obtain the normal dispersion law for surface waves over deep water.

For  $\nu$  and  $\chi$  different from zero, we shall first choose  $k$  in (22) to be real, which means that we consider a wave with amplitude independent on  $x$ , and we expect that it will be damped with increasing time. We introduce two dimensionless quantities  $\theta$  and  $\varepsilon$  by

$$(23) \quad \theta = \frac{\nu k^2}{\sigma}$$

and

$$(24) \quad r = \sigma(1 + \varepsilon)$$

The viscosity parameter  $\theta$  is real, but  $\varepsilon$  may be complex. Eq (22) can then be transformed into:

$$(25) \quad 0 = (i + i\varepsilon + 2\theta)^2 + 1 - 4\theta^2 \frac{m}{k} + \chi \frac{1 + \varepsilon(2 + \varepsilon)mk^{-1}}{(1 + \varepsilon)^2}.$$

and from (8) follows:

$$(26) \quad mk^{-1} = \{1 + i(1 + \varepsilon)/\theta\}^{1/2}$$

Now for the following, we always assume that  $\theta$ , the viscosity parameter, is small as compared to unity. For water, this is true indeed, down to wavelengths of the order of 1 mm (see Table 1).

According to (25) and (26),  $\varepsilon$  becomes a function of  $\theta$  and  $\chi$  only, and we shall consider the continuous solution which is zero for  $\theta = \chi = 0$ . Then it may be seen from (25) and (26) that for small  $\theta$ ,  $\varepsilon$  is also small, irrespective of the value of  $\chi$ . Under these conditions (26) can be approximated by the first term of the series:

$$(27) \quad mk^{-1} = + (1 + i) (2\theta)^{-1/2} \{1 + \frac{1}{2}(\varepsilon - i\theta) + \dots\},$$

since by agreement  $m$  should be the root with positive real part. By developing (25), and neglecting relatively small terms, we obtain the approximate solution for  $\varepsilon$ :

$$(28) \quad \varepsilon = \frac{4i\theta + \chi}{2\{1 - (1 + i)(2\theta)^{-1/2}\chi\}}.$$

Strictly speaking, by (21) and (24),  $\chi$  is still a function of  $\varepsilon$ . In (21) we may, however, replace  $r$  by  $\sigma$ .

In connection with the magnitude of  $\chi$ , we can distinguish two limiting cases:

I.  $\chi = 0$ , or its modulus is sufficiently small, which means that the effect of the surface film is negligible. Then  $\varepsilon = 2i\theta$ . We shall indicate this value by  $\varepsilon_1$ :

$$(29) \quad \varepsilon_1 = 2i\theta.$$

II. The modulus of  $\chi$  is sufficiently large, which means that the influence of the surface film is preponderating. Then we find a value of  $\varepsilon$  which we call  $\varepsilon_2$ :

$$(30) \quad \varepsilon_2 = \frac{1}{4}(i - 1)(2\theta)^{1/2}.$$

In terms of  $\varepsilon_1$  and  $\varepsilon_2$ , eq. (28) may be written:

$$(31) \quad \varepsilon = \frac{2\varepsilon_1 + \chi}{2 + \chi\varepsilon_2^{-1}}.$$

From eq. (28) follows that, unless  $|\chi|$  is very small,  $\varepsilon$  becomes small of the order of  $\theta^{1/2}$ . Consequently, by (27), the next approximation for  $\varepsilon$  from eq. (25) can be given:

$$\varepsilon = \frac{4i\theta(1 + \varepsilon) - (1 + i)(2\theta)^{3/2} + \chi}{2 + \varepsilon - 2\chi\{(1 + i)(1 - \varepsilon)(2\theta)^{-1/2} - 1\}},$$

where, at the right-hand side, the expression (28) may be substituted for  $\varepsilon$ .

The extra time-factor connected with  $\varepsilon$ , figuring in the expression for  $\eta$ , is, according to (10) and (24):  $e^{i\varepsilon\sigma t}$ . Thus, separating  $\varepsilon$  into a real part  $\varepsilon_r$  and an imaginary part  $i\varepsilon_{im}$ , the damping of the wave is determined by this imaginary part of  $\varepsilon$ . The decay factor for the amplitude in a time  $t$  is given by

$$(32) \quad \text{decay factor} = e^{-\varepsilon_{im}\sigma t}.$$

The amplitude is decreased to  $e^{-1} = 0.37$  in a time  $\tau$  given by  $-\varepsilon_{im}\sigma\tau = -1$ , or, introducing the wave-period  $P$ :

$$(32a) \quad P/\tau = 2\pi\varepsilon_{im}.$$

$\tau$  is called the modulus of decay. From (29), by (23), we find for the first limiting case ( $|\chi|$  very small):

$$(33) \quad \tau_1 = \frac{1}{2vk^2},$$

and from (30), by (23), for the second limiting case ( $|\chi|$  large):

$$(34) \quad \tau_2 = \left(\frac{8}{vk^2\sigma}\right)^{1/2}.$$

Table 1 and fig. 1 give the values of the different quantities for wavelengths ranging from 100 cm to 0.1 cm, for two values of the surface tension.

Comparing (30) with (29), we see that for small values of  $\theta$ ,  $\varepsilon_{2im} = \frac{1}{4}(2\theta)^{1/2}$  will become much larger than  $\varepsilon_{1im} = 2\theta$ , indicating that the rate of decay is increased by the presence of a suitable film on the water surface.

TABLE 1  
 $\nu = 0.01 \text{ cm}^2/\text{sec.}$

$T'$ $\text{cm}^2/\text{sec}^2$	$\lambda$ cm	$P$ sec	$C$ cm/sec	$V$ cm/sec	$10^4 \cdot \theta$	$\tau_1$ sec	$\tau_2$ sec	$\frac{\tau_1}{P}$	$\frac{\tau_2}{P}$
73	100	0.80	125.0	62.5	0.050	12650	160	15800	200
73	50	0.565	88.4	44.3	0.142	3160	67.5	5600	119
73	20	0.357	56.0	28.5	0.56	506	21.4	1420	60
73	10	0.249	40.1	21.1	1.56	126.5	9.0	510	36
73	5	0.169	29.5	17.9	4.26	31.6	3.70	188	22
73	2	0.086	23.3	21.6	13.5	5.06	1.05	59	12.2
73	1	0.0403	24.8	31.0	25.3	1.26	0.36	31	9.0
73	0.5	1/63	31.6	44.7	39.9	0.316	0.114	20	7.2
73	0.2	1/241	48.2	71.8	65.5	0.051	0.023	12.2	5.5
73	0.1	1/679	67.9	101.6	92.5	0.013	0.007	8.6	4.7
40	10	0.251	39.9	20.5	1.57	126.5	9.0	506	36
40	5	0.173	28.8	16.2	4.35	31.6	3.74	183	21.6
40	2	0.095	20.9	16.5	15.0	5.06	1.10	53	11.5
40	1	0.0494	20.2	22.5	31.1	1.26	0.40	26	8.1
40	0.5	1/48	24.1	32.8	52.1	0.316	0.129	15.2	6.2
40	0.2	1/180	35.9	52.8	87.4	0.051	0.027	9.1	4.8
40	0.1	1/503	50.3	75.0	125	0.013	0.008	6.4	4.0

We see, moreover, from table 1 and fig. 1 that the effect of a decrease of the surface tension  $T'$  alone is of minor importance in this respect.

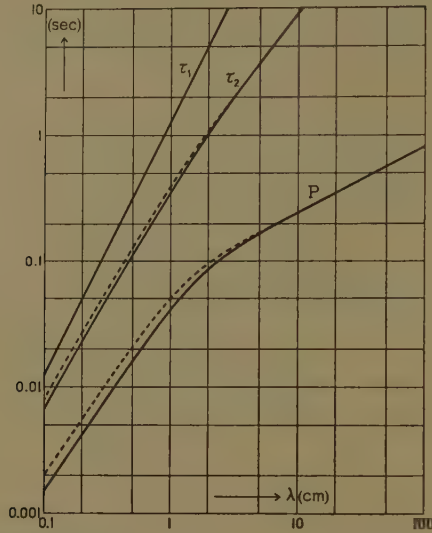


Fig. 1. Period  $P$  and moduli of decay  $\tau_1$  and  $\tau_2$  (eqs (33) and (34)) as functions of wave-length  $\lambda$ . Kinem. viscosity  $\nu = 0.01$  cm<sup>2</sup>/sec (sea water at ca. 22°, fresh water at 20.3°). Solid lines:  $T' = T/\rho = 73$  cm<sup>3</sup>/sec<sup>2</sup>, dotted lines:  $T' = 40$  cm<sup>3</sup>/sec<sup>2</sup>.

We can get an idea of the manner in which a surface film influences the fluid motion by calculating the velocities within the fluid, and especially their horizontal components. From (13), by (24), we obtain the value of  $C/A$  in terms of  $\varepsilon$ :

$$(35) \quad \frac{C}{A} = \frac{i\varepsilon(2+\varepsilon) + 2\theta(1+\varepsilon)}{1 + 2i\theta mk^{-1}(1+\varepsilon)}.$$

Using (27), and neglecting relatively small terms:

$$(36) \quad \frac{C}{A} = 2i\varepsilon + 2\theta.$$

We have always  $|C| \ll |A|$ , and in (9b) the vertical velocity  $v$  appears to be little influenced by the film. In limiting case I., by (29), we have  $C/A = -2\theta$  and, since  $km^{-1}$  is small of the order of  $\theta^{1/2}$ , here the horizontal velocity is also mainly given by the first term in (9a).

Limiting case II occurs if the modulus of  $\chi$  is very large. Then the coefficient of  $\chi$  in (22) and (25) must be zero, and using this in (13) or (35), we get exactly  $C/A = -ikm^{-1}$ , and by (9a), also exactly:  $u_s = 0$ . The wave-motion in this case is therefore characterized by a complete annulment of the horizontal velocity at the surface. Evidently, the rather small viscous shear stresses exerted by the water on the film are not sufficient then to compensate for the great reactive stresses, acting within the surface film, provoked by a noticeable extension or contraction of the surface. According to (21), the second limiting case ( $|\chi|$  large) can be actualized,



either by a small compressibility of the film, or by a large surface viscosity, or both. Fig. 2 gives vertical profiles of the horizontal velocity component in this second limiting case, for  $\theta = 0.005$  and different values of  $(\sigma t + kx)$ , computed from (9a), by putting here  $r = \sigma$ , with  $C/A = -ikm^{-1}$  and  $mk^{-1} = (1 + i)(2\theta)^{-1/2} = 10 + 10i$ .

In the text-book of LAMB (1932, Art. 351) the modulus of decay in the presence of a surface film is calculated, *starting* from the condition that

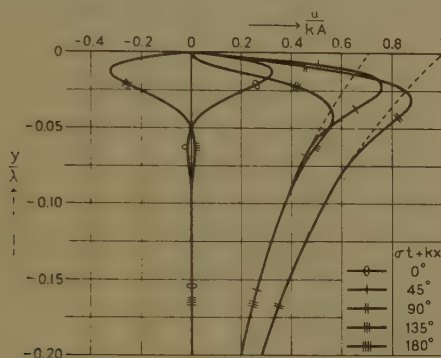


Fig. 2. Horizontal velocity component of wave on deep water with incompressible surface.  $\theta$  (eq (23)) = 0.005. For  $\sigma t + kx \approx 90^\circ$ , a trough is passing if the wave travels to the left, a crest is passing if the wave travels to the right.

Dotted lines indicate first term of eq. (9a) only.

the horizontal velocity is annulled at the surface. Thus, in stead of the second boundary condition (20), the condition  $u_s = 0$ , or, by (9a)

$$(37) \quad 0 = -ikA - mC$$

is put *a priori*. We see that (20) reduces to (37) if in (20) all terms without  $\chi$  can be neglected. Combination of the two equations (13) and (37) obviously leads to the result  $\varepsilon = \varepsilon_2$  and  $\tau = \tau_2$ , according to (30) and (34). This is the result given by LAMB. However, the conditions to be satisfied by the surface film in order that  $u_s$  be zero were not mentioned. Concerning this, there is a reference to an older edition of the book, of 1895. Here, indeed, we find a short derivation which, starting from a hypothesis concerning the behaviour of the surface tension like (18), and supposing the constant  $N$  to be sufficiently large, leads to the result  $\varepsilon = \varepsilon_2$ , and  $u_s = 0$ . The complete formulae (28) or (31) were not given. The effect of a marked surface viscosity was not yet considered.

It is still possible that the surface tension of a film as a function of the available area shows a *hysteresis*-effect, which means that for a fixed value of the surface tension, the area is different, whether a contraction, or an expansion has preceded, being smaller in the latter case, and this more or less independent of time. Such an effect has been shown to exist for several substances (see ADAM (1941) p. 56). We can take this effect readily into account by assuming that  $\delta T/\delta O$ , besides the real factor given by (18),



soon as  $\chi$  is only a little less than  $\frac{1}{2}(2\theta)^{1/2}$ , and that this remains true for all higher values of  $\chi$ . The condition  $\chi > \frac{1}{2}(2\theta)^{1/2}$ , by (21) and (23), corresponds to the condition  $N > N^*$ , with

$$(40) \quad N^* \frac{T'k^3}{\sigma^2} = \frac{1}{2} (2\theta)^{1/2} = \left( \frac{\nu k^2}{2\sigma} \right)^{1/2}.$$

Table 2 gives values of  $N^*$ . The value  $T'k^3/\sigma^2$  measures the relative importance of capillarity in the wave, according to eq. (14). We see that for all waves between 2 cm and 0.1 cm, the value  $N^*$  lies in the neighbourhood of 0.06, whereas for the longer waves where gravity more and more predominates, this value increases rapidly.

TABLE 2  
 $\nu = 0.01 \text{ cm}^2/\text{sec. } T' = 73 \text{ cm}^3/\text{sec}^2$

$\lambda$ cm	$10^2 \frac{T'k^3}{\sigma^2}$	$10^2 \left( \frac{\theta}{2} \right)^{1/2}$	$N^*$
100	0.03	0.16	5.5
50	0.12	0.27	2.3
20	0.72	0.53	0.73
10	2.84	0.88	0.31
5	10.5	1.46	0.14
2	42.2	2.60	0.06
1	74.6	3.56	0.05
0.5	92.1	4.46	0.05
0.2	98.6	5.72	0.06
0.1	99.7	6.80	0.07

Next we consider purely *imaginary* values of  $\chi$ , thus, according to (38), films with constant surface tension, but with a certain surface viscosity. Fig. 3 illustrates that in this case there is a monotonic increase of  $\varepsilon_{im}$  from  $\varepsilon_{1im}$  to  $\varepsilon_{2im}$  as the surface viscosity increases from zero to infinity. Putting  $\chi = i\alpha(2\theta)^{1/2}$  with  $\alpha$  real, we derive from (28)

$$(41) \quad \varepsilon_{im} = \frac{1+\alpha}{1+2\alpha+2\alpha^2} \varepsilon_{1im} + \frac{2\alpha+2\alpha^2}{1+2\alpha+2\alpha^2} \varepsilon_{2im}.$$

For  $\alpha = 1$ , or  $\chi = i(2\theta)^{1/2}$ , formula (41) gives:  $\varepsilon_{im} = 0.4 \varepsilon_{1im} + 0.8 \varepsilon_{2im}$ , so that here the rate of decay has exceeded 80 % of its final value. The value  $\chi = i(2\theta)^{1/2}$  corresponds, by (21) and (23), to a value  $\nu_s = \nu_s^*$  given by

$$(42) \quad \nu_s^* = \frac{(2\nu\sigma)^{1/2}}{k^2}$$

Table 3 gives some values of  $\nu_s^*$ .

TABLE 3  
 $\nu = 0.01 \text{ cm}^2/\text{sec } T' = 73 \text{ cm}^3/\text{sec}^2$

$\lambda$ cm	$\nu_s^*$ cm <sup>3</sup> /sec
100	101
10	1.80
1	0.045
0.1	0.0023

Finally,  $\chi$  will have both a real and an imaginary part if the film has 1°: a variation of surface tension with area, and 2°: either a surface viscosity or a hysteresis effect or both. In this most general case the values of  $\varepsilon$  are intermediate between the values for the two special cases already dealt with, as is illustrated in fig. 3. A hysteresis effect cannot occur without variation of surface tension, in such a way that the factor  $\xi$  in (38) probably will be always much smaller than 1, and then fig. 3 suggests that the effect of hysteresis will always be negligible in comparison with that of the slope of the  $T(O)$ -curve.

In general  $\varepsilon$  has a real part  $\varepsilon_r$  differing from zero, and of the same order as the imaginary part  $\varepsilon_{im}$ . This means that, strictly speaking, the period  $P$  of the wave is no longer given by  $2\pi/\sigma$ , where  $\sigma$  is given by (14), but by  $2\pi/\sigma(1 + \varepsilon_r)$ . Since, however,  $\varepsilon_r$  is at most of the order  $\frac{1}{4}(2\theta)^{1/2}$ , the deviation is very small.

We end this theoretical section with a remark on the decay *with distance* of a *stationary* wave. This case is obtained if we put, instead of  $k$  real, and  $r = \sigma(1 + \varepsilon)$  (equation (24)),  $r$  real, and

$$(43) \quad k = k_0(1 + \delta),$$

where  $|\delta|$  is small and  $k_0$  is a real quantity, defined by

$$(44) \quad r^2 = gk_0 + T'k_0^3.$$

If we now put in the general equation (22):  $\theta = vk^2/r$  and assume  $\theta \ll 1$ , it appears to be most convenient to put  $gk + T'k^3 = \sigma^2 = r^2(1 + \gamma)$  with  $|\gamma|$  small. Then, after collecting the principal terms in the same way as before, we find  $\gamma = -2\varepsilon$ , with  $\varepsilon$  given by (28). The relation between  $\gamma$  and  $\delta$  is given by (from (14) and (43))

$$(45) \quad 1 + \gamma = \frac{\sigma^2}{r^2} \approx 1 + \delta \frac{gk_0 + 3T'k_0^3}{r^2} = 1 + \frac{2\delta k_0 V}{r},$$

where  $V$  is the group-velocity of the undamped wave.

Consequently:  $\delta = -r\varepsilon/k_0V$ , and we have now, instead of a decay factor in time (eq. (32)), a decay factor in distance given by  $e^{\delta_{im}k_0x} = e^{\varepsilon_{im}rx/V}$ . As we have found that  $\varepsilon_{im}$  is always positive, we have a decay in the negative  $x$ -direction, which is the direction of propagation of the wave, and we can find the decay factor from the formulae for  $\varepsilon$  already given, introducing a time, obtained by dividing the distance  $x$  by the group velocity  $V$ . This result could be expected.

(To be continued.)



# INFLUENCE OF ORGANIC COMPOUNDS ON SOAP AND PHOSPHATIDE COACERVATES. XVI <sup>1)</sup>

## EXPERIMENTS ON THE DISTRIBUTION OF ORGANIC MOLECULES IN OLEATE MICELLES. I

BY

H. L. BOOIJ AND P. J. VAN MULLEM \*) <sup>2)</sup>

(Communicated by Prof. H. G. BUNGENBERG DE JONG at the meeting of May 26, 1951)

### 1. *Introduction*

The experiments on the influence of organic compounds on oleate coacervates show that these compounds may be divided in two classes. Some compounds shift the concentration of KCl needed to give a coacervate volume of 50 % to higher values (this has been called a KCl-demanding action), other organic substances have a reverse action (KCl-sparing) <sup>3)</sup>. The experiments in this field have been continued for two reasons:

1. the oleate coacervate is supposed to be a useful model for amphipatic structures in the living cell (e.g. lipoid membranes) and
2. to gain some (indirect) information on the structure of soap micelles.

So far the experiments have suggested that the division of organic substances in KCl-sparing and KCl-demanding compounds is only a provisional one. For the difference between long alcohols (KCl-sparing action) and long fatty acid anions (KCl-demanding action) a plausible explanation has been given. It has been suggested that these compounds will be found in the oleate micelles parallel to the soap molecules, with their polar groups towards the water medium. As the oleate micelle is a result of two opposing forces (Coulomb forces between the charged carboxyl groups of the oleate molecules and LONDON-VAN DER WAALS forces between the hydrocarbon chains), it must be supposed that introduction of a foreign molecule (ion) between the soap molecules will disturb this equilibrium. In the case of fatty acid anions the Coulomb forces will increase (without — e.g. in the case of added laurate — a corresponding

---

\*) Aided by grants from the "Netherlands Organization for Pure Research (Z.W.O.)".

<sup>1)</sup> Publication no. XV of this series will be found in Proc. Kon. Ned. Akad. Wetensch. Amsterdam, 53, 1413 (1950).

<sup>2)</sup> Publication no. 14 of the Team for Fundamental Biochemical Research (under the direction of H. G. BUNGENBERG DE JONG, E. HAVINGA and H. L. BOOIJ).

<sup>3)</sup> For a summary of older experiments see e.g. BOOIJ (1949), page 701.

increase of the LONDON-VAN DER WAALS forces). Then more KCl will be required to produce coacervation (KCl-demanding action). The addition of a long alcohol will, on the other hand, result in an increase of the LONDON-VAN DER WAALS forces (depending on the length of the carbon chain of the alcohol), and an important decrease of the Coulomb forces, as the "heads" of some oleate ions will be brought somewhat farther apart. Then a KCl-sparing action will be noticed (BOOIJ et al. 1950 *a*).

Other KCl-demanding substances do not fit into this scheme. Especially the strong KCl-demanding activity of long paraffins is noteworthy (BOOIJ et al. 1950 *b*). As the oleate micelle is a relatively intricate structure, added organic substances have in principle several "points of attack". Basing ourselves on the work of HESS et al. (1941), who showed that benzene may be taken up in a soap micelle between the  $\text{CH}_3$  end groups of the fatty acid chains (thus forming a "sandwichmicelle") we supposed that aliphatic paraffins were taken up in the same manner. Then for an unknown reason this would result in a KCl-demanding action.

Generally speaking, an organic substance when added to a soap system may be found at three places: *a*) in the medium (practically no influence on coacervation), *b*) parallel to the soap molecules in the micelle (the substances are then anchored to the medium — water — by virtue of their polar groups and the nature of these groups determines the kind of action) and *c*) in between the  $\text{CH}_3$ -planes of the micelle (presumably resulting in a KCl-demanding action). The amount of substance present at these respective places will depend on the strength and number of the polar (hydrophilic) groups as compared with the apolar parts of the molecule. In the homologous series of the alcohols the first members are very soluble in water and will be found in the oleate micelles only at very high concentrations. With increasing length of the carbon chain ever more of the added alcohol is found in the micelle. The alcoholic OH group is still so strongly polar, however, that even long alcohols (e.g. myristic alcohol) seem to be orientated parallel to the soap molecules in the micelle.

In the homologous series of the alkyl-benzenes, however, the first members are only slightly soluble in water, and will concentrate in the micelles consequently. If the alkyl chain is lengthened the compounds develop an ever increasing KCl-demanding action (just like the paraffins) and it has been suggested that the partition of the substance between the two possible places in the micelles shifts in favour of the place between the  $\text{CH}_3$ -planes.

Thus it seems that when adding an organic substance to an oleate coacervate we are dealing with two partition equilibria: *a*) water-micelle and *b*) parallel to the soap molecules — between the  $\text{CH}_3$ -planes in the micelles. In the investigations reported here the latter partition equilibrium has had our attention. We have tried to study this along the following lines. First we measured the action of an organic compound on an oleate coacervate. Then we repeated the experiment with increasing amounts

of a substance, known to concentrate in the micelle only parallel to the soap molecules (e.g. amylalcohol). We expected that the partition equilibrium would be influenced by this procedure. When the substance studied concentrates parallel to the soap molecules, it would be expected that the salt-sparing activity decreases as a result of a "competition" between the substance studied and the added amylalcohol. On the other hand a substance which is originally found between the  $\text{CH}_3$ -planes of the micelle might get some opportunity to find a place parallel to the soapmolecules, when amylalcohol is added. The reason for this is that the amylalcohol cannot fill up the whole space between the soap molecules. The holes in the micelle structure might be filled then with apolar molecules. This might eventually lead to a reversal in the kind of action: a KCl-demanding substance showing a KCl-sparing activity after the addition of amylalcohol.

## 2. *The influence of alcohols on the activity of apolar and polar organic substances*

In the preceding section it has been supposed that apolar and polar organic substances will show a different behaviour — as regards their action on a soap coacervate — when amylalcohol is added to the system. First of all we tried to show this difference for two substances: decane and octylalcohol.

We employed the following method. We made a solution of Na-oleate containing:

$$\left. \begin{array}{l} 20 \text{ g Na-oleate } ^1) \\ 120 \text{ ml KOH } 2 \text{ n} \\ 980 \text{ ml H}_2\text{O} \end{array} \right\} \text{ solution A}$$

Then a series of tubes (with ground glass stoppers) with increasing concentrations of KCl was prepared and put in a thermostat of  $25^\circ \text{C}$ , according to the following scheme:

$$\left\{ \begin{array}{l} x \text{ ml KCl } 3.8 \text{ n} \\ (6.5-x) \text{ ml H}_2\text{O} \\ 3 \text{ ml oleate solution A.} \end{array} \right.$$

After thoroughly shaking the tubes are left in the water bath till the following morning. In high KCl concentrations a coacervate is formed (beginning at approximately 1.6 n KCl), the volume of which is plotted against the KCl concentration. The concentration required for a coacervate volume of 50 % is read off the resulting curve.

If we wish to find the action of *n*-decane a small amount of this substance is weighed in an erlenmeyer flask and 25 ml of solution A is added. With the resulting solution (decane dissolves difficultly in a soap solution) the same experiment is performed with increasing concentrations of KCl.

<sup>1)</sup> We are much indebted to The Rockefeller Foundation for a generous gift of Na-oleate.

The amount of KCl, required for a coacervate volume of 50 % will generally be found at a higher value. This shift of the KCl concentration has been taken as a measure of the action of decane and is plotted against the concentration of decane (fig. 1, blank).

In a previous investigation it was made clear that the action of alcohols increases with increasing number of carbon atoms (BOOIJ et al. 1950 *a*). For the first members of this homologous series this increasing activity is readily explained by a shift in the partition equilibrium of the alcohol between the micelle and the surrounding water. With increasing length of the carbon chain ever more is taken up in the micelle (parallel to the soap molecules, as the alcohol will remain "anchored" to the water by its polar group).

We now investigated the influence of some alcohols on the decane curve. In some flasks a constant volume of alcohol was pipetted <sup>1)</sup>, after which we added small amounts of decane. Then we poured in every flask

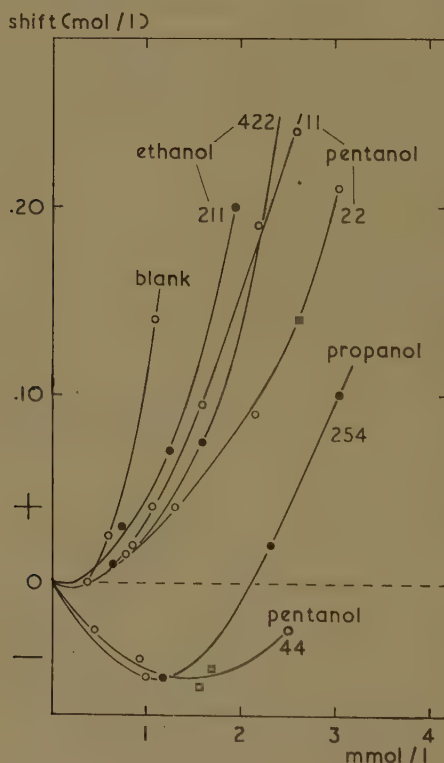


Fig. 1. The action of *n*-decane on an oleate coacervate (the activity is given as the shift of the KCl-concentration required for a coacervate volume of 50 %). The action of *n*-decane was measured after the addition of various alcohols at various concentrations (the numbers attached to the curves give the concentrations of the respective alcohols in mmol/l). Abscissa = concentration of *n*-decane.

<sup>1)</sup> The small amount of amylalcohol was added with the aid of a dripping pipette (BUNGENBERG DE JONG et al. 1949).



25 ml of solution A and measured the KCl coacervation curves in the usual way. As the alcohols themselves have an influence on the KCl concentration required, we must take as a blank the solution A to which the same concentration of alcohol is added. We see (fig. 1) that each alcohol influences the decane curve in the same direction, though the influence of the alcohols grows much higher with increasing chain length. This is exactly what would be expected, as only the amount of alcohol taken up in the micelle is of importance for the action.

The experiments with other organic substances were performed only with amylalcohol (fermentation amylalcohol). When we investigate the influence of *n*-octanol on an oleate coacervate, we see that here amylalcohol has a reverse action (fig. 2). With increasing amounts of amyl-

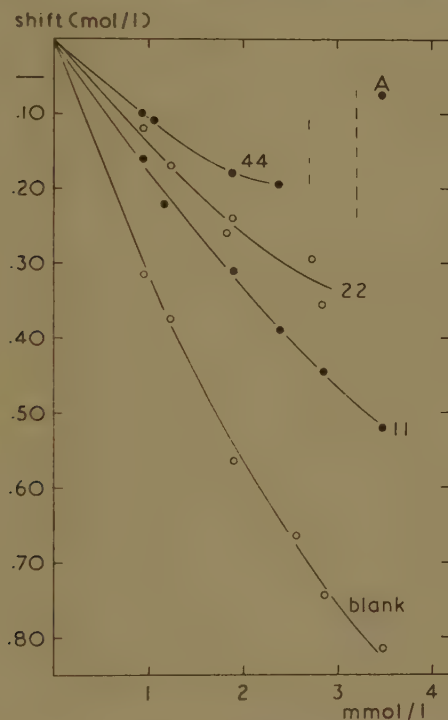


Fig. 2. Octylalcohol has a strong KCl-sparing influence on the oleate coacervate, which influence is decreased by the addition of amylalcohol (added at concentrations of 11, 22 and 44 mmol/l). A = presumably a P-coacervate appearing at high concentrations of amyl- and octylalcohol. Abscissa = concentration of octylalcohol.

alcohol the salt-sparing action of octanol diminishes markedly. At a constant concentration of 44 mmol/l amylalcohol we find at a concentration of approximately 2.5 mmol/l octanol that coacervation is no longer obtained. Many floccules appear in the tubes. At higher octanol concentrations (3.5 mmol) a coacervate is formed once more. Presumably this coacervate is not of the ordinary type, but belongs to the so called *P*-coacervates (see BUNGENBERG DE JONG et al. 1949).

The result of these preliminary experiments was that organic substances may be classified into two types, which we will provisionally call the apolar and the polar type. With the apolar type the action shifts under the influence of added amylalcohol from KCl-demanding to KCl-sparing, with the polar type the shift goes in the other direction. It must be possible with this method to control if the hypotheses regarding the action of organic compounds of several homologous series — framed in previous publications — are true.

### 3. *Aliphatic paraffins*

In the homologous series of the normal paraffins a very remarkable shift has been found by BOOIJ et al. (1950 *b*). Short paraffins have a KCl-sparing activity, but longer paraffins show an ever stronger KCl-demanding action. A comparison with other organic molecules leads to the assumption that short hydrocarbons will be found in the outer regions of the micelles, and that the longer the carbon chain, the more the paraffins tend to concentrate in the inner regions of the micelles (between the  $\text{CH}_3$ -planes). It is far from clear why this would be the case. We framed an *ad hoc* hypothesis, in which it was supposed that short hydrocarbons concentrate at the curved end of the micelles. If these hypotheses were true, it would be found that amylalcohol will make the longer paraffins relatively more KCl-sparing, while the shortest paraffins (e.g. pentane) will get a more KCl-demanding activity. We have already seen that *n*-decane shows the expected behaviour. In fig. 3 we have drawn the curves of the experiments with some members of this homologous series. In some cases it was very difficult or impossible to measure the blank curve. It is obvious, however, that all normal paraffins from heptane upwards show the same character. In every case a strong influence of added amylalcohol is observed. This must in our opinion be explained as a shift of the partition equilibrium within the micelles to the place parallel to the soap molecules.

With *n*-hexane the influence of amylalcohol is only weak. *N*-pentane (fig. 4) shows after addition of amylalcohol a relatively more KCl-demanding character. From these experiments we conclude that our original hypothesis might be true. The influence of amylalcohol is in agreement with the supposition that pentane is relatively more concentrated in the outer regions of the micelles than the longer paraffins.

A closer study of our experiments reveals a peculiar fact. If we compare the action of the paraffins after addition of 11 mmol amylalcohol we see that the curves are not evenly distributed over the graph, but that we always find together a member with an even number of carbon atoms and the adjacent one with an odd number (fig. 5). The only exception of this rule is pentane, which substance behaves abnormally in other respects too (compare figs. 3 and 4). The situation reminds us of the melting points of the paraffins which are also found together in pairs (table I).

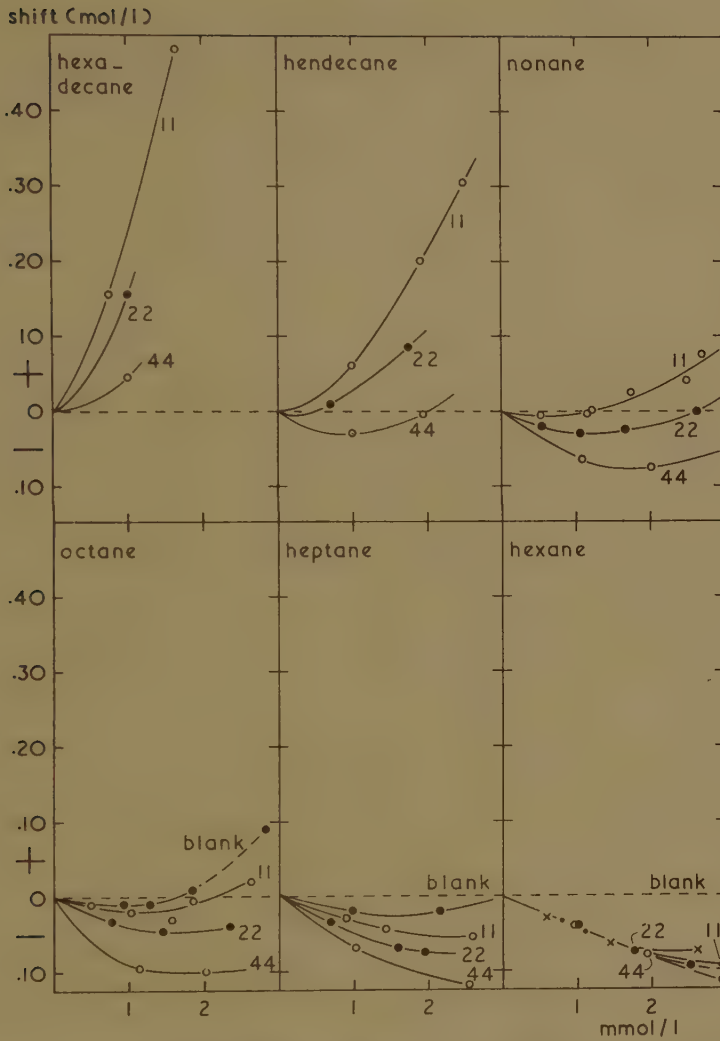


Fig. 3. The action of the normal paraffins under the influence of amylalcohol (concentrations 11, 22 and 44 mmol/l).

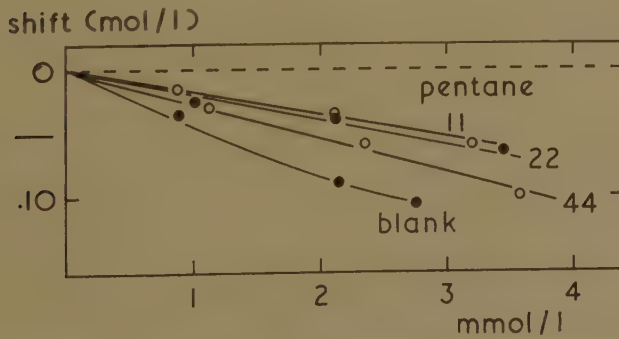


Fig. 4. The influence of amylalcohol on the action of *n*-pentane is abnormal when compared to the longer paraffins.

TABLE I  
Melting points of paraffins (Schoorl, 1935)

<i>n</i> pentane	— 130° C
<i>n</i> hexane	— 95,3° C )
<i>n</i> heptane	— 90,6° C )
<i>n</i> octane	— 57° C )
<i>n</i> nonane	— 53,7° C )
<i>n</i> decane	— 29,7° C )
<i>n</i> hendecane	— 25,6° C )

As the melting points are much lower than the temperature at which the experiments were performed, it seems far fetched to suppose that the paraffins “crystallize” in the micelles. We are inclined to give the following explanation of this phenomenon. We assume that the soap molecules when associated into a micelle may not be seen as an ordinary liquid. On the other hand we agree with STAUFF (1939) that soap micelles may not be regarded as crystalline structures. They seem to be liquid

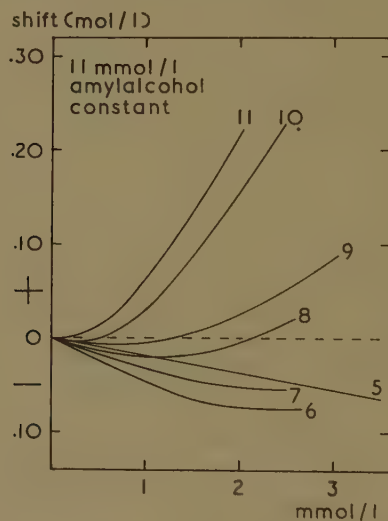


Fig. 5. If we compare the influence of a constant concentration of amylalcohol on the action of the normal paraffins (the numbers denote the number of carbon atoms in the chain), it is seen that the curves lie together in pairs.

structures in which some “crystallinity” is retained. Then a difference in action between odd and even numbered members of a homologous series might be expected. If this hypothesis is true we may go one step further. When the concentration of amylalcohol grows higher (44 mmol) the phenomenon is no longer seen clearly. This would perhaps mean that at high amylalcohol concentrations the micelles begin to lose the rest of their “crystallinity”.

It had been found (BOOLJ et al. 1950 *b*) that various isomers of a paraffin do not influence the oleate coacervate in the same manner. Up till now



it has not been possible to find an explanation of these different actions. Our previous experiments with these isomers had been done after the addition of propylalcohol. After the study of the influence of alcohols on the action of e.g. decane the question was raised whether the differences described might be the result of this added propylalcohol. We have now studied the influence of various isomers of octane after the addition of amylalcohol. Two examples are given in fig. 6. We see that 3,4-dimethylhexane is much less influenced than 2,2,3-trimethylpentane.

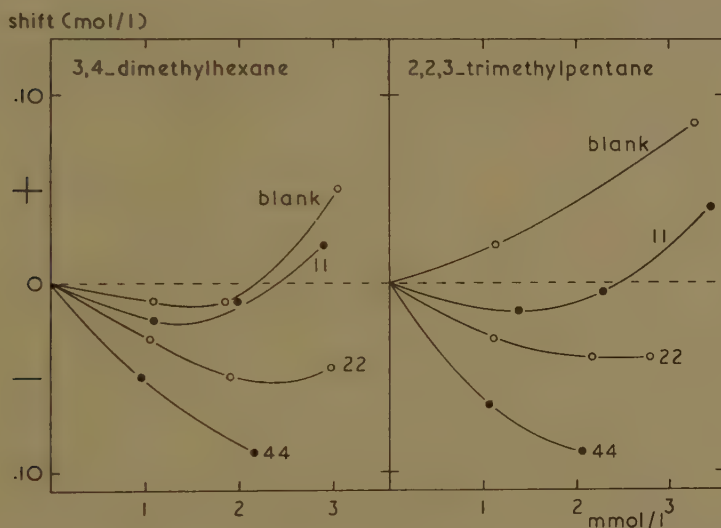


Fig. 6. With two isomers of octane the influence of amylalcohol (concentrations 11, 22 and 44 mmol/l) differs somewhat.

In fig. 7 the results of our experiments with various octanes have been drawn. We plotted the shift of the KCl concentration caused by the isomers (in a concentration of 1 mmol/l) against the concentration of the amylalcohol added. All isomers are influenced in the same direction, but the order of the series does not remain the same. Thus the strongest KCl-demanding member of the series in the blank experiment (2,2,3-trimethylpentane) proves to be the strongest KCl-sparing substance when a high concentration of amylalcohol is added.

From fig. 1 we would deduce that the amount of propylalcohol used in our previous experiments ( $\pm 150$  mmol/l) would have an influence comparable to an amylalcohol concentration between 22 and 44 mmol/l. The series then reported does in fact lie between the last two of fig. 7. So we may conclude that the action of these isomers is dependent on the structure of the micelles, which may be gradually altered by the addition of alcohols. The differences between the various isomers are, however, relatively slight. Even the derivatives of *n*-pentane do not resemble the parent molecule.

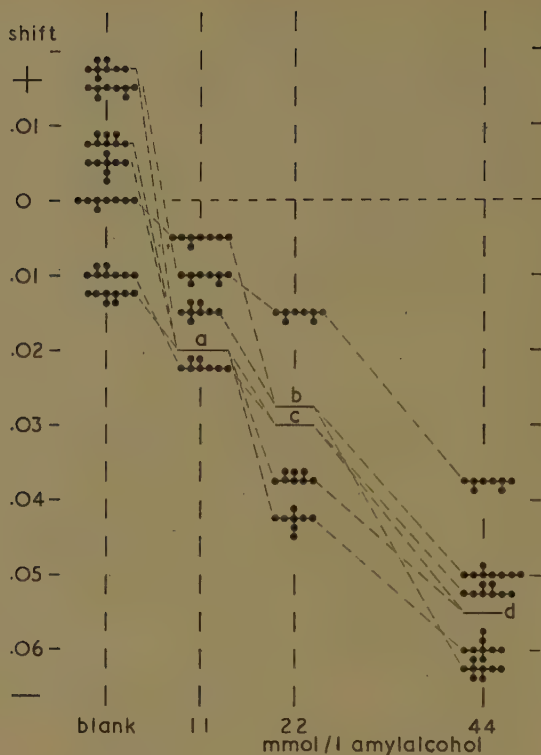


Fig. 7. The action of diverse isomers of octane with increasing amounts of amylalcohol have been studied.

From curves like those in fig. 6 the shifts in KCl concentration caused by the isomers at a concentration of 1 mmol/l were read. These shifts were plotted against the amylalcohol concentration. It is seen that the action of some isomers is much more influenced by amylalcohol than that of others.

At level *a* we find: 2, 3, 4-trimethylpentane, 3-methylethylpentane and 3, 4-dimethylhexane.

At level *b*: 3-methylheptane and 2, 2, 3-trimethylpentane.

At level *c*: 3, 4-dimethylhexane and 2, 3-dimethylhexane.

At level *d*: 2, 3-dimethylhexane and 2, 3, 4-trimethylpentane.

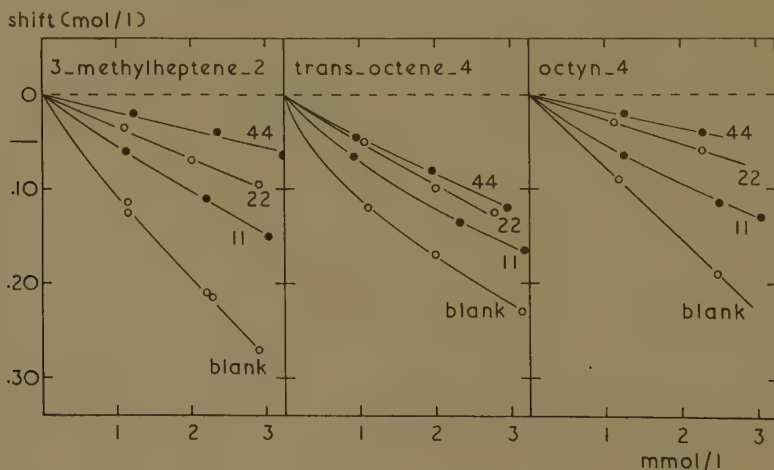


Fig. 8. The influence of unsaturated groups in paraffins is clearly demonstrated by the action of amylalcohol (11, 22 and 44 mmol/l). Note that the curves shift in the other direction as compared with those of normal paraffins (fig. 3).

When a double or triple bond is introduced into a paraffin we find a very marked influence on its activity (BOOIJ et al. 1950 *b*). A strong salt-sparing activity is the result, which would be expected indeed as this polar group will be anchored to the watery medium. Then the action of amylalcohol must be the reverse of its action on saturated paraffins. Three examples of this type of substances have been studied. We compared 3-methylheptene-2 (fig. 8) with 3-methylheptane (fig. 7). Amylalcohol has a strong influence in both cases, but the influence acts in different directions. The same proves to be true for transoctene-4 and octyn-5 when compared with octane (fig. 3). We are inclined to accept these experiments as a strong argument for our hypothesis that apolar and polar substances have totally different partition equilibria in soap micelles.

*(To be continued)*

# INFLUENCE OF ORGANIC COMPOUNDS ON SOAP AND PHOSPHATIDE COACERVATES. XVI <sup>1)</sup>

## EXPERIMENTS ON THE DISTRIBUTION OF ORGANIC MOLECULES IN OLEATE MICELLES. II

BY

H. L. BOOIJ AND P. J. VAN MULLEM \*) <sup>2)</sup>

(Communicated by Prof. H. G. BUNGENBERG DE JONG at the meeting of May 26, 1951)

### 4. *A comparison between some aromatic and aliphatic molecules*

A study of the action of naphtalene, tetrahydronaphtalene and decahydronaphtalene had lead to the hypothesis cited above (BOOIJ, 1949 *b*). There is a remarkable discrepancy between the action of hydrogenated derivatives of naphtalene acetic acid on the one hand and hydrogenated derivatives of naphtalene on the other. BOOIJ and VELDSTRA (1949) found that the decahydro-derivative of naphtalene acetate has a much stronger activity than naphtalene acetate itself. This was readily explained by the assumption that the decahydroderivative was taken up more readily into the soap micelles.

The surprising fact that decalin has a smaller activity than naphtalene was then explained by BOOIJ (1949 *b*). Naphtalene is more polar than decalin and the partition equilibria of the two substances in the micelle will be different. Decalin will partly be present between the CH<sub>3</sub>-planes of the micelle. It seemed to us that this question too might be attacked with the aid of the "amylalcohol method".

The experiments have given a clear answer. The influence of amylalcohol on the action of decahydronaphtalene is the reverse of that on the action of tetrahydronaphtalene and naphtalene (fig. 9). It seems, however, that decahydronaphtalene has a kind of intermediate position between the so called polar and apolar types of substances. It is remarkable that there is no difference between the curves for the various concentrations of amylalcohol.

When BOOIJ et al. (1950 *c*) measured the action of naphtalene and its decahydro-derivative, they found only a small difference in action. The experiments described here make this small difference understandable.

\*) Aided by grants from the "Netherlands Organization for Pure Research (Z.W.O.)".

<sup>1)</sup> Part I of this article will be found in Proc. Kon. Ned. Akad. Wetensch. Amst. C 54, 273, (1951).

<sup>2)</sup> Publication no. 14 of the Team for Fundamental Biochemical Research (under the direction of H. G. BUNGENBERG DE JONG, E. HAVINGA and H. L. BOOIJ).



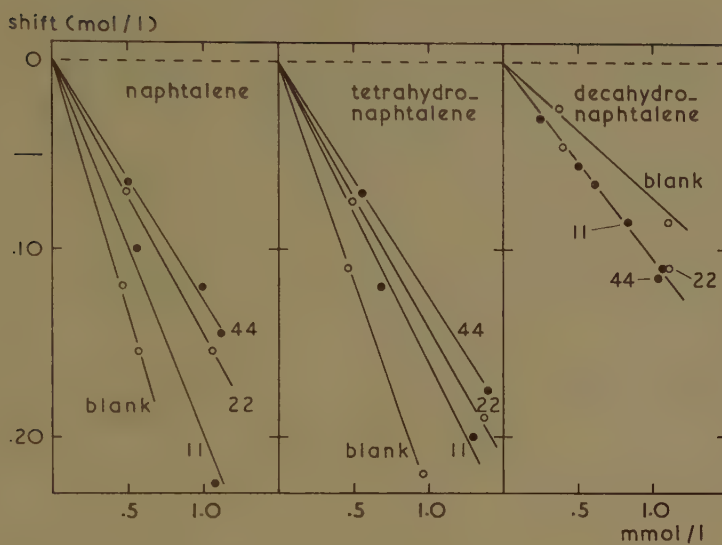


Fig. 9. Experiments with hydrogenated derivatives of naphthalene reveal a striking difference between the decahydro-derivative on the one hand and the tetrahydro-derivative and the parent substance on the other (concentration of amylalcohol 11, 22 and 44 mmol/l).

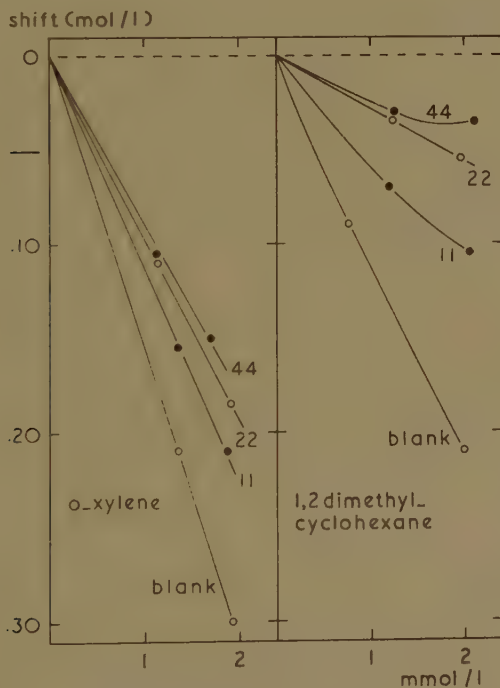


Fig. 10. The influence of amylalcohol on the action of o-xylene and dimethyl-cyclohexane.

They used propylalcohol to dissolve the hydrocarbons. This alcohol will have the same influence as amylalcohol. Thus the naphtalene curve is shifted towards a smaller KCl-sparing activity, while the decalin curve shifts in the other direction. Then the difference in action will be only very small. This once more elucidates the fact that the action of organic molecules on soap coacervates depends very much on the state of affairs in the micelles.

A comparison between *o*-xylene and 1,2-dimethylcyclohexane showed even that a short hydroaromatic molecule (fig. 10) may resemble a "polar type" molecule. Here, the situation reminds one of the action of *n*-pentane. *O*-xylene has a strong KCl-sparing action, which action is decreased somewhat by amylalcohol. The influence of amylalcohol on the action of 1,2-dimethylcyclohexane is much stronger. This is in agreement with the difference in polarity of the two molecules.

### 5. The homologous series of the alkylbenzenes

In the alkylbenzenes we find a combination of a weakly polar group and an apolar chain. As the chain is lengthened the substance will get a more apolar character. This is demonstrated by the action of the members of this homologous series on an oleate coacervate (Booij et al. 1950 c). The short molecules have a pronounced KCl-sparing activity, cetylbenzene was KCl-demanding and heptylbenzene showed a KCl-sparing activity at low and a reverse action at high concentrations.

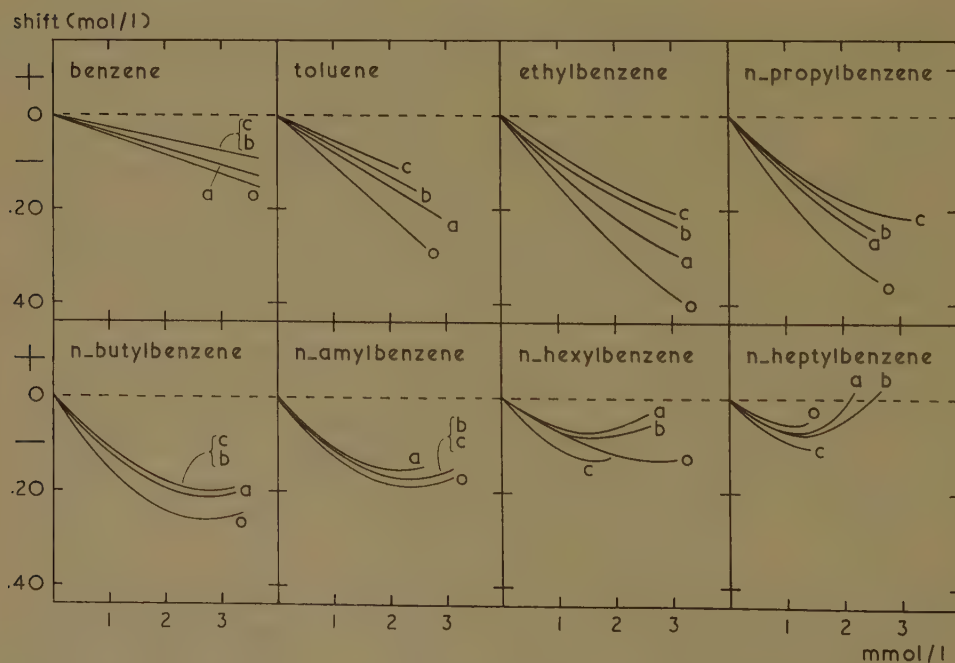


Fig. 11. A comparison of a series of *n*-alkylbenzenes (0 = blank, *a* = 11 mmol/l amylalcohol, *b* = 22 mmol/l amylalcohol, *c* = 44 mmol/l amylalcohol).

We had at our disposal the complete series from benzene up to heptylbenzene <sup>1)</sup>. Fig. 11 gives a survey of our experiments with this group of substances. If we compare, first of all, the blank curves, it is observed that the KCl-sparing activity first increases, which is followed, after *n*-propylbenzene, by a decrease. This homologous series provides a fine example of the two partition equilibria. Benzene is more soluble in water than toluene and thus a noticeable amount of benzene will not enter the micelle. In our case approximately one half of the molecules will remain outside the micelle (see BOOIJ et al. 1950 c). In the case of toluene the partition equilibrium water — micelle shifts in favour of the micelle and we get consequently a stronger KCl-sparing activity. In addition to this we get a shift in the same direction as the molecule is one carbon atom longer (compare the increase in action when we go e.g. from decylalcohol to undecylalcohol). This results in a steady increase of action up to *n*-propylbenzene.

From *n*-butylbenzene upwards the partition equilibrium within the micelles appears to change. The KCl-sparing action decreases again in the same manner as we have already noticed for the normal paraffins.

The study of the influence of amylalcohol is once more in agreement with the hypotheses put forward. Up till *n*-butylbenzene the KCl-sparing action of the substances grows less under the influence of amylalcohol. *N*-heptylbenzene behaves in the reverse manner. Clearly, *n*-amylbenzene and *n*-hexylbenzene take an intermediate position. Thus we might conclude that *n*-heptylbenzene is found for the greater part between the CH<sub>3</sub>-planes of the micelles. On the other hand the greater part of *n*-butylbenzene presumably is found parallel to the soap molecules. The difference between *n*-propylbenzene and *n*-butylbenzene proves that the shift in the partition equilibrium has already started with the latter substance.

We have also studied the action of two branched alkylbenzenes (fig. 12).

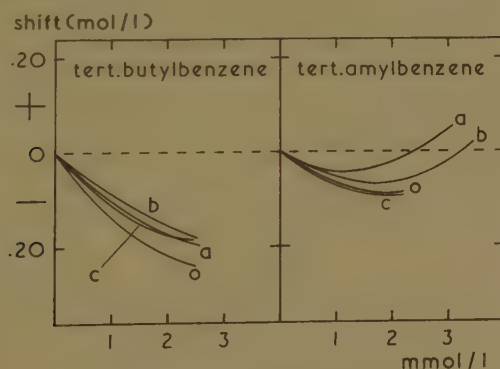


Fig. 12. The influence of amylalcohol (concentrations see fig. 11) on the action of two tert. alkylbenzenes.

<sup>1)</sup> Here we want to thank Mr. J. H. F. BAAK who made several of the compounds required.

In both cases the normal alkylbenzenes (fig. 11) have a stronger action than the branched isomers. This is a well known phenomenon in this field. As regards the influence of amylalcohol, tert.-butylbenzene resembles *n*-amylbenzene and the same may be said of tert.-amylbenzene and *n*-hexylbenzene. This must mean that with tert.-butylbenzene the partition equilibrium is shifted somewhat to the place between the CH<sub>3</sub>-planes in the molecules (as compared with *n*-butylbenzene). Here we have perhaps found a typical difference between the two partition equilibria. With the partition equilibrium water-micelle a branched organic molecule resembles a similar molecule with a lower number of carbon atoms. On the other hand a branched molecule tends to act like a substance with a higher number of carbon atoms if the partition equilibrium within the micelles is involved. In our opinion these two facts may be explained with the hypothesis that normal chains fit best in the orderly structure of the soap molecules in the micelles. They will, therefore, be more concentrated parallel to the soap molecules than branched chains. In the case of the latter molecules the partition equilibrium is shifted, be it to the water or to the place between the CH<sub>3</sub>-planes. Naturally, the direction of this shift is dependent on the presence of polar groups in the molecules.

#### 6. Hexylbromide

If we introduce a bromine atom into *n*-hexane the resulting compound gets a strong KCl-sparing activity as compared with the parent substance (BOOIJ et al. 1950 *d*). This is a general feature of halogen derivatives of apolar substances. We have explained this fact by assuming that the molecule is held parallel to the soap molecules by virtue of its weakly polar group. In this respect *n*-hexylbromide may be compared with *n*-hexylbenzene, though the action of the former substance is much stronger. We expected that the influence of amylalcohol would be stronger too. This proved to be the case (fig. 13). *N*-hexylbromide is influenced like

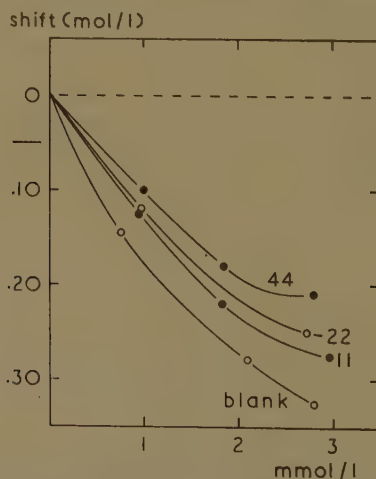


Fig. 13. The influence of amylalcohol on the action of *n*-hexylbromide.



other "polar" substances (compare octylalcohol, fig. 2). As *n*-hexylbenzene takes an intermediate position we must conclude that the bromine atom is more hydrophilic than the benzene nucleus.

This investigation has been made possible thanks to a generous gift of a number of paraffins from the Koninklijke/Shell Laboratory, Amsterdam.

### Summary

1. Long apolar organic molecules (e.g. paraffins) have a different action on oleate coacervates than long organic molecules with a polar group (e.g. alcohols). It has been suggested that the difference in action is caused by a difference in distribution within the micelles, the alcohols concentrating preferentially between the parallel soap molecules, the paraffins going mostly to the place between the CH<sub>3</sub>-planes in the micelles.

2. To test this hypothesis the influence of amylalcohol on the action of many organic molecules has been investigated. Two types could be distinguished: an "apolar" type, which becomes less KCl-demanding and a "polar" type which becomes more KCl-demanding after the addition of amylalcohol (figs. 1 and 2).

3. The hypothesis that in the series of normal paraffins a shift in the partition equilibrium within the micelles takes place could be substantiated by our experiments with amylalcohol. *n*-Pentane shows an abnormal character and *n*-hexane takes an intermediate position.

4. The introduction of a double or triple bond in a longer paraffin has a great influence. The substance changes from an "apolar" to a "polar" type.

5. Decalin seems to belong to the "apolar" type of molecules, while naphthalene is a "polar" molecule. Their activity is influenced by amylalcohol in different directions.

6. In the series of alkylbenzenes we find a combination of an "apolar" and a "polar" group. If the carbon chain is lengthened the substances will ever more resemble the normal paraffins. So we see that *n*-heptylbenzene has the "apolar" type, while *n*-amyl- and *n*-hexylbenzene take intermediate positions. The shorter alkylbenzenes have a "polar" character.

7. With *n*-hexylbromide the polar character is very pronounced. From this we might conclude that the bromine atom is more hydrophilic than the benzene nucleus.

### L I T E R A T U R E

1. BOOIJ, H. L., in KRUYT's Colloid Science II, (Elsevier, Amsterdam), Chapter XIV (1949).
2. ———, Proc. Kon. Ned. Akad. v. Wetensch. Amst. **52**, 1100 (1949b).
3. ———, C. J. VOGELSANG and J. C. LYCKLAMA, Proc. Kon. Ned. Akad. v. Wetensch. Amst. **53**, 59 (1950a).

4. ———, ——— and ———, Proc. Kon. Ned. Akad. v. Wetensch. Amst. **53**, 407 (1950*b*).
5. ———, ——— and ———, Proc. Kon. Ned. Akad. v. Wetensch. Amst. **53**, 882 (1950*c*).
6. ———, ——— and ———, Proc. Kon. Ned. Akad. v. Wetensch. Amst. **53**, 1413 (1950*d*).
7. ——— and H. VELDSTRA, Bioch. et Bioph. Acta **3**, 260 (1949).
8. BUNGENBERG DE JONG, H. G. and L. J. DE HEER, Proc. Kon. Ned. Akad. v. Wetensch. Amst. **52**, 783 (1949).
9. HESS, K., H. KIESSIG and W. PHILIPPOFF, Fette und Seifen, **48**, 377 (1941).
10. SCHOORL, N., Organische analyse I, (Amsterdam 1935).
11. STAUFF, J., Kolloid-Z. **89**, 224 (1939).

ELASTIC-VISCOUS OLEATE SYSTEMS CONTAINING KCl. XVII <sup>1)</sup>

1. Dependence of  $a$ ,  $b$ ,  $e$  and  $f$  in the formula  $\sqrt{G} = a (C_{\text{oleate}} - b)$  and  $n = e (C_{\text{oleate}} - f)$  on the KCl concentration and the temperature

2. Explanation of the typical S-shape of the  $G$ - $C_{\text{KCl}}$  curve at constant oleate concentration

BY

H. G. BUNGENBERG DE JONG, W. A. LOEVEN \* and W. W. H. WEYZEN \*) <sup>2)3)</sup>

(Communicated at the meeting of May 26. 1951)

## 1. Introduction

Hitherto studying the influence of parameters on the elastic behaviour we have kept the oleate concentration constant (practically always 1.2 %).

Fig. 1 gives schematically the dependence of  $G$ ,  $1/\Lambda$  and  $n$  on the KCl concentration (compare part VI of this series).

The other parameters (temperature, pH, added organic substances, substitution of K or Cl in KCl by other cations or anions) have been studied by investigating how they affect the  $G$ ,  $1/\Lambda$  and  $n$  curves in fig. 1.

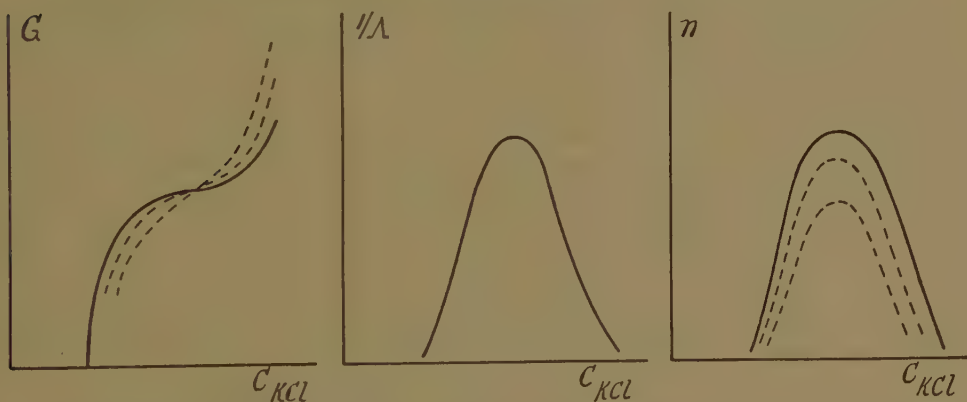


Fig. 1. General character of the dependence of  $G$ ,  $1/\Lambda$  and  $n$  on the KCl concentration at constant oleate concentration (schematically). The influence of increase of the temperature is given by dotted curves.

\*) Aided by grants from the "Netherlands Organization for Pure Research (Z.W.O.)".

<sup>1)</sup> Part I has appeared in these Proceedings 51, 1197 (1948); Part II–VI in these Proceedings 52, 15, 99, 363, 377, 465 (1949); Part VII–XIV in these Proceedings 53, 7, 109, 233, 743, 759, 975, 1122, 1319 (1950); Part XV–XVI in these Proceedings 54, Series B, 1, 240 (1951).

<sup>2)</sup> Publication No. 15 of the Team for Fundamental Biochemical Research (under the direction of H. G. BUNGENBERG DE JONG, E. HAVINGA and H. L. BOOIJ).

<sup>3)</sup> A generous gift of Na-oleate from the ROCKEFELLER Foundation provided the means for the experiments described in this paper.

It was found (parts VI—XIII) that in principle these parameters do not alter the characteristic shape of the curves, though they may shift them in various ways. The dotted curves in fig. 1 give for instance the influence of an increase of the temperature. In this way a convenient survey of the influence of various parameters on the elastic behaviour at constant oleate concentration has been obtained.

Up to now we had no point of attack for the problem how to explain the typical shapes of the  $G - C_{\text{KCl}}$  curves (S-shaped) and the  $1/\lambda - C_{\text{KCl}}$  and  $n - C_{\text{KCl}}$  curves (curves with a maximum). The results in the preceding part XVI, however, show the way how this problem must be handled.

It appeared that quite generally the  $\sqrt{G} - C_{\text{oleate}}$  curve and the lower parts of the  $1/\lambda - C_{\text{oleate}}$  curve and of the  $n - C_{\text{oleate}}$  curve are straight lines intersecting the abscissa at a finite, though small, oleate concentration. Each of the three linear functions is therefore characterized by the slope of the straight line and the part cut off from the abscissa. The two latter are only numerical constants for a given KCl concentration and temperature, but may assume other values when these parameters are varied.

For the shear modulus for instance the formule  $\sqrt{G} = a (C_{\text{oleate}} - b)$  applies. It follows that a change in  $G$ , brought about at constant oleate concentration by varying a parameter (e.g. the KCl concentration as in fig. 1), is not directly accessible for an explanation. For, the change in  $G$  may have been the result of a change in the proportionality factor  $a$ , or of a change in  $b$  (the oleate concentration not taking part in the elastic behaviour), or of a change in both  $a$  and  $b$ .

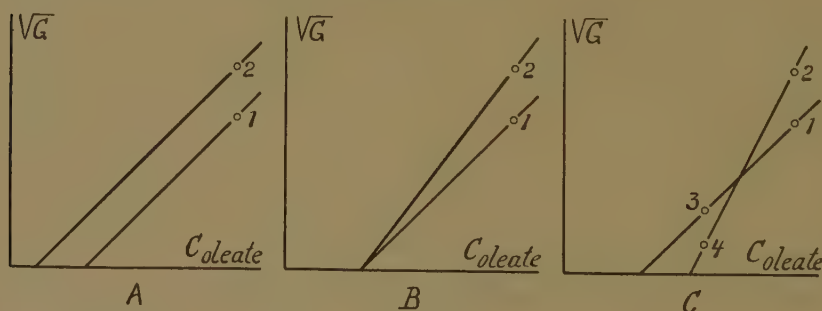


Fig. 2. Schemes to illustrate that a given increase ( $1 \rightarrow 2$ ) of  $\sqrt{G}$  at constant oleate concentration, may have different causes. See text.

Compare the diagrams of fig. 2, in which point 1 may represent the  $\sqrt{G}$  of a given oleate system and point 2 (vertically above point 1, that is at the same oleate concentration) the new value of  $\sqrt{G}$  arisen as a consequence of a change in some parameter other than the oleate concentration. Working at constant oleate concentration we can only state that  $\sqrt{G}$  has increased (from  $1 \rightarrow 2$ ). But why it has increased will remain unknown, until the  $\sqrt{G} - C_{\text{oleate}}$  curves through the points 1 and 2 will actually have been determined. Then we can discriminate between five



possibilities (three of which have been represented in fig. 2), for the increase of  $G$  at the given oleate concentration.

They are:

1. decrease of  $b$  (fig. 2A),
2. increase of  $a$  (fig. 2B),
3. decrease of  $a$  combined with decrease of  $b$ ,
4. increase of  $a$  combined with decrease of  $b$ ,
5. increase of  $a$  combined with increase of  $b$  (fig. 2C).

The diagram fig. 2C shows further, that even the sign of the change in  $\gamma G$  may depend on the arbitrarily chosen oleate concentration. From  $1 \rightarrow 2$  there is increase in  $\gamma G$ , from  $3 \rightarrow 4$  there is decrease in  $\gamma G$ . Reveral in sign is also possible in case No. 3.

The above will suffice to conclude that an insight into the action of parameters on the elastic behaviour can only be gained when their influence is studied on the position of the  $\gamma G - C_{\text{oleate}}$  and the  $1/\lambda - C_{\text{oleate}}$  curve or on the  $n - C_{\text{oleate}}$  curve as substitute for the latter.

The present communication deals in this way with the influence of the KCl concentration and of the temperature, and will enable to give an interpretation of the typical curves in fig. 1.

2. *Influence of the KCl concentration and the temperature on  $a$  and  $b$  in the formula  $\gamma G = a(C_{\text{oleate}} - b)$  and on  $e$  and  $f$  in the formula  $n = e(C_{\text{oleate}} - f)$*

In part XVI table II we gave the results of measurements of  $\gamma G$  and  $n$  as functions of the oleate concentration at three KCl concentrations and four temperatures. Using a statistical method we have calculated

TABLE I  
*Dependence of the values  $a$ ,  $b$ ,  $e$  and  $f$  on the KCl concentration and the temperature*

KCl concentration	temp. ° C	$a$	$b$	$e$	$f$
0.75 N . . . . .	15	6.05	0.17	47.5	0.35
	20	6.13	0.21	46.5	0.42
	25	6.21	0.25	45	0.55
	34.6	6.63	0.38	24.5	0.70
1.05 N . . . . .	15	5.90	0.08	68	0.08
	20	5.95	0.08	60	0.11
	25	6.06	0.09	51	0.14
	34.6	6.20	0.11	29	0.32
1.5 N . . . . .	15	7.01	0.06	47*	0.10*
	20	7.56	0.09	—	—
	25	8.00	0.11	—	—

from the  $\sqrt{G}$  values, the values of  $a$  (slope) and  $b$  (part cut off from the abscissa) for the best fitting straight lines through the experimentally determined points and we have collected them in table I.

Unfortunately the experimental data in part XVI table 2 do not allow to give accurate values for  $e$  and  $f$  in the formula  $n = e (C_{\text{oleate}} - f)$ , which is applying to the lower straight parts of the  $n - C_{\text{oleate}}$  curves. The latter are given in fig. 3 (of part XVI) from which figure the position of the lower straight branches can at least be guessed approximately at 0.75 N KCl and 1.05 N KCl. The value of  $e$  and  $f$  thus obtained are also given in table I.

As at 1.5 N KCl the three experimentally determined points lie probable already on the "second parts" of the  $n - C_{\text{oleate}}$  curve, we cannot give  $e$  and  $f$  values at all here. Fortunately in part XVI we had investigated  $n$ , at 1.5 N KCl and at  $15^\circ$ , as a function of the oleate concentration using a sufficient number of oleate concentrations to locate the lower straight part of the  $n - C_{\text{oleate}}$  curve (compare fig. 2 in part XVI). Calculation of the best fitting straight line gives the  $e$  and  $f$  values supplied with an asterisk in table I.

The  $a$ ,  $b$ ,  $e$  and  $f$  values of table I have been plotted in fig. 3,

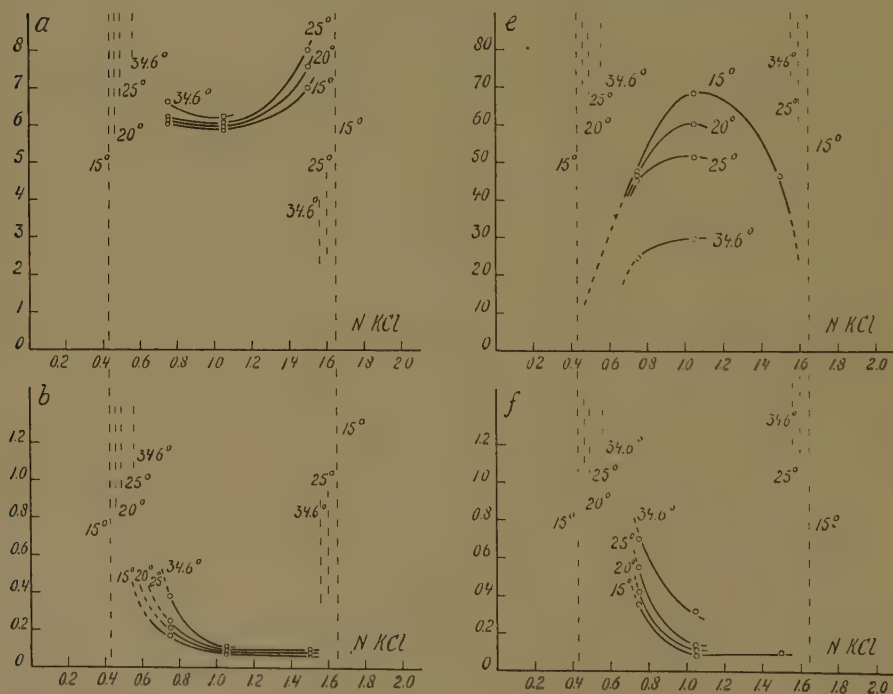


Fig. 3. Influence of the KCl concentration and the temperature on  $a$  and  $b$  of the equation  $\sqrt{G} = a(C_{\text{oleate}} - b)$  and on  $e$  and  $f$  of the equation  $n = e(C_{\text{oleate}} - f)$ .

in which the two vertical dotted lines give the limits of the elastic phenomena for the 1.2% oleate system at  $15^\circ$ , and the short dotted

vertical lines the same limits for the other temperatures. The range of the KCl concentration in which elastic systems are present (appr. 0.43 N KCl — 1.65 N KCl at 15°) thus contracts somewhat at increase of the temperature.

The relative positions of the left branches of the  $b - C_{\text{KCl}}$  and  $f - C_{\text{KCl}}$  curves suggest a direct connection with the displacement of the left limit of the elastic phenomena with the temperature. It seems plausible that by decreasing the KCl concentration below 0.75 N KCl the curves will continue their course upwards to the left with ever more steepness. They will near asymptotically the dotted vertical limits of the same temperature, or at least will not have an intersection point with them below  $b = 1.2\%$  oleate (because the elastic limits were those found with the 1.2% oleate system).

The nature of the  $e - C_{\text{KCl}}$  curves is very probably that of a curve with a maximum. But here further confirmation is certainly desirable, because the only point on the descending branch to the right was borrowed from another experimental series. This confirmation is given in the next section.

The nature of the  $a - C_{\text{KCl}}$  curves is very probably that of a curve with a minimum. The relative position of the curves and the limits of the elastic system at the corresponding temperature suggest that the  $n$  curves have steep ascending branches in the neighbourhood of the elastic limits. Without any doubt the values of  $a$  at 1.5 N KCl are much greater than those at 1.05 N KCl, so that the curves very probably continue to rise in the region between 1.5 N KCl and the elastic limits at the right side. Here, however, measurements are hardly possible because of the greatly increased damping.

The existence of an ascending branch at the left side of the  $a - C_{\text{KCl}}$  curve is strongly suggested by the measurement at 34.6°. At the other temperatures the values of  $a$  at 0.75 N KCl are only slightly higher than those at 1.05 N KCl.

To ascertain the fact that the  $a - C_{\text{KCl}}$  curves really have the character of curves with a minimum, it would be of advantage to have measurements at more than three KCl concentrations, including one at a concentration lower than 0.75 N KCl. Fortunately such measurements are available and they are discussed in the next section.

### 3. *Further experiments concerning the dependence of $a$ , $b$ , $e$ and $f$ on the KCl concentration*

In the next communication we will investigate at 15° or at 17° the influence of a number of organic substances on the  $\sqrt{G} - C_{\text{oleate}}$  and the  $n - C_{\text{oleate}}$  curves at 0.6; 0.9, 1.05 and 1.5 N KCl. The eight independent blank series of these experiments will be considered here, as they can give us further information about the dependence of  $a$ ,  $b$ ,  $e$  and  $f$  on the KCl concentration. The values of  $a$  and  $b$  (calculated from the blank

values of  $\sqrt{G}$  at 0.6; 0.8, 1.0 and 1.2 % oleate) have been given in table II. Inspection of this table conforms the supposition made in section 2 that the  $a - C_{\text{KCl}}$  curve is a curve with a minimum, for without exception we find in each series (No 1—5 at 15° and No 6—8 at 17°) that the  $a$  values both at 0.6 and at 1.5 N KCl are distinctly greater than those

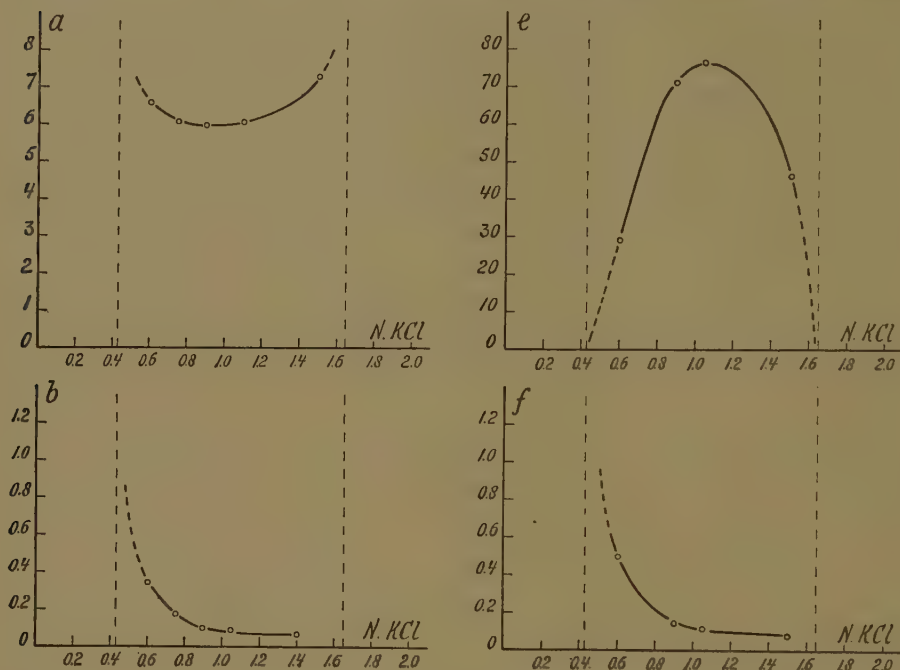


Fig. 4. Influence of the KCl concentration on  $a$  and  $b$  of the equation  $\sqrt{G} = a(C_{\text{oleate}} - b)$  and on  $e$  and  $f$  of the equation  $n = e(C_{\text{oleate}} - f)$ . ( $a$ ,  $b$ ,  $e$  and  $f$  are the means from eight independent series of experiments).

at 0.9 and 1.05 N KCl. The means taken over all values of  $a$  and  $b$ <sup>4)</sup> have been plotted in fig. 4.

<sup>4)</sup> There are reasons to form apart means for the Nos 1—5 and Nos 6—8, not only because the temperatures are slightly different, but also because the samples of the oleate which are used, were not strictly comparable. For the Nos 1—5 we started with a mixture out of 5 bottles of Na-oleate from Baker, for the Nos 6—8 we used a mixture out of 5 other bottles of the same brand. Though all bottles bore the same lot number, we know by experience that the contents may not have precisely identical properties, see part X, section 4, small print.

A further difference is that the experiments Nos 1—5 have been extended over a period of about 4 months, the experiments Nos 6—8 over a period of two weeks. Therefore changes in properties of the oleate powder in store with time were presumably smaller for the Nos 6—8. This may have contributed to the greater uniformity of the results with the Nos 6—8.

Therefore it seems indicated to plot the apart means of  $a$  and  $b$  for the groups Nos 1—5 and Nos 6—8 against the KCl concentration. When this is done it appears that the ascending branch of the  $b$  curve for the group Nos 6—8 (at 17°) lies higher



The  $a - C_{\text{KCl}}$  curve has a very flat minimum, the precise position of the minimum being unknown, but probably lying between 0.9 and 1.05 KCl. The value of  $a$  at 0.75 N KCl from table I has also been designed in fig. 4 and it appears to lie on the curve through the remaining four points.

The blank experiments Nos 1—5 and Nos 6—8 have also been used

TABLE II

Values of  $a$  and  $b$  in  $\log G = a(C_{\text{oleate}} - b)$  at four KCl concentrations from eight independent series of experiments

series No.	$a$				$b$			
	0.6 N KCl	0.9 N KCl	1.05 N KCl	1.5 N KCl	0.6 N KCl	0.9 N KCl	1.05 N KCl	1.5 N KCl
1	6.47	—	5.86	7.11	0.33	—	0.07	0.08
2	6.51	6.00	6.06	7.21	0.32	0.10	0.09	0.06
3	6.45	6.01	6.04	7.47	0.30	0.10	0.08	0.08
4	6.40	5.95	6.00	7.55	0.29	0.09	0.08	0.09
5	6.43	5.97	6.05	7.49	0.30	0.09	0.08	0.09
6	6.68	5.94	6.05	7.10	0.39	0.10	0.09	0.04
7	6.76	5.94	6.04	7.04	0.39	0.11	0.09	0.04
8	6.60	5.90	6.10	7.03	0.38	0.10	0.09	0.04
means 1—5	6.45	5.98	6.00	7.37	0.31	0.10	0.08	0.08
means 6—8	6.68	5.93	6.06	7.06	0.39	0.10	0.09	0.04
means 1—8	6.54	5.96	6.03	7.25	0.34	0.10	0.08	0.07

to estimate the values of  $e$  and  $f$  for the lower parts of the  $n - C_{\text{oleate}}$  curves (Compare table III). Here the same difficulties were met with as are already mentioned in section 2, so that the values recorded in the table are only approximate ones. It may be expected that the nature of the  $e - C_{\text{KCl}}$  and  $f - C_{\text{KCl}}$  curves will be represented fairly well by plotting the means of  $e$  and of  $f$ .

Here too, we have used for fig. 4 the means taken over all values for

than the one for the Nos 1—5 (at 15°), which is in accordance with the known influence of the temperature (compare fig. 3). When one compares the  $a$  curves for the two groups it appears that there is little differences at 0.9 and 1.05 N KCl, but at 0.6 N and 1.5 N KCl the differences have opposite signs. This cannot be the result of the temperature only (compare fig. 3) but points to a quantitative difference between the two oleate mixtures in store which gives rise to a shift of the curves in a horizontal direction. Such a shift may indeed be the result of a slow chemical alteration of the oleate preparation in store.

Therefore it makes little sense to plot apart the curves for the Nos 1—5 and the Nos 6—8.

Instead of the apart means we used in fig. 4 the means taken over all values of the experiments Nos 1—8, which therefore apply to the general mean temperature 15.8°.

TABLE III

Values of  $e$  and  $f$  in  $n = e(C_{\text{oleate}} - f)$  at four KCl concentrations from eight independent series of experiments

Series no.	$e$				$f$			
	0.6 N KCl	0.9 N KCl	1.05 N KCl	1.5 N KCl	0.6 N KCl	0.9 N KCl	1.05 N KCl	1.5 N KCl
1	28	—	87	44	0.44	—	0.14	0.06
2	32	73	77	—	0.51	0.09	0.10	—
3	37	71	73	—	0.55	0.06	0.06	—
4	36	78	85	—	0.54	0.14	0.14	—
5	35	75	80	—	0.56	0.12	0.13	—
6	23	69	66	—	0.51	0.18	0.10	—
7	20	72	72	—	0.46	0.23	0.13	—
8	18	62	68	—	0.46	0.14	0.11	—
means 1—5	34	74	80	44	0.52	0.10	0.11	0.06
means 6—8	20	68	69	—	0.48	0.18	0.11	—
means 1—8	29	71	76	44	0.50	0.14	0.11	0.06

the experiments Nos 1—8<sup>5</sup>). As no  $e$  and  $f$  values could be given at 1.5 N KCl for the Nos 2—8 (the bend in the  $n - C_{\text{oleate}}$  curve lying very disadvantageously here so that the position of the lower part could not be determined) we have only the values from experiment No 1, viz.  $e = 44$  and  $f = 0.06$ . The only other values of  $e$  and  $f$  at 1.5 N are those given in table I with asterisk ( $e = 47$  and  $f = 0.10$ ). The  $e$  and  $f$  curves in fig. 4 have been drawn accordingly through the means of these values ( $e = 45.5$  and  $f = 0.08$ ).

#### 4. Discussion

The results laid down in the figures 3 and 4 are of importance for a future quantitative theory of the viscous elastic oleate systems. Such a theory should for instance reckon with the fact that no very simple quantitative relation of the shear modulus  $G$  and the total oleate concentration can be expected to exist, because the total oleate concentration falls apart in two fractions: “free oleate”, that is oleate not taking part in the elastic phenomena, and “structural oleate”, that

<sup>5</sup>) When the apart means of  $e$  and  $f$  for the groups Nos 1—5 and Nos 6—8 are plotted against the KCl concentration, curves are obtained the relative position of which are in the main in accordance with the difference in temperature (compare fig. 3). In note 4 it was argued that the “differences between group Nos 1—5 and group Nos 6—8 do not reside solely in the difference of the temperature, but that the two mixtures of the oleate powder used were not identical. The occurrence of a shift in horizontal direction was an indication to this. Here the value or “ $f$ ” at 0.6 N KCl is such an indication. This value should be distinctly higher for the group Nos 6—8 than for the group Nos 1—5, whereas it is found to be somewhat lower here.

is oleate taking part in the elastic phenomena. The concentration of the "free oleate" is indicated by  $b$  in the formula  $\sqrt{G} = a (C_{\text{oleate}} - b)$  and the concentration of the "structural oleate" therefore is given by  $(C_{\text{oleate}} - b)$ .

Calling the latter expression the "reduced oleate concentration" and denoting it by  $C_{\text{red.oleate}}$  the expression for  $G$  in its most simple form will be:

$$G = a^2 (C_{\text{red.oleate}})^2$$

Thus future theory has to explain two different points:

1. the transition of "free oleate" into "structural oleate" at increase of the KCl concentration, which is indicated by the decrease of the values for  $b$  in the fig. 3 and 4, and the opposite action at increase of the temperature to this transition as is indicated by the increase of the values  $b$  in fig. 3.

2. the influence of the KCl concentration on the proportionality factor  $a$ , between  $\sqrt{G}$  and the reduced oleate concentration.

This factor is minimal at a KCl concentration which lies somewhere half way in the range of KCl concentrations in which elastic phenomena are present. Compare the  $a$  curves in fig. 3 and 4.

The theory must further elucidate why at all KCl concentrations  $a$  increases at increasing temperature, compare fig. 3.

In a similar way the future theory will also have to reckon with a division of the total oleate concentration in two parts, in order to be able to explain the influence of the KCl concentration and the temperature on the damping. Though it would have been very desirable to possess graphs which give  $c$  and  $d$  in the formula  $1/A = c(C_{\text{oleate}} - d)$  as functions of the KCl concentration and the temperature for the lower straight parts of the  $1/A - C_{\text{oleate}}$  curves, no measurements to derive them are available. But there is no doubt that in principle these curves will bear the same character as the curves for  $e$  and  $f$  (from the formula  $n = e(C_{\text{oleate}} - f)$  in the figures 3 and 4, because  $n$  is an approximate measure for  $1/A$  (for particulars see part XV).

The only difference will be that  $f$ , representing the concentration of the "free oleate", is systematically higher than  $d$ , because  $n$  is only an approximate measure for  $1/A$  (see part XV section 4). We have already discussed, in part XVI, that  $b = d < f$ , and indeed we find in the tables I and II that the values of  $f$  are higher than those of  $b$ . Compared to the changes of  $a$  and  $b$ , the change of  $f$  with the increase of the KCl concentration and the temperature bears the same character as the change of  $b$ , which is quite as is to be expected.

The change of  $e$  is quite different from that of  $a$ , for at increase of the KCl concentration  $e$  follows a curve with a maximum, whereas  $a$  follows a curve with a minimum. The influence of the temperature on  $a$  and  $e$  is also just opposite,  $a$  being increased and  $e$  being decreased at increase of the temperature. It can be expected that the influence of the KCl concentration and the temperature will be qualitatively the same for  $c$  and  $d$  in the formula  $1/A = c(C_{\text{oleate}} - d)$  and this also must be declared by a future theory. Further it appears that the minimum of the  $a$  curve lies at a somewhat lower KCl concentration (between 0.9 and 1.05 N) than the maximum of the  $f$  curve (at approximately 1.05 N).

It is not impossible that this comes from  $n$  being an approximate measure for  $1/A$  only and that the minimum of the  $a - C_{\text{KCL}}$  curve and the maximum of the  $c - C_{\text{KCL}}$  curve will coincide.

5. The shape of the  $G - C_{\text{KCl}}$  and  $n - C_{\text{KCl}}$  curves at constant oleate concentration and the influence of the temperature on them

The characteristic S-shaped  $G - C_{\text{KCl}}$  curve, compare fig. 1, can now be explained as being the resultant of the simultaneous influence of the increasing KCl concentration on the proportionality factor  $a$  in the formula  $\sqrt{G} = a (C_{\text{oleate}} - b)$  and on  $b$ , that is the part cut off from the abscissa.

This may be illustrated by fig. 5, in which for 0.6, 0.75, 0.9; 1.05 and 1.5 N KCl the  $\sqrt{G} - C_{\text{oleate}}$  curves at  $15^\circ$  have been designed (using the mean values of  $a$  and  $b$  for the Nos 1—5 of table II and for 0.75 N the values of  $a$  and  $b$  of table I). A few further dotted straight lines give the presumable position of the  $\sqrt{G} - C_{\text{oleate}}$  curve at lower oleate concentrations.

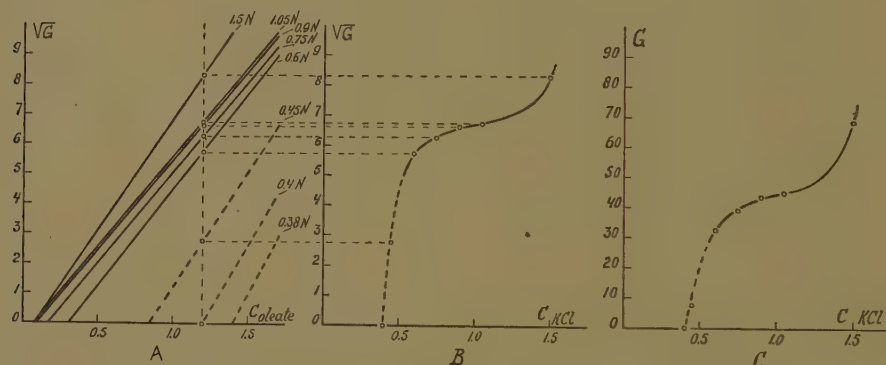


Fig. 5. Explanation of the typical S-shape of the  $G - C_{\text{KCl}}$  curve at constant oleate concentration.

At increase of the KCl concentration up to 1.05 N the  $\sqrt{G} - C_{\text{oleate}}$  curve is shifted to the left, whereby at first  $b$  decreases rapidly and later on more slowly. The slope  $a$  decreases somewhat. At further increase of the KCl concentration  $b$  decreases only slightly, the main effect now being the increase of the slope  $a$  (compare for the changes of  $a$  and  $b$  with the KCl concentration in the figures 3 and 4). We have drawn a dotted vertical line in fig. 5A which may represent an arbitrary chosen constant oleate concentration. The intersection points of this vertical line therefore give the values of  $\sqrt{G}$  at a number of KCl concentrations. The  $\sqrt{G} - C_{\text{KCl}}$  curve at constant oleate concentration in fig. 5B follows from these points. This curve begins at approximately 0.4 N KCl with  $\sqrt{G} = 0$  (the  $\sqrt{G} - C_{\text{oleate}}$  curves in fig. 5A at lower KCl concentrations having presumably no intersection point with the vertical dotted line).

We further see that the  $\sqrt{G} - C_{\text{KCl}}$  curve in fig. 5B has an inflexion point and is therefore S-shaped. It follows that the  $G - C_{\text{KCl}}$  curves at constant oleate concentration must be typically S-shaped too. Compare fig. 5C.



From the influence of increase of the temperature on  $a$  (increase) and  $b$  (increase) it can easily be reasoned that the  $G - C_{\text{KCl}}$  curve at constant oleate concentration takes a steeper course at higher temperatures (compare dotted curve in fig. 1). The shift to the right of the footpoint of this curve on the abscissa is caused by the increase of  $b$ , whereas the increase of  $a$  is the main factor which at 1.5 N KCl leads to an increase of  $G$ .

We now turn to the explanation of the shape of the  $n$  curve at constant oleate concentration (maximum curve, compare fig. 1). This can also be explained from the influence of the KCl concentration on  $e$  and  $f$  in the formula  $n = e (C_{\text{oleate}} - f)$  (compare fig. 3 and 4).

At constant oleate concentration  $n$  will be zero when  $f > C_{\text{oleate}}$ , that is at low KCl concentration<sup>6</sup>). The expression  $(C_{\text{oleate}} - f)$  attains a finite value at a higher concentration which concentration remains finite up to the coacervation limit. But the curve for  $e$  as function of the KCl concentration is a maximum curve and  $e$  becomes probably zero at the coacervation limit. From this follows that the  $n - C_{\text{KCl}}$  curve at constant oleate concentration must be a curve with a maximum.

We have to explain now why at constant oleate concentration increase of the temperature gives rise to a series of  $n - C_{\text{KCl}}$  curves as are depicted in fig. 1 by the dotted curves. For these curves it is characteristic that at any KCl concentration  $n$  is lowered. Increase of the temperature decreases  $e$  and increases  $f$  (compare fig. 3). Both these changes will have a lowering effect on  $n$  at constant oleate concentration. Therefore by the cooperation of these two influences  $n$  will be lowered at increase of the temperature as is depicted by the dotted curves in fig. 1.

Strickly speaking the above reasonings concerning the shape of the  $n - C_{\text{KCl}}$  curves are only valid for such low oleate concentrations that the  $n$  values still lie on the lower straight parts of the  $n - C_{\text{oleate}}$  curves. When at an intermediate KCl concentration  $n$  should move to the second less steep branch, this will practically not alter the above reasonings, but for a considerable flattening of the maximum of the  $n - C_{\text{KCl}}$  curve.

Because  $n$  is an approximate measure of  $1/A$ , it follows that the  $1/A - C_{\text{oleate}}$  curve in fig. 1 must have the same character as the  $n - C_{\text{oleate}}$  curve.

## 6. Summary

1. It has been discussed that the influence of parameters on the elastic behaviour cannot be expressed in a change in the internal equilibrium (free oleate  $\rightleftharpoons$  oleate taking part in the elastic phenomena) and in a change in the proportionality factors between  $\sqrt{G}$ ,  $1/A$ ,  $n$  and the concen-

<sup>6</sup>) The expression  $(C_{\text{oleate}} - f)$  has approximately the same meaning as  $(C_{\text{oleate}} - b)$  in the formula  $\sqrt{G} = a (C_{\text{oleate}} - b)$ , but is somewhat smaller, because  $f > b$  (compare part XVI section 4).

tration of the oleate taking part in the elastic phenomena, when the investigation is performed at only one constant oleate concentration. This becomes possible when the investigation is carried out simultaneously at at least two but preferably at more constant oleate concentrations.

2. The influence of the KCl concentration and the temperature has been investigated on  $a$ ,  $b$ ,  $e$  and  $f$  in the formula  $\sqrt{G} = a (C_{\text{oleate}} - b)$  and  $n = e (C_{\text{oleate}} - f)$ .

The curves representing  $a$ ,  $b$ ,  $c$  and  $f$  as a function of the KCl concentration have the following characters:  $a$  is a curve with a flat minimum,  $e$  is a curve with a flat maximum,  $b$  and  $f$  are curves which consist of a steep descending branch followed by a branch which does not descend much further.

3. At increase of the temperature  $a$ ,  $b$  and  $f$  are increased,  $e$  is decreased.

4. The results are of importance for a future theory of the viscous elastic systems, which has to reckon with the fact that the oleate is present in two different states. Increase of the KCl concentration transforms "free oleate" into oleate taking part in the elastic phenomena and increase of the temperature counteracts this transformation.

5. The results give an explanation why at constant oleate concentration the  $G - C_{\text{KCl}}$  curve is S-shaped and the  $n - C_{\text{KCl}}$  curve has the character of a curve with a maximum. They further explain why increase of the temperature makes the S-shaped  $G - C_{\text{KCl}}$  curve steeper and decreases the maximum of the  $n - C_{\text{KCl}}$  curve.

*Department of Medical Chemistry  
University of Leiden*

ELASTIC-VISCOUS OLEATE SYSTEMS CONTAINING KCl. XVIII <sup>1)</sup>

*The influence of some organic substances on the elastic behaviour investigated with the aid of  $\sqrt{G} - C_{oleate}$  and  $n - C_{oleate}$  curves.*

BY

H. G. BUNGENBERG DE JONG, W. A. LOEVEN \*) AND W. W. H. WEIJZEN \* 2)

(Communicated at the meeting of June 30, 1951)

1. *Introduction*

In the present communication the new method to investigate the influence of parameters on the elastic behaviour — compare part XVII of this series — is applied on the investigation concerning the influence of added organic substances. The following three questions may be put:

1. Does the linear relation between  $\sqrt{G}$  and the oleate concentration and between  $n$  and the oleate concentration (in this last case only for the lower part of the  $n - C_{oleate}$  curve) also exist when organic substances have been added?
2. If question sub 1. is answered in the affirmative, in which way are the slopes of the above-mentioned straight lines for the blanks and the parts cut off from the abscissa altered by organic substances?
3. Is there a connection between the findings sub 2. and the results obtained with the simple method used in the preceding parts VI — XIII (investigation of the influence of organic substances at constant oleate concentration on the  $\sqrt{G} - C_{KCl}$ ,  $1/A - C_{KCl}$  and  $n - C_{KCl}$  curves)?

2. *Methods*

To make a comparison as is mentioned in the above sub 3) possible, the experiments were made at a number of KCl concentrations for which we choose 0.6; 0.9; 1.05 and 1.5 N KCl (in the series with heptane no measurements have been performed at 0.9 N KCl). Measurements were performed at four oleate concentrations for each KCl concentration, namely at 0.6; 0.8; 1.0 and 1.2 % (in the series with heptane we used 0.2; 0.5; 0.8; 1.0 and 1.2 %).

The procedure followed in each series was the following: From a large volume of stock oleate solution we made 540 ml portions of each of the 16 systems which were necessary for the blank determination (4 oleate concentrations at 4 KCl concentrations).

\*) Aided by grants from the "Netherlands Organization for Pure Research (Z.W.O.)".

<sup>1)</sup> Part I has appeared in these Proceedings 51, 1197 (1948); Part II—VI in these Proceedings 52, 15, 99, 363, 377, 465 (1949); Part VII—XIV in these Proceedings 53, 7, 109, 233, 743, 759, 975, 1123, 1319 (1950); Parts XV—XVII in these Proceedings 54, series B, 1, 240, 291 (1951).

<sup>2)</sup> Publication No. 17 of the team for Fundamental Biochemical Research (under the direction of H. G. BUNGENBERG DE JONG, E. HAVINGA and H. L. BOOIJ).

It was seen to that a  $p_H > 12$  was ensured, for which reason each mixture contained 0.05 N KOH. Now 16 spherical vessels of approx. 500 ml capacity (with known radii) were completely filled with the above systems, put in the thermostate until the next morning, whereupon the measurements were performed (electrolytic  $H_2$ -mark, see part X, and contrivance to excite the rotational oscillation, see part VII). As we were not able to make the difficult measurement of the decrement we had to content ourselves with the measurement of  $n$  (compare part XV for the relation between  $n$  and  $1/\lambda$ ). After the measurements the contents of the vessels were poured back in the original 16 flasks (large Erlenmeyer flasks) which still contained the non used rests of the systems and which had been kept closed with rubber stoppers.

Now we added the organic substance that was to be studied, dissolved it by shaking the flasks vigorously and sufficiently long and filled the spherical vessels anew. The latter were put in the thermostate and the measurements were performed the next morning. In some series of experiments we also investigated the influence of a second addition, repeating the above manipulations.

In the way as is given above we investigated the influence of 9 organic substances, the influence of which on the  $\sqrt{G-C_{KCl}}$  and  $n-C_{KCl}$  curves at constant oleate concentration is already known from experiments in the parts VI—XIII. They comprise 6 hydrocarbons, undecylate, n. nonyl alcohol and ethanol. The added quantities of the first seven substances, can be considered to be taken up practically completely or at least for a considerable part (benzene) by the oleate micelles. Therefore the quantities added to the 0.6; 0.8; 1.0 and 1.2 % oleate systems were not taken equal, but proportional to the oleate concentration <sup>3)</sup>.

With ethanol on the other hand the partition equilibrium between micelles and the medium which is bathing them is of a nature that practically all ethanol which is added can be considered to be free in solution in the medium. In the case of ethanol, therefore, the end concentrations which were used were taken the same in the 0.6; 0.8; 1.0 and 1.2 % oleate systems. The experiments with naphtalene, cyclohexane and decahydronaphtalene were performed at 17°, those with the remaining substances at 15°. The oleate which was used for each group was not identical. A mixture of 5 flasks of Na-oleate neutral powder from BAKER <sup>4)</sup> served for the experiments with the first-mentioned group, a mixture of 5 other flasks of the same brand and lotnumber for the second group. All oleate systems measured contained 0.05 N KOH to obtain a  $p_H > 12$ . For reasons mentioned in part XVII (see notes 4 and 5), it is not allowed to compare quantitatively the results of the 8 experimental series with one another, not even within each of the two groups.

---

<sup>3)</sup> As far as the organic substances are liquids, these proportional additions could be done conveniently with the aid of the dripping micropipette described elsewhere, compare these Proceedings 52, 783 (1949).

In the series with ethanol apart blanks and apart mixtures with ethanol were made, because addition of the organic substance to the blanks is not allowed here (the necessary additions would be so large here that the oleate concentration would no longer remain practically constant).

In the series with naphtalene we also made apart mixtures for the blanks for the first addition and for the second addition, in order to give all oleate systems the same heat-time history. We started here from three 2.5 l. portions of the 4 % stock oleate solution. The one from which the blanks were prepared, was heated previously during 5 min. at 80°. The two other 2.5 l. portions got the same heat treatment, which served to dissolve two different additions of the naphtalene. They were used to prepare the mixtures corresponding to the "first addition" and the "second addition" respectively.

<sup>4)</sup> A generous gift of Na-oleate from the Rockefeller Foundation provided the means for the experiments in this paper.



3. The character of the  $\sqrt{G} - C_{\text{oleate}}$  and  $n - C_{\text{oleate}}$  curves in the presence of organic substances

We will not give extensive tables of the results nor reproduce them all graphically. As examples we give here graphically the results with naphthalene (fig. 1) and decahydronaphthalene (fig. 2). We see here — and it also applies for the remaining series — that the  $\sqrt{G} - C_{\text{oleate}}$  curves, which are straight lines for the blanks, remain straight lines after addition of organic substances, though their slopes ( $a$ ) and the parts cut off from the abscissa ( $b$ ) are generally altered.

The same applies for the lower parts of the  $n - C_{\text{oleate}}$  curves. It was shown in part XVI of this series that for the blanks the latter curves have already a more complicated character, consisting of two straight branches. As we are only interested in the influence of organic substances

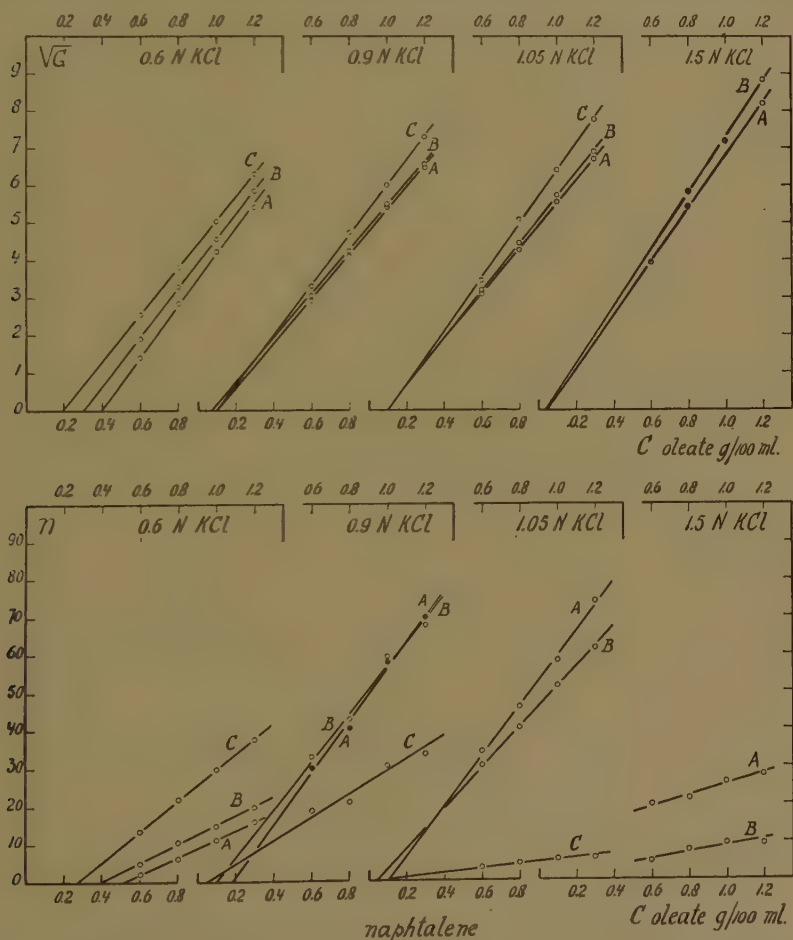


Fig. 1. Influence of naphthalene on the  $\sqrt{G} - C_{\text{oleate}}$  curves (upper) and on the  $n - C_{\text{oleate}}$  curves (lower) at four KCl concentrations.

A = blank; B = after the first addition of naphthalene; C = after the second addition.

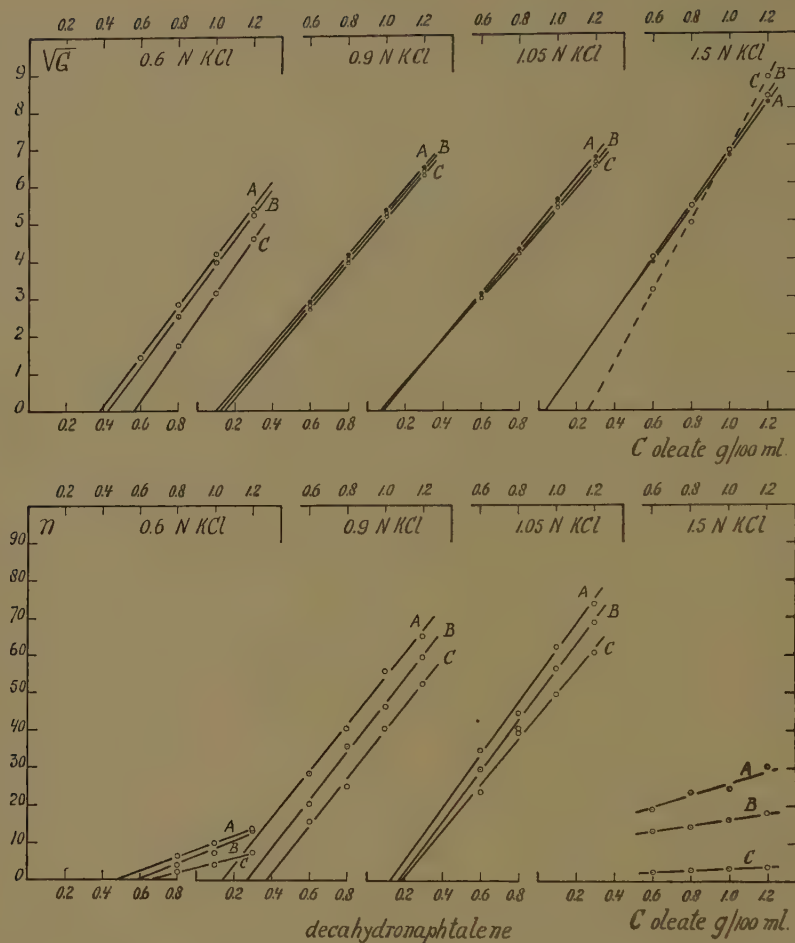


Fig. 2. Influence of decahydronaphthalene on the  $\sqrt{G}$ — $C_{\text{oleate}}$  curves (upper) and on the  $n$ — $C_{\text{oleate}}$  curves (lower) at four KCl concentrations.

A, B and C as in fig. 1.

on the lower straight branch here, the oleate concentrations have been chosen in such a way (0.6; 0.8; 1.0 and 1.2 %) that at least for 0.6; 0.9 and 1.05 N KCl the experimentally determined points are still lying on the lower branch. Sometimes, however, the  $n$  point at 1.2 % (and in few cases the  $n$  point for 1.0 % oleate) was already lying on the second less steep branch or on the bend towards the latter. As only three (or two) experimentally determined points are remaining on the lower branch, then the precise position of the latter remains uncertain.

Nevertheless, the results at 0.6; 0.9 and 1.05 N KCl give the strong impression that the lower branch of the  $n$ — $C_{\text{oleate}}$  curves, which is a straight line for the blanks, retains this character after addition of organic substances, though its slope and the part cut off from the abscissa are generally altered. Compare in fig. 1 and 2 the diagrams for 0.6; 0.9 and 1.05 N KCl. The situation is much more unfavourable at 1.5 N KCl, as the bend in the  $n$  curve lies at much lower oleate concentration here.

The position of the lower branch of the  $n - C_{\text{oleate}}$  curve could only be determined in the series with heptane here, because in this series the oleate concentrations which were used were 0.2; 0.5; 0.8; 1.0 and 1.2 %. In all remaining series the four experimentally determined points are already lying on the second branch, so that the position of the lower branch is not known here (compare in fig. 1 and fig. 2 the  $n$  diagrams at 1.5 N KCl).

4. *Influence of the organic substances on  $a$  and  $b$  in the equation  $\sqrt{G} = a (C_{\text{oleate}} - b)$  and on  $e$  and  $f$  in the equation  $n = e (C_{\text{oleate}} - f)$*

Using a statistical method we have calculated the slope  $a$  and the part cut off from the abscissa  $b$  for the best fitting straight line through the experimentally determined  $\sqrt{G}$  points and we have collected them in Table I. Table II contains the values of  $e$  and  $f$  for the lower straight

TABLE I

Influence of organic substances on  $a$  and  $b$  in the equation  $\sqrt{G} = a (C_{\text{oleate}} - b)$

No.	Substance	Added amount	$a$				$b$			
			0,6 N KCl	0,9 N KCl	1,05 N KCl	1,5 N KCl	0,6 N KCl	0,9 N KCl	1,05 N KCl	1,5 N KCl
1	n-heptane	blank	6,47	—	5,86	7,11	0,33	—	0,07	0,08
		1st add.	5,75	—	5,83	6,62	0,37	—	0,08	0,03?
		2nd „	n.e.	—	5,66	6,21	n.e.	—	0,10	0,07
2	nonanol-1	blank	6,51	6,00	6,06	7,21	0,32	0,10	0,09	0,06
		1st add.	6,26	6,08	6,73	coac	0,21	0,08	0,09	coac
3	benzene	blank	6,45	6,01	6,04	7,47	0,30	0,10	0,08	0,08
		1st add.	6,55	6,19	6,22	8,95	0,28	0,10	0,09	0,11
		2nd „	6,35	6,30	6,90	coac	0,21	0,10	0,12	coac
4	ethanol	blank	6,40	5,95	6,00	7,55	0,29	0,09	0,08	0,09
		1st add.	6,05	6,31	6,36	7,86	0,29	0,12	0,09	0,09
		2nd „	5,50	6,39	6,56	9,48	0,26	0,12	0,11	0,26?
5	n-nonane	blank	6,43	5,97	6,05	7,49	0,30	0,09	0,08	0,09
		1st add.	±n.e.	4,88	5,61	6,34	±n.e.	0,07	0,08	0,06
5*	undecylate-ion	blank	6,43	5,97	6,05	7,49	0,30	0,09	0,08	0,09
		1st add.	—	6,13	6,19	6,30	—	0,16	0,12	0,05
6	naphtalene	blank	6,68	5,94	6,05	7,10	0,39	0,10	0,09	0,04
		1st add.	6,51	5,85	6,23	7,50	0,30	0,07	0,09	0,03
		2nd „	6,26	6,60	7,12	coac	0,19	0,09	0,10	coac
7	cyclohexane	blank	6,76	5,94	6,04	7,04	0,39	0,11	0,09	0,04
		1st add.	6,43	5,94	6,23	—	0,30	0,10	0,09	—
		2nd „	6,50	5,96	6,42	coac	0,30	0,09	0,10	coac
8	decahydro-naphtalene	blank	6,60	5,90	6,10	7,03	0,38	0,10	0,09	0,04
		1st add.	6,73	5,94	5,94	7,12	0,42	0,12	0,08	0,04
		2nd „	7,15	5,95	5,89	9,33?	0,56	0,14	0,09	0,26?

n.e. = not elastic, i.e. number of turning points is zero; coac = coacervated system.

TABLE II

Influence of organic substances on  $e$  and  $f$  in the equation  $n = e(C_{\text{oleate}} - f)$ 

No.	Substance	Added amount	$e$				$f$			
			0,6 N KCl	0,9 N KCl	1,05 N KCl	1,5 N KCl	0,6 N KCl	0,9 N KCl	1,05 N KCl	1,5 N KCl
1	n-heptane	blank	28	—	87	44	0,44	—	0,14	0,06
		1st add.	14	—	74	25	0,51	—	0,16	0,07
		2nd „	n.e.	—	56	25	n.e.	—	0,17	0,09
2	nonanol-1	blank	32	73	77	?	0,51	0,09	0,10	?
		1st add.	51	66	45	coac	0,41	0,14	0,09	coac
3	benzene	blank	37	71	73	?	0,55	0,06	0,06	?
		1st add.	39	65	63	?	0,57	0,05	0,06	?
		2nd „	45	61	(46)	coac	0,38	0,10	?	coac
4	ethanol	blank	36	78	85	?	0,54	0,14	0,14	?
		1st add.	21	77	57	?	0,52	0,30	0,04	?
		2nd „	17	54	46	?	0,56	0,24	0,12	?
5	n-nonane	blank	35	75	80	?	0,56	0,12	0,13	?
		1st add.	8	23	?	53	0,78	0,51	?	0,22
5*	undecylate-ion	blank	35	75	80	?	0,56	0,12	0,13	?
		1st add.	10	32	49	67	0,90	0,26	0,17	(0,11)
6	naphtalene	blank	23	69	66	?	0,51	0,18	0,10	?
		1st add.	24	63	54	?	0,38	0,10	0,04	?
		2nd „	40	31	(4)	coac	0,26	(0,05)	?	coac
7	cyclohexane	blank	20	72	72	?	0,46	0,23	0,13	?
		1st add.	27	70	62	(2)	0,45	0,18	0,16	(0,15)
		2nd „	27	71	55	coac	0,34	0,21	0,14	coac
8	decahydro-naphtalene	blank	18	62	68	?	0,46	0,14	0,11	?
		1st add.	20	64	67	?	0,58	0,27	0,17	?
		2nd „	13	63	61	?	0,65	0,37	0,18	?

coac = coacervated system    n.e. = not elastic, i.e. number of turning points is zero.

part of the  $n - C_{\text{oleate}}$  curves, which values are calculated in the same way. Because of the difficulties mentioned in section 2 the values of  $e$  and  $f$  are approximate ones and besides are in general more uncertain when the KCl concentration is higher (as sometimes only three or even only two experimentally determined points remained for the calculation).

The values  $a$ ,  $b$ ,  $e$  and  $f$  from the Table I and II have been plotted in fig. 3, 4 and 5 against the KCl concentration.

In the figures the curves  $A$  always refer to the blank, the curves  $B$  to the oleate system after the first addition of the organic substance and the curves  $C$  after the second addition. These additions, expressed in percentages of moles organic substance added to one mol oleate (see introduction) amounted to:

heptane 12.7 % and 25.4 %; nonanol 3.3 %; benzene 5.5 % and



16.6 %; nonane 17.3 %; undecylic acid 5.6 %; naphtalene 2.54 % and 11.4 %; cyclohexane 9.1 % and 18.2 %; decahydronaphtalene 2.37 % and 7.1 %.

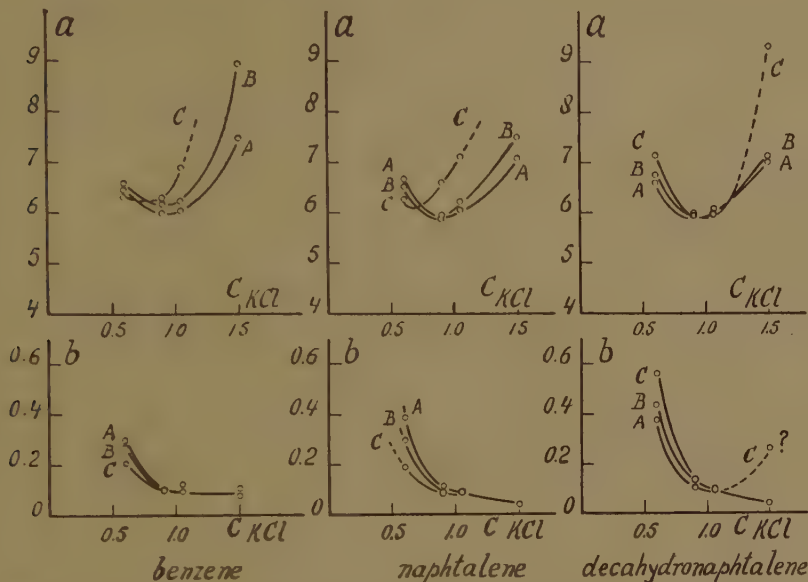


Fig. 3A. Influence of benzene (KCl sparing), naphthalene (KCl sparing) and decahydronaphthalene (transition case) on  $a$  and  $b$  in the equation  $\gamma G = a (C_{\text{oleate}} - b)$ , as a function of the KCl concentration.

A = blank; B = after the first addition; C = after the second addition.

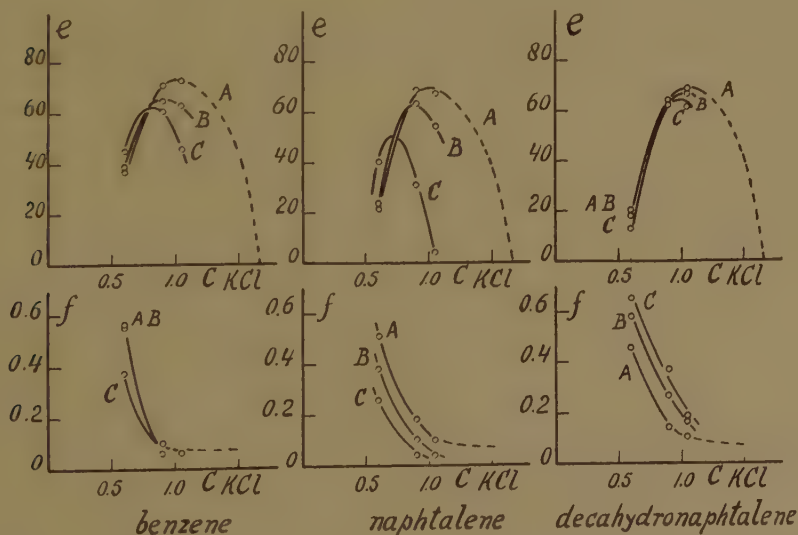


Fig. 3B. Influence of benzene (KCl sparing), naphthalene (KCl sparing) and decahydronaphthalene (transition case) on  $e$  and  $f$  in the equation  $n = e (C_{\text{oleate}} - f)$ , as a function of the KCl concentration.

A, B and C as in fig. 3A.

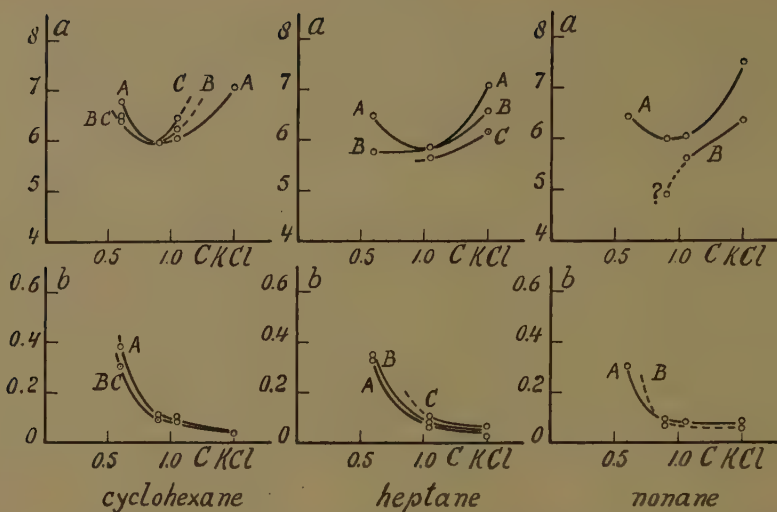


Fig. 4A. Influence of cyclohexane (KCl sparing), *n*-heptane (transition case) and *n*-nonane (KCl demanding) on  $a$  and  $b$  in the equation  $\gamma G = a(C_{oleate} - b)$ , as a function of the KCl concentration.

A, B and C as in fig. 3.

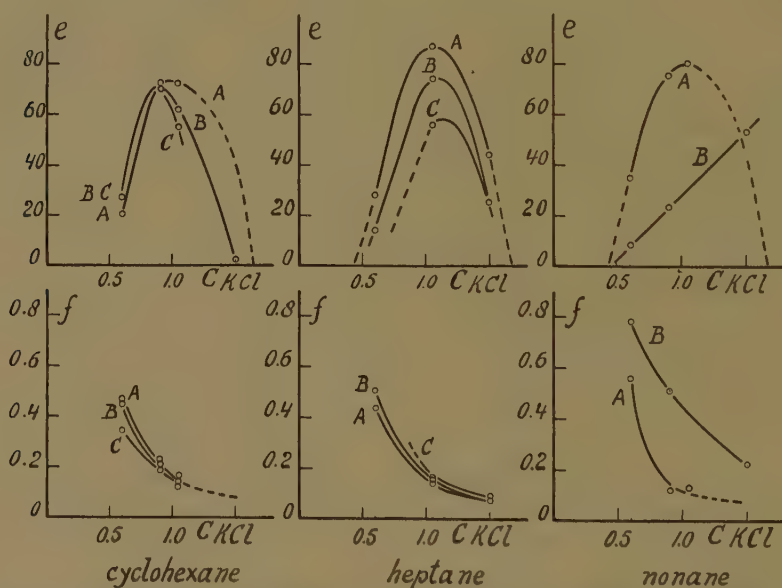


Fig. 4B. Influence of cyclohexane (KCl sparing), *n*-heptane (transition case) and *n*-nonane (KCl demanding) on  $e$  and  $f$  in the equation  $n = e(C_{oleate} - f)$ , as a function of the KCl concentration.

A, B and C as in fig. 3.

In the series with ethanol the concentrations amounted to 0.17 and 0.34 moles/l.

The descending branch of the blank  $e$  curve has been drawn in these figures at 1.5 N through  $e = 44$ , which was actually determined in the blank series with heptane. In the graphs for cyclohexane, naphtalene

and decahydronaphtalene we took 40 here (because all  $e$  values with these three substances were lower) which is perhaps still too high.

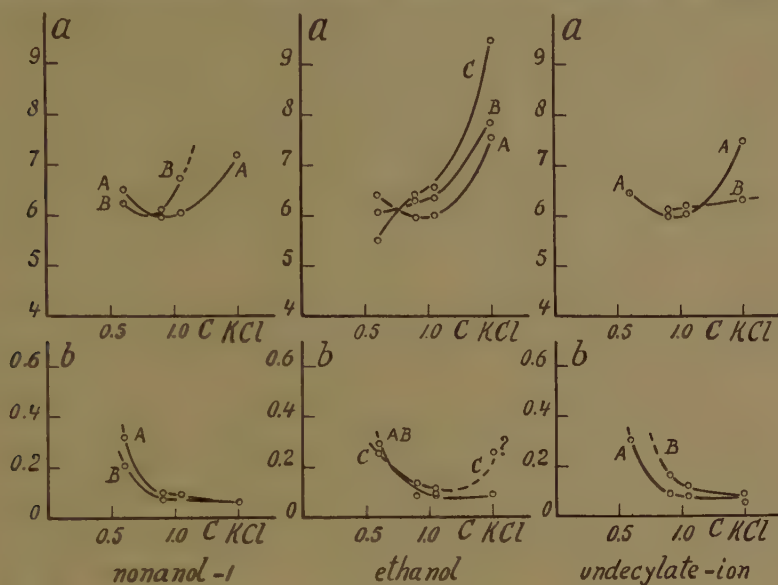


Fig. 5A. Influence of nonanol-1 (KCl sparing), ethanol (transition case; or very weakly KCl sparing) and the undecylate-ion (KCl demanding) on  $a$  and  $b$  in the equation  $\gamma G = a (C_{\text{oleate}} - b)$ , as a function of the KCl concentration.

A, B and C as in fig. 3.

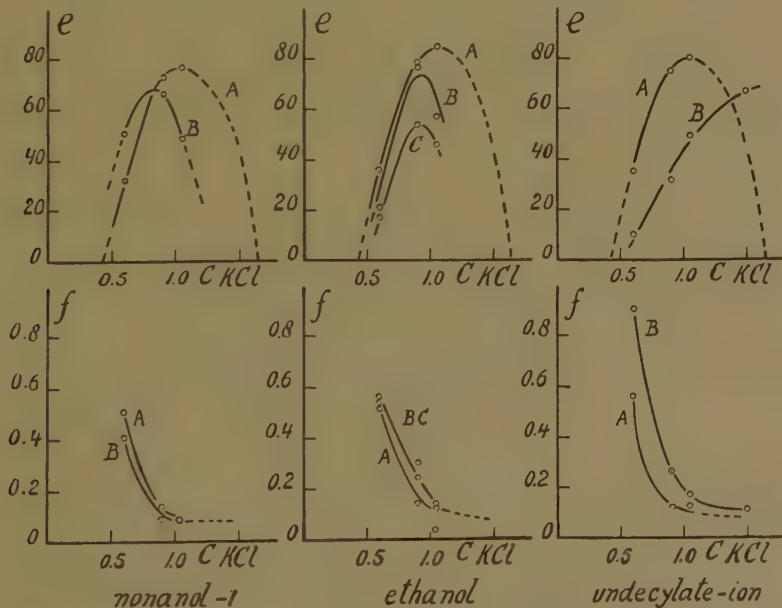


Fig. 5B. Influence of nonanol-1 (KCl sparing), ethanol (transition case, or very weakly KCl sparing) and the undecylate-ion (KCl demanding) on  $e$  and  $f$  in the equation  $n = e (C_{\text{oleate}} - f)$ , as a function of the KCl concentration.

A, B and C as in fig. 3.

The  $f$  curves for the blanks are all drawn at 1.5 N through 0.08, which is the mean of the actually determined value in the heptane series (0.06) and the value found in the part XVI at 1.5 N (= 0.10, compare there fig. 2).

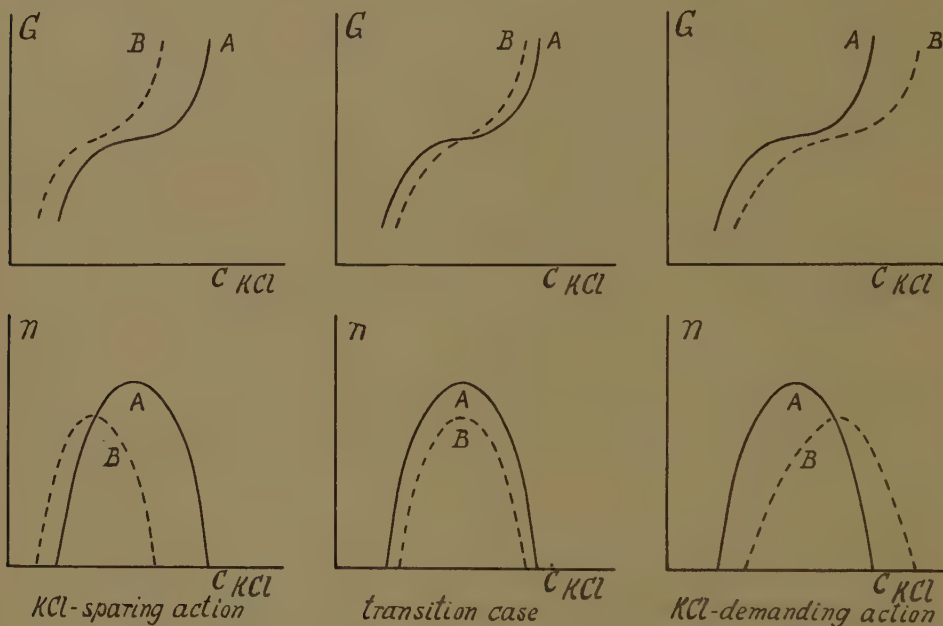


Fig. 6. Schemes to illustrate the influence of organic substances on the elastic behaviour at constant oleate concentration.

A = blank; B = after addition of the organic substance.

### 5. Discussion of the results

In the preceding parts VI — XIII we have studied the influence of added organic substances at constant oleate concentration.

Speaking very generally and leaving details out, the results showed that two opposite kinds of action and transition cases can be discerned:

1. The organic substance exerts a *KCl sparing action* (see dotted curves in fig. 6, left; the drawn curves representing the blanks), that is to say the  $G - C_{KCl}$  curve and the  $\eta - C_{KCl}$  curve are shifted in the direction of lower  $KCl$  concentrations. The shift of the  $\eta - C_{KCl}$  curve is accompanied by a lowering of its maximum.

Distinct examples are: the higher terms of the  $n$ -primary alcohols (therefore also nonanol — 1), benzene, naphtalene and cyclohexane.

2. The organic substance exerts a *KCl demanding action* (see dotted curves in fig. 6, right), that is to say the above-mentioned curves are shifted in the reverse direction. Here too the shift of the  $\eta - C_{KCl}$  curve is accompanied by a lowering of its maximum.



Distinct examples are: the undecylate-anion and the terms of the  $n$ -alkanes higher than heptane, for instance nonane.

3. *Transition cases*, in which no very distinct shifts in either direction do occur. Here the main effect on the  $n - C_{\text{KCl}}$  curve is a lowering of the maximum only (compare fig. 6, middle).

As transition cases we will also reckon those cases in which, depending on the KCl concentration or on the amount of organic substance which is added, the action may change its sign. Examples of transition cases are ethanol, heptane and decahydronaphtalene.

To investigate what lies at the bottom of the above-mentioned shifts at constant oleate concentration, we have applied in the sections 3 and 4 the new method to investigate the influence of parameters on the elastic behaviour (determination of  $\gamma/G - C_{\text{oleate}}$  and of  $n - C_{\text{oleate}}$  curves; compare part XVII of this series) and have chosen as organic substances the examples cited above sub 1., 2. and 3.

This method allows in general to resolve a change of  $\gamma/G$  at constant oleate concentration into changes of  $a$  and (or) of  $b$  in the formula  $\gamma/G = a(C_{\text{oleate}} - b)$ . Similarly a change of  $n$  at constant oleate concentration can be resolved into changes of  $e$  and (or) of  $f$  in the formula  $n = e(C_{\text{oleate}} - f)$ .

The theoretical importance of investigating the changes of  $a$ ,  $b$ ,  $e$  and  $f$  resides in the fact that we obtain more fundamental information, because the influence of the arbitrary chosen oleate concentration is now eliminated<sup>5)</sup>.

The aim was to obtain  $a - C_{\text{KCl}}$ ,  $b - C_{\text{KCl}}$ ,  $e - C_{\text{KCl}}$  and  $f - C_{\text{KCl}}$  curves for the blank and after addition of the organic substance and to consider the relative positions of these curves.

The character of the above-mentioned curves for the blanks is already known from part XVII:  $a - C_{\text{KCl}}$  is a curve with a flat minimum,  $e - C_{\text{KCl}}$  is a curve with a flat maximum,  $b - C_{\text{KCl}}$  and  $f - C_{\text{KCl}}$  are curves which consist of a steep descending branch followed by a branch which does not descend much further.

The results show that in principle added organic substances do not alter the characteristic shape of the curves, though they may shift them in various ways.

Three cases can be discerned here too:

- 1) The  $a - C_{\text{KCl}}$ ,  $b - C_{\text{KCl}}$ ,  $e - C_{\text{KCl}}$  and  $f - C_{\text{KCl}}$  curves are shifted into the direction of lower KCl concentrations, thus the organic substance exerts a *KCl sparing action on all four curves*.

This effect is shown by benzene (fig. 3A and 3B, left), naphtalene (fig. 3A and 3B, middle), cyclohexane (fig. 4A and 4B, left) and

<sup>5)</sup> Compare part XVII, section 1, in which instances are given for the influence of the arbitrarily chosen oleate concentration.

nonanol (fig. 5A and 5B, left); so by the same substances which at constant oleate concentration (1.2 %) exert a KCl sparing action on the  $G - C_{KCl}$  and  $n - C_{KCl}$  curves (fig. 6, left).

- 2) The  $a - C_{KCl}$ ,  $b - C_{KCl}$ ,  $e - C_{KCl}$  and  $f - C_{KCl}$  curves are shifted into the direction of higher KCl concentrations, thus the organic substance exerts a *KCl demanding action on all four curves*.

This effect is shown by nonane (fig. 4A and 4B, right)<sup>6</sup> and by the undecylate-ion (fig. 5A and 5B, right); so by the same substances which at constant oleate concentration (1.2 %) exert a KCl demanding action on the  $G - C_{KCl}$  and  $n - C_{KCl}$  curves (fig. 6, right).

- 3) The  $a - C_{KCl}$ ,  $b - C_{KCl}$ ,  $e - C_{KCl}$  and  $f - C_{KCl}$  curves are not distinctly shifted as a whole in either direction, which we can call *transition cases*.

When we compare the relative positions of the  $a$ -,  $b$ -,  $e$ - and  $f$ -curves for the blanks and after the addition of heptane (fig. 4A and 4B, middle), decahydronaphtalene (fig. 3A and 3B, right) and ethanol (fig. 5A and 5B, middle), one comes to the conclusion that we have transition cases here between typical KCl sparing and KCl demanding actions. Because of the lack of distinct shifts of the  $G - C_{KCl}$  and  $n - C_{KCl}$  curves at constant oleate concentration (1.2 %) in either direction, the same substances were reckoned as transition cases too.

The above results are of importance in two respects.

First, they give a background to and justify the further use of the relatively simple methods (at constant 1.2 % oleate) used in the preceding parts VI — XIII in order to study the connection between the structure of organic substances and their action on the elastic systems (see further small print below).

Second, the results are containing points of interest for a future theory of the viscous elastic oleate (or in general: soap) systems, which theory must also be able to explain the action of added organic substances. We are inclined to consider the shifts of the  $b - C_{KCl}$  curves (and as a substitute for this the shifts of the  $f - C_{KCl}$  curves; compare part XVII why  $f > b$ ) as being of primary importance.

As  $b$  is representing the oleate concentration which does not take part in the elastic phenomena, a shift of the  $b - C_{KCl}$  (and of the  $f - C_{KCl}$ ) curve in the direction of smaller KCl concentration means that the substances in question (benzene, naphtalene, cyclohexane, nonanol-1) are helping KCl to transform "free oleate" into oleate taking part in the elastic phenomena.

Presumably the structure of the elastic system arising in the presence

<sup>6</sup>) The change of the character of the  $a - C_{KCl}$  curve brought about by nonane (the curve has lost its minimum seemingly) is not quite certain. Possibly the experimentally determined point at 0.9 N KCl is erroneous.

of these KCl sparing substances is not or hardly altered, for the  $\alpha - C_{\text{KCl}}$  curve is displaced in the direction of lower KCl concentration without changing the value of  $\alpha$  at the minimum very much.

Organic substances which exert a KCl demanding action (undecylate ion; nonane) counteract KCl to transform "free oleate" into oleate taking part in the elastic phenomena (the  $b - C_{\text{KCl}}$  curves are shifted in the direction of higher KCl concentration).

Since we cannot read the position of the minima of the  $\alpha - C_{\text{KCl}}$  curves in the presence of nonane and the undecylate-ion (fig. 4A and 5A, right), we have no sufficient data here to conclude whether the resulting elastic structure is much altered in these cases.

The relative positions of the  $\alpha - C_{\text{KCl}}$  curves for the transition cases (ethanol, heptane, decahydronaphtalene) neither allow a general conclusion as to a change of the elastic structure by these substances. The value of  $\alpha$  at the minimum is not altered in the case of decahydronaphtalene.

When it is allowed to summarize the effects on the elastic structures, we may say that KCl sparing substances do not lead to a change in the elastic structures brought about by KCl and that it is uncertain whether such a change results from the presence of KCl demanding substances and of substances classed as transition cases.

Therefore there are only two main effects of added organic substances, viz.

- a. they help or they counteract KCl in bringing about the elastic system,
- b. they generally increase the damping (the maximum of the  $e - C_{\text{KCl}}$  curve is always lowered, also by substances classed as transition cases).

Though the method used in the present investigation could in theory be recommended to be used at continuation of the investigation on the connection between structure of an organic substance and its action on the elastic oleate systems, in practice it cannot be recommended. Experience showed that the accuracy of the method followed in the present communication is not very great (compare the often irregular lay of the  $\alpha$ ,  $b$ ,  $e$  and  $f$  points in the fig. 3, 4 and 5). One of the causes certainly is that in reducing the number of vessels to 16, we measured the same oleate system successively as blank, than after the first addition and thereafter after the second addition. The remedy would be to make  $3 \times 16 = 48$  apart mixtures and measure them "simultaneously". But still the number of the oleate concentrations which are used, which number was only four, is too small, strictly spoken, to derive from them accurately the slopes and the parts cut off from the abscissa by the  $\sqrt{G} - C_{\text{oleate}}$  and especially by the  $n - C_{\text{oleate}}$  curves.

The remedy would be to double the number of oleate concentrations. This would bring the number of vessels simultaneously in use to 96. This number should still be larger, as the number of KCl concentrations and the number of additions of the organic substance which is used are too small, strictly spoken. All this makes it practically impossible to use the method of the present investigation for comparison of organic substances. For the latter aim the simple methods used in the parts VI—XIII can still be recommended.

## 6. Summary

1. The influence of nine organic substances on  $a$  and  $b$  in the equation  $\sqrt{G} = a (C_{\text{oleate}} - b)$  and on  $e$  and  $f$  in the equation  $n = e (C_{\text{oleate}} - f)$  at four KCl concentrations has been investigated.

2. Benzene, naphthalene, cyclohexane and nonanol-1 are shifting the blank  $b - C_{\text{KCl}}$  and  $f - C_{\text{KCl}}$  curves in the direction of lower KCl concentrations (KCl sparing action); the undecylate ion and  $n$ -nonane are shifting the mentioned blank curves in the opposite direction (KCl demanding action);  $n$ -heptane, decahydronaphthalene and ethanol form transition cases.

3. The  $a - C_{\text{KCl}}$  curves are shifted in the same directions as the  $b - C_{\text{KCl}}$  and  $f - C_{\text{KCl}}$  curves, while the value of  $a$  at the minimum does not alter very much with benzene, naphthalene, cyclohexane, nonanol and decahydronaphthalene. It is not certain that a change of  $a$  at the minimum occurs with the other substances.

4. The  $e - C_{\text{KCl}}$  curves are also shifted in the same direction as the  $b - C_{\text{KCl}}$  and  $f - C_{\text{KCl}}$  curves. The value of  $e$  at the maximum is always lowered by the organic substance.

5. It follows from the shifts of  $b - C_{\text{KCl}}$  and  $f - C_{\text{KCl}}$  curves that benzene, naphthalene, cyclohexane and nonanol-1 are helping KCl in the transformation of "free oleate" into oleate taking part in the elastic phenomena,  $n$ -nonane and the undecylate-ion, however, counteract this transformation.

6. The results give a background to and justify the further use of the relatively simple methods used in the preceding parts VI — XIII to study the connection between the structure of organic substances and their action on the elastic system.

*Department of Medical Chemistry,  
University of Leiden*



ELASTIC-VISCOUS OLEATE SYSTEMS CONTAINING KCl. XIX <sup>1)</sup>

- 1)  *$\Delta$  as a function of  $R$  at gradually increasing oleate concentrations.*
- 2) *The problem of the nature of the damping in low concentrated oleate systems.*
- 3) *Supplementary notes on subjects investigated in preceding parts of this series.*

BY

H. G. BUNGENBERG DE JONG, H. J. VAN DEN BERG AND H. J. VERHAGEN <sup>2)</sup>

(Communicated at the meeting of June 30, 1951)

1. *Introduction*

J. M. BURGERS <sup>3)</sup> has considered theoretically three possible causes of damping for an oscillating spherical mass of an elastic fluid, viz. (a) purely viscous damping; (b) damping through relaxation of elastic tensions, characterized by a single constant relaxation time  $\lambda$ ; (c) damping through slipping along the wall of the vessel.

In the case of viscous damping the logarithmic decrement  $\Delta$  is inversely proportional to the radius  $R$  of the vessel, in the case of relaxation  $\Delta \propto R$ , while in the case of damping through slipping  $\Delta$  appears to be independent of  $R$ .

From the experimental results in the parts II, III and V of this series it appeared that in higher concentrated oleate systems (1.2 % and 1.6 %)  $\Delta \propto R$ , whereas in lower concentrated oleate systems (0.3 % and 0.6 %)  $\Delta$  is independent of  $R$ .

It, therefore, seemed plausible that the damping in higher concentrated oleate systems is caused by relaxation of elastic tensions, in lower concentrated ones by slipping along the wall of the vessel.

The question whether slip occurs in 0.6% and is absent in 1.2% oscillating oleate systems was thoroughly investigated in part XIV by studying the linear displacements in the equatorplane as a function of the distance from the centre. The results obtained with both systems are exactly alike

---

\*) Aided by grants from the "Netherlands Organization for Pure Research (Z.W.O.)".

<sup>1)</sup> Part I has appeared in these Proceedings 51, 1197 (1948); Parts II—VI in these Proceedings 52, 15, 99, 363, 377, 465 (1949); Parts VII—XIV in these Proceedings 53, 7, 109, 233, 743, 759, 975, 1123, 1319 (1950); Parts XV—XVIII in these Proceedings 54, Series B, 1, 240, 291, 303 (1951).

<sup>2)</sup> Publication No. 18 of the Team for Fundamental Biochemical Research (under the direction of H. G. BUNGENBERG DE JONG, E. HAVINGA and H. L. BOOIJ.)

<sup>3)</sup> J. M. BURGERS; these Proceedings 51, 1211 (1948).

and correspond reasonably well with the theoretical expectations for an oscillating spherical mass of an elastic fluid which does not slip along the wall of the vessel. Therefore slip does not occur in the 0.6 % oleate system. Consequently the problem of the nature of the damping in the low concentrated oleate systems ( $A$  is independent of  $R$  though no slip is present) is still unsolved.

The investigations in the present communication serve to obtain more experimental data which may be of interest for future theoretical efforts to explain the nature of the unknown type of damping occurring in the low concentrated oleate systems (section 3). For this reason the observational data will be given in full.

It seemed of particular interest to investigate in which way, at decrease of the oleate concentration, " $A \propto R$ " (characteristic for the higher oleate concentrations) gradually changes into " $A$  is independent of  $R$ " (characteristic for lower oleate concentrations).

## 2. Methods

For the experimental methods (rotational oscillation, contrivance to excite the oscillation, electrolytic  $H_2$  mark) we refer to preceding parts of this series. The experiments have been performed with completely filled spherical vessels of known capacities ( $A = 1305$ ;  $B = 496$ ;  $C = 315$ ;  $D = 117$ ;  $E = 109$ ;  $F = 73$ ;  $G = 20.8$  ml) and consequently of known radii ( $A = 6.779$ ;  $B = 4.911$ ;  $C = 4.221$ ;  $D = 3.034$ ;  $E = 2.963$ ;  $F = 2.593$ ;  $G = 1.076$  cm).

The use of a stopwatch which allowed the reading of 0.01 sec. diminished the mean error of the mean of the time measurements. As oleate preparation we used Na oleate, neutral powder from BAKER <sup>4</sup>). A mixture of the contents of 5 bottles of Na oleate was made. By examining  $G$  and  $n$  at 1.2 % oleate as a function of the oleate concentration we found for this sample as limits of the elastic systems approximately 0.45 N KCl and 1.8 N KCl and as KCl concentration corresponding to the minimum damping 1.08 N KCl. The main series of experiments has been made at the latter KCl concentration at 20°, two supplementary series of experiments at a lower (0.75 N) and a higher (1.6 N) KCl concentration, both at 15°. In all mixtures free KOH was present at a concentration of 0.05 N. In each series the mixtures were made from one stock solution of oleate and they were measured directly one after another to minimize the influence of time on the oleate. The first series (1.08 N KCl) the results of which have been given in table I and II, took 6 days.

On the last day we repeated the measurements at 0.6 % and at 1.0 % oleate which were already measured on the first and second day respectively. Comparison of the corresponding values in table I (measurements in the first three days) and table II (measurements in the last three days) allows the conclusion that during the 6 days no appreciable changes have taken place. The second (table III) and third (table IV) series have been performed together in three days, some months later than the first series. The room-temperature now allowed to choose a lower temperature of the thermostat (15°), which because of the larger damping at 0.75 and 1.6 N KCl seemed preferable.

The values of the damping ratio  $b_1/b_3$ , from which the logarithmic decrement  $A$  ( $= 2,303 \log b_1/b_3$ ) has been calculated are the means of 20 determinations. The

<sup>4</sup>) A generous gift of Na oleate from The Rockefeller Foundation provided the means for the experiments described in this paper.

TABLE I  
Measurements at 1.08 N KCl (20° C.).

% oleate	vessel	<i>n</i>	T (sec)	G ( $\frac{\text{dyne}}{\text{cm}^2}$ )	$b_1/b_3$	$\Delta$	$\Delta_{\text{ind}}$	$\kappa$	$\lambda$ (sec)
0.6	A	29.5	2.950 ± 0.006	10.9	1.570 ± 0.014	0.451 ± 0.009	0.447	10.5	∞
	B	32.3	2.139 ± 0.006	10.8	1.558 ± 0.015	0.443 ± 0.010			
	D	33.6	1.324 ± 0.002	10.8	1.576 ± 0.010	0.455 ± 0.006			
0.7	A	37.5	2.465 ± 0.005	15.5	1.416 ± 0.011	0.348 ± 0.008	0.292	19.3	21.2
	B	38.6	1.787 ± 0.004	15.5	1.402 ± 0.009	0.338 ± 0.007			
	D	39.7	1.106 ± 0.002	15.5	1.361 ± 0.008	0.308 ± 0.006			
	F	40.6	0.946 ± 0.002	15.5	1.377 ± 0.007	0.320 ± 0.005			
0.8	A	44.5	2.127 ± 0.005	20.9	1.354 ± 0.010	0.303 ± 0.007	0.238	27.5	16.4
	B	44.3	1.544 ± 0.004	20.8	1.328 ± 0.006	0.284 ± 0.005			
	D	45.6	0.954 ± 0.001	20.8	1.306 ± 0.003	0.267 ± 0.002			
0.9	A	50.1	1.853 ± 0.004	27.5	1.305 ± 0.007	0.266 ± 0.005	0.197	38	13.8
	B	51.1	1.345 ± 0.001	27.4	1.273 ± 0.005	0.241 ± 0.004			
	D	52.3	0.831 ± 0.001	27.4	1.257 ± 0.003	0.229 ± 0.002			
1.0	A	56.8	1.646 ± 0.001	34.8	1.265 ± 0.002	0.235 ± 0.002	0.123	69	7.2
	B	59.3	1.195 ± 0.002	34.7	1.234 ± 0.002	0.210 ± 0.002			
	D	59.7	0.740 ± 0.002	34.5	1.187 ± 0.002	0.172 ± 0.002			
1.1	A	65.1	1.491 ± 0.002	42.5	1.223 ± 0.003	0.201 ± 0.003	0.065	146	5.5
	B	65.1	1.087 ± 0.001	42.0	1.183 ± 0.002	0.168 ± 0.002			
	D	64.8	0.671 ± 0.001	42.0	1.133 ± 0.003	0.125 ± 0.003			
1.2	A	65.5	1.360 ± 0.001	51.1	1.170 ± 0.003	0.157 ± 0.003	0	∞	4.2
	B	64.2	0.988 ± 0.001	50.8	1.134 ± 0.003	0.126 ± 0.003			
	D	64.9	0.610 ± 0.001	50.8	1.070 ± 0.002	0.068 ± 0.002			
1.3	A	68.3	1.248 ± 0.001	60.6	1.144 ± 0.002	0.135 ± 0.002	0	∞	4.8
	B	67.9	0.909 ± 0.001	60.0	1.106 ± 0.001	0.101 ± 0.001			
	D	69.4	0.560 ± 0.002	60.3	1.054 ± 0.001	0.053 ± 0.002			
1.5	A	78.0	1.072 ± 0.001	82.1	1.105 ± 0.001	0.100 ± 0.001	0	∞	5.3
	B	79.6	0.777 ± 0.001	82.1	1.073 ± 0.001	0.071 ± 0.001			
	D	81.1	0.481 ± 0.001	81.8	1.048 ± 0.001	0.047 ± 0.001			

values of the period T given in the table follow from the means of 10 determinations of a number of consecutive periods, the number in the group depending on the oleate concentration and the KCl concentration. At 1.1 % oleate and higher we could measure 10 consecutive periods; at lower oleate concentrations this number becomes smaller (e.g. at 1.08 N KCl only 5 periods for the oleate concentrations 0.5–0.9 %; 2.5 periods for 0.3; 0.35 and 0.4 % oleate; 1.5 period for 0.25 % oleate and 0.5 period for 0.2 % oleate. Consequently the mean error of the mean T given in the tables increases with decreasing oleate concentration. The values of *n* (maximum number of turning points observable through the telescope) are the

TABLE II  
Measurements at 1.08 N KCl, continued (20° C.).

% oleate	vessel	<i>n</i>	T (sec)	G ( $\frac{\text{dyne}}{\text{cm}^2}$ )	<i>b</i> <sub>1</sub> / <i>b</i> <sub>3</sub>	<i>A</i>	<i>A</i> <sub>ind</sub>	<i>κ</i>	λ (sec)
0.5	A	22.5	3.710 ± 0.005	6.86	1.790 ± 0.011	0.582 ± 0.006	0.590	6.8	∞
	B	24.0	2.675 ± 0.004	6.92	1.811 ± 0.011	0.594 ± 0.006			
	D	25.7	1.650 ± 0.002	6.95	1.810 ± 0.011	0.593 ± 0.006			
	G	26.3	0.926 ± 0.002	6.97	1.805 ± 0.006	0.591 ± 0.003			
0.4	B	16.5	3.614 ± 0.010	3.80	2.124 ± 0.019	0.753 ± 0.009	0.741	3.8	∞
	D	17.1	2.215 ± 0.009	3.86	2.095 ± 0.008	0.740 ± 0.004			
	G	17.4	1.215 ± 0.004	4.05	2.076 ± 0.006	0.731 ± 0.003			
0.35	B	12.7	4.380 ± 0.008	2.58	2.381 ± 0.014	0.868 ± 0.006	0.872	2.70	∞
	D	14.3	2.642 ± 0.011	2.71	2.393 ± 0.021	0.873 ± 0.009			
	G	15.8	1.458 ± 0.004	2.81	2.395 ± 0.011	0.874 ± 0.005			
0.3	B	10.9	5.451 ± 0.007	1.67	2.862 ± 0.016	1.052 ± 0.006	1.056	1.82	∞
	D	12.0	3.242 ± 0.016	1.83	2.873 ± 0.016	1.056 ± 0.006			
	G	12.7	1.789 ± 0.005	1.87	2.886 ± 0.008	1.060 ± 0.003			
0.25	B	8.0	7.24 ± 0.04	0.95	3.726 ± 0.039	1.316 ± 0.011	1.335	1.08	∞
	C	8.2	6.08 ± 0.05	0.99	3.817 ± 0.011	1.340 ± 0.003			
	D	8.9	4.32 ± 0.02	1.01	3.828 ± 0.012	1.343 ± 0.003			
	G	9.8	2.29 ± 0.02	1.14	3.814 ± 0.017	1.339 ± 0.005			
0.2	C	4.0	9.67 ± 0.19	0.39	8.59 ± 0.27	2.15 ± 0.03	2.16	0.44	∞
	D	4.5	6.58 ± 0.08	0.44	8.70 ± 0.14	2.16 ± 0.02			
	G	5.3	3.53 ± 0.05	0.48	8.89 ± 0.05	2.18 ± 0.01			
0.6	A	29.5	3.018 ± 0.009	10.4	1.564 ± 0.013	0.447 ± 0.008	0.452	10.4	∞
	B	30.3	2.143 ± 0.004	10.8	1.580 ± 0.008	0.458 ± 0.005			
	D	32.3	1.319 ± 0.004	10.9	1.568 ± 0.010	0.450 ± 0.006			
1.0	A	57.6	1.638 ± 0.003	35.2	1.264 ± 0.002	0.234 ± 0.002	0.131	65	8.0
	B	59.5	1.192 ± 0.003	34.9	1.230 ± 0.002	0.207 ± 0.002			
	D	60.6	0.742 ± 0.001	34.4	1.193 ± 0.002	0.177 ± 0.002			

means of 10 determinations. The mean error of the mean is approximately 0.2 here.

The shear modulus *G* has been calculated from  $G = (2\pi/4.493)^2 \cdot (R/T)^2 \cdot \rho$ , which follows from the formula for the rotational oscillation given by J. M. BURGERS for the period. No correction of *T* for *A* has been made, as this is small in general and there where it may have some sense, (large damping) we do not know how *T* must be corrected, because here *A* is independent of *R*.

J. M. BURGERS has given a method to correct *T*, but it is based on the case that "*A* is independent of *R*" is caused by slipping.<sup>5)</sup>

From part XIV it follows, however, that in our oleate systems which show "*A* is independent of *R*" slipping is absent. The density  $\rho$  of the KCl + KOH + oleate systems hardly differ from the corresponding KCl + KOH solutions without oleate

<sup>5)</sup> J. M. BURGERS, these Proceedings 52, 113 (1949).



TABLE III  
Measurements at 0.75 N KCl (15° C.).

% oleate	vessel	$n$	T (sec)	G ( $\frac{\text{dyne}}{\text{cm}^2}$ )	$b_1/b_3$	$A$	$A_{\text{ind}}$	$\kappa$	$\lambda$ (sec)
0.5	A	11.2	$4.579 \pm 0.029$	4.44	$2.845 \pm 0.019$	$1.046 \pm 0.007$	1.051	2.9	$\infty$
	B	12.0	$3.265 \pm 0.014$	4.59	$2.851 \pm 0.014$	$1.048 \pm 0.005$			
	E	12.2	$1.894 \pm 0.007$	4.96	$2.885 \pm 0.010$	$1.060 \pm 0.004$			
0.6	A	16.1	$3.496 \pm 0.021$	7.62	$2.131 \pm 0.013$	$0.757 \pm 0.006$	0.756	5.3	$\infty$
	B	17.0	$2.487 \pm 0.013$	7.91	$2.144 \pm 0.011$	$0.763 \pm 0.005$			
	E	17.8	$1.467 \pm 0.005$	8.27	$2.113 \pm 0.011$	$0.748 \pm 0.005$			
0.7	A	21.4	$2.867 \pm 0.008$	11.3	$1.893 \pm 0.011$	$0.638 \pm 0.006$	0.627	7.8	$\infty$
	B	22.9	$2.046 \pm 0.003$	11.7	$1.851 \pm 0.015$	$0.616 \pm 0.008$			
	E	24.3	$1.202 \pm 0.003$	12.3	$1.874 \pm 0.014$	$0.628 \pm 0.008$			
1.1	A	42.4	$1.644 \pm 0.002$	34.5	$1.390 \pm 0.012$	$0.329 \pm 0.009$	0.142	60	4.5
	B	44.7	$1.175 \pm 0.001$	35.4	$1.295 \pm 0.004$	$0.259 \pm 0.003$			
	E	45.5	$0.701 \pm 0.001$	36.2	$1.255 \pm 0.004$	$0.227 \pm 0.003$			
1.2	A	51.9	$1.466 \pm 0.001$	43.4	$1.255 \pm 0.004$	$0.227 \pm 0.003$	0.067	141	4.6
	B	52.8	$1.061 \pm 0.001$	43.4	$1.193 \pm 0.002$	$0.177 \pm 0.002$			
	E	52.8	$0.626 \pm 0.001$	45.4	$1.148 \pm 0.003$	$0.138 \pm 0.002$			
1.3	A	54.6	$1.331 \pm 0.002$	52.6	$1.171 \pm 0.002$	$0.158 \pm 0.002$	0.004	261	4.3
	B	56.6	$0.956 \pm 0.002$	53.5	$1.123 \pm 0.001$	$0.116 \pm 0.001$			
	E	59.0	$0.571 \pm 0.001$	54.6	$1.074 \pm 0.001$	$0.071 \pm 0.001$			

for which we took  $\varrho = 1.0506$  for the first series (1.08 N KCl + 0.05 N KOH),  $\varrho = 1.0368$  for the second series (0.75 N KCl + 0.05 N KOH) and  $\varrho = 1.0744$  for the third series (1.60 N KCl + 0.05 N KOH).

### 3. Results and discussion

The results of the measurements at 1.08 N KCl have been given in the Tables I and II, those at 0.75 N KCl and 1.6 N KCl in the Tables III and IV respectively. When  $A$  is plotted against  $R$  we obtain the figures 1, 2 and 3.

We first discuss the results at 1.08 N KCl (corresponding to the minimum damping) as this series is the most complete one. It appears from fig. 1 that at low oleate concentration (0.2—0.6 %)  $A$  is independent of  $R$  and at sufficient high oleate concentrations (1.2—1.5 %)  $A$  is proportional to  $R$ . At intermediate oleate concentrations (0.7—1.1 %)  $A$  appears to be a linear function of  $R$ . In this domain of the oleate concentration the two types of damping obviously act simultaneously, as we can consider  $A$  to be composed of two components here; viz.  $A = A_{\text{ind}} + A_{\text{prop}}$ , the indices denoting the  $A$  component which is independent of  $R$  and the  $A$  component which is proportional to  $R$ .

TABLE IV  
Measurements at 1.6 N KCl (15° C.).

% oleate	vessel	<i>n</i>	T (sec)	G $\left(\frac{\text{dyne}}{\text{cm}^2}\right)$	$b_1/b_3$	<i>A</i>	$A_{\text{ind}}$	$\kappa$	$\lambda$ (sec)
0.5	A	11.1	2.777 ± 0.020	12.5	2.432 ± 0.030	0.889 ± 0.012	0.502	10.3	3.5
	B	15.0	1.979 ± 0.006	12.9	2.207 ± 0.030	0.792 ± 0.014			
	E	21.8	1.210 ± 0.003	12.6	1.951 ± 0.018	0.669 ± 0.009			
0.6	A	14.8	2.279 ± 0.017	18.6	2.175 ± 0.023	0.777 ± 0.011	0.309	20.2	2.4
	B	21.3	1.638 ± 0.007	18.9	1.931 ± 0.013	0.658 ± 0.007			
	E	24.6	1.007 ± 0.004	18.2	1.667 ± 0.015	0.511 ± 0.009			
0.7	A	14.7	1.891 ± 0.006	27.0	1.946 ± 0.011	0.666 ± 0.006	0.204	37	2.1
	B	21.6	1.372 ± 0.005	26.9	1.729 ± 0.019	0.548 ± 0.011			
	E	28.3	0.847 ± 0.003	25.7	1.498 ± 0.010	0.404 ± 0.007			
0.8	A	15.7	1.639 ± 0.009	35.9	1.756 ± 0.017	0.563 ± 0.010	0.089	96	1.7
	B	20.6	1.212 ± 0.004	34.5	1.554 ± 0.016	0.441 ± 0.010			
	E	31.0	0.738 ± 0.003	33.9	1.341 ± 0.005	0.294 ± 0.004			
0.9	A	17.5	1.470 ± 0.007	44.7	1.603 ± 0.012	0.472 ± 0.008	0.027	353	1.7
	B	21.7	1.076 ± 0.003	43.8	1.405 ± 0.009	0.340 ± 0.006			
	E	31.5	0.669 ± 0.002	41.2	1.250 ± 0.002	0.223 ± 0.002			

TABLE V

Survey of *G*,  $\gamma G$ ,  $1/A$  and *n* computed from the measurements at 1.08 N KCl.

oleate conc. g/100 ml	G dyne/cm <sup>2</sup> (mean)	$\gamma G$	$1/A$			<i>n</i>		
			R = 3.03	R = 4.91	R = 6.78	R = 3.03	R = 4.91	R = 6.78
0.2	0.44	0.66		0.46*		4.5	4.0**	—
0.25	1.02	1.01		0.75*		8.9	8.0	—
0.3	1.79	1.34		0.95*		12.0	10.9	—
0.35	2.70	1.64		1.15*		14.3	12.7	—
0.4	3.90	1.97		1.35*		17.1	16.5	—
0.5	6.93	2.63		1.69*		25.7	24.0	22.5
0.6†	10.8	3.29		2.22*		33.0	31.3	29.5
0.7	15.5	3.94	3.25	2.96	2.87	39.7	38.6	37.5
0.8	20.8	4.56	3.75	3.52	3.30	45.6	44.3	44.5
0.9	27.4	5.23	4.37	4.15	3.76	52.3	51.1	50.1
1.0†	34.8	5.90	5.73	4.79	4.26	60.2	59.4	57.2
1.1	42.2	6.50	8.00	5.95	4.98	64.8	65.1	65.1
1.2	50.9	7.13	14.7	7.94	6.37	64.9	64.2	65.5
1.3	60.3	7.77	18.9	9.90	7.41	69.4	67.9	68.3
1.5	82.0	9.06	21.3	14.1	10.0	81.1	79.6	78.0

† The values of *G*,  $\gamma G$ ,  $1/A$  and *n* are here the means from those in table I and in table II.

\* Reciprocal of the mean value of  $A_{\text{ind}}$  in table II (column 8).

\*\* In vessel C with *R* = 4.22.

We have calculated by a statistical method (best fitting straight line through the experimentally determined points) the slope (thus  $A_{\text{prop}}/R$ ) and the part cut off from the ordinate axis (thus  $A_{\text{ind}}$ ) and have given the latter values in column 8 of the tables. In this column we also gave the means of the  $A$  values for the oleate concentrations 0.2 — 0.6 %. Here  $A$  is independent of  $R$ , that is in the above formula  $A = A_{\text{ind}}$  because  $A_{\text{prop}} = 0$ .

We now may use the slopes  $A_{\text{prop}}/R$  to calculate  $\lambda$  (the relaxation time) and have given the latter values in column 10 of the tables.

In this column we have also recorded the  $\lambda$  values following from the slopes of the  $A = f(R)$  curves for the 1.2 %, 1.3 % and 1.5 % oleate systems. The values of  $\lambda$  thus obtained have been plotted in fig. 4 as a function of the oleate concentration. It appears that at decrease of the oleate concentration  $\lambda$  first diminishes as long as we remain in the domain in which  $A \propto R$  (thus going from 1.5  $\rightarrow$  1.3  $\rightarrow$  1.2 % oleate).

When at further decrease of the oleate concentration we enter the transition domain (in which  $A$  gradually changes its character, viz. from 1.1 % to 0.7 %),  $\lambda$  no longer decreases but increases and that more and more rapidly as we approach the left limit of this transition domain. At this left limit itself  $\lambda$  must have become infinite.

In a similar way the values of  $A_{\text{ind}}$  in the range of the concentrations 0.2 — 0.6 % oleate and in the transition domain (0.7 — 1.1 % oleate) could be used to calculate the dependence on the oleate concentration of the quantity which characterizes " $A$  is independent from  $R$ , slip being absent". But as this quantity is unknown, this cannot be done at the time present.

It is very interesting to ignore for a moment the fact that no slip is present and to calculate the coefficient  $\kappa$  characterising the friction experienced in slipping from the  $A_{\text{ind}}$  values of the tables with the aid of the formula given by J. M. BURGERS<sup>6)</sup>.

We then obtain the values recorded in column 9 of the tables. These  $\kappa$  values have also been plotted in fig. 4 and it appears that at increase of the oleate concentration in the domain in which  $A$  is independent of  $R$  (0.2  $\rightarrow$  0.6 %)  $\kappa$  increases and that after entering the transition domain (0.7 — 1.1 % oleate)  $\kappa$  still further increases and that more and more rapidly as we approach the right limit of the transition domain. At this right limit itself  $\kappa$  must have become infinite. The transition domain would thus be characterized by  $\lambda$  and  $\kappa$  having finite values simultaneously, the former becoming infinite at the left limit of this domain, the latter becoming infinite at the right limit. This is quite in accordance with the theoretical deductions of J. M. BURGERS, who in deriving the formula for the damping through relaxation from a more general expression only had to consider the case  $\eta = 0$  and  $\kappa = \infty$ ; similarly in deriving the

<sup>6)</sup> J. M. BURGERS, These Proceedings 51, 1211, (1948), compare equation (18).

formula for the damping through slipping only had to consider the case  $\eta = 0$  and  $\lambda = \infty$  <sup>7)</sup>).

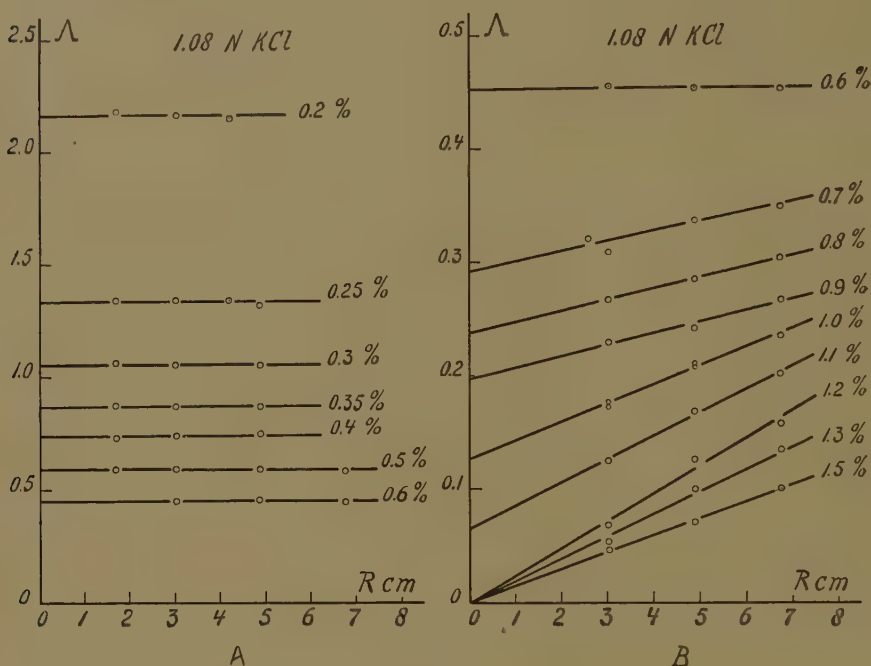


Fig. 1.  $\Lambda$  as a function of  $R$  at increasing oleate concentrations (% = g/100 ml). KCl concentration = 1.08 N and temperature = 20° C.

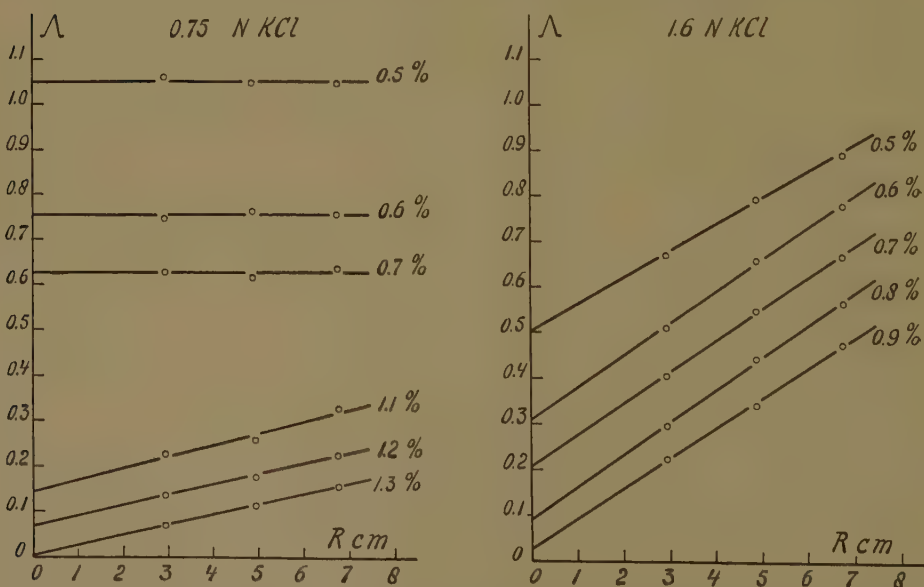


Fig. 2 and 3.  $\Lambda$  as a function of  $R$  at increasing oleate concentrations (% = g/100 ml). KCl concentration = 0.75 N in fig. 2 and 1.6 N in fig. 3. Temperature = 15° C.

<sup>7)</sup> J. M. BURGERS, these Proceedings 51, 1211 (1948), compare equations (15), (17) and (18).



When we add to this that we could confirm in part III of this series quantitative relationships following from the supposition that " $A$  independent of  $R$ " is caused by damping through slipping, it remains quite remarkable that in part XIV decidedly no slip could be observed.

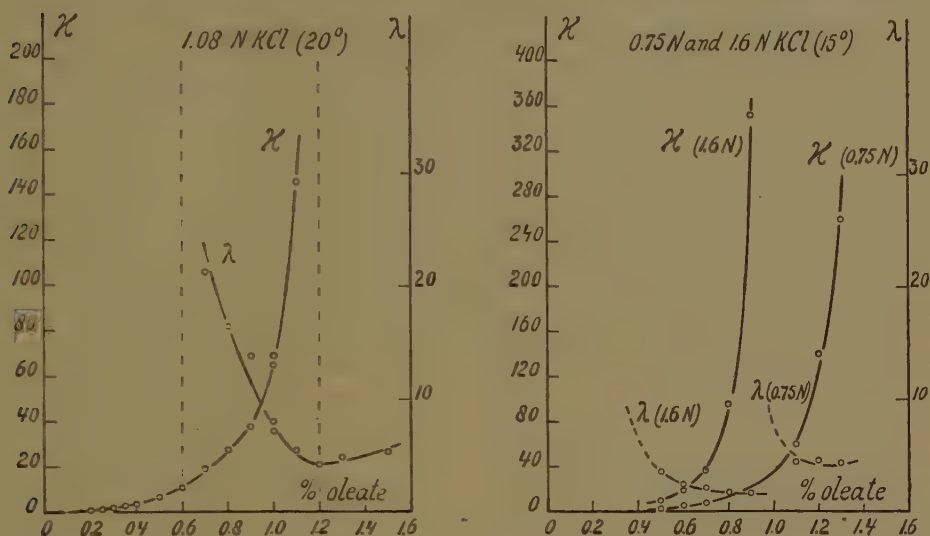


Fig. 4 and 5.  $\kappa$  and  $\lambda$  as a function of the oleate concentration (see text).

A further point against this explanation is that the theory predicts a maximum value of  $A$  of approximately 1.06 for damping through slipping<sup>8)</sup>, whereas it appears from the measurements in table II (compare fig. 1) that " $A$  independent of  $R$ " still is present at 0.25 % and 0.2 % oleate, where  $A$  is 1.34 and 2.16 respectively.

It may be mentioned here that an attempt was made to influence the damping of an 1.2 % oleate system by altering the nature of the wall which is in contact with the oleate system. It formed part of an investigation in which  $T$  and  $A$  as function of the radius of the vessel were measured for 0.6 and 1.2 % oleate systems containing potassium citrate instead of KCl. The concentration which was used of this salt (0.48 mol/l) lies close to the one of the minimum damping.

R cm	0.6 % oleate		1.2 % oleate	
	$T$	$A$	$T$	$A$
3.03	$1.302 \pm 0.003$	$0.449 \pm 0.009$	$0.609 \pm 0.002$	$0.120 \pm 0.002$
4.91	$2.136 \pm 0.008$	$0.439 \pm 0.006$	$0.990 \pm 0.002$	$0.192 \pm 0.003$
4.91*	—	—	$0.989 \pm 0.003$	$0.192 \pm 0.002$
6.78	$2.961 \pm 0.004$	$0.437 \pm 0.007$	$1.360 \pm 0.002$	$0.256 \pm 0.003$

The results (compare survey), when plotted against  $R$ , will show that  $T$  both in the 0.6 % and 1.2 % oleate system is proportional to  $R$  and that  $A$  in the 0.6 % oleate system is independent of  $R$ , whereas in the 1.2 % oleate system  $A$  is

<sup>8)</sup> J. M. BURGERS, these Proceedings 52, 113 (1949).

proportional to  $R$ . The behaviour of  $\Delta$  in the untreated vessels (without asterisk) is therefore comparable to that in fig. 1 with 1.08 N KCl, the transition region lying here too between 1.2 % and 0.6 %. When " $\Delta$  is independent of  $R$ " is caused by slip and assuming that the elastic structures in the oleate system adhere to the polar-glass-wall through intermediary of the polar groups of the oleate, it should be possible with the very 1.2 % oleate system to alter  $\Delta$  by changing the polar glass-wall into a typically apolar hydrocarbon wall.

The adhesion of the oleate structure would then be decreased and as a consequence slip will occur, so that the 1.2 % oleate system in such a vessel will no longer show  $\Delta \propto R$ , but will be in the transition region or will already show " $\Delta$  independent of  $R$ ".

In any of the two cases which are mentioned  $\Delta$  will be increased. To test this, in the above measurements with the 1.2 % oleate system a second vessel with  $R = 4.91$  was included, the inner surface of which had been covered beforehand with a polystyrene film <sup>9)</sup>.

The measurements of this vessel-with asterisk in the above survey-gave exactly the same value of  $\Delta$  as in the untreated glass vessel of the same radius. This result, therefore does not support the supposition that " $\Delta$  independent of  $R$ " is caused by slip.

The experimental series at 0.75 N KCl (Table III) and at 1.6 N KCl (Table IV) are not so extensive as the one at 1.08 N KCl, but they also show the linear dependence of  $\Delta$  on  $R$  in the transition region. Compare figs. 2 and 3. Here too we have calculated  $\lambda$  and  $\kappa$  (compare columns 9 and 10 in Table III and IV) and have plotted them against the oleate concentration in fig. 5. The course of the  $\lambda$  and  $\kappa$  curves is the same here as in fig. 4. When we compare the position of the  $\lambda$  and  $\kappa$  curves in the figs. 4 and 5, it appears that the position of the transition region depends on the KCl concentration. With increase of the latter it is displaced in the direction of lower oleate concentrations.

Taking together all experience regarding " $\Delta$  independent of  $R$ " (parts III, V, XIV and the present part), we are inclined to think that an internal slipping in the oleate system and not a slipping between the system and the wall of the vessel is involved.

#### 4. *Supplementary notes on subjects investigated in the two previous parts of this series*

Using the data of the Tables I and II we give in Table V values of  $G$  (means of the determinations in vessel with different radii),  $\sqrt{G}$ ,  $1/\Delta$  and  $n$  for each oleate concentration at 1.08 N KCl.

---

<sup>9)</sup> A relatively strong adhering film was obtained by evaporating a commercial polystyrene solution diluted with xylol when the inner wall of the vessel was covered previously with a film of soluble starch (evaporating a 1 % aqueous solution). In both steps the evaporation was supported in its final stages by heating the outer wall of the vessel with an electrical hairdryer, while the vessel rotated horizontally around its axis and the air in the vessel was constantly renewed by suction through an horizontal glasstube placed in the axis of the vessel. We controlled that after the above measurements the polystyrene film was still intact.

Fig. 6, in which  $\sqrt{G}$  is plotted against the oleate concentration, confirms that the  $\sqrt{G} - C_{\text{oleate}}$  curve is a straight line, intersecting the abscissa at a finite, though small value of the oleate concentration (compare part XVI). Fig. 6 is the most extensive example hitherto investigated, as it comprises no less than 15 experimental points.

In the only investigated example (part III, compare fig. 5 in part XVI) the  $1/\Lambda - C_{\text{oleate}}$  curve consisted of two straight branches, a lower branch cutting the abscissa at a finite though small value of the oleate concentration and a steeper branch connected with the former by a bend at approx. 1.1 % oleate.

Fig. 7, in which  $1/\Lambda$  is plotted against the oleate concentration for three values of  $R$  (data of Table V), confirms that the lower part of the  $1/\Lambda - C_{\text{oleate}}$  curve is a straight line, intersecting the abscissa at a finite, though small value of the oleate concentration.

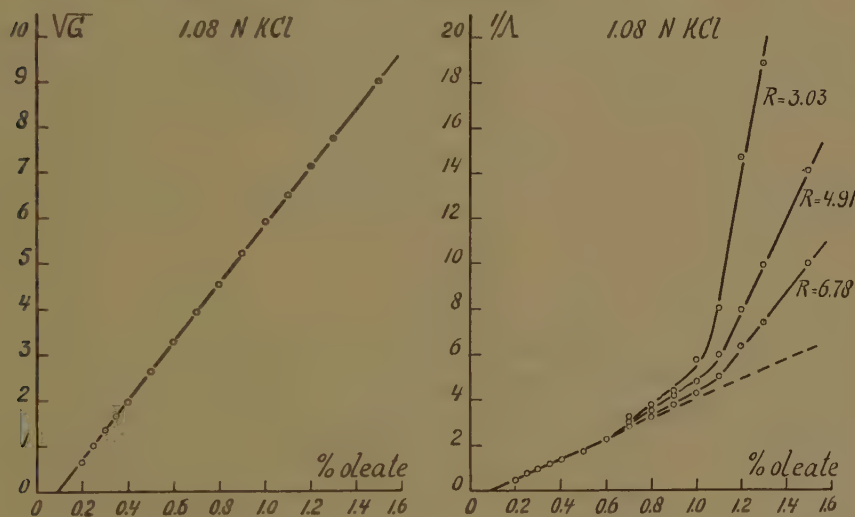


Fig. 6 and 7. Dependence of  $\sqrt{G}$  and of  $1/\Lambda$  on the oleate concentration (1.08 N KCl; 20° C.)

Fig. 7 shows the presence of an intermediate branch, beginning at approx. 0.6 % oleate apart from the lower branch and the steep branch beginning at approx. 1.1 % oleate. Obviously the transition region in which  $\Lambda$  is a linear function of  $R$  (compare section 3) expressed itself here as an apart branch in the  $1/\Lambda - C_{\text{oleate}}$  curve.

Fig. 7 shows clearly the dependence of the position of the intermediate and the upper branch on the radius of the vessel. With the largest vessel — in which  $\Lambda$  is greatest — the angle between the lower and the intermediate branch is the least and the presence of the intermediate branch would have escaped us if we had not had a sufficient number of experimentally determined points. This explains why this detail had actually escaped us in part III using oleate from MERCK.

The number of experimentally determined points was less and the damping was in general much greater with this preparation (though we used 500 ml vessels,  $\Delta$  was even greater in general than the one of analogous systems prepared from oleate from BAKER measured in 1300 ml vessels).

The  $n - C_{\text{oleate}}$  curves show a simpler character — compare fig. 8 in which  $n$  at  $R = 4.91$  is plotted against the oleate concentration (data of Table V). There is no indication that the curve consists of three branches. The change in character of the damping at approx. 0.6 % oleate, therefore, does not come to expression, and only the one in the neighbourhood of 1.1 % oleate is indicated by a bend. The  $n$  values which are actually measured are distributed unusually irregular around the second part of the  $n - C_{\text{oleate}}$  curve.

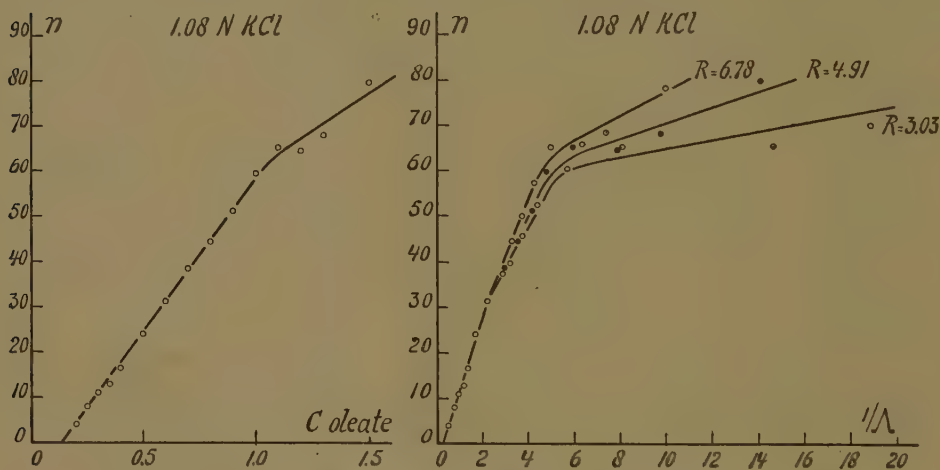


Fig. 8. Dependence of  $n$  on the oleate concentration (1.08 N KCl; 20° C.;  $R = 4.91$  cm).

Fig. 9. Correlation between  $n$  and  $1/\Delta$  (1.08 N KCl; 20° C.;  $R = 3.03, 4.91$  and 6.78 cm respectively).

The lower branch of the  $n - C_{\text{oleate}}$  curve in fig. 8 cuts the abscissa at approx. 0.14 % oleate, whereas the  $\sqrt{G} = C_{\text{oleate}}$  curve (fig. 6) and the lower branch of the  $1/\Delta - C_{\text{oleate}}$  curve (fig. 7) both cut the abscissa at approx. 0.09 % oleate. This confirms for oleate from BAKER the relation  $b = d < f$  found for oleate from MERCK in part XVI (in section 4 an explanation of this relation has been given).

The relation between  $n$  and  $1/\Delta$  was discussed in part XV, using exclusively data obtained with oleate from MERCK. It was found that the  $n - 1/\Delta$  curve consists of two branches, a steeper lower branch cutting the abscissa at a small value of  $1/\Delta$  and an upper less steep branch.

Fig. 9, in which the data of the Table V are used, shows that the  $n - 1/\Delta$  curves consists here of three branches. Obviously the much more damped character of the elastic systems with oleate from MERCK (see above) prevented us to observe that the "lower branch" in reality consists of two branches with slopes that do not differ very much.



### 5. Summary

1. The dependence of  $A$  on  $R$  has been measured at a sufficient number of oleate concentrations and at three KCl concentrations in order to obtain information how “ $A$  independent of  $R$ ” (characteristic for low oleate concentrations) gradually changes into “ $A$  proportional to  $R$ ” (characteristic for higher oleate concentrations).

2. It appears that at intermediate oleate concentrations  $A$  is a linear function of  $R$ . This allows to consider  $A$  to be the sum of two components here, viz. a partial  $A$  which is independent of  $R$  and a partial  $A$  which is proportional to  $R$ .

3. With the aid of the formulae given by J. M. BURGERS — assuming that “ $A$  independent of  $R$ ” is caused in reality here by slipping — the frictional coefficient  $\kappa$  and the relaxation time  $\lambda$  have been calculated and have been plotted against the oleate concentration.

4. The course which the  $\lambda$ - and  $\kappa$ -curves are taking is quite as is to be expected, from the theory given by BURGERS,  $\lambda$  becoming  $\infty$  at the lower limit of the transition domain and  $\kappa$  becoming  $\infty$  at the upper limit of this domain. Other consequences of the theory have already been confirmed quantitatively in part III of this series.

5. Despite the above mentioned sub 4) the nature of the damping shown by the low concentrated oleate systems is still an unsolved problem, because

- (1) “ $A$  independent of  $R$ ” is not accompanied by slipping along the wall of the vessel (compare part. XIV of this series),
- (2) the present investigation shows examples in which “ $A$  independent of  $R$ ” occurs at absolute values of  $A$  (1.34 and 2.06), which are higher than the maximum value of  $A$  (1.06) which would be possible theoretically in the case of slipping.
- (3) an attempt to influence the damping by the nature of the wall which is in contact with the oleate system (glass, polystyrene) had a completely negative result.

The suggestion has been made that there is “internal” slipping in the low concentrated oleate systems.

6. The experimental data have been used to supplement some subjects treated in the parts XV and XVI. The most important contributions are (1) a fair example of the strict linear relation between  $\sqrt{G}$  and the oleate concentration as is expressed by  $\sqrt{G} = a (C_{\text{oleate}} - b)$ , (2) the shape of the  $1/A - C_{\text{oleate}}$  curve, which appears to consist of three branches.

*Department of Medical Chemistry,  
University of Leyden*

# CHEMISTRY

## THE OZONOLYSIS OF PYRROLE AND SOME OF ITS HOMOLOGUES IN CONNECTION WITH THE STRUCTURE OF THE RING SYSTEM <sup>1)</sup>

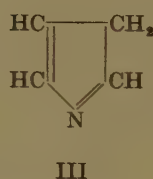
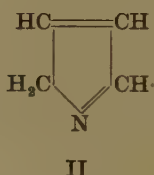
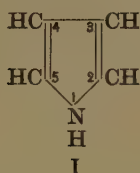
BY

J. P. WIBAUT AND A. R. GULJÉ

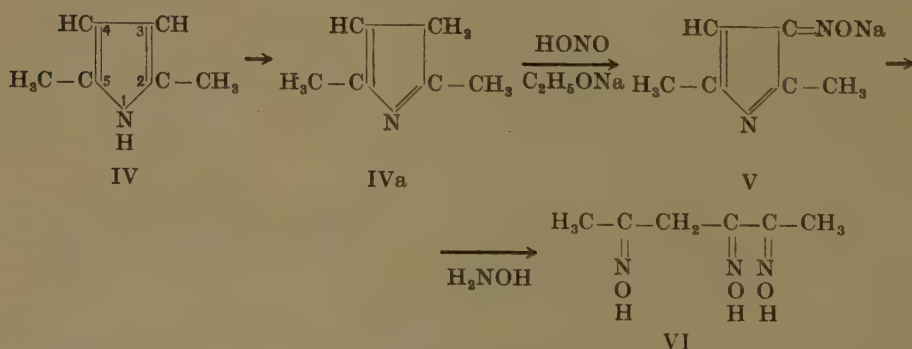
(Communicated at the meeting of June 30, 1951)

### § 1. Introduction

Pyrrole and its homologues show in some respects an aromatic character, but are in general less saturated in their behaviour than benzene and its derivatives. To pyrrole itself the imine structure (I) is assigned; there are indications that certain pyrrole derivatives can react according to a pyrrolenine structure (II) or (III):

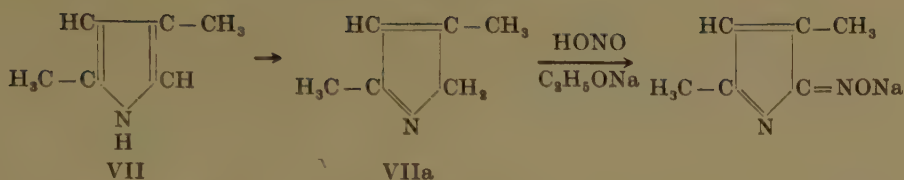


ANGELI, ANGELICO and CALVELLO [1] treated 2,5-dimethylpyrrole (IV) with amyl nitrite and sodium ethylate and obtained the sodium salt of an isonitroso compound, to which they assigned structure (V), because this substance can be converted into the trioxime of hexanetrione-2, 3, 5 (VI).



Therefore they assume that the 2,5-dimethylpyrrole in this case reacts according to the tautomeric structure (IVa). Also from 2,4-dimethylpyrrole (VII) the sodium salt of an isonitroso compound was obtained, a similar reaction being assumed.

<sup>1)</sup> Compare the thesis of A. R. GULJÉ, (Amsterdam 1950).



Afterwards efforts were made to find out by physical measurements whether the pyrrole occurs in tautomeric forms. BONINO, MANZONI-ANSIDEI and PRATESI [2] concluded from the study of the Raman spectrum of pyrrole and its homologues that these forms do not occur. STERN and THALMAYER [3], who repeated these measurements, came to the opposite conclusion. LORD and MILLER [4] made an accurate investigation of the Raman and infra-red spectra of pyrrole and some deuteropyrroles; they did not find indications of tautomerism.

A study of the ozonolysis of aromatic compounds may show according to which valency structures the ring system can react [5]. Therefore we carried out an extensive investigation into the action of ozone on pyrrole and its homologues and examined the decomposition products obtained <sup>1)</sup>.

FRERI [6] investigated the action of ozone at 0° on pyrrole in an undiluted condition, on a suspension of pyrrole in water and on a solution of pyrrole in acetic acid, in dilute sulphuric acid or in ether. He only obtained amorphous, undefined reaction products and observed resinification. This resinification was also found during the action of ozone on some methyl homologues of pyrrole.

We found that the action of ozone on pyrrole and its homologues proceeds satisfactorily if the reaction is carried out at -60° C in dry, pure chloroform as solvent. Even at this low temperature resinification takes place to some extent. In all cases investigated by us, however, we succeeded in isolating the characteristic decomposition products formed during ozonolysis.

In our experiments a mixture of ozone and oxygen, containing 12-15 % by *wt* of ozone, was passed through a solution of 20 millimols of pyrrole or pyrrole derivative in 30 ml of chloroform. After introducing 40 millimols of ozone the cold chloroform was poured into a solution of nitrophenylhydrazine and sulphuric acid in ethanol cooled to -60° C. The dicarbonyl compounds formed by ozonolysis are converted into *p*-nitrophenylosazones, which are isolated from pyridine by recrystallization and identified by mixed melting point. It is impossible, however, in this way to effect a quantitative separation of the *p*-nitrophenylosazones. To determine the relative quantities of dicarbonyl compounds formed we isolated them in the form of the dioximes. For this purpose the cold chloroform solution, as obtained after the action of ozone, was poured

<sup>1)</sup> The experimental details will be published in the *Recueil des Travaux chimiques des Pays-Bas*.

into a solution of hydroxylamine hydrochloride and soda in water cooled at 0° C, after which the mixture was shaken for a considerable time. For the working-up and analysis of the dioximes formed we refer to previous publications.

The *p*-nitrophenylosazones have a low solubility and are therefore easier to isolate than the dioximes. The total yield of dicarbonyl compounds is higher on the basis of the quantity of *p*-nitrophenylosazones than on that of the quantity of dioximes. The total yield of dicarbonyl compounds calculated from the dioximes therefore represents a minimum value. By analysis of the mixture of dioximes, however, the relative quantities of the dicarbonyl compounds formed are found to a first approximation.

In the ozonolysis of pyrrole and its homologues not only dicarbonyl compounds are formed, but also ammonia, which was in some cases determined quantitatively, in addition to formic acid or acetic acid, which were identified qualitatively. In some cases also very slight quantities of nitric acid were identified and determined as nitron nitrate. From the pyrroles substituted to nitrogen no ammonia is formed, but a primary amine.

The ozonizations were carried out at -60° C, except 2,5-dimethylpyrrole, which was ozonized at -45° C.

From the isolated quantity of *p*-nitrophenylosazones it is impossible to estimate which percentage of the original pyrrole derivative has reacted with ozone. Neither is it possible to determine which quantity of pyrrole derivative is still unchanged after the experiment. Therefore we tried a different method to gain some insight into the quantitative development of the reaction. For a number of pyrrole homologues which do not show resinification during the action of ozone, we made an accurate determination of the quantity of ozone taken up at a constant temperature and of that of ammonia (methylamine) formed after the ozonides have split off<sup>1</sup>). The results are summarized in table I.

TABLE I

Pyrrole derivative	Temp. °C	Millimols of ozone taken up per millimol of pyrrole	Millimols of amm. formed per millimol of pyrrole
2,4-dimethylpyrrole . . . . .	- 60°	1.60	0.79
2,4-       "       . . . . .	- 60°	1.59	0.79
2,3-       "       . . . . .	- 60°	1.65	0.85
2,3-       "       . . . . .	- 60°	1.66	0.87
2,5-       "       . . . . .	- 45°	1.67	0.84
2,5-       "       . . . . .	- 45°	1.68	0.81
1,2-       "       . . . . .	- 60°	1.66	0.83 <sup>2</sup> )

<sup>1</sup>) For the experimental procedure of the quantitative ozone determinations we refer to a paper by SIXMA to be published in the Recueil des Travaux chimiques des Pays Bas. For the ammonia determinations see H. BOER, F. L. J. SIXMA and J. P. WIBAUT, Rec. Trav. chim. 70, 457 (1951).

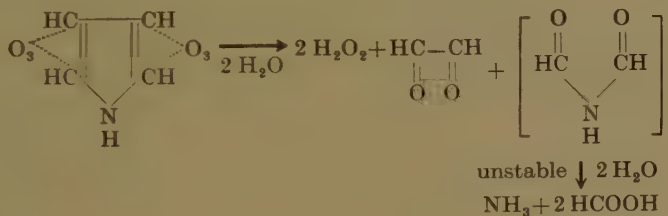
<sup>2</sup>) methylamine



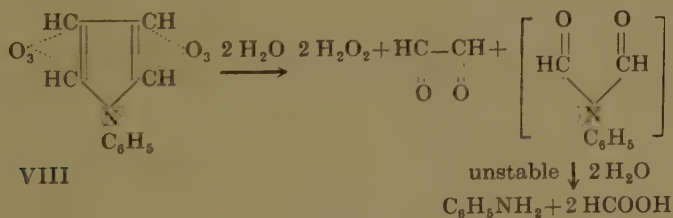
Assuming that the quantity of ammonia (methylamine) found is a measure of the quantity of pyrrole which has reacted with ozone, it may be concluded from the figures that one mol of pyrrole derivative has reacted with two mols of ozone. The deviations from this ratio may have been caused by analytical errors.

We shall now discuss some scission products formed during the ozonolysis of the pyrrole derivatives examined.

Ozonolysis of pyrrole is accompanied by resinification; on decomposition of the ozonized product glyoxal is formed in a yield of 15 % (isolated in the form of the *p*-nitrophenylosazone melting at 308°), in addition to formic acid and ammonia. These decomposition products can be formed according to the imine formula of pyrrole, assuming that one molecule of ozone acts on each of the C = C bonds and that the diozonide formed is decomposed according to the following scheme:

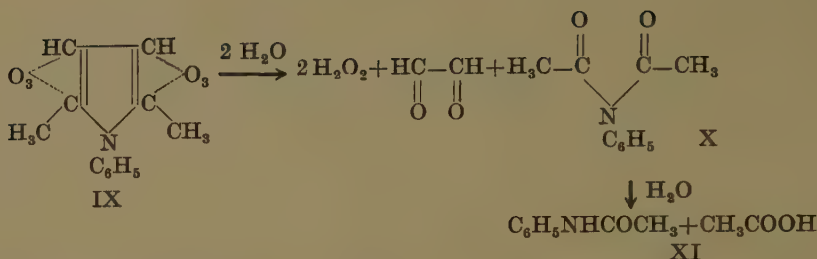


In the ozonolysis of N-phenylpyrrole (VIII) we obtained not only glyoxal (38 %, isolated as *p*-nitrophenylosazone), but also aniline in a yield of 58 % (isolated in the form of tribromoaniline); formic acid was identified qualitatively. This result is in very good agreement with the imine formula of the pyrrole ring:

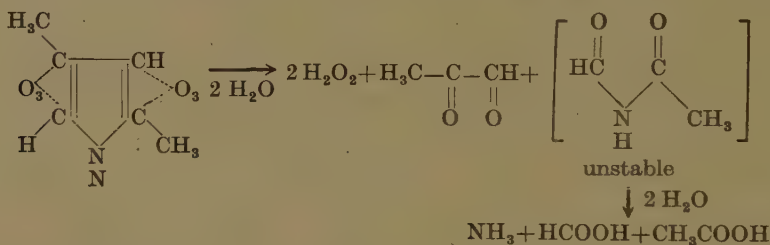


As the action of ozone takes place at  $-60^\circ$ , the phenyl group occurring in the N-phenylpyrrole is hardly attacked by ozone.

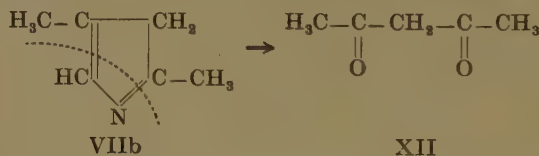
The 1-phenyl-2,5-dimethylpyrrole (IX) also reacts according to the imine structure. In this case we isolated the 2,4-dibromoacetanilide in a yield of 4.5 % after adding bromine water to the reaction product. This proves the formation of acetanilide (XI) as scission product of the ozonolysis; under the experimental conditions one acetyl group is apparently split off from the primarily formed diacetylaniline (X):



During ozonolysis of 2,4-dimethylpyrrole (VII) methylglyoxal is formed and isolated as *p*-nitrophenylosazone (yield 41 %) and as methylglyoxime (yield 36.5 %), formic acid, acetic acid, ammonia, and nitric acid (0.8 %), isolated in the form of the nitron nitrate ( $\text{C}_{20}\text{H}_{16}\text{N}_4 \cdot \text{HNO}_3$ ). This result is in very good agreement with the imine structure:



If the 2,4-dimethylpyrrole should partly react according to a  $\beta$ -pyrrole-nine form (VIIb) the decomposition product might be expected to be acetylacetone (XII), which can be identified by its characteristic blue copper compound. However we could not identify acetylacetone.



The formation of a small quantity of nitric acid shows that slight oxidation of the nitrogen atom has taken place.

The above experiments are in perfect agreement with the classical concept of the structure of the pyrrole ring, namely the imino formula. The following experiments show that also other structures have to be considered.

In the ozonolysis of 2,5-dimethylpyrrole glyoxal and methylglyoxal are formed in a total yield of about 33 %, calculated on the basis of the quantity of *p*-nitrophenylosazones formed. Calculated on the basis of the isolated dioximes the yield of glyoxal was 3.2 % and that of methylglyoxal 20.6 %. Moreover, we found acetic acid, 84 % of the nitrogen present in the pyrrole derivative being recovered as ammonia. The glyoxal can be formed from the imine structure (IV), in which the carbon atoms 3 and 4 are linked by a single bond. The methylglyoxal must, however,

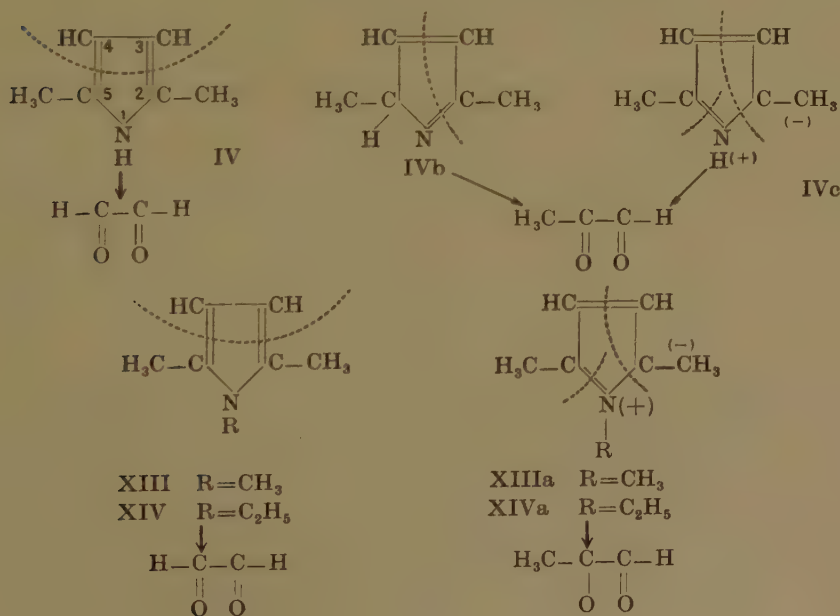
be formed from a structure in which the carbon atoms 2 and 3 are linked by a single bond.

In this connection one might consider the  $\alpha$ -pyrrolenine structure IVb formed from the imine structure by the shifting of a proton. It is impossible to imagine, however, how from this structure the nitrogen could be split off as ammonia, for investigations into the ozonolysis of pyridine homologues showed that the  $C=N$  bond does not react with ozone, but that this bond undergoes hydrolytic splitting in the latter stage of the reaction, i.e. during decomposition of the ozonide. Oxidative splitting of the  $C=C$  bond, together with hydrolytic splitting of the  $C=N$  bond would result in the formation of  $\alpha$ -aminopropione aldehyde (or  $\alpha$ -aminopropionic acid) from the pyrrolenine structure, but not of ammonia.

The 1,2,5-trimethylpyrrole (XIII), whose nitrogen atom carries a methyl group cannot be converted into a pyrrolenine form. Ozonolysis of 1,2,5-trimethylpyrrole, however, not only yielded 1 % of glyoxal, but also 2 % of methylglyoxal (determined as dioximes). The low yields are caused by pronounced resinification during ozonization of the pyrrole derivative.

After ozonolysis of 1-ethyl-2,5-dimethylpyrrole (XIV), in which resinification was less pronounced than in the former case, we found 1.6 % of glyoxal and 4.4 % of methylglyoxal.

It must be assumed that the methylglyoxal has been formed from a polar form XIIIa or XIVa, for in this structure the carbon atoms 2 and 3 are linked by a single carbon bond. In the polar structure the nitrogen atom carries a positive charge, the carbon atom 5 carrying a negative charge. Now we can also assume for the 2,5-dimethylpyrrole a polar structure IVc, from which methylglyoxal can be formed.

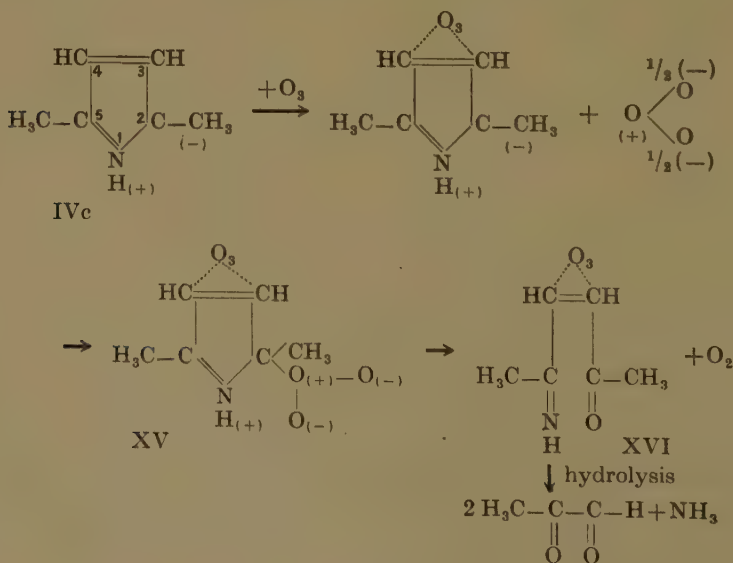


The question arises how ozonolysis must be assumed to take place if the pyrrole derivative reacts according to a polar structure. The double bond between the C atoms 3 and 4 will react with one molecule of ozone; we cannot imagine, however, that the double bond between the nitrogen atom and the carbon atom 2 should react with ozone. If this were the case it might be expected that nitrous acid or nitric acid would be formed during ozonolysis. We have not succeeded, however, in identifying the presence of nitrous acid, while only small quantities of nitric acid are formed. Most of the nitrogen present in the pyrrole nucleus is split off as ammonia.

Kinetic investigations into the action of ozone on benzene and benzene derivatives [7], including the influence of catalysts such as  $\text{AlCl}_3$ ,  $\text{BF}_3$  and  $\text{FeCl}_3$  led to the conclusion that the action of ozone on the aromatic nucleus proceeds according to an electrophilic mechanism. If a similar mechanism is assumed for the action of ozone on pyrrole, it is quite plausible also to assume electrophilic addition of the ozone molecule to the carbon atom 2.

Also in the nitration of pyrrole, which may be considered as an electrophilic substitution, the substituent preferably occupies the  $\alpha$ -position.

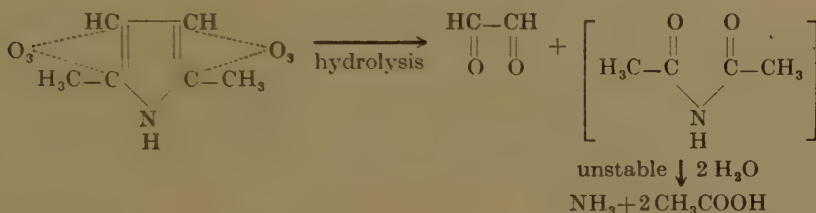
We further assume that the primary addition product XV decomposes in such a way that an oxygen molecule is split off and an oxygen atom is linked by a double bond to the carbon atom 2, the single bond between the nitrogen atom and carbon atom 5 being broken. Hydrolysis of the hypothetical intermediate product XVI leads to the formation of two molecules of methylglyoxal and of one molecule of ammonia, because the group  $\text{H}_3\text{C}-\overset{\textstyle |}{\text{C}}=\text{O}$  will be formed from the atom group  $\text{H}_3\text{C}-\overset{\textstyle |}{\text{C}}=\text{NH}$  present in XVI, the nitrogen bound by the imino group being split off as ammonia.





According to this reaction scheme, which contains various unproved assumptions, the polar form of the pyrrole homologue will react with two molecules of ozone, while on decomposition of the reaction product the nitrogen will be split off as ammonia with formation of methylglyoxal. From one molecule of the polar form two molecules of methylglyoxal can be formed. This is in agreement with the experimental fact that ozonolysis of 2,5-dimethylpyrrole is accompanied by formation of a considerable quantity of methylglyoxal.

The imino form (IV) of 2,5-dimethylpyrrole can also take up 2 molecules of ozone: after hydrolysis of the diozonide glyoxal, ammonia and acetic acid are formed:



As according to the proposed theory both the polar and the imino form of 2,5-dimethylpyrrole react with two molecules of ozone, the nitrogen being split off from the two forms as ammonia, this theory is in agreement with the experimental data mentioned in table I.

Similar results were obtained in the ozonolysis of some other homologues of pyrrole.

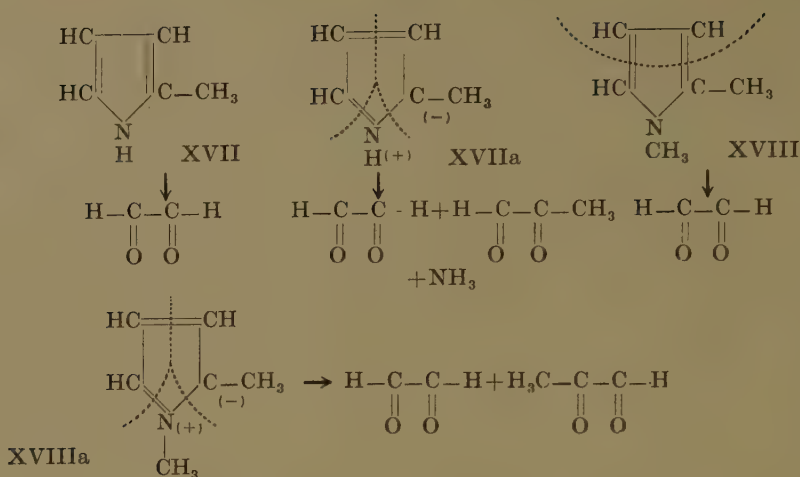
The action of ozone on 2-methylpyrrole XVII at  $-60^\circ$  is accompanied by pronounced resinification. However, we still succeeded in isolating the characteristic scission products; from 15 millimols of 2-methylpyrrole we obtained 1.08 millimols of glyoxal and 0.18 millimol of methylglyoxal, both isolated in the form of the dioximes.

The action of ozone on 1,2-dimethylpyrrole (XVIII) proceeded without resinification; ozonolysis of 28.4 millimols of this pyrrole homologue yielded 1.45 millimols of glyoxal (5.1 %) and 2.37 millimols of methylglyoxal (8.3 %).

These results are in agreement with the assumption that the above-mentioned pyrrole homologues can react both according to the imino structure and according to a polar structure: (See following page).

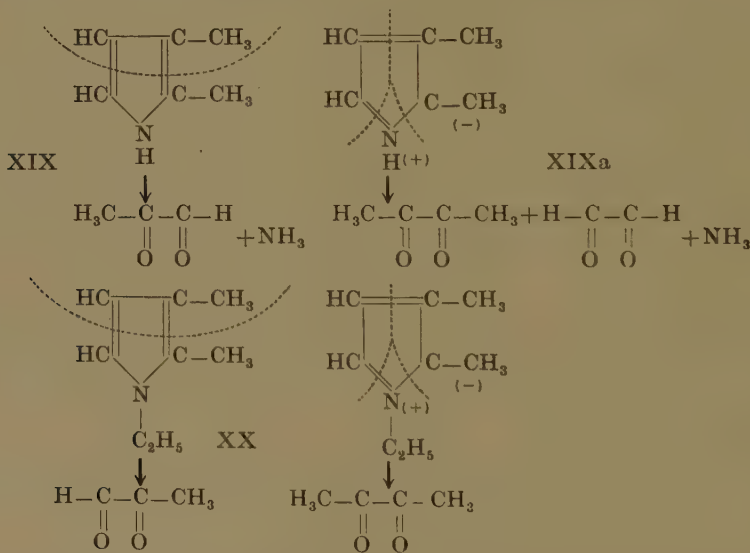
In the ozonolysis of 2,3-dimethylpyrrole (XIX) we obtained from 43 millimols of the pyrrole homologue 4.94 millimols of dimethylglyoxal (11.5 %), 1.86 millimols of methylglyoxal (4.3 %) and some glyoxal. The dioximes of dimethylglyoxal and of methylglyoxal were identified by their mixed melting points; the dioxime of glyoxal was identified by the infrared spectrum. The mixture of the scission products contained ammonia (86 %, see table I) and a very slight quantity of nitric acid.

In the ozonolysis of 14 millimols of 1-ethyl-2,3-dimethylpyrrole (XX),



we obtained 0.4 millimol of methylglyoxal (2.9 %) and 1.2 millimols of dimethylglyoxal (8.6 %), isolated as dioximes. Glyoxal, which was expected to be present in the reaction mixture, could not be identified with certainty.

Also these pyrrole homologues therefore react to a considerable degree according to a polar structure.



Our investigation has therefore shown that in the reaction with ozone some pyrrole homologues not only react according to the imino structure, but also to a considerable degree according to a structure in which the carbon atoms 2 and 3 are linked by a single bond. The experimental results cannot be made to agree with a reaction according to a pyrrolenine structure; this conclusion is in agreement with the investigations by BONINO, MANZONI-ANSIDEI and PRATESI and with the investigations

by LORD and MILLER mentioned in § 1. The question arises how the experiments by ANGELI, ANGELICO and CALVELLO, discussed in § 1 are to be accounted for. In this connection we would only observe that the action of amyl nitrite on 2,5-dimethylpyrrole can also be formulated by starting from the imino structure. A further investigation of this reaction will possibly clarify this point.

*Laboratory for Organic Chemistry of the  
University of Amsterdam*

June 1951

#### L I T E R A T U R E

1. ANGELI, A., and F. ANGELICO, R.A.L. (5) 11, II, 16 (1902).  
ANGELICO, F. and E. CALVELLO, Gazz. 31, II, 4 (1901).
2. BONINO, G. B., R. MANZONI-ANSIDEI and P. PRATESI, Zeits. f. Phys. Chem. B 22, 21 (1933).
3. STERN, A. and K. THALMAYER, Zeits. f. Phys. Chem. B 31, 403 (1936).
4. LORD JR., R. C. and F. A. MILLER, J. Chem. Phys. 10, 328 (1942).
5. HAAYMAN, P. W. and J. P. WIBAUT, Rec. trav. chim. 60, 842 (1941).  
KOORYMAN, E. C. and J. P. WIBAUT, *ibid* 66, 705 (1947).  
WIBAUT, J. P. and J. VAN DIJK, *ibid* 65, 413 (1946).  
——— and H. BOER, Proc. Kon. Ned. Akad. v. Wetensch. 53, 19 (1950).  
——— and L. W. F. KAMPSCHMIDT, *ibid* 53, 1109 (1950).  
———, Bull. Soc. Chim. 1950, 996.
6. FRERI, M., Gazz. 62, 600 (1932); 63, 281 (1933).
7. WIBAUT, J. P., F. L. J. SIXMA, L. W. F. KAMPSCHMIDT and H. BOER, Rec. trav. chim. 69, 1355 (1950).

THE SULPHONE OF THIOPHENE <sup>1)</sup>

BY

H. J. BACKER AND J. L. MELLES <sup>2)</sup>

(Communicated at the meeting of June 30, 1951)

The isolation of the sulphone of thiophene (I) has been the subject of many publications. Whenever the preparation was described, the results could not be reproduced by others.

The first paper on this sulphone appeared in 1911. LANFRY <sup>3)</sup> oxidized thiophene by means of hydrogen peroxide in acetic acid and claimed to have isolated a liquid boiling at 130°, which he took for the sulphone. STEINKOPF and STENDE <sup>4)</sup>, however, repeating LANFRY's work, could not isolate definite reaction products other than sulphuric acid.

In 1934 the isolation of the sulphone was published again. VAN MEEUWEN <sup>5)</sup> oxidized thiophene with perbenzoic acid and isolated an oil boiling at 129—131° with the composition  $C_4H_4SO_2$ . This result could not be confirmed by STEVENS <sup>6)</sup>, who obtained a white solid m.p. 177°, having the composition of a sesquioxide ( $C_4H_4SO_{1\frac{1}{2}}$ ) and the formula  $C_8H_8S_2O_3$ . The same compound had probably been isolated by DE ROY VAN ZUYDEWIJN <sup>7)</sup>, who, on account of the analysis, took it for the sulphone.

The results of STEVENS could be reproduced by us with a somewhat higher yield of the sesquioxide; an oil with the properties described by LANFRY was not obtained.

The same peculiar behaviour was observed with the oxidation of the mono-alkyl and -aryl derivatives of thiophene, which also gave a "sesquioxide"  $C_8H_6R_2S_2O_3$  ( $R = CH_3$  or  $C_6H_5$ ) <sup>1)</sup>.

As the oxidation of thiophene does not result in the formation of a sulphone, we tried another method of preparation, viz. the elimination of two molecules of hydrogen bromide from 3,4-dibromo-thiacyclopentane-1,1-dioxide (II).

Since we had found that the elimination of hydrogen bromide from

---

<sup>1)</sup> For experimental details see: J. L. MELLES, Thesis Groningen (May 1951).

<sup>2)</sup> Present address: N.V. Aagrunol, Groningen.

<sup>3)</sup> M. LANFRY, *Compt. rend.* 153, 821 (1911).

<sup>4)</sup> W. STEINKOPF and A. STENDE, *Ann.* 430, 96 (1923).

<sup>5)</sup> C. VAN MEEUWEN, Thesis Delft (1934).

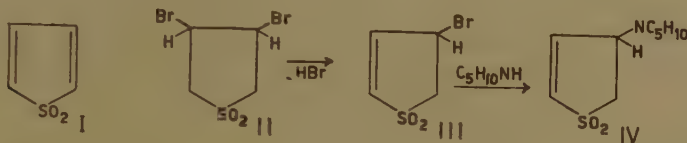
<sup>6)</sup> W. STEVENS, Thesis Groningen (1940).

<sup>7)</sup> E. DE ROY VAN ZUYDEWIJN, Thesis Delft (1936).



3,4-dibromo-3,4-dimethyl-thiacyclopentane-1,1-dioxide with piperidine in benzene gives the sulphone of 3,4-dimethylthiophene with a good yield <sup>1)</sup>, the same procedure was chosen here. It proved to be practical to eliminate first one molecule of hydrogen bromide by means of pyridine <sup>8)</sup>; this reaction gives 3-bromo-thiacyclopentene-4,1,1-dioxide (III).

When treated with piperidine in water, the sulphone III does not give the sulphone of thiophene (I) but the amine IV, the picrate of which can be isolated in a pure form.



The sulphone III is added to an aqueous solution of the equivalent amount of piperidine and dissolved by gentle heating. After filtration the amine IV is precipitated by adding concentrated alkali and cooling to  $0^\circ$ . Recrystallized from water, the product (m.p.  $108-109^\circ$ ) is not yet pure. Crystallization from various solvents always gave a coloured product and insoluble residues. The amine is isolated in pure form as the picrate, which can be recrystallized from acetone.

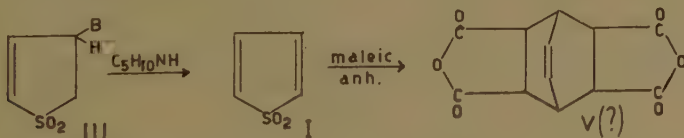
The picrate of 3-(N-piperidino)-thiacyclopentene-4,1,1-dioxide (IV) melts at  $203-204^\circ$  (decomposition).

Found N 13.11, 12.90

$\text{C}_9\text{H}_{15}\text{O}_2\text{NS} \cdot \text{C}_6\text{H}_3\text{O}_7\text{N}_3$  (430.39). Calc. N 13.02

Treatment of the sulphone III with piperidine in benzene gives an almost quantitative precipitate of piperidinium bromide within a minute; after some minutes the solution smells of sulphur dioxide. Apparently the sulphone of thiophene (I) is unstable and decomposes at room temperature. Therefore we tried to prove its existence by preparing derivatives.

Since we had observed that several thiophene dioxides add two molecules of maleic anhydride with loss of sulphur dioxide <sup>1)</sup>, the application of this reaction to the unstable sulphone of thiophene was expected to give bicyclo-(2,2,2)-octene-7-2,3,5,6-tetracarboxylic anhydride (V). This compound and its tetramethyl ester had been prepared in another way by DIELS and ALDER <sup>9)</sup>.



The isolated anhydride, however, contained sulphur; the analysis corresponded to 3a,4,5,6,7,7a-hexahydro-4,7-endovinylene-thianaphtene-1,1-dioxide-5,6-dicarboxylic anhydride (VI). The analysis of the dimethyl ester was also in good agreement with this formula.

<sup>8)</sup> TH. A. H. BLAAS, Thesis Groningen (1941).

<sup>9)</sup> O. DIELS and K. ALDER, Ann. 490, 257 (1931).

A solution of piperidine in anhydrous benzene is at once added to a benzenic suspension of the equivalent amount of the sulphone III. The mixture is cooled with water. After one minute the crystallized piperidinium bromide is filtered off quickly. The solution of the sulphone I is added to a solution of maleic anhydride in bromobenzene and the benzene is distilled quickly. Sulphur dioxide is evolved. The remaining solution is boiled for 7 hours. A tarry brown mass and a white crystalline product separate. After decantation of the benzene and boiling of the residue with acetone, the crystals are collected. Crystallization from ethyl acetate gives 3a,4,5,6,7,7a-hexahydro-4,7-endovinylene-thianaphtene-1,1-dioxide-5,6-dicarboxylic anhydride (VI) as colourless compact crystals, melting at 305–306°, soluble only in large amounts of ethyl acetate. At a high temperature sulphur dioxide escapes; with boiling maleic anhydride no reaction occurs. The compound is soluble in alkali.

Found C 53.88; H 3.98; S 12.09

$C_{12}H_{10}O_5S(266.26)$ . Calc. C 53.69; H 3.76; S 12.03

The dimethyl ester is prepared by saturating a methanolic suspension of the anhydride with anhydrous hydrogen chloride. The anhydride dissolves quickly; in one day the ester separates as a fine white powder. It is filtered and washed with methanol. The dimethyl ester can be crystallized from water in fine white needles and melts at 228.5–229.5°. The ester is very stable; it boils without decomposition.

Found C 53.50, 53.49; H 5.29, 5.33; S 10.33

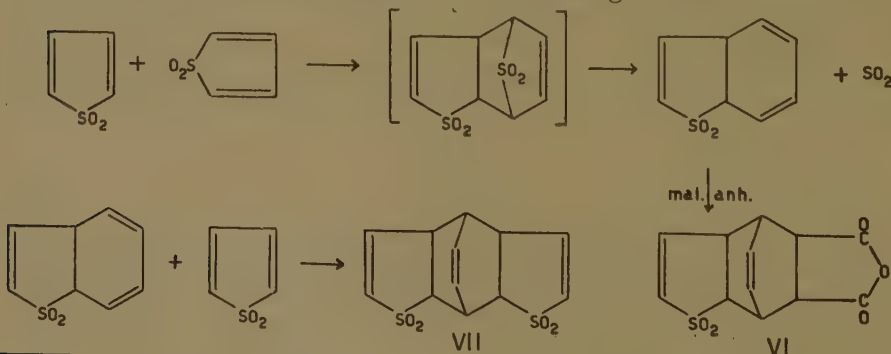
$C_{14}H_{16}O_6S(312.33)$ . Calc. C 53.84; H 5.13; S 10.26

Thus we conclude that the unstable thiophene dioxide dimerises quickly, one molecule reacting as diene and another as dienophilic compound. That  $\alpha$ -unsaturated sulphones are dienophilic was demonstrated by ALDER<sup>10</sup>.

An analogous dimerisation has been observed with cyclopentadienones<sup>11</sup>). The dimeric sulphone, however, differs from these compounds by being unstable and losing the endo-sulphonyl group. The resulting 3a,7a-dihydro-thianaphtene dioxide adds maleic anhydride.

From a solution of thiophene dioxide we could isolate, after one day, another addition product: 3a,4,4a,7a,8,8a-hexahydro-4,8-endovinylene-benzdithiophene-1,1,7,7-tetroxide (VII). This has been formed from the dihydrothianaphtene dioxide by addition of a third molecule of thiophene dioxide.

The reactions are summarized in the following scheme:



<sup>10</sup>) K. ALDER, H. F. RICKERT and E. WINDEMUTH, Ber. 71, 2451 (1938).

<sup>11</sup>) C. F. H. ALLEN, Chem. Rev. 37, 209 (1945).

A solution of piperidine in dry benzene is at once added to a benzenic suspension of the equivalent amount of the sulphone III. After two minutes the crystallized piperidinium bromide is filtered off. The clear solution smells of sulphur dioxide. At room temperature a brown viscous mass has separated in one day. The benzene is decanted, the residue boiled with acetic acid and the insoluble white flakes are collected. The product may be crystallized from a large quantity of water or from diallylsulphone and toluene. When heated over  $350^{\circ}$  the compound decomposes without melting.

3a,4,4a,7a,8,8a-Hexahydro-4,8-endovinylene-benzdithiophene-1,1,7,7-tetroxide forms colourless thin plates <sup>12)</sup>.

Found C 50.45; H 4.50; S 22.37, 22.43

C<sub>12</sub>H<sub>12</sub>O<sub>4</sub>S<sub>2</sub>(284.34). Calc. C 50.70; H 4.23; S 22.53

*University of Groningen, Laboratory  
for organic chemistry*

---

<sup>12)</sup> According to a private communication of Dr J. STRATING this disulphone can also be prepared by reaction of 3,4-dibromo-cyclopentane-1,1-dioxide with aqueous alkali.

## SOME REMARKS ON THE INTERNAL CONSTITUTION OF THE BODIES OF THE SOLAR SYSTEM

BY

H. P. BERLAGE

(Communicated at the meeting of June 30, 1951)

### *Summary*

A diagram containing the mean densities of the bodies of the solar system in function of their masses, is shown to give significant information on their internal constitution.

KUHN and RITTMANN [1] suggested that a distinct core in the Earth, the presence of which was proved by seismologic methods, might be not composed of iron, as was almost generally accepted at the time, but might equally well be explained by a high percentage of hydrogen kept in store from solar matter below a certain level. Since then several other investigators [2] [3] took up and developed the view that the core of the Earth is determined by pressure rather than by a discontinuity in chemical composition.

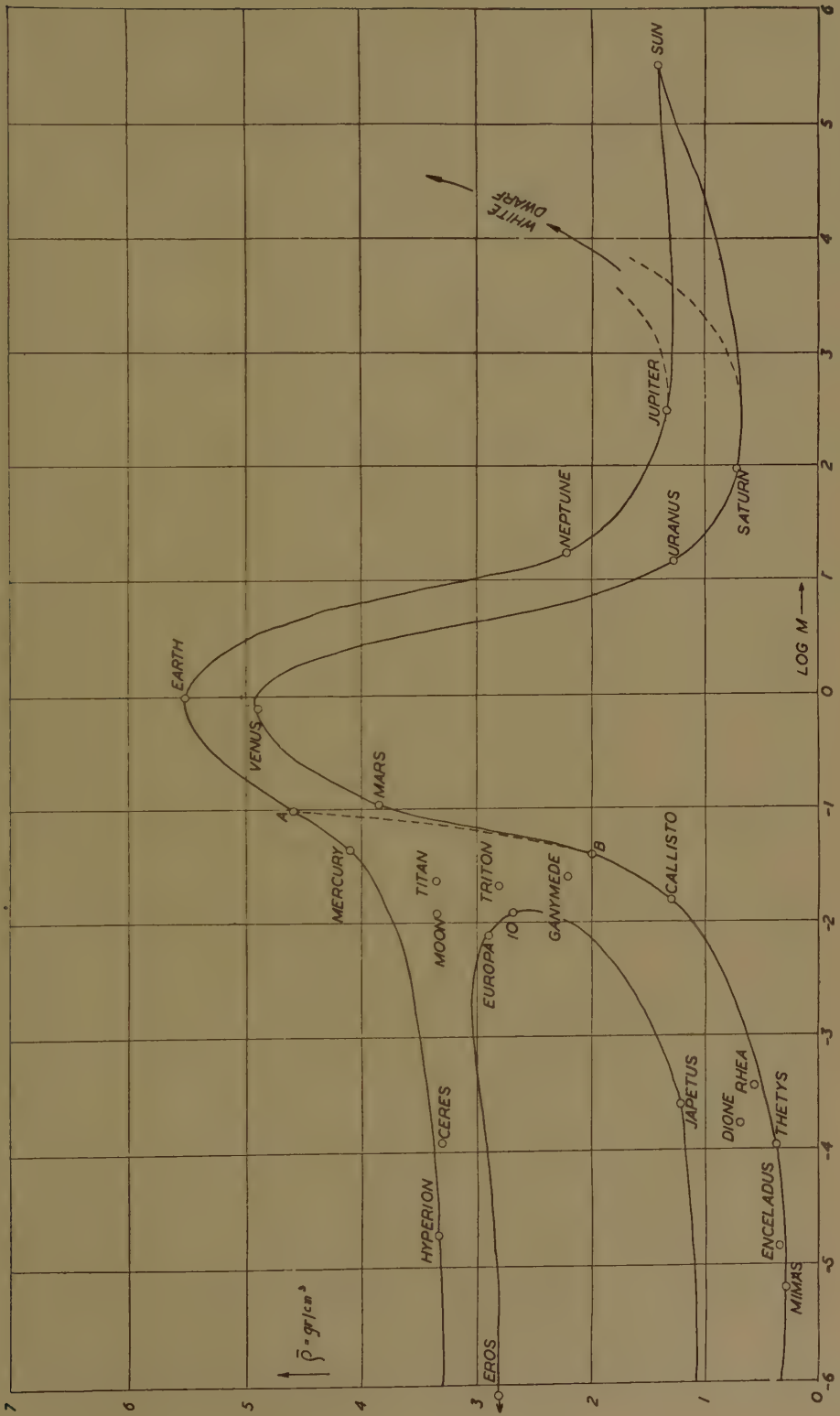
It was stated that the four terrestrial planets, Mercury, Venus, the Earth and Mars show relations between mass, mean density, angular velocity, oblateness and moments of inertia which indubitably invite an explanation by the compressibility of one and the same substance, aided by transitions of elements from molecular to atomic phases [4] [5] [6] [7]. It was tried to include the Moon in the same scheme, or arguments are brought forward for a composition of the Moon widely differing from the composition of the terrestrial planets [8].

However, the idea of similar gross composition of the minor bodies in the solar system, such as the terrestrial planets and the Moon, might become overstressed by a priori arguments. As a matter of fact in papers on this subject, with few exceptions [9], it has thus far been overlooked that it is quite impossible to keep close to the same idea when the study of bodies of similar or smaller mass is extended to the satellites of the giant planets.

This becomes evident as soon as we compare the mean density of the Moon (3.34) with the mean densities of the Jovian satellites Callisto (1.3) and Ganymede (2.2), which differ greatly from the former value, although the masses of these satellites are greater than the mass of our Moon, or, in fact, 1.32 and 2.11 respectively, when expressed in lunar masses.

Now, Callisto and Ganymede can have easily assimilated a quantity of lighter substances, superior to the quantity which our Moon contains,





since these substances could condense under the temperature conditions prevailing at Jupiter's distance from the Sun, but not at the Earth's distance. However, the outstanding difference between the mean densities of Callisto and Ganymede remains a puzzling question which cannot be answered by an appeal to the greater compression of the bigger one of the two satellites, because the maximum mean density found in Jupiter's satellite system (2.9) is associated with the smallest of the four Galileian satellites (Europa), whose mass is only 0.64, when expressed in lunar masses.

There can be no essential equality in the chemical composition of the bodies of the Jovian system. Moreover, the trend of the mean density of the four bodies, from 2.7 through 2.9 to 2.2 and 1.3, when we cross the system in outward direction, reminds us rather strongly of a similar trend through a maximum, when we pass from Mercury to Venus, the Earth and Mars, as if this trend were of a fundamental nature.

In Saturn's system of satellites the highest mean density (3.4) is also associated with a satellite in intermediate position (Titan), but, as this satellite is also by far the most massive there may be other reasons for meeting the same parallelism in this case.

In the figure we have plotted the mean density of all the bodies in the solar system of which this value is known with tolerable accuracy, in function of the logarithm of their masses in terrestrial units. The diagram is based on the table below. The data have been taken from the 1945 edition of H. N. RUSSELL, R. S. DUGAN, J. Q. STEWART, *Astronomy*, account being taken of KUIPER's recent correction of Neptune's mean density [10]. The masses of Saturn's satellites are those given by STRUVE [11]; the densities have been calculated on the assumption that the albedo of the three very small bodies, Mimas, Enceladus and Hyperion is 0.59, as high as the albedo of Venus, the albedo of the other satellites is assumed to be 0.45, equal to the known albedo of Titan. This places the density of Hyperion at the level of the density of Titan, which is reasonable for a satellite revolving round Saturn at only slightly greater distance than Titan, so that it must have condensed from almost the same original material. It raises the mean density of Mimas and Enceladus to at least 0.28 and 0.33 respectively, which, however, are still very low values on which we will have to comment later.

In the diagram boundaries have been drawn along the zones of actually occurring mean densities. These zones are strikingly narrow.

We see that three distinct kinds of small bodies exist, with mean densities of roughly 1, 3 and 7 g/cm<sup>3</sup>. The latter category contains the iron meteorites. The stony meteorites, followed upward to bigger masses, enter the diagram through the asteroids Eros and Ceres and the Saturnian satellite Hyperion.

With the density 1 we enter the diagram through the majority of the satellites of Saturn. Expecting to find a density of, say, 0.8 as an absolute

TABLE  
*Masses and mean densities of bodies in the solar system*

	log m	$\bar{\rho}$		log m	$\bar{\rho}$
Sun . . . . .	5.52	1.41	Io . . . . .	- 1.91	2.7
Mercury . . . . .	- 1.35	4.1	Europa . . . . .	- 2.11	2.9
Venus . . . . .	- 0.09	4.9	Ganymede . . . . .	- 1.59	2.2
Earth . . . . .	0	5.52	Callisto . . . . .	- 1.79	1.3
Mars . . . . .	- 0.96	3.85	Mimas . . . . .	- 5.19	0.28
Jupiter . . . . .	2.50	1.33	Enceladus . . . . .	- 4.84	0.33
Saturn . . . . .	1.98	0.71	Thetys. . . . .	- 3.96	0.35
Uranus . . . . .	1.16	1.26	Dione . . . . .	- 3.75	0.70
Neptune . . . . .	1.24	2.22	Rhea . . . . .	- 3.42	0.55
			Titan . . . . .	- 1.62	3.35
Ceres . . . . .	- 3.90	3.3 ?	Hyperion . . . . .	- 4.71	3.32
Eros. . . . .	- 8.70	2.8 ?	Japetus . . . . .	- 3.59	1.22
Moon . . . . .	- 1.91	3.34	Triton. . . . .	- 1.66	2.8

lower limit among the smaller solid bodies — ice might be a frequent constitutive substance and several organic compounds possess comparable densities — we become tempted to deny the truly solid character of at least Mimas, Enceladus and Thetys. The planetesimal origin of satellites and planets gaining probability, the question arises, whether these satellites are perhaps merely clusters of meteorites, revolving outside Roche's limit, whereas the particles of Saturn's ring, rotating within Roche's limit, could not unite.

We can, however, not venture to suggest that all these Saturnian satellites might be clusters of meteorites, the latter ones individually possessing densities of nearly 3, since it is inconceivable that the same view could hold in the case of Callisto, a satellite of Jupiter greater than our Moon and yet possessing a mean density of 1.3.

I therefore consider as placed beyond doubt the existence of a distinct group of small solid bodies of a density of approximately 1. On the other hand, converging evidence pointing to a passage of satellites and planets through the meteoric state, we might well ask, whether meteorites consisting of ice and other substances of low specific weight are not a very common occurrence far away from the Sun.

Following the two kinds of satellites and asteroids towards the bigger masses, we see how both groups combine into one group of bodies, which, after the inclusion of the Moon, Triton, Titan and Ganymede acquire planetary dimensions.

It looks more than a mere chance that the zone of planets is bounded by two almost parallel curves, the superior one passing through Mercury, the Earth, Neptune and Jupiter, the inferior one passing through Mars, Venus, Uranus and Saturn. This typical fact does, at any rate, suggest

that it would be impracticable and even incorrect to look for one theoretical relation fitting strictly with all observed values, without leaving room for possible inequalities in the chemical composition of these planets. However, the zone being narrow, we may expect and it should not be difficult to find a mathematical formula representing the average trend of the planetary densities and allowing for a margin of error which is not negligible but small.

The main sequence finds, through the giant planets, its logical and remarkably unstrained asymptotic termination in 1.41, the mean density of the Sun. The boundaries have been tentatively extended by dashed ends pointing towards an imaginative central star representing the case in which the Sun would have degenerated into a white dwarf. It may remind us of KOTHARI's theory of white dwarf constitution extended to planetary constitution [4]. Moreover it is instructive to look at the present diagram as the "cold" entry to the HERTZSPRUNG-RUSSELL diagram of stellar evolution.

The descending branch in the diagram should obviously be explained by the greater gravitative power of the major planets to hold together the lighter and volatile constituents. The ascending branch between the Moon and Titan on the lower end and the Earth and Venus on the upper end may now be explained by compression, aided by the transition of one or more of the constituting elements from molecular into atomic phases at very high pressures. We found, however, such outstanding differences among the mean densities of satellites of comparable mass in one and the same secondary system that we must conclude that the matter available for the different bodies at the time of condensation was of rather different composition. By some cause or other, one or more substances have not been evenly distributed through the nebulae surrounding their primaries out of which the satellites assembled their constituents. Neither is there, consequently, a sufficient foundation for the assumption that materials were evenly distributed through the nebula rotating round the Sun at the time when the planets were created.

From the cosmogonic point of view it remains perfectly well conceivable that iron is a major constituent of the inner planets and has built up their cores, whereas it may prove to be scarce in the interior of the outer planets.

That iron plays a specific role in the internal constitution of heavenly bodies is proved by the puzzling existence of iron meteorites, the only particles which have been left out of our picture so far.

On the other hand, whether terrestrial planets born in the outer region of the solar system possess the same internal constitution as the inner planets might only be proved by a reliable determination of Pluto's mass. As a matter of fact Pluto, with a diameter, intermediate between the diameters of Mars and Mercury according to recent measurements made by KUIPER [12], poses still a dubious case. Without straining matters



it may find its place on any point of the dashed line between the points *A* and *B* in the diagram, its possible density ranging from 2.0 to 4.6. Once Pluto's mass being fixed at less than 0.1 of the mass previously calculated from its pretended perturbations, it would be of the utmost interest, with regard to the origin of the planetary system, to know whether Pluto is a body similar to Mars or Mercury or similar to Gany-mede.

## REFERENCES

1. KUHN, W. and A. RITTMANN, Ueber den Zustand des Erdinnern und seine Entstehung aus einem homogenen Urzustand, *Geol. Rdsch.* 32, 215, (1941).
2. RAMSEY, W. H., On the constitution of the terrestrial planets, *Mon. Not. R.A.S.* 108, 406 (1948).  
 ———, On the nature of the Earth's core, *M.N. Geoph. Suppl.* 5, 409 (1949).  
 ———, The planets and the white dwarfs, *Mon. Not. R.A.S.* 110, 444 (1950).
3. BULLEN, K. E., Compressibility-pressure hypothesis and the earth's interior, *M.N. Geoph. Suppl.* 5, 355, (1949).  
 ———, On the constitution of Venus, *Mon. Not. R.A.S.* 109, 457 (1949).  
 ———, On the constitution of Mars, *Mon. Not. R.A.S.* 109, 688 (1949).  
 ———, An Earth model based on a compressibility-pressure hypothesis, *M.N. Geoph. Suppl.* 6, 50 (1950).  
 ———, Venus and the Earth's inner core, *Mon. Not. R.A.S.* 110, 256 (1950).
4. KOTHARI, D. S., The internal constitution of the planets, *Mon. Not. R.A.S.* 96, 833 (1936).  
 ———, The theory of pressure-ionization and its applications *Proc. Roy. Soc. A*, 165, 486 (1938).
5. PRITAM SEN, A note on the internal constitution of the planets, *Zs. f. Astroph.* 16, 297 (1938).
6. KRONIG, R., J. DE BOER and J. KORRINGA, On the internal constitution of the earth, *Physica* 12, 245 (1946).
7. SCHOLTE, J. G., On the internal constitution of the planets, *Mon. Not. R.A.S.* 107, 237 (1947).
8. HARRISON BROWN, On the composition and the structure of the planets, *Astroph. J.* 111, 641, (1950).
9. WILDT, R., Reports, The constitution of the planets, *Mon. Not. R.A.S.* 107, 84, (1947).
10. KUIPER, G. P., The diameter of Neptune, *Astroph. J.* 110, 93, (1949).
11. STRUVE, G., Neue Untersuchungen im Saturnsystem, *Veröff. Univ. Sternw. Berlin-Babelsberg*, Bd. 6, Heft. 4.
12. KUIPER, G. P., The diameter of Pluto, *P.A.S.P.* 62, 133 (1950).

GENERAL LINEARIZED THEORY OF THE EFFECT OF  
SURFACE FILMS ON WATER RIPPLES. II

BY

R. DORRESTEIN

(Communicated by Prof. F. A. VENING MEINESZ at the meeting of May 26, 1951)

§ 3. *Experimental verification.* Direct accurate quantitative experiments on the decay of small water waves have been performed by R. C. BROWN (1936). He generated a stationary train of ripples of period  $P = \frac{1}{300}$  sec (wave-length  $\lambda = 0.172$  cm), and very low amplitude ( $2 - 3 \cdot 10^{-5}$  cm). By an optical method he examined the decay of the amplitude  $a$  with the distance  $x$ , and he found  $a = a_0 e^{-\kappa x}$ , with, for distilled water of 20° C with a clean surface,  $\kappa = 0.451$  cm $^{-1}$  or  $\kappa^{-1} = 2.22$  cm. Dividing this modulus of decay in distance by the group velocity, which can here be put equal to  $3\lambda/2P = 77.4$  cm/sec, we obtain the modulus of decay in time:  $\tau_1 = 0.029$  sec. Fig. 1 gives  $\tau_1 = 0.038$  sec. Thus the rate of decay experimentally found exceeds the theoretical value by about 30 %. Taking into account that all conceivable disturbances, as: some turbulence, some air friction, traces of surface films, will tend to increase the decay, the accordance between experiment and theory can be called reasonably good. When a surface layer was present, BROWN observed a much stronger decay of the waves, but he gave no quantitative data.

The present author could not find in literature any more accurate experimental data on the decay of water waves by internal friction.

§ 4. *Discussion and conclusions*

Before drawing conclusions from the theoretical result of § 2, we should be well aware of the fact that the present theory is the *linearized* theory, and thus is only valid for waves with sufficiently small steepness. The estimation of the errors made if the steepness has a finite value is a different problem, which is not examined here. The theory of deep water waves of finite amplitude in the absence of surface films has been rather well elaborated (see LAMB (1932)), and we can be sure that the formula (29) for the decay constant will be substantially right for waves with a steepness up to, say 0.05. Considering, however, the very large vertical gradients of horizontal velocity near the surface in the presence of a surface film, as given by fig. 2, we are suggested to be especially cautious when extrapolating the results of the linear theory to waves of finite steepness in the

presence of a surface film. For the present, however, more than this cannot be said concerning this point.

Another point of interest is the eventual occurrence of turbulence in the water motion. It is very probable (GROEN and DORRESTEIN, 1949, BOWDEN, 1950) that in the large swell waves of the oceans the wave motion is turbulent, resulting in a rate of decay larger than that given by eq. (29). As BOWDEN already suggested, it is probable that the beginning of turbulence is determined by a "Reynolds number", which must exceed some critical value, just as in cases of stationary flow.

One might describe a surface wave as a primary *horizontal* oscillatory motion parallel to the surface, the accompanying vertical velocities and the crests and troughs being a consequence of the incompressibility of the fluid. Then, in analogy with the stationary "Grenzschicht"-flow (PRANDTL) occurring when a flat plate would move uniformly along the surface, one might define the "Reynolds number" for wave motion (when no surface film is present) by

$$Re_w = \frac{(2\pi a/P) (\lambda/2\pi)}{\nu} = \frac{Ca}{\nu},$$

where  $2\pi a/P$  is the amplitude of the horizontal velocity at the surface ( $a$  = wave amplitude,  $P$  = wave period) and  $\lambda/2\pi$  is the "Verdrängungsdicke" (PRANDTL)<sup>10</sup>, that is: the effective depth of the motion;  $C$  is the phase velocity. If the wave steepness  $2a/\lambda$  is not very small, one might assume that the critical value of  $Re_w$  would be dependent on this steepness.

As long as there are no more available data, we dispose of two indications concerning the magnitude of the critical value of  $Re_w$ . First, for stationary "Grenzschicht"-flow, it is known to be about 1000 (see e.g. PRANDTL)<sup>10</sup>. For the oscillatory motion there is some reason to suppose a larger value, since eddies have got only a limited time to develop.

Secondly, if we attribute the observed decay of ocean swell entirely to energy dissipation by eddy viscosity, we find a maximum value for the eddy viscosity  $\nu_e$ , which, for waves of a certain steepness, can be assumed to be some increasing function of the wave-length. If we substitute in this function such a value of the wave length that this computed eddy viscosity  $\nu_e$  becomes equal to the molecular viscosity  $\nu$ , we cannot be far from the transition situation. GROEN and DORRESTEIN (1950), assuming  $\nu_e \sim \lambda^{4/3}$ , and using the swell observations mentioned by SVERDRUP and MUNK (1947), came to the formula  $\nu_e = .000075 \lambda^{4/3}$  (c.g.s. units), so that  $\nu_e$  would become equal to  $\nu = 0.01$  for  $\lambda = 39$  cm; then, with a steepness 0.02,  $Re_w = 3000$ . BOWDEN (1950), using the same observations, postulated  $\nu_e = .000056 Ca$ , so that  $\nu_e$  would become equal to  $\nu$  for  $Re_w = 18000$ . We can conclude that the critical value of  $Re_w$  will be of the order  $10^3 - 10^4$ . With a steepness 0.10 this means:  $\lambda = 6 - 30$  cm, with a steepness 0.02:  $\lambda = 19 - 86$  cm. Consequently the transition between laminar and turbulent wave motion very probably occurs for wave lengths between 10 and 100 cm. At any rate, for wave lengths less than 10 cm the wave motion is laminar as was assumed in § 2.

The main conclusions to be drawn from the results of § 2 are:

1. In all cases considered (wavelengths between 0.1 and 100 cm) the modulus of decay  $\tau$  turns out to be large compared with the period  $P$ . The damping is never so serious that the waves would lose their wave-character.

2. For wave lengths increasing from 0.1 to 1.7 cm (capillary ripples), the ratio  $\tau_1/\tau_2$  increases from 1.6 to about 4. For longer waves this ratio increases more considerably. Thus, for the capillary waves the influence of a film on the rate of decay is relatively small. This is remarkable, since it is the general impression that an oil film affects especially the smaller ripples. However, we must now distinguish between the two phenomena 1. and 2., mentioned in § 1. A closer consideration makes evident that the conspicuous prohibitive action of an oil film on small waves manifests itself not so much by the phenomenon 2. (the increased damping), but rather by the phenomenon 1.: the prevention of the formation of short waves by the *wind*.

This phenomenon may be explained, either by an impeded transfer of energy by the wind, or by an enhanced rate of decay by friction.

Now, without a surface film, the theoretical rate of decay increases by almost a factor 2 if the temperature decreases from 20° to 0°, since the viscosity of water does so. As far as the author knows, there are no indications whatever that waves are markedly more easily formed by the wind on warmer water than on colder water. Thus, a factor 2 in the rate of decay seems insignificant in this respect, and the relatively small ratio between  $\tau_1$  and  $\tau_2$  indicates that the second possibility mentioned above may be excluded.

The transfer of energy from the wind, blowing over an undisturbed water surface, into initial wavelets is conceivable in two ways:

a. Turbulent *pressure* fluctuations with a certain periodicity in time and/or in space cause, primarily, a vertical momentum of the water particles at the surface, of the same periodicity, and, consequently (by almost immediate propagation of pressure differences through the water), wavelets are formed.

b. Turbulent variations in the *skin friction* at the surface with a certain periodicity in time and/or in space cause, primarily, a horizontal momentum of the water particles at the surface, of the same periodicity, and, consequently, convergencies and divergencies of the water along the surface, crests and troughs, pressure differences, wavelets.

These initial wavelets will travel at random in all directions. It is in the next stage that the wind favors the growth of wavelets with a component of propagation in its own direction, and prevents the growth of other wavelets.

It is not to be seen why an oil film at the surface would exert an appreciable impeding influence on the process mentioned under a., but it seems very natural that a limited compressibility of such a film will suppress the process b. to a large extent.



So the following important conclusion must be drawn: In the formation of initial capillary ripples (wave-lengths less than 2 cm) on a water surface by the wind, turbulent fluctuations in the *skin friction* exerted by the wind at the surface play a predominating role.

It must be noticed that this conclusion is not necessarily applicable to the first waves formed by the very weakest wind capable of forming waves. These waves seem to have a wave length between 5 and 10 cm. Here the ratio between  $\tau_1$  and  $\tau_2$  is about 10, and the increase of decay by the film may be an important factor.

3. An eventual film on the surface has to satisfy very moderate conditions in order to be effective on waves. This explains the wide variety of effective oils. A variation of the surface tension  $T$  with the available surface-area  $O$ , as small as according to  $T \sim O^{0.06}$ , or a surface-viscosity of about 0.1 c.g.s. units, is sufficient to make the rate of decay exceed its final value, for waves between 0.1 and 2 cm.

The value 0.06 for the exponent in (18a) seems surprisingly low. Thus it seems that not only condensed films must be effective, but also many liquid-expanded and vapour-expanded films (terminology of ADAM (1941)). One might even think of gaseous films.

In a later paper, the author hopes to discuss in some detail the consequence of this result in connection with known data on  $T(O)$ -curves (and on surface-viscosities), and its bearing on some special phenomena occurring mostly on coastal waters in light or moderate winds, as described by various authors.

*Acknowledgement.* The author is indebted to the Director-in-Chief of the Royal Netherlands Meteorological Institute, for his permission to publish this paper, and to Dr P. GROEN for helpful criticisms.

May 1951.

*Section of Oceanography,  
Koninklijk Nederlands Meteorologisch Instituut, De Bilt*

Appendix 1. *Introduction of two velocity-potentials  $\Phi$  and  $\vec{\Psi}$  in the linearized equation of Navier-Stokes.*

The derivation in the three-dimensional case can readily be written down if we use the vector-notation. Assuming incompressibility, we have for the velocity vector  $\vec{V}$  (components  $u, v, w$ )

$$(1-1) \quad \text{div } \vec{V} = 0$$

The equation of motion, neglecting terms which are quadratic in the velocity, is then:

$$(1-2) \quad \frac{\partial \vec{V}}{\partial t} = -\text{grad} \left( U + \frac{p}{\rho} \right) + \nu \Delta \vec{V},$$

where  $U = gy$ , if only gravity is present as an extraneous force.

Any vector function of space can be expressed as a sum of an irrotational and a divergence-free field. Substituting

$$(1-3) \quad \vec{V} = -\text{grad } \Phi - \text{curl } \vec{\Psi},$$

where  $\Phi$  and  $\Psi$  are functions of space and time, in eq. (1-1), we get:

$$(1-4) \quad \Delta \Phi = 0$$

Substituting the same expression for  $\vec{V}$  in eq (1-2), remembering that  $\partial/\partial t$  and  $\Delta$  as scalar operators can be commutated with grad and curl, we obtain an equation which can be put in the following form, using (1-4):

$$(1-5) \quad \text{grad} \left( U + \frac{p}{\rho} - \frac{\partial \Phi}{\partial t} \right) = \text{curl} \left( \frac{\partial \vec{\Psi}}{\partial t} - \nu \Delta \vec{\Psi} \right)$$

The most general equations to be satisfied by  $p$ ,  $\Phi$  and  $\vec{\Psi}$  in order that (1-3) be a solution of (1-1) and (1-2) are thus given by (1-4) and

$$(1-6) \quad U + \frac{p}{\rho} - \frac{\partial \Phi}{\partial t} = \Phi^*,$$

$$(1-7) \quad \frac{\partial \vec{\Psi}}{\partial t} - \nu \Delta \vec{\Psi} = \vec{\Psi}^*$$

where the two new functions  $\Phi^*$  and  $\vec{\Psi}^*$  of space and time are connected by the relation

$$(1-8) \quad \text{grad } \Phi^* = \text{curl } \vec{\Psi}^*$$

but otherwise are arbitrary. Taking both  $\Phi^*$  and  $\vec{\Psi}^*$  equal to zero, a special class of solutions is selected.

Restricting ourselves to the two-dimensional case, we have  $w = 0$  and  $\partial/\partial z = 0$ , and we have only to deal with the  $z$ -component of  $\vec{\Psi}$ , which may simply be called  $\Psi$ . Then, with  $\Phi^* = \vec{\Psi}^* = 0$ , we obtain the formulae (4), (5) and (6).

A system of solutions where  $\Phi$ ,  $\Psi$ ,  $\Phi^*$ ,  $\Psi^*$  are all of the special form (7a) or (7b) proves not to be possible, unless  $\Phi^*$  and  $\Psi^*$  are zero.

## Appendix 2. *Surface stresses and surface viscosity.*

The linear theory of viscosity can be written down in two dimensions just in the same way as it is done in three dimensions (cf. LAMB, (1932), Art. 323-326).

In general, the stresses acting within the surface will form a two-dimensional symmetrical tensor of the second order:

$$\begin{pmatrix} T_{xx} & T_{xz} \\ T_{xz} & T_{zz} \end{pmatrix}$$

and the surface tension will, by definition, be given by  $T = \frac{1}{2}(T_{xx} + T_{zz})$ .

From the differential quotients of the velocities in the surface, we can form another two-dimensional tensor of the second order:

$$\begin{pmatrix} \frac{\partial u_s}{\partial x} & \frac{1}{2} \left( \frac{\partial u_s}{\partial z} + \frac{\partial w_s}{\partial x} \right) \\ \frac{1}{2} \left( \frac{\partial u_s}{\partial z} + \frac{\partial w_s}{\partial x} \right) & \frac{\partial w_s}{\partial z} \end{pmatrix}$$

If the surface has isotropic properties and is in uniform motion, the second tensor is zero,  $T_{xx} = T_{zz} = T$  and  $T_{xz} = 0$ . If there exist linear relations between the elements of both tensors, these must then be of the form (cf. LAMB (1932) Art. 326):

$$T_{xx} = T + \lambda_s \left( \frac{\partial u_s}{\partial x} + \frac{\partial w_s}{\partial z} \right) + 2\mu_s \frac{\partial u_s}{\partial x}$$

$$T_{zz} = T + \lambda_s \left( \frac{\partial u_s}{\partial x} + \frac{\partial w_s}{\partial z} \right) + 2\mu_s \frac{\partial w_s}{\partial z}$$

$$T_{xz} = \mu_s \left( \frac{\partial u_s}{\partial z} + \frac{\partial w_s}{\partial x} \right)$$

where  $\lambda_s$  and  $\mu_s$  are constants.

By adding the first two of these equations, it follows that  $\lambda_s = -\mu_s$ , and if  $w_s$  and  $\partial/\partial z$  are zero, as in the case of § 2, we have  $T_{zz} = T_{xz} = 0$  and

$$T_{xx} = T + \mu_s \frac{\partial u_s}{\partial x}.$$

The coefficient  $\mu_s$  is called the "surface viscosity" of the film. Values have been measured for several films by means of different methods (see ADAM (1941)).

We can make clear the physical meaning of this surface viscosity and its relation to the normal viscosity  $\mu$  of the fluid by means of a simple example. Consider a volume of fluid with a free surface, enclosed between two vertical walls  $z = \text{const.}$  which move in the  $x$ -direction with different speeds. In the case of laminar motion the fluid will then assume a velocity  $u(z)$  with  $\partial u/\partial z = \text{const.}$  The shearing force exerted on a rectangular part of one of the walls extending from the surface to a depth  $D$ , and with length  $L$  in the  $x$ -direction will then be:

by the fluid:

$$LD\mu \frac{\partial u}{\partial z},$$

by an eventual surface film:

$$LT_{xz} = L\mu_s \frac{\partial u}{\partial z},$$

and thus together:

$$L \frac{\partial u}{\partial z} (D\mu + \mu_s)$$

The c.g.s. unit of  $\mu$  is gram/cm sec (or poise), that of  $\mu_s$  is gram/sec (or "surface poise").

### Summary

Extending a short calculation given already in the text-book "Hydrodynamics" of LAMB (1932), the complete linearized theory of the decay of surface waves on water by friction, if a surface film is present, is elaborated (§ 2). The theory includes the effects of a limited compressibility of the film (i.e. variation of surface tension with area available for a certain part of the film), of a noticeable "surface viscosity", and of a hysteresis in the surface tension. These effects appear together, linearly combined, in one complex parameter  $\chi$  (eqs. (21) and (38)).

Without surface film this parameter is zero, and the modulus of decay  $\tau$  (defined as the time by which the amplitude of a wave has decreased by a factor  $e^{-1}$ ) is given by eq. (33). If the modulus of  $\chi$  exceeds a certain value, the modulus of decay is practically given by eq. (34), which value corresponds to  $\chi = \infty$ ; in this case the horizontal motion at the surface is practically annulled by the film. Numerical results for wave-lengths between 100 cm and 0.1 cm are given in fig. 1 and in table 1.

For capillary ripples with wave-lengths between 0.1 and 2 cm, a very slight dependence of surface tension on available surface area appears to be already sufficient to let  $\tau$  be given by (34). This indicates that a large variety of surface films is capable of causing the increased decay.

It seems evident that the rather moderate increase of decay of capillary ripples by the presence of a surface film cannot be put responsible for the apparent effect of oil on wind-waves, but that the essential thing must be here the prohibition of horizontal velocity gradients along the surface, which prevents the arising of wind-induced irregular movements along the surface. A consequence of this concept is that the turbulent skin friction exerted by the wind is the essential agent in forming initial capillary ripples on clean water surfaces (§ 4).

### REFERENCES

1. FRANKLIN, B., a.o., On the stilling of waves by means of oil, *Philos. Trans.* London **64**, 445–460 (1774).
2. REYNOLDS, O., *Brit. Ass. Rep.* (1880), cited by H. LAMB<sup>6</sup>), 631. To his regret, the present author did not succeed in obtaining the loan of this paper in the Netherlands.
3. AITKEN, J., On the Effect of Oil on a Stormy Sea, *Proc. Roy. Soc. Edinb.* **12**, 56–75 (1883).
4. POCKELS, A., Surface Tension, *Nature* **43**, 437–439 (1891).
5. ADAM, N. K., *The Physics and Chemistry of Surfaces*, 3rd Ed. (Oxford, 1941).
6. LAMB, H., *Hydrodynamics*, 6th Ed. (Dover Publ., New York, 1932).
7. BROWN, R. C., A method of measuring the amplitude and damping of ripples, *Proc. Phys. Soc.* **48**, 323–328 (1936).
8. GROEN, P. and R. DORRESTEIN, Ocean Swell: its Decay and Period Increase, *Nature* **165**, 445–447 (1950).
9. BOWDEN, K. F., The effect of Eddy Viscosity on Ocean Waves, *Phil. Magaz.* Ser. 7, **41**, 907–917 (1950).
10. PRANDTL, L., *Führer durch die Strömungslehre*, 3e Aufl., p. 108 (1949).
11. SVERDRUP, H. U. and W. H. MUNK, U.S. Hydrogr. Office, Pub. No. 601 (1947).



## NOTES ON SOME REPRESENTATIVES OF MIOGYPSINELLA

BY

C. W. DROOGER

(Communicated by Prof. G. H. R. VON KOENIGSWALD at the meeting of Sept. 29, 1951)

Abstract: In addition to the description of a new species, *Miogypsina* (*Miogypsinella*) *bermudezi*, new data are being furnished on *Miogypsina* (*Miogypsinella*) *complanata* SCHLUMBERGER. Suggestions are given about the development of primitive *Miogypsinidae*, mainly by taking into account the early ontogenetic features.

In 1940 HANZAWA established the genus *Miogypsinella* for those primitive species of the *Miogypsinidae*, which have simple, non-lamellar lateral walls (type species: *Miogypsinella borodinensis*). So he separated these species from those of *Miogypsinoides* YABE and HANZAWA, 1928, whose type species, *Miogypsina dehaarti* VAN DER VLERK, is different from typical *Miogypsinella* by possessing lateral walls of distinctly lamellar structure. We may briefly say that all species, included by HANZAWA in his new genus, are characterized by the lack of distinct lateral chambers, in stead of which are found thick and ornamented outer walls; furthermore the early coiled chambers are arranged in a trochoid spiral.

By courtesy of Dr P. J. BERMUDEZ the present author received a number of specimens of a sample from a well, drilled in western Cuba. These specimens appeared to possess characteristics, which place them close to the known species of *Miogypsinella*, but after all it was impossible to identify them with any of these previously described species. The new species, described below, is very interesting, as it certainly should be seen as another morphologically intermediate form between the early *Miogypsinidae* and *Rotalia*, from which the former family has been derived. Because of the observed features it appears to be closer to the *Rotaliidae* than the other known species of *Miogypsinella*.

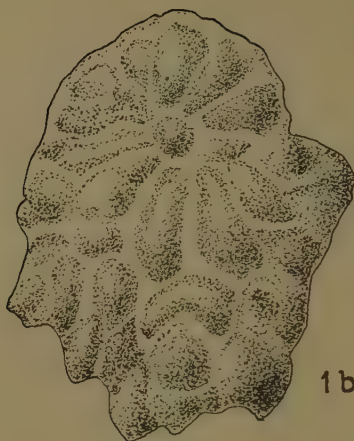
*Miogypsina* (*Miogypsinella*) *bermudezi* n.sp.

Figs. 1a—6

*Description*: Test small, thin-walled, irregularly fan-shaped, about as long as broad, with the early portion rounded and the frontal margin crenulate, consisting of a large trochoid initial part — where the test is thickest — and a variable number of equatorial chambers on one side of this spiral portion of the test. Early coiled chambers distinctly trochoid, later ones tending to become planispiral and slightly evolute ventrally, 15—19 spiral chambers (5 observations) present in  $1\frac{1}{2}$ —2 whorls, very rapidly increasing in size as added, except the last-formed one or two, which are usually somewhat smaller, 10—12 chambers in the final



1a



1b



1c



2a



2c



2b



3a



3b



Figs. 1a—6: *Miogypsina* (*Miogypsinella*) *bermudezi* n. sp.; Early Middle Oligocene, Pinar del Río Province, Cuba; 1, holotype; 1a, 2a, 3a: dorsal views, 1b, 2b, 3b: ventral views, 1c, 2c: side views, 4: median section, 5, 6: transverse sections; figs. 1—3, 65 x, figs. 4—6, resp. approx. 50 x, 85 x and 70 x.  
Fig. 7: *Miogypsina* (*Miogypsinella*) *complanata* SCHLUMBERGER; Middle Oligocene, S. W. Trinidad; transverse section; approx. 60 x.





convolution, later coiled chambers elongated to a blunt point. Ventral umbilicus filled with a distinct plug, the latter occasionally subdivided into less distinct pillars. Equatorial chambers 5–30 in number, placed along one third to half of the circumference of the coiled part, elongately arcuate in shape, arranged in a rather irregular pattern. Chambers inflated throughout, both the later ones of the coiled stage and the median chambers often strongly elevated; sutures correspondingly depressed. Wall smooth, distinctly perforate and of a thickness, not exceeding that, observed in most species of *Rotalia*. Maximum observed diameter 1.0 mm, thickness up to 0.25 mm.

In median sections the protoconch appears circular, measuring 50–70  $\mu$  (including half of the walls); the larger diameter of the deuteroconch is of nearly the same size. The equatorial chambers vary considerably in size and shape, the larger ones measuring about 200  $\mu$  longitudinally and about 135  $\mu$  in transverse direction, which dimensions are about the same for the larger spiral chambers. In sections, perpendicular to the median plane, the early chambers appear distinctly trochoid and the thickness of the outer walls proves to amount to 10–15  $\mu$ . In the sections only occasionally faint traces of a canal system in the walls could be observed, but no further details could be ascertained by means of canada-balsam preparation, as all hollows of the test are filled by light coloured calcareous material. In the thin sections this usually also somewhat effaces the contrasts between the hollows and the walls of the test, as may be seen in the photographs.

*Occurrence:* The specimens were derived from a well near Baños in Pinar del Río Province, western Cuba, at a depth of 3687–3697'. The age is not exactly known, but it is considered as Early Middle Oligocene by BERMUDEZ. Holotype and paratypes have been deposited in the collection of the Geological Institute, State University of Utrecht, Netherlands. Collection numbers D 33680–33686.

*Remarks:* As only 12 specimens were available, future studies with more material may very well prove that the variation, as to the counted numbers, given in the description above, is somewhat wider than indicated here.

*M. bermudezi* is different from the earlier described representatives of the subgenus *Miogypsinella* mainly because of the thin walls, which are without surface ornamentation. These features serve to distinguish it from *M. borodinensis* HANZAWA, which is otherwise closest to the Cuban species, but differing in the possession of a thicker wall with pustules. According to the figures of median sections of *M. borodinensis*, given by HANZAWA, this species possesses about 15 chambers in the coiled stage. *M. bermudezi* is more easily separable from *M. complanata* SCHLUMBERGER, which, in addition to generally still thicker outer walls than *M. borodinensis*, is different from the other two species for its usually higher average number of coiled chambers.

*Miogypsina (Miogypsinella) complanata* SCHLUMBERGER

Fig. 7

*Miogypsina complanata* SCHLUMBERGER, 1900, Bull. Soc. géol. France, sér. 3, tome 28, p. 330, pl. 2, f. 13—16, pl. 3, f. 18—21; SILVESTRI, 1923, Boll. Soc. Geol. It., vol. 42, pl. 1, f. 19; NUTTALL, 1933, Journ. of Pal., vol. 7, p. 176, pl. 24, f. 9, 11, 13, 14 (not f. 7); BARKER and GRIMSDALE, 1937, Ann. Mag. Nat. Hist., ser. 10, vol. 19, p. 162, pl. 5, f. 6, pl. 6, f. 1—6, 8, pl. 7, f. 1, pl. 8, f. 6; COLE, 1938, Florida State Dept. Conserv., Geol. Bull. 16, pl. 8, f. 10; COSIJN, 1942, Leidsche Geol. Meded., vol. 13, pt. 1, p. 144.

*Miogypsinella sanjosensis* HANZAWA, 1940, Micropaleontological studies of drill cores from a deep well in Kita-Daito-Zima (North Borodino Island), p. 766.

A large number of specimens from a Middle Oligocene sample of a subsurface section in S.W. Trinidad, depth 3790', kindly offered to the author by Dr P. BRONNIMANN, could be determined as *M. complanata*. Briefly described these specimens from Trinidad show the following characteristics.

Test irregularly rounded in outline, 0.75—1.25 mm diameter, with a thickness varying between 0.35 mm and 0.75 mm, in adult specimens the thickest portion situated somewhat eccentrically. Surface covered by closely-set low pustules, which vary in diameter from 25  $\mu$  to 140  $\mu$ , both in a single individual and among different specimens. In transverse sections the early coiled portion of the test is seen to be distinctly trochoid and the lateral walls appear to be of considerable thickness (45—130  $\mu$ ), the latter usually clearly showing the separate pillars as well as the perforations; in some specimens few, irregularly placed, hollows in the outer walls could be observed. In horizontal sections the spherical protoconch measures 60—75  $\mu$  in diameter (including half of the walls). The number of spirally arranged chambers varies between 18 and 30 (always including the protoconch in these countings); they gradually increase in size as added, the last-formed 1—5 usually being somewhat smaller. The equatorial chambers are arranged along half to 3/4 of the circumference of the trochospiral part, irregularly arcuate to ogival in shape, strongly variable in size from 100—200  $\mu$  in greatest dimension, which is directed apically-frontally, especially near the frontal margin exceeding the transverse dimension with up to 50 %.

Collection numbers D 33687—33692.

Just as in other larger Foraminifera the early ontogenetic features are thought to be the most reliable characteristics for determination and comparison of species, when taking into account the existing variation of these characteristics in the individuals of each fossil assemblage. Thus the number of coiled chambers may be highly important in our case and it has been used as the main feature in the comparison of the *Miogypsina*'s involved. As a matter of fact, during this study it became evident that this characteristic was less variable and less irregularly distributed among different assemblages — also in other groups of the

*Miogypsinidae*, not dealt with in this paper — than others, as for instance size and shape of the separate chambers, thickness of the walls and surface ornamentation. However, from our few data the extent of influences of environmental factors on the observed changes of this characteristic in the course of time cannot yet be estimated, but probably future research on this subject will give similar results as those, acquired from this study. Thus it would be possible to conclude with greater certainty that these influences are of minor importance only, in connection with the changes in *Miogypsinella*, discussed below. As to *M. complanata* the following additional data on the numbers of coiled chambers could be obtained either from literature or from own investigation.

In the pictured megalospheric specimen of SCHLUMBERGER about 22 chambers can be counted, which number is in accordance with the statement he observed in all made sections: a spiral "composée d'une vingtaine de loges formant deux tours autour de la loge primordiale". Two macrospheric individuals from SCHLUMBERGER's type-locality at St. Etienne d'Orthes, Landes, southwestern France, obtained through the mediation of Prof. H. SCHOELLER and Dr A. MAGNE (Bordeaux), showed spirals, consisting of respectively 18 and 23 chambers. BRONNIMANN's *M. complanata* var. *mauretanica* from Morocco possesses 11—18 spirally arranged chambers, which are relatively low numbers in the species. In material from Villa Sacco, Turin, Italy, lent to the writer by the Naturhistorisches Museum of Basel, Switzerland, in five sectioned specimens a range of variation was ascertained of 20—26 in the number of coiled chambers. The specimen pictured by SILVESTRI from Vasciano, Province of Perugia, Italy, has 24 spiral chambers; and in a specimen from St. Géours, S. W. France, borrowed from the Naturhistorisches Museum of Basel, 23 chambers were counted in the coiled part of the test.

Some good observations could be made on a large collection from yet another part of the Mediterranean area. Prof. VAN DER VLIERK kindly enabled me to investigate at the Rijksmuseum voor Geologie en Mineralogie, Leiden, COSIJN's ample material from Puente Viejo, Spain, which gave very interesting results. COSIJN sectioned a large number of specimens of *M. complanata* from three separate samples (408—410, 408 being the oldest), belonging to a short section along the southern bank of the Guadalquivir. Of about 180 specimens of each of the samples the numbers of spiral chambers could be counted, which gave the following results, concerning these numbers:

Sample number	Number of specimens	Observed range	Mean	Standards error of the mean ( $\sigma_M$ )	$d/\sigma_d$ <sup>1)</sup>
410	186	11—24	17.33	$\pm 0.19$	3.1 11.0
409	183	9—25	16.45	$\pm 0.20$	
408	171	9—21	13.58	$\pm 0.17$	

<sup>1)</sup>  $\sigma_d$  calculated from  $\sigma_d = \sqrt{\sigma_{M_1}^2 + \sigma_{M_2}^2}$ .



From this we see that the ranges remain fairly constant throughout the section, but that a marked increase in the average number of coiled chambers has taken place in the course of time. Furthermore it is worth mentioning that in COSIŶN's collection of the oldest Puente Viejo sample 408 some specimens had been picked out by this author as "*Miogypsina* sp. with lateral chambers", though during the re-investigation the present writer was unable to obtain many more details about this, except that in one of these specimens a spiral of 11 chambers was distinguished. Moreover it should be remarked that occasionally among the specimens of the three samples, but especially among those of 408, traces were observed of a commencing development of a second auxiliary chamber (TAN's HAK), and even short spirals from it, in the angle between protoconch and deuterococonch, opposite to the third chamber.

As to the American occurrences of *M. complanata*, we have the following data. NUTTALL, in his description indicates a variation of 16—26 for the number of coiled chambers in the specimens from the Meson formation of Mexico.<sup>1)</sup> The pictured specimen shows 25 chambers. Plate 6, fig. 5 of BARKER and GRIMSDALE shows us a specimen with 24 chambers, COLE's figure one with 22 in the coiled part, both specimens also coming from Mexico.

Recapitulating all these data, we have to conclude that in the specimens of one and the same fossil assemblage the beginning development of equatorial chambers and correspondingly the termination of spiral growth, occur at rather widely divergent stages of individual development. This leads us to a short discussion of HANZAWA's classification of the described American representatives of *M. complanata*. HANZAWA proposed in his paper of 1940 to separate from SCHLUMBERGER's species the forms, described by NUTTALL, and BARKER and GRIMSDALE, and he established a new species, *Miogypsinella sanjosensis*, for them. This he based on slightly differing numbers of chambers in the various whorls of the pictured specimens from France and Central America and on the differences in the order of the chambers, counted from the protoconch, that are situated at the apical part of the test of these specimens. From the individuals of Trinidad and Spain (and also from all observed similar forms of other localities), where sufficiently large numbers occur, it proves that just as the total numbers of spirally arranged chambers show considerable variation in the specimens of a single assemblage, also variation exists in the numbers of whorls and in the numbers of chambers in each convolution, and even more widely than the values, considered to be critical

---

<sup>1)</sup> However, the numbers, given by NUTTALL, are not fully reliable, as this author probably confused in his paper *M. complanata* with a form, resembling in horizontal section *M. panamensis* (CUSHMAN) (NUTTALL's fig. 7). Nevertheless, from a re-study of the latter species from its type-locality in Panama, it proved that *M. panamensis* possesses about the same average number of coiled chambers as *M. complanata*, being different because of other features.



for specific separation by HANZAWA. Equally variable are the angles, formed by the axis of the first two chambers and the apical-frontal line, and thus the places occupied by the separate chambers, counted from the proloculus, in connection with the apical part of the test. For these reasons it is considered to be preferable to leave the American occurrences in *M. complanata*; evidently a rather variable species, but without important primary differences between its representatives in Europe and America. It is even probable that *M. ubaghsi* TAN SIN HOK, described from the Upper Oligocene of Borneo, should also be placed in the synonymy of *M. complanata*, but the single median section of TAN's species with about 20 spiral chambers, gives no conclusive evidence as to the range of variation of the Indonesian form.

Regarding the present knowledge of *Miogypsinella* it can be safely assumed that the features, shown by *M. bermudezi*, indicate that we are dealing here with the most primitive representative of the *Miogypsinidae*, known so far. Morphologically *M. borodinensis* (HANZAWA) occupies an intermediate position between the Cuban species and *M. complanata*, though the frequently recorded *M. complanata* has a much wider species conception, being in some extreme variants very close to *M. borodinensis*. It is possible that these three species represent rapidly succeeding stages in the phylogenetic development of the primitive members of the family. In assuming such a development we have to conclude to the remarkable fact that from *M. bermudezi* and *M. borodinensis* to part of the assemblages, considered to belong to *M. complanata*, an increase in the average number of spirally arranged chambers has taken place.<sup>1)</sup> A similar increase is found in the representatives of *M. complanata* from Puente Viejo. This development in *Miogypsinella* is remarkable as, on the other hand, much evidence has been found in the younger *Miogypsina* s.str. for a general decrease of the number of chambers in the primary coil during phylogenetic development, at the cost of new spirals, originating from the opposite side of the deuteroconch.

As to the descent of the family *Miogypsinidae* it should be borne in mind that BARKER and GRIMSDALE proposed that this family had been derived directly from some *Rotalia* ancestor, basing their opinion on a study of the canal systems in some species of *Miogypsina* and *Rotalia*. Their conclusion is further substantiated by the characters, observed in *M. bermudezi*. From these characters it is very likely that the latter species descended directly from a form, closely allied to *Rotalia mexicana* NUTTALL, which species strongly resembles the early portion of the Cuban *Miogypsinella*; the *Rotalia* species, however, shows a distinct surface ornamentation. No doubt, the other known representatives of *Miogypsinella* should be considered as having further developed, on account of their

<sup>1)</sup> On the other hand, however, some of the samples (as for instance Puente Viejo 408) have an average, which is lower than the stated range of *M. bermudezi*.

thicker and ornamented lateral walls. In *M. complanata* hollows and occasionally even development of lateral chambers in the thick outer walls have been observed. From this species another step leads us immediately to primitive representatives of *Miogypsina* s.str., as for instance *M. gunteri* COLE, where lateral chambers are distinctly developed, whereas the coiled ones become arranged planispirally. Considering the number of coiled chambers in *M. gunteri* (about 13) to be characteristic for the most primitive *Miogypsina* s.str. and estimating the larger number of the ascertained changes of this feature in *Miogypsinella* not to be caused by environmental alterations, it would be obvious to think of a genesis of *Miogypsina* s.str. from early *M. complanata*, rather than to see it as a further development from the last representatives of this species with theoretically the highest average number of chambers in the coiled part of the test. The indications in this direction found in COSJN's Spanish collection are unfortunately too weak to support this supposition.

The more we shall know in future about these primitive forms, the more the gaps between the presently known species will be bridged. A clear indication for this opinion we see already in each investigated assemblage. Here we generally find individuals which are more primitive and others that are more advanced than the average type. Thus, on account of these partly ascertained and partly assumed, gradual changes, it is preferable to give to *Miogypsinella* no more than subgeneric rank within the genus *Miogypsina*. A similar position is recommended for *Miogypsina* s.str., *Miogypsinoides* and *Miolepidocyclina*.

Concerning the age of the early members of the *Miogypsinidae* the available data still give a somewhat confused picture. In America probably all known occurrences of the subgenus *Miogypsinella* are of ages, considered to be earlier than Upper Oligocene, that of *M. bermudezi* being most ancient. The occurrences of the western Pacific, including those of *M. ubaghsi* and *M. borodinensis*, have been recorded from Upper Oligocene and Lowermost Miocene, while in the Mediterranean area *M. complanata* is reported from Upper Oligocene <sup>1)</sup> and Lower Miocene. Though partly these differences may be the consequences of incorrect long-distance correlations, it is certain that the most frequently recorded species, *M. complanata*, had a relatively long stratigraphical range, which might have been somewhat different in the several, widely separated regions of the world. In Indonesia (MOHLER) and in Marocco (BRONNIMANN) this species, respectively a variety of this species, are recorded to occur together with species of *Miogypsina* s.str., which are generally considered to be more highly developed and to have appeared later than early *M. complanata*. If we assume that from the latter species the younger species of the *Miogypsinidae*, mainly belonging to *Miogypsina* s.str., have developed, it has to

<sup>1)</sup> The Aquitanian is considered to be Uppermost Oligocene.

be borne in mind that this *Miogypsinella* still existed some time afterwards together with the early species of the subgenus *Miogypsina*. No doubt future investigation will reveal the existence of several geographical and chronological subspecies in *M. complanata*, but at the moment both the available data and the criterions for further subdivision are considered to be generally insufficient, for which reasons it is thought more important at present to recognize the close relations between the various described occurrences, than to introduce new names for the different, till now insufficiently known, types.

*Acknowledgements:* The author is gratefully indebted to Dr P. J. BERMUDEZ (Caracas), Dr P. BRONNIMANN (Trinidad), Dr E. RITTER (Basel), Prof. I. M. VAN DER VLERK (Leiden), Prof. H. SCHOELLER and Dr A. MAGNE (Bordeaux), who, by their valuable support, offered the opportunity to study this interesting material. Furthermore many thanks are due to Dr P. MARKS for his critical suggestions as well as the careful drawing of the figures and to Mr J. H. VAN DIJK for the making of the photographs.

#### REFERENCES

- BARKER, R. WRIGHT and T. W. GRIMSDALE, Studies of Mexican fossil Foraminifera, *Ann. and Mag. of Nat. Hist.*, ser. 10, **19**, 161—178 (1937).
- BRONNIMANN, P., Über die tertiären Orbitoididen und die Miogypsiniden von Nordwest-Marokko, *Schweiz. Pal. Abh.*, **63** (1940).
- COSIJN, A. J., On the phylogeny of the embryonic apparatus of some Foraminifera, *Leidsche Geol. Meded.*, **13**, pt. 1, 140—171 (1942).
- HANZAWA, S., Micropaleontological studies of drill cores from a deep well in Kita-Daito-Zima (North Borodino Island) (1940).
- MOHLER, W. A., *Floresculinella reicheli* n. sp. aus dem Tertiär e5 von Borneo, *Ecl. Geol. Helv.*, **42**, no. 2, 521—527 (1949).
- TAN SIN HOK, Zur Kenntnis der Miogypsiniden, *De Ingenieur in Ned. Indië IV*, *De Mijningenieur*, **3**, no. 3, 45—61 (1936).

## VISCOSITY OF BINARY LIQUID MIXTURES

BY

N. L. BALÁZS <sup>1)</sup>

(Laboratory for General and Inorganic Chemistry of the University of  
Amsterdam, Netherlands)

(Communicated by Prof. C. H. MAC GILLAVRY at the meeting of September 29, 1951)

§ 1. *Introduction*

In a recent article [1] (abbreviated as I.) the author has given an approximate expression relating the viscosity coefficient of a mixture to that of the pure components.

The properties of the actual mixture were supposed to be approximated sufficiently well by the assumptions of the strictly regular solutions [2]; whilst the statistical model used for the calculation of the viscosity coefficient gave results which resembled the equation deduced by EYRING [3].

In this article, which is based on a different mixture model, we give proofs of statements which were used in I. The results will approximately be the same, though in the final equation an additional term appears which for practical purposes is negligible. Notwithstanding, from a theoretical standpoint it is of some interest since it shows the relative importance of different effects.

§ 2. *The model used for the description of viscous flow*

The properties of the actual system are compared with the properties of an ideal gas moving in an external field of force. This latter is adjusted in such a way that it shall represent the average force acting on a particle in the liquid due to its neighbours and to the shearing forces.

This can be specified more precisely with the help of the following assumptions:

1) It is sufficient to account for the interaction with the closest neighbours, whose average number,  $z$ , is identical for every particle and independent of temperature in the temperature region concerned. The closest neighbours are supposed to take up every position with equal probability on the surface of a sphere of radius  $a$ , around the particle concerned. This corresponds to the well-known cell model of LENNARD-JONES and DEVONSHIRE [4].

2) The average field, averaged over all positions of the neighbours on the sphere, is identical around every particle. This will be the case for

---

<sup>1)</sup> Present adress: Dublin Institute of Advanced Studies, Dublin.



pure liquids except for a negligible fraction near the walls of the container.

3) The shearing forces do not appreciably disturb the equilibrium structure of the liquid, (e.g. the spherical cells are not deformed into ellipsoids).

4) Equilibrium statistics may be used, though we deal with a transport process. This implies that the "activation energy" of viscous flow (see later) shall be large compared with  $kT$ . So one should not use this expression at elevated temperatures, e.g. near the critical temperature, as it is not infrequently done.

5) The unit mechanism of flow consists of an interchange of neighbouring particles.

6) The unit mechanisms are independent of each other. Then the macroscopic viscosity coefficient measured during the flow of  $N$  particles is the arithmetic mean of the microscopic coefficients defined in terms of unit mechanisms. In virtue of the above assumptions, for pure liquids all the microscopic viscosity coefficients are equal to each other and to the macroscopic viscosity coefficient. Hence, during the calculation it is sufficient to consider only one cell of the liquid. (This simplicity — which is a rough approximation — is due to the smoothing out effect of the early partial averaging by introducing an average field of force.) We then exclude the cases of laminar flow and other anomalies.

Using these assumptions, it is possible to deduce the following expression (5)

$$(1) \quad \eta = v^{-1} (2\pi mkT)^{1/2} \left( \int_R \exp -U(r)/kT \, dr \right)^{1/3} \exp U(r_c)/kT,$$

where  $\eta$  = viscosity coefficient;  $v = V/N$ , volume per particle;  $m$  = mass of the moving particle;  $U(r)$  = potential energy of the moving particle at the point  $r$ ;  $U(r_c)$  is the potential energy at a point  $r_c$  where a transition from a relatively stable position to an other relatively stable position may occur. If  $U(r_c)$  is the potential energy at a relatively stable position, (and will be the energy zero),  $U(r_c) - U(r_c) = U(r_c)$  can be denoted as the activation energy for viscous flow. The integration is performed over a region  $R$  enclosing a point  $r_c$ . The vagueness of the above terms arises from the fact that equilibrium states are defined for the system as a whole and *not* for the particles composing the system.

The integral is identical with the free volume as used by LENNARD-JONES and DEVONSHIRE, but not with that of EYRING and HIRSCHFELDER [6].

The evaluation of  $U(r)$  is given in detail in (5). The idea is briefly the following: We calculate the potential energy,  $w(v, r)$ , of a particle in a cell of radius  $a$  at a distance  $r$  from the center of the cell ( $v = V/N = a^3/\gamma$ , where  $\gamma$  is a packing factor). At sufficiently low temperatures, compared to  $U(r_c)/k$ , this will be that of an isotropic harmonic oscillator,  $w(v, r) - w(v, 0) = (z/2) \varepsilon k(v) r^2 = (A/2) k(v) r^2$ . Here the value of the constant  $\varepsilon$  and the form of the force constant  $k(v)$  will depend on the intermolecular

potential function used. We take the LENNARD-JONES potential  $\varphi(r) = \varepsilon[(r/r_0)^{-12} - 2(r/r_0)^{-6}]$ ;  $\varepsilon$  is the potential energy at the separation  $r_0$ , which is the root of  $d\varphi/dr = 0$ ;  $\Lambda = z\varepsilon$ . Since  $v$  is temperature dependent and the force constant  $k(v)$  is a function of  $v$ , the potential energy in the cell is an implicit function of  $T$ .

Substituting this expression in Eq (1), and performing the integration from  $-\infty$  to  $+\infty$ , we obtain

$$(2) \quad \left\{ \begin{aligned} \eta &= v^{-1}(2\pi mkT)^{1/2}(\gamma v)^{1/3}(2\pi kT/\Lambda k(v))^{1/2} \exp(\Lambda k(v_c) r_c^2/2kT) = \\ &= (2\pi kT) v^{-2/3} \gamma^{1/3} (m/\Lambda k(v))^{1/2} \exp(\Lambda k(v_c) r_c^2/2kT), \end{aligned} \right.$$

where  $v_c$  is the volume of the cell if the moving particle is at  $r_c$ .

Although in this expression every term is temperature dependent, it is possible to show (5), that over a limited temperature range (see assumption 4)) Eq (2) is equivalent to

$$(3) \quad \eta = (m\Lambda)^{1/2}/r_0^2 \alpha \exp(\beta\Lambda/kT),$$

taking into account the local density changes around the moving particle to calculate  $v_c$ , and, assuming that  $r_c$  is located midway between the original positions of the two interchanging particles. In Eq (3)  $\alpha$  and  $\beta$  are constants, independent of temperature, and have the same values for different liquids, provided they satisfy the above assumptions. This means that these liquids have the same viscosity coefficient if the temperature is measured in units  $\Lambda/k$ , and the viscosity coefficient in units  $(m\Lambda)^{1/2}/r_0^2$ . (This is a particular case of the Law of Corresponding States as defined by J. DE BOER [7].)

### § 3. The model for binary mixtures

Our system is composed of  $N_A$   $A$  particles and  $N_B$   $B$  particles. In this case assumption 2) cannot be maintained any longer and we have to replace it by a more suitable one. The simplicity of the treatment used for pure liquids arose from the situation that in view of the assumptions we had to deal with one "representative cell" only. Similarly, we obtain a simple situation for mixtures if we suppose that

7) the average molecular distribution (averaged over time in a small volume element) is random and this random distribution is preserved throughout the process.

The first part of this assumption will probably be valid if the energy of interaction between two  $A$  particles is not too different from that of two  $B$  particles, and at temperatures far above the temperature of critical mixing if the latter exists. (See also I. footnote 5.) The second part will be satisfied if the original distribution is random, and the shearing forces are sufficiently low which is anyway a necessary condition in virtue of assumption 3).

Accepting assumption 7) we have only two representative cells, one

in which an  $A$ , another in which a  $B$  particle is oscillating. This model, which is a logical extension of the cell model for mixtures was developed by PRIGOGINE and GARIKIAN [8].

The potential energy between two particles is now given as

$$(4) \quad \varphi_{kl}(r) = \varepsilon_{kl} [(r/r_{okl})^{-12} - 2(r/r_{okl})^{-6}] ; \quad (k, l, = A, B).$$

If

$$(5) \quad r_{okl} = r_{okk} = r_{oIl} = r_o,$$

then

$$(6) \quad \varepsilon_k = (\varepsilon_{kk} \varepsilon_{ll})^{1/2}.$$

to the first approximation (9).

We suppose further

8) the average number of closest neighbours,  $z$ , is the same in both pure liquids  $A$  and  $B$ , and in their mixture respectively; it is independent of temperature in the temperature region concerned.

Introducing the abbreviations

$$(7a) \quad \begin{cases} z\varepsilon_{AA} \equiv \Lambda_{AA} & x_A \equiv N_A/(N_A + N_B) \\ z\varepsilon_{BB} \equiv \Lambda_{BB} & x_B \equiv N_B/(N_A + N_B) \end{cases}$$

$$(7b) \quad \begin{cases} z(x_A \varepsilon_{AA} + x_B \varepsilon_{AB}) = (x_A \Lambda_{AA}^{1/2} + x_B \Lambda_{BB}^{1/2}) \Lambda_{AA}^{1/2} \equiv \Lambda_A^{AB} \\ z(x_A \varepsilon_{AB} + x_B \varepsilon_{BB}) = (x_A \Lambda_{AA}^{1/2} + x_B \Lambda_{BB}^{1/2}) \Lambda_{BB}^{1/2} \equiv \Lambda_B^{AB} \end{cases}$$

$$(7c) \quad x_A \Lambda_A^{AB} + x_B \Lambda_B^{AB} = (x_A \Lambda_{AA}^{1/2} + x_B \Lambda_{BB}^{1/2})^2 \equiv \Lambda_{AB}$$

we may simply write (with  $v_{AB} = V/(N_A + N_B)$ )

$$(8) \quad \begin{cases} w_A^{AB}(v_{AB}, r) - w_A^{AB}(v_{AB}, 0) = (z/2) (x_A \varepsilon_{AA} + x_B \varepsilon_{BB}) k(v_{AB}) r^2 = \\ = (\Lambda_{AB}/2) k(v_{AB}) r^2, \\ w_B^{AB}(v_{AB}, r) - w_B^{AB}(v_{AB}, 0) = (\Lambda_B^{AB}/2) k(v_{AB}) r^2 \end{cases}$$

for the average field acting on an  $A$  resp  $B$  particle in the mixture  $AB$ .

#### § 4. Calculation of the viscosity coefficient

According to assumption 5) the following mechanisms will contribute to the flow:

- 1) The interchange of an  $A$  particle with an  $A$  particle;
- 2) „ „ „ „  $A$  „ „ „  $B$  „ ;
- 3) „ „ „ „  $B$  „ „ „  $B$  „ ;
- 4) „ „ „ „  $B$  „ „ „  $A$  „ .

An elementary consideration shows that in our case 2) and 4) cancel. If we denote the microscopic viscosity coefficient arising from the flow

of an  $A$  particle in the mixture  $AB$  due to 1) with  $\eta_A^{AB}$ , and similarly for  $\eta_B^{AB}$ , we obtain:

$$(9) \quad \left\{ \begin{aligned} \eta_K^{AB} &= (2\pi kT) v_{AB}^{-2/3} \gamma^{1/3} (m_K/k(v_{AB}) \Lambda_K^{AB})^{1/2} \exp(\Lambda_K^{AB} k(v_{cAB}) r_{cAB}^2/2kT) \\ &\quad (K = A, B) \end{aligned} \right.$$

$$(10) \quad \left\{ \begin{aligned} \eta_{AB} &= x_A \eta_A^{AB} + x_B \eta_B^{AB} = (2\pi kT) v_{AB}^{-2/3} \gamma^{1/3} \cdot \\ &\quad \cdot \{x_A [m_A/k(v_{AB}) \Lambda_A^{AB}]^{1/2} \exp[\Lambda_A^{AB} k(v_{cAB}) r_{cAB}^2/2kT] + \\ &\quad + x_B [m_B/k(v_{AB}) \Lambda_B^{AB}]^{1/2} \exp[\Lambda_B^{AB} k(v_{cAB}) r_{cAB}^2/2kT]\}. \end{aligned} \right.$$

where  $\eta_{AB}$  is the viscosity coefficient of the mixture.

One may try to evaluate Eq (10) as it stands, but it seems more expedient to evaluate  $\eta_{AB}$  in terms of  $\eta_A$  and  $\eta_B$ . In addition we may hope that some of the inadequacies due to the adapted model will cancel.

Eq (10) shows immediately that formulas like  $\eta_{AB} = x_A \eta_A + x_B \eta_B$ , cannot hold generally since  $\eta_A \neq \eta_A^{AB}$ ,  $\eta_B \neq \eta_B^{AB}$ . This is fairly obvious if one realizes that as long as in the case of a pure liquid  $\eta$  arises from the interaction of similar particles, then, in the case of a mixture we have to account for an interaction between unlike particles also. If  $\eta_A^{AB}$  does not differ appreciably from  $\eta_A$  the difference between the field of force of an  $A$  resp  $B$  particle must be small, hence the difference  $\eta_A - \eta_B$  is small, and expanding the above expression in powers of this difference, we obtain neglecting higher terms

$$(11) \quad \eta_{AB} = (\eta_A)^{x_A} (\eta_B)^{x_B}.$$

Eq (11) suggests that it is worth while to try to find an approximate solution of Eq (10) in the form

$$\eta_{AB} = \eta_A^{x_A} \eta_B^{x_B} g(x_A, x_B, \Lambda_{AA}, \Lambda_{BB}, v_{AB}, T).$$

Returning to Eq (10) we may observe that in view of the relation

$$x_a a + x_b b = a^{x_a} b^{x_b} + (1/2) x_a x_b (a - b)^2/a + \dots \quad (x_a + x_b = 1),$$

we may use the geometric mean instead of the arithmetic one if  $a$  does not differ from  $b$  more than about 30 %. Then

$$(12) \quad \left\{ \begin{aligned} \eta_{AB} &= (2\pi kT) \gamma^{1/3} v_{AB}^{-2/3} (m_A/\Lambda_A^{AB} k(v_{AB}))^{x_A/2} (m_B/\Lambda_B^{AB} k(v_{AB}))^{x_B/2} \cdot \\ &\quad \cdot \exp(\Lambda_{AB} k(v_{cAB}) r_{cAB}^2/2kT), \end{aligned} \right.$$

using Eq (7c).

This approximation will be certainly valid if  $(1/2)|H_v^A - H_v^B|/kT < 1$ , where  $H_v^A$  is the heat of vaporization of the pure  $A$  component.

If we define a function  $f(x_A, x_B, \Lambda_A^{AB}, \Lambda_B^{AB})$ , so that

$$(13) \quad (\Lambda_A^{AB})^{x_A} (\Lambda_B^{AB})^{x_B} = f \Lambda_{AB},$$

we may write in place of Eq (12)

$$(14) \quad \eta_{AB} = (2\pi kT) \gamma^{1/3} v_{AB}^{-2/3} (m_A^{x_A} m_B^{x_B} / f \Lambda_{AB} k(v_{AB}))^{1/2} \exp(\Lambda_{AB} k(v_{cAB}) r_{cAB}^2/2kT).$$

We assume now that



a)  $r_{cAB}$  is still located midway between the original positions of the interchanging particles in  $v_{cAB}$ .

We know that  $v_{AB}/r_0^3$  is the same function of the reduced temperature  $kT/\Lambda_{AB}$  as  $v_A/r_0^3$  and  $v_B/r_0^3$  of  $kT/\Lambda_{AA}$  and  $kT/\Lambda_{BB}$ . Then, since  $f$  is independent of  $T$ , by comparing Eq (14) with Eq (2) we immediately see that the temperature dependence of  $\eta_{AB}$  will be the same as that of  $\eta_A$  or  $\eta_B$  if we measure the temperature in units  $\Lambda_{AB}/k$ , and the viscosity in units  $((m_A^{x_A} m_B^{x_B}/f)\Lambda_{AB})^{1/2}/r_0^2$ , (using, of course, the corresponding units for the pure liquids). We may look upon  $(m_A^{x_A} m_B^{x_B}/f)$  as being the "effective mass" of a hypothetical particle. In the "pure liquid" composed from these particles such a particle has a potential energy  $(\Lambda_{AB}/2) k(v_{AB})r^2$  at the point  $r$  relative to the center of its cell.

This justifies the fundamental assumption of I., though there the function  $f$  did not appear due to the different connection between the free volumes of the pure liquids and the free volume of the mixture, as defined in the theory of strictly regular solutions.

Then, ad analogiam of the step from Eq (2) to Eq (3) we may write

$$(15) \quad \left\{ \begin{aligned} \eta_{AB} &= [(m_A^{x_A} m_B^{x_B}/f) \Lambda_{AB}]^{1/2}/r_0^2 \alpha \exp (\beta \Lambda_{AB}/kT) = \\ &= (m_A^{x_A} m_B^{x_B} \Lambda_{AB}^2/(\Lambda_{AA}^{x_A} \Lambda_{BB}^{x_B})^{1/2} r_0^{-2} \alpha \exp (\beta \Lambda_{AB}/kT), \end{aligned} \right.$$

where  $\alpha$  and  $\beta$  are the *same* constants as for pure liquids.

Using Eq (3) for the viscosity coefficient of pure liquids  $A$  and  $B$ , we obtain

$$(16) \quad \eta_{AB}/(\eta_A)^{x_A} (\eta_B)^{x_B} = (\Lambda_{AB}/\Lambda_{AA}^{x_A} \Lambda_{BB}^{x_B})^{3/4} \exp (-\beta x_A x_B (\Lambda_{AA}^{1/2} - \Lambda_{BB}^{1/2})^2/2kT)$$

using Eq's (7).

According to the cell model of liquids the heat of vaporization is equal to

$$(17) \quad H_v^A = \Lambda_{AA} \{ (v/v_0)^{-4} - 2(v/v_0)^{-2} \} - kT/2.$$

At low temperatures we may expand the term in curly brackets in powers of  $v - v_0$ . Retaining the linear term only we obtain

$$(18) \quad H_v^A \sim \Lambda_{AA} - kT/2 \sim \Lambda_{AA},$$

since at low temperatures  $kT/2$  is negligible compared with  $\Lambda_{AA}$ . This shows that the constant  $\beta$  defined by Eq (3) is approximately equal to the constant  $1/n$  used *empirically* for pure liquids by EWELL and EYRING [10] and which has the value  $n \sim 2.5 - 3$ .

Furthermore, to the above used approximation the excess energy of mixing and the excess entropy of mixing, (the latter being due to the change of frequency of vibration, and excess over the values given for perfect solutions) will be ( $P-G$ . Eq (5.2), (5.3))

$$(19) \quad \left\{ \begin{aligned} E^e/NkT &\sim H^e/NkT = x_A x_B (\Lambda_{AA}^{1/2} - \Lambda_{BB}^{1/2})^2/2kT, \\ S_v^e/Nk &= -(3/4) \log \Lambda_{AB}/(\Lambda_{AA})^{x_A} (\Lambda_{BB})^{x_B}, \quad (\text{index } v \text{ for vibration}). \end{aligned} \right.$$

Substituting them in Eq (16) we obtain

$$(20) \quad \log (\eta_{AB}/(\eta_A)^{x_A}(\eta_B)^{x_B}) = -(\beta E^e + TS_v^e)/NkT.$$

Expanding  $-S_v^e$  in powers of  $(\Lambda_{AA}^{1/2} - \Lambda_{BB}^{1/2})$ , and neglecting higher order terms we obtain

$$S_v^e/Nk = -x_A x_B (\Lambda_{AA}^{1/2} - \Lambda_{BB}^{1/2})^2 / \Lambda_{AA}. \quad ^1)$$

Thus,

$$\log (\eta_{AB}/(\eta_A)^{x_A}(\eta_B)^{x_B}) = -(\beta + 3kT/2\Lambda_{AA}) x_A x_B (\Lambda_{AA}^{1/2} - \Lambda_{BB}^{1/2})^2 / 2kT.$$

In the limited temperature range where this expression is valid, the average value of  $kT/\Lambda_{AA}$  will be about 1/20 for liquids approximately satisfying the conditions 1) to 7), while  $\beta$  is about 1/3 for the same liquids. Then, since the factor  $(\beta + 3kT/2\Lambda_{AA})$  will hardly vary with the temperature in this limited temperature range, and its value will be slightly higher than the value of  $\beta$ , it will appear as a constant which has nearly the value of  $\beta$ , confirming the empirical findings of POWELL, ROSEVEARE and EYRING [11]. (In their notation  $\beta = 1/n$ .)

### § 5. Discussion of the results

Using the theory of strictly regular solutions, with the additional assumption of random mixing we obtained in I. (Eq (16))

$$(21) \quad \log (\eta_{AB}/(\eta_A)^{x_A}(\eta_B)^{x_B}) = -\beta G^e/NkT,$$

where  $G^e \sim F^e$  is the excess free energy of mixing.

Since with the assumptions used in I.  $S_e = 0$ , Eq (21) differs by a term of  $-S_v^e/Nk$  from Eq (20). As we saw, this term is usually very small, and is more interesting theoretically than practically. If  $E^e \sim 0$ ,  $\eta_{AB} = (\eta_A)^{x_A}(\eta_B)^{x_B}$ , which definitely settles the long discussion for the mixing law of viscosities of perfect solutions (12).

There are four interesting points to notice in the interpretation of Eq (20).

- a) We seemingly did not make use of any assumption regarding the additivity of volumes.
- b) There is a term  $\beta E^e/NkT$  but no  $\beta S_v^e/Nk$ .
- c) There is a term  $S_v^e/Nk$ , but no  $E^e/NkT$ , only  $\beta E^e/NkT$ .
- d) The terms containing  $S_v^e$  and  $E^e$  do not appear in the combination  $E^e - S_v^e T$ , but  $\beta E^e + S_v^e T$ .

Ad point a).

During the course of this work we used the assumption that  $r_c$  is located halfway between the positions of the two particles to be interchanged.

<sup>1)</sup> Do not be surprised that this expression is not symmetric in  $A$  and  $B$  though Eq (19) is. This is due to the approximation of retaining only the first term in the series expansion.

This assumption, though valid for pure liquids, is only an approximation for mixtures, where this point will be probably displaced, if there is an excess volume of mixing. The error involved in this is usually negligible.

Ad point b).

The term  $\beta E^e/NkT$  accounts for the fact that the changed interaction between the particles changed the height of the potential barrier surrounding the equilibrium position of a particle. On the other hand, the fact that the factor  $\beta$  is identical in both pure liquids and mixtures shows that the activation energy for viscous flow in our hypothetical liquid is the same fraction of the potential energy at the center of the cell as for pure liquids.

Using further this model composed of hypothetical particles, we see at once that a term  $\lambda S^e/Nk$  would appear if and only if there would be an entropy difference, proportional to the entropy per particle of the initial state, between the initial state and activated state. If this proportionality factor  $\lambda$  happens to be the same as for the energy, we would obtain a term  $\beta S^e/Nk$ . Since according to our model 1) the particles move independently, 2) the internal degrees of freedom of the particles are not affected by the process, no such entropy change could arise.

Ad point c).

The excess entropy of mixing, due to the change in frequency of vibration at an equilibrium position, clearly must enter and with its full value, since a change in frequency will change the probability of a transition.

A term  $E^e/NkT$  cannot arise, since the transition does not depend explicitly on the absolute value of the energy of a particle at an equilibrium position, but only on the potential energy difference between the initial and activated states.

Ad point d).

A positive excess energy of mixing decreases the interaction between the particles and, hence, lowers the viscosity coefficient of the mixture. This explains the sign of the term containing  $E^e$ . On the other hand, a negative excess entropy of mixing, due to the change in frequency of vibration, ( $S_v^e$  is always negative as given by Eq (19)) corresponds to the stiffening of the oscillator, representing the particle, and hence, raises the viscosity of the mixture. This explains the negative sign of the term containing  $S_v^e/Nk$ .

Summing up, the term  $\beta E^e/NkT$  measures the change in height of the potential barrier, and the term  $S_v^e/Nk$  measures the change in shape of the potential barrier compared with a potential barrier made up additively from that of the pure liquids. The missing term containing  $v_e$ , the excess volume of mixing, would measure the change of the position of the top of the potential barrier.

It seems impossible to compare the results of this paper with satisfactory experimental measurements, since they simply do not exist for mixtures where the particles are spherical, have about identical radii, and dispersional forces are acting between them. It would be of considerable theoretical interest to perform viscosity measurements in the liquid phase on such systems at different temperatures and compositions. Such systems are, besides the heavy inert gas mixtures, the mixtures  $\text{CCl}_4 - \text{C}(\text{CH}_3)_4$ ;  $\text{CCl}_4 - \text{CBr}_4$ , etc.

The author wishes to express his thanks to Prof. Dr C. H. MACGILLAVRY and Prof. Dr J. A. A. KETELAAR for reading the manuscript and giving helpful advice and criticism, and to the U. A. F. for financial assistance.

### *Summary*

The article gives a description of viscous flow in a binary liquid mixture using a) the LENNARD-JONES DEVONSHIRE [4] cell model and its extension to mixtures due to PRIGOGINE and GARIKIAN [8] to calculate the thermodynamical properties of the mixture; b) a theory [5] similar to that of EYRING [3] to deal with the viscous flow itself.

The results show that 1) for perfect solutions the logarithms of the viscosity coefficients are additive; 2) the deviation from this additivity is proportional to the excess energy and entropy of mixing (but not to the excess free energy of mixing); 3) as far as the viscosity coefficient is concerned the mixture can be identified with a hypothetical pure liquid where each particle in the liquid has a concentration-dependent mass and potential energy, thereby justifying this assumption given by the author in another paper [1]. The conditions to be satisfied for the validity of the results are listed in § 2 and 3.

### REFERENCES

1. BALÁZS, N. L., *Rec. Trav. Chim.* **70**, 412 (1951).
2. See e.g. R. H. FOWLER, E. A. GUGGENHEIM, *Statistical Thermodynamics*, p. 351. (Cambridge 1939). (Abbreviated as F—G).
3. GLASSTONE, S., K. J. LAIDLER, H. EYRING, *The Theory of Rate Processes*. International Chemical Series, p. 485 (1941).
4. LENNARD—JONES, J. E., A. F. DEVONSHIRE, *Proc. Roy. Soc.* **A163**, 53 (1937); **A165**, 1 (1938).
5. BALÁZS, N. L., (Thesis. Amsterdam. 1951).
6. EYRING, H., J. O. HIRSCHFELDER, *J. Phys. Chem.* **41**, 249 (1937).
7. BOER, J. DE, (Thesis. Amsterdam. 1940).
8. PRIGOGINE, I., G. GARIKIAN, *Physica* **16**, 239. (1950). (P—G).
9. LONDON, F., *Trans. Faraday Soc.* **33**, 19 (1937).
10. EWELL, R. H., H. EYRING, *J. Chem. Phys.* **5**, 726 (1937).
11. POWELL, R. F., W. F. ROSEVEARE, H. EYRING, *Ind. Eng. Chem.* **33**, 430 (1941).
12. HATSCHKE, E., *The viscosity of Liquids*. Chapter IX (1928).



## PALEONTOLOGY

### ARENONIONELLA, A NEW ARENACEOUS GENUS OF FORAMINIFERA FROM THE MIOCENE OF ALGERIA

BY

P. MARKS JR

(Communicated by Prof. G. H. R. VON KOENIGSWALD at the meeting of June 30, 1951)

#### *Introduction*

During the summer of 1947 a number of samples was taken by Mr C. VOÛTE, from the Miocene of the Algerian tableland near Constantine, on behalf of the Geological Survey of Algeria. These samples were handed over to the present writer for a micropaleontological investigation, in the course of which a number of arenaceous Foraminifera were detected which could not be assigned to any existing genus.

The accompanying fauna was found to be closely related to that encountered in the Miocene of Egypt, in beds which are considered by MACFADYEN (Miocene Foraminifera from Egypt and the Clysmic area of Sinai, 1930/1931) to be of Lower Vindobonian age. The affinity to the Vindobonian faunae from Central and Southern Europe is also unmistakable, so that an approximate Middle Miocene age may be assumed.

The samples were taken from the top part of a profile, which covers the marine section of the local Miocene; the basal beds of this formation are considered to be continental.

#### *Systematic discussion*

The Foraminifera for which a new genus is being proposed, consist of forms of numerous occurrence and every outward appearance of *Nonionella*, except for the fact that they are in the possession of an arenaceous wall, which, being moreover very flexible, causes most of the specimens found to be much distorted, often almost beyond recognition.

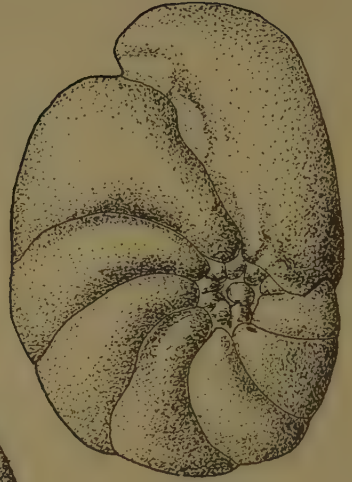
When subjected to a treatment with hydrochloric acid, most of the fragmentary material the wall is composed of, dissolves with much effervescence, leaving quite a complete skeleton of chitinous material, and some insoluble inorganic fragments. Strong magnification also distinctly shows the fragmentary, and therefore truly arenaceous, character of the wall.

In thin-section the chambers are found to be simple, not labyrinthic.

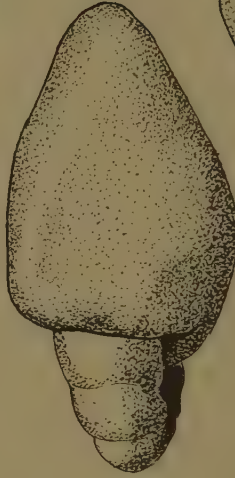
Though the author was at first inclined to place the new genus, for which the name *Arenonionella* is proposed, in the *Trochamminidae*, it was on second thoughts considered to be more appropriate to classify the new



1a



1b



1c



2b



2a



2c



3a



3b



3c

genus under the *Lituolidae*, because of the similarity of its morphological relations to those of *Nonionella* in the *Nonionidae*, and as the peripheral position of its aperture is inconsistent with the generally ventral one in the *Trochamminidae*.

The composition of the wall would point to an affinity to *Endothyra* rather than to *Haplophragmoides*, but the exclusive Paleozoic to Early Mesozoic occurrence of the first-mentioned genus makes it a rather doubtful ancestor. As the relative amount of cement in arenaceous Foraminifera is very variable anyway, a relation to *Haplophragmoides* seems to be more probable, and it is therefore proposed to include *Arenonionella* in the subfamily *Haplophragmiinae*.



Subordo FORAMINIFERA  
Family LITUOLIDAE  
Subfamily Haplophragmiinae  
Genus *Arenonionella*, gen. nov.  
Genotype *Arenonionella voutei*, sp. nov.

Test free, subtrochoid, close-coiled, consisting of several spiral turns, not quite involute on the dorsal side, completely so on the ventral side; chambers numerous, several to a coil, simple, undivided, on the ventral side in the adult stage extending a well-developed lobe, covering the umbilicus. Wall thin, more or less flexible, arenaceous with dominating calcareous cement; a chitinous inner coating may be present. Aperture simple, a low slit at the base of the apertural face. Monotypic.

Explanation of the figures:

In all the figures 'a' indicates the ventral view, 'b' the dorsal view, 'c' the apertural view. The magnification is X 124 for all of the figures.

1. *Arenonionella voutei*, MARKS, holotype, Miocene Djebel Ferroukh, Constantine area, Algeria.

2. *Id.*, paratype, same locality.

3 and 4. *Id.*, distorted specimens from the same locality.

The drawings have been made with the help of a *camera lucida* by the author.

## ARENONIONELLA VOUTEI gen. nov., sp. nov.

(figs. 1a—4c.)

Test free, trochoid, nearly biconvex, rather involute on the dorsal side, only showing a small portion of the preceding coils; completely involute on the ventral side; periphery subacute in the young, rounded in the adult; adult individuals consisting of  $1\frac{1}{2}$  to 2 whorls, typically 8—9 chambers in the last-formed whorl. Chambers distinct, undivided, somewhat inflated, regularly but rather rapidly increasing in size as added, the last-formed one extending a well-developed lobe over the ventral umbilicus. Sutures distinct, depressed, rather strongly, often somewhat angularly, curved backwards. Wall thin, very finely arenaceous, smoothly finished, with a relatively large amount of calcareous cement and a thin chitinous inner coating, very flexible. Aperture simple, a low slit at the base of the apertural face.

Largest diam.: 0.35 mm to 0.51 mm.

Thickness: 0.14 mm to 0.26 mm.

*Type locality*: About 5 km. S of Ain Fakroun, on the Western slope of the Djebel Ferroukh, near Constantine, Algeria.

*Type level*: Miocene, probably Vindobonian.

The species is named for Mr C. Voûte, from the State University of Utrecht, who collected the samples.

The types are in the collection of the "Geologisch-Mineralogisch Museum" of the State University of Utrecht, Netherlands. Registry numbers: D. 33588 to D. 33591.



## CHEMISTRY

### ADDITION REACTIONS OF ALKENES IN SILENT ELECTRICAL DISCHARGES <sup>1)</sup>

BY

H. J. DEN HERTOOG <sup>2)</sup> AND P. BRUIN

(Communicated by Prof. J. P. WIBAUT at the meeting of June 30, 1951)

#### § 1. *Introduction*

It is well known that alkenes of the type  $\text{CH}_2 = \text{CRR}'$  (R and R' = hydrogen or alkyl) add on readily hydrogen-compounds such as hydrogen chloride, hydrogen bromide and water in the gas phase when a suitable catalyst is present. In these reactions almost exclusively the secondary and tertiary halogenocompounds and alcohols are formed in accordance with MARKOWNIKOFF's rule. The "abnormal addition-reaction" is reported only in one case: by irradiating a gaseous mixture of alkene and hydrogen bromide with ultraviolet light the primary bromoalkanes were obtained [1]. Whereas the normal additions are considered to be ionic processes, the course of the abnormal reaction is explained by the following radical mechanism:

- (1)  $\text{HBr} \rightarrow \text{H} + \text{Br}$
- (2)  $\text{CH}_2 = \text{CRR}' + \text{Br} \rightarrow \text{CH}_2\text{Br} - \dot{\text{CRR}}'$
- (3)  $\text{CH}_2\text{Br} - \dot{\text{CRR}}' + \text{HBr} \rightarrow \text{CH}_2\text{Br} - \text{CHRR}' + \text{Br}$

Thus the photochemical dissociation (1) introduces a chain reaction which proceeds rapidly, both reactions (2) and (3) being exothermic. Hydrogen chloride and water do not enter into such a chain reaction as both compounds are more stable than hydrogen bromide. They do not dissociate quickly in ultraviolet light neither part easily with their hydrogen in a reaction analogous to reaction (3) the last process being endothermic <sup>3)</sup>.

We have studied now the behaviour of mixtures of lower alkenes and hydrogen compounds as mentioned above when exposed to silent electrical discharges under different conditions. As it might be expected that not

---

<sup>1)</sup> This investigation will be published in detail in the *Recueil des Travaux chimiques des Pays-Bas*; it was carried out for the greater part during 1948 and 1949 in the Laboratory of Organic Chemistry of the Municipal University of Amsterdam (Director: Prof. Dr J. P. WIBAUT).

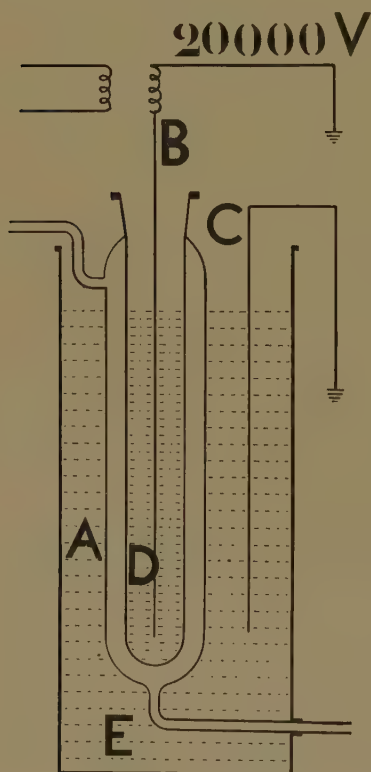
<sup>2)</sup> Present address: Laboratory of Organic Chemistry, Agricultural University, Wageningen.

<sup>3)</sup> The energies of the HCl- and the HO-bond (102.7 and 110.2 Cals./mole according to Pauling [2]) are larger than the energy of the HC-bond (87.3 Cals./mole); the energy of the HBr-bond (87.3 Cals./mole) is equal to it.

only hydrogen bromide but also the other addends would dissociate into radicals, we intended to investigate what would be the result of the reaction of these radicals on alkene molecules.

There are only a few papers in the literature dealing with reactions of alkenes and hydrogen-compounds in electrical discharges [3]. LOSANITSCH has published some articles in which he described experiments on the reactivity of ethene towards hydrogen chloride, ammonia and hydrogen sulphide in electrical discharges [4]. As the reaction time chosen amounted to several hours, he obtained very complicate mixtures of high-boiling compounds, only one or two of which were isolated and identified. An addition reaction has been carried out by FRANCESCONI and CIURLO. These investigators report the synthesis of ethyl amine from ethene and ammonia in an ozoniser according to BERTHELOT [5]; in a yield of 10 %.

In this paper we communicate some results obtained in experiments in which we reacted propene with hydrogen bromide, hydrogen chloride and water vapour in a glass ozoniser according to SIEMENS. The shape and size of the ozoniser are given in the figure; the voltage was applied in all experiments by a high tension transformer of 20000 V connected to a supply of alternating current of 220 V (50 cycles per second).



A = ozoniser according to SIEMENS; thickness of the wall of the glass tubes = 1.5 mm; inner diameter of the outer tube = 40 mm; distance between the inner and the outer tube = 2.5 mm; volume exposed to silent electrical discharges = 120 ml.

B and C = copper electrodes

D = aqueous solution of copper sulphate

E = water

### § 2. *Reaction of propene and hydrogen bromide*

When a gaseous mixture of propene and a slight excess of hydrogen bromide was passed through the ozoniser at room temperature, 1-bromopropane was formed as the only reaction product in a yield of 100 %. In this reaction an induction period of some minutes was observed. After that the gas current could be accelerated up to a rate of 0.25 l/min (residence time of the gas mixture = 30 sec. See the table, Exp. 1), while the addition reaction continued to be a quantitative process.

When the experiment was carried out at an elevated temperature, 1-bromopropane was obtained in a lower yield. Together with this addition product a higher boiling liquid was formed and a quantity of partially unsaturated gaseous products could be captured. (See the table, Exp. 2).

The data given above make it probable that the formation of 1-bromopropane in the ozoniser proceeds according to a mechanism which corresponds to the photochemical reaction of propene and hydrogen bromide described in the introduction.

### § 3. *Reaction of propene and water*

We have studied the reaction of propene and water only at an elevated temperature (80°–90°) as we wished the reaction to proceed in the gas phase. Our first experiments were carried out at reduced pressure (see the table, Exp. 3). So we could investigate only the reaction products which condensed in the acceptor connected to the ozoniser. A complicated mixture was formed. When it was subjected to fractional distillation the following substances were successively isolated: propanal, propanol-2, propanol-1, a hexanol fraction (boiling range: 140–150°,  $n_D^{20} = 1.423$ ) and a small quantity of a higher boiling liquid.

In collaboration with S. HERZBERG we have shown that the hexanol fraction consisted chiefly of 2,3-dimethylbutanol-1, for the liquid could be converted into a 3,5-dinitrobenzoate (m.p. 52.5–53.5°) and an acid 3-nitrophthalate (m.p. 167–168°) which compounds gave no depression of the melting point when mixed with the corresponding esters of 2,3-dimethylbutanol-1 (boiling range: 143–146°,  $n_D^{20} = 1.420$ ) prepared according to GORSKI by reducing the ethyl ester of 2,3-dimethylbutyric acid [6].

In subsequent experiments the reaction of propene and water vapour was carried out at atmospheric pressure. It appeared that in this case the yield was improved when hydrogen was added as a diluent (see Exp. 4). In these experiments the gaseous products escaping from the ozoniser were collected. It was found, that a considerable quantity of propene had passed unchanged and that a mixture of alkane and alkyne was formed. The same liquid reaction products were present (in about the same ratio) as in the experiment at lower pressure.

Apart from the processes leading to the formation of the gaseous products (which we have not investigated in detail) two different reactions

*Reactions in the ozoniser connected to 20000 V transformer.*

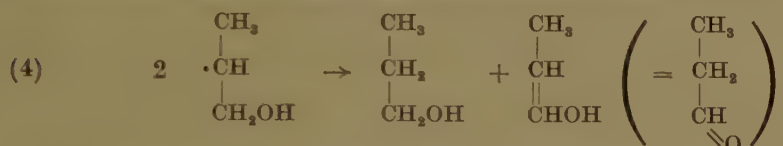
Exp.	Reaction of propene with	Temperature of thermostat	Pressure (atm)	Composition of reaction mixture	Residence time <sup>1)</sup> (sec)	Compounds isolated from the reaction product (quantities calc. on 1 mole of propene introduced)
1	hydrogen	20°	1	1 pr: 1.5HBr	30	1-bromopropane (100 %).
2	bromide	90°	1	1 pr: 1.5HBr	30	1-bromopropane (40–50 %), higher boiling liquid (25–30 g), gaseous compounds (4 l, partially unsaturated).
3	water	90°	0.65	1 pr: 6H <sub>2</sub> O	10–15	propanal (2–3 %), propanol-2 (1–2 %), propanol-1 (4–5 %), hexanol (9–10 %), higher boiling liquid (3–4 g).
4	vapour	90°	1	1 pr: 7H <sub>2</sub> O : 1H <sub>2</sub>	10	propanal (2–3 %), propanol-2 (1–2 %), propanol-1 (3 %), hexanol (8 %), gas mixture containing i.a. unsaturated hydrocarbons (alkene + alkyn (70–75 %)) and alkanes (10–15 %).
5	hydrogen chloride	0°	1	1 pr: 4HCl	30	2 chloropropane (5–10 %), 1-chloropropane (0.5 %), chlorohexane + chloroalkene of the same b.p. (20 %), dichlorohexane (> 20 %), higher boiling liquid (2–3 g), gas mixture containing alkene, alkyn and alkane.
6		90°	1	1 pr: 4HCl	30	2-chloropropane (15–20 %), 1-chloropropane (3 %), higher boiling liquid (about the same quantity as in Exp. 5), gas mixture (as in Exp. 5).
7		80°	1	1 pr: 7HCl : 1HBr	30	1-chloropropane (20–25 %), 1-bromopropane (15–20 %), higher boiling liquid (55–60 g), gas mixture (20–25 l, partially unsaturated).

<sup>1)</sup> Residence time = the period during which the gas mixture introduced into the ozoniser would have been exposed to electrical discharges if it had passed the reaction space unchanged  $\left( = \frac{\text{volume of the ozoniser}}{\text{volume of gas introduced/sec}} \right)$ .

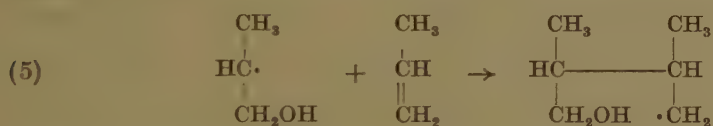


can be distinguished here: an addition reaction according to MARKOWNIKOFF and the formation of the substances in which oxygen is bound to a primary carbon atom. It seems probable that the latter starts with the dissociation of water into hydroxyl and hydrogen, followed by the addition of hydroxyl to a propene molecule. The 1-hydroxypropyl radical formed cannot remove a hydrogen atom from a water molecule and so a chain reaction — as in the addition of hydrogen bromide — fails to occur. The radical can be converted, however, in a slower reaction e.g. with a propene molecule or a second 1-hydroxypropyl radical.

Propanol-1 may originate from the reaction of the two radicals; together with the primary alcohol the aldehyde is formed:



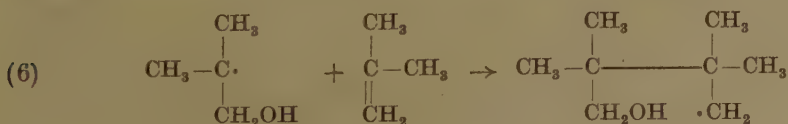
The hexanol may result from the reaction of the radical with a propene molecule. According to (5) a hydroxyhexyl radical is formed which is converted into 2,3-dimethylbutanol-1, taking possession of hydrogen in some way.



It is remarkable that in this reaction the *secondary* carbon atoms of hydroxypropyl and propene are linked together.

A similar coupling process was observed in collaboration with C. JOUWERSMA when isobutene was reacted with water vapour in the ozoniser. A liquid reaction product was formed which contained together with 2-methylpropanol-2, 2-methylpropanol-1 and 2-methylpropanal, an octanol. This octanol has been converted into a 3,5-dinitrobenzoate (m.p. 87.5–89°) and this ester could be identified as the dinitrobenzoate of 2,2,3,3-tetramethylbutanol-1 by mixed melting point determination with a specimen of this substance synthesised according to WHITMORE, MARKER and PLAMBECK [7] from 2,2,3,3-tetramethylbutane.

The octanol may originate from the addition of a 1-hydroxy-2-methylisopropyl radical (formed by addition of hydroxyl to isobutene) to a second isobutene molecule according to equation (6). In this reaction the tertiary carbon atoms of the radical and the alkene-molecule are linked together.



#### § 4. *Reaction of propene and hydrogen chloride*

The reaction of propene and hydrogen chloride in the ozoniser has been investigated at 0° and 90° (see the table, Exp. 5 and 6). It appeared that the course of this process corresponded in several respects to that of the reaction of propene and water vapour. Again a complicated reaction mixture consisting of a liquid and gaseous compounds was formed. It contained, together with the secondary propane derivative, a small quantity of the primary compound and as the main product a higher boiling liquid; the gaseous hydrocarbons were belonging to the series of alkanes, alkenes (= for the greater part unchanged propene) and alkynes.

While the last mentioned constituents of the reaction mixture have not yet been studied fully, we have obtained some results on the composition of the high boiling liquid formed at 0° (in collaboration with L. BRAVENBOER and J. D. BIJLOO (Wageningen)). We found that this liquid could be separated by fractional distillation chiefly into two fractions (boiling ranges: 110–125° and 175–185°,  $n_D^{20}$  respectively = 1.425 and 1.458. The first fraction was partially unsaturated. Analysis showed that it consisted probably of a chlorohexane together with an unsaturated chloro compound (Found: C = 60.3 %, H = 10.2 %, Cl = 30.0 %; calc. for  $C_6H_{13}Cl$ : C = 59.7 %, H = 10.8 %, Cl = 29.5 %). When the fraction was brominated, the chlorohexane could be isolated from it by distillation. The structure of the chlorohexane was established by converting it into a hexanol via the acetate. It appeared that the 3,5-dinitrobenzoate and the acid 3-nitrophtalate of this alcohol were identical with the esters of the hexanol formed in the reaction of propene and water. Therefore the chlorohexane is 1-chloro-2,3-dimethylbutane. The second fraction appeared from its analysis to be a dichlorohexane (Found: C = 47.0 %, H = 7.8 %; calc. for  $C_6H_{12}Cl_2$ : C = 46.5 %, H = 7.9 %).

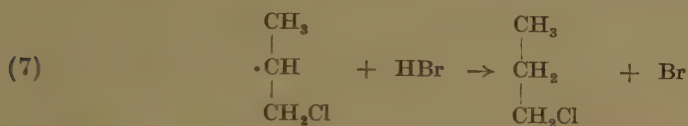
Awaiting the result of the determination of the structure of the dichlorohexane, it can be stated already that also in the reaction of propene with hydrogen chloride a considerable quantity of primary alkane derivatives is formed. It seems likely that the series of reactions leading to these compounds starts with the dissociation of hydrogen chloride and the addition of chlorine to propene. The 1-chloropropyl radical thus formed is converted only to a slight degree into 1-chloropropane. It reacts chiefly with propene (or perhaps with a second radical) so that hexane derivatives are formed.

Our supposition that the 1-chloropropyl radical is present in the ozoniser as an intermediate is affirmed in a series of experiments (in collaboration with J. TH. DRILLING) in which hydrogen bromide was added to the mixture of propene and hydrogen chloride (see Exp. 7 as an example). When a mixture of propene, hydrogen chloride and hydrogen bromide in the molar ratio 1 : 7 : 1 is passed through the ozoniser, a considerable amount of 1-chloropropane together with 1-bromopropane is formed while 2-chloropropane has disappeared completely from the

reaction product. The series of experiments given in the table below shows the gradual change of the composition of the reaction mixture when hydrogen bromide is added in increasing quantity.

Gas mixture introduced			Reaction product		
HBr : HCl : C <sub>3</sub> H <sub>6</sub>			2-chloro-propane	1-chloro-propane	1-bromo-propane higher boiling liquid
0 : 4 : 1			15—20 %	3 %	— 30 g
0.06 : 4 : 1			5—10 %	5—10 %	0.5 % 35 g
0.25 : 4 : 1			0.5 %	15—20 %	3.5 % 30—35 g
1 : 7 : 1			0 %	20—25 %	15—20 % 55—60 g

Thus the formation of 1-chloropropane may result from the conversion of the chloropropyl radical by hydrogen bromide acting as a hydrogen donor:



#### § 5. Survey of results obtained

It was found that propene reacts easily in the ozoniser with hydrogen compounds such as hydrogen bromide, hydrogen chloride and water.

The most simple process is the reaction of propene and hydrogen bromide. According to a chain reaction 1-bromopropane is formed; 2-bromopropane could not be detected in the reaction product. The lacking of the secondary addition compound was also observed in the reaction of propene and hydrogen sulphide at room temperature in the ozoniser. In a preliminary experiment it was found that only the primary thiol was formed, though in a poor yield, together with higher boiling compounds.

The more stable substances such as hydrogen chloride, water and also ammonia, which possess larger bond energies than the energy of the H-C-bond, differ in their behaviour from the hydrogen compounds just mentioned. They act on propene in several ways at the same time. Firstly a normal addition reaction proceeds. Under comparable conditions (90°, residence time 30 sec, excess of the hydrogen compound) 15—20 % 2-chloropropane and 2—5 % propanol-2 were formed, while in a preliminary experiment 10—15 % 2-aminopropane (together with < 0.5 % 1-aminopropane and some higher boiling liquid) was obtained from the reaction of ammonia and propene. Secondly some reactions occur side by side, probably starting with the dissociation of the hydrogen compounds and the reaction of the radicals so obtained on propene. In the

case of water as well as hydrogen chloride this initial process is more important than the normal addition reaction. The 1-chloro- and 1-hydroxypropyl radicals are converted into stable molecules (primary derivatives of propane and 2,3-dimethylbutane). It seems that the chloropropyl radicals are chiefly converted into branched hexane derivatives; in the conversion of hydroxypropyl disproportionation into derivatives of propane moreover acts a part.

The investigation is being continued.

We wish to express our thanks to the Management of the Koninklijke/Shell Laboratory Amsterdam, for enabling us to carry out this investigation and to Dr J. OVERHOFF for stimulating this study.

*Wageningen, May 1951.*

#### B I B L I O G R A P H Y

1. VAUGHAN, W. E., F. F. RUST and TH. W. EVANS, *J. Org. Chem.* **7**, 477 (1942).
2. PAULING, L., *The Nature of the Chemical Bond* p. 53 (1945).
3. See the survey of chemical reactions in electrical discharges given by G. GLOCKLER and S. C. LIND (*The Electrochemistry of gases and other dielectrics* (1939)) and also C. L. THOMAS, G. EGLOFF and J. C. MORRELL, *Reactions of Hydrocarbons in Electrical Discharges*, *Chem. Rev.* **28**, 1 (1941).
4. LOSANITSCH, S. M., *Ber.* **40**, 4656 (1907); *ibidem* **41**, 2683 (1908); *Bulet. Socet de Stiinte din Bucuresti* **22**, 5 and *Chem. Zentr.* **1913** II, 754.
5. FRANCESCONI, L. and A. CIURLO, *Gazz. chim.* **53**, 598 (1923).
6. GORSKI, A., *J. Russ. Phys. Chem. Ges.* **45**, 168 (1913); *Chem. Zentr.* **1913** I, 2022.
7. WHITMORE, F. C., R. E. MARKER and L. PLAMBECK Jr., *J. Am. Chem. Soc.* **63**, 1626 (1941).



## PHYSICS

### EXPERIMENTAL DETERMINATION OF LONG-RANGE ATTRACTIVE FORCES

(Provisional communication)

BY

J. TH. G. OVERBEEK AND M. J. SPARNAAY

(*van 't Hoff Laboratory, University of Utrecht*)

(Communicated by Dr E. J. W. VERWEY at the meeting of June 30, 1951)

Several phenomena, among them the flocculation of hydrophobic colloids <sup>1)</sup>, point to the existence of long-range attractive forces. These attractive forces, which may be interpreted as LONDON-VAN DER WAALS forces, have now been measured between objects of macroscopic dimensions.

For the force between two parallel flat plates DE BOER <sup>2)</sup> and HAMAKER <sup>3)</sup> obtain:

$$(1) \quad F = \frac{A}{6\pi d^3}$$

where  $F$  = the force in dynes/cm<sup>2</sup>,  $d$  = the distance between the plates in cm,  $A = \pi^2 q^2 \lambda$ ,  $\pi = 3.141\dots$ ,  $q$  = number of atoms per cm<sup>3</sup> and  $\lambda$  is the LONDON-VAN DER WAALS constant. For solid substances  $A$  is expected to be of the order of  $10^{-13} - 10^{-11}$  dynes.cm.

#### *Experiments*

In our experiments two highly polished glass plates (refr. ind. D line 1.5209;  $d_{15^\circ} = 2.556$ ) were very carefully adjusted over a surface of the order of 1 cm<sup>2</sup> at distances varying from 6000 to 15000 Å. NEWTON rings in white light were used to estimate the parallelism and the distance between the plates. One of the plates was attached to a rather stiff spring. The force  $F$  was obtained by determining the bending of this spring by an electrical capacity method capable of measuring the bending with an accuracy of 12 Å. In order to diminish the viscosity of the air and to remove water vapour the system was placed in a vacuum of 0.04 mm Hg. Dust particles and gel-layers formed in a wet atmosphere were the major causes of difficulties in the experiments.

In the following table some of our results are given. The values have been reproduced several times during a period of approximately one year.

---

<sup>1)</sup> E. J. W. VERWEY and J. TH. G. OVERBEEK, Theory of the stability of lyophobic colloids, Chapter 6 (Elsevier, Amsterdam 1948).

<sup>2)</sup> J. H. DE BOER, Trans. Faraday Soc., **32**, 21 (1936).

<sup>3)</sup> H. C. HAMAKER, Physica, **4**, 1058 (1937).

TABLE

Force  $F$  between parallel glass plates at a distance  $d$ , and the LONDON—VAN DER WAALS constant  $A$  calculated with eq (1).

$d$ in Å	$F$ in dynes/cm <sup>2</sup>	$A$ in dynes.cm
$\sim 200$	7500—150000	$0.11 - 2.3 \times 10^{-11}$
6000	3.5 — 8.5	$1.4 - 3.5 \times 10^{-11}$
8000	1.8 — 3	$1.7 - 2.9 \times 10^{-11}$
10000	0.8 — 1.5	$1.5 - 2.8 \times 10^{-11}$
12000	0.25 — 1	$0.8 - 3.3 \times 10^{-11}$
15000	0.15 — 0.3	$1.0 - 1.9 \times 10^{-11}$

In the range from 6000—15000 Å the glass plates were completely free from one another. The distance between them could be changed continuously. At 200 Å a strong cohesion existed and a different measuring technique had to be used, in which the force necessary to draw the plates suddenly apart was measured. The difficulty in measuring these small distances with precision explains the wide spread in the values of the force.

### Conclusion

Attractive forces of the expected order of magnitude exist, although the force constant  $A$  is somewhat larger than expected. This might be due to a certain roughness of the plates, which would tend to make the force larger than corresponds to the average distance measured.

It seems very unlikely that electrostatic effects are responsible for our results. Electrostatic forces would be expected to depend only slightly upon the distance, and very strongly upon the treatment of the glass plates, whereas the reverse was found to be the case.

Moreover the air inside the measuring apparatus was made conducting by the presence of a radioactive preparation.

The investigations are being continued.

THEORETICAL AND EXPERIMENTAL AVERAGES OF  
TURBULENT FUNCTIONS

BY

J. KAMPÉ DE FÉRIET <sup>1)</sup> AND R. BETCHOV*(Institute for Fluid Dynamics and Applied Mathematics, University of Maryland)**(Communicated by Prof. J. M. BURGERS at the meeting of September 29, 1951)*1. *Introduction*

One of the accepted bases for the study of turbulent flows is the system of equations given by O. REYNOLDS in 1895 [11]. As is well known, REYNOLDS assumed that the motion of a viscous incompressible fluid satisfies the NAVIER-STOKES equations, but the flow being much too complicated for a complete knowledge of all small details, one must replace the true value of all the functions involved (3 components of the velocity and the pressure) by mean values or averages.

The notion of mean value is very old in mathematics and physics, but usually one takes for the mean value of a function some constant quantity. The new idea of REYNOLDS was to introduce for the mean value of a function  $f(x, y, z, t)$  a new function  $\bar{f}(x, y, z, t)$  called the mean value of  $f$  and still depending on some or all variables. For instance, for the turbulent flow in pipes, one speaks of the "profile" of the mean velocities  $\bar{u}, \bar{v}, \bar{w}$  and in meteorology, one studies the mean velocity of the wind as a function of the altitude, etc.

Once these mean values have been introduced, it is logical to define the corresponding fluctuations by the relation:

$$(1) \quad f'(x, y, z, t) = f(x, y, z, t) - \bar{f}(x, y, z, t).$$

To obtain new equations containing only mean values REYNOLDS used certain rules of computation. The senior author of this note has proved [5] that these rules are based on the following set of assumptions, which we will call for brevity: "Reynolds' axioms":

$$(2) \quad \left\{ \begin{array}{l} R\ 1 \quad \overline{\bar{f} + g} = \bar{\bar{f}} + \bar{g}, \\ R\ 2 \quad \overline{a\bar{f}} = a\bar{\bar{f}}, \text{ } a \text{ being a constant,} \\ R\ 3 \quad \overline{\bar{f}g} = \bar{\bar{f}}\bar{g}, \\ R\ 4 \quad \overline{\text{Lim } f_n} = \text{Lim } \bar{f}_n \text{ for some convenient definition of the} \\ \quad \quad \quad \text{limiting process.} \end{array} \right.$$

---

<sup>1)</sup> Visiting Research Professor from the University of Lille.

The axioms  $R\ 1$  and  $R\ 2$  are obvious, and a special consequence of  $R\ 3$ , if  $g = 1$  is:

$$(3) \quad \overline{\overline{f}} = \overline{f},$$

from which we obtain:

$$(4) \quad \overline{f'} = \overline{f} - \overline{\overline{f}} = 0.$$

The axiom  $R\ 4$  is necessary to replace the mean value of a partial derivative by the partial derivative of the mean value.

If any one of those four axioms is not satisfied, the equations of REYNOLDS are no longer a logical consequence of the NAVIER-STOKES equations for a viscous incompressible fluid; and it is not at all easy to find all the possible definitions of mean values compatible with the four axioms. This problem of definition of averages has two completely different aspects:

a) the first one, purely mathematical, is concerned with a constructive definition of the averaging process satisfying the REYNOLDS axioms for a given class of functions,

b) the second one, purely experimental, is to prove that every result of measurements, interpreted as a mean value or as a fluctuation, has been obtained by a process compatible with the four axioms.

## 2. The theoretical approach

The difficulties arising with the definition of an averaged quantity were pointed out first by C. W. OSEEN in 1930 [10] and we should also mention the interesting contribution by BURGERS and ISAKSON [4]. But it was not really possible to understand the full meaning of this problem till it was written in a general abstract form [6] and [7]; it appeared then as a problem of abstract algebra.

Let us consider a set  $X$  and a set of functions defined for every  $x \in X$  and taking values in some field  $F$ . We will consider this set of functions as a topological ring  $R$ , that is a set in which three operations are defined: an *addition*, symbolized by  $f + g$ , commutative, for which the set is an abelian group;

a *scalar multiplication*, symbolized by  $af$  with  $a$  belonging to the field  $F$ ; a *product* symbolized by  $f \cdot g$ , distributive for the addition and the scalar multiplication.

We will also suppose that the ring  $R$  contains functions 0 and 1 with the properties that  $f + 0 = f$  and  $f \cdot 1 = f$ ; moreover, according to the topology existing in  $R$  we will represent by  $N(f)$  a neighborhood of  $f$ .

Then the problem of finding a convenient definition of mean values can be stated as follows:



"Find a transformation of the ring  $R$  into itself, that is define for every  $f \in R$  a transform  $Tf$  with  $Tf \in R$  having the following properties:

$$(5) \quad \left\{ \begin{array}{l} R1 \quad T(f + g) = Tf + Tg, \\ R2 \quad T(\alpha f) = \alpha Tf, \text{ if } f = 1, \\ R3 \quad T(fTg) = Tf \cdot Tg, \\ R4 \quad \text{If } g \in N(f) \text{ then } Tg \in N(Tf)'' \end{array} \right.$$

The solution of the elementary case, where all the functions  $f$  take on only a finite number of values (the same for all functions of  $R$ ), was given in [7] and the more refined case where all the functions could take a finite number of values, this number being not bounded for the whole ring, was solved in [8]. In this case a partition  $\Pi(f)$  of the set  $X$  corresponds to every function  $f(x)$  belonging to  $R$ , partition in a finite number of subsets such that  $f$  is constant over each subset. The solution can be summarized in the following way:

"To every REYNOLDS transformation  $T$  corresponds a partition  $\theta_T$ , finite or not, of the set  $X$  and, if we call  $\theta(f)$  the finest partition containing  $\Pi(f)$  and  $\theta_T$ , then  $Tf$  takes constant values over every set of the finite partition  $\theta(f)$ ."

A much more difficult case was solved by GARRETT BIRKHOFF [1] for the case that  $R$  is the ring of all continuous functions on a compact set. A very interesting contribution was also given by J. SOPKA [12].

There are still many interesting questions connected with the abstract algebraic problem posed by REYNOLDS axioms, but actually, one has already a general idea of the definition of mean values, in agreement with the axioms, for some of the most important classes of functions.

### 3. The experimental approach

The experimental physicist is limited to the use of a small number of sensitive instruments, and he cannot always use a convenient averaging process. Usually he is only able to measure  $f(x, y, z, t)$  at a fixed point in the turbulent flow as, for example, with a Pitot tube or a hot-wire anemometer; and we shall consider that the functions to be averaged depend only on the time. To him, these functions  $f(t)$  appear to belong to a class introduced by NORBERT WIENER [13], that is the class of functions such that

$$(6) \quad \lim_{T \rightarrow \infty} \frac{1}{2T} \int_{-T}^{+T} [f(t)]^2 dt \quad \text{exists.}$$

More precisely, this class is the set of all complex-valued functions<sup>1)</sup> defined for  $-\infty < t < +\infty$  and satisfying the three conditions:

<sup>1)</sup> The \* will represent the complex conjugate quantity.

- H1  $f(t) \in L^2(a; b)$  for every finite interval  $(a, b)$ ,  
 H2 for every real  $h$  the limit  $\varrho(h)$  exists such that

$$(7) \quad \varrho(h) = \lim_{T \rightarrow \infty} \frac{1}{2T} \int_{-T}^{+T} f(t+h) f^*(t) dt,$$

H3  $\varrho(h)$  is continuous for  $h = 0$  which implies that it is uniformly continuous for every  $h$ .

This function  $\varrho(h)$  is called "autocorrelation" of  $f(t)$ .

In general, the functions belonging to the Wiener class are not square integrable in the whole interval  $-\infty$  to  $+\infty$  and it is impossible to apply an ordinary Fourier transformation. The figure 1 represents such a function and the cases  $f = \text{constant}$  or  $f = \sin \omega t$  are more trivial examples.

To avoid the difficulty introduced by infinite intervals we consider "truncated" functions as illustrated in figure 2, such that

$$(8) \quad \begin{cases} f_T(t) = f(t), & \text{if } |t| \leq T; \\ f_T(t) = 0, & \text{if } |t| \geq T. \end{cases}$$

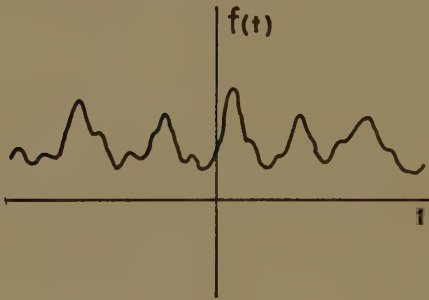


Fig. 1  
Turbulent function

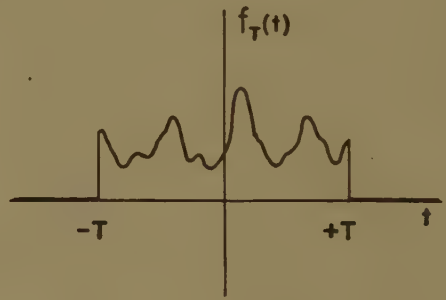


Fig. 2  
Truncated function

Evidently,  $f_T$  is square integrable for finite  $T$  and tends towards  $f$  if  $T \rightarrow \infty$ . Let us now introduce the Fourier transform  $a_T(\lambda)$  of  $f_T(t)$  and the spectral density  $s_T(\lambda)$  defined by

$$(9) \quad a_T(\lambda) = \frac{1}{\sqrt{2\pi}} \int_{-\infty}^{+\infty} f_T(t) e^{i\lambda t} dt,$$

$$(10) \quad s_T(\lambda) = \frac{1}{2T} |a_T(\lambda)|^2.$$

Then we have

$$(11) \quad \int_{-\infty}^{+\infty} s_T(\lambda) d\lambda = \frac{1}{2T} \int_{-T}^{+T} |f(t)|^2 dt.$$

It is interesting to note that, not only from the theoretical point of view as shown in [9] but also for practical applications, it is very

convenient to approximate the autocorrelation  $\varrho(h)$  by the autocorrelation  $\varrho_T(h)$  of the truncated function  $f_T$

$$(12) \quad \varrho_T(h) = \frac{1}{2T} \int_{-T+\frac{|h|}{2}}^{T-\frac{|h|}{2}} f\left(t+\frac{h}{2}\right) f^*\left(t-\frac{h}{2}\right) dt, \quad \text{if } |h| < 2T;$$

$$\varrho_T(h) = 0, \quad \text{if } |h| \geq 2T.$$

One has still (see (7))

$$(13) \quad \varrho(h) = \lim_{T \rightarrow \infty} \varrho_T(h);$$

but for numerical computations, this method reduces by 50 % the number of operations. Moreover, the spectral density  $s_T(\lambda)$  can be directly computed from  $\varrho_T(h)$  by

$$(14) \quad s_T(\lambda) = \frac{1}{2\pi} \int_{-2T}^{+2T} e^{-i\lambda h} \varrho_T(h) dh.$$

A fundamental fact is that, if  $T$  tends towards infinity and  $f_T$  towards  $f$ ,  $s_T(\lambda)$  does not in general tend toward a limit, but its integral does. One can define a function  $S(\lambda)$  by

$$(15) \quad S(\lambda) = \lim_{T \rightarrow \infty} \int_{-\infty}^{\lambda} s_T(\zeta) d\zeta.$$

This function  $S(\lambda)$  is real, non-decreasing, and corresponds to the superposition of a normal band spectrum, and of a line spectrum, the set of lines being void, finite, or at most countable. A general expression for  $S(\lambda)$  is

$$(16) \quad S(\lambda) = \int_{-\infty}^{\lambda} s(\lambda) d\lambda + \sum_1^{\infty} A_n \sigma(\lambda - \lambda_n),$$

where

$$(17) \quad \begin{cases} \sigma(\lambda) = 0, & \text{if } \lambda \leq 0; \\ \sigma(\lambda) = 1, & \text{if } \lambda > 0. \end{cases}$$

This function  $S(\lambda)$  was called by N. WIENER "energy spectrum" or "periodogram" and it is related to the autocorrelation of  $f(t)$  by the relation

$$(18) \quad \varrho(h) = \int_{-\infty}^{+\infty} e^{i\lambda h} dS(\lambda),$$

where the use of a Stieltjes integral is necessary if lines are present in the spectrum. For  $h = 0$  we have

$$(19) \quad \varrho(0) = \lim_{T \rightarrow \infty} \frac{1}{2T} \int_{-T}^{+T} |f(t)|^2 dt = \int_{-\infty}^{+\infty} dS(\lambda),$$

which justifies the name "energy spectrum" for  $S(\lambda)$ , if we call "energy" of  $f(t)$  the limit considered in (6) (this terminology is quite natural if  $f$  is a velocity). The contribution to the "energy" of the function having wave numbers in the interval  $\mu_1 \leq \lambda \leq \mu_2$  is given by

$$(20) \quad \int_{\mu_1}^{\mu_2} dS(\lambda).$$

When it will be necessary to stress that  $S(\lambda)$  corresponds to a particular function  $f$  we shall write  $S(\lambda|f)$ .

In experimental research we never operate with the function  $f$  itself, or even with truncated functions, but we obtain from  $f$ , by applying some operator, new functions which we call "mean value", "fluctuation", or "spectral density" and which we compare to theoretical expressions. Our purpose here is to focus attention on some aspects of this problem and to clarify certain definitions.

For instance, in order to obtain a mean value of some function  $f(t)$ , various processes are used, all equivalent to a low-pass filter. This operation in its simplest form (see J. M. BURGERS and R. BETCHOV [2] and R. M. FANO [3]) is equivalent to the following definition of  $\bar{f}(t)$

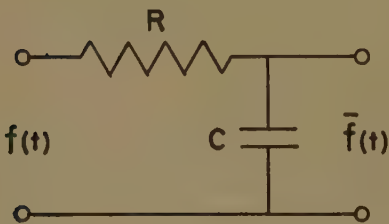
$$(21) \quad \tau \frac{d\bar{f}(t)}{dt} + \bar{f}(t) = f(t),$$

where  $\tau$  is a constant, with the dimension of time. If  $f(t)$  is the difference of electrical potential across a hot-wire anemometer, one may apply it to the network of figure 3 in order to obtain the averaged quantity  $\bar{f}(t)$ . More often a network of the type illustrated in figure 4 is used in order to obtain a fluctuation  $f'(t)$  such that

$$(22) \quad \tau \frac{df'(t)}{dt} + f'(t) = \tau \frac{df(t)}{dt},$$

and this is fully equivalent to our definition of  $\bar{f}$  (21) if we suppose

$$(23) \quad \bar{f}(t) = f(t) - f'(t).$$



$$T = RC$$

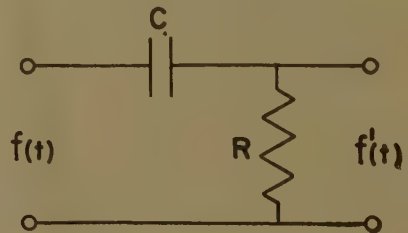


Fig. 3

Definition of a mean value

Fig. 4

Definition of a fluctuation



It is convenient to write the definition of  $\bar{f}$  as follows:

$$(24) \quad \tau \frac{d}{dt} (e^{t/\tau} \bar{f}) = e^{t/\tau} f;$$

and, by integration, we obtain

$$(25) \quad \bar{f}(t) = A e^{\frac{t_0 - t}{\tau}} + \frac{1}{\tau} \int_{t_0}^t e^{\frac{s-t}{\tau}} f(s) ds.$$

Let us suppose that for  $t_0 \rightarrow -\infty$ ,  $A$  is finite; then we have

$$(26) \quad \bar{f}(t) = \frac{1}{\tau} \int_{-\infty}^t e^{\frac{s-t}{\tau}} f(s) ds.$$

This supposition on the initial value of  $\bar{f}(t)$  means that we observe  $\bar{f}(t)$  after a time long enough to eliminate the usual transients.

We see that our definition of  $\bar{f}$  is of the following general type:

$$(27) \quad \bar{f}(t) = \int_{-\infty}^{+\infty} K(t-s) f(s) ds,$$

where  $K$  is a kernel such that

$$(28) \quad \begin{cases} K(\xi) = \frac{1}{\tau} e^{-\xi/\tau}, & \text{if } \xi \leq 0; \\ K(\xi) = 0 & \text{if } \xi > 0. \end{cases}$$

More intricate networks could be used to define  $\bar{f}$  or many other functions or mechanical processes could serve the same purpose, but most of them will be equivalent to some kernel  $K(t-s)$  similar to the one defined. In other words, the experimental definition of the mean value  $\bar{f}$  is a particular case of a functional operator which transforms every function  $f$  (belonging to some given class of functions) into another function  $Tf$  given by

$$(29) \quad Tf = \int_{-\infty}^{+\infty} K(t-s) f(s) ds.$$

For such transforms  $Tf$ , N. WIENER has proved an important result [13]: if  $S(\lambda|f)$  is the energy spectrum of  $f$  according to (15) and if  $S(\lambda|Tf)$  is the energy spectrum of  $Tf$ , then

$$(30) \quad S(\lambda|Tf) = \int_{-\infty}^{\lambda} \varphi(\mu) dS(\mu|f),$$

where  $\varphi(\mu)$  is related to  $K$  by

$$(31) \quad \varphi(\mu) = \left| \int_{-\infty}^{+\infty} K(\xi) e^{i\mu\xi} d\xi \right|^2.$$

For the validity of this last equation, we have only to assume that  $\xi K(\xi)$  belongs to  $L(-\infty; +\infty)$  and to  $L^2(-\infty; +\infty)$ .

In the case where  $f$  is a turbulent quantity, our definition of  $\bar{f}$  must satisfy the REYNOLDS' axioms. The comparison of (2) and (26) shows that all are satisfied, but the third one, that is,

$$(32) \quad \overline{\bar{f}g} \neq \bar{f}\bar{g}$$

If we consider the particular and essential case  $g = 1$ , we have

$$(33) \quad \bar{f}' = \bar{f} - \bar{\bar{f}} \neq 0$$

This is a defect in our definition of  $\bar{f}(t)$  by a kernel, or in other words, by a physical apparatus such as an anemometer. This point needs careful examination.

For the energy distribution of the function  $\bar{f}$  we have, according to WIENER'S formula (30) and to our particular kernel (28)

$$(34) \quad S(\lambda|\bar{f}) = \int_{-\infty}^{\lambda} \frac{1}{1+\mu^2\tau^2} dS(\mu|f).$$

On the other side, for  $\bar{\bar{f}}(t)$ , one obtains easily

$$(35) \quad \tau^2 \frac{d^2}{dt^2} (e^{t/\tau} \bar{\bar{f}}) = \tau \frac{d}{dt} (e^{t/\tau} \bar{f}) = e^{t/\tau} f,$$

or

$$(36) \quad \bar{\bar{f}} = \frac{1}{\tau^2} \int_{-\infty}^t (t-s) e^{\frac{s-t}{\tau}} f(s) ds.$$

Whence, for  $\bar{f}'$  according to (33),

$$(37) \quad \bar{f}' = \frac{1}{\tau^2} \int_{-\infty}^t (s-t+\tau) e^{\frac{s-t}{\tau}} f(s) ds.$$

The energy spectrum of  $\bar{f}'(t)$  can now be obtained, by using WIENER'S formula (30) together with the kernel of (37) and the result is

$$(38) \quad S(\lambda|\bar{f}') = \int_{-\infty}^{\lambda} \frac{\mu^2 \tau^2}{(1+\mu^2 \tau^2)^2} dS(\mu|f).$$

From the shape of the curve  $y = x^2/(1+x^2)^2$  one sees immediately that the only important contribution to  $s(\lambda|\bar{f}')$  comes from small wave numbers of the order of magnitude of  $1/\tau$ . The function  $\bar{f}'$ , therefore, is not equal to zero for every  $t$  as required by the REYNOLDS' axioms, but we can say that these axioms are approximately satisfied if the major contributions to  $S(\lambda|f)$  are due to wave numbers such that  $|\lambda| \gg 1/\tau$ . Then  $\bar{f}'$  is negligible compared with  $f$ .

This supposition means also that the energy spectrum of  $\bar{f}(t)$ , except for the contribution at  $\lambda = 0$  is a small fraction of the energy spectrum of  $f$ .

This case is illustrated in figure 5 where we choose a particular form for  $S(\lambda|f)$ , which then determines the various other energy spectra shown. For comparison with the more usual notion of energy density, we represent by dotted lines the "derivatives" of the various energy spectra, although their existence is not always certain.

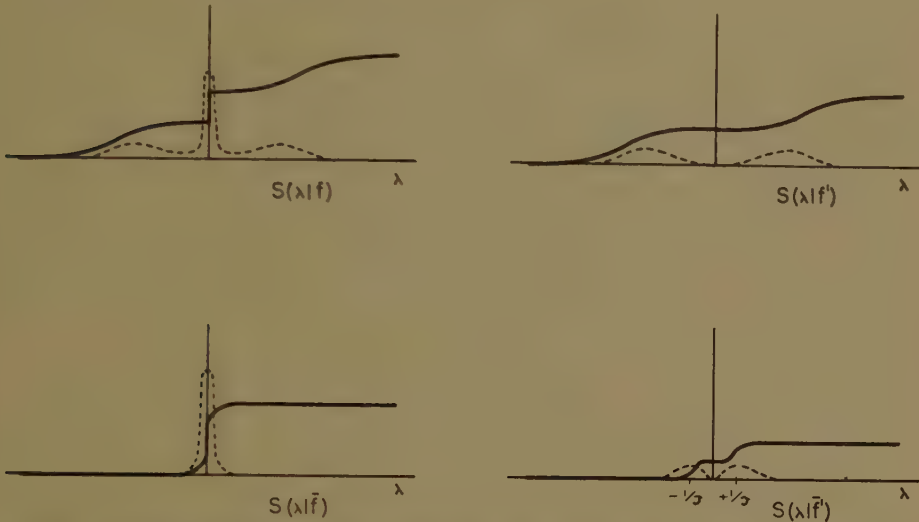


Fig. 5. Energy spectra of various spectra. The dotted lines are the analogues of energy densities.

As far as the function  $\bar{f}\bar{g} - \overline{\bar{f}g}$  is concerned, one can obtain the following formula

$$(39) \quad \bar{f}\bar{g} - \overline{\bar{f}g} = \iint_{-\infty}^{+\infty} \frac{i\lambda\tau e^{i(\lambda+\mu)t}}{(1+i\lambda\tau)(1+i\mu\tau)(1+i(\lambda+\mu)\tau)} dS(\lambda|f) dS(\mu|g),$$

and it is clear that similar assumptions about the energy spectra of  $f(t)$  or  $g(t)$  permit us to admit that the left member of (39) is negligible.

This means that the third axiom of REYNOLDS is approximately satisfied, if the energy of  $f(t)$  is principally due to wave numbers much larger than  $1/\tau$ ; or, if

$$(40) \quad S(+\infty|f) \gg S(+\infty|\bar{f}).$$

As an example of other transformed functions, we may mention the so-called "experimental energy density" obtained with some band-pass filters; it would be very desirable to study their properties together with their significance in fluid dynamics.

### Summary

The notion of averaged quantities as used in the dynamics of turbulent flows, is studied in this paper; axioms are stressed which must be satisfied by every averaging process.

One knows suitable definitions for some theoretical cases but in the

experimental investigation a definition of averaged quantities is used that does not satisfy exactly the axioms mentioned. In general the functions to be averaged are not square integrable, but it is possible to study this problem if they belong to a certain class introduced by N. WIENER; in the analysis one uses FOURIER-STIELTJES integrals.

### Résumé

Les quantités moyennes utilisées dans l'étude des fluides turbulents font ici l'objet d'une étude théorique qui dégage les axiomes auxquels doit satisfaire toute définition de quantité moyenne.

Dans certains cas théoriques, on sait définir des moyennes satisfaisantes, mais les travaux expérimentaux utilisent une définition de la moyenne qui ne vérifie pas exactement les axiomes mentionnés. Ces problèmes impliquent des fonctions de carré non intégrable, mais il est possible de les traiter si l'on se limite à une classe de fonctions introduite par N. WIENER et si l'on utilise les intégrales de FOURIER-STIELTJES.

### L I T E R A T U R E

1. BIRKHOFF, G., Moyennes des fonctions bornées. Colloque d'Algèbre et de théorie des Nombres. (Paris, Sept. 1949).
2. BURGERS, J. M. and R. BETCHOV, L'analyse spectrale de la turbulence and Spectral Analysis of an irregular Function, *Proceed. Kon. Nederl. Akad. van Wetensch.* **51**, (1948).
3. FANO, R. M., Short time autocorrelation function and power spectra. *Journal Acoustical Soc.* **22**, (Sept. 1950).
4. ISAKSON, A. A., (Exposé de J. M. BURGERS). 3me Congrès Int. Mec. Ap. Stockholm 18—21 (1930).
5. KAMPÉ DE FÉRIET, J., L'état actuel du problème de la turbulence *La Science Aérienne*. **3**, 9—34 (1934) et **4**, 12—52 (1935).
6. ———, La notion de moyenne dans les équations du mouvement turbulent d'un fluide. 6me Congrès Int. Mec. Ap. (Paris 1946).
7. ———, *Turbulencia*. Instituto Nacional de Tecnica Aeronautica Madrid (1949).
8. ———, Sur un Problème d'algèbre abstraite posé par la définition de la moyenne dans la théorie de la turbulence. *Annales Société Scientifique de Bruxelles, Série I*, **63**, 165 (1949).
9. ———, Sur l'analyse harmonique des fonctions à carré moyen fini. *Internat. Congress of Mathematicians*, (Cambridge, 1950).
10. OSEEN, C. W., Das Turbulenzproblem. 3me Congrès Int. Mec. Ap. Stockholm, **1**, 3—18 (1930).
11. REYNOLDS, O., On the dynamical theory of incompressible viscous fluids and the determination of the criterion. *Philos. Trans. R. Soc. A. T.* **186**, Partie I, 123—164 (1895).
12. SOPKA, J., On the Characterization of REYNOLDS' Operators on the Algebra of all continous Fonctions on a compact Hausdorf Space. (Thesis, Harvard, 1950).
13. WIENER, N., The Fourier integral and certain of its applications. (Cambridge, 1933).

J. KAMPÉ DE FÉRIET  
*Université de Lille and  
 University of Maryland*

R. BETCHOV  
*Institute for Fluid Dynamics & Applied  
 Mathematics, University of Maryland*



ELASTIC-VISCOUS SOAP SYSTEMS CONTAINING SALTS. XXa <sup>1)</sup>

*Comparison of the elastic behaviour of elastic-viscous systems of K-laurate, K-myristate, K-palmitate, K-stearate and K-oleate containing K<sub>2</sub>CO<sub>3</sub>*

BY

H. G. BUNGENBERG DE JONG, H. J. v. D. BERG, W. A. LOEVEN\* and  
W. W. H. WEYZEN\*) <sup>2)</sup> <sup>3)</sup>

(Communicated at the meeting of October 27, 1951)

1. *Introduction*

It is to be expected that in a future theory of the elastic-viscous soap systems the rôle played by the carbon chain of the soap will take a central place. In all previous parts of this series we investigated elastic-viscous systems of one soap only, namely oleate.

We have thus gained a thorough knowledge of the many parameters which have an influence on the elastic behaviour and are thus prepared to choose methods which seem adequate for a comparison of elastic-viscous systems of different soaps. We will compare elastic systems of K-laurate, K-myristate, K-palmitate, K-stearate and K-oleate, using K<sub>2</sub>CO<sub>3</sub> as the potassium salt which is added. In section 3 the comparison will be made at constant soap concentration. A more fundamental comparison follows in section 4, using methods based upon the results in Part XVII of this series.

2. *Methods*

For the experimental methods (completely filled spherical vessels, rotational oscillation, contrivance to excite the oscillation, electrolytic H<sub>2</sub> mark) we refer to preceding parts of this series. Compare e.g. section 2 in Part XIX. To increase

\*) Aided by grants from the "Netherlands Organization for Pure Research (Z.W.O.)."

<sup>1)</sup> The preceding parts of this series appeared under the title "Elastic-viscous oleate systems containing KCl". The title is changed into a more general form here. Part I has appeared in these Proceedings 51, 1197 (1948); Parts II—VI in these Proceedings 52, 15, 99, 363, 377, 465 (1949); Parts VII—XIV in these Proceedings 53, 7, 109, 233, 743, 759, 975, 1122, 1319 (1950); Parts XV—XIX in these Proceedings 54, Series B, 1, 240, 291, 303, 317 (1951).

<sup>2)</sup> Publication No. 19 of the Team for Fundamental Biochemical Research (under the direction of H. G. BUNGENBERG DE JONG, E. HAVINGA and H. L. BOOIJ).

<sup>3)</sup> A generous gift of reasonably pure preparations of lauric acid, myristic acid, palmitic acid, stearic acid and oleic acid from the Rockefeller Foundation provided the means for the experiments in this paper.

the accuracy of the measurements of the period, we used the means of 20 determinations of a number of consecutive periods. (if possible 10, but at larger damping 5 or a lower number).

We started from C. P. preparations from Eimer and Amend of stearic acid, palmitic acid, myristic acid, lauric acid and oleic acid. Stock solutions of the K-soaps were made by dissolving the acids in the equivalent amount of KOH. In all soap systems which were measured we provided for a concentration of 0.05 N. free KOH, which served to prevent hydrolysis. This precaution is necessary in order to obtain a simple behaviour of the soap systems as hydrolysis complicates matters considerably (compare Part XIII).

In order to further an economic use of the fatty acids the measurements were performed in 110 ml. vessels.

### 3. Experiments at constant soap concentration

In all experiments in this section, the soap concentration amounted to 40 millimoles/l. They were of two kinds:

a. the usual measurements of the period and of  $n$ , (the maximum number of turning points which is observable through the telescope ( $n$  is an approximate measure for  $1/\Delta$ , compare Part XV);

TABLE I

*Survey of the characteristic points from the measurements with 40 millimoles/l. systems of some potassium soaps*

Soap	Coacervation limit		Lower limit of the elastic systems		Minimum damping		Values of $n$ , $G$ and $\gamma G$ at the $K_2CO_3$ concentrations corresponding to the ones of minimum damping			
	$C_{K_2CO_3}$	Temp. $^{\circ}C.$	$C_{K_2CO_3}$	Temp. $^{\circ}C.$	$C_{K_2CO_3}$	Temp. $^{\circ}C.$	$n$	$G$	$\gamma G$	Mean $\gamma G$ at mean temp.
K-laurate	2.48	21.8	1.84	6.0	—	—	—	—	—	} 6.69 at 18.8° C
	—	—	1.93	8.8	2.18	8.7	3.9	44.7	6.69	
	—	—	1.98	11.8	2.15	11.8	1.5	—	—	
	—	—	(2.01)	15.0	2.10	15.0	(0.3)	—	—	
K-myristate	1.87	29.5	0.95	24.0	1.38	24.0	31.5	52.0	7.21	} 6.87 at 29.8° C
	1.82	35.5	1.02	29.8	1.36	29.8	20.0	48.8	6.99	
	1.76	45.5	1.03	35.5	1.34	35.5	7.5	41.2	6.42	
K-palmitate	1.18	45.2	0.40	40.0	(0.76)	40.0	(53.5)	48.9	6.99	} 6.89 at 47.3° C
	1.15	50.8	0.44	45.0	0.75	45.0	42.5	48.4	6.95	
	1.13	55.0	0.49	49.7	0.74	49.7	24.5	47.2	6.87	
	1.10	59.9	0.52	54.6	0.73	54.6	11.5	45.6	6.75	
K-stearate	0.775	60.	0.19	61.2	0.485	61.2	80	60.1	7.75	} 7.57 at 66.1° C
	0.75	65	0.21	65.3	0.475	65.3	50.5	57.6	7.59	
	0.715	69.9	0.24	71.8	0.455	71.8	31	54.2	7.36	
K-oleate	1.12	15	0.41	15	0.805	15	61.5	50.5	7.11	} 7.03 at 25.4° C
	1.08	25.5	0.45	25.5	0.775	25.5	43	50.1	7.08	
	1.06	35.6	0.48	35.6	0.735	35.6	20	47.7	6.91	

b. determination of the coacervation limit. Both kinds of investigations were performed at a few temperatures for each soap. Some characteristic data derived from these measurements have been collected in Table I. In fig. 1 we give for each soap at one temperature only the coacervate volume— $C_{K_2CO_3}$  curve, the  $n$ — $C_{K_2CO_3}$  curve and the  $G$ — $C_{K_2CO_3}$  curve.

It appears that the character of these curves is the same for all soaps. Just as with oleate the coacervate volume becomes 100 % (the coacervation limit) at the point where the right descending branch of the  $n$ -curve cuts the abscissa. Thus in general the coacervation limit is at the same time the limit to the right of the region of  $K_2CO_3$  concentrations in which elastic phenomena are observable.

Just as with oleate the  $n$ — $C_{K_2CO_3}$  curves are curves with a maximum. The  $G$ — $C_{K_2CO_3}$  curves have the same typical  $S$ -shape as with oleate and their inflexion points also coincide approximately with the maxima of the

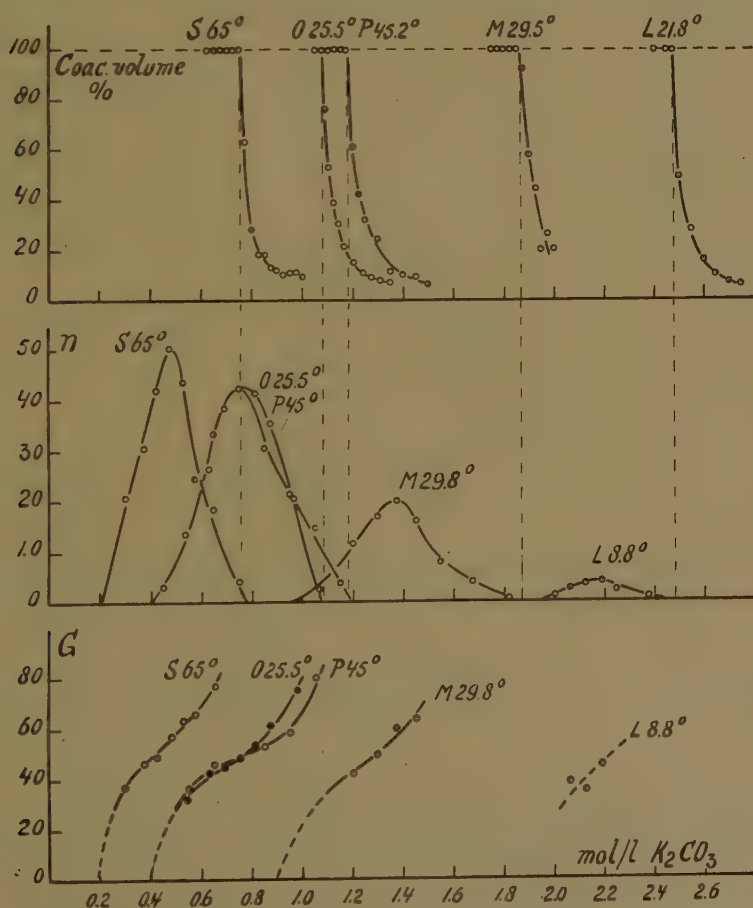


Fig. 1. Coacervate volume and elastic properties of 40 millimoles/l systems of K-stearate (S), K-oleate (O), K-palmitate (P), K-myristate (M), and K-laurate (L) as a function of the  $K_2CO_3$  concentration. Temperatures are given in centigrades.

$n$ - $C_{K_2CO_3}$  curves. Because of difficulties inherent with the laurate systems (see below) no reliable measurements of  $G$  could be obtained here, therefore the above mentioned phenomena could not be controlled with laurate, the position of its  $G$ - $C_{K_2CO_3}$  curve not being known here.

The influence of the temperature is also of equal nature for all soaps. Compare Table I, from which we see that at increase of the temperature the coacervation limit shifts somewhat into the direction of smaller  $K_2CO_3$  concentrations. This also occurs with the position of the maximum of the  $n$ -curve, whereas the left footpoint of the  $n$ -curve shifts into the opposite direction on increasing temperature. Therefore at increase of the temperature the region of  $K_2CO_3$  concentrations in which elastic phenomena are observable, contracts somewhat. Compare fig. 2, in which for each soap ( $S$  = stearate,  $O$  = oleate,  $P$  = palmitate,  $M$  = myristate,  $L$  = laurate) the coacervation limit (letters with suffix "coac"), the maximum of the  $n$ -curve (letters with suffix "max") and the left footpoint of the  $n$ -curve (letters with suffix "l.fpt.") have been given in a  $K_2CO_3$ -temperature diagram.

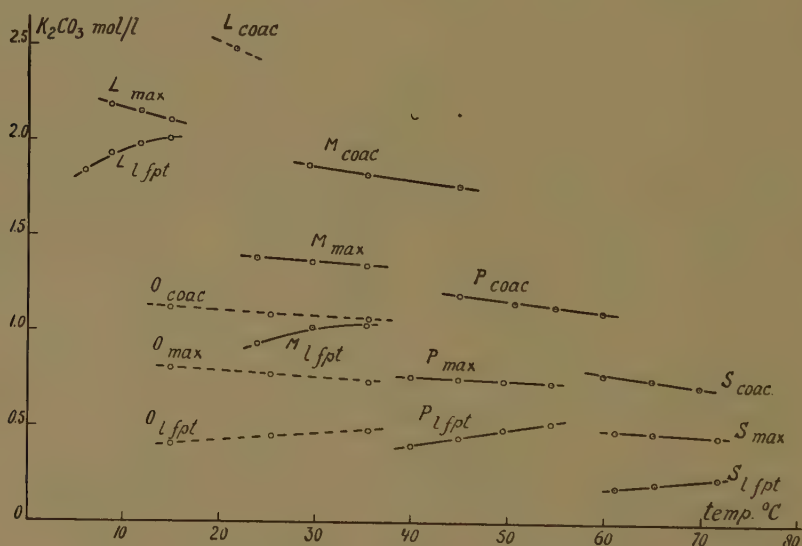


Fig. 2. Regions of temperatures and of  $K_2CO_3$  concentrations where measurements of the elastic properties of the different soaps are practicable. (Compare Table I).

Increase of the temperature causes the  $S$  shaped  $G$ - $C_{K_2CO_3}$  curve to take a steeper course and to lower the value of  $n$  at the maximum of the  $n$ -curve. (Compare for oleate, Part XIII). The latter of these effects limits the range of temperatures in which measurements of the elastic properties are practicable with a given soap. For if  $n$  becomes too low the accuracy of the measurement of the period decreases.

On the other hand we have (with exception perhaps of oleate) a lower limit of the above-mentioned range of temperatures for each soap on



account of the elastic systems becoming instable (crystallisation, curd formation). This complication was seriously felt with laurate, as a result of which the tract of temperatures in which (with difficulty on account of the very low  $n$ -values) measurements could be performed was only 1—2 centigrades. These complications also occurred with myristate and palmitate at  $K_2CO_3$  concentrations higher than those corresponding to the ones of minimum damping.

The tract of temperatures in which measurements are practicable is here at least some 10 centigrades.

We see from fig. 2 that the above-mentioned tracts for the different soaps do not overlap in general (except for oleate).

This means that *a comparison of the elastic behaviour of the five different soaps cannot be made at one and the same temperature.*

Therefore the comparison can only be made when the elastic properties of each of the soaps are measured as a function of the temperature, the results are plotted against the temperature and the relative courses of the curves are considered.

Let us first discuss fig. 2 from this point of view. Though it seems likely to conclude from the upper part of fig. 1 that the coacervation limits of the soaps with saturated carbon chain decrease with increase of the number of carbon atoms, this conclusion can only be verified by plotting the coacervation limits as a function of the temperature, a plotting which has actually been done in fig. 2. The relative position of the corresponding curves (letters  $L$ ,  $M$ ,  $P$  and  $S$  with the suffix "coac") appears to be such that we do not doubt any longer, that when the measurements could be done at the same temperature, we would find:

stearate < palmitate < myristate < laurate.

When we apply the above to the curves in fig. 2 representing the positions of the maxima of the  $n$ -curves (letters  $L$ ,  $M$ ,  $P$  and  $S$  with the suffix "max") or to the curves which give the positions of the left footpoints of the  $n$ -curves (letters  $L$ ,  $M$ ,  $P$  and  $S$  with the suffix "l.fpt.") we come to quite the same sequence.

Generalizing we may therefore conclude (apart from the influence of the temperature) that *the region of salt concentrations in which elastic phenomena are observable lies at a lower concentration when the carbon chain of the soap is longer:*

stearate < palmitate < myristate < laurate.

When one compares in fig. 2 in the same way the relative positions of the three kinds of curves (with suffixes "coac", "max" and "l.fpt") for oleate and stearate, one concludes that *introduction of a double bond into the carbon chain shifts the above-mentioned region into the same direction as does shortening of the carbon chain.* This shift, however, is not very great, for the regions of the elastic phenomena for oleate and palmitate

lie in fig. 2 at about equal ordinate values (compare in particular the curves with suffix "max"). Thus introduction of the double bond is, roughly spoken, equivalent to shortening the saturated carbon chain with two carbon atoms<sup>1)</sup>.

We now proceed to a proper comparison of elastic properties, but have first to consider how to compare the shear modulus or the damping, these quantities being functions of the  $K_2CO_3$  concentration (compare fig. 1). Obviously we have to compare the above-mentioned quantities of the different soaps at such  $K_2CO_3$  concentrations, that the soap systems can be considered to be in *corresponding states*. It seems very probable that at the  $K_2CO_3$  concentration corresponding to the one of minimum damping (maximum of the  $n$ -curve, which practically coincides with the inflexion point of the  $G$ -curve) the soap systems are in corresponding states.

We therefore will compare the values of  $G$  and of  $n$  of the different soaps at the  $K_2CO_3$  concentrations corresponding to the ones of minimum damping.

Compare the figures 3 and 4, in which we have plotted the values of  $\sqrt{G}$  (data from the last column in Table I) and of  $n$  (column 8 of Table I) against the temperature.

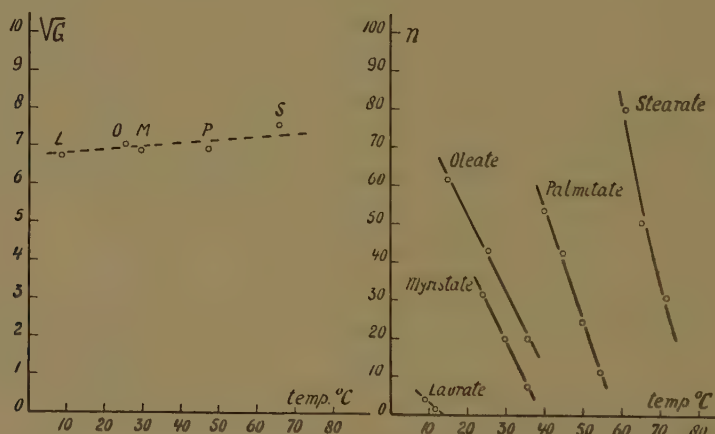


Fig. 3 and 4. Comparison of laurate, myristate, palmitate, stearate and oleate as regards  $\sqrt{G}$  and  $n$  at the  $K_2CO_3$  concentrations corresponding to the ones of minimum damping. (see text).

We first discuss fig. 4. This figure clearly demonstrates the usefulness of comparing the elastic properties of the different soaps with the aid of the temperature functions of these properties.

Because of instability of the elastic systems at somewhat lower temperatures as are corresponding to the upper ends of the  $n$ -curves, these

<sup>1)</sup> It is remarkable, that in quite another field of investigations one comes to an analogous conclusion. Compare H. L. BOOIJ in H. R. KRUYT, Colloid Science (Elsevier publishing company, Amsterdam 1949), Vol. II p. 709—710.

$n$ -curves cannot be investigated further upwards (except oleate). This means that it is not possible to compare the damping of all soaps at one and the same temperature. It is not even possible to find a temperature at which two saturated soaps can be investigated. The  $n$ -temp. diagram now allows to conclude that (apart from the temperature) *the damping decreases very considerably with increase of the number of carbon atoms in the carbon chain of the soap.*

stearate < palmitate < myristate < laurate.

We find here the same succession as above for the  $K_2CO_3$  regions in which elastic phenomena are observable.

When we compare the relative position of the  $n$ -temperature curves for oleate and stearate, we conclude that *introduction of a double bond into the carbon chain of a soap increases the damping very considerably.*

With regard to the shift of the salt region in which elastic phenomena are observable, the influence of the introduction of a double bond on the damping seems more pronounced, the  $n$ -curve for oleate lying even in the neighbourhood of the one for myristate.

Still we must consider this with some reservation. For the damping is very sensitive to chemical alterations, and it is not excluded that such alterations have already proceeded to some extent in the oleic acid which was used for the experiments.

We now turn to a discussion of fig. 3, in which the mean of  $\sqrt{G}$  over the temperatures at which was measured has been plotted for each soap against the mean temperature. We deviate here from the principles given above, according to which the elastic properties of each soap should be plotted as a function of the temperature in order to compare the relative position of the curves which are obtained. Certainly considerable errors were introduced by the method which was followed in order to obtain the  $G$ -values recorded in column 9 of Table I <sup>2)</sup> and the decrease of  $G$  with temperature which these values suggest cannot be trusted to be real.

We know from previous more accurate measurements with oleate (Part XIII, using 500 ml vessels) that  $G$  at the salt concentration corresponding to the one of minimum damping, does not decrease but increases slightly with increasing temperature. Through each of the soap points (letters  $L, M, P, S, O$ ) in fig. 3 we must therefore imagine lines sloping slightly up to the right (e.g. lines parallel to the dotted line in fig. 3) and we should consider their relative position.

Though these  $\sqrt{G}$ -temperature curves cannot be drawn actually, we may conclude that they lie relatively close together, but one cannot give the succession of these lines in the vertical direction (the mean  $G$  values may still contain relatively large errors).

<sup>2)</sup> This method comprises as a first step to find graphically the  $K_2CO_3$  concentration at which the maximum of the  $n$ - $C_{K_2CO_3}$  curve is situated and thereafter to interpolate the corresponding value of  $G$  on the  $G$ - $C_{K_2CO_3}$  curve.

When we summarize the results in this section, it appears that the measurements at constant soap concentration clearly show the influence of the length of the carbon chain and the influence of the introduction of a double bond into the carbon chain, on the  $\text{K}_2\text{CO}_3$  regions in which elastic phenomena are observable (fig. 2) and on the damping (fig. 4), but that a distinct answer cannot be given with regard to the shearmodulus. We can only conclude that at corresponding states the shearmodulus for all five soaps is of the same order of magnitude.

*(To be continued)*



## ELASTIC-VISCOUS SOAP SYSTEMS CONTAINING SALTS. XXb

*Comparison of the elastic behaviour of elastic-viscous systems of K-laurate, K-myristate, K-palmitate, K-stearate and K-oleate containing  $K_2CO_3$*

BY

H. G. BUNGENBERG DE JONG, H. J. v. D. BERG, W. A. LOEVEN \*) and  
W. W. H. WEYZEN \*)

(Communicated at the meeting of October 27, 1951)

4. *Experiments in which the elastic properties are investigated as a function of the soap concentration*

In the present section quite other methods are followed to compare the elastic behaviour of the soap systems and the results will be used to answer the question which was left undecided in the preceding section. Strictly spoken the answer will not be in the same terms as are used in section 3 (relative position of the  $\eta$ - $G$ -temperature curves), but in terms that are more fundamental (relative position of the  $a$ -temperature curves — for the meaning of  $a$  see below).

The method is based on the results of part XVI and XVII of this series. It was shown in the former of the two that the relation between the shear modulus  $G$  and the oleate concentration  $C_{\text{oleate}}$  is quite generally expressed by linear formulae of the type  $1/G = a(C_{\text{oleate}} - b)$ . In this formula  $b$  is the part cut off by the straight line from the abscissa and thus represents the concentration of the "free oleate", that is the oleate which does not take part in the elastic structure. Hence  $(C_{\text{oleate}} - b)$  is the concentration of the oleate which does take part in the elastic structure and  $a$  is a proportionality factor, characteristic of the elastic behaviour.

How  $a$  and  $b$  are depending on the salt concentration and on the temperature was studied in part XVII of this series. It appears that the  $a-C_{\text{salt}}$  curve is a curve with a very flat minimum, which coincides practically with the salt concentration corresponding to the one of minimum damping. A not too large error in the estimation of the salt concentration corresponding to the one of minimum damping (in fig. 1 estimation of the position of the maximum of the  $n$ -curve) will, therefore, hardly be felt in the value of  $a$ .

The  $a-C_{\text{salt}}$  curve is shifted upwards at increase of the temperature, but in a tract of 10–20 centigrades this shift is only small.

The above two points are making  $a$ , at the salt concentration correspond-

\*) Aided by grants from the "Netherlands Organization for Pure Research (Z.W.O.)."

ing to the one of minimum damping, a very apt quantity for the comparison of the elastic behaviour of different soaps.

Based upon the results of section 3 (Table I) we took for the following experiments as  $K_2CO_3$  concentrations corresponding to the ones of minimum damping for stearate 0.475, for oleate 0.80, for palmitate 0.75, for myristate 1.375 and for laurate 2.18 moles/l. The mixtures were measured at three temperatures successively <sup>3)</sup>. Though the above measurements

TABLE II  
Results obtained with *K*-stearate

Temp.	Soap. conc. mmol/l	0.35 mol/l $K_2CO_3$			0.475 mol/l $K_2CO_3$			0.60 mol/l $K_2CO_3$		
		$\gamma G$	$a$	$b$	$\gamma G$	$a$	$b$	$\gamma G$	$a$	$b$
60 °	50	9.15 $\pm$ 0.02	0.199	4.3	9.60 $\pm$ 0.01	0.202	2.4	10.36 $\pm$ 0.01	0.217	2.6
	40	7.00 $\pm$ 0.01			7.58 $\pm$ 0.01			8.14 $\pm$ 0.05		
	30	5.13 $\pm$ 0.01			5.58 $\pm$ 0.01			5.59 $\pm$ 0.01		
	20	3.14 $\pm$ 0.01			3.54 $\pm$ 0.01			3.98 $\pm$ 0.01		
64.8°	50	9.09 $\pm$ 0.02	0.206	6.3	9.63 $\pm$ 0.02	0.207	3.2	10.49 $\pm$ 0.01	0.219	1.6
	40	6.83 $\pm$ 0.03			7.67 $\pm$ 0.02			8.69 $\pm$ 0.06		
	30	4.97 $\pm$ 0.01			5.50 $\pm$ 0.01			6.09 $\pm$ 0.02		
	20	2.83 $\pm$ 0.02			3.47 $\pm$ 0.01			4.05 $\pm$ 0.02		
70.8°	50	8.68 $\pm$ 0.02	0.209	8.6	9.63 $\pm$ 0.01	0.206	3.2	10.61 $\pm$ 0.05	0.220	1.7
	40	6.44 $\pm$ 0.03			7.61 $\pm$ 0.02			8.41 $\pm$ 0.05		
	30	4.51 $\pm$ 0.02			5.57 $\pm$ 0.02			6.17 $\pm$ 0.02		
	20	—			3.44 $\pm$ 0.02			4.04 $\pm$ 0.03		
		$\Delta$	1/ $\Delta$	$n$	$\Delta$	1/ $\Delta$	$n$	$\Delta$	1/ $\Delta$	$n$
60 °	50	0.104 $\pm$ 0.001	9.62	74.1	0.071 $\pm$ 0.001	14.1	107	—	—	69.4
	40	0.134 $\pm$ 0.002	7.46	52.7	0.111 $\pm$ 0.001	9.01	83.8	—	—	—
	30	0.346 $\pm$ 0.008	2.89	35.0	0.162 $\pm$ 0.004	6.17	62.2	—	—	—
	20	0.769 $\pm$ 0.008	1.30	20.8	0.425 $\pm$ 0.005	2.35	36.2	—	—	22.8
64.8°	50	0.155 $\pm$ 0.004	6.45	58.7	0.136 $\pm$ 0.002	7.35	73.0	0.221 $\pm$ 0.003	4.53	45.0
	40	0.405 $\pm$ 0.016	2.47	36.8	0.163 $\pm$ 0.003	6.14	58.9	—	—	—
	30	0.535 $\pm$ 0.018	1.87	27.6	0.291 $\pm$ 0.004	3.44	38.4	0.711 $\pm$ 0.014	1.41	24.6
	20	1.231 $\pm$ 0.013	0.81	10.6	0.673 $\pm$ 0.010	1.49	22.4	1.174 $\pm$ 0.012	0.85	16.3
70.8°	50	0.378 $\pm$ 0.010	2.65	35.9	0.209 $\pm$ 0.003	4.78	44.9	—	—	22.6
	40	0.743 $\pm$ 0.006	1.35	18.8	0.343 $\pm$ 0.004	2.92	34.6	—	—	18.9
	30	1.289 $\pm$ 0.018	0.78	11.5	0.711 $\pm$ 0.016	1.41	24.6	—	—	16.2
	20	—	—	(3)	0.948 $\pm$ 0.020	1.06	13.3	—	—	6.0

<sup>3)</sup> Table I shows that the  $K_2CO_3$  concentration corresponding to the one of minimum damping shifts slightly with increase of the temperature. We should, therefore, have to prepare three different series of soap mixtures each with the  $K_2CO_3$  concentration corresponding to the one of minimum damping at the respective temperatures (e.g. 0.485, 0.475, and 0.455 moles/l at 60°, 65° and 69.9°C. respectively for *K*-stearate). But as the shift with the temperature is small and the minimum of

would have sufficed for our purposes, we also prepared for each soap mixtures at a  $K_2CO_3$  concentration lower than and higher than the concentration corresponding to the one of minimum damping and such that one could suppose  $n$  to have roughly half the value of the  $n$  at the maximum of the  $n$ -curve. These two extra sets of measurements were made to control that the measurements of the main series really will give the minimum value of  $a$ . The results of the measurements have been given in the tables II—VI.

TABLE III  
*Results obtained with K-palmitate*

Temp.	Soap. conc. mmol/l	0.6 mol/l $K_2CO_3$			0.75 mol/l $K_2CO_3$			0.9 mol/l $K_2CO_3$		
		$ G$	$a$	$b$	$ G$	$a$	$b$	$ G$	$a$	$b$
45.8°	30	4.15 ± 0.01	0.189	7.6	4.76 ± 0.01	0.195	5.8	5.40 ± 0.01	0.183	0.5
	40	6.29 ± 0.02			—			—		
	50	7.87 ± 0.03			8.43 ± 0.01			—		
	60	9.91 ± 0.01			10.65 ± 0.02			10.89 ± 0.04		
50.6°	30	3.81 ± 0.02	0.201	10.9	4.68 ± 0.02	0.200	6.4	5.31 ± 0.05	0.188	2.4
	40	5.98 ± 0.04			6.76 ± 0.01			6.87 ± 0.03		
	50	7.63 ± 0.03			8.75 ± 0.01			—		
	60	9.96 ± 0.01			10.68 ± 0.02			10.89 ± 0.03		
55.7°	30	3.58 ± 0.03	0.187	10.5	4.73 ± 0.02	0.200	6.3	5.35 ± 0.02	0.195	2.6
	40	5.64 ± 0.02			6.77 ± 0.02			7.30 ± 0.06		
	50	7.32 ± 0.04			8.77 ± 0.03			—		
	60	—			10.74 ± 0.02			(10.34 ± 0.07)		
		$\Delta$	$1/\Delta$	$n$	$\Delta$	$1/\Delta$	$n$	$\Delta$	$1/\Delta$	$n$
45.8°	30	1.163 ± 0.019	0.86	12.4	0.635 ± 0.008	1.57	27.4	0.735 ± 0.022	1.36	20.3
	40	0.588 ± 0.017	1.70	25.5	—	—	—	—	—	—
	50	—	—	30.8	0.166 ± 0.003	6.02	49.9	—	—	—
	60	0.250 ± 0.002	4.00	39.4	0.146 ± 0.004	6.85	53.9	0.268 ± 0.005	3.73	40.1
50.6°	30	1.715 ± 0.021	0.58	7.5	0.938 ± 0.016	1.07	14.4	1.502 ± 0.021	0.67	9.9
	40	0.901 ± 0.009	1.11	14.5	0.615 ± 0.008	1.63	29.0	1.191 ± 0.021	0.84	14.3
	50	0.871 ± 0.011	1.15	18.6	0.431 ± 0.008	2.32	39.7	—	—	—
	60	0.428 ± 0.007	2.34	29.6	0.225 ± 0.002	4.44	47.6	0.712 ± 0.015	1.40	20.7
55.7°	30	—	—	(3—4)	1.477 ± 0.022	0.68	9.7	—	—	4.3
	40	1.730 ± 0.022	0.58	8.3	1.057 ± 0.005	0.95	15.3	—	—	6.3
	50	1.534 ± 0.012	0.65	9.4	0.799 ± 0.007	1.25	19.1	—	—	—
	60	—	—	—	0.601 ± 0.010	1.66	22.8	—	—	8.0

the  $a$ - $C_{K_2CO_3}$  curve is very flat (compare text above), the simplification to make only one series of mixtures and to measure them at three temperatures, will not give  $a$ -values which differ from the value of  $a$  at exactly the  $K_2CO_3$  concentration corresponding to the one of minimum damping.

TABLE IV

*Results obtained with K-myristate*

Temp.	Soap conc. mmol/l	1.15 mol/l K <sub>2</sub> CO <sub>3</sub>			1.375 mol/l K <sub>2</sub> CO <sub>3</sub>			1.6 mol/l K <sub>2</sub> CO <sub>3</sub>		
		$\gamma G$	$a$	$b$	$\gamma G$	$a$	$b$	$\gamma G$	$a$	$b$
25.5°	40	6.41 $\pm$ 0.03			6.98 $\pm$ 0.01			7.06 $\pm$ 0.05		
	60	10.10 $\pm$ 0.03	0.188	5.9	10.56 $\pm$ 0.03	0.187	2.8	11.16 $\pm$ 0.06	0.205	5.6
	80	13.91 $\pm$ 0.07			14.44 $\pm$ 0.10			—		
31.0°	40	6.13 $\pm$ 0.03			6.77 $\pm$ 0.02			—		
	60	9.74 $\pm$ 0.04	0.184	6.3	10.42 $\pm$ 0.06	0.186	3.8	—	—	—
	80	13.74 $\pm$ 0.11			14.22 $\pm$ 0.06			—		
38.0°	40	—			6.57 $\pm$ 0.06			—		
	60	—	—	—	10.67 $\pm$ 0.10	0.205	7.9	—	—	—
	80	14.17 $\pm$ 0.20			—			—		
		$\Delta$	1/ $\Delta$	$n$	$\Delta$	1/ $\Delta$	$n$	$\Delta$	1/ $\Delta$	$n$
25.5°	40	0.802 $\pm$ 0.008	1.25	16.8	0.320 $\pm$ 0.007	3.13	32.6	—	—	12.0
	60	0.295 $\pm$ 0.007	3.39	36.7	0.202 $\pm$ 0.002	4.95	50.8	—	—	18.3
	80	—	—	43.3	—	—	54.1	—	—	( $\pm$ 20)
31.0°	40	1.454 $\pm$ 0.007	0.69	10.7	0.855 $\pm$ 0.020	1.17	19.4	—	—	4
	60	0.654 $\pm$ 0.005	1.53	19.9	0.495 $\pm$ 0.009	2.02	25.7	—	—	7
	80	—	—	25.0	—	—	33.6	—	—	(5–6)
38.0°	40	—	—	(3)	—	—	(5)	—	—	0
	60	—	—	(6–7)	—	—	(11–12)	—	—	( $\pm$ 1)
	80	—	—	11.7	—	—	(12–13)	—	—	( $\pm$ 1)

TABLE V

*Results obtained with K-laurate*

Soap conc. mmol/l	K <sub>2</sub> CO <sub>3</sub> mol/l.	Temp. °C.	$\gamma G$	$\gamma G$ mean	$a$	$b$	$\Delta$	1/ $\Delta$	$n$		
50	2.05	7.6	7.84 ± 0.05	8.09	0.192	8	2.55 ± 0.03	0.39	4		
		9.5	7.26 ± 0.10				—	Mean 0.40	3		
	2.18	7.6	8.61 ± 0.03				2.27 ± 0.10	0.44	5.3		
		9.5	8.64 ± 0.05				2.65 ± 0.02	0.38	4		
60	2.05	7.6	9.82 ± 0.06	10.01			0.192	8	1.74 ± 0.02	0.57	7.5
		9.5	9.71 ± 0.10						2.42 ± 0.02	0.41	4.3
	2.18	7.6	10.26 ± 0.07						—	Mean 0.45	7.6
		9.5	10.26 ± 0.06						2.67 ± 0.02	0.37	4



When the values of  $|G|$  are plotted against the soap concentration it will be seen that straight lines are obtained which cut the abscissa at a small soap concentration. The slopes  $a$  and the parts cut off from the abscissa  $b$ , have been calculated with a statistical method (best fitting straight line through the experimentally determined points). Because of the irregular results in the case of laurate, Table V, we used the mean of all values at 50 millimoles/l and the mean of all values at 60 millimoles/l for this calculation. The values of  $a$  and  $b$  therefore apply here to the mean of the two slightly different temperatures and to the mean of the two slightly different  $K_2CO_3$  concentrations.

The errors in the calculated values of  $a$  and  $b$  in the tables II–VI are certainly greater than in the analogous experiments with oleate in part

TABLE VI  
*Results obtained with K-oleate*

Temp.	Soap conc. mmol/l	0.6 mol/l $K_2CO_3$			0.8 mol/l $K_2CO_3$			1.0 mol/l $K_2CO_3$		
		$ G $	$a$	$b$	$ G $	$a$	$b$	$ G $	$a$	$b$
13.5°	25	3.94 ± 0.01			4.46 ± 0.01			5.13 ± 0.02		
	35	5.76 ± 0.02	0.183	3.4	6.34 ± 0.01	0.187	1.0	7.21 ± 0.02	0.210	0.6
	40	6.75 ± 0.03			7.26 ± 0.02			8.29 ± 0.02		
	50	8.51 ± 0.02			9.23 ± 0.02			10.38 ± 0.03		
25.3°	25	3.48 ± 0.01			4.46 ± 0.01			5.50 ± 0.04		
	35	5.42 ± 0.04	0.199	7.6	6.50 ± 0.03	0.200	2.6	7.96 ± 0.07	0.226	0.6
	40	6.40 ± 0.02			7.46 ± 0.02			8.56 ± 0.03		
	50	8.45 ± 0.04			9.46 ± 0.03			11.25 ± 0.13		
35.5°	25	3.01 ± 0.02			4.53 ± 0.03			—		
	35	4.96 ± 0.02	0.201	10.1	6.54 ± 0.02	0.205	3.0	—		
	40	6.00 ± 0.04			7.64 ± 0.04			—		
	50	8.02 ± 0.03			9.65 ± 0.05			—		
		$\Delta$	$1/\Delta$	$n$	$\Delta$	$1/\Delta$	$n$	$\Delta$	$1/\Delta$	$n$
13.5°	25	0.758 ± 0.007	1.32	18.6	0.250 ± 0.005	4.00	39.3	0.332 ± 0.007	3.01	33.0
	35	0.414 ± 0.006	2.42	31.4	0.154 ± 0.004	6.49	59.3	0.251 ± 0.004	3.98	42.7
	40	0.257 ± 0.004	3.89	39.6	0.133 ± 0.002	7.52	67.7	0.231 ± 0.002	4.33	46.9
	50	0.174 ± 0.003	5.75	55.2	0.103 ± 0.002	9.62	87.4	0.192 ± 0.003	5.21	56.4
25.3°	25	1.426 ± 0.008	0.70	9.8	0.482 ± 0.015	2.07	28.3	1.347 ± 0.010	0.74	11.5
	35	0.741 ± 0.007	1.35	19.7	0.340 ± 0.006	2.94	39.5	0.805 ± 0.009	1.24	17.0
	40	0.512 ± 0.005	1.95	25.4	0.251 ± 0.002	3.98	44.5	0.817 ± 0.011	1.22	17.6
	50	0.255 ± 0.006	3.92	39.3	0.196 ± 0.003	5.08	53.9	—	—	(14 ± 4)
35.5°	25	—	—	5	1.358 ± 0.008	0.74	10.4	—	—	1.5
	35	1.486 ± 0.018	0.67	9.9	0.928 ± 0.014	1.08	16.2	—	—	2.5
	40	1.089 ± 0.010	0.92	14.0	0.809 ± 0.005	1.24	18.6	—	—	3.2
	50	0.728 ± 0.002	1.37	19.3	0.615 ± 0.005	1.63	21.5	—	—	3.2

XVII of this series. The values of  $a$  have been given in three decimals, but the last decimal may be uncertain up to several units. The percentual error of the  $b$ -values is probably much greater <sup>4)</sup>.

5. Comparison of the soaps as regards  $a$  and  $b$  in the formula  $\sqrt{G} = a(C_{\text{soap}} - b)$

a. General shape of the  $a = f(C_{\text{K}_2\text{CO}_3})$  and  $b = f(C_{\text{K}_2\text{CO}_3})$  curves

We have collected in the next survey (Table VII) all  $a$  and  $b$  values from the tables II—VI. We will now first control that the dependence of  $a$  and of  $b$  on the salt concentration bears in principle the same character for all soaps. To minimize the influence of the experimental errors we have used in fig. 5 the mean values of  $a$  and  $b$  over all temperatures at which

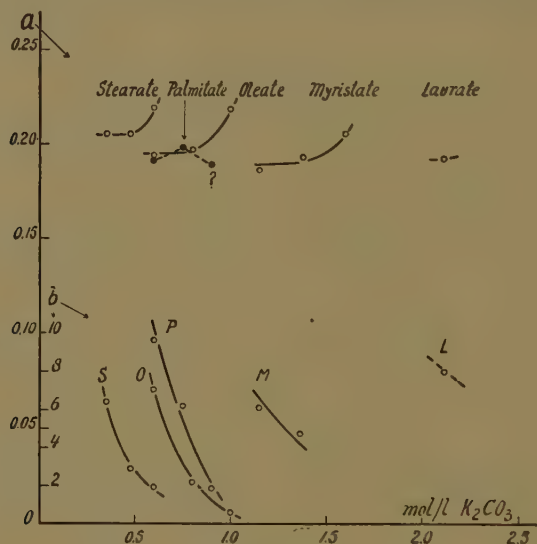


Fig. 5. Values of  $a$  and  $b$  from the formula  $\sqrt{G} = a(C_{\text{soap}} - b)$  as a function of the  $\text{K}_2\text{CO}_3$  concentration.

measurements were performed (these means have also been given in Table VII). We recognize in this figure the characteristic shape of the  $a = f(C_{\text{salt}})$  curve (curve with a very flat minimum, though in fig. 5 the ascending branch to the left has not been reached), and of the  $b = f(C_{\text{salt}})$  curve (curve with a steep descending branch to the left), which we have studied already for oleate in part XVII of this series.

There are two interesting points in fig. 5. First the succession of the  $a$ - and  $b$ -curves from left to right; second the nearly same value of  $a$  at the minimum of the  $a$ - $C_{\text{K}_2\text{CO}_3}$  curves of the different soaps. These points will be discussed further below.

<sup>4)</sup> The following reasons can be given for the larger experimental errors:

1) the use of small spherical vessels (110 ml.) instead of the usual 500 ml. vessels, 2) the often much higher temperatures at the measurements, 3) the difficulties connected with the tendency to instability (especially with laurate, and at the highest salt concentrations also with myristate and palmitate).

TABLE VII

*Survey of the values of a and of b of the Tables II-VI*

	Temp. C.	a			b		
		$C_{K_2CO_3} < \min.$ damping.	$C_{K_2CO_3} = \min.$ damping.	$C_{K_2CO_3} > \min.$ damping.	$C_{K_2CO_3} < \min.$ damping.	$C_{K_2CO_3} = \min.$ damping.	$C_{K_2CO_3} > \min.$ damping.
Oleate ( $K_2CO_3 = 0.6; 0.8;$ 1.0 mol/l)	13.5	0.183	0.187	0.210	3.4	1.0	0.6
	25.3	0.199	0.200	0.226	7.6	2.6	0.6
	35.5	0.201	0.205	—	10.1	3.0	—
		Mean 0.194	Mean 0.197	Mean 0.218	Mean 7.0	Mean 2.2	Mean 0.6
Stearate ( $K_2CO_3 = 0.35;$ 0.475; 0.60 mol/l)	60.0	0.199	0.202	0.217	4.3	2.4	2.6?
	64.8	0.206	0.207	0.219	6.3	3.2	1.6
	70.8	0.209	0.206	0.220	8.6	3.2	1.7
		Mean 0.205	Mean 0.205	Mean 0.219	Mean 6.4	Mean 2.9	Mean 2.0
Palmitate ( $K_2CO_3 = 0.6; 0.75;$ 0.9 mol/l)	45.8	0.189	0.195	0.183	7.6	5.8	0.5
	50.6	0.201	0.200	0.188	10.9	6.4	2.4
	55.7	0.187	0.200	0.195	10.5	6.3	2.6
		Mean 0.192	Mean 0.198	Mean 0.189	Mean 9.7	Mean 6.2	Mean 1.8
Myristate ( $K_2CO_3 = 1.15; 1.375;$ 1.6 mol/l)	25.5	0.188	0.187	0.205	5.9	2.8	5.6?
	31.0	0.184	0.186	—	6.3	3.8	—
	38.0	—	0.205	—	—	7.9	—
		Mean 0.186	Mean 0.193	Mean 0.205	Mean 6.1	Mean 4.8	
Laurate ( $K_2CO_3 =$ 2.12 mol/l)	8.6	—	0.192	—	—	8	—

b. Comparison of the different soaps as regards  $b$  in the formula  $\sqrt{G} = a(C_{\text{soap}} - b)$

As  $b$  represents the concentration of the soap which does not take part in the elastic structure, the general decrease of  $b$  with increase of the  $K_2CO_3$  concentration indicates the transformation of "free soap" into soap taking part in the elastic structure. From the succession of the  $b$  curves in fig. 5 follows that this transformation is easier as the carbon chain of the saturated soap is longer. It follows too from the relative position of the  $b$  curves of stearate and oleate, that this transformation is made less easy by introduction of a double bond into the carbon chain. Thus the succession of the  $b$  curves in fig. 5 explains why the left limits of the elastic systems were found to follow the same rules in section 3 (compare fig. 2).

In the above comparison of the  $b$ -curves the influence of the temperature on  $b$  has been completely neglected (e.g. the  $b$ -curve for oleate in fig. 5 represents its approximate position at the mean temperature of about 25° C; that for stearate at the mean temperature of about 65° C).

It follows that we ought to construct a three dimensional diagram in

which  $b$  is represented as a function of the  $K_2CO_3$  concentration and of the temperature. Such a figure would allow to make a decision whether the succession of the  $b$  curves in fig. 5 is the expression of a different position of the  $b$ -surfaces of the individual soaps, or whether the succession in fig. 5 is caused only by the different mean temperatures.

The relatively big errors in the values of  $b$  do not allow to construct such a three dimensional diagram, though the data are sufficient to get an impression how the relative position of the  $b$ -surfaces of the investigated soaps in such a diagram must be. We begin with oleate and stearate, because the  $b$  values seem the most reliable ones in this case.

In fig. 6A the  $b$  values for the three  $K_2CO_3$  concentrations which were investigated have been plotted against the temperature.

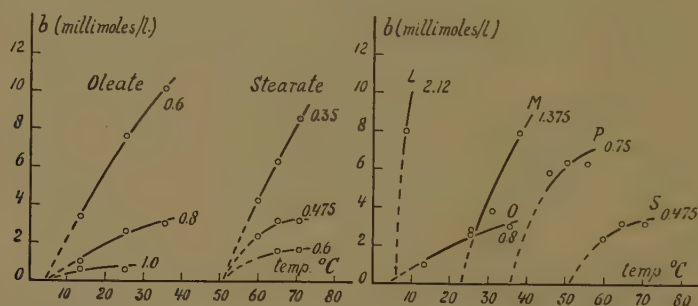


Fig. 6. Comparison of the different soaps as regards  $b$  in the formula  $V'G = a(C_{\text{soap}} - b)$ . Fig. 6A: comparison of stearate and oleate; Fig. 6B: comparison of the five soaps at the  $K_2CO_3$  concentrations of minimum damping. Salt concentrations have been given in moles/l.

The figure thus obtained can be regarded as the projection of a three dimensional  $b-C_{K_2CO_3}$ -temperature diagram upon the  $b$ -temperature face of the diagram.

It is obvious that we need not doubt any longer that the  $b$ -surfaces for oleate and for stearate have very different positions in the three dimensional diagram.

Moreover fig. 6A depicts the influence of the temperature and of the salt concentration on  $b$ . The upward to the right course of the curves and their relative position in each bundle show that for both stearate and oleate  $b$  increases with temperature and decreases with increase of the salt concentration. We knew this already for oleate from the results of part XVII.

Inspection of Table VII will show that with stearate as well as with myristate and palmitate the influence of the temperature and of the  $K_2CO_3$  concentration on  $b$  is alike (not taking into account the certainly erroneous values of  $b$  which are provided with a question mark).

A remarkable point in fig. 6A is that the three curves in each bundle seem to emerge from one point (or three points closely situated together)



on (or slightly above) the temperature axis. This may be connected with the fact which was already discussed in section 3, that the temperature regions in which elastic phenomena are observable, are limited at their lower end by the then occurring instability of the elastic systems (crystallisation, curd formation). It seems therefore that for the stability of the elastic systems a small value of  $b$  is necessary, i.e. some "free soap" must be present within the elastic structure. We will, however, not speculate further on this question, but we will assume that for the other soaps (laurate, myristate, palmitate) too analogous bundles exist as is the case for oleate and stearate, viz. bundles which emerge from the point on the temperature axis below which, for a given soap, crystallisation or curd formation sets in.

As these temperatures are approximately known (they lie a few degrees below the lowest temperature which was used for laurate, myristate and palmitate), we know roughly the points on the abscissa from where the bundles emerge.

Now the  $b$  values for these soaps at the lowest and highest salt concentration have probably large errors. For this reason we have plotted in fig. 6B only the values of  $b$  at the  $K_2CO_3$  concentrations corresponding to the ones of minimum damping. The curves through them give roughly the probable course of the  $b$  curves at these  $K_2CO_3$  concentrations.

Thus fig. 6B supplements fig. 6A and we may conclude that in a  $b-C_{K_2CO_3}$ -temp. diagram the  $b$  surfaces of the investigated soaps have very different positions. Those belonging to the saturated fatty acids (laurate, myristate, palmitate, stearate) do not intersect. Introduction of a double into the carbon chain shifts the  $b$ -surface mainly into the direction of smaller temperatures, without much altering its slope (compare also fig. 6A).

c. Comparison of the different soaps as regards  $a$  in the formula  $1/G = a(C_{\text{soap}} - b)$

In section 5a we mentioned already that the minima of the  $a = f(C_{K_2CO_3})$  curves at the  $K_2CO_3$  concentrations corresponding to the ones of minimum damping lie roughly spoken at about the same height above the abscissa (compare fig. 5).

Thus once more a similar result as we obtained in section 3. ( $G$  values of equally concentrated soap systems are of the same order of magnitude), but now for a much more fundamental quantity ( $a$ , the proportionality factor in the formula  $1/G = a(C_{\text{soap}} - b)$ ).

We must now proceed to compare the relative positions of the  $a$  curves for the five soaps in a  $a$ -temperature diagram. To this aim the values of  $a$  at the  $K_2CO_3$  concentrations corresponding to the ones of minimum damping have been plotted in fig. 7A against the temperature. Now we had to draw curves through always three experimentally determined points obtained with one soap (except in the case of laurate, where only

one point is available). But because of the small horizontal distance of the three points for one soap and the relative great errors in the  $a$  values (possibly 5 units in the third decimal) it has actually no sense to draw the curves for each soap.

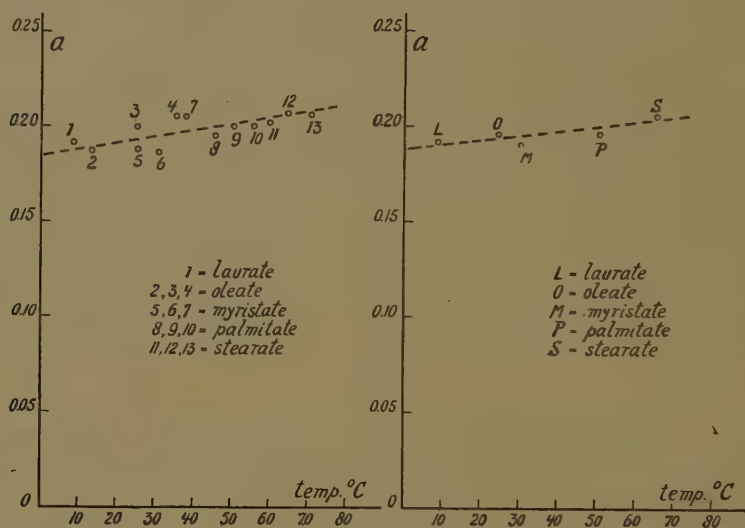


Fig. 7A. Values of  $a$  at the salt concentrations corresponding to the ones of minimum damping as a function of the temperature.

Fig. 7B. General influence of the temperature on  $a$  at the salt concentrations corresponding to the ones of minimum damping. (each point represents for one soap the mean value of  $a$  at the mean of the temperatures at which measurements were performed.)

Instead of it we have drawn a straight line (dotted) through all experimentally determined points, which actually lie distributed at both sides of it.

We know already from Part XVII of this series that for oleate  $a$  increases slightly with the temperature. When we consider in fig. 7A the relative position of always three  $a$  values obtained with one soap at three temperatures, the tendency of  $a$  to increase with temperature is generally present (e.g. oleate  $2 \rightarrow 3 \rightarrow 4$ , myristate  $5 \rightarrow 7$ , palmitate  $8 \rightarrow 9 \rightarrow 10$ , stearate  $11 \rightarrow 12 \rightarrow 13$ ).

We do not believe to be erroneous very far when we conclude that the individual  $a$ -temperature curves of the five soaps lie close together. Thus apart from the general increasing influence of the temperature on  $a$ , the conclusion seems probable that the proportionality factor  $a$  in the equation  $\sqrt{G} = a(C_{\text{soap}} - b)$  is practically independent of the length of the carbon chain and of the presence of a double bond in the carbon chain of the soap.

To get some idea of the temperature function of  $a$ , fig. 7B has been drawn in which each soap is represented by one mean  $a$  value only. This was done to diminish the influence of the errors of the individual  $a$  values.

The mean  $a$  value is here the mean of 6  $a$  values, namely of the values of  $a$  at the lowest  $K_2CO_3$  concentration <sup>5)</sup> at three temperatures and of the values of  $a$  at the  $K_2CO_3$  concentration corresponding to the one of the minimum damping at three temperatures.

The five  $a$  points in fig. 7B lie now more regularly distributed at both sides of the dotted straight line. The slope of this line suggests that  $a$  depends on a power of the absolute temperature which is smaller than one. (The slope of the drawn line corresponds approximately to a proportionality with  $\sqrt{T}$ ).

In the present communication we have always expressed the soap concentration in millimoles/l. Thus the numerical values of  $b$  in the formula  $\sqrt{G} = a (C_{\text{soap}} - b)$  are given in the tables also in millimoles/l, and the numerical values of  $a$  — which is approx. 0.2 for all soaps (at the  $K_2CO_3$  concentration corresponding to the one of minimum damping) — are also calculated with this concentration unit as a basis. This means that when the expression  $(C_{\text{soap}} - b)$  has a value of one — thus when the concentration of the soap taking part in the elastic structure is 1 millimol/l — the shearmodulus will be approx.  $(0.2)^2$ , that is approx. 0.04 dyne/cm<sup>2</sup>. This value of  $G$  can be called the *millimolar shearmodulus*.

When we express the soap concentration in moles/l the numerical value of  $a$  becomes  $10^3$  times greater, hence the *molar shearmodulus*  $10^6$  times greater. The result of the measurements can therefore be expressed by saying that at the  $K_2CO_3$  concentration corresponding to the one of minimum damping the molar shearmodulus has approx. the same value for the five investigated soaps, viz.  $4 \cdot 10^4$  dynes/cm<sup>2</sup>. It need not to be emphasized that molar solutions of the soaps cannot be handled and that, therefore, the introduction of the term molar shearmodulus can only be defended by the wish to use the customary concentration unit.

## 6. Comparison of the soaps as regards the damping

When  $n$  at the concentration of 50 millimoles/l soap is plotted against (at the  $K_2CO_3$  concentration corresponding to the one of minimum damping) the temperature — compare fig. 9 — we obtain of course a figure

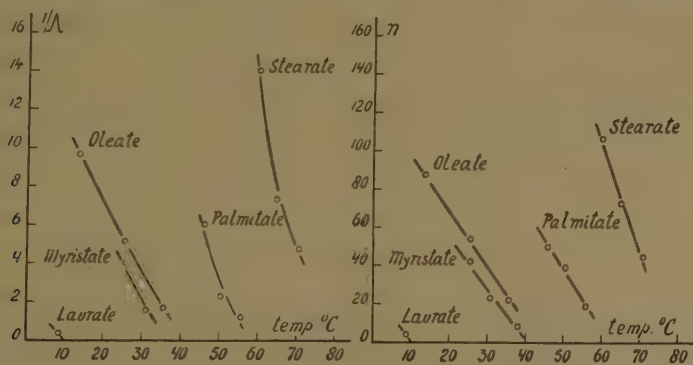


Fig. 8 and 9. Values of  $1/A$  and of  $n$  of 50 millimoles/l soap systems (at the  $K_2CO_3$  concentrations corresponding to the ones of minimum damping) as a function of the temperature.

<sup>5)</sup> From fig. 3 it appears that the values of  $a$  at the lowest  $K_2CO_3$  concentration hardly differ from the values of  $a$  at the  $K_2CO_3$  concentration corresponding to the one of minimum damping.

quite analogous to fig. 4<sup>6</sup>). But  $n$  is only an approximate measure for  $1/\Delta$  (compare part XV) and we are desirous to know if  $1/\Delta$  plotted against the temperature gives a similar figure. For this reason  $\Delta$  has been determined as well in the experiments in section 4. When  $1/\Delta$  at the concentration of 50 millimoles/l (at the  $K_2CO_3$  concentration corresponding to the one of minimum damping) is plotted against the temperature we obtain fig. 8, which shows the same general aspect as fig. 9, the sequence of the curves being also the same from left to right: laurate – myristate – oleate – palmitate – stearate<sup>7</sup>).

## 7. *Final remarks*

It need not to be emphasized that the results of the present investigation must be important for a future theory of the viscous elastic soap systems. The fact that the damping depends very strongly on the length of and the eventual presence of a double bond in the carbon chain of the soap, suggests that the point of attack for the damping is mainly located in the interior of the soapmicelles. It is a much surprising fact that the proportionality factor  $a$  (which, with  $b$  and the soap concentration determines the shear modulus) seems to be approximately independent of the length and nature of the carbon chain. This suggests that, what the different soaps have in common — the ionized carboxylgroup — is the factor of primary importance here.

With the present communication we end for the time being this series of experiments on the properties of elastic-viscous oleate (more generally-soap) systems. The aim of this series was in the first place to become acquainted with the many parameters which influence the elastic behaviour. Theoretical considerations have been avoided in general, as one must first have a survey of the facts which should be explained. We hope in due time to return to this question, but it seems that other information will be necessary before an attempt can be made. As for a future theory a comparison of the elastic behaviour of the viscous-elastic soap systems and of macromolecular gels might be of some interest, we have also made investigations on the latter systems. A communication on this subject will also be published in these Proceedings.

## 8. *Summary*

### 1. The elastic properties of $K_2CO_3$ containing viscous-elastic systems

<sup>6</sup>) Measurements with myristate at 50 millimoles/l have not been performed. The values of  $n$  in fig. 8 and of  $1/\Delta$  in fig. 9 have been obtained by interpolation between these values at 40 and at 60 millimoles/l.

<sup>7</sup>) The determinations of the decrement are not sufficiently numerous to derive from the  $1/\Delta$  values in a similar way as with  $\sqrt{G}$ , a proportionality factor and a part cut off from the abscissa.

The  $1/\Delta - C_{\text{soap}}$  curve is much more complicated than the  $\sqrt{G} - C_{\text{soap}}$  curve (compare Part XIX) and the four soap concentrations used in section 4 are far too few to locate sufficiently the position of three branches of the  $1/\Delta - C_{\text{soap}}$  curves.



of K-laurate, K-myristate, K-palmitate, K-stearate and K-oleate have been compared.

2. The temperature regions in which measurements are practicable do not overlap in general. This implies that the elastic properties must be measured as functions of the temperature, and the comparison must be done with the aid of graphs which give the results as functions of the temperature.

3. When the limits of the elastic systems are designed in a  $K_2CO_3$ -temperature diagram, it appears that the region of salt concentrations in which elastic phenomena are observable lies at lower salt concentrations when the carbon chain of the soap is longer.

stearate < palmitate < myristate < laurate.

4. Introduction of a double bond into the carbon chain shifts the region mentioned sub 3) into the same direction as does the shortening of the carbon chain, the shift being roughly equal here to the one caused by shortening the carbon chain with 2 carbon atoms.

5. The shape of the  $G-C_{K_2CO_3}$  curve (*S*-shaped) and of the  $n-C_{K_2CO_3}$  curve (curve with a maximum, the maximum coinciding with the inflexion point of the  $G-C_{K_2CO_3}$  curve), the influence of the temperature on them, the coincidence of the right footpoint of the  $n-C_{K_2CO_3}$  curve with the coarservation limit are the same for all soaps. This shows that the elastic-viscous soap systems are comparable objects.

6. Because of the dependence of the elastic properties on the  $K_2CO_3$  concentration, it is necessary to compare these properties at the  $K_2CO_3$  concentrations (for each soap a different one) at which the systems are in corresponding states. As such have been chosen the  $K_2CO_3$  concentrations corresponding to the ones of minimum damping (maximum of the  $n-C_{K_2CO_3}$  curve at constant soap concentration).

7. From a comparison of the elastic systems at constant soap concentration (40 millimoles/l) it appears that:

- a. the damping decreases considerably with increase of the number of carbon atoms in the carbon chain.

stearate < palmitate < myristate < laurate

(the successive  $n$ -curves in a  $n$ -temperature diagram lie 20 centigrades or more apart).

- b. the damping increases considerably by introduction of a double bond into the carbon chain of the soap (the  $n$ -curve for oleate was found to lie between those for palmitate and myristate).
- c. the number of carbon atoms in the carbon chain and the introduction of a double bond into it have no pronounced influence on the shear modulus. The method used did not allow to come to a conclusion regarding the succession of the curves in the  $G$ -temperature diagram.

8. A comparison of the elastic systems has also been made with methods based on the results of part XVII of this series. In this investigation the elastic properties (shear modulus, logarithmic decrement and  $n$ ) have been measured as functions of the soap concentration at appropriate  $K_2CO_3$  concentrations and temperatures.

9. The results have been used to evaluate the values of  $a$  and  $b$  of the equation  $\sqrt{G} = a(C_{\text{soap}} - b)$ .

It appears that in a  $b-C_{K_2CO_3}$  diagram the  $b$  curves lie wide apart, showing that the transformation of "free soap" into "soap taking part in the elastic structure" is easier as the carbon chain of the soap is longer and that introduction of a double bond into it acts in the opposite direction.

Particularities of the  $b$ -temperature diagrams have been discussed.

10. The values of  $a$  at the  $K_2CO_3$  concentrations corresponding to the ones of minimum damping are of the same order of magnitude for all investigated soaps.

11. When plotted in an  $a$ -temperature diagram the  $a$  values of the different soaps lie distributed in a narrow band with a slope coming near a proportionality with the square root of the absolute temperature.

12. It was not possible to discern with certainty the succession of the  $a$ -temperature curves of the investigated soaps. They must lie close together or may even coincide.

13. As regards the damping, similar results were obtained as mentioned sub 7. The succession of the  $1/\Delta$  curves in a  $1/\Delta$ -temperature diagram is the same as that of the  $n$ -curves in a  $n$ -temperature diagram.

14. The remarkable contrast between the damping (very large influence of the nature of the carbon chain) and the shearmodulus (no or a very small influence) suggest that the point of attack for the damping is situated in the soapmicelles, the rigidity of the elastic system, however, is connected with the ionized carboxylgroups.

*Department of Medical Chemistry  
University of Leiden*

## MISLEADING COLOUR-REACTIONS

BY

J. H. DE BOER AND G. M. M. HOUBEN

(Communicated at the meeting of November 24, 1951)

1. *Introduction*

Some 20 years ago, one of the authors <sup>1)</sup>, experimenting in the field of adsorption of organic molecules with peripheric dipoles (OH-groups), found that p-nitrophenol, when adsorbed on the surface of an inorganic salt exhibited an intense yellow colour. It was established that this colour was not caused by the formation of a salt, viz an alkali or alkaline earth p-nitrophenolate, but that the absorption spectrum of the p-nitrophenol molecule itself was shifted towards longer wave lengths, thus causing an absorption of light in the blue part of the spectrum and rendering the yellow colour which was observed. The salt-layers which served as adsorbents in these experiments were made by sublimation in a high vacuum, by which method they are obtained in thin, completely transparent and optically clear layers <sup>2)</sup>. They, nevertheless, possess a highly developed surface area — of about 250 m<sup>2</sup>/g — and they belong, therefore, to the class of adsorbents of high capacity. Because of this high capacity and of their own transparency, also in the ultra-violet region of the spectrum, these salt layers, when used as adsorbents, make it possible to measure the absorption spectra of adsorbed molecules. Systematic investigations in the then following years revealed that many organic- and also inorganic molecules — suffered a shift of their absorption spectra, when adsorbed on these salt layers. It was found that adsorption on a BaF<sub>2</sub>-layer always resulted in a stronger shift than adsorption on a CaF<sub>2</sub>-layer; p-nitrophenol e.g. showing the following data

maximum of absorption when dissolved in hydrochloric acid <sup>3)</sup>	316 mμ
maximum of absorption when adsorbed on CaF <sub>2</sub> <sup>4)</sup>	365 mμ
maximum of absorption when adsorbed on BaF <sub>2</sub> <sup>5)</sup>	413 mμ

<sup>1)</sup> J. H. DE BOER, Z. physikal. Chem. (B) 16, 397 (1932).

<sup>2)</sup> J. H. DE BOER, Physica 8, 145 (1928); Proc. Roy. Acad. (Amsterdam) 31, 906 (1928), Z. physikal. Chem. (B) 13, 314 (1931); (B) 14, 149 (1931); (B) 14, 457 (1931); (B) 15, 281 (1932); (B) 15, 300 (1932); See also J. H. DE BOER, Electron Emission and Adsorption Phenomena, (Cambridge 1935), Chapter VIII (German translation, Kap. VIII (Leipzig 1937)).

<sup>3)</sup> J. EISENBRAND and H. VON HALBAN, Z. physikal. Chem. (A) 146, 101 (1930).  
J. H. DE BOER and J. F. H. CUSTERS, Z. physikal. Chem. (B) 25, 238 (1934).

<sup>4)</sup> J. H. DE BOER and J. F. H. CUSTERS, loc. cit.

<sup>5)</sup> J. F. H. CUSTERS and J. H. DE BOER, Physica 3, 407 (1936).

It may, for comparison, be mentioned that the maximum of absorption of the p-nitrophenolate ion (in alkaline solution) is at  $400\text{ m}\mu$  <sup>6)</sup>. Similarly phenolphthalein <sup>7)</sup>, when adsorbed on  $\text{CaF}_2$  shows a bright red colour and has a maximum of absorption at  $475\text{ m}\mu$ , whilst it is redviolet coloured when adsorbed on  $\text{BaF}_2$  with a maximum of absorption at  $536\text{ m}\mu$ . Thymolphthalein is brown-red coloured, when adsorbed on  $\text{CaF}_2$ .

The explanation of these phenomena was given in 1932 <sup>7)</sup> by considering the difference in adsorption energy between the ground states and the excited states of the molecules. If the excited state of the molecule is adsorbed more strongly than the ground state, the act of adsorption decreases the energy difference between the ground level and the excited level, hence causes a shift of the absorption spectrum towards red. When applying this simple principle, it must be observed that also the Franck-Condon-principle will hold here and that, therefore, in extreme cases these two principles may counteract each other.

Apparently without knowing this former work WEITZ and collaborators <sup>8)</sup> rediscovered this effect in 1939, when they examined the changes in colour of various organic molecules when adsorbed on  $\text{Al}_2\text{O}_3$  and similar adsorbents. They describe e.g. also the adsorption of phenolphthalein on aluminium oxide, resulting in a bright red coloration of the surface.

## 2. *The nature of the surface of aluminiumoxide*

Partly as a continuation of the older experiments of the first author and his collaborators, which came to an end by the war, the adsorption of p-nitrophenol and of phenolphthalein on aluminiumoxide was examined by the second author during the experimental work for his thesis <sup>9)</sup>. The nature of the surface of aluminiumoxide may be modified in two different ways. The results of these studies will be published separately, the following summarizing remarks may, however, be given, in order to understand the colour changes which are observed. Starting from so-called  $\gamma$ -aluminiumoxide, which in its purest, stoichiometric form, must be written  $\text{HAL}_5\text{O}_8$ , the oxide may be heated at a certain temperature in an atmosphere of water vapour of a given tension, such that the surface will only contain O-atoms(ions) and OH-groups in equal quantities. This state may e.g. be obtained by heating at  $184^\circ\text{ C.}$  in an atmosphere of water vapour of  $4.57\text{ mm Hg}$  or by heating at  $345^\circ\text{ C.}$  in an atmosphere of water vapour of  $18.6\text{ mm Hg}$ . Whilst the formula  $\text{HAL}_5\text{O}_8$  must then be given to the bulk of the material, the surface-layer consists of  $\text{AlO(OH)}$ . Heating at a higher temperature and/or at a lower water

<sup>6)</sup> J. EISENBRAND and H. VON HALBAN, loc. cit.

<sup>7)</sup> J. H. DE BOER, Z. physikal. Chem. (B) **18**, 49 (1932).

<sup>8)</sup> E. WEITZ and F. SCHMIDT, Ber. d.d. chem. Ges. **72**, 2099 (1939).  
E. WEITZ, F. SCHMIDT and J. SINGER, Z. Elektrochem. **46**, 222 (1940).

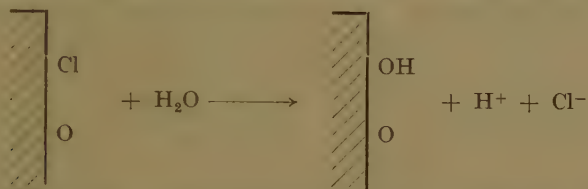
E. WEITZ, Z. Elektrochem. **47**, 65 (1941).

<sup>9)</sup> G. M. M. HOUBEN, Thesis Delft (1951).

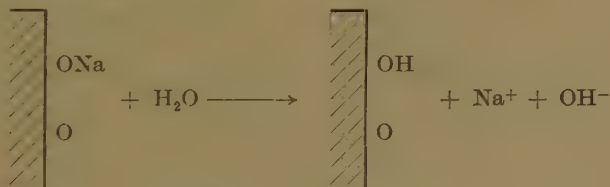


vapour pressure results in a partial loss of HO-groups, which are converted into O-atoms (ions) by liberation of water molecules. The OH-groups do not give the surface an acid or an alkaline reaction, the surface being completely amphoteric in character for all practical purposes. The O-atoms, which are certainly largely ionic in character cause the surface to adsorb predominantly such organic molecules which possess peripheric dipoles having the positive end of the dipole sticking outwards, such as OH-,  $\text{NH}_2$ -, NH- or  $\text{N}(\text{CH}_3)_2$ -groups<sup>10</sup>).

When aluminiumoxide is treated with an acid, like hydrochloric acid, part of the OH-groups are exchanged for  $\text{Cl}^-$ -ions. If, afterwards, such an oxide is studied in aqueous solutions, the surface shows an acid reaction caused by the hydrolysis of the  $\text{Cl}^-$ -ions on the surface:



When, on the other hand, aluminiumoxide is treated with a sodium hydroxide solution (or when it is originally made by precipitation by alkali), it contains partially ONa-groups in stead of OH-groups. In aqueous solutions these groups cause the surface to behave as an alkaline surface, again by hydrolysis:



### 3. The adsorption of phenolphthalein (Alkalinity)

Any aluminiumoxide, which is sufficiently dried, such that no water molecules are physically adsorbed on the surface, adsorbs, from their solutions in organic solvents, p-nitrophenol with a yellow colour and phenolphthalein with a red colour of some description. o-Nitrophenol, which is yellow of its own in non-alkaline solutions, is adsorbed with a deep orange colour. The shade of the colour may change with the nature of the solvent from which the substance is adsorbed and with the nature of the surface of aluminiumoxide, as described in the preceding section. The colour is stronger and deeper the less OH-groups the surface has and the less polar is the solvent from which the molecules are adsorbed. There is always a competition between the adsorption of the molecules of the solvent itself and of the molecules of the solute, but even from alcoholic solutions phenolphthalein is adsorbed to some extent, colouring

<sup>10</sup>) J. H. DE BOER and J. F. H. CUSTERS, Z. physikal. Chem. (B) 25, 225 (1934).

the surface of aluminium oxide red. Water molecules, however, are so strongly adsorbed that phenolphthalein molecules are displaced by them. This behaviour was already found with the adsorption on  $\text{CaF}_2$  or  $\text{BaF}_2$  surfaces and is also reported by WEITZ with the adsorption on  $\text{Al}_2\text{O}_3$ .

The development of a red colour, when a solution of phenolphthalein is applied to a surface of an adsorbent, might be — and is sometimes — mistaken as an indication of an alkaline reaction of that surface. This colour reaction may, therefore, lead to erroneous conclusions. If, however, after the application of the phenolphthalein and development of the colour, water is added, the colour will disappear. This bleaching may, sometimes, take some time because of the slowness of diffusion, like also the development of the red colour may take some time. If the original sample contains ONa-groups at its surface, the colour will not disappear but change into the shade of that of an alkaline phenolphthalein solution.

#### 4. *The adsorption of an azo-dye (Proton-activity)*

As already stated in Section 2, the OH-groups on the surface of aluminium oxide do not give an acid reaction. Whilst aluminium silicates may contain quite active hydrogenions (protons) at their surfaces the two components aluminium oxide and silicium dioxide do not show this behaviour. Aluminium silicates, when possessing protons at their surfaces are industrially used for bleaching or for catalytic reactions and in both cases it is the protons which make the surfaces "active". Quite a number of attempts have been made to estimate the number or the "strength" of these protons. It is known that azo-dyes are strongly adsorbed by them and that the colour of these dyes is often distinctly changed by this adsorption. TAMELE<sup>11)</sup>, using p-dimethyl-amino-azobenzene as an indicator based a titrimetric estimation of protons on this colour change. The colour of dimethyl-amino-azobenzene changes from yellow to red when adsorbed on a proton-active surface. In accordance with its failure of any proton-active effect, TAMELE observed that the surface of aluminium oxide did not cause this colour change. If, however, aluminium oxide is previously heated to a high temperature, it will adsorb dimethyl-amino-azobenzene with a red colour and one might be inclined to conclude that protons are formed at the surface by this heat treatment. Here, again, we meet another example of a misleading colour reaction. The normal adsorption of dimethyl-amino-azobenzene on aluminium oxide leads to a shift of the absorption spectrum to longer wave lengths resulting in the development of a red colour. The shade of the colour, however, is different from that which is developed when the azo-dye is bound to a proton of the surface. It takes, moreover, only place on the surfaces of aluminium oxides which, by heating, have lost a sufficiently great number of their OH-groups. Addition of water again makes the red colour disappear.

<sup>11)</sup> M. W. TAMELE, Disc. Far. Soc. 8, 270 (1950).

### 5. Adsorption of a leuco-compound ("Atomic oxygen")

In the course of studies about the development of atomic oxygen by photochemical reactions at surfaces, WEYL<sup>12)</sup> used some leuco-compounds of triphenyl-methane dyes as reagents on atomic oxygen. Whilst undoubtedly atomic oxygen will oxidise these leuco-compounds and turn them into coloured molecules, the development of colour, when such leuco-compounds are adsorbed at surfaces, may not be taken as proof that atomic oxygen is present. This colour reaction, however, has lately been used by WEYL<sup>13)</sup>, as a proof that atomic oxygen is liberated when quartz is ground or when silica-gel is dehydrated and most unlikely reaction schemes are given to explain these effects. HAUSER and collaborators<sup>14)</sup> found, using the same colour reaction, that aluminium oxide did not, but silicium dioxide and all aluminium silicates did show this colour reaction and they concluded that atomic oxygen was present in all such cases. WEYL even suggested that the professional lung disease of "silicosis" might be explained by atomic oxygen. This suggestion has induced denials in literature to the effect that atomic oxygen has nothing to do with "silicosis"; the occurrence of atomic oxygen at the surface of silicium containing minerals has, however, not been disputed<sup>15)</sup>.

The reagent is either applied from its benzene solution or from the vapour phase by heating a sample of the material with a small amount of the leuco-dye gently at about 150° C. In both cases also normal adsorption takes place and it is again this adsorption which leads to the development of colour. As heating may easily lead to discoloration itself, we studied the colour changes when a solution of p.p'-tetramethyl-diamino-triphenyl-methane (the leuco-base of malachite-green) in benzene is applied to the surfaces of the oxides. Silica-gel, dried beforehand at 110° C., gave a beautiful olive-green colour. On application of water, however, the colour disappears completely, as the adsorbed molecules are displaced by water molecules. If, however, the coloured system is kept too long in daylight in the presence of air the colour does not disappear completely. Similarly if, after the complete disappearance of colour by addition of water, the system is kept in light and in the presence of air, a new colour, completely different from the first one, develops. This oxidation, however, takes only place in the presence of oxygen and of light<sup>16)</sup>.

Aluminium oxide, when normally dried at 110° C. does not give any coloured adsorption of p.p'-tetramethyl-diamino-triphenyl-methane from

<sup>12)</sup> W. A. WEYL and T. FÖRLAND, *Ind. Eng. Chem.* **42**, 257 (1950).

<sup>13)</sup> W. A. WEYL, *Research (Suppl.)* **3**, 230 (1950).

<sup>14)</sup> E. A. HAUSER, D. S. le BEAU and P. P. PEVEAR, *J. Phys. and Colloid Chem.* **55**, 68 (1951).

<sup>15)</sup> B. M. WRIGHT, *Nature* **166**, 538 (1950).

J. EWLES and R. F. YOEELL, *Trans. Far. Soc.* **47**, 1060 (1951).

<sup>16)</sup> These experiments have been executed by Mr P. ZWIETERING of the Central Laboratory of "Staatsmijnen", Geleen (L.), the Netherlands.

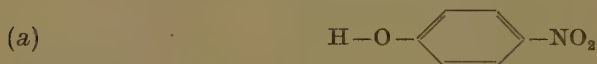
benzene solution. If, however, aluminium oxide is heated beforehand at 450° C. application of the benzene solution of the leuco-dye results in the development of a dark green colour. Application of water makes this colour disappear completely.

#### 6. *The cause of the colour-shifts*

The explanation of the colour changes by adsorption, described here, runs along the lines already developed in 1932 <sup>17)</sup>.

Modern developments in the nature of the chemical bonds in organic molecules, especially the concept of mesomerism (or "resonance") makes it possible to develop these lines somewhat further. The effect must not, as WEITZ <sup>8)</sup> does, be ascribed to a change (polarization) of the normal constitution of the adsorbed molecule, but one must rather look for the difference in adsorption energy between the ground- and excited levels of these molecules.

The normal ground level of p-nitrophenol is mainly governed by the conventional structure formula:



with the well-known "resonance" between the two possible Kékulé-structures of the benzene ring and with "resonance" between

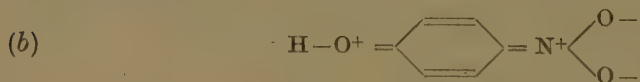


in the OH-group and between



in the NO<sub>2</sub>-group; both these last mentioned cases of "resonance" leading to the well-known dipole moments of these groups.

The excited level of p-nitrophenol may, however, mainly be presented by the formula



hence a more strongly polar structure. Light absorption causes, according to this conception an electron transition from the oxygen of the OH-group to the oxygen of the nitro-group.

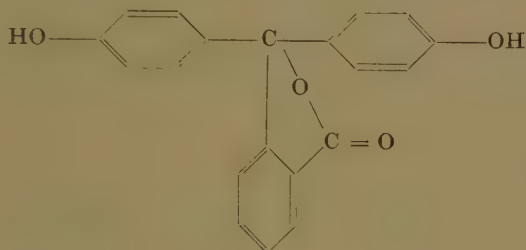
When adsorbed, p-nitrophenol has its OH-group directed towards negative ions of the surface. In the excited state, therefore, the positively charged oxygen of this group is situated opposite the negative ion of the

<sup>17)</sup> (Loc. cit. 7); see also: J. H. DE BOER, Z. Elektrochem. 44, 488 (1938).

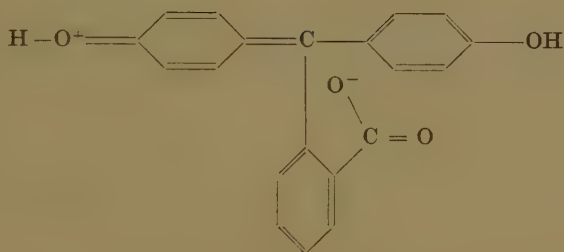


surface to which the OH-group is attached. The excited state of the molecule, consequently, is stronger bound than the ground state and this results in a shift of the light-absorption to longer wave-lengths. The F-ions of  $\text{BaF}_2$  exercise a stronger negative action than those of  $\text{CaF}_2$ , hence a stronger shift with  $\text{BaF}_2$ .

A similar explanation may be given for phenolphthalein when the ground state is written as



and an excited state as



The ground state of the azo-dye, dimethyl-amino-azobenzene may be written as



with the normal resonance structure for the benzene rings and the  $\text{N}(\text{CH}_3)_2$ -group, leading to a dipole moment of the latter.

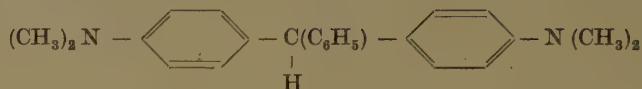
The excited state will mainly have the structure:



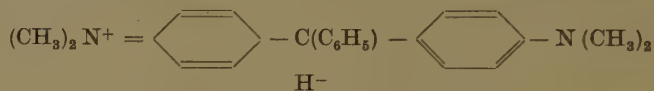
light absorption causing a transition of an electron from the N of the dimethyl-amino-group to an N of the azo-group. As the molecule is adsorbed on to the negative ions of the surface by the dipole-bearing  $(\text{CH}_3)_2\text{N}$ -group, the excited state is adsorbed more strongly than the ground state and adsorption leads to a shift of the absorption spectrum to longer wave-lengths.

In the case of the leuco-compound we must ascribe the following

formula to the ground state:



whilst the excited state may be given the formula:

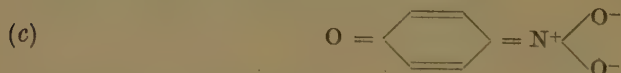


The explanation of the development of colour on adsorption is then exactly the same as in the case of the azo-dye, mentioned above.

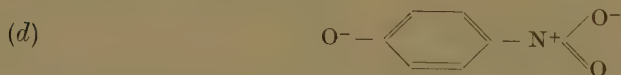
#### 7. The energy scheme of ionization of *p*-nitro phenol and of phenolphthalein

In older publications<sup>1) 4)</sup> we have compared the yellow colour of *p*-nitrophenol, adsorbed on  $\text{CaF}_2$ , with that of *p*-nitrophenolate ion by considering that the effect of the addition of a  $\text{H}^+$ -ion to the ion is counteracted by the negative fluorine ion on which the molecule is adsorbed. The argument was that addition of a  $\text{H}^+$ -ion to the yellow *p*-nitrophenolate ion results in shifting the absorption spectrum completely into the ultra-violet, but that the presence of a  $\text{F}^-$ -ion in the immediate proximity would nullify this shift. As we have mentioned in Section 1, however, the absorption of *p*-nitrophenol, when adsorbed on  $\text{BaF}_2$ , is even at longer wavelengths than that of the ion. A more satisfactory explanation may now be given along the lines, developed in the previous Section.

In alkaline solution, when  $\text{H}^+$ -ions are taken away and phenolate ions form, we have to consider the formula:



as the ground level and



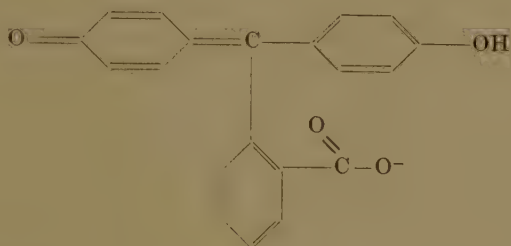
as the excited level. The normal (Kékulé) structure and the chinoide structure, therefore, reverse places with respect to ground- and excited level when the molecule is ionised. Such a reversion can easily be understood when one realises that the addition of a  $\text{H}^+$ -ion to structure *d* of the excited level of the ion will result in a very strong bond, the energy of which is comparable to that of the binding of a  $\text{H}^+$ -ion to an  $\text{OH}^-$ -ion, which is about 350 kcal/mol<sup>18)</sup>. When, however, a  $\text{H}^+$ -ion is bound to the  $\text{O} =$  of structure *c*, the energy is comparable to that of the binding of a  $\text{H}^+$ -ion to a  $\text{H}_2\text{O}$ -molecule, hence about 165 kcal/mol<sup>18)</sup>. In fig. 1 we give the ground- and excited levels of both the ions and the molecule,

<sup>18)</sup> F. J. GARRICK, Phil. Mag. (7) 8, 102 (1929).

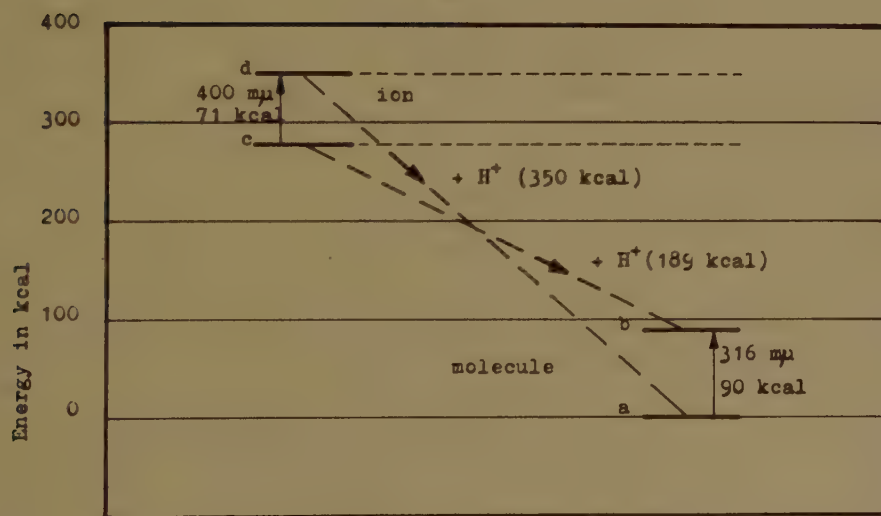
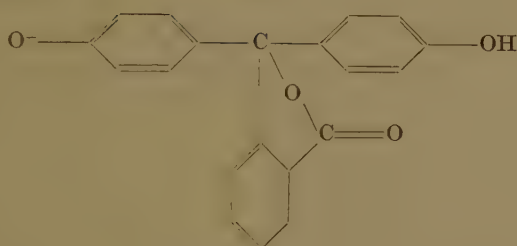
Cf. A. E. VAN ARKEL and J. H. DE BOER, La Valence et l'Electrostatique, 245 (Paris 1936).

separated by an energy distance as follows from their absorption spectra <sup>19)</sup>. It may be seen that the reversion of the structures for the ground- and the excited levels is a normal consequence of the binding of a  $H^+$ -ion to form the OH-group.

A similar reversion takes place when phenolphthalein or thymolphthalein are brought into alkaline solution and their ions are formed. The ground level, therefore, of the phenolphthalein ion may be considered as



its excited level as



*Geleen (L.) and Delft, November 1951*

<sup>19)</sup> The distance between the ground- and excited levels of the molecule (*a* and *b*) and of the ion (*c* and *d*) are taken from the maximum of the absorption bands. In order to make a more precise scheme the thermal levels should be taken, hence the Franck-Condon-principle should be applied. Fig. 1 serves only for purposes of understanding why a reversion of structures will occur.

## PHYSICS

### INCREASE OF COSMIC RAY INTENSITY IN CORRELATION WITH METEORIC ACTIVITY ON NOV. 6-7, 1951

BY

J. CLAY, H. F. JONGEN AND A. J. DIJKER

(*Natuurkundig Laboratorium Universiteit van Amsterdam*)

(Communicated at the meeting of November 24, 1951)

*Summary.* On Nov. 6-7, 1951 in the course of intensity measurements of cosmic radiation a simultaneous increase of intensity was found in 3 ionisation vessels under different shieldings of iron. This increase coincided with a period of meteoric activity of the Taurids.

Some time ago we mentioned an otherwise unexplained sudden increase of cosmic ray intensity during the passage through the atmosphere of meteoric debris following the Giacobini Zinner comet on Oct. 10, 11, 1946.<sup>1)</sup> We could not give an explanation of this coincidence, but a recent observation has strengthened the notion of a possible correlation between meteoric activity and cosmic ray intensity.

Solar activity has been reported on magnetic evidence on Nov. 6, 09.42-10.04 GMT. Simultaneous ionospheric disturbances were registered. As a solar flare is commonly followed within 20 min. to 2 h. by an increase of cosmic ray intensity lasting several hours, we may ascribe the intensity change in the unshielded ionisation vessel starting after 10.00 GMT (fig. 1 and 2) to this solar flare. The radiation of this flare evidently contained no very penetrating particles, under 12 and 110 cm Fe no appreciable enhancement was found. A striking case of this type of flare occurred May 11<sup>th</sup> 1949<sup>2)</sup>.

The continued heightened intensity in the unshielded vessel and the sudden increment of 3 % for the harder components at 17.00 GMT cannot be reasonably ascribed to this flare. We suggest that this enlarged intensity may be due to the activity of the Taurid meteors, which from 1-10 Nov. showed an extended and flat maximum with a possible peak value on Nov. 5, as was kindly reported to us by Mr. C. DE JAGER of the Utrecht Observatory. The only way in which we can imagine that this phenomenon arrived at making itself felt, was by a variation induced in the STÖRMER current by the meteors, altering the STÖRMER pass for higher energy particles.

The question arises what may be the reason, that the increase did

<sup>1)</sup> JONGEN, H. F., Proc. Kon. Ned. Ak. v. Wetensch. Series B 54, 253 (1951).

<sup>2)</sup> M. SCHEIN, Como Conference (Sept. 1949).

J. CLAY, H. F. JONGEN, A. J. DIJKER. Proc. Kon. Ned. Akad. v. Wetensch. 52, 906 (1949).



not last the whole period of 1-10 Nov. We must own we cannot answer this. From 18.00-24.00 GMT on Nov. 6 the intensity of the weaker components of cosmic radiation remains nearly constant at the

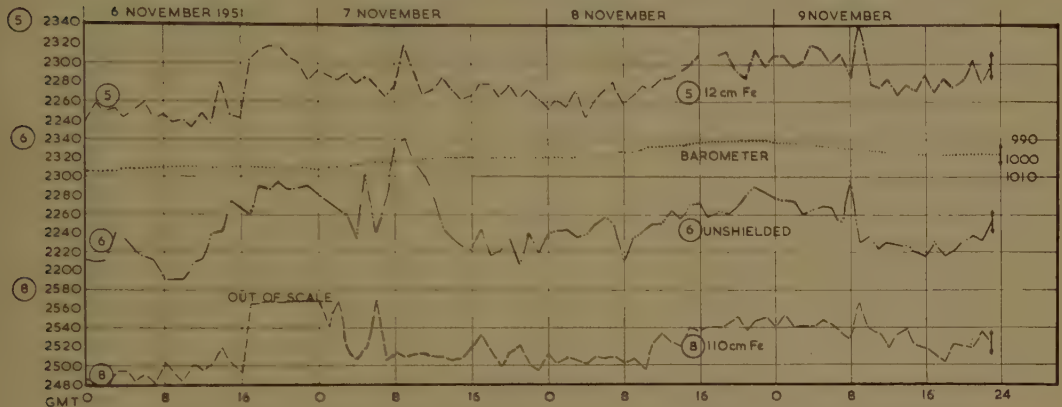


Fig. 1. Cosmic ray intensity in differently shielded vessels during meteoric activity on 6-9 Nov. 1951.

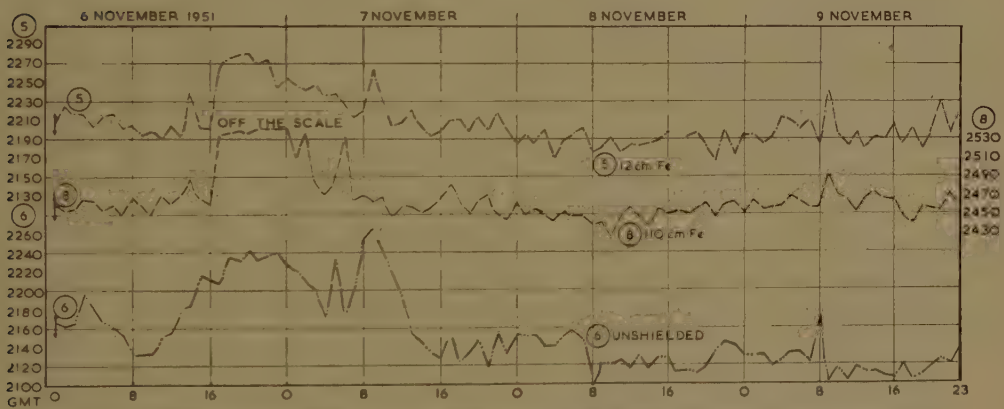


Fig. 2. Cosmic ray intensity in differently shielded vessels during meteoric activity on 6-9 Nov. 1951, corrected for barometric effect.

heightened level, the hard component keeps increasing. The exact value for the maximum of the hard component escaped registration, our instrument being unable to follow the excessive increase.

To permit an idea of the sensibility of the methods employed, in fig. 1 and 2 the intensity is given resp. without and with correction for barometric changes. The figures show at first glance that the enhancement in intensity on Nov. 8 and 9 is for the greater part due to low atmospheric pressure.

During the first part of Nov. 7 the intensity shows an irregular decrease interrupted by another maximum for the softer radiation at 09 G.M.T. This maximum, as well as the sudden peak recorded by all our instruments between 07 and 09 G.M.T. on Nov. 9 '51 may perhaps be due to the same meteor stream.

# A THIRD ARC IN MANY ISLAND ARC AREAS

BY

F. A. VENING MEINESZ

(Communicated at the meeting of November 24, 1951)

## *Summary*

In several island-arc areas a third arc seems to be present; it reaches hardly above sea-level. Three instances are dealt with, the Aves swell inside the Antillean arc, a ridge to the west of the Marianas arc and the Lucipara islands ridge in the Banda Sea which can probably be continued over the Tukang Besi Islands, south of the Tiger Islands, over the Kangean Islands and possibly over North Java. This would agree with Umbgrove's views about the idio-geosyncline of N. Java being the continuation of the Banda basin.

The writer thinks that their origin can probably be explained by crustal compression caused by the drag exerted on the crust by local convection-currents already formerly assumed by him for explaining the sinking of the basins inside the arcs, as e.g. the Banda basin, and the deep and intermediate earthquake-foci in these areas. His view is that these currents do not last long enough for crustal compression to bring about much more than a thickening of the crust; for the formation of a geosyncline and for a crustal downbulging longer periods are probably needed and, therefore, larger scale convection-currents.

As far as the writer knows it hitherto has found little or no attention <sup>1)</sup> that volcanic island-arcs which, on the outside, are often accompanied by a tectonic arc showing strong folding and overthrusting, may, at least over part of its length, be accompanied on the inside by a third arc. As far as the indications go, this third arc is neither characterized by strong folding nor by strong volcanicity; it usually shows a less irregular topography than the other arcs and it seldom comes more above sea-level than in a few isolated spots. The distance from the volcanic arc to this third arc is often somewhat larger than to the tectonic arc on the other side although other ratios of these distances may also occur. The third arc usually seems not to show marked seismicity of the shallow type as the outer arc often does.

---

<sup>1)</sup> Special mention may here be made of the study of H. H. HESS on "Major structural features of the western north Pacific, an interpretation of H. O. 5485, Bathymetric chart, Korea to New Guinea, Bull. G. S. A. 59, (May 1948); in this study HESS makes mention of the third arc in the Marianas area.

We find a clear instance of such a third arc in the Aves swell running north-south in the Caribbean sea some 200—300 km to the west of the north-south part of the main volcanic Antillean arc. Aves island is the only spot where it rises above sea-level. The swell is separated from the main arc by depths of some 3000 m.

We see a second instance on the bathymetric map of the area between Korea and New Guinea mentioned in the foot-note about the paper of H. H. HESS on page 432; the Marianas arc is accompanied by a parallel ridge some 300 km to the west of it. Farther to the north, in the Bonin and Nanpo Shoto arc area, it seems to disappear or to merge in the volcanic arc but there are slight indications of elevations to the west of this volcanic arc — though at a smaller distance from it — which might perhaps be its true continuation. The main third ridge, to the west of the Marianas arc, does not show islands rising above sea-level, but there are several spots where the depth is less than a few tens of fathoms. It is separated from the Marianas arc by an area of a depth of some 3500—4000 m.

A third instance occurs in the Banda arc, i.e. in the eastern part of the Indonesian archipelago where we have a double arc of the classical type. The Timor-Ceram arc represents the outer belt where the islands, as far as they have been investigated, show strong folding and overthrusting. Inside we find the volcanic arc which is the continuation of the row of volcanoes on the larger and smaller Sunda Islands; the active volcanic character of the arc is only interrupted in the islands north of Timor. The arc ends in the Banda Islands.

Inside the volcanic arc we find the great depths of the Banda Sea of some 4500—5000 m but directly north of this deep belt we see a third ridge rising above sea-level in the Lucipara and Turtle Islands which we may compare to the other instances already mentioned. The distance of this third ridge to the volcanic arc is here 200—250 km i.e. about  $1\frac{1}{2}$  to 2 times the distance between the volcanic and tectonic arcs. So we find similar distances here as in the former cases.

It is remarkable that this third ridge seems to continue over a great distance to the west in a course persistently parallel to the curved tectonic belt while the volcanic arc deviates in this area and continues in a nearly straight direction westwards. If this interpretation of the bathymetric map of this area is right, the ridge continues over the southeastern part of the Tukang Besi Islands, where the direction of a not intensive plio-pleistocene folding seems to be in harmony with this supposition, further over the islands Kalaotua, Kalao and Tanahdjampea, i.e. to the SE, the S. and the SW. of the Tiger Islands, and, continuing to follow the northern border of the Flores Deep and the Bali Sea, over the Postillion and Paternoster Islands to the Kangean Islands.

Whether we may perhaps even assume it to continue still further over the island of Madura and over the northern border of the oil-bearing



idio-geosyncline of Java, may be left an open question here. The distance of this border to the corresponding part of the tectonic belt south of Java of about 350 km checks well with the distance between the tectonic and the third belts in the Banda Sea area. We shall come back to this point.

The most remarkable feature in this whole area to the west of the ridge of the Lucipara Islands and of E. Timor is that the volcanic arc does not follow the curves of the tectonic and third arcs but that it continues more or less independently in a nearly straight course towards the west. It thus draws nearer and nearer to the supposed continuation of the third arc, while at the same time it draws away from the tectonic belt. This curious behaviour of the volcanic belt — of which perhaps the situation north of the Marianas is another instance — seems to indicate that the third belt is more narrowly related to the tectonic belt than to the volcanic one.

We may perhaps find more indications of a third arc in the topography of the Sea of Japan and in the Pacific southwest of the Samoa Islands and west of the Tonga Islands. We shall however, confine ourselves here to the three instances already mentioned.

In two of these three areas gravity has been determined viz. in the East and West Indies. Examining the fields of anomalies obtained we see that the third ridge does not show up by strong deviations. In both areas the anomalies over the ridge are, in the algebraic sense, somewhat less than on both sides. In the Caribbean area the Aves swell shows practically no deviation after local isostatic reduction but assuming regional isostatic compensation we find weak negative anomalies over the ridge and weak positive ones on both sides.

In the Banda area the whole field is positive but the anomalies over the third ridge are less than on both sides. Towards the north the difference is small, towards the south it is somewhat larger: supposing local compensation it is only 10—20 mgal but for regional compensation with a large degree of regionality it comes up to 60—70 mgal. In this last case the difference towards the north is 20—30 mgal. Over the supposed continuation towards the west the first part, near the Tukang Besi Islands, shows the same picture but further to the west it becomes uncertain; south of the Gulf of Bone the net of stations does not allow conclusions. Still further westwards the normal situation is again present: the anomalies over the belt are somewhat lower than on both sides and the difference is more marked for regional than for local isostatic reduction. Near the Kangean Islands the problem becomes more complicated and the same is true for a possible continuation over Madura and the north of Java, between Surabaya and Semarang.

If this last hypothesis is right, the deep basin of the idio-geosyncline of Java would have the same character as the deep Banda basin with the important difference, however, that in Java the basin has been filled up entirely with light sediments while the ridge north of it has perhaps



also been covered by them. This must have brought about changes in the field of anomalies, causing moderately negative anomalies over the basin instead of the positive ones over the Banda basin and, possibly, also reducing those over the ridge: in this last area values around zero are found. The gravity anomalies obtained are, therefore, not contradictory to the hypothesis dealt with here. We may mention that it is similar to that presented recently by UMBGROVE <sup>1)</sup>.

The question now arises what is the origin of these third ridges and how did the basins between these ridges and the other arcs come into being. We shall first take up this problem for the clearest cases where the third ridge follows a fairly straight course and where the basin has not been filled up, viz. the instances in the Caribbean, in the Marianas area and in the Banda Sea.

It seems to the writer that we can look for an explanation in two directions. In the first place we can suppose the basin to be a second downward wave of the crust inside the main one which bulged downwards in the tectonic arc. If we consider the crust to behave as an elastic plate floating on the plastic substratum, we can understand that if the lateral compression in the crust exceeds the buckling-limit, a wave-formation will occur and so, if the thickness and elastic properties are constant over a broader belt than the main downbuckling occupies, a second wave will come into being besides this main one and only a small difference in strength will decide which of the two will bulge downwards; the second one will continue to keep its shape as a crustal wave.

A deeper study of the crustal deformation makes it, however, probable that the buckling-limit far exceeds the elasticity-limit of the crust <sup>2)</sup> and that, therefore, the character of the crustal deformation has to be that of plastic flow or creep, but it can be proved that this too leads to the formation of a wave bulging downwards. Perhaps also a second wave besides this main wave is possible but whether such a second wave can indeed thus come into being is difficult to decide.

This explanation, raises serious difficulties if we try to apply it to the Banda Sea belt here considered and to the similar deeps between the third arc and the volcanic arc in the Caribbean and in the Marianas area. Instead of the gravity field showing negative anomalies over the deep and positive ones over the third ridge and the volcanic ridge, as we ought to find if we had to do with a wave-formation kept in position by the lateral compression in the crust, we see the reverse to be true; in the Caribbean and in the Banda Sea the third ridge shows smaller anomalies, algebraically speaking, than the basin and this shows positive anomalies.

Another objection is that we can not easily explain a second wave

<sup>1)</sup> See e.g.: UMBGROVE, The Origin of deep-sea troughs in the East Indies, Intern. Geol. Congress, Report of the Eighteenth Session, Pt 8, (1948).

<sup>2)</sup> F. A. VENING MEINESZ, Earth's crust deformations in geosynclines, Proc. Kon. Ned. Akad. v. Wet., Amsterdam 53, No. 1 (1950).

systematically originating on the inside of the other arcs and never on the outside.

A different explanation of the origin of the deep basins inside the island-arcs may be given by assuming convection-currents in the sub-crustal layer in these areas which must bring about temperature differences and cooling in that layer and thus, by thermal shrinking, cause differences of level at the surface. The writer has dealt with this hypothesis at some length in previous publications <sup>1)</sup> and so he may give here only a summary, referring for details to these papers. The hypothesis has the advantage to give also an explanation for the intermediary and deep earthquake-foci. Here the problem is added of the origin of the third ridge inside these basins which has formerly not been dealt with and we shall see that it can give a good explanation of it.

Before starting this summary, however, it is necessary to point out that in those areas where the main tectonic belt is rising, as it is e.g. strongly the case in the Indonesian arc east of Sumba — the cause is no doubt the tendency to readjust the highly disturbed isostatic equilibrium — deeps alongside of this belt are developing which are evidently brought about by the fact that if the belt is disengaging itself sufficiently from the neighbouring areas for being able to start such a readjustment, these adjoining areas, originally lifted up by the upward tendency of the belt, will sink back. In such a way we can simply explain the deeps on the outside of the outer Banda arc as well as those on the inside between this arc and the inner, volcanic, belt. The depth-profiles are in good agreement with this interpretation; they indicate that these deeps have another origin than the deep basin inside the volcanic arc; the profiles have a more local character than the latter, as e.g. the profiles of fig. 1 and fig. 2 show. If we lower the areas of the Kay Is. (fig. 1) and of the Tanimbar Is. (fig. 2) and raise the floor of the deeps on both sides, the remaining profile shows a gradual slope downwards towards the Banda Sea.

The base of the convection-hypothesis for explaining the deep basins inside the volcanic arc is the thermal disturbance brought about in these areas by the concentration of sialic matter in the main tectonic belt where the crust is downbulging; sial has a higher content of radio-activity than the deeper layers and so the downbulge must act as a cause of heating. Thus temperature gradients come into being in the subcrustal layer with horizontal components and this must provide a trigger-effect for the overcoming of the stabilizing effect caused by the small strength-

---

<sup>1)</sup> F. A. VENING MEINESZ, Deep-focus and intermediate earthquakes in the East Indies, *Proc. Kon. Ned. Akad. v. Wetensch.*, Amsterdam **49**, No. 8 855—864 (1946).

F. A. VENING MEINESZ, Convection-currents in the Earth, *Proc. Kon. Ned. Akad. v. Wetensch.*, Amsterdam **50** No. 3, 237—245 (1947).

F. A. VENING MEINESZ, Gravity Expeditions at Sea, 1923—1938, WALTMAN (A. J. MULDER), 37—63 (Delft, 1948).

limit of this layer which must otherwise prevent this layer to come into convection movement under the effect of the vertical temperature gradient brought about by the Earth's cooling. It is clear that another condition for convection is the homogeneity over sufficient thickness of the subcrustal layer.

The writer has made an estimate of the time needed for a newly developed sialic downbuckle of the size as now present in the Banda area to lead to a sufficient temperature disturbance for the overcoming of the

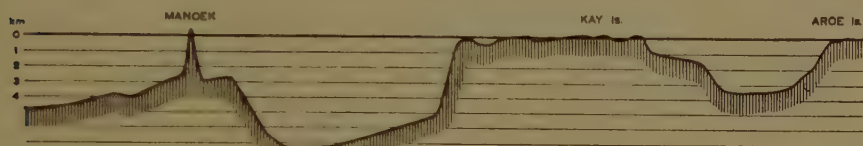


Fig. 1. Depth-profile *Banda Sea—Aroe Is.* hor. scale 1 : 5,000,000; vert. scale 1 : 500,000; line-interval 1000 m.

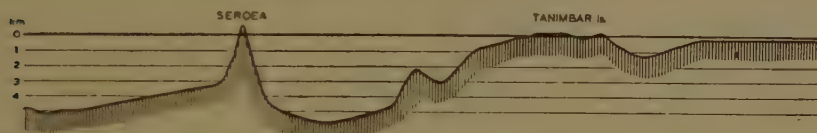


Fig. 2. Depth-profile *Banda Sea—Tanimbar Is.* hor. scale 1 : 5,000,000; vert. scale 1 : 500,000; line-interval 1000 m.

strength-limit mentioned and he found a figure of some 10—12 million years. The data required for this computation are uncertain and so no precise figure can be obtained. We thus come to the conclusion that we may expect a period of strong folding to lead to a convection-current in the subcrustal layer but only after a considerable time-lag of the order as mentioned.

We may further expect such a current to reach a maximum speed after having made a quarter of a revolution and to come to a stop after about half a turn; after a quarter of a turn we may expect the temperature difference of the sinking and the rising columns to be a maximum and after about half a turn stability must have been reestablished, the denser matter of lower temperature being down and the lighter matter of higher temperature on top. In this schematic picture temperature-conduction has been considered to play only a subordinate part with regard to the effect of heat transport by the current.

Figure 3 gives a cross-section of the two-dimensional current-system as derived on the base of supposing stable convection, i.e. assuming a convection-current of constant speed continuing indefinitely, working in cells of which only one is represented and brought about by a vertical gradient diminishing according to an *e*-function towards the depth. If we assume the gradient to have been caused by cooling since a previous convection-system had destroyed an older gradient system, the last



supposition seems reasonable. The first, however, is certainly not true as we have mentioned above that the current must have a temporary character with variable speed. Neither can it be right that the convection-current occurs in a row of cells; the way the current is started by a trigger-effect overcoming the strength-limit of the subcrustal layer, must bring about only one cell with a rising current under the tectonic belt and developing towards the side of least resistance which no doubt must be the inside of the arc. Both deviations from the real conditions must

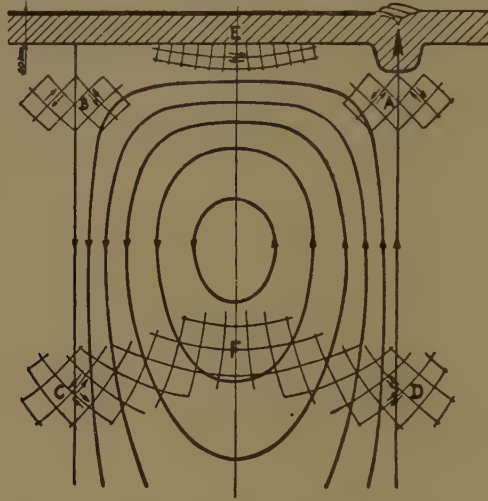


Fig. 3. Cross-section of supposed convection-current in substratum under the Banda Sea; A, B, C, D, E, and F areas of maximum shearing-stress, directions of shearing-stress indicated.

evidently affect the shape of the current. It is, however, difficult to derive a better approximation but, in drawing conclusions, this uncertainty must be kept in mind.

Figure 3 shows the crust with the downbulge near *A* and below it the substratum with the streamlines of the current and the direction of the shear in the areas *A*, *B*, *C*, *D* and *E* where it has maximum values.

The following consequences of such a convection-current may be expected. In the first place we must expect a general speeding up of the Earth's cooling in these areas. We may say it also in this way that the lower temperature must be transported downwards and that this, by conduction, must have a cooling effect on the layer below the current-system while the higher temperature transported upwards disappears for a great part by radiation. The result of this excess of cooling must be a thermal shrinking and, therefore, a sinking of the Earth's surface over the whole area. This mean subsidence may be estimated at roughly some 1500 m; the figure is uncertain.

In the second place we may expect that during the period the current is there, the lower temperature in the sinking column must give a sub-



sidence at the surface above it and the higher temperature in the rising column a rise. The difference in elevation thus brought about may be estimated at some 4000—5000 m. Combined with the former effect we find a subsidence over the sinking column, viz. over the area on the inside of the arc, of some 4000 m and a much smaller rise of about 1000 m over the tectonic belt. Both figures are uncertain, the figure for the sinking gives an order of magnitude, that for the rising may also disappear entirely and possibly even be slightly negative.

We thus see that the convection-hypothesis can give a good explanation of the sinking down of the Banda basin and also of the period of its formation at the end of the pliocene or in the pleistocene, i.e. with a time-lag of some 10—20 million years after the last period of strong folding in the main tectonic arc which took place in the tertiary ( $f 2^1$ ). The recent rising of this last arc and of the volcanic arc can thus likewise be understood.

A third consequence of the presence of the subcrustal current must be the causing of tension in the crust over the rising column, i.e. in the area of the tectonic arc, by the horizontal drag exerted by the current. This is in remarkably good agreement with the actual data. In the first place the strong rise of the tectonic belt in the pleistocene and the sinking down of the deeps on both sides points, as it has already been mentioned, to a sufficient disengaging of the tectonic belt from its environment for allowing a beginning of its isostatic readjustment and a sinking back of the neighbouring belts. Besides this evidence of at least a decrease of the compression we have also that of the graben formed in the tectonic belt during the pliocene pointing in the same sense. This appears to indicate that the current started already at that time.

In the fourth place we may mention the location of the strongest shear, as indicated in fig. 3 in *A* and *C*, which checks with the position of the earthquake foci of the deep and intermediate earthquakes, while the direction of the shear-planes and the sense of the relative movement in these foci <sup>2</sup>) are also in good agreement with the available data. We shall not go deep into these questions here, nor in possible explanations of the fact that the areas *B* and *D* of maximum shear do not usually seem to be characterized by earthquake foci although perhaps a few instances do occur: for these questions the writer may refer to the papers mentioned above.

The number of facts which can be understood by means of the hypothesis of convection-currents appears to be such that it deserves certainly

<sup>1</sup>) For these and other statements about the geology of Indonesia the writer is indebted to UMBROVE's papers on this subject, e.g. *Structural History of the East Indies* (Cambridge Univ. Press. 1949).

<sup>2</sup>) See L. P. G. KONING, *Het mechanisme in den haard van diepe aardbevingen* (Van Campen, Amsterdam 1941), also a doctor's thesis by Drs A. R. RITSEMA, *Over diepe aardbevingen in de Indische Archipel* (Univ. of Utrecht, 1952).

serious consideration. If accepted they would point to dimensions of these current-systems corresponding to a distance of the axis of the rising and sinking currents of 300—600 km and depths of about the same size or slightly greater. Their presence would involve the assumption of a homogeneous subcrustal layer of sufficient thickness to allow such currents to develop, i.e. of at least some 600 km. It is true that the seismic results seem to show that below a depth of about 200 km a gradual increase of density occurs <sup>1)</sup> but there is a possibility that this is caused by a change of phase of the same substance and so this result need not be considered as an unsurmountable obstacle against the hypothesis of convection. We shall not further enlarge here on this problem.

For the subject of this paper it is of special importance that the drag exerted by the current on the crust must be considerable. For a speed in the axis of the current of the order of 5 cm/year, corresponding to a time of 4.000.000 years for a quarter revolution — which is possibly about the time-interval elapsed since its beginning — we find a maximum shear exerted on the crust (in point *E* of fig. 3) of about 1600 kg/cm<sup>2</sup>. Assuming the distance from rising to sinking axis to be ten times the thickness of the rigid crust, we could thus expect a compressional stress in the crust over the sinking current of the order of 10.000 kg/cm<sup>2</sup>. There can be no doubt that the crust can not stand such a stress and so it must have given way by plastic flow or by creep. As it has been dealt with by the writer in a previous paper <sup>2)</sup> such a deformation must have started as a thickening of the crust in such a way that upward and downward crustal bulges develop in the ratio needed for isostatic balance. Though present from the start it is only after a long time-interval, possibly to be counted in millions of years and dependent on the coefficient of apparent viscosity (or creep?) of the crust, that another tendency becomes perceptible, viz. a downward bending which gradually gains in speed and takes the upper hand, thus leading to the development of a geosyncline and, in a still later period, its major downbulging.

It seems likely that in our case of the formation of the third ridge these latter stages are never developing because the local current-systems here dealt with do not last more than a few million years, i.e. not long enough for bringing about the geosyncline or downbulging stages, and that thus the phenomenon stops after having caused a crustal thickening in isostatic equilibrium, or perhaps with a slightly larger root than would correspond to the upper ridge, because of the beginning of a downbending tendency. When the current stops, isostasy, probably never strongly disturbed, must reestablish itself. According to this view-point only large

---

<sup>1)</sup> See e.g. FRANCIS BIRCH, Remarks on the Structure of the Mantle and its bearing upon the possibility of convection currents, *Trans. Am. Geophys. Union*, 32, No. 4, 533, (1951); see also *ibid.* p. 531 by the writer.

<sup>2)</sup> F. A. VENING MEINESZ, Earth's crust's deformation in Geosynclines, *Proc. Kon. Ned. Akad. v. Wetensch.* 53, No. 1 (1951).

scale convection-currents of depth-dimensions comparable to the thickness of the mantle of the Earth and lasting several tens of millions of years can bring about the great geosyncline developments.

If the writer is right in his conjecture — he is conscious of its speculative character — the third ridge in island-arc areas could well originate in the way here described as a result of local convection, but it would be possible that they may not be the result of only one current-system but of several consecutive systems, each one being an after-effect of a major tectonic deformation in the main belt.

According to our view-point the third ridge ought more or less to occur over the sinking current, i.e. over the area where the deep foci occur. As the relation is only an indirect one and the coupling agent a temperature distribution, we can not expect a strong correlation. In general we find this rough correlation to be present. A satisfactory side of our hypothesis is that it provides for a stronger relation of the third ridge to the tectonic arc than to the volcanic one.

A last point may shortly be touched on, viz. the question whether, as Umbgrove supposes, the idio-geosyncline in Java is the continuation of the Banda basin and the ridge in North Java between Surabaya and Semarang the prolongation of the third ridge in the Banda Sea. There is much in favour of this hypothesis. It would e.g. explain the presence also in the Java Sea of deep earthquake-foci as, according to this view, the local convection-current would continue here. This current would have brought about the idio-geosynclines in the same way as it caused the Banda basin to sink down. This view about the development of the idio-geosynclines seems attractive; it appears more acceptable than the formation as a second wave accompanying the main wave in the tectonic belt, especially since this main wave is now considered to have originated as a deformation of the plastic or creep type. This view-point does not affect the idea that lateral compression in the crust must also have its effect and must tend to deepen waves already present; such a deepening must be accompanied by a moderate folding of the sedimentary contents of the idio-geosyncline. The folding towards the end of the pliocene or the beginning of the pleistocene may well have had this character, the crustal compression being brought about by the combination of the general large-scale convection and the local convection.

If this view about the origin of the idio-geosynclines is right, it appears likely <sup>1)</sup> that the formations of this type in Indonesia have developed in at least three stages; during the first stage, in the eocene, the idio-geosynclines of N. Sumatra and E. Borneo, during the second, in the tertiary, those in middle and S. Sumatra and in W. Java, and during the last that of E. Java, brought about, at least partly, by the current which is still there.

<sup>1)</sup> See e.g. J. H. F. UMBGROVE, Geological history of the East Indies, Bull. A. A. P. G., p. 39 e.s. and map p. 41 (Jan. 1938).

A deeper study of the problems raised in this paper and especially of the extension of the formation towards E. Java via the curved course between the Banda Sea and E. Java as mentioned may be reserved for a later paper. The same may be done for the investigation of the problem we shall not further deal with here, why the course of the volcanic belt between the tectonic arc and the third ridge is so erratic, being near to the first in the Banda area, avoiding the curved course of the other two ridges further westwards and approaching the third ridge in Java, thus nearly coinciding there with the axis of the idio-geosyncline. As we have already mentioned an analogous curious behavior of the volcanic ridge is found in the Marianas-Nanpo Shoto arc.



## A MODEL OF THE EARTH'S CRUST

BY

J. H. F. UMBGROVE

(Communicated at the meeting of October 27, 1951)

Stimulating discussions during and after the "COPEI" meetings<sup>1)</sup> which were held in Hershey, Penns. (1950) and in Brussels (1951) lead the present author to re-study the various aspects of the crust-substratum concept. Such a procedure is needed, time and again, when prevailing views do no longer stand the accumulating evidence of new data. The new data belong to different fields of research (gravimetric, seismic, thermal, experimental, petrological and volcanological).

In the following preliminary communication a strongly condensed summary of the results obtained so far is presented for further discussion. A full treatment of the subject will be published elsewhere in due time.

The fundamental basis of the crust-substratum concept was laid by BARRELL in his classical papers on the strength of the earth's crust, published in 1914. He clearly showed the necessary acceptance of lateral displacement of material accomplished by flow in a layer which is unable "to resist stress-differences above a certain small limit. Its name, therefore, is the sphere of weakness — the asthenosphere."

BARRELL's conclusion is supported by an ever growing accumulation of evidence. For, indeed, geological observations lead to the irrefutable conclusion that sub-crustal material is able to become displaced over appreciable distances in both vertical and horizontal directions. We need only think of such phenomena as the formation of deep basins, geosynclines, mountain-roots and the reverse movements of the earth's surface accompanying mountain-building elevation, denudation, the formation of marginal troughs along one or either side of a rising mountain belt, subsiding border-lands and shelf areas.

The many-sided main problem concerns the thickness of the crust and the material of which crust and substratum consist. A picture of the outer layers of the earth ought to be consistent with a great variety of geophysical and geological phenomena. Among these are the distribution of high standing continents and deep lying oceans floors, the character and distribution of volcanic and plutonic phenomena, the temperature of extruded lavas, the velocities of seismic waves as well as the density-distribution, elasticity, bulk modulus, and strength of the corresponding

---

<sup>1)</sup> Committee on Physics of the Earth's Interior.

material, the presence of discontinuities as deduced from seismograms, the gravity observations at sea and on the continents, the heat flow observed at the earth's surface and on the floor of the oceans, and experimental results on high pressure and temperature. Last but not least our picture ought to be consistent with a multitude of phenomena known from the unravelling of the geological history of the earth's surface features.

The model of the earth's crust which is tentatively and diagrammatically depicted in the accompanying textfigure, fig. 1, shows four crustal columns, viz. a normal sea-level continent, a continental section across a mountain root, the continental margin, and a typical oceanic cross-section of the crust.

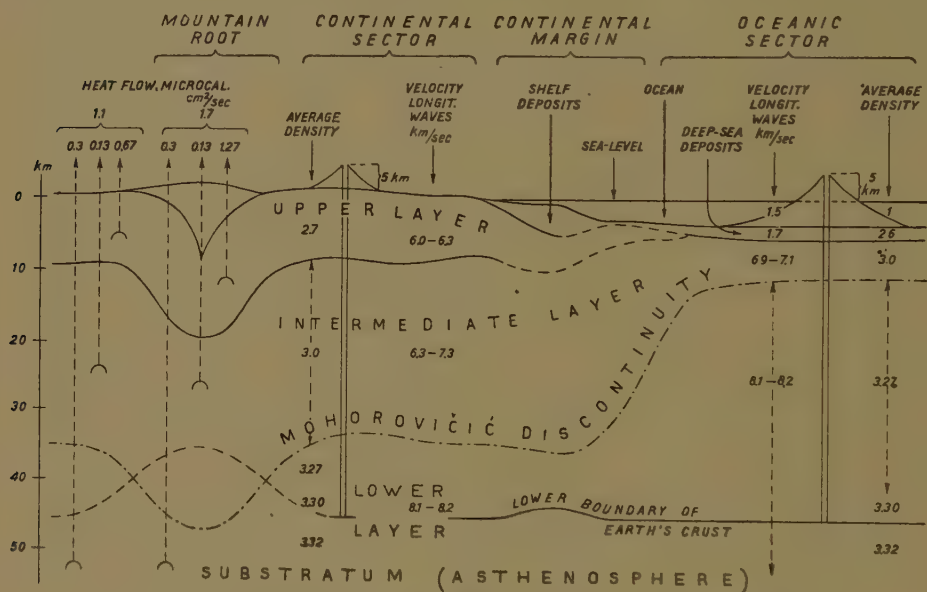


Fig. 1. Tentative and diagrammatic model of the earth's crust.

On gravimetric evidence the boundary between crust and substratum lies at a depth of a few tens of kilometres, and is probably of the same thickness in both continental and oceanic sectors (VENING MEINESZ). A crustal thickness in the order of a few km or of a few hundreds of kilometres seems out of question.

The concept of isostasy postulates comparatively heavy material at a higher level under the oceans than under the continents. And the oceanic sectors appear to be largely in isostatic balance with the continents. This is corroborated by seismic evidence.

Seismological evidence points to the existence of an upper layer in the continents with average thickness of 10 km resting on an "intermediate" layer with thickness 25 km, which in turn rests on a so-called lower layer. The velocities of longitudinal waves are up to about 6.3 km/sec. in the

upper layer, they increase up to about 7.3 km/sec. at the Mohorovičić discontinuity which is the boundary between the intermediate and lower layers.

Admittedly the idea that the material of the crust lies in essentially horizontal layers is a purely statistical concept. Actually the structure of the crust is much more complex. The thickness of the upper layer shows considerable variation. In some areas a distinction of the boundary between upper and intermediate layers is hardly possible.

The density of the upper layer which is also designated by the name "granitic layer" is about 2.7, the average density of the intermediate layer is taken at 3.0 corresponding with basic rocks such as basalt, gabbro and diabase. The average density of the lower layer is about 3.30 to 3.32. The suggested thicknesses and densities of the layers are approximations liable to change. The lower layer is usually identified as "ultra-basic" by seismologists. This is probably a premature conclusion inasmuch as similar velocities may occur in basic rocks in a dense phase.

Seismologists usually consider the Mohorovičić discontinuity as the lower boundary of the crust. This is not necessarily so. In the oceanic sectors the lower boundary of the crust lies decidedly much deeper than the Mohorovičić discontinuity. Probably it lies also at a deeper level under the continents.

Thermal evidence is found to be consistent with the thicknesses of the granitic and intermediate layers as indicated by seismology (JEFFREYS).

The "upper" layer of seismologists is probably non-existent in the oceanic sectors. The intermediate layer appears to be comparatively thin, in the order of 5 km. It rests on the "lower layer". In the Atlantic velocities of 6.9 — 7.1 and 8.1 — 8.2 were found characteristic of the intermediate and lower layers respectively.

This oceanic type of crust was found in the Atlantic west and east of the Mid-Atlantic Ridge (EWING, TEIXEIRA). Probably the Pacific Basin proper, i.e. the area within the boundaries of the andesite line has the same type of crust. The same probably holds good for the Arctic Basin and part of the Indian Ocean.

At our present state of knowledge any theory on the petrographic composition of the dense layer in the crust below the Mohorovičić discontinuity is a pure speculation. The possibility remains that it represents the dense phase of one or more basic rocks, but it would be a mere speculation to introduce terms like eclogite or amphibolite for it.

Possibly a thin "upper" layer does exist in part of the northern Atlantic (HILL). Certain parts of the Pacific, for example between the Easter Island Rise and South America, and between the Marianas and the Asiatic continent show indications of the existence of a thin "upper" layer, according to GUTENBERG and RICHTER. Between the Carlsberg Ridge and the African continent is another area where a thin "upper" layer is supposed to be present, in the opinion of POISSON and ROTHÉ.

More data are needed in order to furnish either confirmation or negation of these suppositions.

Volcanoes and outflows of lava appear to be bound to certain limits of height. But the elevation of the volcanoes in the Pacific (if measured from the floor of the ocean on which they rest) greatly surpasses the average elevation of basaltic volcanoes on the continents. The upper limit of volcanic growth is a quite self-evident fact if we accept that the maximum height is controlled by the total pressure exerted by the crust on the top layer of the substratum whence the basaltic material is supposed to derive (DALY). If an average density of 2.7 is taken for basalt in the molten condition it follows that the thickness of the continental crust is in the order of 45 km, accepting the densities of the crustal layers mentioned in fig. 1. For the sake of argument the lower boundary of the crust has been taken at that level in fig. 1.

The same height above sea-level can be reached in the oceanic sectors if we accept a column 33 km thick of density 3.27 between the Mohorovičić discontinuity, as found by EWING, and the lower boundary of the crust (or 28 km density 3.27 plus 5 km density 3.3). However, if we accept 2.6 as the density of fluid lava the best value for the lower boundary of the earth's crust is approximately 40 km. And if the density of fluid lava were 2.5 the lower boundary of the continental crust could coincide with the Mohorovičić discontinuity at a depth of approximately 35 km.

The wide distribution of basaltic lava in space and time, both on the continents and in the ocean sectors shows that reservoirs or pockets of basaltic material in a potentially eruptible state must have originated practically everywhere under the crust, though temporarily and locally.

The ultimate source of the basaltic material as well as of the volatiles and heat involved may lie deeper down in the mantle. This conclusion is quite consistent with the considerations advanced by RUBEY, KULP, and BIRCH concerning the source of water and other volatiles. Transfer to higher levels may possibly take place along zones of shear including those along which deep-focus earthquakes originate. Whether the material of the uppermost part of the substratum is crystalline, vitreous, or in a two-phase condition (DALY) remains an open question.

Whatever the situation may be it appears that ultra-basic material, like peridotite or dunite exists at a comparatively short distance beneath the crust. For with very violent eruptions dunitic material is brought up to the surface together with other less deep-seated material (e.g. in the kimberlite pipes of S. Africa). And a second argument is found in the remarkable time-relations of ultra-basic intrusions in fold-belts (H. H. HESS).

From the temperature estimates it would appear that throughout the earth's crust the temperature is everywhere well below those required for melting the material, either granitic or basaltic.

The temperature distribution changes very much as soon as the granitic



layer is thickened in down-warped areas (geosynclines and basins) and — *a fortiori* — in areas where a mountain root formed.

In a thickened crust the granitic root will disintegrate due to the temperature in the root. The disintegrated material will force its way upward and after denudation appear as granite batholiths.

The conception of a mountain root originally based on the interpretation of the isostatic anomalies (VENING MEINESZ) is supported by seismic evidence (GUTENBERG) and thermal evidence (BIRCH).

The left-hand side of the model shows BIRCH's data on heat flow in a normal continental area and in a fold-belt, and his analysis of the flow of heat into three components.

In previous publications the present author tried to show that an adequate model of the earth's crust ought to account for the remarkable phenomenon known as magmatic cycles. The explanation which was then put forward still holds good in its main outlines, though a few minor changes have to be introduced. In a few words the following general picture may be sketched.

If the crust becomes thickened due to the formation of a mountain root the crustal basalt of the intermediate layer probably will push sideways the material of the substratum. Hence temporarily the boundary between densities 3.0 and 3.27 — 3.32 (i.e. the Mohorovičić discontinuity) will shift downward. At this stage ultra-basic material may intrude the root and the overlying sediments. But due to the extra radioactive heat furnace of the root the mobility boundary will shift to a higher level. The fusing downward bulge of the lower part of the crust may give rise to basaltic extrusives. After folding of the contents of the geosyncline the sialic root of the upper layer disintegrates and gives rise to the gradual ascent of granite batholiths.

The author feels sincerely indebted to several colleagues for their elucidating and stimulating discussions of problems of the earth's crust. He owes special thanks to Dr FRANCIS BIRCH, Dr WALTER H. BUCHER, Dr M. EWING, Dr W. HEISKANEN and Dr F. A. VENING MEINESZ.

#### REFERENCES

- BARREL, J., The strength of the earth's crust. *The Journal of Geology*, 22, 655—683 (1941).
- BIRCH, F. and BANCROFT, D., The elasticity of glass at high temperature, and the vitreous basaltic substratum. *Americ. Journ. of Sc.* 240, 457—490 (1942).
- , et al. Handbook of physical constants. *Geol. Soc. of America. Special Paper* 36 (1943).
- , Flow of heat in Front Range, Colorado. *Bull. Geol. Soc. of America*, 61, 567—630 (1950).
- , Recent work on the radioactivity of Potassium and some related geophysical problems. *Journ. of geoph. research*, 56, 107—126 (1951).
- DALY, R. A., The roots of volcanoes. *Transact. Americ. Geoph. Union Rep. General Assembly* (1938).

- , Nature of the asthenosphere. *Bull. Geol. Soc. of America* **57**, 707—726 (1946).
- EWING, M., et al. Crustal Structure and Surface-wave dispersion. *Bull. Seismology Soc. of America*, **40**, 271—280 (1950).
- , Seismic investigations in great ocean depths. U.G.G.I., Assoc. d'Océanogr. physique. Abstracts of communications. Assembly Brussels 1951, 45—46 (1951).
- GUTENBERG, B., Seismological evidence for roots of mountains. *Bull. Geol. Soc. of America* **54**, 473—496 (1943).
- , Crustal layers of the continents and oceans. *Bull. Geol. Soc. of America* **62**, 427—440 (1951).
- HEISKANEN, W., On the isostatic structure of the earth's crust. *Ann. Acad. Sci. Fennicae. Ser. A* **3**, 22, 1—59 (1950).
- HILL, M. N., Seismic refraction shooting at a point in the eastern Atlantic. U.G.G.I. Assoc. d'Océanogr. physique. Abstracts of communications. Assembly Brussels, 55 (1951).
- JEFFREYS, H., Earthquakes and mountains, sec. ed. (Methuen London) (1950).
- KULP, J. L., Origin of the hydrosphere. *Bull. Geol. Soc. of America* **62**, 326—328 (1951).
- ROTHÉ, J. P., Discussion sur la structure du fond de l'océan Atlantique, U.G.G.I. Assoc. d'Océanogr. physique. Abstracts of communications. Assembly Brussels, 59—60 (1951).
- RUBEY, W. W., Geological History of Sea-water. *Bull. Geol. Soc. of America*, **62**, 1111—1147 (1951).
- TEIXEIRA, C., A propos d'une hypothèse sur la structure de l'Océan Atlantique. *Museu e Laboratório Mineralógico e Geológico da Universidade de Lisboa. Bull. no. 18*, 1—13 (1950).
- UMBROVE, J. H. F., The Pulse of the Earth 78—81 (2d Ed. Nijhoff, The Hague, 1947).
- , Symphony of the Earth 138—142 (Nijhoff, the Hague, 1950).
- VENING MEINESZ, F. A., Gravity over the Hawaiian archipelago and over the Madeira area; conclusions about the earth's crust. *Proceed. Nederl. Akad. v. Wetensch.* **44**, 1—12 (1941).

## CRYSTALLOGRAPHY

THE MOLECULAR STRUCTURE OF TRANS  $\beta$  IONYLIDENE CROTONIC ACID

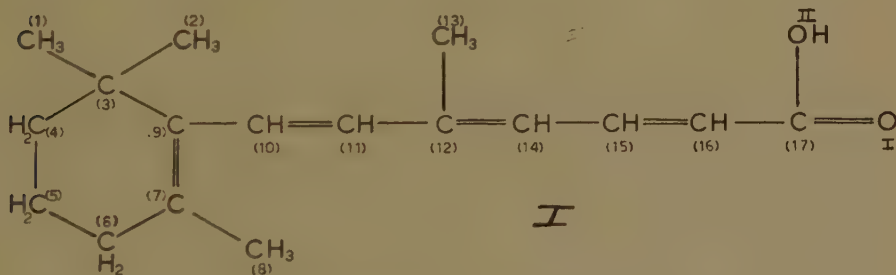
BY

CAROLINE H. MacGILLAVRY, A. KREUGER AND E. L. EICHHORN

(Communicated at the meeting of Nov. 24, 1951)

*Trans*- $\beta$ -Ionylidene Crotonic acid (I) was prepared by D. A. VAN DORP and J. F. ARENS<sup>1</sup>) as a first step in their vitamin A synthesis. In view of the interest centered around the question of isomerism of the carotenoids and related compounds<sup>2</sup>) it was thought worthwhile to start with an investigation of this comparatively simple compound, which, however, shows already some of the characteristics of the carotenoid structures: i.e. the substituted cyclohexene ring and a beginning of the long conjugated bond system with a "side chain" at every fourth carbon atom.

According to L. PAULING<sup>3</sup>), double bonds such as 10 = 11 can only be *trans* on account of steric hindrance between the methyl group C (13) and the hydrogen atom at C (10). The same evidently holds for the double bond 15 = 16 in the acid (I).



The morphology of  $\beta$  Ionylidene Crotonic acid and its optical properties were described by W. G. PERDOK<sup>4</sup>). In accordance with his results we found the acid to be triclinic. Weissenberg diagrams about the *c*- and *a*-axes gave the following cell dimensions:

$$\begin{array}{ll} a = 9,90 \pm 0,04 \text{ \AA} & \alpha = 109^\circ \\ b = 12,87 \pm 0,05 \text{ \AA} & \beta = 128^\circ \\ c = 7,24 \pm 0,03 \text{ \AA} & \gamma = 67^\circ \end{array}$$

<sup>1</sup>) DORP, D. A. VAN, and J. F. ARENS; Rec. Trav. Chim. **65**, 338 (1946).

<sup>2</sup>) KARRER, P. and E. JUCKER, "Carotenoids" p. 39 (Elsevier 1950).

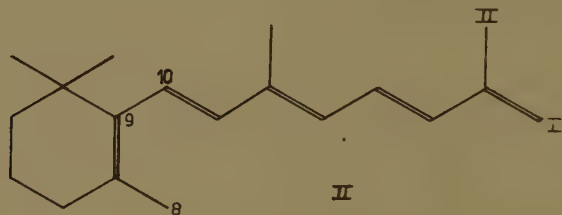
<sup>3</sup>) PAULING, L., Fortschr. Chemie Org. Naturstoffe, **3**, 203 (1939).

<sup>4</sup>) PERDOK, W. G., private communication.

The space group was assumed to be  $P\bar{1}$  for the following reasons:

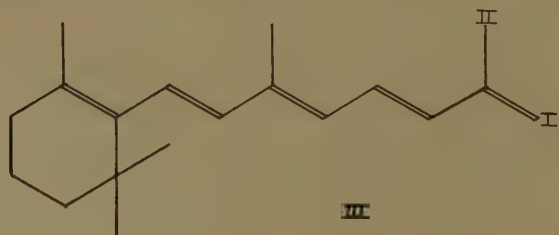
1. The development of the crystals shows no indication of polarity.
2. Carboxylic acids are mostly linked by a symmetry centre; there are two molecules per unit cell.
3. The intensities show great variety; there are strong ones and a considerable number of possible diffraction spots is missing.

The solution of the crystal structure, with nineteen about equally heavy atoms in general position, is made comparatively easy because of some striking features in the diagrams. In the equator about the  $a$ -axis, the plane  $(0\bar{3}1)$  gives strong reflections in the first, second and third order. This indicates that both molecules lie in this plane: indeed, the spacing,  $d_{0\bar{3}1} = 3,64 \pm 0,02 \text{ \AA}$  is a very plausible value for the thickness of a practically plane molecule. The position of the molecules was further specified by some reflexions  $hk0$  at high  $\theta$  values, which evidently correspond with the periodicity of the conjugated zigzag chain.



Starting from the "conventional" formula (II) no refinement of parameters could be obtained in the  $c$ -projection. We then tried configuration (III) which has been advocated by BRAUDE c.s.<sup>5)</sup> on not too convincing spectroscopic and sterical grounds. It is clear that configuration (II) with a *cis*-arrangement about the single bond 9—10 gives the same sort of steric hindrance between  $\text{CH}_3$  (8) and H at C (10) as discussed by PAULING with respect to the double bonds. Indeed, if the conjugation is sufficiently strong, rotation about the single bonds ought to be appreciably hindered so that *cis-trans* isomerism can be expected for them as well.

It was found that configuration (III) could be rapidly refined by repeated twodimensional Fourier summations. Fig. 1 shows the 5th



<sup>5)</sup> BRAUDE, E. A., E. R. H. JONES, H. P. KOCH, R. W. RICHARDSON, F. SONDEHEIMER and J. B. TOOGOOD, J. chem. Soc. London, 1890 (1949).





Fig. 1. Electron density of *trans*- $\beta$ -ionylidene crotonic acid projected along the *c*-axis. Contour levels on arbitrary scale. No contour lines have been drawn below the  $F_{00}$  level.



Fig. 2. Electron density projected along the *a*-axis. Contour lines as in Fig. 1. The repetition of the molecule by *c*-translation, in the upper left hand corner of the figure, has been omitted for simplicity.



synthesis of the structure projected along the  $c$ -axis, fig. 2 the second synthesis in  $a$ -projection. The latter shows the layerlike arrangement of the molecules in plane  $(0\bar{3}1)$ .

We wish to thank Dr D. A. VAN DORP who not only drew our attention to the problem but also provided the substance and gave us most generous and enthusiastic support in this research. We also gratefully acknowledge financial support from the Organisation ZWO and from the Rockefeller Foundation.

A three-dimensional synthesis is now in the course of preparation. Full details will be given elsewhere.

*Lab. for general and inorganic Chemistry  
University of Amsterdam*

# THE STERICAL CONFIGURATION OF TROPINE AND $\psi$ -TROPINE <sup>1)</sup>

BY

F. L. J. SIXMA, C. M. SIEGMANN AND H. C. BEYERMAN

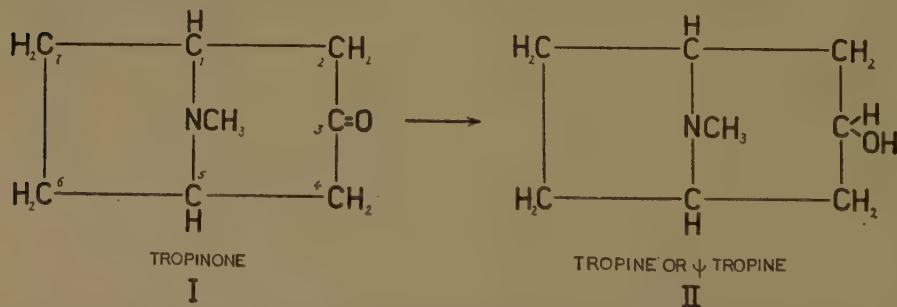
(Communicated by Prof. M. W. WOERDERMAN at the meeting of November 24, 1951)

The probable stereochemical configuration of tropine and  $\psi$ -tropine and their methiodides has been established by measuring the saponification velocities of the corresponding benzoic and *p*-nitrobenzoic esters.

## § 1. Introduction

Though the constitution of the stereoisomeric alcohols tropine and  $\psi$ -tropine was established already fifty years ago [1], their complete stereochemical configuration has not been elucidated so far. In connection with the investigations of J. P. WIBAUT and his collaborators in this laboratory into the tropane alkaloids [2], we have tried to solve this problem, which is also of considerable interest in connection with the differences in pharmacological action shown by the tropeines and the  $\psi$ -tropeines.

Tropine occurs in very small quantities in *Atropa Belladonna* [3] and is found as *l*-tropyatropeine (hyoscyamine) in various *Solanaceae*; it is the alcohol of the well-known mydriatic atropine (*dl*-tropyatropeine).  $\psi$ -Tropine occurs as benzoyl- $\psi$ -tropeine (tropacocaine) in the leaves of a species of *Erythroxylon Coca* in Java and as tiglyl- $\psi$ -tropeine (tigloidine) in *Duboisia Myoporoides*. Both alcohols (II) have been prepared by reduction of the corresponding ketone tropinone (I) under suitable conditions.



When reduced by sodium amalgam and dilute hydrochloric acid  $\psi$ -tropine is formed [4], whereas reduction with hydrogen and platinum

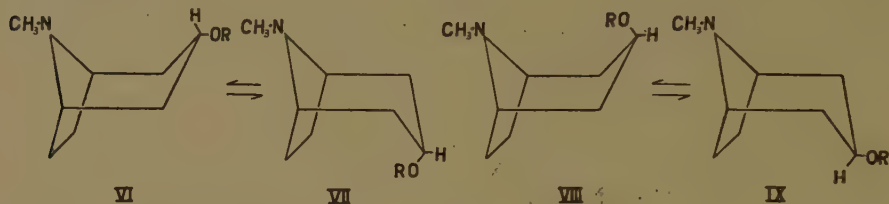
<sup>1)</sup> Details of this investigation will be published in the *Recueil des Travaux Chimiques des Pays-Bas*.





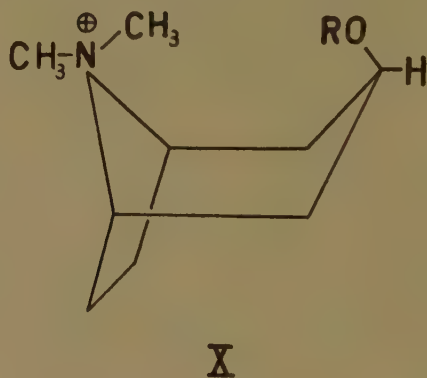
will be small. This is in agreement with the experience that a stereoisomer of tropinone has never been found.

As both tropine and  $\psi$ -tropine have been produced by reduction of tropinone, we have to consider four configurations for these alcohols (VI — IX, R = H).



Inspection of the corresponding STUART models shows that none of these configurations can *a priori* be excluded. Attempts to ascribe one of these configurations to tropine or  $\psi$ -tropine based on their physical properties and their rates of esterification do not give satisfactory results, because these properties show only very small differences [7].

We have investigated the chemical properties of some tropine and  $\psi$ -tropine derivatives, which show much greater differences. The benzoic and the *p*-nitrobenzoic esters appeared to suit our purpose very well. For these esters too we have to take into consideration the four configurations VI—IX (R = C<sub>6</sub>H<sub>5</sub>CO— and NO<sub>2</sub>·C<sub>6</sub>H<sub>4</sub>CO— respectively). Moreover, the methiodides of these esters gave very important information. Here one of the four structures (X) can be excluded on account of the very great steric overlapping between the ester group and one of the methyl groups (fig. 1).



## § 2. Determination of the sterical configuration from reaction rates

From a consideration of the formulae VI — IX for the tropeines and  $\psi$ -tropeines it is apparent that in structures VII and VIII the ester group is partly screened off by the —CH<sub>2</sub>—CH<sub>2</sub>— and the >NCH<sub>3</sub> bridge respectively. As VAVON [8] has shown for an extensive series of compounds, such a screening effect very often results in a lower saponification velocity

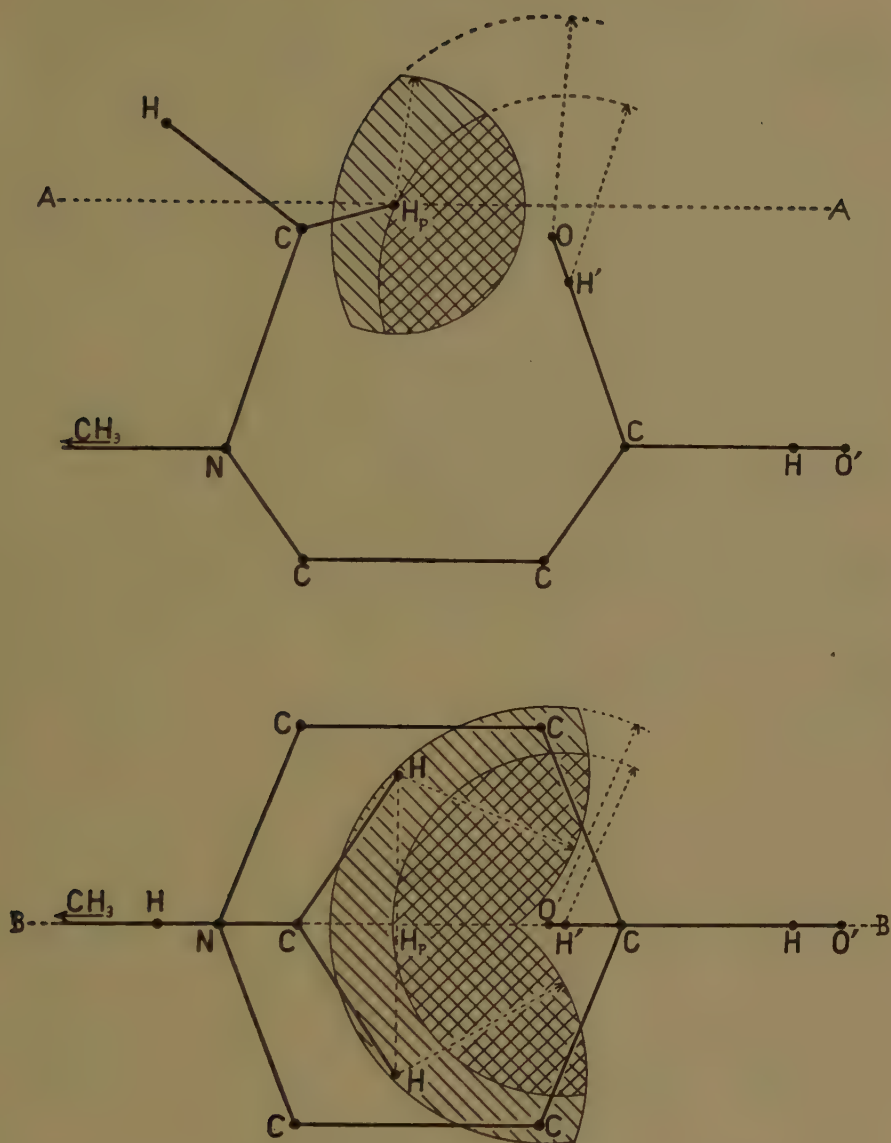


Fig. 1.

Above: projection of structure X in the vertical plane BB  
(see lower part of the figure).

Below: projection of structure X in the horizontal plane AA.

of the "sterically hindered" esters. This property has been used by several investigators to establish the stereo-chemical configuration of alcohols [9].

For our investigations we chose the benzoic and *p*-nitrobenzoic esters, as we expected these to have a suitable reaction rate for the base catalysed hydrolysis. These compounds are moreover easy to isolate and purify. The saponification velocities have been measured at 29.0° with 0.025 molar solutions of the esters in approximately 88 % ethanol to which

the equivalent amount of sodium hydroxide had been added. The reaction follows the overall equation



At regular intervals small amounts were pipetted from the reaction mixture and added quickly to excess 0.025 n. sulphuric acid in order to stop the reaction. The excess sulphuric acid was titrated with 0.025 n. sodium hydroxide solution. The reaction constant was computed with the formula:  $k = \frac{1}{at} \cdot \frac{x}{a-x}$ , where  $a$  is the concentration of the ester at zero time and  $x$  the same concentration after  $t$  minutes.

For comparison we also determined the saponification velocities of ethyl benzoate and of the *p*-nitrobenzoate of ethanol. The results of our measurements have been collected in table I.

TABLE 1

Compound	Melting point	Ethanol	Number of Exper.	k(min <sup>-1</sup> mol <sup>-1</sup> litre)
Ethyl benzoate	(B.pt. 90—91° at 12 mm)	87.97%	3	(42.4 ± 1.1) × 10 <sup>-3</sup>
Benzoyl- <i>ψ</i> -tropine	49.7°	87.97%	3	(38.7 ± 0.8) × 10 <sup>-3</sup>
Benzoyltropine. $\frac{1}{3}$ <i>aq</i>	37°	87.97%	2	(0.98 ± 0.05) × 10 <sup>-3</sup>
Ethyl <i>p</i> -nitrobenzoate	55.5—56.5°	88.56%	3	(42.6 ± 1.1) × 10 <sup>-1</sup>
<i>p</i> -nitrobenzoyl- <i>ψ</i> -tropine	120°	88.56%	2	(46.6 ± 0.5) × 10 <sup>-1</sup>
<i>p</i> -nitrobenzoyl-tropine. $\frac{1}{3}$ <i>aq</i>	131.5—132.5°	88.56%	3	(2.70 ± 0.05) × 10 <sup>-1</sup>
Ethyl benzoate	(B.pt. 90—91° at 12 mm)	88.56%	2	(43.5 ± 0.8) × 10 <sup>-3</sup>
Benzoyl- <i>ψ</i> -tropine methiodide	266—268°	88.56%	3	(34.5 ± 0.3) × 10 <sup>-3</sup>
Benzoyltropine methiodide	271—272.5°	88.56%	2	(40.8 ± 0.1) × 10 <sup>-3</sup>

### § 3. Discussion of the results

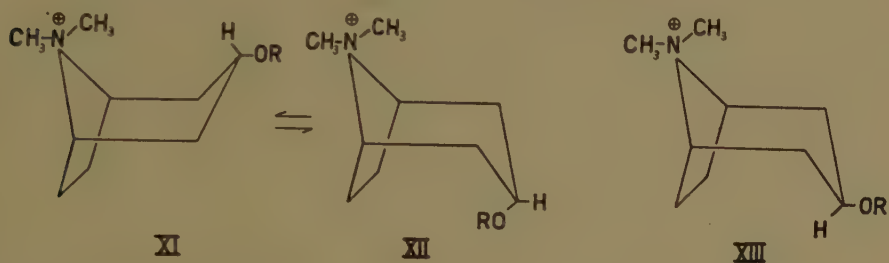
Table I shows that both the benzoic ester and the *p*-nitrobenzoic ester of *ψ*-tropine have a much higher saponification velocity than the corresponding tropeines. Therefore we conclude that the ester group of the tropeines is more sterically hindered (screened off), so that to tropine one of the structures VII or VIII has to be ascribed. For *ψ*-tropine the structures VI and IX are possible, both of which have a "sterically unhindered" ester group. This is in agreement with the fact that the saponification constant of benzoyl *ψ*-tropine is of the same order of magnitude as that of ethyl benzoate.

For the methiodides, however, table I shows quite different results. Here the tropine derivative shows a somewhat greater reaction velocity than the *ψ*-tropine, but *both reaction constants are of the same order of*

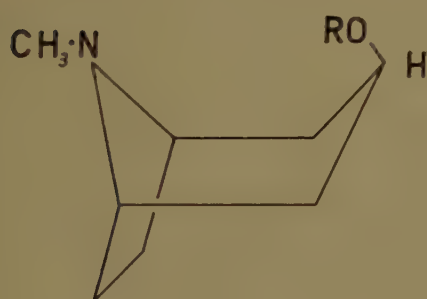


magnitude as those for the compounds with an unhindered ester group.

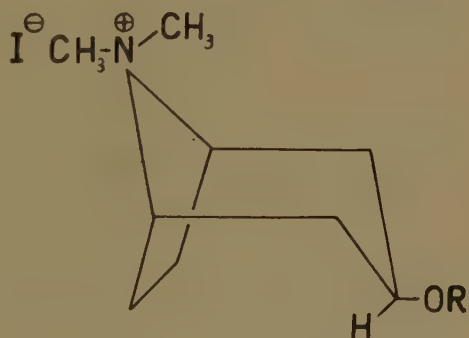
As has been shown in § 1 only three configurations are sterically possible for the methiodides (XI — XIII).



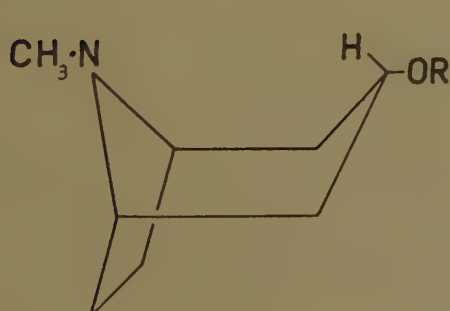
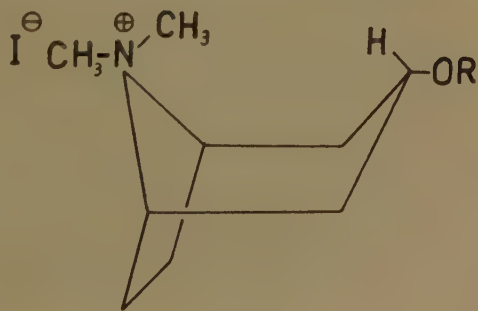
Configuration XII, however, can be excluded on account of the saponification rate. Apparently structure XI is energetically more favorable than XII; this is somewhat surprising as one might expect a certain overlapping between the VAN DER WAALS-radii of the hydrogen atom at C — 3 and one of the methyl groups at the nitrogen atom in structure XI, though this will be smaller than the overlapping between the ester group and the methyl group in configuration X. The conclusion seems justified that the tropeines and  $\psi$ -tropeines will show the same preference for the con-



BENZOYL TROPEINE



BENZOYL TROPEINE METHIODIDE

BENZOYL  $\psi$  TROPEINEBENZOYL  $\psi$  TROPEINE METHIODIDE

figurations VI and VIII, which have the same sterical model as XI. Here the lower part of the molecules is identical with that of the methiodide XI, whereas the sterical overlapping at the upper part of VI and VIII is much smaller than in configurations X and XI or even totally absent.

If this conclusion is correct we conclude from the saponification velocities of the tropeines and  $\psi$ -tropeines that configuration VIII has to be ascribed to tropine and its derivatives and configuration VI to  $\psi$ -tropine.

Summarizing, we conclude that the derivatives under investigation have predominantly the foregoing structures.

Our conclusions are in no way modified by the fact that besides these predominating structures the corresponding equilibrium forms may occur to some extent.

### *Acknowledgement*

Our thanks are due to Professor J. P. WIBAUT for his stimulating interest in this investigation, to the Management of the Nederlandse Cocaïne Fabriek for a sample of  $\psi$ -tropine and to A. F. VAN DEN HOVEN and R. VAN VELZEN for their assistance in performing the measurements.

Amsterdam, September 1951

*Laboratory for Organic Chemistry of the  
University of Amsterdam*

### BIBLIOGRAPHY

1. WILLSTÄTTER, R., Ber. **34**, 129, 3163 (1901).  
For a complete review of the literature on tropine,  $\psi$ -tropine and their derivatives reference is made to T. A. HENRY, "The Plant Alkaloids", Churchill Ltd., London, 4th Ed. p. 64 (1949) and H. L. HOLMES, in R. H. F. MANSKE and H. L. HOLMES, "The Alkaloids", Academic Press, Inc., New York, vol. I, p. 271 (1950).
2. WIBAUT, J. P., A. L. VAN HULSENBECK and C. M. SIEGMANN, Proc. Kon. Ned. Akad. v. Wetensch., **53**, 989 (1950).
3. KING, H. and L. L. WARE, J. Chem. Soc., 331 (1941).
4. WILLSTÄTTER, R., Ber. **29**, 936 (1896).
5. LE ROY C. KEAGLE and W. H. HARTUNG, J. Am. Chem. Soc., **68**, 1608 (1946).
6. WILLSTÄTTER, R. and M. BOMMER, Ann. **421**, 15 (1921).  
cf. also M. BARROWCLIFF and F. TUTIN, J. Chem. Soc., **95**, 1966 (1909).
7. SMITH, P. F., thesis, Univ. of Maryland, (1947).
8. VAVON, G., Bull. Soc. Chim. Fr. [4], **49**, 937 (1931).
9. HÜCKEL, W., H. HAVEKOS, K. KUMETAT, D. ULLMANN and W. DOLL, Ann. **533**, 128 (1938).  
MIESCHER, K. and W. H. FISCHER, Helv. Chim. Acta **21**, 336 (1938).  
RUZICKA, L., M. FURTER and M. W. GOLDBERG, *ibid.* **21**, 498 (1938).

## THE INFLUENCE OF CRYSTAL ORIENTATION ON POLYGONIZATION OF ALUMINIUM SINGLE CRYSTALS

BY

W. G. BURGERS, Y. H. LIU AND T. J. TIEDEMA

(Communicated by Prof. J. M. BURGERS at the meeting of November 24, 1951)

1. Much work has recently been done on polygonization of aluminium, in particular by CAHN, GUINIER, CRUSSARD and co-workers (see CHALMERS, 1950), but the exact nature of the process is still not clarified. CRUSSARD (1944) has found polygonization in annealed single crystals of aluminium, which had been extended to a few per cent. GUINIER and TENNEVIN (1948) have shown that the minimum temperature required to bring about detectable polygonization in crystals of pure aluminium was about  $450^{\circ}$  C. and that the foreign atoms present in crystals of low purity retarded the process of polygonization very considerably. They have also observed that in heavily deformed specimens recrystallization took place before any perceptible polygonization had been detected. No marked effect of the crystal orientation relative to the direction of deformation was found in their experiments. However, in the light of the theory of dislocations, it seems practically certain that the occurrence of polygonization is essentially associated with lattice curvatures. Consequently a predominant effect of the crystal orientation would be expected. With this in view, the following experiments were carried out.

2. In order to get more detailed information about polygonization the focussing Laue-method developed by GUINIER and TENNEVIN (1949) was used in the present investigation. A divergent X-ray beam was generated from a point source, the diameter of which was 0.3 mm. The specimen was set at a distance of 50 cm from the source and the surface area irradiated by the divergent beam was a circle with a diameter of 4 mm.

The crystals with definite orientations were prepared according to the method described by TIEDEMA (1949, 1951). They were in plate form, 1 mm in thickness, about 10 cm in length and 2 cm in width, and were of 99.6 % purity. The orientations of the crystals used in the investigation are approximately (fig. 1) as follows:

Crystal	Plane— specimen surface	Direction— length direction
<i>A</i>	(100)	[100]
<i>B</i>	(100)	[110]
<i>C</i>	(111)	[110]

The width of the focussed diffraction spots of the crystals in the annealed state indicated that they were undeformed. The crystals were then extended to 10 % elongation in the length direction. After extension, the Laue photograph of crystal *A* (fig. 2*a*) showed practically no asterism

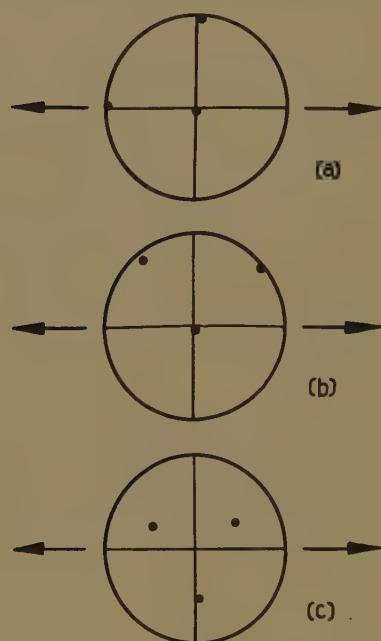


Fig. 1. Stereographic projection (cube-poles) of crystals *A*, *B* and *C*.

whereas those of crystals *B* (fig. 3*a*) and *C* (fig. 4*a*) showed pronounced asterisms. This is in agreement with the work of BURGERS and PLOOS VAN AMSTEL (1933) and is obviously due to the fact that the number of active glide systems is larger in crystal *A* than in crystals *B* and *C*. As fig. 2*b*, 3*b* and 4*b* show, the focussed diffraction spots of all the deformed crystals were very broad and diffuse.

All the crystals were subsequently subjected to successive annealing treatments at 625° C. and an X-ray investigation was made at frequent intervals. After each anneal the specimen under investigation was always placed in the same position in the specimen holder, so that the progressive change in the same spot could be studied.

*Crystal A* (fig. 2*a-e*). Already after annealing at 625° C. for  $\frac{1}{2}$  hour, the focussed diffraction spot showed an indication of diffuse striations superimposed on a continuous background (fig. 2*c*). This implies that crystalline blocks (sub-grains, polygons) had grown big enough and sufficiently strain-free to give distinct diffractions against the continuous background. On continued annealing, the striations became gradually sharper, shorter and more intense; the relative intensity of the background decreased very slightly. After 115 hours annealing (fig. 2*d*), the striations became fairly sharp and a number of small spots, which were very faint and not quite resolved, began to appear. When the annealing treatment was





Fig. 2*a*



Fig. 3*a*



Fig. 4

as  
deformed



Fig. 2

625 °C  
11.5 h



Fig. 3

as  
deformed

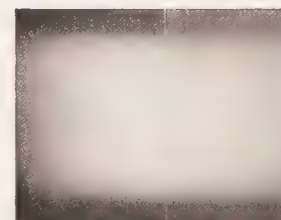


Fig. 3*b*

as  
deformed

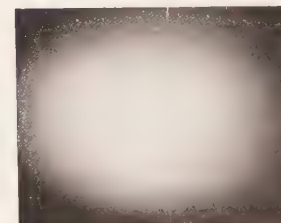


Fig. 4*b*

625 °C  
11.5 h



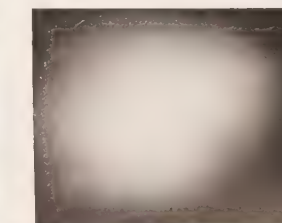
625 °C  
11.5 h



625 °C  
180 h



625 °C  
180 h





continued to 180 hours, an assembly of separate spots made its appearance in place of the original focussed diffraction spot and the continuous background almost disappeared (fig. 2e). At this stage, the crystal was transformed into an assembly of sub-grains of slightly differing orientations (about 1 minute of arc). As can be seen from a comparison of fig. 2b and 2e, the total range of orientations was smaller than that present in the deformed crystal before annealing. Judging from the sharpness of the spots, the sub-grains were almost strain-free. The ordinary Laue-photograph taken at this stage exhibited a peculiar appearance, some spots being split-up, some striated and a few with one or two dashes across them.

*Crystal B* (fig. 3a-c), after annealing at 625° C. for 180 hours, showed an indication of striations in the focussed diffraction spot comparable with that of crystal *A* after 115 hours annealing, whereas *crystal C* (fig. 4a-c) showed hardly any striations in the focussed spot after the same heat treatment. This indicates that polygonization in these crystals took place at a much lower speed than in crystal *A*.

From these results it is clear that a deformed crystal, which exhibits no pronounced asterism, polygonizes much more readily than those which show asterism. Hence, a dependence of polygonization on the orientation of a crystal relative to the direction of deformation is clearly shown.

3. It can be concluded from the results obtained that polygonization is essentially connected with the nature of the lattice distortion. A deformation involving a large number of glide combinations (crystal *A*) apparently provides a more favorable condition for polygonization than a deformation whereby gliding is confined to one or at least a small number of glide combinations (crystals *B* and *C*). At present it seems not well possible to give a precise reason for this behaviour. Tentatively the following suggestion is advanced (BURGERS, 1951):

NYE (1949), in his paper on stresses in silverchloride, points to the necessity of a bent lattice region to straighten out when it forces dislocations to its edges. This straightening out cannot occur without stresses being set up in neighbouring lattice regions. In an analogous way polygonization of definite lattice regions in a deformed single crystal may be hindered by neighbouring regions and it seems possible that those regions are privileged, the polygonization of which does not require a relatively large "straightening-out" in a definite "direction", but a more restricted change of shape. Reasoning along these lines it might be conceived that a lattice region, which has suffered glide along one definite set of glide planes and which thus is curved rather strongly about one definite axis, is less apt for polygonization than regions, which have been subjected to several intersecting glide systems and therefore possess a more "all-round" curvature.

Although we realize the vagueness of this suggestion, nevertheless considerations of this kind seem to us essential for understanding the

occurrence of sharp recrystallization textures when recrystallizing severely cold-worked metals. As pointed out elsewhere (TIEDEMA, 1951), we expect that the orientations found in these textures correspond to those lattice regions in the coldworked test-piece, which polygonize first. Here again both the type of deformation, which a lattice region has suffered, and the way, in which it is embedded in the surrounding grains, may be expected to determine its polygonization capacity. The experimental fact that recrystallization textures generally contain lattice orientations, which have a highly symmetrical orientation with regard to the main directions of flow, might be connected with the suggestion put forward above <sup>1</sup>). In particular the occurrence, in rolled cubic face-centred metals, of the so-called cube-texture seems of special interest in view of the pronounced capacity for polygonization of a crystal with this orientation, as found for crystal *A* in this investigation <sup>2</sup>).

To confirm our point of view experiments with polycrystalline specimens are required, with a view to find out whether differences in polygonization-capacity can be detected between grains of different orientation and position. Preliminary investigations in this direction seem to indicate that this is actually the case.

One of the authors (T. J. TIEDEMA) is associate worker of the "Stichting voor Fundamenteel Onderzoek der Materie" (F.O.M.). The present investigation is part of its research program and was made possible by financial support from the Netherlands Organisation for Pure Research (Z.W.O.).

---

<sup>1</sup>) Quite recently, DECKER and HARKER (1951) on somewhat other grounds concluded that those grains in the deformed material, which have undergone what they call "complex" deformation by slippage on several sets of slip-planes, will recrystallize first and thus constitute the recrystallization texture.

<sup>2</sup>) It was clearly shown by COHEUR and LEJEUNE (1949) that the cube-texture can be formed when recrystallizing rolled aluminium if only lattice domains in this orientation are present in the rolled state.

*Note added in proof.*

In a recent paper SCHMID and THOMAS, Z. Physik 130, 293 (1951), come to the conclusion that this condition is of minor importance for the formation of the cube-texture. Their conclusion is based upon the observation that recrystallization of a cold-rolled nickel-iron strip, which already possessed the cube-texture *before* rolling, always results in a material with a far *less*-pronounced cube-texture. In our view, however, this might be due to the fact that in such material a larger part of the nuclei with "cube-orientation" are embedded in grains with (approximately) the same orientation. Under such conditions growth of these nuclei is impossible (cf. Tiedema, May and Burgers, Acta Cryst. 2, 151, 1949), so that nuclei with other orientations may develop, resulting in a less-pronounced texture.



## REFERENCES

- BURGERS, W. G., Report for the Solvay Congress on the Solid State, held at Brussels. (1951).
- BURGERS, W. G. and PLOOS VAN AMSTEL, J. J. A., *Z. Physik* **81**, 43 (1933).
- CHALMERS, B., "Progress in Metal Physics", Vol. 2, Chapters 5, 6 and 7 (Butterworth, London) (1950).
- COHEUR, P. AND LEJEUNE, L. M., *Rev. de Métall.* **46**, 439 (1949).
- CRUSSARD, C., *Rev. de Métall.* **41**, 111 and 133 (1944).
- DECKER, B. F. and HARKER, D., *J. Appl. Physics* **22**, 900 (1951).
- GUINIER, A. and J. TENNEVIN, *Acta Cryst.* **1**, 188 (1948).
- and ———, "Progress in Metal Physics", Chapter 6 (1950).
- NYE, J. F., *Proc. Roy. Soc. A* **200**, 47; in particular p. 63 (1949).
- TIEDEMA, T. J., *Acta Cryst.* **2**, 261 (1949).
- , Thesis Delft (1951).

ON GRAMMEL'S LINEARISATION OF THE EQUATIONS FOR  
TORSIONAL VIBRATIONS OF CRANKSHAFTS

BY

W. T. KOITER

(Communicated by Prof. C. B. BIEZENO at the meeting of November 24, 1951)

1. *The complete equations and their linearisation*

The equations for torsional vibrations of a crankshaft may be written in the form <sup>1)</sup> <sup>2)</sup>

$$(1) \quad \left\{ \begin{aligned} \Psi_k \ddot{\psi}_k + \frac{1}{2} \frac{d\Psi_k}{d\psi_k} \dot{\psi}_k^2 - \frac{C_k}{l_k} (\psi_{k-1} - \psi_k) + \frac{C_{k+1}}{l_{k+1}} (\psi_k - \psi_{k+1}) &= M_k, \\ (k = 1, 2, \dots, n) \quad (C_0 = C_{n+1} = 0) \end{aligned} \right.$$

where  $\psi_k$  is the angular coordinate of crank  $k$ ,  $\Psi_k$  is the corresponding inertia coefficient ( $\frac{1}{2} \Psi_k \dot{\psi}_k^2$  being the kinetic energy of crank, connecting rod and piston),  $C_k$  and  $l_k$  are torsional stiffness and length of the crankshaft between cranks  $k-1$  and  $k$  and  $M_k$  is the external moment working on crank  $k$ . Differentiations with respect to time are indicated by dots. The inertia coefficient  $\Psi_k$  is a periodic function with period  $2\tau$  of the angular coordinate  $\psi_k$ . Putting

$$(2) \quad \psi_k = \omega t + \vartheta_k,$$

where  $\vartheta_k$  is the angular displacement of crank  $k$  from a uniform rotation, equations (1) may be written

$$(3) \quad \Psi_k \ddot{\vartheta}_k + \frac{1}{2} \frac{d\Psi_k}{d\vartheta_k} (\omega + \dot{\vartheta}_k)^2 - \frac{C_k}{l_k} (\vartheta_{k-1} - \vartheta_k) + \frac{C_{k+1}}{l_{k+1}} (\vartheta_k - \vartheta_{k+1}) = M_k,$$

where  $\Psi_k$  and  $\frac{d\Psi_k}{d\vartheta_k}$  are periodic functions of  $\vartheta_k = \omega t + \vartheta_k$ .

In order to linearize the highly nonlinear equations (3) GRAMMEL assumes  $\vartheta_k$  to be small, then argues that  $\dot{\vartheta}_k$  may be neglected compared with  $\omega$ , and finally puts

$$\begin{aligned} \Psi_k(\psi_k) &\cong \Psi_k(\omega t) \\ \frac{d\Psi_k}{d\psi_k} &\cong \frac{d\Psi_k(\omega t)}{d(\omega t)} = \Psi'_k(\omega t). \end{aligned}$$

---

<sup>1)</sup> R. GRAMMEL. Die kritischen Drehzahlen der Kolbenmotoren. Z. angew. Math. Mech. 15, 47 (1935).

<sup>2)</sup> C. B. BIEZENO und R. GRAMMEL. Technische Dynamik, Berlin 976, (1939).

The resulting *linear* equations with periodic coefficients are

$$(4) \quad \Psi_k(\omega t) \ddot{\vartheta}_k - \frac{C_k}{l_k} (\vartheta_{k-1} - \vartheta_k) + \frac{C_{k+1}}{l_{k+1}} (\vartheta_k - \vartheta_{k+1}) = M_k - \frac{1}{2} \Psi'_k(\omega t) \cdot \omega^2.$$

Except for the second term in (3) this procedure seems entirely satisfactory, granted the assumption that  $\vartheta_k$  is small. However, development of the second term in (3) with respect to  $\vartheta_k$  and  $\dot{\vartheta}_k$  yields with retention of *all* linear terms

$$(5) \quad \left\{ \begin{aligned} & \frac{1}{2} \frac{d\Psi_k}{d\varphi_k} (\omega + \dot{\vartheta}_k)^2 = \frac{1}{2} \left[ \left( \frac{d\Psi_k}{d\varphi_k} \right)_{\varphi_k=\omega t} + \left( \frac{d^2\Psi_k}{d\varphi_k^2} \right)_{\varphi_k=\omega t} \cdot \vartheta_k + \dots \right] \times \\ & \times (\omega^2 + 2\omega\dot{\vartheta}_k + \dots) = \frac{1}{2} \Psi'_k \omega^2 + \frac{1}{2} \Psi''_k \omega^2 \vartheta_k + \Psi'_k \omega \dot{\vartheta}_k + \dots \end{aligned} \right.$$

Only the first term of (5) appears in (4). In the frame of the linearised theory (4) should therefore be replaced by

$$(6) \quad \left\{ \begin{aligned} & \Psi_k \ddot{\vartheta}_k + \Psi'_k \omega \dot{\vartheta}_k + \frac{1}{2} \Psi''_k \omega^2 \vartheta_k - \frac{C_k}{l_k} (\vartheta_{k-1} - \vartheta_k) + \\ & + \frac{C_{k+1}}{l_{k+1}} (\vartheta_k - \vartheta_{k+1}) = M_k - \frac{1}{2} \Psi'_k \omega^2, \end{aligned} \right.$$

where accents attached to  $\Psi_k$  indicate differentiations with respect to  $\omega t = \tau$ .

Usually the lower natural frequencies are of the same order of magnitude as the rotational speed of the crankshaft. It is then easily seen that the second and third terms of (6) are of the same order of magnitude as the contribution to the first term, that is due to the *fluctuating* part of  $\Psi_k$ .

Hence, as soon as the fluctuation of the inertia coefficients has to be taken into account, equations (4) *cannot be used even as a first approximation but they must be replaced by equations (6)*.

It is therefore to be feared that Grammel's analysis of critical speeds, based on equations (4) will lead to results that may be seriously in error when the effect of the fluctuating part of the inertia coefficients is not negligible. However, it will be shown that to a first approximation the critical speeds are — quite unexpectedly — not affected by the second and third terms of (6) *together* because they cancel each other's effect. It should be noted that the effect of each term separately is not negligible. Therefore the omission of these terms is fundamentally incorrect.

## 2. The perturbation method

Introducing nondimensional time

$$(7) \quad \tau = \omega t,$$

equations (6) may be rewritten in the form<sup>1)</sup>

$$(8) \quad \vartheta_k'' + \frac{\Psi'_k}{\Psi_k} \vartheta_k' + \frac{1}{2} \frac{\Psi''_k}{\Psi_k} \vartheta_k - \lambda \frac{\Theta_k}{\Psi_k} U_k(\vartheta) = F_k(\tau),$$

<sup>1)</sup> Cf. footnote 2, p. 1038.

where

$$\lambda = 1/\omega^2$$

$$\frac{1}{\Theta_k} = \frac{1}{2\pi} \int_0^{2\pi} \frac{1}{\Psi_k(\tau)} d\tau = \text{mean value of } \frac{1}{\Psi_k}$$

$$U_k(\vartheta) = \frac{C_k}{l_k \Theta_k} (\vartheta_{k-1} - \vartheta_k) - \frac{C_{k+1}}{l_{k+1} \Theta_k} (\vartheta_k - \vartheta_{k+1})$$

$$F_k(\tau) = \frac{1}{\Psi_k} [M_k - \frac{1}{2} \Psi'_k \omega^2]$$

and accents indicate differentiations with respect to  $\tau$ . For two-stroke engines <sup>1)</sup> the right-hand side of (8) is a periodic function of  $\tau$  with period  $2\pi$ . The critical speeds are now characterized by those values of  $\lambda = 1/\omega^2$  (eigenvalues) for which the *reduced* equations admit a solution with period  $2\pi/j$  ( $j = 1, 2, \dots$ ). Following GRAMMEL we write

$$\frac{1}{\Psi_k} = \frac{1}{\Theta_k} (1 + e \varrho_k),$$

where  $e\varrho_k$  represents the fluctuating part of  $1/\Psi_k$ . The Fourier expansion of  $\varrho_k$  may be written in the form

$$(9) \quad \varrho_k = \sum_{n=1}^{\infty} (A_{kn} \cos n\tau + B_{kn} \sin n\tau).$$

We now assume that the periodic solutions of the reduced equations (8) and the corresponding eigenvalues may be expanded in power series with respect to  $e$ , the parameter that indicates the "amplitude" of the fluctuating part of  $1/\Psi$

$$\vartheta_k = \vartheta_{k0} + e \vartheta_{k1} + e^2 \vartheta_{k2} + \dots$$

$$\lambda = \lambda_0 + e \lambda_1 + e^2 \lambda_2 + \dots$$

As a first approximation we retain only the linear terms in  $e$ , noting that to the same approximation we may then write

$$\frac{\Psi'_k}{\Psi_k} = -e \varrho'_k \quad \frac{\Psi''_k}{\Psi_k} = -e \varrho''_k$$

The reduced equations (8) may now be written

$$(10) \quad \left\{ \begin{aligned} \vartheta''_{k0} - \lambda_0 U_k(\vartheta_0) + e [\vartheta''_{k1} - \lambda_0 U_k(\vartheta_1) - \lambda_1 U_k(\vartheta_0) - \lambda_0 \varrho_k U_k(\vartheta_0) - \\ - \varrho'_k \vartheta'_{k0} - \frac{1}{2} \varrho''_k \vartheta_{k0}] + \dots = 0 \end{aligned} \right.$$

The terms of zero order vanish identically because  $\vartheta_{k0}$  and  $\lambda_0$  are the known solution for  $e = 0$

$$\vartheta_{k0} = u_{k0} \cos(j\omega t + \varphi) = u_{k0} \cos(j\tau + \varphi).$$

<sup>1)</sup> For 4-stroke engines the period of  $F_k(\tau)$  is  $4\pi$  and the arguments must be correspondingly modified, see footnote 2, p. 1043.



The first order terms yield the equation

$$(11) \quad \vartheta_{k1}'' - \lambda_0 U_k(\vartheta_1) = (\lambda_1 + \lambda_0 \varrho_k) U_k(\vartheta_0) + \varrho_k' \vartheta_{k0}' + \frac{1}{2} \varrho_k'' \vartheta_{k0} = R_k(\tau),$$

the solution of which is periodic, i.e. contains no secular terms, only if the right-hand sides satisfy the equations

$$(12) \quad \sum_k \int_0^{2\pi} R_k(\tau) u_{k0} \cos j\tau d\tau = \sum_k \int_0^{2\pi} R_k(\tau) u_{k0} \sin j\tau d\tau = 0.$$

These equations now are equivalent to Grammel's equations

$$(13) \quad \begin{cases} \sum_k \int_0^{2\pi} (\lambda_1 + \lambda_0 \varrho_k) U_k(\vartheta_0) u_{k0} \cos j\tau d\tau = \\ = \sum_k \int_0^{2\pi} (\lambda_1 + \lambda_0 \varrho_k) U_k(\vartheta_0) u_{k0} \sin j\tau d\tau = 0 \end{cases}$$

because, as will be shown presently, for each crank separately, the following equalities hold

$$(14) \quad \int_0^{2\pi} (\varrho_k' \vartheta_{k0}' + \frac{1}{2} \varrho_k'' \vartheta_{k0}) \cos j\tau d\tau = \int_0^{2\pi} (\varrho_k' \vartheta_{k0}' + \frac{1}{2} \varrho_k'' \vartheta_{k0}) \sin j\tau d\tau = 0.$$

Therefore Grammel's first order correction  $\lambda_1$ , deduced from eq. (13) is not affected by the second and third terms in (6) *together*.

To prove (14) we use the Fourier-expansion of  $\varrho_k$  (9) and write

$$\begin{aligned} \varrho_k' \vartheta_{k0}' + \frac{1}{2} \varrho_k'' \vartheta_{k0} &= -ju_{k0} \sin(j\tau + \varphi) \sum_{n=1}^{\infty} n(-A_{kn} \sin n\tau + B_{kn} \cos n\tau) - \\ &\quad - \frac{1}{2} u_{k0} \cos(j\tau + \varphi) \sum_{n=1}^{\infty} n^2 (A_{kn} \cos n\tau + B_{kn} \sin n\tau) = \\ &= u_{k0} \sum_{n=1}^{\infty} [A_{kn} \{(\frac{1}{2}jn - \frac{1}{4}n^2) \cos[(n-j)\tau - \varphi] - \\ &\quad - (\frac{1}{2}jn + \frac{1}{4}n^2) \cos[(n+j)\tau + \varphi]\} + \\ &\quad + B_{kn} \{(\frac{1}{2}jn - \frac{1}{4}n^2) \sin[(n-j)\tau - \varphi] - \\ &\quad - (\frac{1}{2}jn + \frac{1}{4}n^2) \sin[(n+j)\tau + \varphi]\}]. \end{aligned}$$

Multiplying by  $\cos j\tau$  or  $\sin j\tau$  and integrating over the period  $2\pi$  gives non-vanishing integrals

$$\int_0^{2\pi} \begin{matrix} \cos \\ \sin \end{matrix} [(n-j)\tau - \varphi] \begin{matrix} \cos \\ \sin \end{matrix} j\tau d\tau$$

only for  $n = 2j$  but for this value of  $n$  the coefficient  $\frac{1}{2}jn - \frac{1}{4}n^2$  of the integral is zero, so that (14) holds true.

## ASTRONOMY

# ON THE ELECTRON TEMPERATURE OF THE CHROMOSPHERE AND PROMINENCES

BY

D. KOELBLOED AND W. VELTMAN

(Circular No. 3 of the Astronomical Institute of the University of Amsterdam)

(Communicated by Prof. H. ZANSTRA at the meeting of Nov. 24, 1951)

### *Summary*

The method proposed by H. ZANSTRA to obtain electron temperatures for the chromosphere makes use of the intensities of the Ba<sub>2</sub> spectrum, the other recombination and electron switch spectra and the scattering of photospheric light by free electrons. With this method electron temperatures are derived for the chromosphere, using films taken by DAVIDSON during the solar eclipse of January 14, 1926. For the electron temperature of the chromosphere a value of at most 10,000° to 16,000° is obtained. This is a good deal lower than the kinetic temperature of 30,000° found by REDMAN, as was also expected by ZANSTRA. For the prominences investigated an electron temperature of about 5,000° was obtained, while the concentration of electrons and protons seems higher than the mean values usually adopted.

### 1. *Introduction. The characteristic curve*

In circular No 1 of the Astronomical Institute of the University of Amsterdam, Professor H. ZANSTRA drew attention to the value of observations of continuous spectra of the chromosphere and prominences during solar eclipses <sup>1)</sup>.

At his request, the Astronomer Royal put the films of the eclipse of January 14, 1926, obtained by Mr. DAVIDSON, at our disposal for the derivation of some preliminary results, using ZANSTRA's method. For the derivation of characteristic curves only a film of the solar spectrum (centre of disc), with exposures of 1, 2 and 4 seconds, was available. This calibration film was not developed together with the eclipse films, so that our measures cannot give accurate photometric results. But it is believed that they may have some value as an orientation, in particular for the coming eclipse of February 25, 1952, at Khartoum, where REDMAN and

---

<sup>1)</sup> H. ZANSTRA, Proc. Kon. Ned. Akad. v. Wetensch., Amsterdam, 53, 1289, (1950) (Circular No. 1 of the Astronomical Institute of the University of Amsterdam).

We will refer to this paper as Circular No. 1. (See also the errata at the end of the present paper).

ZANSTRA intend to use the same ultraviolet spectrograph. As the Schwarzschild exponent  $p$  is not accurately known, the computations were carried out for  $p = 0,8$  and  $1,0$ , as had been done by DAVIDSON, MINNAERT, ORNSTEIN and STRATTON, who reduced the films for other purposes <sup>1)</sup>.

The derivation of the characteristic curve was first carried out in the usual way by plotting the transmission  $T$  vertically against  $\log It^p$ , after which a horizontal displacement of corresponding points was applied to bring all points on a single curve. By transmission is meant the galvanometer deflection, expressed as a percentage of the deflection for the clear plate. The density is therefore  $100 - T$ . The part of medium transmission could only be obtained for the spectral region  $\lambda < 3300 \text{ \AA}$ , as the spectra were too black for longer wavelengths. So we must assume that the shape of the curve is valid for the longer wavelengths used in the computations.

The sensitivity of the films, the absorption in the earth's atmosphere and the absorption and reflection in the instrument vary with wavelength. In principle all these complications can be eliminated by expressing the intensities in terms of the intensity at the same wavelength in the solar spectrum, if the latter is taken immediately after the eclipse, provided that the intensity as a function of wavelength is exactly known for the solar continuous spectrum. The solar film was taken at the same altitude one day after the eclipse. The variation of the absorption of the atmosphere with wavelength was therefore only imperfectly eliminated.

In the region studied, the solar spectra were very black. So the solar intensities are lying in the far toe of the characteristic curve, and its shape is difficult to determine by the method of horizontal displacements mentioned above.

For this part of the characteristic curve we therefore applied the following method. We call  $T_t$  the transmission of the photographic plate for a certain wavelength region in the solar spectrum, taken with an exposure of  $t$  seconds. For a large number of points with  $T < 20 \%$ , we measured  $T_1$  and  $T_2$  and plotted  $T_1 - T_2$  against  $T_1$ . From the points plotted mean values were computed. It was seen that these mean points were represented very well by a straight line through the origin. So

$$(1) \quad T_1 - T_2 = kT_1 \quad \text{or} \quad T_2/T_1 = 1 - k,$$

for all intensities larger than a certain value. Relation (1) is equivalent to

$$(2) \quad T = c(I t^p)^n$$

where

$$(3) \quad 2^{np} = 1 - k$$

---

<sup>1)</sup> C. R. DAVIDSON, M. MINNAERT, L. S. ORNSTEIN and J. F. M. STRATTON, M. N. 88, 536 (1928).

so that  $n$  is known in terms of  $p$  and  $k$ . The value of  $k$  found was  $+0.38$ , from which follows  $np = -0.69$ .

Formula (2) is used to determine the characteristic curve for the toe-parts, adjusting the constant  $c$  in such a way that a smooth transition to the medium transmission part is derived. The transmissions of the solar continuous spectrum (exp. 1 sec.) at the wavelengths studied,  $\lambda 3646$  and  $4010$ , are 3.2 and 1.7 %. According to (2) the difference in  $\log I$  for the two transmissions is 0.396 (for  $p = 1$ ) and 0.317 (for  $p = 0.8$ ).

The intensity of the continuous solar spectrum (continuous background between Fraunhofer lines) at both wavelengths (table 1) are derived from:

- a. MULDER'S curve (Diss., fig. 2, or Circular No 1, fig. 1),
- b. Table II of CHALONGE-CANAVAGGIA and their collaborators<sup>1)</sup>.

TABLE 1

Intensity per wave-length unit of the solar continuous spectrum at the centre of the disc, in  $\text{ergs cm}^{-2} \text{sec}^{-1}$

$\lambda$	a. (Mulders)	b. (Chalonge)
3646	$2.47 \times 10^{14}$	$3.31 \times 10^{14}$
4010	$4.50 \times 10^{14}$	$4.60 \times 10^{14}$

According to MICHARD, MULDER'S values may be improved<sup>2)</sup>. His corrections of PETTIR's radiometric measurements are in agreement with the spectrophotometric results of the French observers, so that case  $b$  may be given larger weight.

Then, adopting the characteristic curve for  $\lambda 3646$  as a standard, the curve may be used for  $\lambda 4010$ , if the readings of the logarithmic intensity scale are diminished by 0.136 ( $p = 1$ ) in case  $a$  and by 0.253 ( $p = 1$ ) in case  $b$ . For  $p = 0.8$  the values are 0.057 and 0.174. For wavelengths between  $\lambda 3646$  and  $4010$  the continuous solar spectrum cannot be measured on account of the numerous Balmer lines (cf 1), and we therefore assume the horizontal displacement of the characteristic curve to be a linear function of the wavelength in this region.

## 2. Determination of the electron temperature $T_e$ of the chromosphere

In Circular No 1, figures 2—5, ZANSTRA gives the intensities of the continuous spectra  $Ba_c$ ,  $c$  and  $C$  for different electron temperatures, wavelengths and concentrations. The  $C$  spectrum is caused by all recombinations (except  $Ba_c$ ) and electron switches and the  $c$  spectrum by scattering of photospheric light by free electrons, with the Fraunhofer lines entirely fuzzed out. All his computations refer to a chromospheric height of 1300 km. For the height  $h$  needed in this paper we have used his formulae (8) and (6).

<sup>1)</sup> R. CANAVAGGIA, D. CHALONGE, M. EGGER—MOREAU, H. OZIOU—PELLEY, *Ann. d'Astrophys.* 13, 355 (1950).

<sup>2)</sup> R. MICHARD, *B.A.N.* 9, 228 (1950).



For wavelengths shorter than 3646 Å the observed continuous spectrum consists of  $Ba_c + c + C$ , for longer wavelengths of  $c + C$ . We computed the theoretical ratio  $(Ba_c + c + C)_{3646}/(c + C)_\lambda$  for different electron temperatures and plotted these values for the chosen wavelength against  $T_e$ . This graph served for determining the electron temperature, using the observed intensity ratio.

Tracings were made of the chromospheric spectrum at  $h = 400$  km above the solar limb. The regions 3784—3785 and 4000—4020 Å give the lowest intensities. For  $\lambda$  3785 and 4010 we supposed that we have reached the continuous background. Faint emission lines, if present there, will result in finding a too high temperature and therefore our temperatures will be upper limits.

For the chromospheric intensities we find the ratios given in table 2, for  $p = 1$  and 0.8, both for case *a* and *b*.

TABLE 2

Observed chromospheric intensity ratios  $(Ba_c + c + C)_{3646}/(c + C)_\lambda$ ,  $h = 400$  km.

$\lambda$	transm.	case <i>a</i>		case <i>b</i>		uncorrected	
		$p = 1$	$p = 0.8$	$p = 1$	$p = 0.8$	$p = 1$	$p = 0.8$
3646	17.8 %						
3646/3785		9.60	5.85	10.62	6.38	8.5	5.6
3785	82.2 %						
3646/4010		6.80	4.10	8.85	5.30	4.9	3.6
4010	64.8 %						

The uncorrected values are obtained from one characteristic curve, thus with the approximation that the relation between the density and the spectral intensity is treated as independent of  $\lambda$  for this region.

With the intensity ratios of table 2 we find the electron temperatures for the various cases, given in table 3.

TABLE 3

Electron temperatures  $T_e$  for the chromosphere,  $h = 400$  km.

		3646/3785	3646/4010	$\Delta T_e$
case <i>a</i> . . . . .	$p = 1$	11800°	13000°	+ 1200°
	$p = 0.8$	16400°	19200°	+ 2800°
case <i>b</i> . . . . .	$p = 1$	10900°	10100°	— 800°
	$p = 0.8$	15600°	15900°	+ 300°
uncorr. . . . .	$p = 1$	13000°	17000°	+ 4000°
	$p = 0.8$	17000°	23500°	+ 6500°

The last column shows for cases *a* and *b*, that, with the procedure adopted for the toe and the assumption of the same atmospheric absorption during and outside the eclipse, we get nearly the same value of  $T_e$  from the two

wavelengths  $\lambda 3785$  and  $\lambda 4010$  as compared with  $\lambda 3646$ . For the uncorrected case, the difference in the two values of  $T_e$  is much larger. This gives some confidence that notwithstanding the difficulties encountered with the large densities of the solar spectra, the procedure adopted in § 1 seems justified. Case *b* gives the smallest  $\Delta T_e$ , suggesting that CHALONGE's values are to be preferred.

We conclude that ZANSTRA's method gives electron temperatures between  $10,000$  and  $16,000^\circ K$  for the chromosphere at a height of  $400$  km. However it should be remembered that undetected narrow emission lines and wings of adjacent broad emission lines contribute to the measured intensity. Also the possibility should be kept in mind that the continuous spectrum due to the formation of negative hydrogen or even spectra of unknown origin play a part. For this reason it is best to look upon the result as an upper limit. These results point to a much lower electron temperature than the kinetic temperature of  $30,000^\circ$  found by REDMAN. They are more in agreement with the determinations of MIYAMOTO and KAWAGUCHI, who found from the degree of ionization of metals electron temperatures not higher than  $10,000^\circ$ . A more uncertain result is their temperature of about  $6000^\circ$ , derived from the curve of growth for the Calcium ion <sup>1)</sup>. From the non-appearance of forbidden lines in the lower and medium chromosphere, WURM surmises also a electron temperature lower than  $10,000^\circ$  for these regions <sup>2)</sup>.

### 3. *The prominences*

Two prominences are investigated, the prominence in the chromosphere at the height of  $700$  km and the prominence in the coronal region at about  $14,000$  km <sup>3)</sup>. On both sides of the spectrum of the high prominence a continuous coronal spectrum is seen, which becomes stronger towards the longer wavelengths. This background must be subtracted in order to obtain the intensity of the prominence itself.

For the prominence in the flash spectrum we adopt as background the intensity of the chromospheric spectrum immediately below the prominence. For the region just above the prominence only an unmeasurable small region of chromospheric origin seems to be present. So the correction for background is more uncertain.

Using Circular No 1, fig. 2—5, for the proton or electron concentration of prominences adopted there, the electron temperatures become impossibly low. This certainly points to much higher concentrations of protons or electrons which, on account of the high hydrogen abundance, are assumed equal. If the concentration is  $m$  times larger than adopted

<sup>1)</sup> S. MIYAMOTO and I. KAWAGUCHI, Publ. Astron. Soc. of Japan, **1**, 114 (1949).

<sup>2)</sup> K. WURM, Zs. f. Ap. **25**, 109, (1948), Ann. de Phys. **3**, 139 (1948).

<sup>3)</sup> C. R. DAVIDSON, M. MINNAERT, L. S. ORNSTEIN and J. F. M. STRATTON, M.N. **88**, 536 (1928).

in Circular No 1, the intensity ratio becomes

$$(4) \quad I_{3646}/I_{\lambda} = (Ba_c + c/m + C)_{3646}/(c/m + C)_{\lambda}$$

This ratio is a function of the electron temperature  $T_e$  and the concentration  $n$ . In principle therefore, intensity measures for two different wavelengths should give  $T_e$  and  $n$ .

In Table 4 we give the results for the concentrations computed for electron temperatures of  $5000^\circ$  and  $10,000^\circ$ , obtained with formula (4) for case  $b$ .

TABLE 4  
Concentrations  $n$  of electrons or protons for prominences

	Intensity ratio		Concentration $\times 10^{-10}$				
	3646/3785	3646/4010	3646/3785		3646/4010		
			5000°	10,000°	5000°	10,000°	
High	16.3	5.55	4.4	65.5	2.3	8.7	$p = 1$
prominence . .	14.2	5.46	3.8	34.2	2.2	8.4	$p = 0.8$
Low	47.1	20.6	15.7	$\infty$	10.2	$\infty$	$p = 1$
prominence . .	27.3	12.0	7.8	$\infty$	5.4	41.1	$p = 0.8$

For  $5000^\circ$  both wavelengths give approximately the same concentrations. For  $10,000^\circ$   $\lambda$  3785 gives much larger concentrations than  $\lambda$  4010, especially for the low prominence. Both wavelengths give for the high prominence the same concentration  $n = 1.9 \times 10^{10}$  at  $4700^\circ$  for  $p = 0.8$  and  $n = 2.0 \times 10^{10}$  at  $4800^\circ$  for  $p = 1$ . For the low prominence we adopt  $5000^\circ$  and  $n = 9 \times 10^{10}$ . The high prominence seems to have smaller concentration, which seems reasonable. The value usually adopted is  $n = 10^{10}$  about.

The foregoing method was partly proposed by WURM, who estimated from the reproduction of the 1926 spectrum of the high prominence a value between 1 and 100 for the ratio  $Ba_c/c$  near the head <sup>1)</sup>. Adopting the value 10 and assuming  $T = 5000^\circ$ , he found  $\log n = 10.75$ .

DAVIDSON, MINNAERT, ORNSTEIN and STRATTON derived from line intensities of ionized Titanium with the help of the Boltzmann formula,  $4200^\circ$  for the high prominence, adopting  $5000^\circ$  for the low prominence <sup>2)</sup>. From the distribution of intensity in the continuous spectrum for  $\lambda < 3646$ , these authors derived electron temperatures of  $4000^\circ$  and  $3200^\circ$  for the low, resp. high prominence according to the Kramers theory, not taking account of scattering by free electrons.

Low kinetic temperatures in prominences were found by BRÜCK and

<sup>1)</sup> K. WURM. Mitt. Hamb. Sternw. Bergedorf 21, Nr. 206, 103 (1948).

<sup>2)</sup> C. R. DAVIDSON, M. MINNAERT, L. S. ORNSTEIN and J. F. M. STRATTON, M.N. 88, 543 (1928).

Moss <sup>1)</sup>. The intensities of the lines hydrogen  $H_a$  and helium  $D_3$ , observed by them, are in agreement with a curve of growth for a kinetic temperature of 5000°.

The writers wish to express their thanks to The Astronomer Royal, Sir HAROLD SPENCER JONES, for placing the films at their disposal and to Professor F. J. M. STRATTON for his aid in this matter. They also thank Professor ZANSTRA for suggesting the problem and for valuable discussions.

ERRATA to the paper by H. ZANSTRA, Proc. Kon. Akad. v. Wetensch., Amsterdam, 53, 1289 (1950) (Circular No. 1 of the Astronomical Institute of the University of Amsterdam).

p. 1294 (fig. 3) for  $\frac{T_e}{10^4} \cdot \frac{10^{10}}{n_1}$  read  $\left(\frac{T_e}{10^4}\right)^{3/2} \cdot \frac{10^{10}}{n_1}$

p. 1296 row 8, for  $\left(\frac{T_e}{10^4}\right)^3$  read  $\left(\frac{T_e}{10^4}\right)^{3/4}$

---

<sup>1)</sup> H. A. BRÜCK and W. MOSS, M.N. 105, 17 (1945).



# NOTE SUR UNE ROCHE FILONNIENNE DU TYPE DES AÏOUNITES DE LA RÉGION DE TAOURIRT ET SUR L'ORIGINE DES LAVES BASIQUES ALCALINES NÉOGÈNES ET QUATERNAIRES DU MAROC FRANÇAIS. I

PAR

J. WESTERVELD, E. TEN HAAF ET C. J. MULDER

(Communicated by Prof. H. A. BROUWER at the meeting of September 29, 1951)

## Introduction

Parmi des échantillons de roches volcaniques provenant des environs du Jebel Narguechoum au Sud de Taourirt dans le Nord-est du Maroc, que le premier auteur (W.) reçut par l'intermédiaire de la Direction de la mine de manganèse de Narguechoum, il se trouva une lave basique alcaline du type remarquable des aïounites décrites par M. L. DUPARC (1925—26, p. 119) et Mme. E. JÉRÉMIANE (1948, p. 67), évidemment prélevée sur un filon coupant les marnes argileuses bajociennes à l'Ouest de la route de Taourirt à la mine, au pied d'un promontoire au flanc nord des Hauts Plateaux, où cette même roche a été observée par lui (W.) lors d'une visite à cette région.

Dans un autre article (J. WESTERVELD, 1951, p. 28), il a été relevé que l'aïounite de Narguechoum fut reconnue à juste titre comme telle par Messrs. L. U. DE SITTER et R. LAGAAIJ (1948).

Les lignes suivantes servent à fournir une description pétrographique, aussi bien qu'une analyse chimique, du spécimen en question, tandis que dans la deuxième partie du présent article il sera démontré au moyen de diagrammes composés à l'aide des paramètres proposés par M. P. NIGGLI (1923, p. 51, 52; 1936 a) que l'ensemble des laves basiques alcalines issues de centres d'éruption distribués sur de vastes étendues au Maroc représente une seule tribu pétrochimique nettement caractérisée et bien différente de celle des basalto-dolérites dites du Permo-Trias.

Comme nous l'apprennent les descriptions géologiques, pétrographiques et pétrochimiques déjà existantes, notamment celles de M. L. DUPARC (1925—26), M. H. TERMIER (1936, pp. 1521—1545), Mme. E. JÉRÉMIANE (1948), M. H. et Mme. G. TERMIER et M. G. JOURAVSKY (1948) et M. J. AGARD (1950), le „clan" basique alcalin se compose de coulées, filons, dômes et cônes de phonolites, murites phonolitiques, néphélinites, tahitites, ordanchites, basanites, limburgites, fasinites, fasinites doléritiques, aïounites, mestigmérites, ankaratrites, talzastites, etc., dont l'âge semble varier entre le Néogène et le Quaternaire. TERMIER (1936, p. 1527) incline

à ranger les venues phonolitiques de la région d'Oulmès dans le Quaternaire ancien, tandis que pour AGARD (1950) les essais de sills et de dykes d'aïounites et de mestigmérîtes recoupant des terrains jurassiques dans le couloir de Taza-Oujda au Maroc Oriental sont distinctement anté-helvétiques.

Comme les roches basiques alcalines citées plus haut doivent leur origine probablement à un processus de différenciation partant en premier lieu d'un magma basique de la composition du substratum basaltique, leur composition chimique sera encore comparée, dans la IIe partie, à celle des basalto-dolérîtes (ou mélaphyres, d'après la dénomination de DUPARC, 1925—26) développées en intercalations plus ou moins concordantes dans le Permo-Trias gréseux des deux Atlas calcaires et représentées par six analyses chimiques dans les travaux de DUPARC (1925—26, p. 133) et TERMIER (1936, pp. 1491—1501). Nous verrons que les deux tribus en discussion forment des unités pétrochimiques très indépendantes l'une de l'autre; phénomène ressortant nettement de la coördination en deux systèmes séparés des points indiquant la position des analyses dans les diagrammes déjà cités, qui révèlent, en outre, que les différenciations du magma paraissent avoir suivi des cours divergeants dans les deux cas.

Pour expliquer l'origine du magma secondaire qui, par des changements chimiques internes, à ce qu'il semble, produisit la diversité des roches basiques alcalines mentionnées ci-dessus, nous renvoyons à la théorie élaborée par le volcanologue américain G. A. MACDONALD (1949) pour élucider le mode de formation des laves basiques à mélilite et (ou) néphéline sorties pendant la dernière phase des activités volcaniques sur quelques-unes des îles Hawaï, où les éruptions commencèrent invariablement par l'effusion de masses considérables de basaltes à olivine suivies fréquemment de variétés d'andésite, de basalte picritique à phénocristaux d'augite et de trachytes et se terminèrent, par endroits, après une phase assez prolongée de dénudation, par la formation de cônes de roches basiques alcalines.

Comme des observations récentes du premier auteur (W.) et de deux de ses élèves dans la région au Sud du Grand Atlas s'accordent mieux avec une mise en place des basalto-dolérîtes du Domaine Atlasique par intrusion pendant le Supracrétacé ou l'Infratertiaire qu'avec une sortie à ciel ouvert pendant le Permo-Trias (ou Infralias), conception encore prévalante, il y a lieu de considérer des relations plus directes entre l'éruption du magma basalto-doléritique et la formation des roches basiques alcalines néogènes et quaternaires du même Territoire. Les deux ensembles de roches volcaniques représenteraient donc, d'après cette nouvelle manière de voir, des produits de manifestations successives d'une même grande période d'activités magmatiques.

*Description pétrographique de l'aïounite de Narguechoum* (par C. J. MULDER)

A l'oeil nu, cette roche se montre assez profondément altérée et se

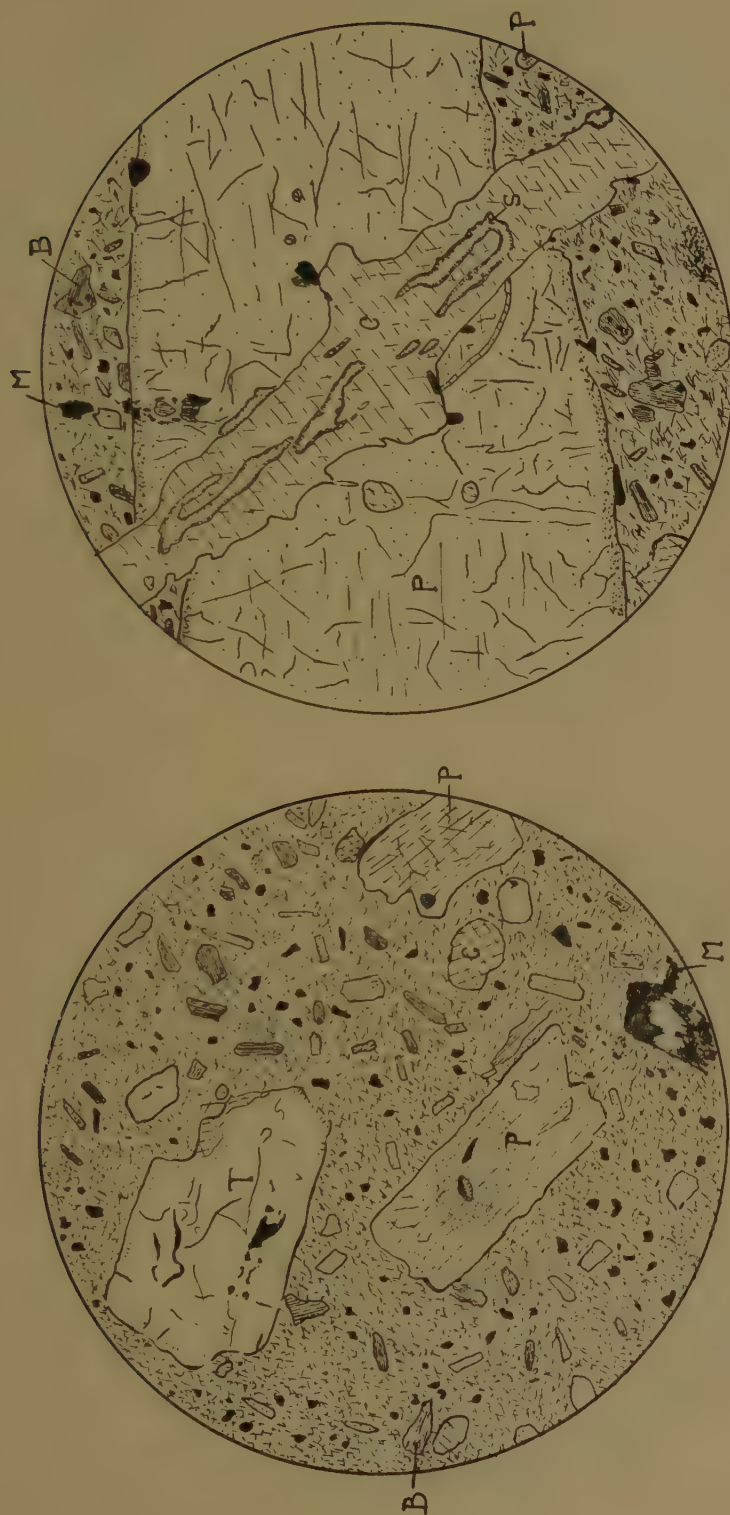


Fig. 1. Aspect général de l'aïounite de Narguechoum. Phénocristaux zonés d'augite et olivines remplacées par du talc dans une pâte consistant principalement en augite, biotite, magnétite, talc, carbonate et zéolite. *B* = biotite; *M* = magnétite; *P* = augite; *T* = talc. Grossissement 31.

Fig. 2. Veinule de carbonate traversant un cristal d'augite zoné et renfermant des trainées de serpentine. *B* = biotite; *C* = carbonate; *P* = augite; *S* = serpentine. Grossissement 25.



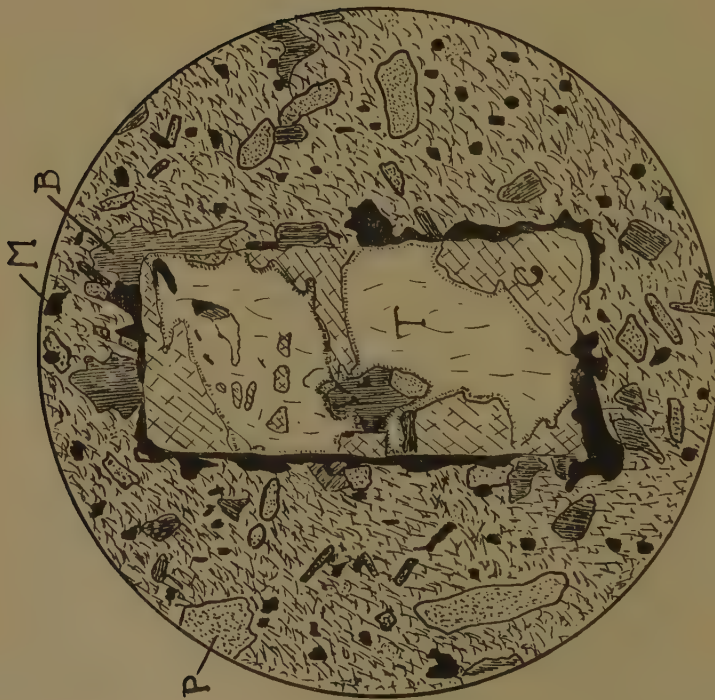


Fig. 3. Phénocristal d'olivine substitué principalement par du talc et du carbonate, avec un enduit de magnétite. *B* = biotite; *C* = carbonate; *M* = magnétite; *P* = augite. Grossissement 83,9.

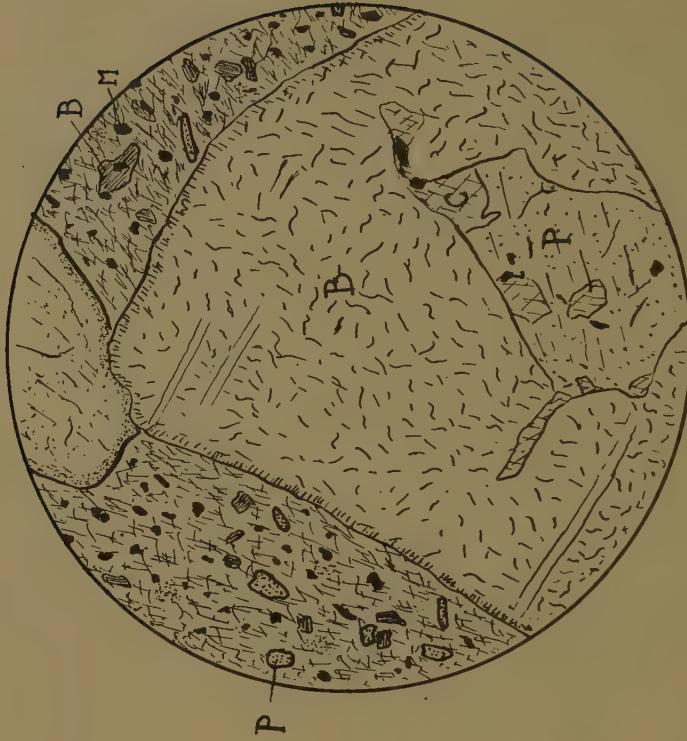


Fig. 4. Grand phénocristal de biotite renfermant un noyau d'augite partiellement carbonatisée. *B* = biotite; *C* = carbonate; *M* = magnétite; *P* = augite. Grossissement 17,9.



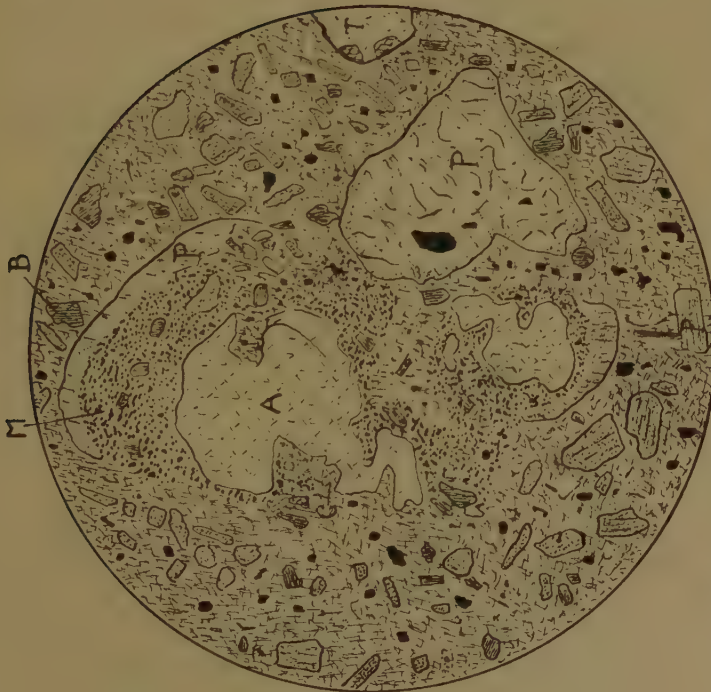


Fig. 5. Cristal d'amphibole corrodé et enveloppé par un grand individu d'augite largement remplacé par de la magnétite et par des minéraux de la pâte, de sorte qu'il ne reste presque que la bordure titanifère de la pyroxène. *A* = amphibole; *B* = biotite; *M* = magnétite; *P* = augite; *T* = talc. Grossissement 32,9.

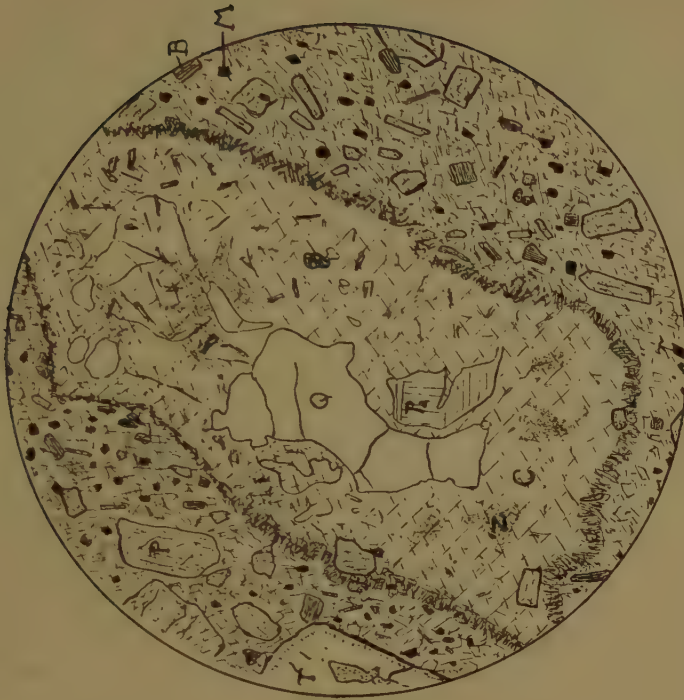


Fig. 6. Amygdale contenant principalement du carbonate, du quartz, du plagioclase et une zéolite. *B* = biotite; *C* = carbonate; *M* = magnétite; *P* = augite; *Pa* = plagioclase; *Q* = quartz; *T* = talc. Grossissement 24,5.

distingue par un développement de phénocristaux de pyroxène et d'olivine altérée, ainsi que de biotite et d'amphibole, dans une pâte fine grisâtre. Elle est striée de veinules de carbonate.

Au microscope, la pâte apparaît holocristalline, consistant en premier lieu en augite et en magnétite, auxquelles espèces se joignent de la biotite, de l'olivine altérée, de l'apatite, du talc, des carbonates secondaires, de la serpentine et une zéolite. On note, de plus, de petites amygdales d'une composition différente.

*Augite.* Espèce développée en formes bien idiomorphes composées d'enveloppes de trois variétés: 1) Augite verte, avec pléochroïsme  $n_a$  vert bleuâtre,  $n_\beta$  vert et  $n_\gamma$  jaune verdâtre, formant le noyau des phénocristaux; 2) Augite titanifère, avec  $n_a = n_\beta$  brun violacé et  $n_\gamma$  beige clair, formant les pyroxènes de la pâte et la bordure des noyaux verts; 3) Augite à peu près incolore, avec  $n_\gamma/c$  et 2V petits, formant parfois une étroite zone de transition entre les deux variétés teintées (voir Figs. 1, 2, 5).

*Olivine.* Espèce toujours complètement remplacée sous conservation de ses contours originels. L'altération a produit principalement du talc incolore ou verdâtre (Figs. 1, 3) accompagné de quelques écailles très pléochroïques d'une couleur vert jaune, qui représentent probablement de la bowlingite. Le chrysotile, en fibres à peu près incolores, surtout dans la pâte, se présente comme un produit intermédiaire dans ce phénomène d'altération (voir T. DU RIETZ, 1935). Autour des individus d'olivine altérés on observe souvent des enduits de petits grains de magnétite et d'hématite formés par la libération de la teneur en fer des cristaux originels. Au contact des filonnets de carbonate, les olivines altérées se trouvent être partiellement ou complètement carbonatisées (Fig. 3).

*Biotite.* Les individus de biotite se trouvent surtout dans la pâte, en écailles pléochroïques ( $n_a$  beige clair,  $n_\beta = n_\gamma$  brun rougeâtre foncé) renfermant de nombreux granules de magnétite, mais on observe également un développement en phénocristaux dispersés (Fig. 4).

*Amphibole.* Minéral développé presque exclusivement en phénocristaux formant parfois le noyau d'individus d'augite (Fig. 5). Le pléochroïsme se distingue par  $n_a$  brun jaune,  $n_\beta$  brun rougeâtre et  $n_\gamma$  brun foncé, tandis que le centre des cristaux est souvent plus clair. On distingue en forme d'inclusions de l'ilménite en petits grains. Les indices de réfraction de l'amphibole, déterminés d'après la méthode SCHROEDER VAN DER KOLK, sont  $n_a = 1,680$ ,  $n_\beta = 1,701$ ,  $n_\gamma = 1,703$ .

*Magnétite.* Minéral abondant dans la pâte en petits cubes et en octaèdres idiomorphes, mais aussi formé, avec un peu d'hématite, par des phénomènes d'ex-solution, comme il est indiqué dans ce qui précède. Les individus de magnétite peuvent atteindre des dimensions assez considérables. L'espèce est probablement titanifère, vue la forte teneur en  $TiO_2$  de la lave et le caractère titanifère de l'augite de la pâte.

*Chrysotile.* Minéral incolore associé au talc dans les olivines altérées. Là où des veinules de carbonate traversent des augites, les premières contiennent du chrysotile vert clair, à biréfringence plus forte (Fig. 2).

*Talc.* Matière incolore ou vert clair remplaçant l'olivine et développée en de nombreuses petites écailles dans la pâte.

*Zéolite.* De petits individus xénomorphes d'une zéolite incolore à biréfringence faible, 2V petit, signe optique positif et indice de réfraction  $< 1,531$  s'observent en petite quantité dans la pâte et dans le contenu des amygdales. Il s'agit probablement de phillipsite ou de harmotome; la teneur relativement élevée en potasse de la roche rend en effet la présence de phillipsite la plus probable.

*Carbonate.* Matière de remplissage de veinules où le carbonate s'est développé en lamelles appliquées perpendiculairement aux parois. De part et d'autre des filonnets, la roche se montre fortement carbonatisée, surtout dans les olivines altérées.

*Les amygdales.* Vacuoles minéralisées, généralement de petites dimensions et aux contours accentués par des granules prismatiques d'augite. Parfois, elles renferment des cristaux plus grands d'augite et d'olivine altérée associés à du carbonate — matière prépondérante —, du quartz, de l'oligoclase-andésine et de la zéolite fibroradiée (Fig. 6). On observe, en outre, un grand nombre de petits grains et d'aiguilles minuscules indéterminables représentant probablement de la biotite, de l'ilménite et des oxydes de fer.

### Analyse chimique

La composition chimique de l'aïounite de Narguechoum (moyenne de deux analyses) est indiquée dans la première colonne de la Table I, celle

TABLE I  
Analyses chimiques d'aïounites du Maroc

	Aïounite de Narguechoum; analyse par E. TEN HAAFF	Aïounite d'El Aïoun; analyse par A. SULZER
SiO <sub>2</sub> . . . . .	38,30	39,06
TiO <sub>2</sub> . . . . .	4,91	3,73
Al <sub>2</sub> O <sub>3</sub> . . . . .	12,11	11,75
Fe <sub>2</sub> O <sub>3</sub> . . . . .	4,81	8,21
FeO . . . . .	5,52	4,49
MnO . . . . .	0,09	0,15
MgO . . . . .	10,49	10,27
CaO . . . . .	14,67	13,61
K <sub>2</sub> O . . . . .	1,85	1,58
Na <sub>2</sub> O . . . . .	0,92	1,76
P <sub>2</sub> O <sub>5</sub> . . . . .	0,62	1,08
H <sub>2</sub> O <sup>+</sup> . . . . .	2,72	3,75
H <sub>2</sub> O <sup>-</sup> . . . . .	0,59	
CO <sub>2</sub> . . . . .	2,82	
S . . . . .	0,17	
	100,59	99,44

de l'aïounite de DUPARC (1925—26, p. 120) dans la seconde à titre de comparaison.

Comme on voit, le titre de la roche filonienne de Narguechoum diffère très peu de celui de l'aïounite de DUPARC, les principaux écarts consistant en une teneur plus faible en soude et en un excès de matières volatiles dans la première; phénomènes qui s'expliqueraient probablement tous les deux, en partie ou entièrement, par des altérations épigéniques.

*(A continuer)*



# NOTE SUR UNE ROCHE FILONNIENNE DE TYPE DES AÏOUNITES DE LA RÉGION DE TAOURIRT ET SUR L'ORIGINE DES LAVES BASIQUES ALCALINES NÉOGÈNES ET QUATERNAIRES DU MAROC FRANÇAIS. II

PAR

J. WESTERVELD, E. TEN HAAF ET C. J. MULDER

(Communicated by Prof. H. A. BROUWER at the meeting of September 29, 1951)

*Les qualités chimiques d'ensemble de la tribu des roches basiques alcalines du Maroc comparées à celles des basalto-dolérites dites du Permo-Trias*

Afin de pouvoir nous servir de moyens de comparaison graphiques d'une disposition claire, les analyses chimiques déjà connues des roches appartenant aux deux tribus discutées ici ont été réduites aux paramètres *si*, *al*, *fm*, *c*, *alk*, *ti*, *p*, *L*, *M* et *Q* élaborés par NIGGLI (1923, p. 50, 51; 1936a). Les résultats des calculs se trouvent réunis dans la Table II, laquelle indique, de plus, la classification de chacun des groupes de paramètres dans le système des types magmatiques d'après le même auteur (1936b). La figure 7 représente une esquisse géologique du Maroc montrant la répartition des deux familles de roches éruptives et les lieux où les spécimens analysés furent prélevés.

Bref, il suffit de répéter que les valeurs *si*, *al*, *fm*, *c*, *ti* et *p* représentent les proportions moléculaires des teneurs en  $\text{SiO}_2$ ,  $\text{Al}_2\text{O}_3$ ,  $(2 \text{Fe}_2\text{O}_3 + \text{FeO} + \text{MnO} + \text{MgO})$ ,  $\text{CaO}$ ,  $(\text{K}_2\text{O} + \text{Na}_2\text{O})$ ,  $\text{TiO}_2$  et  $\text{P}_2\text{O}_5$ , la somme *al* + *fm* + *c* + *alk* étant réduite à 100. Les chiffres *k* et *mg*, ensuite, représentent les quotients

$$\frac{\text{K}_2\text{O}}{\text{K}_2\text{O} + \text{Na}_2\text{O}} \text{ et } \frac{\text{MgO}}{2\text{Fe}_2\text{O}_3 + \text{FeO} + \text{MnO} + \text{MgO}},$$

également en termes moléculaires. *L*, *M* et *Q* indiquent finalement les proportions mutuelles des sommes suivantes de molécules de base sous-saturées en silice.

$$L = Kp + Ne + Cal = \text{KAlSiO}_4 + \text{NaAlSiO}_4 + \text{CaAl}_2\text{O}_4$$

$$M = Cs + Fs + Fa + Fo = \text{Ca}_2\text{SiO}_4 + \text{Fe}_2\text{SiO}_5 + \text{Fe}_2\text{SiO}_4 + \text{Mg}_2\text{SiO}_4$$

$$Q = Qu + Ru = \text{SiO}_2 + \text{TiO}_2$$

$$L + M + Q = 100$$

Les représentations graphiques des paramètres, Figs. 8 et 9, dont la première illustre la variation des valeurs *al*, *fm*, *c* et *alk* en fonction de *si*, tandis que la seconde indique les positions des compositions chimiques des roches en question dans le système ternaire *L* — *M* — *Q*, montrent clairement une séparation très nette entre l'ensemble des analyses 1—14

représentant les roches basiques alcalines et celui des analyses A — F relatives aux basalto-dolérites. C'est dire que ces deux tribus doivent leur diversité chimique et pétrographique à des mécanismes de différenciation mutuellement indépendants.

La figure 8 et la Table II nous apprennent que les membres les plus acides du groupe des roches basiques alcalines, les mestigmérites, murites phonolitiques et phonolites, se distinguent au contraire des basalto-dolérites par des valeurs relativement élevées pour *al*, *alk* et *L*, tandis que dans la direction des ankaratrites on note un accroissement prononcé de *fm*, *c* et *M*, joint à une décroissance des chiffres pour *al*, *alk*, *L* et *Q*; ces deux phénomènes tiennent aux teneurs élevées des ankaratrites en oxydes de fer, de magnésium et de calcium et à leur pauvreté en silice et aluminium. On remarque, d'ailleurs, que les deux courbes pour *alk*, ainsi que celles pour *c*, tendent à diverger dans la direction de l'accroissement de *si*.

Pour marquer les dernières différences remarquables entre le titre des basalto-dolérites et celui des roches basiques alcalines il nous reste d'attirer l'attention sur la haute teneur en  $\text{TiO}_2$ , souvent aussi en  $\text{P}_2\text{O}_5$ , et finalement en substances volatiles ( $\text{H}_2\text{O}$ ) de celles-ci. La teneur en  $\text{TiO}_2$  monte jusqu'à plus de 3 et même au-delà de 4 p.c. chez la tribu basique alcaline, tandis que chez les basalto-dolérites elle dépasse à peine 2 p.c.

La figure 9 montre que les points représentant les basalto-dolérites, exception faite de l'échantillon A, se trouvent tous très rapprochés de la ligne de saturation P — F, au-dessous de laquelle on passe dans le champ des roches sous-saturées où sont cantonnés tous les membres de la tribu basique alcaline. Cela indique que, normativement, les basalto-dolérites tendent à des teneurs très faibles en feldspathoïdes et olivine, ou même à l'absence de ces espèces dans la norme. Le rassemblement des points représentant le groupe basique alcalin au-dessous de la ligne P — F, au contraire, est parfaitement en harmonie avec la richesse des membres de cette tribu en espèces comme l'haüyne, la néphéline, la leucite, l'analcite, la mélibite et l'olivine, et en partie en zéolites.

La direction générale de la forme serrée et allongée de la ligne de contour du champ des points représentant les analyses 1—14 dans la figure 9 semble correspondre à des cours de différenciation à peu près identiques et parallèles suivis par les membres de la tribu basique alcaline. La ligne médiane à pointes de flèche tirée à travers le centre dudit champ indiquerait la direction idéale des changements chimiques subis par une matière liquide mère hypothétique. Tandis que les différenciations des magmas basiques alcalins semblent s'être effectuées plus ou moins parallèlement à la direction P — F en plein milieu du cadre M — P — F — L, la composition du magma basalto-doléritique semble plutôt avoir suivi le cours de la ligne brisée. Malgré le nombre encore restreint des analyses de basalto-dolérites, les données disponibles permettent pourtant de distinguer clairement deux systèmes d'évolution magmatique notablement divergeants.

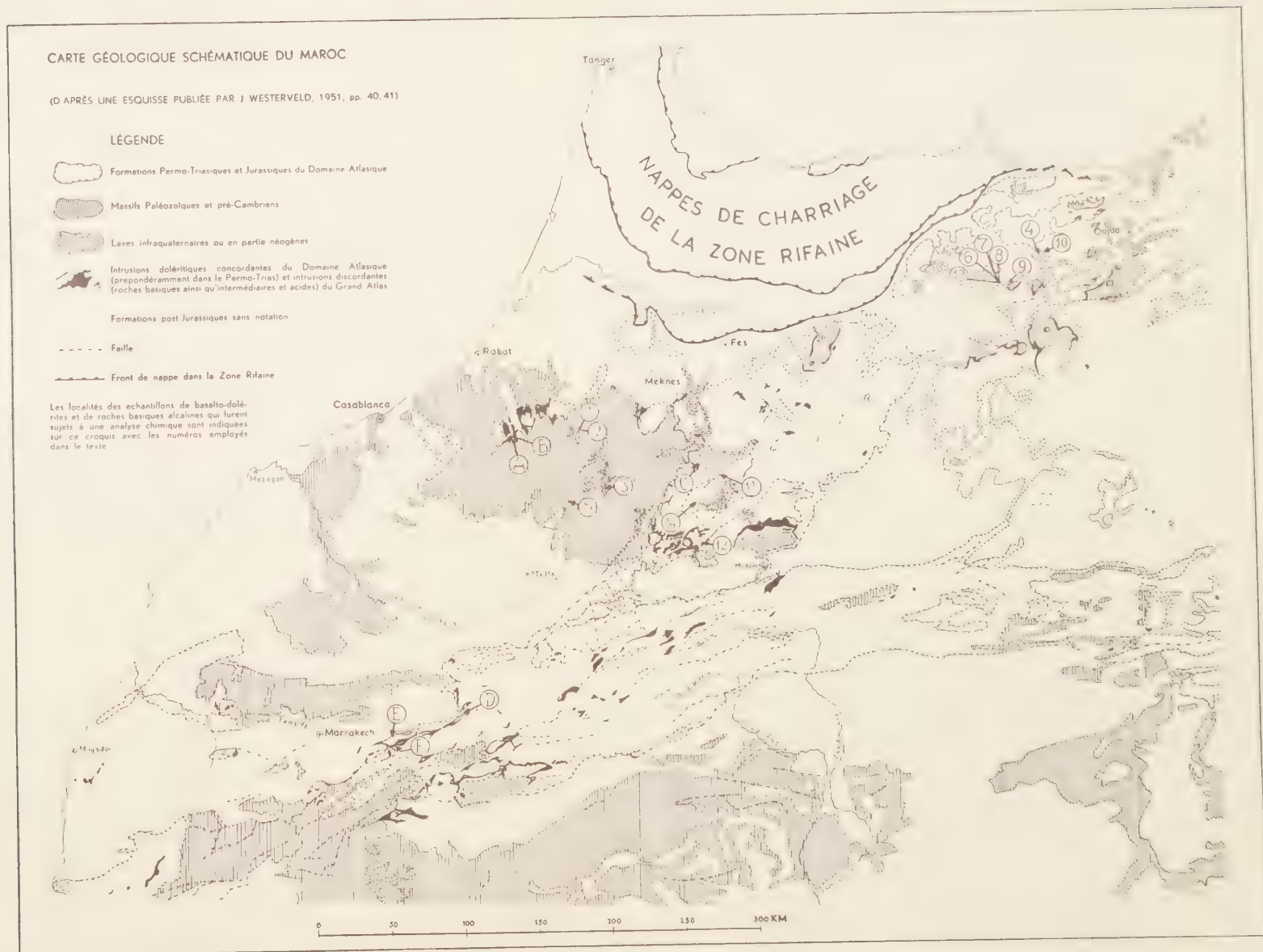


Fig. 7





TABLE II

Tableau des paramètres et de la classification selon P. NIGGLI des analyses de basalto-dolérites et de roches basiques alcalines marocaines.  
Auteurs: TERNIER 1936 (T.), DUPARC 1925-1926 (D.) et Mme. JÉRÉMIÉ 1948 (J.)

No.	Roche et localité	Auteur	si	al	fm	c	alk	ti	p	k	mg	L	M	Q	Type du magma d'après P. NIGGLI (1936b)
1	Phonolite, Volcan d'Harcha (Oulmès)	T., p. 1523	144	39½	14½	16½	29½	2.5	1.5	0.16	0.10	65.8	10.1	24.1	± monmouthitique
2	Phonolite, Volcan d'Harcha (Oulmès)	T., p. 1524	135	32	20½	20½	27	2.5	0.3	0.33	0.28	59.7	17.8	22.5	± ijolithique normal
3	Murite phonolitique, Dj. Tiousirt	T., p. 1526	104	22½	33	24	20½	5.5	0.8	0.25	0.37	51.1	32.8	16.1	théralitique normal
4	Mestignérine, Mestigner	D., p. 122	95	20½	42	27	10½	5.5	1.5	0.16	0.50	40.8	35.9	23.3	gabbro-dioritique essexitique
5	Tahitite, Gara Rehaña	T., p. 1528	91	19	35	32	14	6	2	0.25	0.37	44.1	37.9	18.0	melégitique
6	Fassinite, Volcan Taourirt-Taberichent	T., p. 1539	83	19	39	33	9	6	1	0.11	0.51	38.9	41.5	19.6	bérondritique
7	Fassinite doléritique, ibidem	T., p. 1538	82	14½	42	33½	10	6	1	0.30	0.54	34.7	48.6	16.7	e-gabbro-théralitique
8	Fassinite, Taourirt	J., p. 70	76	13	52	29½	5½	5.5	0.6	0.33	0.63	28.1	55.1	16.8	issitique
9	Aïounite, N de Narguechoum	79½	14	49	33	4	7.5	0.5	0.57	0.67	27.7	51.4	20.9	± issitique ou polzénitique	
10	Aïounite, El Aïoun	D., p. 120	79	14	51	29½	5½	5.5	1	0.37	0.60	29.0	51.7	19.3	potassique ± issitique
11	Ankaratrite limbourgitique, Dj. Tarbalou	T., p. 1543	75	15½	48½	28	8½	4	0.8	0.17	0.62	34.3	52.3	13.4	ankaratritique
12	Ankaratrite, Dj. Tasfaït et Tastafait	T., p. 1535	72	14	46½	33½	6	5	1	0.23	0.62	31.1	53.3	15.6	± issitique
13	Ankaratrite, Volcan Taourirt-Taberichent	T., p. 1536	67½	10½	57	25½	7	4.5	0.5	0.23	0.68	27.7	62.3	10.0	± hornblenditique
14	Ankaratrite à méllite, Dj. Anach	T., p. 1541	62½	10	52½	32	5½	3.5	1	0.29	0.70	26.6	63.9	9.5	± polzénitique vésécitique
A	Basalte labradorique, S d'Azrou	T., p. 1498	95½	17	52½	23	7½	3	0.4	0.20	0.62	33.3	43.8	22.9	± gabbroïde essexitique
B	Basalte labradorique, OuedSbeida	T., p. 1494	117½	21	47	28	4	2	0.14	0.20	0.57	30.6	35.7	33.7	± miharaitique
C	Dolérite à pigeonite, Oued Khenoussa	T., p. 1496	123½	20	45½	30	4½	2.5	0.14	0.19	0.54	29.6	35.8	34.6	± miharaitique
D	Mélaphyre, Dennaat	D., p. 135	117	21	47½	25½	6	1.8		0.13	0.62	33.1	35.4	31.5	± gabbroïde normal
E	Mélaphyre, Sidi Réhal	D., p. 139	128½	21	46	25	8	2.9		0.27	0.57	33.6	33.0	33.4	± gabbro-dioritique normal
F	Mélaphyre, Sidi Réhal	D., p. 137	132	20	45	27½	7½	2.4		0.19	0.53	31.4	34.0	34.6	± miharaitique

Roches basiques alcalines infraquaternaires et néogènes

Basalte dolérites dites du Perno-Trias

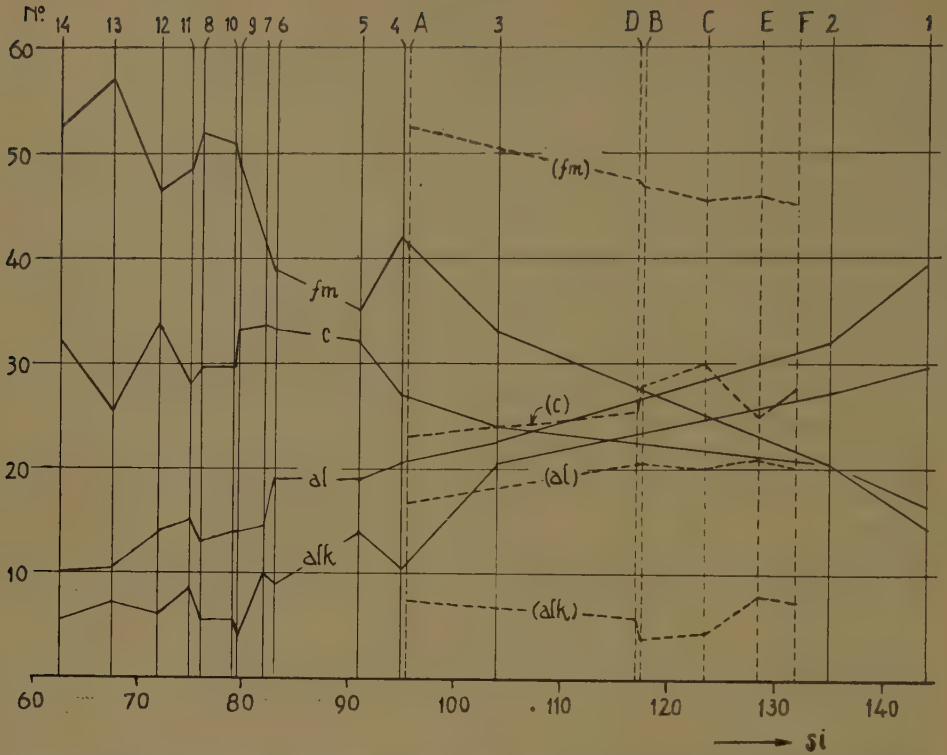


Fig. 8. Diagramme des valeurs  $al$ ,  $fm$ ,  $c$  et  $alk$  en fonction de  $si$ . Lignes brisées: Basalto-dolérîtes dites du Permo-Trias. Lignes pleines: Roches basiques alcalines néogènes et infraquaternaires

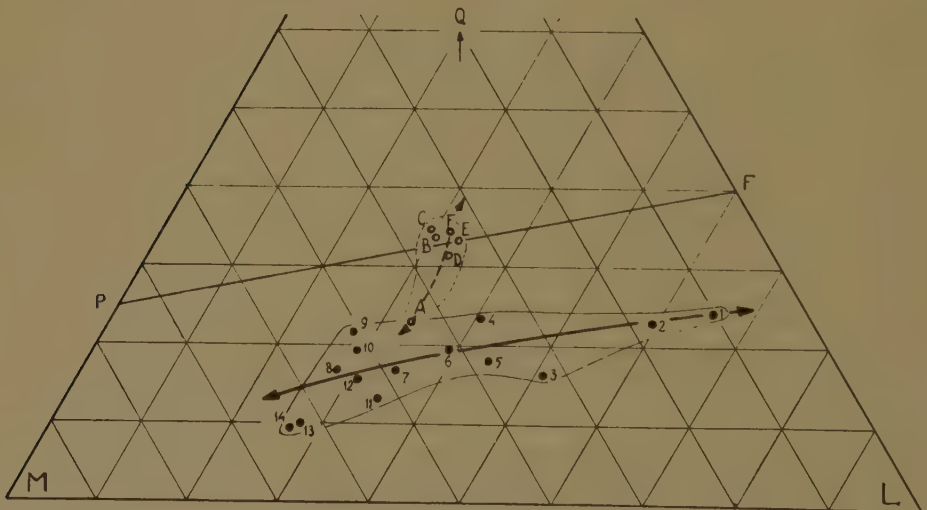


Fig. 9. Diagramme du système ternaire  $L - M - Q$ . Cercles ouverts: Basalto-dolérîtes dites du Permo-Trias. Cercles noirs: Roches basiques alcalines néogènes et infraquaternaires.  $L = Kp + Ne + Cal$ ;  $M = Cs + Fs + Fa + Fo$ ;  $Q = Qu + Ru$ ;  $P = \text{pyroxènes } (Wo + En + Hy)$ ;  $F = \text{feldspaths } (Or + Ab + An)$ .

### *Mode de formation des roches basiques alcalines*

L'apparition de roches effusives d'une composition basique et de caractère soudique au milieu des centres d'éruption de basaltes à olivine dans les régions océaniques, ou bien parfois dans un environnement continental, reste un des phénomènes encore mal expliqués de la pétrogenèse, comme l'ont affirmé encore tout récemment F. J. TURNER et J. VERHOOGEN (1951, p. 139).

Si l'on s'en tient, en attendant la fixation d'une opinion commune sur cette question, au point de vue soutenu par le premier auteur (W.) du présent article, selon lequel les basalto-dolérites du Domaine Atlasique devraient leur mise en place à des intrusions néocrétacées ou infratertiaires liées à l'orogénèse alpine, il y aurait lieu de considérer celles-ci comme des manifestations d'une phase antérieure et gigantesque du volcanisme marocain précédant l'extrusion (ou l'intrusion) beaucoup moins violente des laves basiques alcalines sorties pendant le Néogène ou le Quaternaire inférieur. Dans ce cas, les relations assez intimes que nous devrions admettre entre ces deux groupes de roches éruptives seraient à peu près analogues, du point de vue de la succession des compositions chimiques et aussi jusqu'à un certain degré des phénomènes d'éruption, à celles qu'on a constaté en plusieurs régions océaniques, notamment dans l'archipel des îles Hawaï.

Les compositions chimiques des basalto-dolérites du Domaine Atlasique, pour autant qu'on les connaît à présent, ne s'opposent guère à des relations génétiques plus ou moins rapprochées par rapport au groupe postérieur, néogène et quaternaire, des roches basiques alcalines. L'origine commune et la mise en place des deux tribus en relation immédiate avec les poussées alpines, présumées ici, font supposer des affinités entre la composition des basalto-dolérites intercalées dans le Permo-Trias gréseux du Maroc et celle des basaltes à olivine des îles océaniques plutôt qu'une conformité de celle-là au titre des basaltes des plateaux ou tholéiites, pour confirmer la séparation entre ces deux types de magmas faite par W. Q. KENNEDY (1933). En passant la revue des compositions chimiques des basalto-dolérites marocaines, on constate que celles données par TERMIER (1936, pp. 1494, 1496, 1498) se rapprochent plus, à ce qu'il paraît, de celles des basaltes à olivine que de celles des tholéiites, tandis que les chiffres publiés par DUPARC (1925—26, pp. 135, 137, 139) montrent en partie plutôt l'inverse. Le titre du basalte à labrador d'Azrou (no. A), par exemple, démontre l'affinité essexitique de cette roche et sa ressemblance chimique avec les basaltes à olivine de la sub-province peu déformée de la région d'Otago Oriental en Nouvelle Zélande (voir les moyennes de 8 analyses chez TURNER et VERHOOGEN, 1951, p. 144); celui de la dolérite à pigeonite de l'Oued Khenoussa (no. C) démontre une certaine identité avec la composition du basalte à olivine de la série de Waianae sur l'île d'Oahou dans l'Archipel Hawaïen (analyse chez TURNER et VERHOOGEN, p. 127); celui du „mélaphyre" de Demnat (no. D) démontre enfin, quelque ressem-

blance avec la moyenne de 11 analyses de basaltes à olivine de l'île Hawaï (voir TURNER et VERHOOGEN, p. 137). Le titre des „mélaphyres” de Sidi Réhal (nos. E et F), par contre, par sa ressemblance avec la moyenne de 5 analyses de diabases dans le système du Karroo, ou bien avec la composition de la diabase non-différenciée du „Palisade sill” (voir TURNER et VERHOOGEN, p. 187), se rapproche plus de celui du magma tholéïtique de KENNEDY. Les basalto-dolérites du Maroc paraissent donc être en partie conformes aux types accompagnés en plusieurs cas par des roches basiques soudiques.

L'image présentée par la figure 9 amène facilement à la conclusion que les membres individuels de la tribu basique alcaline se laissent dériver de matières liquides mères sujettes à des différenciations par cristallisation. D'une part, on arriverait à supposer la formation de magmas alcalins basiques ou ultrabasiques (ceux des ankaratrites) par la résorption de cristaux d'olivine et de pyroxène s'enfonçant vers la base de réservoirs de ce qu'on appelle magmas primaires; d'autre part, à concevoir la ségrégation de liquides résiduels riches en feldspathoïdes et en feldspaths (les magmas phonolitiques, par exemple) par l'élimination de ces premières cristallisations. Reste la difficulté principale, celle d'expliquer la dérivation du substratum basaltique de sub-magmas alcalins qui auraient pu donner naissance, à leur tour, à la formation de roches basiques alcalines à feldspathoïdes et sous-saturées en haut degré en silice; question pour la solution de laquelle maintes hypothèses ont été rédigées par divers auteurs (voir, par exemple le résumé de ces théories par TURNER et VERHOOGEN, 1951, pp. 134—140).

La tentative récente de G. A. MACDONALD (1949) de jeter quelque lumière sur les causes des éruptions très localisées de basaltes à néphéline, basaltes à néphéline et mélilite, basanites à néphéline, basaltes à picrite du type des mimosites, etc., dans les îles d'Oahou et de Kaouai de l'Archipel Hawaïen, où ces roches firent leur apparition après un long intervalle de tranquillité volcanique, utilisé par les forces d'érosion pour altérer considérablement le relief morphologique des volcans pré-existants, offre peut-être aussi des perspectives pour l'interprétation du „clan” basique alcalin du Maroc. Comme dans le cas de l'exemple du Pacifique, le volcanisme néogène-infracratérien du Domaine Atlasique et de la Meseta marocaine s'est manifesté comme un phénomène tardif et beaucoup moins vaste en comparaison avec l'éruption des basalto-dolérites. En se basant sur des calculs pétrochimiques très minutieux, MACDONALD, sans prétendre vouloir dire le dernier mot sur la question, arrive à la conclusion que les basaltes et basanites à néphéline, etc., de la série de Honolulu sur Oahou et des roches semblables sur Kaouai représentent en premier lieu des produits engendrés par la cristallisation à peu près complète d'un sub-magma cafémique formé auparavant, ou peut-être simultanément, par l'assimilation de cristaux d'olivine, de pyroxène et de plagioclase basique s'enfonçant dans un liquide de la composition des basaltes à olivine;



processus qui aurait été secondé peut-être, mais pas nécessairement, par l'assimilation de petites quantités de roches calcaires et par le transport d'alcalis et de fer par des agents volatils. Le mélange de roches basiques alcalines et de basaltes à olivine sorti lors des éruptions postérieures à la phase de dénudation sur Kaouai et Oahou s'expliquerait peut-être par la co-existence de plusieurs foyers magmatiques de petites dimensions se trouvant en des phases différentes de cristallisation et soumis à des conditions de température et de pression variées.

Par la voie de la comparaison, on arrive donc à s'imaginer que, comme sur les îles Hawaï, les éruptions des ankaratrites, aïounites, fasinites, tahitites, mestigmérites, murites, phonolites, etc., du Maroc Français sont parties de réservoirs magmatiques isolés que des éruptions antérieures des basalto-dolérites et la décroissance graduelle des poussées orogéniques ont empêchés de percer jusqu'à la surface; foyers où la matière liquide basaltique eut l'occasion et le temps de subir des modifications chimiques considérables par suite de l'assimilation des premières cristallisations près du fond des cuvettes, et de différenciations prolongées succédant à la ségrégation dans le même milieu de nouvelles générations de phénocristaux.

## R É F É R E N C E S

- ACARD, J., *Sur l'âge et le mode de gisement des aïounites et mestigmérites du Maroc Oriental*. Notes du Service Géologique, III (Notes et Mém. du Serv. Géol. du Maroc, 76), 189—195 (1950).
- DUPARC, L., *Contribution à la connaissance de la pétrographie et des gîtes minéraux du Maroc*. Ann. Soc. Géol. de Belgique, 49, 114—119 (1925—26).
- JÉRÉMINÉ, Mme. E., *Sur quelques roches provenant du Maroc Oriental: aïounite et mestigmérite*. Notes du Service Géologique, I (Notes et Mém. du Serv. Géol. du Maroc, 71), 67—71 (1948).
- KENNEDY, W. Q., *Trends of differentiation in basaltic magmas*. Amer. Journ. of Science, 5th series, 25, 239—256 (1933).
- MACDONALD, G. A., *Hawaiian petrographic province*. Bull. Geol. Soc. of America, 60, 1541—1596 (1949).
- NIGGLI, P., *Gesteins- und Mineralprovinzen*, 1 (1923).
- , *Über Molekularnormen zur Gesteinsberechnung*. Schweiz. Min. und Petr. Mitt. 16, 295—317 (1936a).
- , *Die Magmentypen*. Schweiz. Min. und Petr. Mitt., 16, 335—399 (1936b).
- RIETZ, T. DU, *Peridotites, serpentines, and soapstones of Northern Sweden*. Geol. Förl. i Stockholm Förl., 57, 133—260 (1935).
- SITTER, L. U. DE et LAGAAIJ, R., *Sur le mode de gisement des laves permotriassiques dans le Maroc Oriental*. C.R. somm. d. Séances, Soc. Géol. de France, 13—14, 279—281 (1948).
- TERMIER, H., *Études géologiques sur le Maroc Central et le Moyen Atlas Septentrional, III, Pétrographie*. Notes et Mém. du Serv. Géol. du Maroc, 33, 1423—1566 (1936).
- , H. et G. et JOURAVSKY, G., *Une roche volcanique à gros grain de la famille des ijolites: la talzastite*. Notes du Service Géol., I (Notes et Mém. du Serv. Géol. du Maroc, 71), 81—120 (1948).
- TURNER, F. J. et VERHOOGEN, J., *Igneous and Metamorphic Geology* (1951).

- WESTERVELD, J., *Sur la position géologique des laves soi-disant permotriasiques ou infra-liasiques du Domaine Atlasique et leurs rapports avec la métallogénie marocaine*. Proc. Kon. Ned. Akad. v. Wetensch., **51**, 565—574 (1948).
- , *Les gîtes de manganèse du Domaine Atlasique au Maroc Français et leur classification géologique*. Geologie en Mijnbouw, Nieuwe Serie, **13**, 25—52 (1951).

*Amsterdam, Institut Géologique de l'Université*

# INDEX

(*Proceedings, Series B, Vol. LIV, 1951*)

## Astronomy

- BERLAGE, H. P.: "Some remarks on the internal constitution of the bodies of the solar system", p. 344.
- KOELBLOED, D. and W. VELTMAN: "On the electron temperature of the chromosphere and prominences", p. 468.
- PANNEKOEK, A.: "Periodicities in lunar eclipses", p. 30.

## Chemistry

- ARENS, J. F. and P. MODDERMAN: "Synthesis of a lower homologue of citral and of pseudo-ionone", p. 236.
- BACKER, H. J. and Th. J. DE BOER: "A new method for the preparation of diazo-methane", p. 191.
- BACKER, H. J. and J. L. MELLES: "The sulphone of thiophene", p. 340.
- BALÁZS, N. L.: "Viscosity of binary liquid mixtures", p. 366.
- BOOIJ, H. L. and P. J. VAN MULLEM: "Influence of organic compounds on soap and phosphatide coacervates". XVI, I, p. 273.
- BOOIJ, H. L. and P. J. VAN MULLEM: "Influence of organic compounds on soap and phosphatide coacervates". XVI, II, p. 284.
- BUNGENBERG DE JONG, H. G.: "Elastic viscous oleate systems containing KCl". XV, p. 1.
- BUNGENBERG DE JONG, H. G. and W. W. H. WEYZEN: "Soap coacervates with special properties, hitherto only known in coacervates of phosphatides". III, p. 81.
- BUNGENBERG DE JONG, H. G. and A. M. VAN LEEUWEN: "Influence of exposure of a gelatin solution to various temperatures or to the action of pepsin on the subsequent complex coacervation with Gum Arabic", p. 91.
- BUNGENBERG DE JONG, H. G., W. A. LOEVEN and W. W. H. WEYZEN: "Elastic-viscous oleate systems containing KCl". XVI, p. 240.
- BUNGENBERG DE JONG, H. G., W. A. LOEVEN and W. W. H. WEYZEN: "Elastic-viscous oleate systems containing KCl". XVII, p. 291.
- BUNGENBERG DE JONG, H. G., W. A. LOEVEN and W. W. H. WEYZEN: "Elastic-viscous oleate systems containing KCl". XVIII, p. 303.
- BUNGENBERG DE JONG, H. G., H. J. VAN DEN BERG and H. J. VERHAGEN: "Elastic-viscous oleate systems containing KCl". XIX, p. 317.
- BUNGENBERG DE JONG, H. G., H. J. VAN DEN BERG, W. A. LOEVEN and W. W. H. WEYZEN: "Elastic-viscous soap systems containing salts". XXa, p. 399.
- BUNGENBERG DE JONG, H. G., H. J. VAN DEN BERG, W. A. LOEVEN and W. W. H. WEYZEN: "Elastic-viscous soap systems containing salts". XXb, p. 407.
- HERTOG, H. J. DEN and P. BRUIN: "Addition reactions of alkenes in silent electrical discharges", p. 379.
- HONIG, P.: "The heat conductivity of scales in evaporators", p. 110.
- MAASSEN, A. P.: "Insulin and growth", p. 160.
- SIXMA, F. L. J., C. M. SIEGMANN and H. C. BEYERMAN: "The sterical configuration of tropine and  $\psi$ -tropine", p. 452.
- STRATING, J. and H. J. BACKER: "A new homologue of provitamin D<sub>3</sub>", p. 13.
- WIBAUT, J. P. and A. STRANG: "Autoxidation of saturated hydrocarbons in the liquid phase". (First communication), I, p. 102.

WIBAUT, J. P. and A. STRANG: "Autoxidation of saturated hydrocarbons in the liquid phase". (First communication), II, p. 229.

WIBAUT, J. P. and A. R. GULJÉ: "The ozonolysis of pyrrole and some of its homologues in connection with the structure of the ring system", p. 330.

### Chemistry, Physical

BOER, J. H. DE and G. M. M. HOUBEN: "Misleading colour-reactions", p. 421.

BURGERS, W. G., Y. H. LIU and T. J. TIEDEMA: "The influence of crystal orientation on polygonization of aluminium single crystals", p. 459.

PEERDEMAN, A. F., A. J. VAN BOMMEL and J. M. BIJVOET: "Determination of absolute configuration of optical active compounds by means of X-rays", p. 16.

### Crystallography

MACGILLAVRY, CAROLINE H., A. KREUGER and E. L. EICHHORN: "The molecular structure of trans  $\beta$  ionylidene crotonic acid", p. 449.

### Dynamics

KAMPÉ DE FÉRIET, J. and R. BETCHOV: "Theoretical and experimental averages of turbulent functions", p. 389.

### Elasticity

BAX STEVENS, O.: "Elementary derivation of the shearing stress distribution, the angle of twist and the warping in a prismatic shaft of elliptical cross section twisted by a torque", p. 120.

### Geology

BROUWER, H. A. et C. G. EGELER: "Sur le métamorphisme à glaucophane dans la nappe des schistes lustrés de la Corse", p. 130.

UMBROGROVE, J. H. F.: "A model of the earth's crust", p. 443.

WESTERMANN, J. H.: "The water bore of Oranjestad 1942–1943, and its implication as to the geology and geohydrology of the island of Aruba (*Netherlands West Indies*)". I, p. 140.

WESTERMANN, J. H.: "The water bore of Oranjestad 1942–1943, and its implication as to the geology and geohydrology of the island of Aruba (*Netherlands West Indies*)". II, p. 151.

WESTERVELD, J., E. TEN HAAF et C. J. MULDER: "Note sur une roche filonienne du type des aïounites de la région de Taourirt et sur l'origine des laves basiques alcalines néogènes et quaternaires du Maroc français". I, p. 475.

WESTERVELD, J., E. TEN HAAF et C. J. MULDER: "Note sur une roche filonienne du type des aïounites de la région de Taourirt et sur l'origine des laves basiques alcalines néogènes et quaternaires du Maroc français". II, p. 483.

ZWART, H. J.: "Postglaciale land- en zeeniveau-veranderingen", p. 162.

### Geophysics

VENING MEINESZ, F. A.: "A remarkable feature of the earth's topography, origin of continents and oceans". I, p. 212.

VENING MEINESZ, F. A.: "A remarkable feature of the earth's topography, origin of continents and oceans". II, p. 220.

VENING MEINESZ, F. A.: "A third arc in many island arc areas", p. 432.

### History of Science

CITTERT, P. H. VAN and J. G. VAN CITTERT-EYMERS: "Some remarks on the development of the compound microscopes in the 19th century", p. 73.



**Hydrodynamics**

- DORRESTEIN, R.: "General linearized theory of the effect of surface films on water ripples". I, p. 260.
- DORRESTEIN, R.: "General linearized theory of the effect of surface films on water ripples". II, p. 350.

**Mechanics**

- KOITER, W. T.: "On GRAMMEL's linearisation of the equations for torsional vibrations of crankshafts", p. 464.

**Meteorology**

- BOER, H. J. DE: "Treering measurements and weather fluctuations in Java from A.D. 1514". I, p. 194.
- BOER, H. J. DE: "Treering measurements and weather fluctuations in Java from A.D. 1514". II, p. 203.

**Paleontology**

- DROOGER, C. W.: "Foraminifera from the tertiary of Anguilla, St. Martin and Tintamarre (Leeward Islands, West Indies)", p. 54.
- DROOGER, C. W.: "Upper cretaceous foraminifera of the Midden-Curaçao beds near Hato, Curaçao (N.W.I.)", p. 66.
- DROOGER, C. W.: "Notes on some representatives of *Miogypsinella*", p. 357.
- JONGMANS, W. J.: "Fossil plants of the island of Bintan (with a contribution by J. W. H. ADAM)", p. 183.
- MARKS JR, P.: "Arenonionella, a new arenaceous genus of Foraminifera from the Miocene of Algeria", p. 375.
- RITSEMA, L.: "Description de quelques Alvéolines de Timor: résultat d'une élaboration de la méthode des courbes d'indice de REICHEL", p. 174.

**Physics**

- CLAY, J.: "Similarity of initial processes of continuous cosmic radiation and showers", p. 20.
- CLAY, J.: "Similarity of initial processes of continuous cosmic radiation and showers". II, p. 210.
- CLAY, J., H. F. JONGEN and A. J. DIJKER: "Increase of cosmic ray intensity in correlation with meteoric activity on Nov. 6—7, 1951", p. 430.
- GROOT, S. R. DE and H. A. TOLHOEK: "Electric and chemical potentials; different methods of treatment and their relation", p. 42.
- JONGEN, H. F.: "Sudden increase of cosmic ray intensity following large meteoric activity", p. 253.
- NIJBOER, B. R. A. et L. VAN HOVE: "Sur la fonction de distribution radiale d'un gaz imparfait et le principe de superposition", p. 256.
- OVERBEEK, J. TH. G. and M. J. SPARNAAY: "Experimental determination of long-range attractive forces", p. 387.

# AUTHOR-INDEX

## A

ARENS, J. F., 236.

## B

BACKER, H. J., 13, 191, 340.

BALÁZS, N. L., 366.

BAX STEVENS, O., 120.

BERG, H. J. VAN DEN, 317, 399, 407.

BERLAGE, H. P., 344.

BETCHOV, R., 389.

BEYERMAN, H. C., 452.

BOER, H. J. DE, 194, 203.

BOER, J. H. DE, 421.

BOER, TH. J. DE, 191.

BOMMEL, A. J. VAN, 16.

BOOIJ, H. L., 273, 284.

BROUWER, H. A., 130.

BRUIN, P., 379.

BUNGENBERG DE JONG, H. G., 1, 81,  
91, 240, 291, 303, 317, 399, 407.

BURGERS, W. G., 459.

BIJVOET, J. M., 16.

## C

CITTERT, P. H. VAN, 73.

CITTERT-EYMERS, J. G. VAN, 73.

CLAY, J., 20, 210, 430.

## D

DORRESTEIN, R., 260, 350.

DROOGER, C. W., 54, 66, 357.

DIJKER, A. J., 430.

## E

Egeler, C. G., 130.

EICHHORN, E. L., 449.

## G

GROOT, S. R. DE, 42

GULJÉ, A. R., 330.

## H

HAAF, E. TEN, 475, 483.

HERTOG, H. J. DEN, 379.

HONIG, P., 110.

HOUBEN, G. M. M., 421.

HOVE, L. VAN, 256.

## J

JONGEN, H. F., 253, 430.

JONGMANS, W. J., 183.

## K

KAMPÉ DE FÉRIET, J., 389.

KOELBLOED, D., 468.

KOITER, W. T., 464.

KREUGER, A., 449.

## L

LEEUEWEN, A. M. VAN, 91.

LIU, Y. H., 459.

LOEVEN, W. A., 240, 291, 303, 309, 407.

## M

MAASSEN, A. P., 160.

MACGILLAVRY, CAROLINE H., 449.

MARKS JR, P., 375.

MELLES, J. L., 340.

MODDERMAN, P., 236.

MULDER, C. J., 475, 483.

MULLEM, P. J. VAN, 273, 284.

## N

NIJBOER, B. R. A., 256.

## O

OVERBEEK, J. TH. G., 387.

## P

PANNEKOEK, A., 30.

PEERDEMAN, A. F., 16.

## R

RITSEMA, L., 174.

## S

SIEGMANN, C. M., 452.

SIXMA, F. L. J., 452.

SPARNAAY, M. J., 387.

STRANG, A., 102, 229.

STRATING, J., 13.

## T

TIEDEMA, T. J., 459.

TOLHOEK, H. A., 42.

## U

UMBROVE, J. H. F., 443.

## V

VELTMAN, W., 468.

VENING MEINESZ, F. A., 212, 220, 432.

VERHAGEN, H. J., 317.

## W

WESTERMANN, J. H., 140, 151.

WESTERVELD, J., 475, 483.

WEYZEN, W. W. H., 81, 240, 291, 303,  
399, 407.

WIBAUT, J. P., 102, 229, 330.

## Z

ZWART, H. J., 162.









3 8198 305 321 448

UNIVERSITY OF ILLINOIS AT CHICAGO

